PHARMACOLOGY AND CHEMICAL PROBE DEVELOPMENT OF THE K-26 FAMILY OF NATURAL PRODUCT ANGIOTENSIN-I CONVERTING ENZYME INHIBITORS

By

Glenna J. Kramer

Dissertation

Submitted to the Faculty of the

Graduate School of Vanderbilt University

in partial fulfillment of the requirements

for the degree of

DOCTOR OF PHILOSOPHY

in

Chemistry

December, 2014

Nashville, Tennessee

Approved:

Professor Brian O. Bachmann, Ph.D.

Professor Lawrence Marnett, Ph.D.

Professor Gary A. Sulikowski, Ph.D.

Professor Borden Lacy, Ph.D.

TABLE OF CONTENTS

To my family, for all of your love.

“You don't even have to understand the desert: all you have to do is *contemplate* a simple *grain of sand,* and you will see in it all the *marvels of creation.”*

-Paulo Coelho, The Alchemist

ACKNOWLEDGEMENTS

First and foremost, I would like to thank the Vanderbilt chemistry department for giving me the opportunity to follow my dream to pursue a PhD in chemistry. Without the guidance, encouragement and support of all faculty, staff and students in the department my pursuit would have been much more difficult. Specifically, I would like to thank Dr. Stone and Dr. Rizzo for working to accommodating me when I followed the not traditional path of having a baby in graduate school. The demands of a career in science are notoriously not conducive to raising a family, so I deeply appreciate that they have tried to make this department friendly to graduate students with children. I must thank Sandra Ford for patiently answering all of my questions ranging from class registration to defense scheduling and the storeroom and front office personnel for helping me order any chemical or reagent that I needed and for getting my packages shipped on time. Your assistance has been invaluable.

I would especially like to thank those that I have worked with on teaching assignments throughout the years. I have enjoyed working under Dr. Phillips and Dr. Todd throughout my graduate school career. I truly appreciate all of the light-hearted conversations and the reminders that there is more to science than my research project. I have learned much about myself as an educator in science from working with them. Also, I must say thank you for all of the pizza for compensation for the long days spent proctoring and grading general chemistry exams. I may have complained about grading days, but to be truthful, I enjoyed the opportunity to get to know the other graduate students in the department.

Secondly, I would like to thank the people that have been more directly involved in my research. To my thesis committee, thank you for all of the insight and input along the way. From committee meetings to informal one-on-one conversations about research you have always provided me with a fresh new perspective on my project. I have also had the opportunity to work with fantastic and enthusiastic collaborators throughout my time at Vanderbilt including scientists from the laboratories of Dr. E.D. Sturrock at University of Cape Town, Dr. Ravi Acharya at Bath and Dr. Jens Meiler at Vanderbilt. It has been a pleasure to share excitement with this group of scientists about ongoing research and their scientific insight has been invaluable. I would like to thank Dr. Sturrock specifically for welcoming me into his lab for a period of time for research collaboration and to the members of his lab for making me feel at home when I was so far away from home.

I also would like to thank my advisor, Brian Bachmann for his guidance both with regard to my project and with regards to life. Throughout my graduate school career, he has shared his excitement about science with me, and this excitement has helped me push to complete challenging experiments. Ever since my first day in his lab, I was captivated by the multi-disciplinary perspective that Brian takes on science, a trait that I continuously aspire to develop further, for pushing me to accomplish more than I thought possible and for helping me grow in to a more confident person. Also, I would like to thank Brian for the sometimes brutally honest perspective on balancing a career as a scientist and a family. Most of all, I look up to Brian for being able to balance a career as successful scientist, while being dedicated to his wife and children.

I also must thank my co-workers and lab mates. I consider myself lucky to have spent the last few years surrounded by such a great group of people. Thank you especially for all of the lab lunches, trips to get coffee, games of where's Waldo and politically incorrect debates. I will certainly miss all of you. A special thanks to David Nanneman and Vanessa Phelan for making me feel at home in the lab while introducing me to the wonders of Fantasy Pizza. I truly looked up to you as a younger student in the lab. Also, thank you to Kasia, Emilianne McCranie and Will Birmingham for your friendship and for making my last few years fun.

Lastly, I must thank my friends and family for their love and support. Kerri Grove and Gongping Chen, thank you for your friendship over our journey as graduate students together, for all those morning workouts, and for always listening and cheering me up. Thank you also to Kevin Perzynski for all of the music recommendations that have kept my lab playlist fresh and for providing a listening ear when I have needed a break. To Vanessa Phelan, thank you for being so positive and encouraging and for your honest perspective on being a female in science. I cannot express how I value your friendship. And to my flood friends, the honey badgers, who have been my adopted family for the last four years. Thank you for all of the holiday celebrations, random Thursday night fireworks, trivia, group dinners, bourbon and just general ridiculousness and debauchery. When I had been most frustrated with my lab work and graduate school career you helped me keep the situation in perspective and encouraged me to see the end goal. I might be leaving Nashville, but you are not getting rid of me.

To my parents, I think at times you may have not understood why I wished to pursue a career as a scientist, but you have stood behind me as my biggest cheerleaders every step of the way. Ever since I was young you have encouraged me to have a curiosity in the world around me, to work hard and to follow my dreams. Thank you for all of your dedication, support, and love, for without your guidance I would not be here today.

Thank you also to my husband, Brandon, who has been my rock during the process of graduate school. In many ways you have saved me from myself by reminding me that there is more to life than my lab work. You have been my friend, partner in crime, soul-mate and have given me one of the best gifts, our handsome son. Thank you for your love and encouragement. I am so lucky to have you and I look forward to our future adventures.

Lastly, to my little man, Jude, you have filled a void in my life that I didn't even realize was there. I am so proud of you and I love you so much. Thank you for all of the smiles, laughs and bringing me so much joy over the last year.

LIST OF TABLES

LIST OF FIGURES

LIST OF SCHEMES

LIST OF ABBREVIATIONS

ACE	Angiotensin converting enzyme
AHEP	(R)-1-amino-2-(4-hydroxyphenyl)ethylphosphonic acid
AnCE	ACE homologue in *Drosophila melanogaster*
Ang I	Angiotensin I
Ang II	Angiotensin II
CDC	Center for Disease Control
C-ACE	C-domain ACE
C-dom	C-domain
dAcK-26	Des-acetyl-K-26
DCM	Dichloromethane
DCP	Dicarboxypeptidase
DIPCl	Diisopropylcarbodiimide
DMF	Dimethylformamide
EcDCP	*E. coli* dicarboxypeptidase
EDC	1-ethyl-3-(3-dimethylaminopropyl)carbodiimide
FAPGG	Furylacryloyl-phenylalanyl-glycyl-glycine
HABA	4'-hydroxyazobenzene-2-carboxylic acid
HHL	Histadyl-histadyl-leucine
HOBT	Hydroxybenzotriazole
HPLC	High-performance liquid chromatography
IC_{50}	Half maximal inhibitory concentration

I-TMSi	Iodotrimethylsilane
K26DCP	*Actinomycete K-26* DCP
K_i	Inhibitory constant
LB	Luria broth
LC	Liquid chromatography
MS	Mass spectrometry
MR1DCP	*Schwanella* DCP
N-ACE	N-domain ACE
N-dom	N-domain
NHS	*N*-hydroxysuccinimide
NMR	Nuclear magnetic resonance
PCR	Polymerase chain reaction
Pd/C	Palladium on carbon
PEG	Polyethylene glycol
PEP	Phosphoenolpyruvate
RAS	Renin angiotensin system
sACE	Somatic ACE
SDS-PAGE	Sodium dodecylsulfide polyacrylamide gel electrophoresis
TAEA	Tris(2-aminoethyl)amine
tACE	Testicular ACE
TEA	Triethylamine
TFA	Trifluoroacetic acid
TLC	Thin layer chromatography

TtACE	*T. tessulatum* ACE
tRNA	Transfer ribonucleic acid
WHO	World Health Organization
XcACE	*Xanthamonas* ACE-like enzyme

CHAPTER I

INTRODUCTION

Natural products and natural product derived structures have been a source of many new drug leads for the treatment of human diseases.[1] One pharmacological target which has been employed in natural product bioactivity screens with is angiotensin-I converting enzyme (ACE), EC 3.5.15.1, an enzyme best known for its role in blood pressure modulation in mammals.[2] As part of the renin-angiotensin system (RAS), ACE is responsible for the hydrolysis of the vasodilator bradykinin to inactive peptides, and for cleaving the inactive decapeptide angiotensin I (ang I) to the vasoconstrictor angiotensin II (ang II) (Figure I-1). Ang II not only raises blood pressure directly, it activates the release of the hormone aldosterone from the adrenal cortex, which increases the absorption of sodium and water, thereby increasing blood volume and raising blood pressure. As hypertension is a widespread health concern that is estimated by the Center for Disease Control to effect 1 in 3 adults in the US and believed by the World Health Organization to affect one billion people worldwide and claim nine million lives annually, effectively modulating the function of this enzyme is beneficial to human health.[3-4]

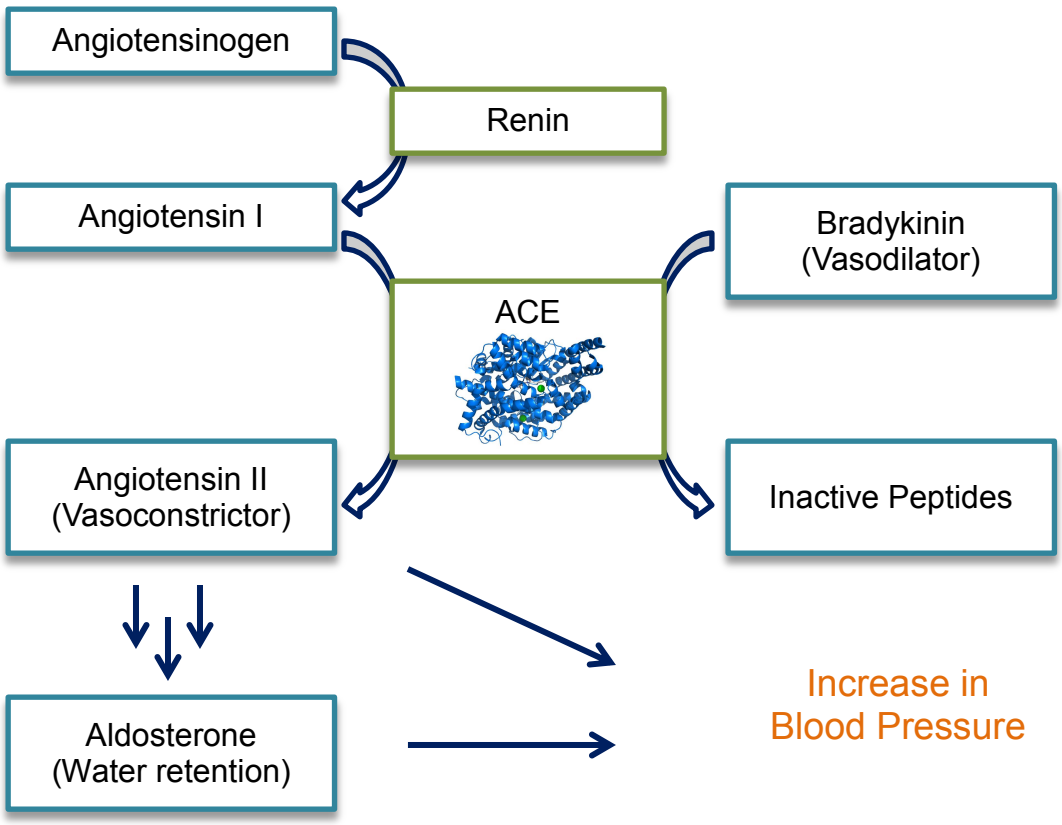

Figure I-1. Schematic of the renin angiotensin aldosterone system emphasizing the role of ACE in blood pressure regulation.

ACE inhibitors have been developed as a means of treatment for hypertension, a condition that is a risk factor for cardiovascular disease including heart attack, heart disease and stroke. However, recent literature has focused on biological functions of ACE outside of the realm of blood pressure regulation, shedding light on why current ACE inhibitor pharmaceuticals are not without side effects, such as angioedema and a dry cough, attributed both to off target effects of these inhibitors and poor modulation of other biological functions of ACE.[2, 5] Despite the relevance of this enzyme to human health, the question of ACE inhibition has not yet been fully answered.

A search of the dictionary of natural products reveals a cohort of over 50 known natural products that have been noted for their inhibitory activity towards ACE.[6] These bioactive natural products have been isolated from a variety of sources including bacteria, fungi, plants and animals. Of these isolated ACE inhibitors, many are peptides or peptide derivatives, including our potent ACE inhibitor and molecule central to this study, K-26 (I-1) (Figure I-2).[7] However, a handful of these natural products that have been noted for their potent ACE inhibitory activity contain other scaffolds. In the following paragraphs, ACE inhibitory natural products and their sources will be discussed.

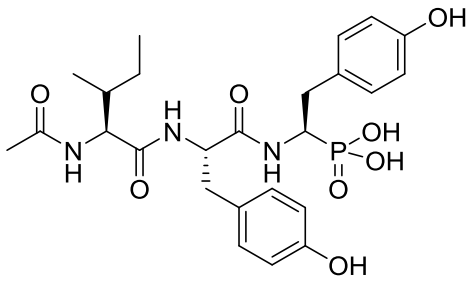

K-26 (I-1)

Figure I-2: Structure of the potent ACE inhibitory natural product, K-26 (I-1).

Unmodified peptides as ACE inhibitors

ACE inhibitory peptides have been isolated and characterized from a broad array of sources including animals, fungi and food products. Tryptic digests of human serum albumen have revealed several ACE inhibitory peptides including Acein I, Acein II, and Albutensin I.[8-10] ACE inhibitory peptides have been isolated from the digestive system of the bonito fish and tuna.[11-14] Viper venom from the species *Bothrops jararaca , Vipera*

aspis, and Agkistrodon halys blomhof, has also been noted for its ACE inhibiting peptides.[15-17] Fungal sources of peptidic natural products with ACE inhibitory activity include the Asian medicinal mushroom *Tricholoma giganteum* and the edible mushroom *Pleurotus cornucopiae.*[18-19] Furthermore, milk, fish, and meat have also been discovered as a source of many bioactive ACE inhibitory peptides.[20-21] Generally, isolated ACE inhibitory peptides range from 3 amino acids to just under 20 amino acids in length and have reported IC_{50}s which fall in the low- to mid- micromolar range. Perhaps the wide array of diverse peptides which have exhibited micromolar inhibitory concentrations towards ACE is a testament to the promiscuity of the enzyme.

Fungal and plant ACE inhibitors

Only a handful of non-peptidic ACE inhibitory natural products have been isolated from fungal and plant sources (Figure I-3). Study of the Chinese medicinal mushroom, *Ganoderma lucidum*, a species known as a rich source of bioactive natural products, have revealed a series of ACE inhibitory triterpenoids.[22] These natural products are variants of Ganolucidic acid A (I-2) and Ganderol B (I-3).[23] Also, an iridoid-type metabolite, oleacein (I-4), was isolated from the olive species *Olea europaea* and *Olea lancea,* and the jasmine species, *Jasminium azoricum and Jasminus grandiflorum* and noted for its ACE inhibitory activity.[24-25] Natural product screening of the jasmine species yielded an additional three bioactive iridoid compounds, sambacein I, II and III (I-5, I-6, I-7), with an IC_{50} for ACE of 26-36 μM.[24] The most potent ACE-inhibitor isolated from a fungal species is a modified peptide with a C-terminal tyrosine, WF 10129. (I-8)

This metabolite is produced by *Doratomyces putredinis*, and is reported to have an IC_{50} of 14 nM.[26-27]

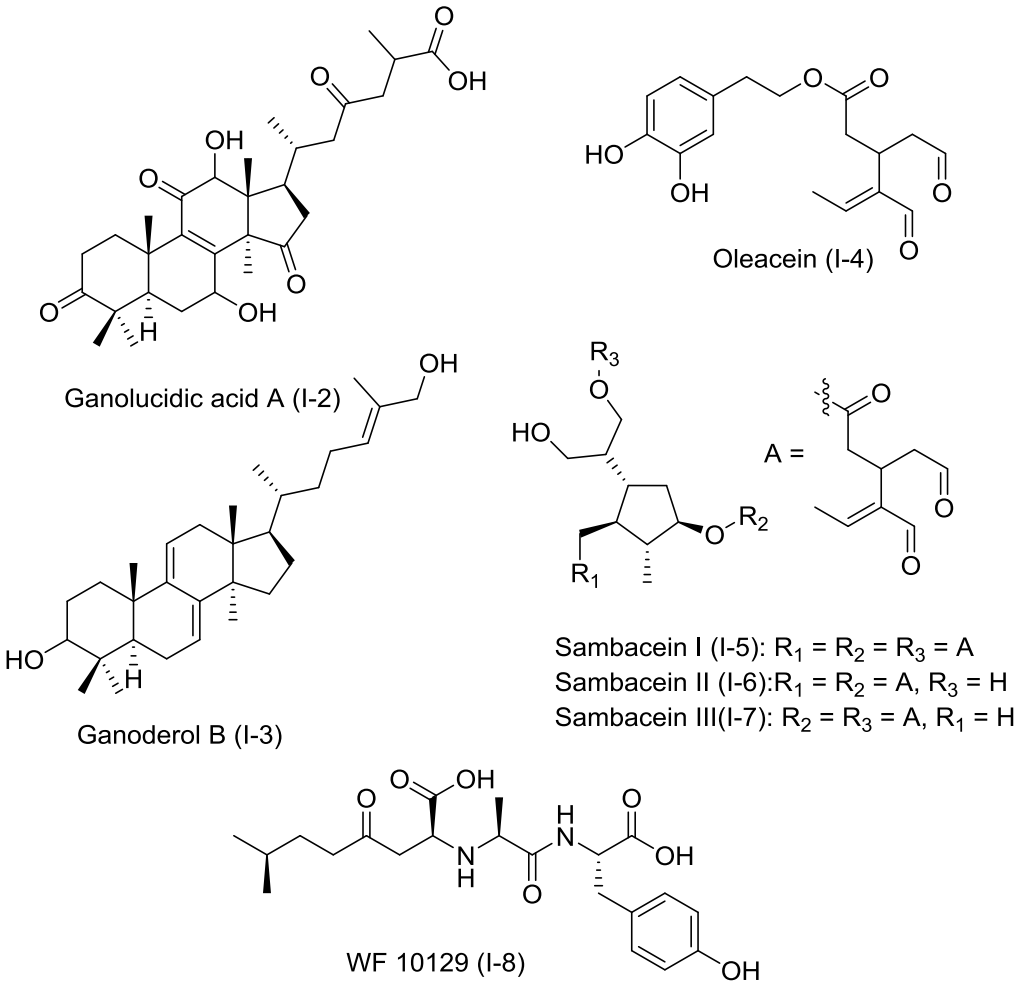

Figure I-3. ACE inhibitory compounds isolated from fungal and plant species.

Microbially produced ACE inhibitors

Microbially produced ACE inhibitory natural products have more structural diversity than those isolated from animal, plant or fungal sources. Although most of these natural products are modified peptides, two scaffolds of non-peptidic natural products have

been isolated for their ACE inhibitory activity, both from *Streptomyces* (Figure I-4). The first is a tricyclic natural product produced by *Streptomyces tanashiensis-zaomyceticus* with a phenazine scaffold. This natural product, phenacein (I-9), inhibits ACE with a K_i of 580 nM.[28-29] The second class consists of A58365A (I-10) and A58365B (I-11), two 3-pyridinyl propanoic acid containing natural products which have been isolated from the organism *Streptomyces chromofuscus.*[30] The discovery of the A58365 series of compounds was particularly interesting due to the structural similarity with captopril (I-12), a benchmark ACE inhibitor (IC_{50} = 7.7 nM) developed for the treatment of hypertension and one of the first pharmacological successes of ligand based drug design.[31]

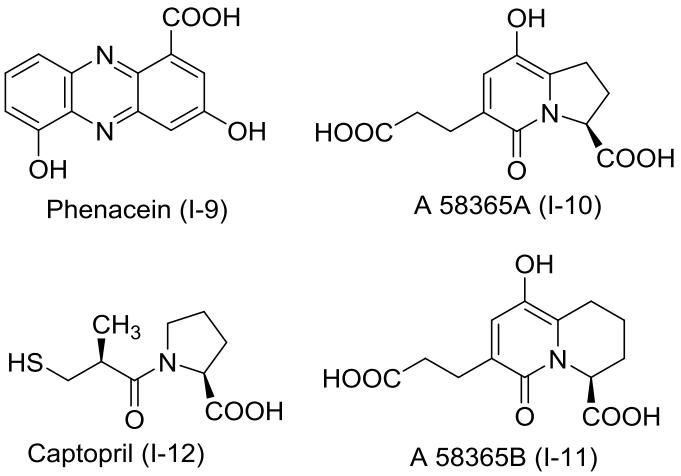

Figure I-4. Non-peptidic natural products isolated from *Streptomyces.* The commonly prescribed ACE inhibitor, captopril (I-12), is shown to highlight structural similarities with the A 58365 series of compounds (I-10, I-11).

Several peptidic natural products have been isolated from *Streptomyces* strains (Figure I-5). Foroxymithine (I-13) has been isolated from both *Streptomyces nitrosporeus* and *Streptomyces zaomyceticus* and has an IC_{50} of 200 μM.[32] L 681176

(I-14), isolated from *Streptomyces* sp. MA5143a has an IC50 of 3.72 μM.[33-34] Also, the siderophore Tsukubachelin (I-15) is reported as an ACE inhibitor isolated from *Streptomyces* sp. TM-34.[35] Other peptidic ACE inhibitors include Ancovenin (I-16), a 16-amino acid containing tricyclic molecule.[36-37] This ACE inhibitor, produced by *Streptomyces* sp. No. A647P-2 is unique due to the prevalence of dehydroalanine and sulfide containing amino acids. This large peptide was discovered to inhibit ACE with an IC_{50} of 870 nM.

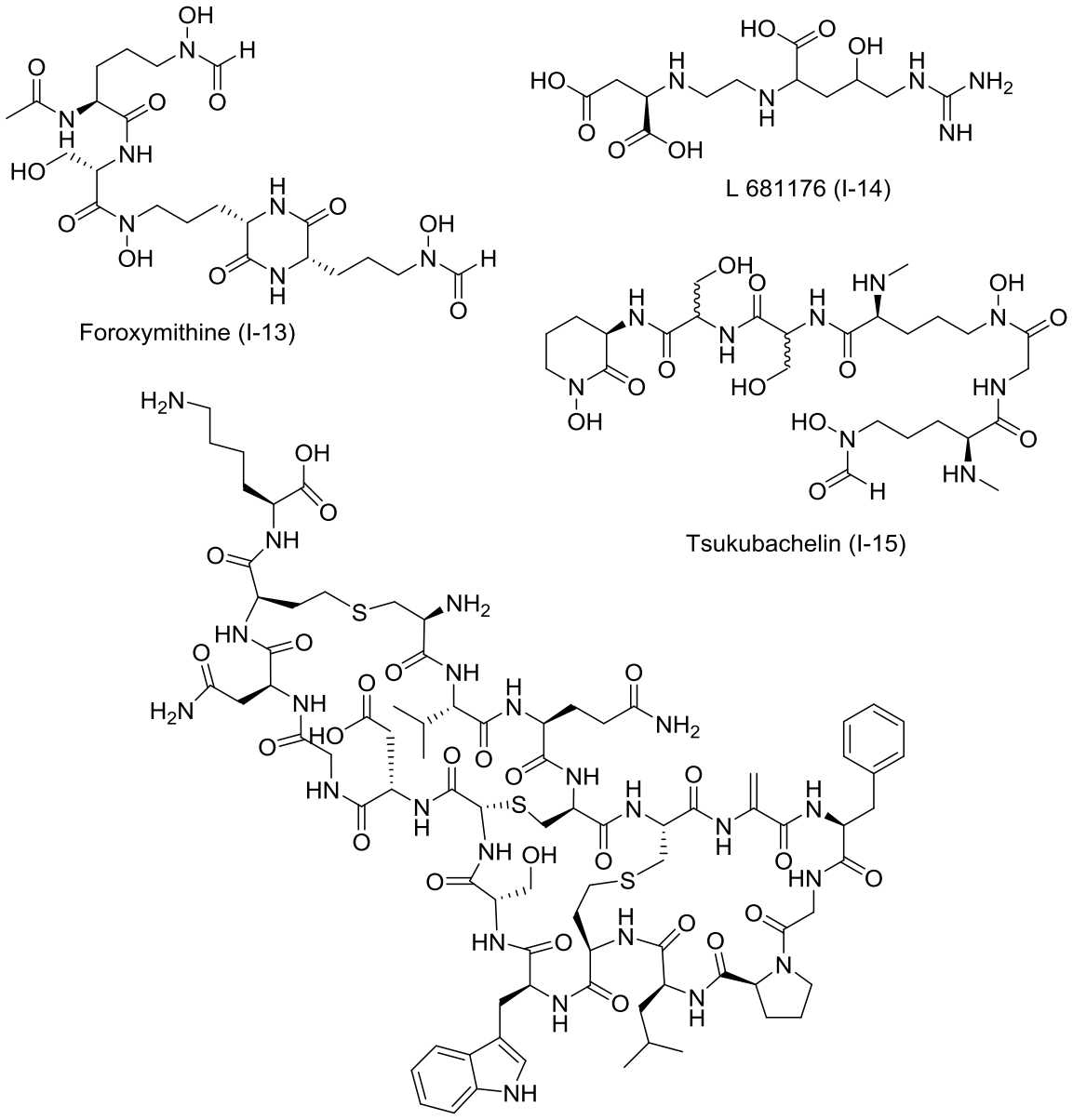

Figure I-5. Peptidic natural products with ACE inhibitory activity which have been isolated from *Streptomyces*.

Other peptidic ACE inhibitory natural products consist of a series of glycopeptides, which have been isolated from *Nocardia orentalis* (Figure I-6). These muramyl peptides, contain three structural variants, muracein A (I-17), muracein B (I-

18), and muracein C (I-19) with ranges in ACE inhibition from 280 nM to 170 μM.[38-39] Interestingly, the muraceins have been shown to exhibit selectivity for mammalian ACE as they do not inhibit carboxypeptidase A at concentrations of 150 μM.

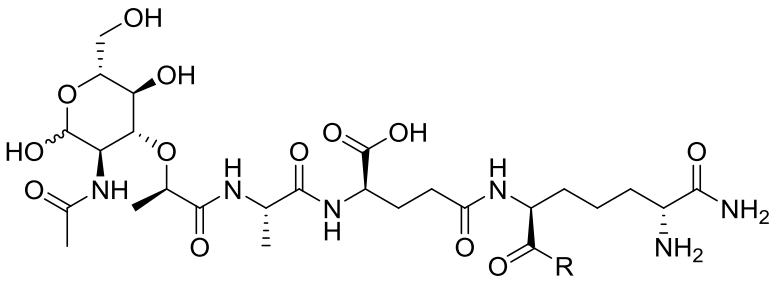

Muracin A (I-17): R = OH

Muracin B (I-18): R =$NHCH(CH_3)CONHCH(CH_3)COOH$

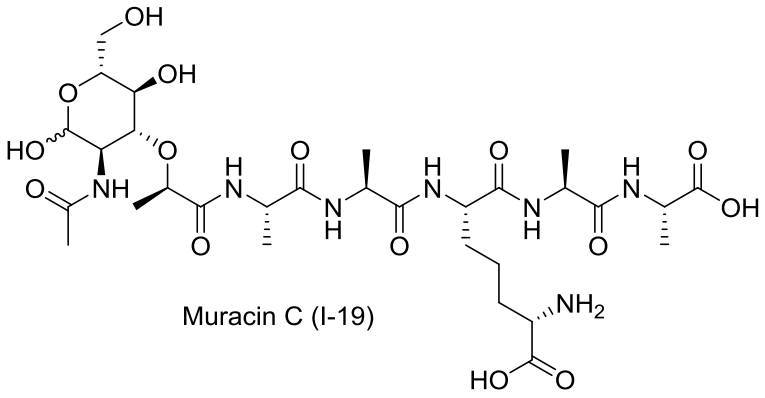

Muracin C (I-19)

Figure I-6. The muracins, a series of ACE inhibitory glycopeptides.

One structural feature common to many peptidic ACE inhibitors is a carboxy-terminal tyrosine (Figure I-7). The microginin series of ACE inhibitors (I-20 to I-24), isolated from the bluegreen algae Microcystis aeruginosa, are noted not only for their low μM inhibiton of ACE, but also for their selectivity.[40-45] The microginins were found not to inhibit other peptidases including trypsin, plasmin, chymotrypsin and, carboxypeptidase A. The inhibitor K-13 (I-25) was isolated from *Micromonospora halophytica subsp. exilisia K-13.*[46-47] This inhibitor, with a K_i of 349 nM, was also reported to be selective for the

mammalian enzyme as it did not potently inhibit carboxypeptidase A or trypsin, among other proteases. Lastly, there is K-26 (I-1), a representative of a family of 6 natural products characterized by a unique phosphonic acid analog of tyrosine. K-26 (I-1) is of particular interest as, to the best of our knowledge, it is the most potent ACE inhibitory natural product discovered to date.[7]

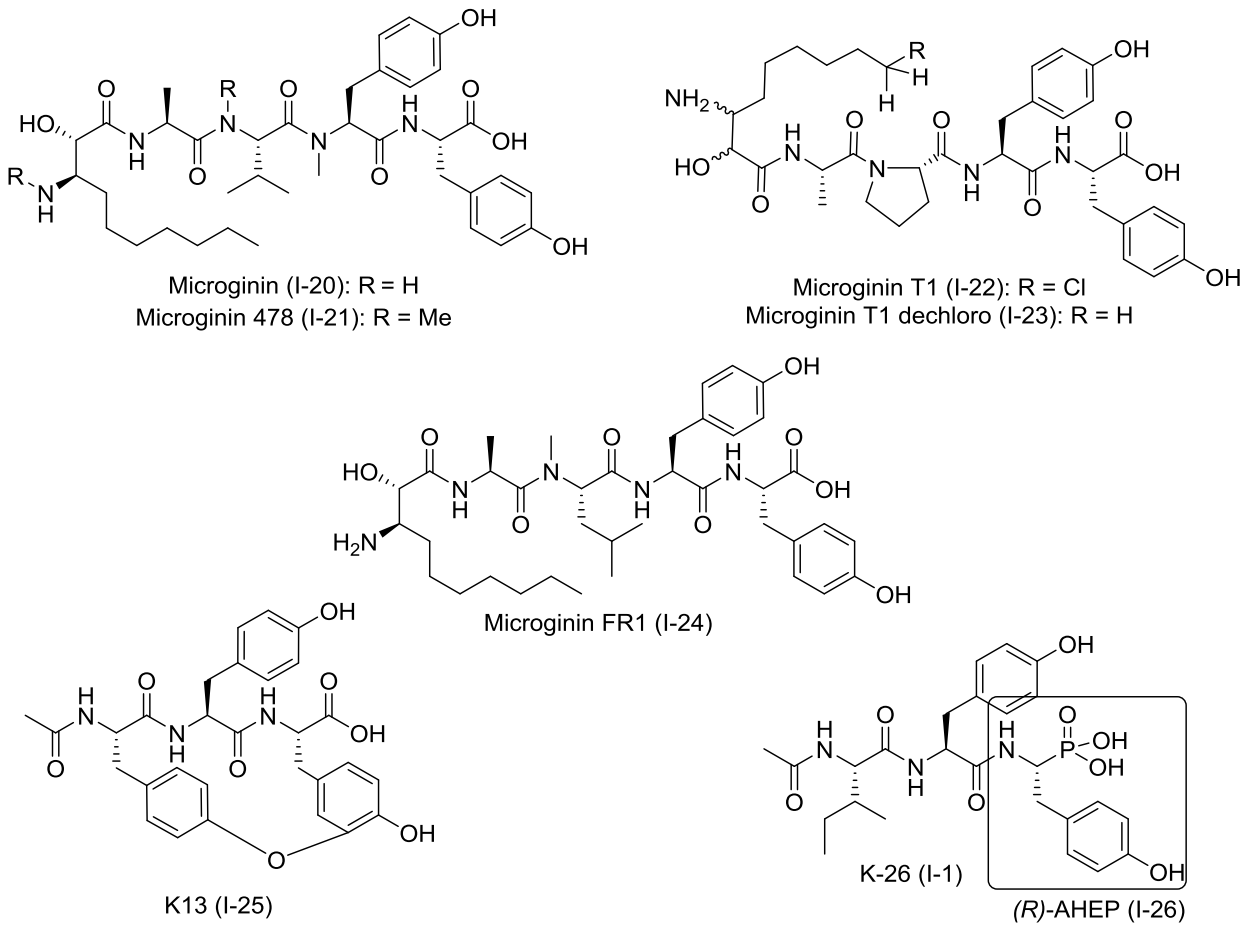

Figure I-7. Peptidic ACE inhibitory natural products that are terminated by a tyrosine-like moiety.

The K-26 family of natural products

The representative natural product from this family, K-26 (I-1) was initially discovered through bioactivity guided fractionation and determined to have an IC_{50} in the low nanomolar range (12.5 nM), comparable to the widely prescribed pharmaceutical, captopril (IC_{50} = 7.7 nM).[7] The tripeptidic structure was elucidated through NMR, mass spectrometry and degradation.[48] Synthetic investigations confirmed that this tripeptide was comprised of *N*-acetylated isoleucine, tyrosine and the non-proteinogenic amino acid (*R*)-1-amino-2-(4-hydroxyphenyl)ethylphosphonic acid (AHEP) (I-26).[49] Testing with the substrate HHL revealed K-26 (I-1) to be a non-competitive inhibitor of ACE. Furthermore, K-26 was reported as a specific inhibitor of ACE, as carboxypeptidase A was only slightly inhibited by K-26 (I-1) and all as other proteases tested showed no degree of inhibition. When administered to a normotensive rat intravenously, K-26 (I-1) was able to inhibit the pressor response in a similar manner to captopril (I-12). This potent inhibition of ACE was postulated to be the result of interactions between the phosphonate of the AHEP (I-26) and the active site zinc.[7]

Structure activity relationship studies of synthetic K-26 (I-1) and variants have revealed features necessary for potent ACE inhibition.[50] Inverting the stereochemistry of (*R*)-AHEP to (*S*)-AHEP yielded a K-26 (I-1) variant that was 10 fold less active than K-26 (I-1). Replacing (*R*)-AHEP (I-26) with L-tyrosine resulted in a 1500 fold decrease in activity and removal of the N-acetyl group afforded des-acetyl K-26 (dAcK-26) which displayed a 15 fold decrease in activity compared to K-26 (I-1). The stereochemistry of AHEP (I-26), the presence of the phosphonate, and the N-acetyl functionality were

deemed to be important structural aspects for the potent inhibition of ACE by K-26 (I-1). Interestingly, AHEP (I-26) alone is not a potent inhibitor of ACE (IC_{50} > 10μM).

Although the production of the K-26 family of metabolites is low, 6 members of this family have been isolated and described from species of, presumably closely related, soil dwelling actinomycetes (Figure I-8). K-26 (I-1) has been isolated from the actinomycete *Astrosporangium hypotensionis* (NRRL 12379) whereas SF2513 A (I-27), SF2513 B (I-28) and SF2513 C (I-29) were isolated from *Streptosporangium nondiastaticum.*[51] K-4 (I-30) was isolated from *Actinomadura spiculosospora* and *Actinomadura* sp. No. 937ZE-1 was found to produce both K-4 (I-29) and 15-B-2 (I-31).[52-53]

All 6 characterized K-26 family metabolites are all classified as tripeptidic natural products, with N-terminal modification and AHEP (I-26) as the terminal moiety. Furthermore, all of these described AHEP (I-26) containing natural products have been noted for their potent nanomolar inhibition of mammalian ACE (Figure I-8). Despite the potent activity towards mammalian angiotensin-I converting enzyme, an unusual interkingdom target for a microbially produced metabolite, the endogenous target of the K-26 family of bacterial metabolites, if any, has not been identified leaving the native significance of these fascinating metabolites a mystery.

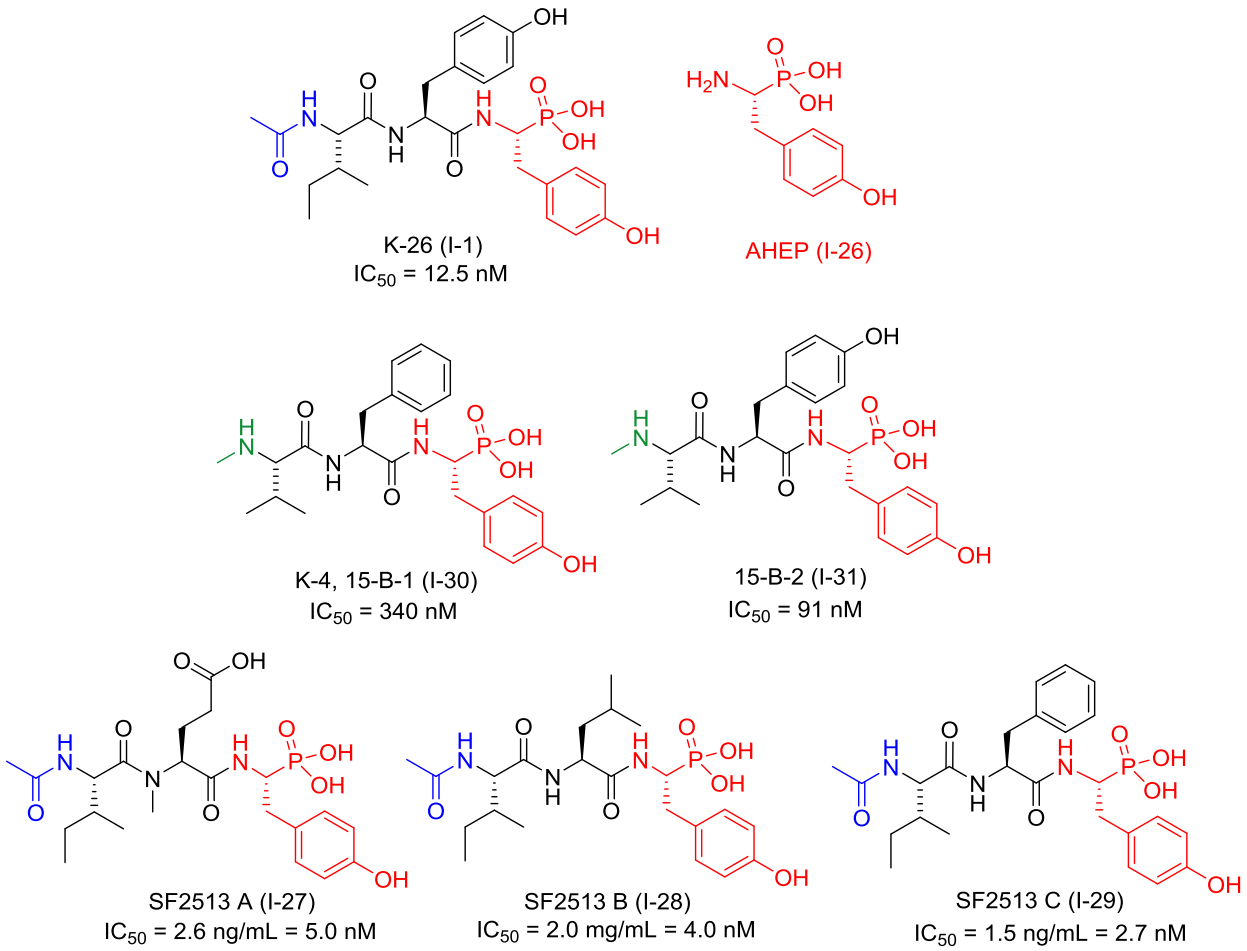

Figure I-8. The K-26 family of natural products. AHEP (I-26) is highlighted in red. The N-acetyl is highlighted in blue in and the N-methyl is highlighted green. Initially reported activity is presented with the structure.

The carbon-phosphorus (C-P) bond in K-26 family allows the classification of these tripeptides with a diverse group of C-P bond containing natural products. Many C-P bond containing natural products are bioactive and have broad utility ranging from antibacterial compounds to herbicides.[54-58] Recently there have been insights into the biosynthesis of several phosphonate containing natural products revealing a common biosynthetic route for the formation of the C-P bond.[59] Central to this process is phosphonenolpyruvate mutase (PEP mutase), an enzyme responsible for the

intramolecular rearrangement of phosphoenolpyruvate (I-32) to phosphonopyruvate (I-33) (Figure I-9A).[59] This enzyme is responsible for a phosphono-transfer, which is hypothesized to occur via two possible mechanisms allowing for the conservation of stereochemistry at both the phosphorus and the C3 carbon. In the first proposed mechanism, a nucleophilic residue in the active site of the PEP mutase would participate in forming a phosphoenzyme intermediate (I-34) (Figure I-9B).[60-61] This intermediate is then attacked by the pyruvate enolate (I-35) to yield the product. In the second proposed mechanism, dissociated metaphosphate (I-36) would be held in place by enzymatic active site residues while a C1-C2 bond rotation occurs in the pyruvate enolate (I-35) (Figure I-9C).[62] This would allow for attack of the pyruvate enolate C3 on the metaphosphate (I-36) with the appropriate retention of stereochemistry. Despite insights and advances into the biosynthesis of phosphorus containing natural products, little is known about the biosynthesis of natural products from the K-26 family, in particular the AHEP (I-26) moiety.

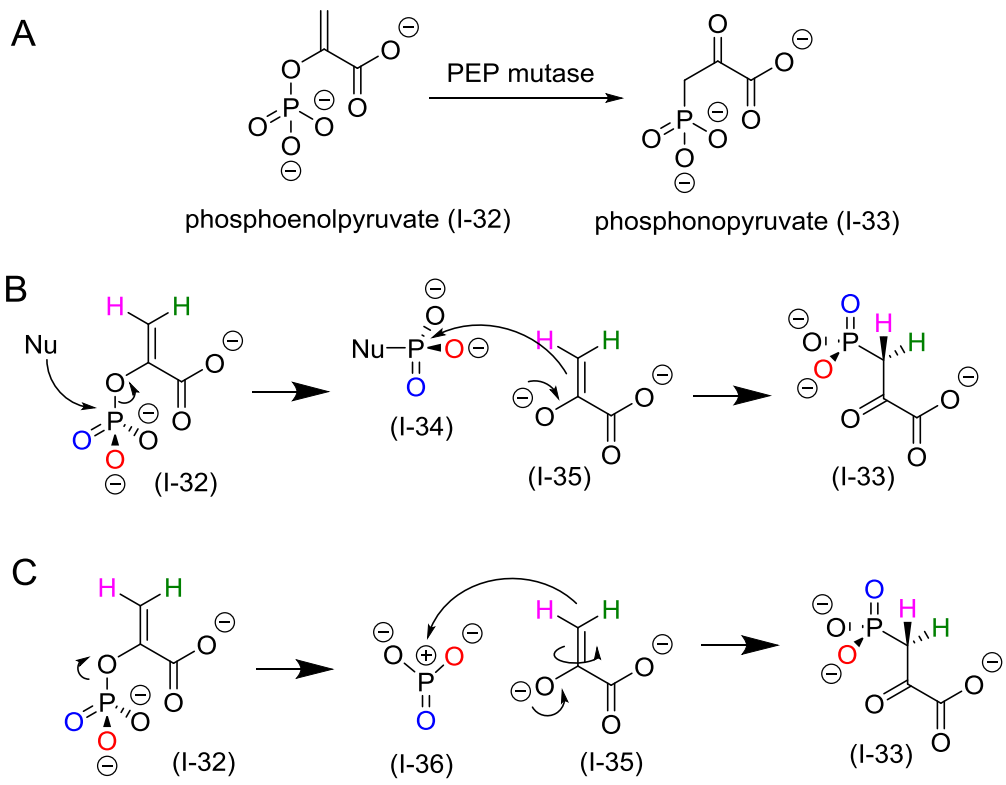

Figure I-9. C-P bond formation by PEP mutase A. Intramolecular rearrangement carried out by PEP mutase to give phosphonopyruvate. B. Mechanism proposed via nucleophilic attack by an enzymatic active site residue. C. Mechanism proposed via dissociation of metaphosphate. Hydrogens and oxygens are colored to highlight the retention of stereochemistry in this transformation.

Some information has been gleaned about the biosynthesis of K-26 (I-1) and AHEP (I-26) using precursor incorporation studies. Feeding studies with isotopically labeled tyrosine has suggested that AHEP (I-26) is a discrete biosynthetic intermediate for K-26 (I-1) that is derived from tyrosine or a closely related metabolite.[49, 63] The nitrogen, the hydrogens on both the aromatic ring and the β-carbon of tyrosine were all incorporated into AHEP (I-26) moiety of K-26 (I-1) isolated from *Astrosporangium hypotensionis*.[49] Synthetic AHEP (I-26) was also incorporated directly into K-26 (I-1), whereas tyramine, the decarboxylated product of tyrosine, was not.[63] These results suggest that in the biosynthesis of AHEP (I-26), a tyrosine-like AHEP (I-26) precursor must undergo

phosphonylation without the formation of an elimination intermediate. Although all previously investigated carbon-phosphorus bond containing natural products have a biosynthetic route incorporating PEP mutase, it is difficult to rationalize a possible biosynthetic pathway utilizing phosphonopyruvate to generate AHEP (I-26) due to the placement of the aromatic ring, a hypothesis that is supported by the feeding studies. This supports the notion that a PEP mutase or an analogous enzyme may not be responsible for the biosynthesis of AHEP (I-26). Presently, the biosynthesis of AHEP (I-26) is not well understood and the gene cluster has not been identified. As a result, the biosynthesis of K-26 (I-1) still remains cryptic leaving many unanswered questions about the origin of the unique carbon-phosphorus bond in this interesting bioactive molecule.

Angiotensin converting enzyme domains and function

Somatic ACE (sACE) was originally discovered by Leonard T. Skeggs Jr. in the mid 1950's as the last of the ""traditional components" of the RAS.[64-65] Once this membrane bound protein was successfully cloned from human endothelial cells and mouse kidney, it was determined to contain two homologous domains, a phenomenon believed to be the result of gene duplication.[66-67] This approximately 1300 amino acid protein was unexpectedly discovered to have two internal areas of homology, which for human ACE, is 612 amino acids in length. These internal regions of homology have 60% of both the DNA and amino acid sequence in common with 89% homology being apparent in the region comprised of amino acids making up the active site.[67] Within each of these two catalytic domains, there is a conserved HEXXH zinc binding motif. The two histidines

in that motif, along with a glutamate found in its own characteristic EXIXD motif to the C-terminal side of the HEXXH motif, are responsible for coordinating zinc in the active site. Each of these areas of homology and corresponding active sites on the somatic ACE have been termed N-domain (N-dom) ACE and C-domain (C-dom) ACE (Figure I-10A). A second tissue specific ACE isoform was discovered in 1971, testes ACE (tACE) (Figure I-10B).[68] This ACE variant was found to be about half the size of somatic ACE, and to contain only one active site and be nearly identical to C-domain of sACE.[69]

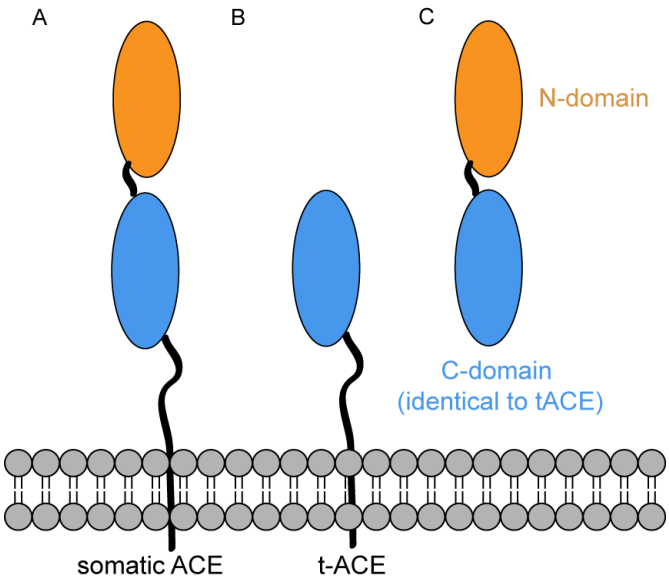

Figure I-10. ACE isoforms present in mammals. The N-domain is colored orange and the C-domain is colored blue. A. Somatic ACE (sACE) tethered to the cell membrane through a C-terminal linker region. B. tACE tethered to the cell membrane through a C-terminal linker region. C. sACE after being cleaved off of the cell membrane.

ACE is tethered to the cell membrane through a C-terminal amino acid sequence, however this enzyme is found in plasma, suggesting that ACE is cleaved off of the cell membrane and released into the bloodstream as an active form of the enzyme (Figure I-10C).[70-71] It is believed that there is an enzymatic factor responsible

for cleaving ACE off of the cell membrane through hydrolysis of the C-terminal amino acid stalk.[72] This factor, which has not been identified with certainty, is referred to ACE sheddase, a hypothesized membrane associated enzyme.[73-75]

Although the physiological role of ACE is the regulation of blood pressure through the degradation of bradykinin and the hydrolysis of ang I to ang II is well established, this promiscuous enzyme is believed to play a role in many other physiological processes.[2, 76-78] As both N-dom and C-dom ACE have been shown to have different substrate preferences, it suggests that these two domains also have different functions *in vivo* (Figure I-11).

The N-dom of ACE is believed to be more efficient at cleaving the β amyloid peptide suggesting a possible role for ACE in Alzheimer's disease, a disease characterized by an accumulation of amyloid plaques in the brain.[79] However mouse studies and the clinical analysis of a large body of elderly patients concluded that pharmacological treatment with an ACE inhibitor did not encourage the accumulation of plaques in the brain.[80-81] Furthermore, the peptide Ac-Ser-Asp-Lys-Pro (AcSDKP) is also preferentially cleaved by the N-domain with a k_{cat} 40 times higher than that of the C-domain.[82] AcSDKP is a peptide that is believed to be a natural regulator of hematopoietic stem cell proliferation, and has also been recently discovered to have a role in inflammation and fibrosis of the pulmonary system through its role in preventing the proliferation of fibroblasts.[83-86] N-dom ACE is believed to be the primary means of degrading this peptide *in vivo*.[77]

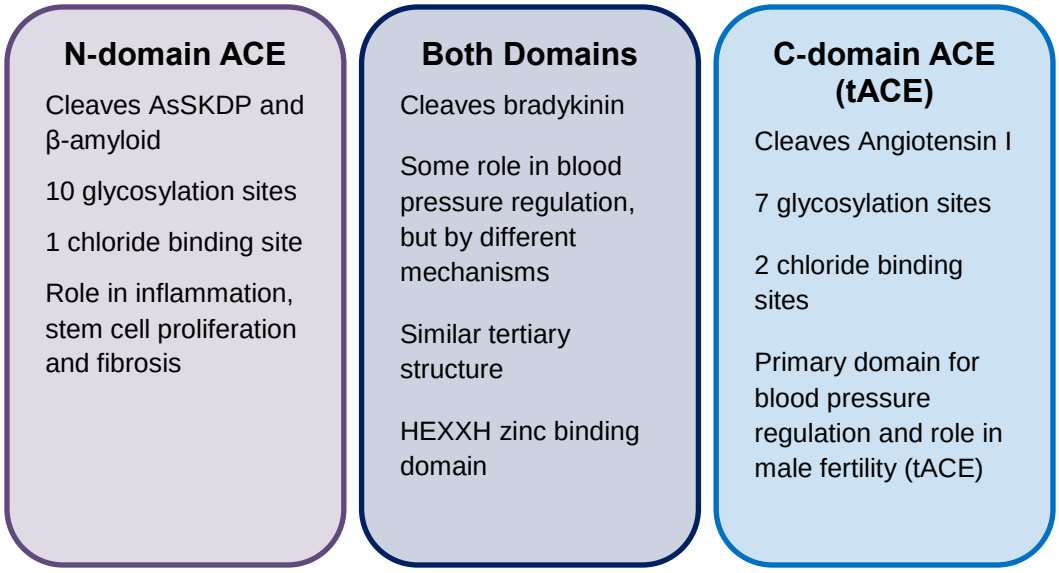

Figure I-11. Substrate and structural differences between N-dom and C-dom ACE.

C-dom ACE has been shown to be 3 times more efficient at catalyzing the hydrolysis of the decapaptide Ang I into the vasoconstrictor Ang II, highlighting the role of this domain in blood pressure regulation.[87] Furthermore, the C-dom ACE, including the tissue specific tACE, has been shown to be absolutely necessary for fertility as male C-dom ACE knockout mice were shown to be sterile.[88]

Despite the pharmacological interest in this enzyme the heavy glycosylation of this enzyme, with 10 glycosylation sites in the N-domain and 7 sites in the C-domain, has contributed to the difficulties in expression and crystallization.[89-91] However, tACE and the N-domain of ACE have been successfully crystalized in 2003 and 2006, respectively, through the use of minimally glycosylated ACE mutants.[92-93] These crystal structures show that both tACE and C-dom structures are comprised of α-helices which surround a zinc binding motif and active site buried in the interior of the enzyme (Figure I-12). C-domain ACE requires substantially more chloride for activity than the N-dom

ACE, a characteristic explainable by the two chloride ions apparent in the crystal structure near the active site in tACE versus the one chloride ion in N-dom ACE.[87] As expected the crystal structures revealed differences in the amino acid residues present in the binding pocket, which likely contribute to the substrate and inhibitor preference of these two individual ACE domains.

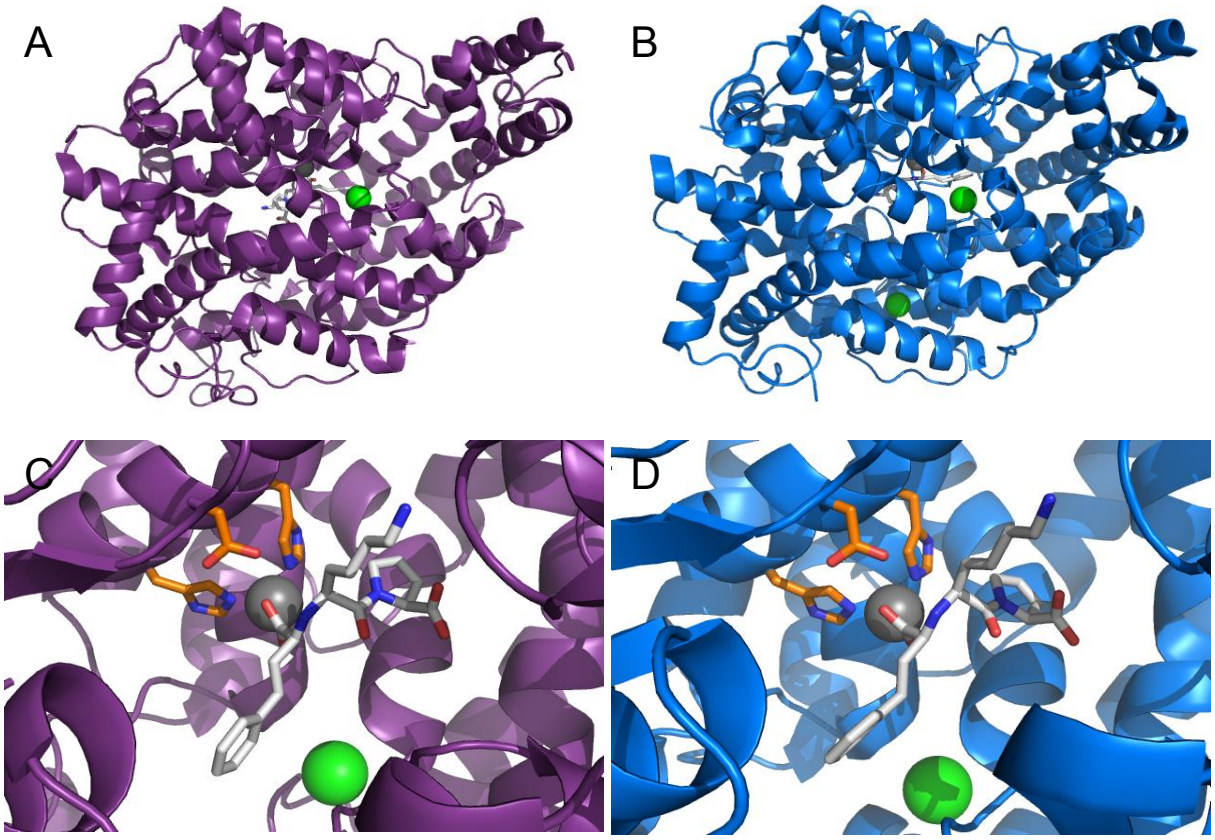

Figure I-12. Crystal structures of N-dom (purple) and C-dom (blue) ACE. Zinc present in the active site is colored grey and chloride is colored green. Active site residues which coordinate zinc as part of the HEXXH motif are colored orange. A. N-domain ACE. B. C-domain (tACE). C. Lisinopril bound in the active site of N-dom ACE. D. Lisinopril bound in the active site of C-dom ACE (tACE).

Early ACE inhibitors

The first ACE inhibitor developed was captopril, in 1975 by Miguel Ondetti, Bernard Rubin and David Cushman who were working for the drug company Squibb.[94-95] The development of this inhibitor was one of the first successful drug designs using the revolutionary ligand-based approach. The initial inspiration for this ACE inhibitor came from natural product peptides from the pit viper venom, *Bothrops jararaca*.[96] This deadly venom, which was purposed as arrowhead poison by an indigenous Brazilian tribe, would cause a sudden drop in blood pressure causing the victim to collapse.

ACE inhibitor design is rationalized using a subsite notation. The catalytic zinc is at the center of the binding pocket, with the prime subsites, S1' and S2', extending off to one side and the non-prime binding sites, S1 and S2, extending off to the other side. Studying inhibitor functionality at these ACE subsites was important in the design of inhibitors, in particular domain selective inhibitors, prior to the successful crystallography of ACE. The first generation of ACE inhibitor pharmaceuticals, including captopril (I-12), lisinopril (I-37), and enalprilat (I-38) (administered as the esterified prodrug, enalapril) did not show significant preference for either ACE domain.[97] However, these initial inhibitors relied on a sulfhydryl (captopril (I-12)) or carboxyl (lisinopril (I-37) and enalprilat (I-38)) functionalities to coordinate the zinc and inhibit the enzyme by occupying the S1', S2' and in the case of some inhibitors, the S1 subsite (Figure I-13A).[92-93, 97-98]

Domain selective ACE inhibitors

The first domain selective inhibitors, which were not developed until the late 1990s, made use of phosphinic moiety to coordinate the catalytic zinc and explored the S2 subsite for its potential in domain selective inhibitor development, leading to the design of RXP 407 (I-39) and RXPA 380 (I-40).[99-101]

RXP 407 (I-39) was the first N-domain selective inhibitor discovered, through a process of screening a phosphinic peptide library.[99] (Figure I-13B). This peptide was able to inhibit N-dom ACE with a K_i of 7 nM and a 1000 fold preference for the N-domain. The potent and selective inhibiton of N-dom ACE by this peptide was attributed to the C-terminal carboxamide along with the N-acetyl group and presence of an aspartic acid side chain at the S2 subsite.[102]

The first C-dom inhibitor, RXPA 380 (I-40), was designed based on the observation that inhibitors containing a proline which would bind in the S1' position had a binding preference for the C-dom (Figure I-13C).[100] RXPA 380 was found to have K_i of 3 nM and a 3000 fold preference for the C-domain, with the pseudo-proline in the S1' position and a tryptophan in the S2' position necessary structural aspects of the inhibitor for potent and selective C-dom inhibition.[103]

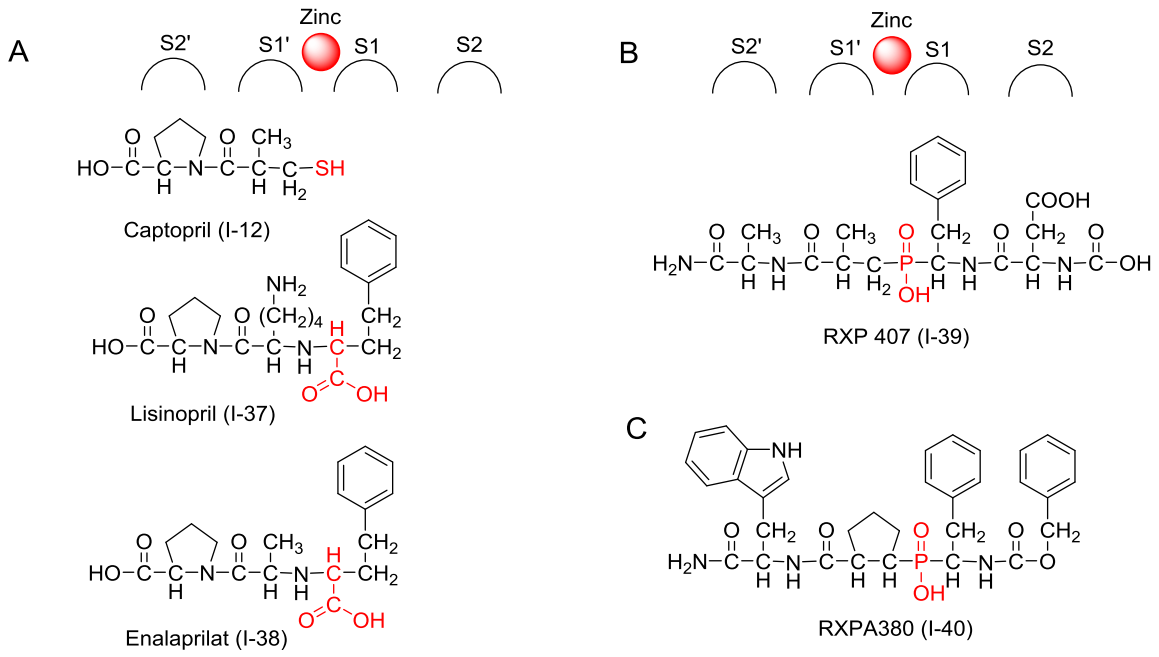

Figure I-13. Structures of ACE inhibitors and their binding subsites. Zinc binding region of the inhibitor is highlighted in red. A. Common ACE pharmaceuticals captopril (I-12), lisinopril (I-37) and enalaprilat (I-38). B. N-dom selective inhibitor RXP 407 (I-39) C. C-dom selective inhibitor. RXPA 380 (I-40)

Domain selective ACE inhibition is enticing from a pharmacological standpoint as each ACE domain has a different biological function. Not only will domain selective inhibitors provide the ability to study the biological functions of the two domains *in vivo,* but they may be more appropriate when treating patients when only the inhibition of one ACE active site is necessary.[76] It is possible that a domain selective ACE inhibitor could reduce the occurrence of side effects which are attributed with the current general ACE inhibitors on the market.[5]

ACE as an evolutionarily conserved enzyme

The role of ACE in the mammalian cardiovascular system is well established with the other roles of this enzyme in mammalian physiology being more obscure. Supporting

the notion that ACE has a broad role in physiology is the evolutionary analysis of this enzyme. Due to the increase of the availability of DNA characterization of many species, primary sequence analysis has revealed that there are many variants of ACE in nature.[76, 104] These ACE-like enzymes, which are widely distributed through various classes of organisms, are noted for their high sequence similarity with the human ACE isoforms. Searching available databases for proteins with sequence similarities to human ACE, single domain ACE-like enzymes are found in an enormous number of species ranging from mammals, insects and invertebrates and even in protozoa and bacteria.[105-112] Interestingly, many of these orthologs are present in prokaryotic organisms suggesting that this zinc dependent enzyme became necessary at a point in evolution long before its modern function in the role of blood pressure regulation.[76]

Human ACE is characterized as an M2 metallopeptidase. This enzyme falls into the broad classification of zincin due to the HEXXH residues that are responsible for binding the catalytic zinc.[113] An additional glutamate residue, found 29 residues towards the C-terminal side of the HEXXH motif is believed to be responsible for coordinating the zinc in the active site of ACE further classifying this enzyme as a distinct member of its own family, the angiotensin converting enzyme family. Other families of zincins include the closely related enzymes in the thermolysin family, the neurotoxin family, the endopeptidase-24.11 family and the endopeptidase 24.15 family.[114] Each one of these families have an additional glutamate residue outside the HEXXH motif which coordinates the zinc in the active site, however they differ due to the proximity of this glutamate residue to the HEXXH motif in the primary enzyme sequence.

A handful of ACE-like enzymes have been purified and biochemically characterized *in vitro* demonstrating that these enzymes retain their ability to hydrolyze angiotensin I, among other ACE substrates, and are inhibited by pharmacologically relevant ACE inhibitors. Particularly well characterized ACE-like enzymes include the *Drosophila melanogaster* homologs AnCE and Acer, an ACE-like enzyme from *Leishmania* (LdDCP), the ACE2 homolog from humans, an ACE homolog from the leech *Theromyzon tessulatum* (TtACE), and the bacterial ACE-like enzymes from *Escherichia coli* (EcDCP) and *Xanthamonas citri* (XcACE)[106-112, 115] Based on sequence similarities with human ACE, most of these enzymes fall into the M2 metalopeptidase family with ACE, with the exception of LdDCP and EcDCP, which are characterized as M3 metallopeptidases. BLAST and ClustalW analysis of the sequences of these ACE-like enzymes show a high degree of coverage and identity despite their presence in organisms from different kingdoms (Figure I-14).[116-117] Regardless of the high sequence similarity and shared substrates between these ACE orthologs and mammalian ACE, in most cases the function of these evolutionarily conserved enzymes is unknown or poorly understood.[76]

	N-ACE	C-ACE	ACE2	AnCE	Acer	EcDCP	XcACE	LdDCP
TtDCP	96% (48%)	98% (48%)	74% (41%)	96% (41%)	92% (39%)	7% (37%)	88% (35%)	34% (24%)
LdDCP	18% (33%)	17% (38%)	13% (36%)	20% (32%)	26% (24%)	99% (45%)	13% (38%)	
XcACE	91% (38%)	97% (38%)	73% (33%)	95% (31%)	78% (35%)	11% (41%)		
EcDCP	20% (26%)	15% (44%)	8% (35%)	11% (32%)	7% (32%)			
Acer	96% (39%)	97% (41%)	76% (36%)	99% (50%)				
AnCE	95% (42%)	99% (45%)	97% (36%)					
ACE2	96% (42%)	99% (42%)						
C-ACE	96% (55%)							

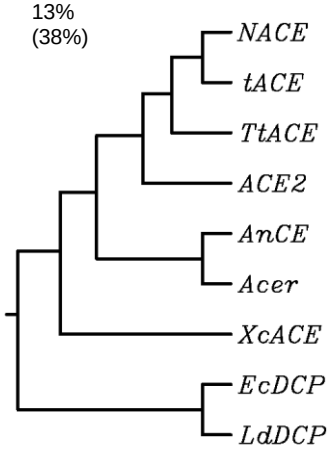

Figure I-14. Sequence identity and coverage (from BLAST) of biochemically characterized ACE-like enzymes and phylogenetic tree (from ClustalW) showing the relationship of ACE-like enzymes in nature. Shown in the table is percent identity (percent coverage).

One particularly useful example of an ACE ortholog was discovered in the fruit fly, *Drosophila melanogaster.* This enzyme, AnCE, was first described in 1995 and has since been crystallized and used extensively in the study of ACE substrates and ACE inhibitors due to its similarity to C-dom ACE, along with its amenability to heterologous expression by the yeast strain *Pichia pastoris* as an unglycosylated, yet active enzyme.[108, 110] This enzyme was shown to hydrolyze Ang I to Ang II (Km = 265 µM) and degrade bradykinin (K_m = 22 µM), similar to mammalian ACE. AnCE was also shown to be potently inhibited by the known ACE inhibitors captopril (I-12) (IC_{50} = 1.1 nM) and trandolaprilat (IC_{50} = 16 nM). Furthermore, the crystal structure of this enzyme revealed a nearly identical tertiary structure when compared to human C-dom ACE.[118] Interestingly, despite the ability of AnCE to turnover substrates hydrolyzed by

mammalian ACE, none of these substrates are relevant in *Drosophilia* leaving the question of the physiological function of this ACE ortholog unanswered.[76]

Co-crystal structures of AnCE with known ACE inhibitors on the pharmaceutical market show a preference of binding for the S2' and S1' subsites.[119] These inhibitors also showed preference for the prime subsites in mammalian ACE, as shown by later crystal structures.[93, 97-98] However, the co-crystalization of our inhibitor of interest, K-26 (I-1), in AnCE showed that this small molecule adopts a novel conformation in the binding pocket of AnCE, occupying only the non-prime subsites (Figure I-15).[120] As K-26 (I-1) is the only known inhibitor to solely fill the non-prime binding pockets, it sets the stage for ACE inhibitor development focusing on the unique phosphonic acid moiety and the underexplored non-prime binding pockets.

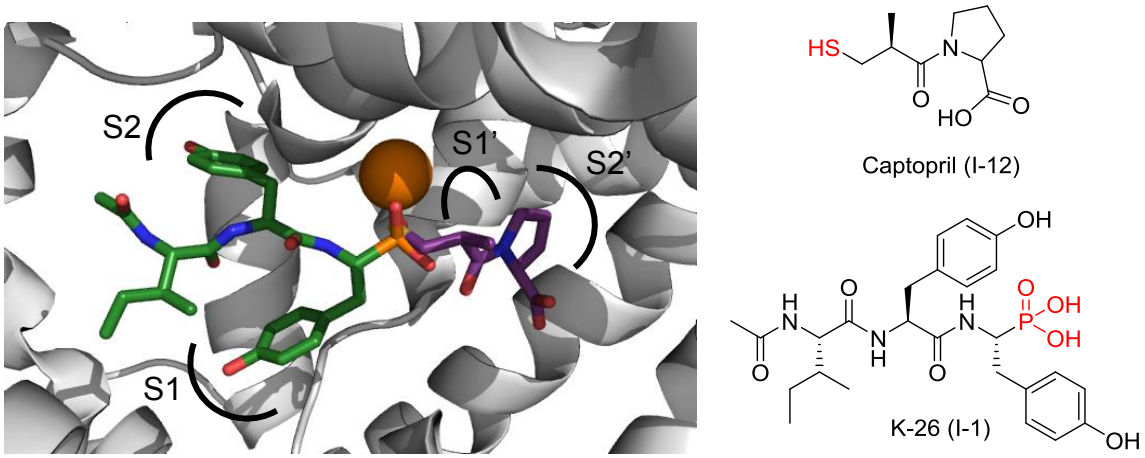

Figure I-15. Co-crystal structure of K-26 (I-1), captopril (I-12) and AnCE. K-26 (I-1) is shown in dark green. Captopril is shown in purple. The active site zinc is colored orange. Binding subsites are labeled on the diagram and structures of the inhibitors are shown with the zinc binding region highlighted in red.

Dissertation statement

K-26 (I-1) has been established as one of the most potent natural product inhibitors of the pharmacological target ACE. The structural features responsible for this bioactivity by the K-26 family of natural products have not been fully studied. The potential for domain selective inhibition by these natural products has not been evaluated, especially in the context of the unique binding conformation that K-26 (I-1) has been shown to adopt in AnCE. Also, questions remain unanswered regarding the biosynthesis of these AHEP containing compounds. Furthermore, the native target of these microbially produced peptides is unknown. In this thesis, we strive to glean insight into the pharmacology of the K-26 family of natural products with both mammalian ACE and bacterial ACE orthologs and progress towards the development of tools that may be applicable in unraveling the biosynthesis and in target identification of this fascinating metabolite.

Chapter II describes the pharmacology of K-26 (I-1) and other related AHEP containing natural products with both mammalian and bacterial ACE.

Chapter III describes the application of the computational tool Rosetta in structural activity relationship studies on an extensive set of K-26 variants and the experimental validation of the Rosetta predictions.

Chapter IV describes the design of a chemical probe using K-26 (I-1) and initial applications for target and biosynthetic enzyme identification.

Chapter V describes the possible future studies and directions with regards to structural activity relationships of potent ACE inhibition by K-26 family of natural products and K-26 target identification.

CHAPTER II

INTERKINGDOM PHARMACOLOGY OF K-26

Introduction

A significant number of secondary metabolites produced by bacteria are potent and selective inhibitors of enzymes and receptor targets in organisms classified in other kingdoms.[121] Whether these activities are the result of adaptive evolutionary pressures or coincidence is unknown, but increasing evidence is accumulating that microbial secondary metabolites play central roles in interkingdom chemical ecological relationships.[122] The significance of this interkingdom pharmacology is also evident in the role of bacterial natural products in clinically approved therapies. A striking example of such interkingdom activity are the microbial natural products, K-26, (II-1) and related compounds (II-2 – II-7) which are produced by actinomycetes isolated from soil-based ecosystems[51, 123-125] (Figure II-1). These tripeptides contain a conserved terminal phosphonic acid analog of tyrosine, (*R*)-1-amino-2-(4-hydroxyphenyl) ethylphosphonic acid ((*R*)-AHEP,II-8). This non-proteinogenic amino acid, unique to this family, is the zinc-binding pharmacophore that renders these compounds among the most potent reported natural product inhibitors of the two domain human enzymatic target, ACE. The potency of the K-26 family against ACE, produced by a soil microbe for unknown purposes, raises questions pertaining to the structural origin of the potency and selectivity within the K-26 family and the chemical ecological roles of these compounds across kingdoms.

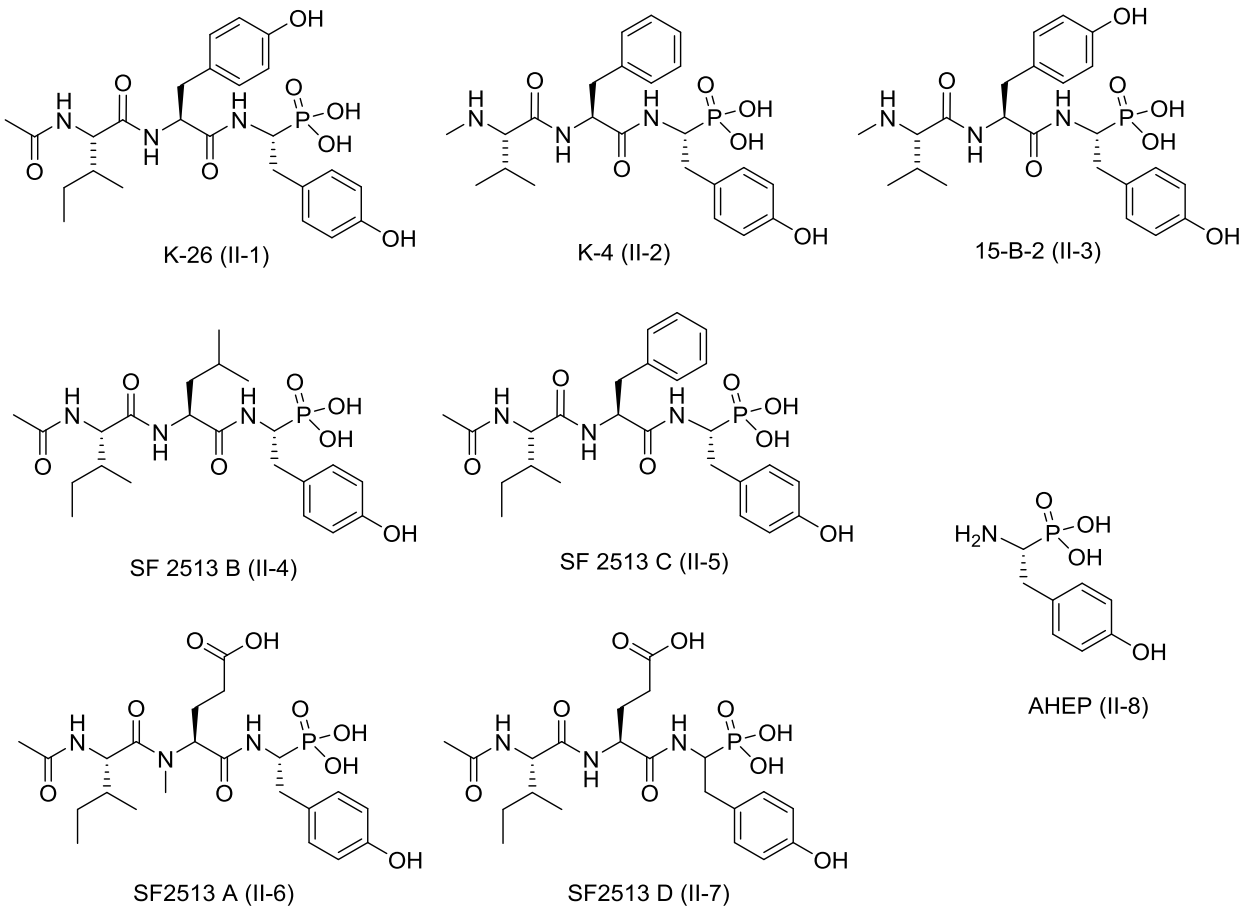

Figure II-1. K-26 analogs of interest. K-26 (II-1), K-4 (II-2), 15-B-2 (II-3), SF2513 B (II-4), SF2513 C (II-5), and SF2513 A (II-6) have been isolated from actinomycete cultures and noted for their potent ACE inhibitory activity. SF2513 D (II-7) was a synthetic analog used as a replacement for SF2513A in this study. All analogs are characterized by a non-proteogenic phosphonate analog of tyrosine, 1-amino-2-(4-hydroxyphenyl)-ethylphosphonic acid, (AHEP) (II-8). This figure has been adapted from Kramer et. al.[126] and is used with permission.

Here we investigate the structural basis for K-26 inhibition of human ACE and the domain selectivity within the K-26 family of secondary metabolites. Chemical synthesis of five naturally produced structural variants of K-26 and analysis of their domain-selective inhibition properties facilitates the determination of the structure-activity relationships within the natural product family. The co-crystallization of the most potent

member K-26, in both N- and C-domains, provides the first structural data of a natural product inhibitor in human ACE, and reveals a new mode of inhibitor binding. To investigate interkingdom structure-activity relationships, we also explore the activity of K-26 and synthetic ACE inhibitors against a panel of bacterial zinc metalloenzyme analogs of human ACE. Structural departures from the K-26/hACE inhibitor complex, engendered either within the inhibitor or the enzyme, resulted in significantly decreased binding affinity, confirming previous studies.[127] Understanding the biochemical and structural basis for K-26 inhibition provides an avenue for the future development of domain-selective inhibitors for improved ACE-targeting therapies and the groundwork for future studies to elucidate the biological mechanism for the selectivity of K-26 for a mammalian enzyme.

Results

Synthesis of K-26 family natural products

With the exception of *A. hypotensionis,* the producing organisms are not publically available, and as K-26 metabolites are generated at very low production levels their total synthesis was necessary for study. The full complement of the six known naturally occurring K-26 variants were synthesized, with the exception of the compound SF2513 A (II-6) (Scheme II-1), which was not readily accessible to us using an array of standard peptide coupling conditions. Despite the usage of a variety of peptide coupling reagents including HATU, PyBrop, EDC, and acid chloride generation, bases including collidine and triethylamine, glutamate protecting group schemes, reaction times and conditions including microwave, the coupling of the N-Ac-isoleucine

to the N-methyl glutamate-AHEP did not result in the desired peptide. Instead, either the original starting peptides were recovered or a peptide containing a cyclization product of the glutamate side chain resulted. Therefore, a close structural analog of SF2513 A (II-6) was generated lacking methylation on the penultimate amide nitrogen, and designated SF2513 D (II-7) (Scheme II-2). Both synthetic schemes yielded the desired K-26 analogs as mixtures of two major diastereomers, which were separated by preparative C_{18}-HPLC. Comparison of ^{1}H- and ^{13}C-NMR acquired from synthetic (natural diastereomeric) natural products were consistent with extant literature spectral data, confirming the originally proposed structures and stereochemistries of these natural compounds. Details of the synthesis are given in the methods section.

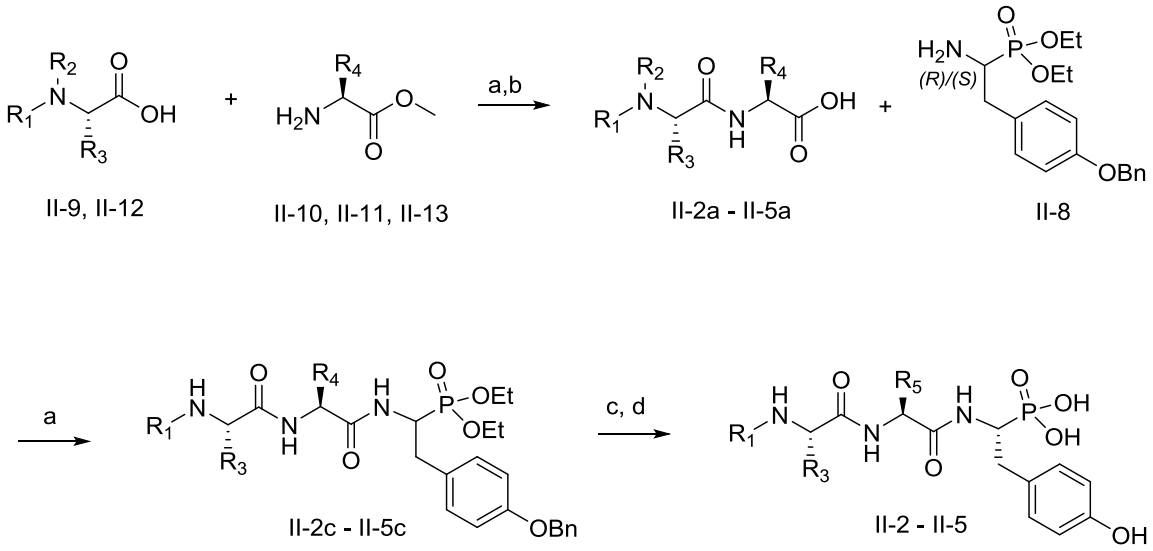

Scheme II-1. Chemical Synthesis of K-4, 15-B-2, SF2513 B and SF2513 C. Reagents and Conditions: (a) method A; HOBt, EDC, 2,4,6-trimethylpyridine, DMF, 0°C for 1 hr, then rt overnight. (b) method B; 3% $NaCO_3$ in H_2O, CH_3CN, rt overnight. (c) method C; 10% Pd/C, H_2, MeOH, rt overnight (d) method D; I-TMSi, thioanisole, CH_3CN, 0°C, 3 hours. K-4 II-**2**: R_1=Me, R_2=Cbz, R_3=Val, R_4=Phe, R_5=Phe. 15-B-2 II-**3**: R_1=Me, R_2=Cbz, R_3=Val, R_4=Tyr(OBn), R_5=Tyr. SF2513B II-**4**: R_1=Ac, R_2=H, R_3=Ile, R_4=Leu, R_5=Leu. SF513C **5**: R_1=Ac, R_2=H, R_3=Ile, R_4=Phe, R_5=Phe. This figure has been adapted from Kramer et. al.[126] and is used with permission.

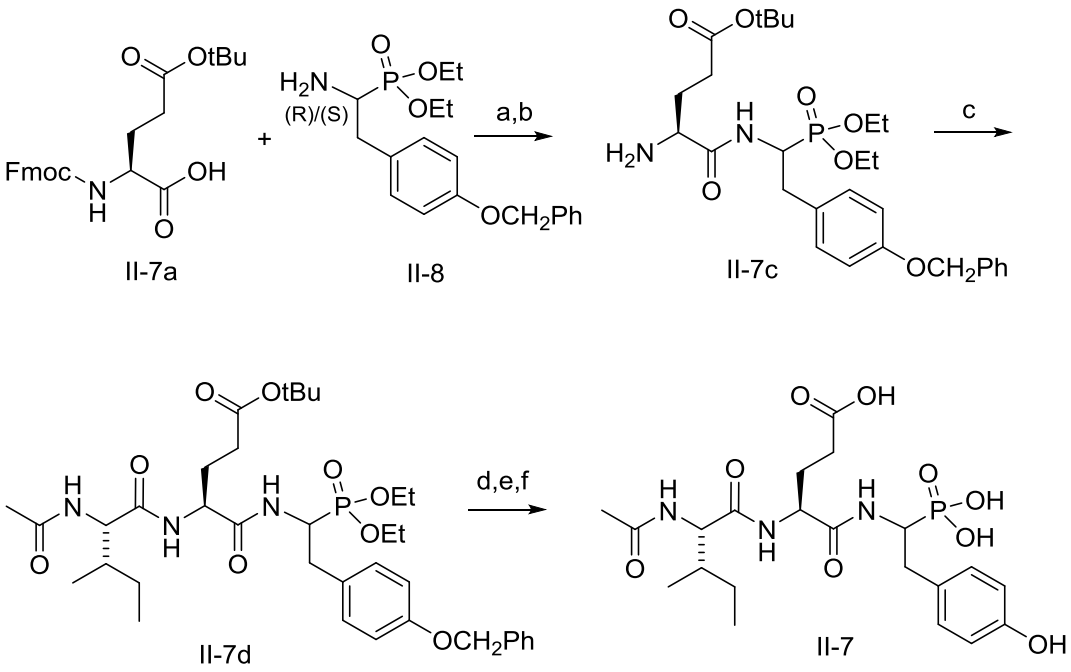

Scheme III-2. Chemical Synthesis of SF2513 D (II-7). Reagents and conditions: (a) method A; HOBt, EDC, 2,4,6-trimethylpyridine, DMF, 0°C for 1 hr, then rt overnight. (b) method E; TAEA, DCM, rt, 20 min. (c) method A; N-Ac-Ile, HOBt, EDC, 2,4,6-trimethylpyridine, DMF, 0°C for 1 hr, then rt overnight. (d) method C; 10% Pd/C, H_2, MeOH, rt overnight. (e) method F; TFA, DCM, rt, 30 min. (f) method D; I-TMSi, thioanisole, CH_3CN, 0°C, 3 hours. This figure has been adapted from Kramer et. al.[126] and is used with permission.

ACE inhibitory activity of the K-26 family

Chemically synthesized K-26 family phosponotripeptides were initially assayed for mammalian ACE inhibition using the benchmark chromogenic substrate furylacryloyl-phenylalanyl-glycyl-glycine (FAPGG) and rabbit lung somatic ACE extract.[127-128] Consistent with previous data from K-26 SAR studies, diastereomers terminated by the naturally occurring (*R*)-AHEP amino acid were 10- to 400-fold more potent than the those terminated by (*S*)-AHEP (Table II-1, Table II-2).

(S)-diastereomer	IC_{50} (M)
K-4 (II-2)	4.2×10^{-6}
15-B-2 (II-3)	5.4×10^{-5}
SF2513 B (II-4)	1.7×10^{-6}
SF2513 C (II-5)	2.4×10^{-6}

Table II-1. IC_{50} values calculated for least active (*S*)- diastereomers of the K-26 family of natural products using the substrate FAPGG with somatic ACE. This figure has been adapted from Kramer et. al.[126] and is used with permission.

With the exception of SF2513 D (II-7) (desmethyl SF2513 A), all synthesized natural products were potent nanomolar inhibitors of somatic rabbit lung ACE. SF2513 A (II-6) was previously reported to be a nanomolar inhibitor of ACE, with initial structure of SF2513 A (II-6) being elucidated using ^{1}H NMR, ^{13}C NMR and chemical degradation.[51] With these results in mind, if the originally published structure of SF2513 A (II-6) is correct, the N-methyl substituent must have an important role in promoting binding of SF2513 A (II-6) in the active site of ACE. In general, N-acetylated family members were markedly more potent than their respective N-methylated congeners using the substrate FAPGG. Of the N-acetylated variants, K-26 was found to be the most potent inhibitor of rabbit lung somatic ACE, with an IC_{50} of 25 nM, followed by SF2513 C (II-5) then SF2513 B (II-4).

	IC_{50} Data (nM)			K_i Data (nM)	
Compound	sACE[a]	C-dom[b]	N-dom[b]	C-dom[b]	N-dom[b]
K-26 (II-1)	25[d]	11[d]	110[e]	11[f]	75[d]
K-4 (II-2)	370[e]	590[d]	220[c]	NT[g]	NT
15-B-2 (II-3)	140[e]	54[e]	52[c]	NT	NT
SF2513 B (II-4)	100[e]	12[d]	76[c]	21[e]	33[d]
SF2513 C (II-5)	35[e]	7[e]	88[e]	12[f]	170[d]
SF2513 D (II-7)	5200[d]	NT	NT	NT	NT

Table II-2. ACE inhibitory activity of synthesized K-26 variants. [a]Rabbit lung sACE was tested for inhibition with the substrate FAPGG. [b]Z-FHL was used as a substrate with purified N- and C- domain ACE constructs. Standard deviations, reported in supporting information on S89-S93, are [c]1-10%, [d]10-25%, [e]25-50% or [f]50-75%, of the mean. [g]NT is not tested. This figure has been adapted from Kramer et. al.[126] and is used with permission.

Each of the synthesized natural products that exhibited nanomolar somatic ACE inhibition were also tested for domain selectivity by measuring the IC_{50} of inhibition using the substrate Cbz-Phe-His-Leu-OH (Z-FHL) (Table II-2)[129-131] with purified N-domain and C-domain human ACE constructs. Analogs showing promising domain selectivity were reevaluated via measurement of the inhibition constant K_i. The N-methylated analogs, K-4 (II-2) and 15-B-2 (II-3), did not exhibit a large degree of domain-selectivity and SF2513 B only showed a slight preference for the C-domain, whereas N-acetylated analogs K-26 (II-1) and SF2513 C (II-5), showed approximately 7- and 15-fold higher affinities for the C-domain, respectively.

Co-crystal structures of K-26 with N-domain and C-domain ACE

To further understand the structural basis for inhibition of human ACE by the most potent member of this family of bacterial natural products, K-26 (II-1) was separately co-crystalized in the N-domain and the C-domain. As shown in the resulting crystal structures, K-26 (II-1) adopts a similar conformation in both domains (Figure II-

2), conserving nearly identical potential hydrogen bond networks between the two domains (Table II-3). K-26 (II-1) has a unique binding motif as it occupies the “non-prime” binding pockets of this mammalian ACE construct (Figure II-3). The phosphonate coordinates the zinc, the side chain of the AHEP (II-8) sits in the S1 binding pocket, the tyrosine side chain fills the S2 binding pocket and the N-acetyl isoleucine occupies a S3 binding pocket. Other known inhibitors of the enzyme, including the synthetic phosphinic inhibitor RXPA380 (II-14), and the clinically relevant captopril (II-15) and lisinopril, and fill the ‘prime’ binding pockets.[103, 132-133] The binding pattern of K-26 in human ACE is almost identical to that adopted by K-26 in the active site of *Drosophila* ACE (AnCE).[120]

Ligand atom	Interacting atom from the C-domain sACE	Distance (Å)	**Ligand atom**	Interacting atom from the N-domain sACE	Distance (Å)
OAG	Zinc ion	2.3	**OAG**	Zinc ion	2.1
OAJ	Zinc ion	2.3	**OAJ**	Zinc ion	2.5
OAG	Y523 OH	2.5	**OAG**	Y501 OH	2.5
OAJ	H387 NE2	3.3	**OAJ**	H365 NE2	3.0
OAJ	H383 NE2	3.2	**OAJ**	H361 NE2	3.3
OAD	D358 N	2.8	**OAD**	D336 N	2.8
N	A356 O	3.1	**N**	A334 O	3.1
O	A356 N	2.9	**O**	A334 N	2.8

Table II-3. Hydrogen bond interactions of C- and N- domains of ACE with K-26. Used with permission from Kramer et al.[126]

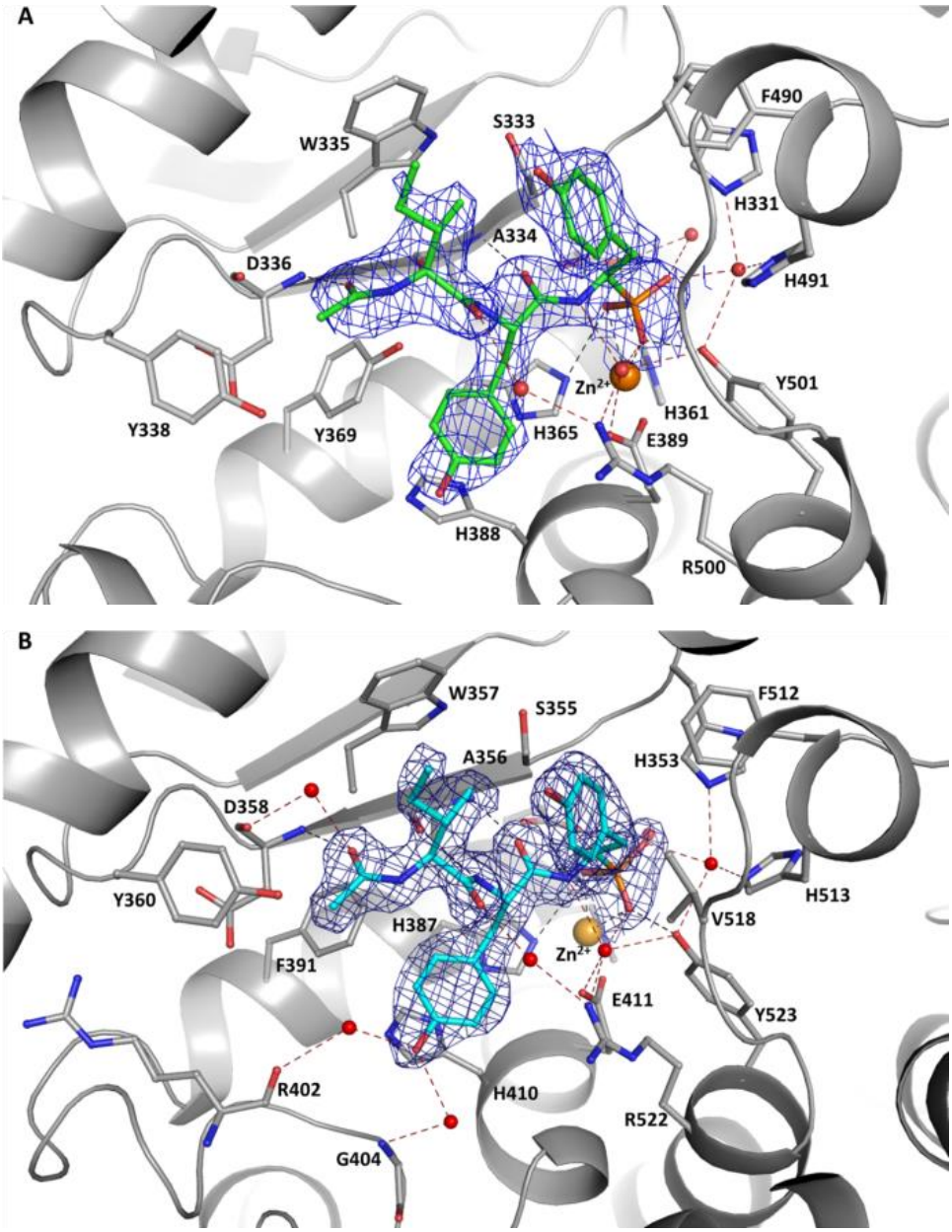

Figure II-2. K-26 binding in both domains of ACE. A. K-26 (green) bound in the N-domain of ACE. B. K-26 (cyan) bound in the C-domain of ACE. Residues involved in K-26 interactions are shown as grey sticks. The zinc ion is shown as an orange sphere and water molecules in red. Potential hydrogen interactions and water mediated ones are presented with black and red dashed lines, respectively. Omit maps for K-26 bound to N- and C-domain are shown at 1σ contour level. Used with permission from Kramer et al.[126]

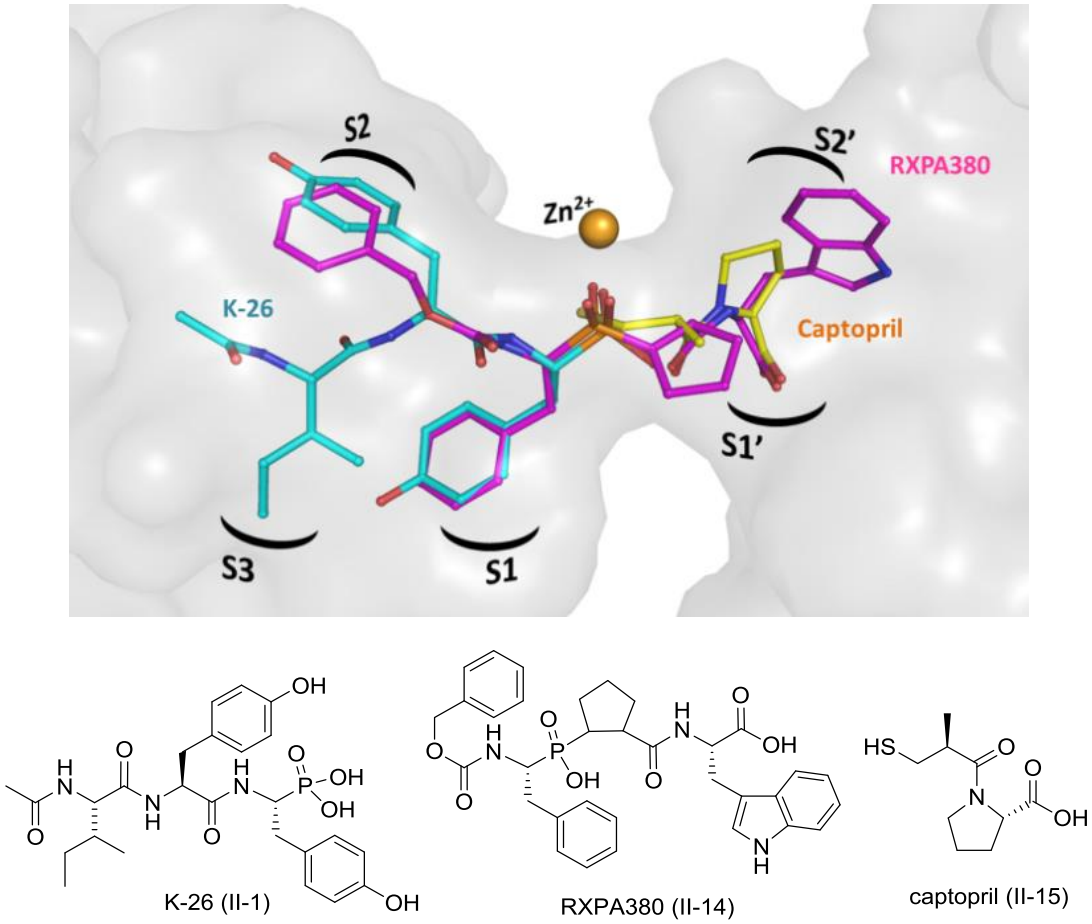

Figure II-3. Binding motifs of K-26 (II-1), RXPA380 (II-14) and captopril (II-15) in the active site of ACE. K-26 is shown in cyan, captopril (PDB 1UZF) in green and RXPA380 in pink (PDB 2OC2). Zinc is shown as an orange sphere. Binding pockets of the enzymes are labeled within the surface-rendered catalytic channel of C-domain ACE. Adapted from Kramer et al.[126] Used with permission.

Overexpression and characterization of dicarboxypeptidases

As K-26 family natural products are of microbial origin, and likely have not evolved to specifically inhibit human ACE, we endeavored to assay their interkingdom ACE-like activity. Biochemical characterization of several bacterial dicarboxypeptidases shows remarkable similarities in substrate and inhibitor preferences in comparison to mammalian ACE.[107, 134] In support of these observations, sequence alignment of several bacterial dicarboxypeptidases reveals a high degree of sequence homology between mammalian ACE and bacterial dicarboxypeptidases (Table II-4, Figure II-4). This

encouraged us to explore the potential of the known potent mammalian ACE inhibitor, K-26, as an inhibitor of bacterial analogs of ACE. In order to explore the scope of interkingdom activity of K-26, we have recombinantly expressed, purified, and assayed a panel of ACE-like enzymes represented by phylogenetically distinct, bacterial zinc-dependent dicarboxypeptidases for inhibition by captopril (II-15) and K-26 (Figure II-5).

	N-domain	tACE	AnCE	ACE2	K26DCP	EcDCP
MR1DCP	95%, 43%	97%, 43%	95%, 38%	74%, 38%	11%, 35%	18%, 45%
EcDCP	20%, 41%	15%, 56%	11%, 55%	10%, 38%	99%, 46%	
K26DCP	17%, 83%	16%, 56%	12%, 33%	11%, 33%		
ACE2	73%, 42%	73%, 42%	77%, 41%			
AnCE	95%, 42%	99%, 45%				
tACE	96%, 55%					

Table II-4. Sequence coverage and identity for ACE-like enzymes. N-ACE, tACE and ACE2 are human enzymes. AnCE is a *Drosophila* homolog. K-26, E.coli and MR-1 are dicarboxypeptidases from the respective bacteria. Adapted from Kramer et al.[126] Used with permission.

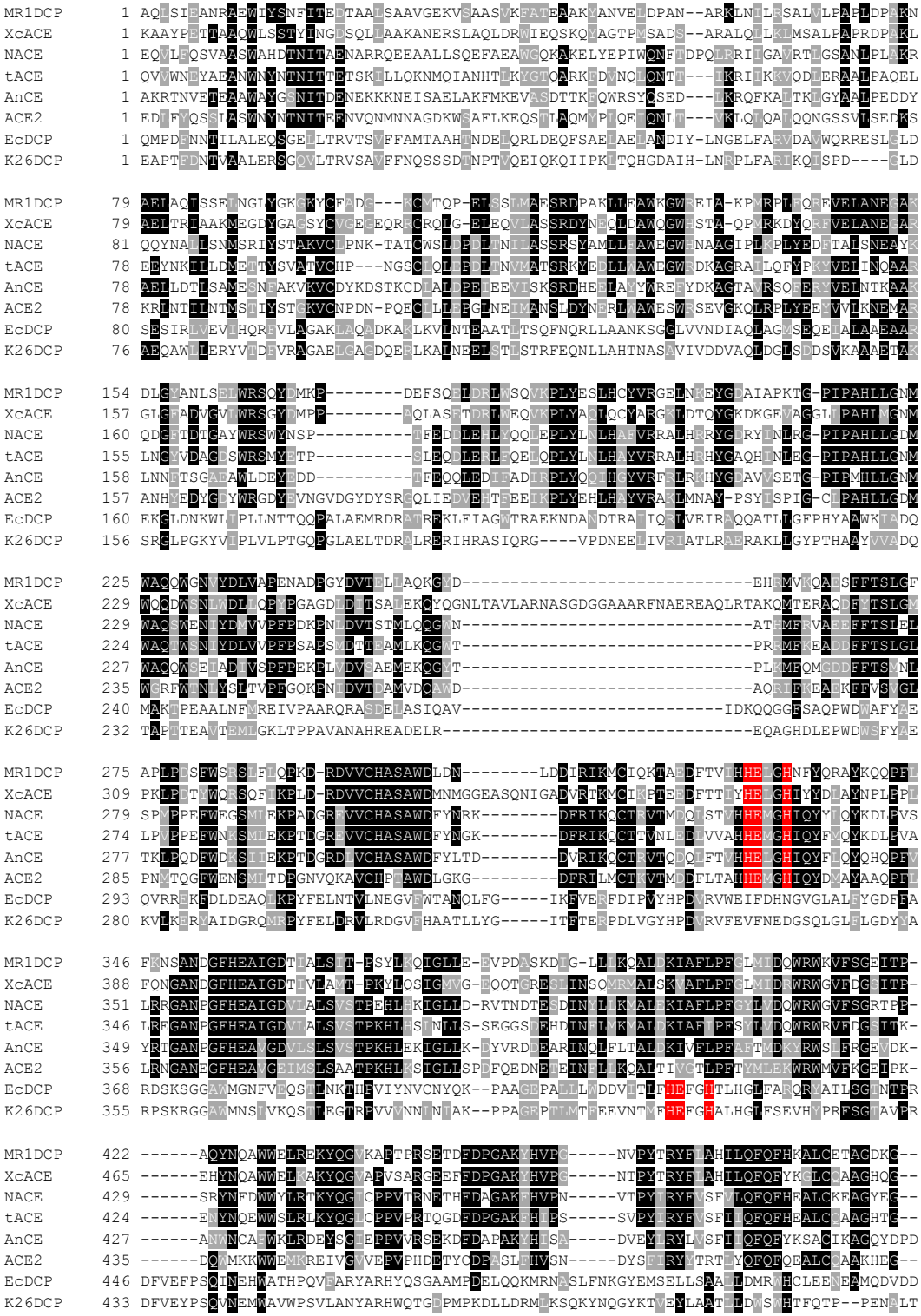

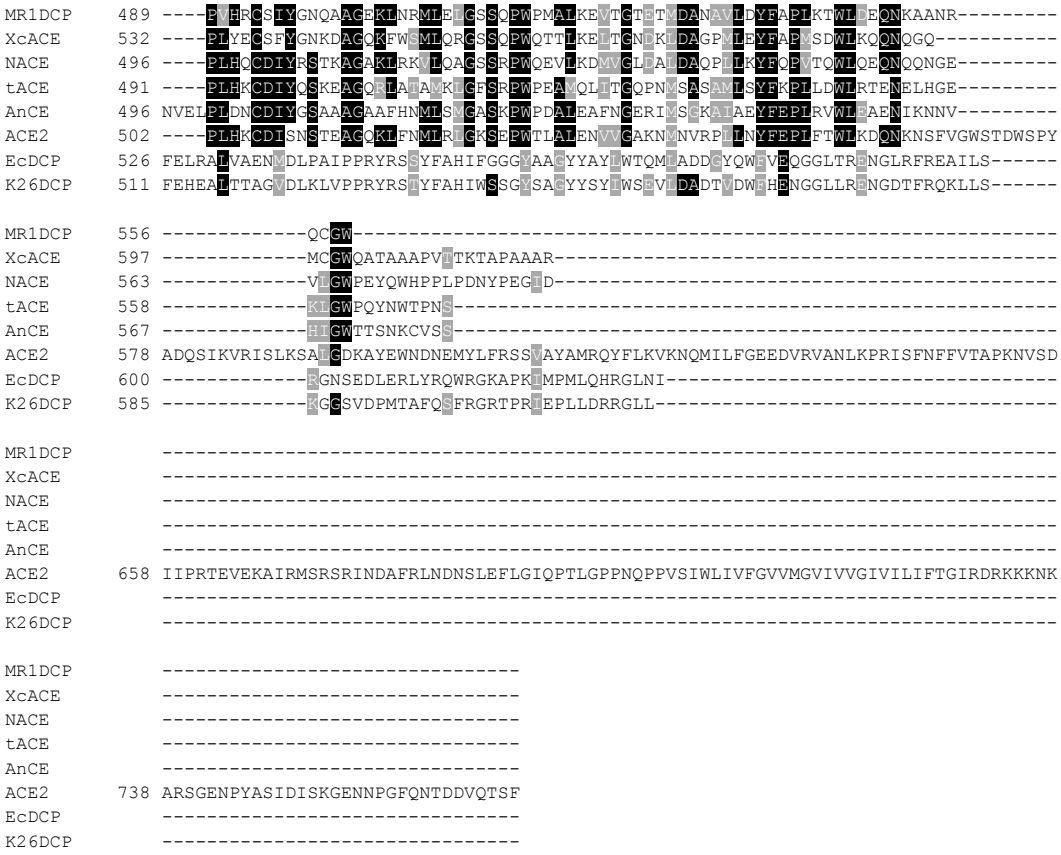

Figure II-4: Boxshade sequence alignment for ACE and ACE-like enzymes in this study. The HEXXH zinc binding motif is highlighted in red. This figure has been adapted from Kramer et. al.[126] and is used with permission.

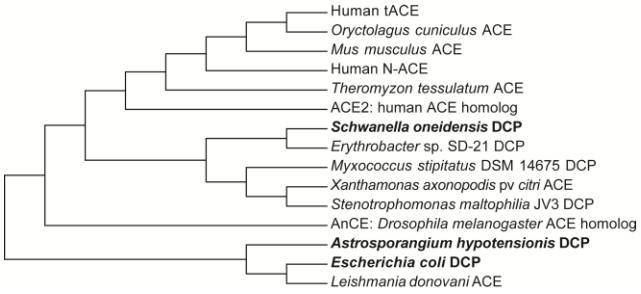

Figure II-5. Phylogenetic tree comparing ACE and related bacterial dicarboxypeptidases (DCP). Dicarboxypeptidases which have been overexpressed and purified in this study are shown in bold text. The optimal tree with the sum of branch length = 6.39523051 is shown. This figure has been adapted from Kramer et. al.[126] and is used with permission.

Three bacterial enzymes were chosen: dicarboxypeptidases from the K-26 producing organism (K26DCP), from *E.coli* st. K-12 sbstr. MG1655 (EcDCP)[134] and from *Schwanella onedesis str. MR-1* (MR1DCP). K26DCP is the only putative zinc metallopeptidase present in the genome of the actinomycete *Astrosporangium hypotensionis,* the organism from which the tripeptide K-26 was originally isolated. MR1DCP was selected for the high similarity with human ACE as it has a 43% sequence identity with both the N- and C- domain of human ACE. All three enzymes contain the characteristic HEXXH zinc-binding domain, characteristic of the zincin family of zinc metalloproteases. The dicarboxypeptidases EcDCP and the K-26 producer K26DCP both are both classified specifically as a M3 zinc metalloproteases due to the presence of two additional glutamate residues, 30 and 37 amino acids C-terminal to the HEXXH zinc-binding domain that are believed to aid in coordinating the zinc in the active site of the enzyme.[135] A glutamate residue present 29 residues downstream from the HEXXH zinc-binding domain, believed to be a ligand for zinc coordination in both MR1DCP and mammalian ACE, distinguishes these enzymes within the M2 subfamily of ACE zinc metalloproteases.

All three bacterial dicarboxypeptidases were found to efficiently hydrolyze the substrate FAPGG. Captopril (II-15) was shown to be a potent, low nanomolar inhibitor of all the purified overexpressed dicarboxypeptidases (Table III-5). However, K-26 (II-1) was found to be a potent inhibitor of the mammalian ACE, but a poor inhibitor of the bacterial ACE-like enzymes, including the dicarboxypeptidase encoded in the genome of the K-26 producer.

Dicarboxypeptidase	Type	Captopril IC_{50} (M)	K-26 IC_{50} (M)
Somatic ACE	M3	7.7×10^{-9}	2.5×10^{-8}
K26DCP	M2	5.2×10^{-9}	4×10^{-5}
EcDCP	M2	1.6×10^{-8}	1.5×10^{-4}
MR1DCP	M3	9.2×10^{-9}	1.1×10^{-5}

Table II-5. Inhibition of overexpressed bacterial dicarboxypeptidases by K-26. Adapted from Kramer et al.[126] Used with permission.

Discussion

The shared activity of K-26 family metabolites is largely determined by the terminal non-proteinogenic amino acid (*R*)-AHEP, which has been demonstrated to be an essential component for potent ACE inhibitory activity. On its own, AHEP (II-8) does not possess potent activity (IC_{50} > 1 μM), however, replacement of AHEP (II-8) by tyrosine causes a 1500-fold decrease in ACE inhibitory activity.[127] Alteration of stereochemistry also decreases the activity 10 fold. The crystal structure reveals the importance of the phosphonate for potent binding as this is shown to coordinate with the zinc in the active site of the enzyme and form a hydrogen bond network with several conserved amino acids in both domains of ACE (Figure II-6). The AHEP (II-8) side chain fits into the S1 binding pocket, where the aromatic group of AHEP (II-8) may form hydrophobic interactions with Val 518 (Thr 496 in N-ACE). Furthermore, the high resolution of the crystallographic data allowed for the identification of several key water molecules which may have a role in inhibitor binding. The AHEP (II-8) seems to be stabilized at the active site by a network of water molecules anchoring K-26 (II-1) at S1 in both crystal structures. Interestingly, additional water molecules interacting with K-26 (II-1) were visible in the C-domain.

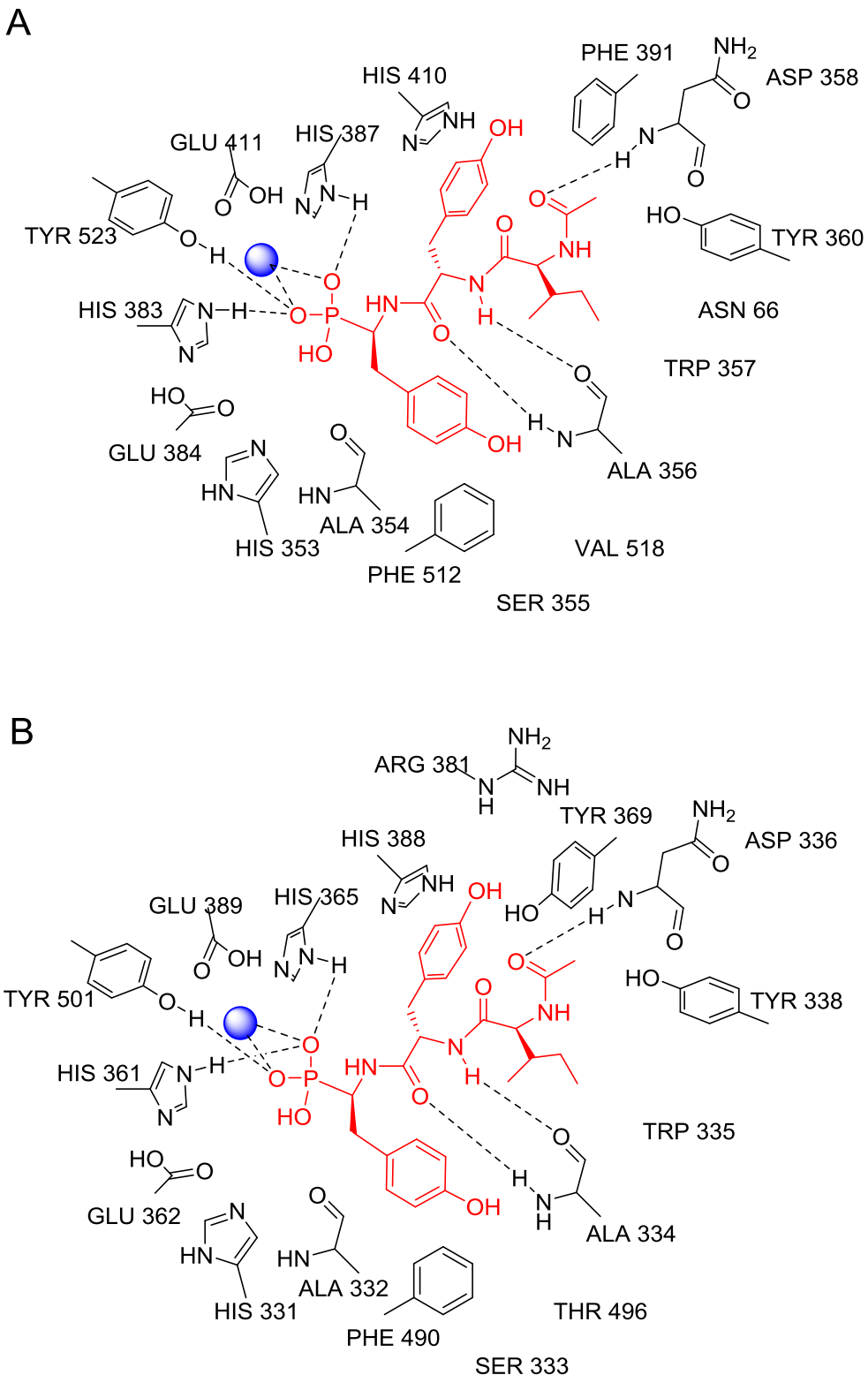

Figure II-6. Ligand plot of K-26 bound in both domains of ACE. K-26 is shown in red and the zinc present in the active site is shown as a blue sphere. A. K-26 bound in the C-domain of ACE B. K-26 bound in the N-domain of ACE

In the S2 binding pocket, the tyrosine side chain may form conserved aromatic stacking interactions with His 387 and His 410 (His 365 and His 388 in N-domain) and hydrophobic interactions with Phe 391 (Tyr 369 in N-ACE). Interestingly, synthesis of a phosphinic inhibitor library analogous to the inhibitor RXPA380 (II-14) showed that a Phe or Tyr in the S2 position of the inhibitor encouraged the most ACE binding potency in both domains, suggesting the importance of these interactions.[103] Hydrogen bonds between the backbone of the tyrosine in K-26 (II-1) with the backbone of Ala356 (Ala 334 in N-ACE) are also evident. Additionally, the hydroxyl group of the tyrosine side chain makes water-mediated interactions with the backbone of Arg 402 and Gly 404 (Figure II-2B). These two residues are conserved in both domains of ACE, however, Glu 403 (C-domain) is occupied by Arg 381 in the N-domain. The long polar side chain of Arg 381 may thus prevent these water-mediated interactions in the N-domain, decreasing the binding affinity for K-26.

The remaining structural features of K-26 class of natural products are the third amino acid side chain and the N-terminal substitution, which occupies the S3 position. The N-terminal substitution has an effect on potency as shown with K-4 and 15-B-2, which have an N-terminal methyl group and inhibit somatic ACE with a 5 – 10 fold decrease in ACE inhibition, than the corresponding N-acetyl analogs. The origin of this activity difference likely derives from the ability of the N-acetyl carbonyl to form a hydrogen bond with backbone nitrogen of Asp 358 (Asp 336 in N-domain) and the OH from Tyr 369 in the N-domain. These hydrogen bonding interactions with the N-acetyl tail are likely important interactions for the increased potency of the N-acetylated analogs in comparison to cationic N-methylated congeners.

Additionally in previous studies, in the insect homolog of ACE, AnCE (*Drosophila melanogaster)*, captopril (II-15) has been shown to be a more potent inhibitor (K_i of 1.1 nM) of the enzyme than K-26 (II-1) (K_i of 160 nM).[120, 136] Sequence alignment of human tACE with the most similar bacterial enzyme, MR1DCP, reveals five mutations in residues near the K-26 binding site (Figure II-7). In the binding pocket, Y360, F391, R402, G404 and F512 in tACE are mutated to D365, Q396, K407, S409, and Y515 altering the polarity of the pocket. However, the difference in potency between the mammalian and bacterial enzyme likely arises from mutations which increases the net negative charge in the active site, and likely deleteriously effects binding of our negatively charged substrate, K-26 (II-1).

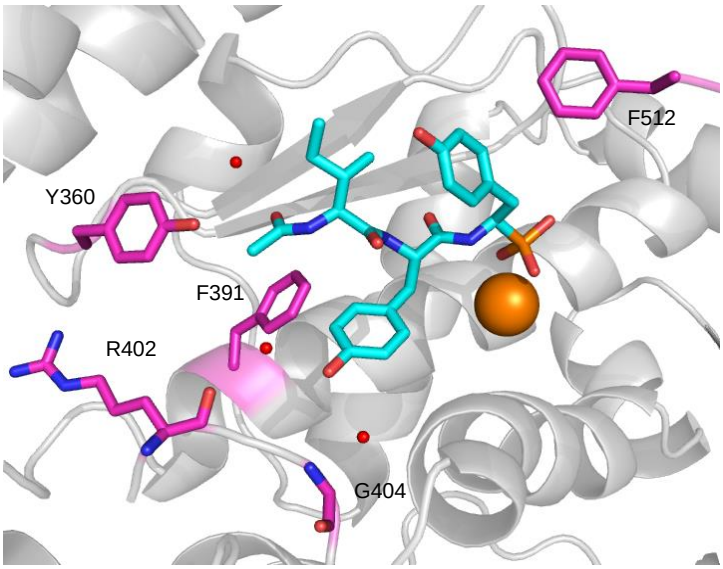

tACE	N-ACE	MR1DCP
Y360	Y338	D365
F391	Y369	Q396
R402	R380	K407
G404	G382	S409
F512	F490	Y515

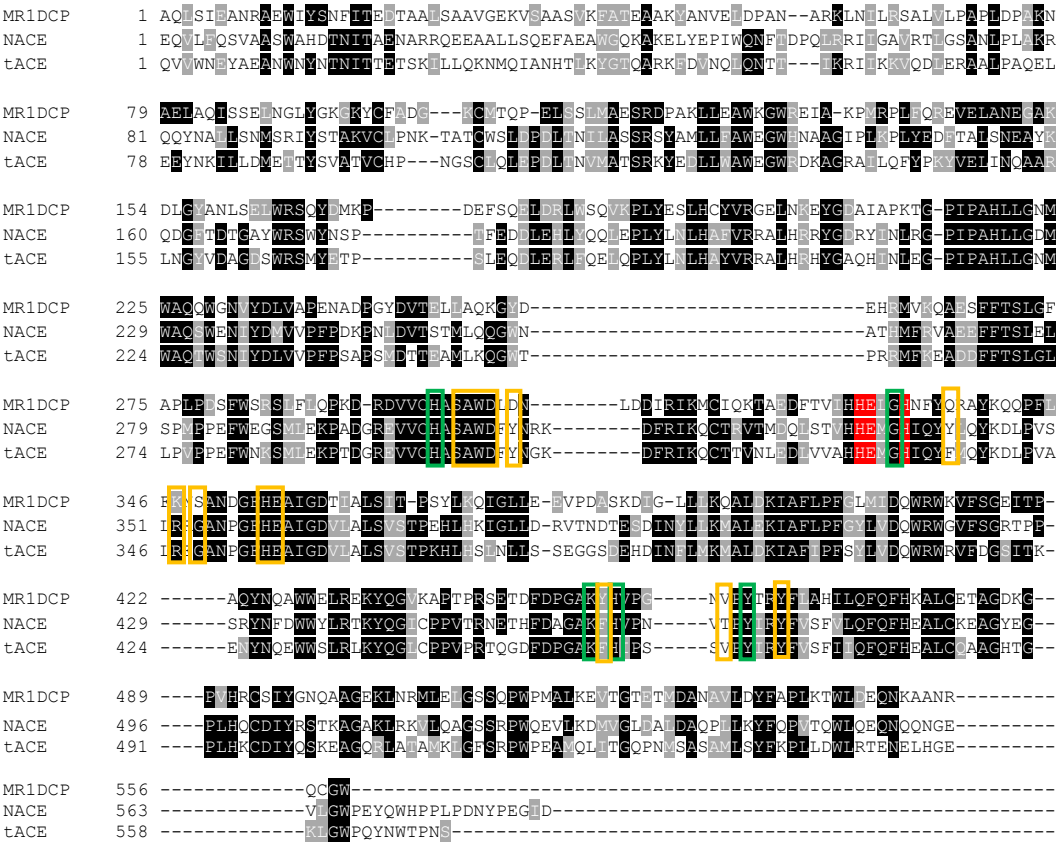

Figure II-7: Sequence homology between human tACE and N-ACE and MR1DCP. Residues in proximity to K-26 (cyan) in the binding pocket of tACE that are mutated in MR1DCP are shown in magenta. Specific residue mutations between tACE, NACE and MR1DCP are shown in the table. In the sequence alignment, the HEXXH binding motif is shown in red. Residues directly interacting with captopril in the binding pocked are highlighted in green. Residues in proximity to K-26 in the binding pocket are shown in orange. Adapted from Kramer et al.[126] Used with permission.

In conclusion, we have illuminated the structure-activity relationships of the K-26 family of natural products in mammalian ACE, the enzyme target that was originally used in screening for their discovery from Actinomycetes. These results provide structural insight that can be applied toward future development of potential domain-selective inhibitors through improving binding in the unexplored non-prime pockets of ACE. The inhibition data from bacterial ACE-like dicarboxypeptidases, together with previous data from *Drosophila* ACE, emphasize that, among all known groups of ACE-like dicarboxypeptidases, mammalian ACE seems uniquely inhibited by K-26 (II-1). Indeed, the combined enzyme and substrate structural activity data suggest that the natural target for K-26 (II-1) possesses an active-site architecture similar to mammalian ACE, prompting questions regarding potential interkingdom chemical ecological roles for natural target of K-26 (II-1). Future studies will investigate the potential for generation of improved domain selective analogs building from the AHEP (II-8) pharmacophore into the unique binding pose of this family of natural products, and work to identify potential chemical ecological targets for AHEP functional natural products.

Materials and Methods

Synthesis of K-26 family of natural products

General Experimental

Reactions were carried out in oven or flame dried glassware. All solvents were reagent grade. Amino acids and peptide coupling agents were purchased from EMD or Bachem. All reagents were commercially available and used without purification unless specified otherwise. AHEP (II-8) and K-26 (II-1) were synthesized as previously

described.[127] Silica gel (35-70 mm) from EM Science was used for column chromatography. Silica gel 60 TLC plates were purchased from EMD and plates were visualized by UV. HPLC purification was carried out using a Phenomonex C_{18} semi-preparative HPLC column on a Waters instrument using a flow rate of 5 mL/min. The purified analogs were tested for somatic ACE inhibitory activity using the substrate FAPGG. The most potent inhibitor was taken to be the desired (*R*)-diastereomer. All analogs were characterized by NMR and HRMS and quantitated, prior to inhibition studies, using an attenuated time delay proton NMR experiment (relaxation d_1 = 15 s) with dioxane added as an internal standard. NMR spectra were acquired on a Brucker DRX-400, AV-400, DRX-500, or AV-II-600 instrument. NMR spectra of synthetic intermediates and analogs are available in Appendix A.

Method A: Peptide Coupling[125, 127, 137]

The corresponding amino acids or peptides were dissolved in dimethylformamide (DMF) with N-hydroxybenzotriazole (HOBt) and the reaction mixture was cooled to 0 ^{o}C. Under inert atmosphere, 1-ethyl-3(3'-dimethylaminopropyl)carbodiimide hydrochloride (EDC) and 2,4,6-trimethylpyridine were added and the reaction was allowed to proceed for 1 hour at 0 ^{o}C and then overnight at room temperature. Unless otherwise specified, the reaction was dissolved in ethyl acetate and washed with 1N HCl, 1N $NaHCO_3$, and brine. The organic layer was then dried over $MgSO_4$, and then concentrated to give the desired product.

Method B: Saponification.[127]

The dipeptide methyl ester was dissolved in acetonitrile. An aqueous solution of 3% Na_2CO_3 was added and the reaction was stirred overnight at room temperature. The reaction was washed with hexane, acidified with 1 N HCl to pH = 3, then extracted with chloroform. The combined chloroform fractions were washed with brine and dried over $MgSO_4$, then concentrated to yield the product.

Method C: Hydrogenation.[125]

The corresponding tripeptide and palladium on activated carbon (Pd/C) were combined in anhydrous methanol and allowed to stir overnight under 1atm hydrogen gas. After filtering through Celite, the filtrate was evaporated to give the product.

Method D: Phosphonate Deprotection.[127, 138]

The corresponding ethyl phosphonate was dissolved in anhydrous acetonitrile and thioanisole at 0 ^{o}C. Iodotrimethyl silane (I-TMSi) was added dropwise, and the reaction was allowed to proceed for 3 hours at 0 ^{o}C, after which the solvent was removed under vacuum to give a brown oily residue of the phosphonate trimethylsilyl ester. After hydrolysis of the trimethylsilyl ester, the solvent was evaporated and residue was redissolved in methanol ant the product was purified via preparative HPLC.

Method E: Fmoc Deprotection.[139]

The corresponding Fmoc protected dipeptide was dissolved in anhydrous DCM (5 mL) and under inert atmosphere tris(2-aminoethyl)amine (TAEA) (3.5 mL) was added dropwise. The reaction was allowed to stir for 30 minutes at room temperature then was dissolved in additional DCM, washed with brine and phosphate buffer (pH 5.5). The aqueous portion was collected and back extracted with additional DCM. The organic layers were combined, dried over $MgSO_4$ and concentrated to give the product.

Method F: t-Butyl Deprotection.[140]

The corresponding t-butyl protected peptide was dissolved in DCM (5 mL) and trifluoroacetic acid (TFA) (5 mL). The reaction was stirred for 30 minutes at room temperature and the solvent was removed *in vaccuo* to give the product.

N-benzyloxycarbonyl-N-methyl-L-valyl-L-phenylalanine methyl ester (II-2a).

Synthesized using N-benzyloxycarbonyl-N-methyl-L-valine II-9 (200 mg, 0.753 mmol), L-phenylalanine methyl ester hydrochloride II-10 (156 mg, 0.791 mmol), HOBt (121 mg, 0.791 mmol), EDC (151 mg, 0.791 mmol) and 2,4,6-trimethylpyridine (200 μL, 1.51 mmol) in DMF (6 mL) using method A. Clear oil. Yield: 321 mg, 84.1%. Rotamers ^{1}H NMR (600 MHz, $CDCl_3$) δ 7.42-7.03 (m, 10H), 5.18-5.12 (m, 2H), 4.90-4.85 (m, 1H), 4.12 (d, *J* = 11.0 Hz, 0.8H), 3.97 (d, *J* = 10.7 Hz, 0.2H), 3.72 (s, 3H), 3.17-3.14 (m, 1H), 2.96-2.92 (m, 1H), 2.80 (s, 0.7H), 2.71 (s, 2.3H), 2.25-2.20 (m, 1H), 0.96-0.88 (m, 3H), 0.85--0.82 (m, 3H); ^{13}C NMR (150 MHz, $CDCl_3$) δ 171.68, 169.63, 157.30, 136.57, 135.96, 129.11, 128.57, 128.10, 127.67, 126.95, 67.50, 54.93, 52.76, 52.31, 38.03,

29.53, 25.92, 19.50, 18.52; HRMS calculated for $C_{24}H_{31}N_2O_5$ ($M+H^+$) 427.2228 found 427.2426.

N-benzyloxycarbonyl-N-methyl-L-valyl-L-phenylalanine (II-2b).

Synthesized using N-benzyloxycarbonyl-N-methyl-L-valyl-L-phenylalanine methyl ester II-2a (702 mg, 1.64 mmol), acetonitrile (85 mL) and 3% Na_2CO_3 (130 mL) using method B. Clear oil. Yield: 522 mg, 77.2%. Rotamers. ^1H NMR (600 MHz, $CDCl_3$) δ 7.45-6.90 (m, 10H), 5.20-5.15 (m, 2H), 4.93-4.89 (m, 1H), 4.20 (d, *J* = 11.2 Hz, 0.8H), 4.01 (d, *J* = 10.4 Hz, 0.2H), 3.24 (dd, *J* = 14.0, 5.0 Hz, 1H), 2.89 (dd, *J* = 14.0, 8.2 Hz, 1H), 2.78 (s, 0.7H), 2.71 (s, 2.3H), 2.26-2.19 (m, 1H). 0.92 (d, *J* = 6.5 Hz, 3H), 0.83 (d, *J* = 6.7 Hz, 3H); ^{13}C NMR (150 MHz, $CDCl_3$) δ 174.21, 169.75, 157.54, 136.29, 136.21, 129.34, 128.70, 128.43, 128.32, 127.81, 126.91, 67.95, 64.88, 52.83, 37.83, 29.60, 26.10, 19.44, 18.48; HRMS calculated for $C_{23}H_{29}N_2O_5$ ($M+H^+$) 413.2071 found 413.2282.

Diethyl N-(N-benzyloxycarbonyl-N-methyl-L-valyl-L-phenylalanyl)-1-amino-2-(4-enzyloxyphenyl)ethyl phosphonate (II-2c).

Synthesized using N-benzyloxycarbonyl-N-methyl-L-valyl-L-phenylalanine II-2b (309 mg, 0.75 mmol), diethyl 1-amino-2-(4-benxyloxyphenyl)ethylphosphonate II-8 (288.4 mg, 0.788 mmol), HOBt (120.6 mg, 0.788 mmol), EDC (130 mg, 0.68 mmol) and 2,4,6-trimethylpyridine (172 μL, 1.30 mmol) in DMF (5 mL) using method A. The product was further purified by flash chromatography (4% methanol in DCM, R_f = 0.23) to give a mixture of diastereomers. Clear oil. Yield: 360 mg, 64.0%. ^1H NMR (400 MHz, $CDCl_3$) δ

7.43-6.82 (m, 19H), 5.19-5.06 (m, 2H), 5.03-4.93 (m, 2H), 4.81-4.70 (m, 2H), 4.17-4.01 (m, 5H), 3.23-3.15 (m, 1H), 3.12-3.06 (m, 0.5H), 2.92-2.81 (m, 1.5H), 2.70-2.62 (m, 1H), 2.59-2.55 (m, 3H), 2.17-2.12 (m, 1H), 1.37-1.25 (m, 6H), 0.87-0.74 (m, 6H); ^{13}C NMR (150 MHz, $CDCl_3$) δ170.84-170.54, 169.97, 169.50, 158.30-157.64, 157.36-157.14, 137.15-136.98, 136.73-136.50, 130.36, 130.27, 129.24, 129.14, 129.11, 128.56, 128.40, 128.20, 128.15, 127.92, 127.73, 127.68, 127.45, 126.92-126.59, 70.02, 69.91, 67.54, 67.49, 64.95, 64.79, 62.95-62.41, 54.04-52.88, 47.34-45.74, 38.28, 37.99, 34.87, 29.74-29.35, 25.85, 19.62,19.50, 18.43, 18.39, 16.59-16.29; ^{31}P NMR (162 MHz, $CDCl_3$) δ 24.92, 24.89. 24.82; HRMS calculated for $C_{42}H_{53}N_3O_8P$ ($M+H^+$) 758.3565 found 758.3983.

Diethyl N-(N-methyl-L-valyl-L-phenylalanyl)-1-amino-2-(4-hydoxyphenyl)ethyl phosphonate (II-2d).

Synthesized using diethyl N-(N-benzyloxycarbonyl-N-methyl-L-valyl-L-phenylalanyl)-1-amino-2-(4-benzyloxyphenyl)ethyl phosphonate II-2c (371 mg, 0.489 mmol), Pd/C (10% Pd, 37 mg) in methanol (7 mL) using method C, to yield a mixture of diastereomers. White solid. Yield: 206 mg, 78.9%. ^{1}H NMR (600 MHz, $CDCl_3$) δ 7.27-6.98 (m, 7H), 6.74-6.67 (m, 2H), 4.73-4.64 (m, 2H), 4.16-4.01 (m, 4H), 3.18-3.07 (m, 2H), 2.96-2.84 (m, 1H), 2.80-2.74 (m, 1H), 2.66 (dd, *J*=15.5. 4.5 Hz, 1H) 2.23 (s, 1.5H), 2.10 (s, 1.5H), 1.92-1.83 (m, 1H), 1.33-1.25 (m, 6H), 0.83-0.56 (m, 6H); ^{13}C NMR (150 MHz, $CDCl_3$) δ 174.37, 174.30, 171.39-171.19, 155.88, 155.79, 136.69, 136.62, 130.41, 130.30, 129.34, 129.29, 128.63, 128.58, 127.45-127-21, 126.93, 115.61, 115.52, 70.87, 70.48, 63.14-62.75, 53.98, 53.66, 47.32, 46.29, 37.77, 37.72, 36.05, 34.92, 34.86,

31.30, 31.14, 19.45, 19.42, 17.77, 17.48, 16.59-16.45; ^{31}P NMR (162 MHz, $CDCl_3$) δ 25.52, 25.39; HRMS calculated for $C_{27}H_{41}N_3O_6P$ ($M+H^+$) 534.2728 found 534.2973.

K-4: N-(N-methyl-L-isoleucyl-L-phenylalanyl)-1-amino-2-(4-hydoxyphenyl)ethyl phosphonic acid (II-2).

Synthesized using diethyl N-(N-methyl-L-valyl-L-phenylalanyl)-1-amino-2-(4-hydoxyphenyl)ethyl phosphonate II-2d (30.1 mg, 0.0564 mmol), acetonitrile (6 mL), thioanisole (0.6 mL) and I-TMSi (3.0 mL) using method D. The phosphonate trimethylsilyl ester was hydrolyzed by treatment with 8:2 methanol in water (30 mL). Purified by HPLC, using a gradient of 5% acetonitrile in water to 25% acetonitrile in water containing ammonium acetate (10 mM) over 30 minutes. White solid. Yield: 3.45 mg, 12.8%. ^{1}H NMR (600 MHz, D_2O pD = 11.9) δ 7.35-7.29 (m, 4H), 7.26 (t, *J* = 7.11, 1H), 7.14 (d, *J* = 8.5 Hz, 2H), 6.70 (d, *J* = 8.5 Hz, 2H), 4.72 (m, 1H), 4.06 (m, 1H), 3.29 (dd, *J* = 14.2, 3.5 Hz, 1H), 3.21 (dt, *J* = 14.2, 2.8 Hz, 1H), 2.73 (dd, *J* = 14.1, 11.9 Hz, 1H), 2.64-2.57 (m, 2H), 1.68 (s, 3H), 1.64-1.57 (m, 1H), 0.74 (d, *J* = 6.8 Hz, 3H), 0.60 (d, *J* = 6.8 Hz, 3H); ^{13}C NMR (150 MHz, , D_2O pD = 11.9) δ 174.68, 171.53, 171.49, 154.89, 137.09, 130.61, 130.51, 130.32, 129.23, 128.53, 126.72, 115.42, 69.49, 54.09, 51.99, 51.07, 37.76, 36.41, 32.85, 30.80, 18.30; ^{31}P NMR (162 MHz, D_2O pD = 11.9) δ 15.15; HRMS calculated for $C_{23}H_{33}N_3O_6P$ ($M+H^+$) 478.2102 found 478.2169.

N-benzyloxycarbonyl-N-methyl-L-valyl-O-benzyl-L-tyrosine methyl ester (II-3a).

Synthesized using N-benzyloxycarbonyl-N-methyl-L-valine II-9 (200 mg, 0.753 mmol), *O*-benzyl-L-tyrosine methyl ester hydrochloride II-11 (231 mg, 0.718 mmol),

HOBt (121 mg, 0.791 mmol), EDC (151 mg, 0.791 mmol) and 2,4,6-trimethylpyridine (200 μL, 1.51 mmol) in DMF (6 mL) using method A. Clear oil. Yield: 321 mg, 84.1%. Rotamers. ^{1}H NMR (600 MHz, $CDCl_3$) δ 7.49-7.22 (m, 10H), 7.03-6.64 (m, 4H), 5.22-5.12 (m, 2H), 5.03-4.90 (m, 2H) 4.89-4.79 (m, 1H), 4.20 (d, *J* = 11.2 Hz, 0.8H), 4.01 (d, *J* = 10.7 Hz, 0.2H), 3.70 (s, 3H), 3.13-3.07 (m, 1H), 2.94-2.87 (m, 1H), 2.85 (s, 0.7H), 2.75 (s, 2.3H), 2.24 (m, 1H), 0.98-0.89 (m, 3H), 0.88-0.83 (m, 3H); ^{13}C NMR (150 MHz, $CDCl_3$) δ 171.61, 169.55, 157.66, 157.13, 136.87, 136.43, 130.03, 128.44, 128.38, 128.11, 127.95, 127.74, 127.52, 127.24, 114.69, 69.66, 67.36, 64.70, 52.77, 52.10, 37.06, 29.38, 26.87, 19.35, 18.44; HRMS calculated for $C_{31}H_{37}N_2O_6$ ($M+H^+$) 533.2647 found 533.2981.

N-benzyloxycarbonyl-N-methyl-L-valyl-O-benzyl-L-tyrosine (II-3b).

Synthesized using N-benzyloxycarbonyl-N-methyl-L-valyl-O-benzyl-L-tyrosine methyl ester II-3a (610 mg, 1.15 mmol), acetonitrile (67 mL) and 3% Na_2CO_3 (101 mL) using method B. Clear oil. Yield: 467 mg, 78.3%. Rotamers. ^{1}H NMR (400 MHz, $CDCl_3$) δ 7.43-7.29 (m, 10H), 7.02 (d, *J* = 7.9 Hz, 2H), 6.79 (d, *J* = 8.2 Hz, 2H), 5.19 (s, 2H), 4.92-4.84 (m, 2H), 4.22 (d, *J* = 11.1 Hz, 0.8H), 4.02 (d, *J* = 10.3 Hz, 0.2H), 3.18 (dd, *J* = 13.9, 4.62 Hz, 1H), 2.88-2.80 (m, 1H), 2.72 (s, 3H), 2.60 (s, 2H), 2.29-2.19 (m, 1H), 0.93 (d, *J* = 6.2 Hz, 3H), 0.85 (d, *J* = 6.4 Hz, 3H); ^{13}C NMR (150 MHz, $CDCl_3$) δ 174.08, 169.75, 157.72, 157.47, 136.95, 136.16, 130.32, 128.62, 128.48, 128.24, 127.86, 127.73, 127.39, 114.69, 69.77, 67.90, 64.81, 52.93, 36.93, 29.51, 26.02, 19.35, 18.43; HRMS calculated for $C_{30}H_{35}N_2O_6$ ($M+H^+$) 519.2490 found 519.2781.

Diethyl N-(N-benzyloxycarbonyl-N-methyl-L-valyl-O-benzyl-L-tyrosyl)-1-amino-2-(4-benzyloxyphenyl)ethyl phosphonate (II-3c).

Synthesized using N-benzyloxycarbonyl-N-methyl-L-valyl-L-tyrosine II-3b (315 mg, 0.861 mmol), diethyl 1-amino-2-(4-benxyloxyphenyl)ethylphosphonate II-8 (131 mg, 0.861 mmol), HOBt (132 mg, 0.861 mmol), EDC (165 mg, 0.861 mmol) and 2,4,6-trimethylpyridine (216 μL, 1.64 mmol) in DMF (5 mL) using method A. The product was further purified by flash chromatography (4% methanol in DCM, R_f = 0.21) to give a mixture of diastereomers. Clear oil. Yield: 425 mg, 60.0%. ^{1}H NMR (600 MHz, $CDCl_3$) δ 7.46-6.69 (m, 23H), 5.19-5.09 (m, 2H), 5.08-5.01 (m, 2H), 4.94-4.83 (m, 2H) 4.77-4.65 (m, 2H), 4.18-4.00 (m, 5H), 3.20-3.13 (m, 1H), 3.03-2.97 (m, 1H), 2.90-2.83 (m, 1H), 2.66-2.58 (m, 1H), 2.55 (s, 3H), 2.20-2.13 (m 1H), 1.36-1.24 (m, 6H), 0.87-0.75 (m, 6H); ^{13}C NMR (150 MHz, $CDCl_3$) δ; 170.53, 170.50, 170.06,, 157.77, 157.64, 157.40, 157.30, 137.07-136.97, 136.45, 130.34, 130.16, 128.79-128.60, 127.98, 127.81, 127.56, 127.43, 114.80, 114.77, 69.93, 69.82, 67.68, 64.95, 62.88, 62.83, 62.70, 62.66, 53.84, 46.66, 45.63, 37.03, 34.89, 29.78, 29.54, 25.82, 19.66, 18.51, 25.71, 19.56, 18.41, 16.55-16.47; ^{31}P NMR (162 MHz, $CDCl_3$) δ 25.01, 24.95, 24.86; HRMS calculated for $C_{49}H_{59}N_3O_9P$ ($M+H^+$) 864.3984 found 864.4500.

Diethyl N-(N-methyl-L-valyl-L-tyrosyl)-1-amino-2-(4-hydoxyphenyl)ethyl phosphonate (II-3d).

Synthesized using diethyl N-(N-benzyloxycarbonyl-N-methyl-L-valyl-O-benzyl-L-tyrosyl)-1-amino-2-(4-benzyloxyphenyl)ethyl phosphonate II-3c (134 mg, 0.155 mmol), Pd/C (10% Pd, 14 mg) in methanol (3 mL) using method C, to yield a mixture of

diastereomers. White solid. Yield: 69 mg, 81.0%. ^{1}H NMR (600 MHz, MeOD) δ 6.97 (t, J = 8.5 Hz, 4H), 6.58 (dd, J = 15.4, 8.5 Hz, 4H), 4.61 (q, *J* = 7.5, 4.6 Hz, 1H), 4.45-4.39 (m, 1H), 4.08-4.01 (m, 4H), 3.06-3.00 (m, 1H), 2.86 (dd, *J* = 14.0, 5.3 Hz, 1H), 2.71-2.64 (m, 1H), 2.59 (dd, *J* = 14.0, 9.8 Hz, 1H), 2.52 (d, *J* = 6.8 Hz, 1H), 1.87 (s, 3H), 1.65-1.59 (m, 1H), 1.20-1.14 (m, 6H), 0.71 (d, *J* = 6.8 Hz, 3H), 0.64 (d, *J* = 6.8 Hz, 3H); ^{13}C NMR (150 MHz, MeOD) δ 175.37, 173.31, 173.29, 157.32, 157.29, 131.38, 131.05, 128.86, 128.78, 116.25, 116.14, 71.45, 64.21-64.16, 55.16, 48.00, 39.03, 32.59, 19.63, 19.20, 16.88-16.76; ^{31}P NMR (162 MHz, MeOD) δ 25.57, 25.40; HRMS calculated for $C_{27}H_{41}N_3O_7P$ ($M+H^+$) 550.2677 found 550.2920.

15-B-2: N-(N-methyl-L-valyl-L-tyrosyl)-1-amino-2-(4-hydoxyphenyl)ethyl phosphonic acid (II-3).

Synthesized using diethyl N-(N-methyl-L-valyl-L-tyrosyl)-1-amino-2-(4-hydoxyphenyl)ethyl phosphonate II-3d (31.2 mg, 0.0599 mmol), acetonitrile (6 mL), thioanisole (0.6 mL) and I-TMSi (3.0 mL) using method D. The phosphonate trimethylsilyl ester was hydrolyzed by treatment with 8:2 methanol in water (30 mL). Purified by HPLC, using a gradient of 5% acetonitrile in water to 25% acetonitrile in water containing ammonium acetate (10 mM) over 30 minutes. White solid. Yield: 3.01 mg, 10.2%. ^{1}H NMR (600 MHz, D_2O pD = 11.9) δ 7.13 (d, *J* = 7.9 Hz, 4H), 6.76 (d, *J* = 8.5 Hz, 2H), 6.72 (d, *J* = 8.5 Hz, 2H), 4.65-4.61 (m, 1H),4.05-4.00 (m, 1H), 3.21-3.16 (m, 2H), 2.65-2.56 (m, 3H), , 1.71 (s, 3H), 1.64-1.58 (m, 1H), 0.74 (d, *J* = 6.8 Hz, 3H), 0.59 (d, *J* = 6.8 Hz, 3H); ^{13}C NMR (150 MHz, , D_2O pD = 11.9) δ 174.03, 171.61, 171.57, 155.60, 153.92, 131.11, 130.52, 130.33, 128.03, 115.79, 115.10, 69.37, 54.21,

51.91, 50.99, 36.96, 36.37, 32.66, 30.71, 18.27, 18.19; ^{31}P NMR (162 MHz, D_2O pD = 11.9) δ 16.47; HRMS calculated for $C_{23}H_{33}N_3O_7P$ ($M+H^+$) 494.2039 found 494.2039.

N-acetyl-L-isoleucyl-L-leucine methyl ester (II-4a).

Synthesized using N-acetyl-L-isoleucine II-12 (112 mg, 0.65 mmol), L-leucine methyl ester hydrochloride II-13 (99 mg, 0.68 mmol), HOBt (104 mg, 0.68 mmol), EDC (130 mg, 0.68 mmol) and 2,4,6-trimethylpyridine (172 μL, 1.30 mmol) in DMF (5 mL) using method A. White solid. Yield: 130 mg, 69%. ^{1}H NMR (600 MHz, $CDCl_3$) δ 6.89 (d, *J* = 7.4 Hz, 1H), 6.60 (d, *J* = 8.8 Hz, 1H) 4.57-4.52 (m, 1H), 4.40 (q, *J* = 0.8, 7.9 Hz, 1H), 3.72 (s, 3H), 2.00 (s, 3H), 1.84-1.76 (m, 1H), 1.65-1.60 (m, 2H), 1.60-1.51 (m, 2H), 1.19-1.09 (m, 1H), 0.96-0.85 (m, 12H); ^{13}C NMR (150 MHz, $CDCl_3$) δ 173.12, 171.66, 170.17, 57.564, 52.27, 50.99, 41.11, 37.73, 25.10, 24.88, 23.25, 22.81, 21.96, 15.22, 11.37; HRMS calculated for $C_{15}H_{29}N_2O_4$ ($M+H^+$) 301.2122 found 301.2284.

N-acetyl-L-isoleucyl-L-leucine (II-4b).

Synthesized using N-acetyl-L-isoleucyl-L-leucine methyl ester II-4a (67.6 mg, 0.225 mmol), acetonitrile (12 mL) and 3% Na_2CO_3 (20 mL) using method B. Clear oil. Yield: 51.0 mg, 79.1%. ^{1}H NMR (600 MHz, DMSO-d^6) δ 4.24-4.16 (m, 2H), 1.84 (s, 3H), 1.71-1.66 (m, 1H), 1.65-1.57 (m, 1H), 1.57-1.51 (m, 1H), 1.50-1.45 (m, 1H), 1.45-1.38 (m, 1H), 1.10-1.02 (m, 1H), 0.90-0.86 (m, 3H), 0.86-0.75 (m, 9H); ^{13}C NMR (150 MHz, DMSO-d^6) δ 173.93, 171.42, 171.34, 169.09, 169.01, 56.52-56.39, 50.22, 50.13, 39.84, 36.81, 36.79, 24.33, 24.28, 22.86, 22.49, 22.44, 21.37, 15.28, 10.99; HRMS calculated for $C_{14}H_{27}N_2O_4$ ($M+H^+$) 287.1966 found 287.2097.

Diethyl N-(N-acetyl-L-isoleucyl-L-leucyl)-1-amino-2-(4-benzyloxyphenyl)ethyl phosphonate (II-4c).

Synthesized using N-acetyl-L-isoleucyl-L-leucine II-4b (80 mg, 0.28 mmol), diethyl 1-amino-2-(4-benxyloxyphenyl)ethylphosphonate II-8 (105 mg, 0.29 mmol), HOBt (44 mg, 0.29 mmol), EDC (56 mg, 0.29 mmol) and 2,4,6-trimethylpyridine (74 μL, 0.56mmol) in DMF (3 mL) using method A. The product was further purified by flash chromatography (4% methanol in DCM, R_f = 0.15) to give a mixture of diastereomers. White solid. Yield: 112 mg, 63.3%. ^{1}H NMR (600 MHz, $CDCl_3$) δ 7.44-7.27 (m, 5H), 7.17 (d, *J* = 8.58 Hz, 1H), 7.14 (d, *J* = 8.58 Hz, 1H), 6.87 (d, *J* = 8.64 Hz, 1H), 6.79 (d, *J* = 8.64 Hz, 1H), 5.01-4.97 (m, 1H), 4.94-4.88 (m, 1H), 4.87-4.82 (m, 0.5H), 4.71-4.56 (m, 1.5H), 4.46-4.36 (m, 1H), 4.15-3.97 (m, 4H), 3.22 (dt, *J*= 14.2 Hz, 0.5H), 3.16-3.10 (m, 0.5H), 2.93-2.81 (m, 1H), 2.05 (s, 1.5H), 1.98 (s, 1.5H), 1.79-1.71 (m, 1H), 1.71-1.58 (m, 1H), 1.55-1.49 (m, 1.5H), 1.41-1.35 (m, 0.5H), 1.32-1.22 (m, 6H), 1.20-1.15 (m, 1H), 1.14-1.06 (m, 1H), 1.04-0.96 (m, 0.5H), 0.91-0.79 (m, 9H), 0.74-0.66 (m, 3H);^{3}C NMR (150 MHz, $CDCl_3$) δ 172.02-1.71.99, 171.52, 171.28, 170.39, 170.28, 157.83, 157.65, 137.06, 130.31, 130.13, 129.53-129.20, 128.66, 128.57, 128.05, 127.95, 127.55, 127.44, 114.79, 114.76, 70.05, 69.86, 62.99, 62.94, 62.63-62.46, 57.78, 51.62, 51.35, 47.29, 47.21, 46.26, 46.18, 42.61, 42.00, 37.84, 37.72, 34.86, 34.62, 29.78, 29.39, 24.48, 24.47, 23.27, 23.05, 22.95, 22.84, 22.63, 22.17, 16.64-16.40, 15.34, 11.49, 11.41; ^{31}P NMR (162 MHz, $CDCl_3$) δ 23.88, 23.69; HRMS calculated for $C_{33}H_{51}N_3O_7P$ ($M+H^+$) 632.3460 found 632.3539.

Diethyl N-(N-acetyl-L-isoleucyl-L-leucyl)-1-amino-2-(4-hydoxyphenyl)ethyl phosphonate (II-4d).

Synthesized diethyl N-(N-acetyl-L-isoleucyl-L-leucyl)-1-amino-2-(4-benzyloxyphenyl)ethyl phosphonate II-4c (49 mg, 0.078 mmol Pd/C (10% Pd, 5 mg) in methanol (1 mL) using method C, to yield a mixture of diastereomers. White solid. Yield: 33 mg, 78.0%. ^{1}H NMR (600 MHz, MeOD) δ 6.94 (dd, *J* = 8.5, 4.8 Hz, 2H), δ 6.59 (dd, *J* = 11.6, 8.5 Hz, 2H) 4.48-4.40 (m, 1H), 4.38-4.32 (m, 0.5H), 4.28-4.24 (m, 0.5H), 4.12-3.99 (m, 5H), 3.08-2.98 (m, 1H), 2.75-2.64 (m, 1H), 1.91 (s, 1.5H), 1.90 (s, 1.5H), 1.75-1.64 (m 1H), 1.60-1.50 (m, 1H), 1.48-1.33 (m, 2H), 1.28-1.20 (m, 6H), 1.17-1.10 (m, 2H), 0.89-0.76 (m, 9H), 0.75-0.68 (m, 3H); ^{13}C NMR (150 MHz, MeOD) δ 174.36, 174.04, 173.42-173.29, 158.21, 157.96, 131.13, 130.94, 128.51-128.15, 116.56, 116.52, 64.16, 64.12, 59.41, 59.37, 52.73, 52.68, 47.85, 42.56, 42.17, 37.79, 37.71, 35.03, 34.90, 26.07, 25.95, 25.55, 25.52, 23.40, 23.22, 22.41, 22.20, 21.94, 16.89-16.67, 15.98, 15.93, 11.30, 11.24; ^{31}P NMR (121 MHz, MeOD) δ25.94, 25.71; HRMS calculated for $C_{26}H_{45}N_3O_7P$ ($M+H^+$) 542.2995 found 542.3144.

SF2513 B: N-(N-acetyl-L-isoleucyl-L-leucyl)-1-amino-2-(4-hydoxyphenyl)ethyl phosphonic acid (II-4)

Synthesized using diethyl N-(N-acetyl-L-isoleucyl-L-leucyl)-1-amino-2-(4-hydoxyphenyl)ethyl phosphonate II-4d (34.1 mg, 0.063 mmol), acetonitrile (6 mL), thioanisole (0.6 mL) and I-TMSi (3.0 mL) using method D. The phosphonate trimethylsilyl ester was hydrolyzed by treatment with 8:2 methanol in water (30 mL). Purified by HPLC, using a gradient of 5% acetonitrile in water to 25% acetonitrile in

water containing ammonium acetate (10 mM) over 30 minutes. White solid. Yield: 4.85 mg, 15.8%. ^{1}H NMR (600 MHz, D_2O) δ 7.15 (d, *J* = 8.5 Hz, 2H), 6.78 (2, *J* = 8.5 Hz, 2H), 4.37 (dd, *J* = 10.6, 4.6 Hz, 1H), 4.18 (m, 1H), 3.98 (d, *J* = 8.6 Hz, 1H), 3.18 (dt, *J* = 11.3, 3.1 Hz, 1H), 2.66 (td, *J* = 13.2 6.2 Hz, 1H), 2.02 (s, 3H), 1.73-1.65 (m, 1H), 1.60-1.53 (m, 1H), 1.52-1.46 (m, 1H), 1.45-1.39 (m, 2H), 1.15-1.07 (m, 1H), 0.90 (d, *J* = 6.6 Hz, 3H), 0.84 (m, 6H), 0.65 (d, *J* = 6.8 Hz, 3H); ^{13}C NMR (150 MHz, D_2O) δ 173.97 173.12, 173.09, 172.79, 153.76, 130.30, 130.10, 130.00, 115.05, 58.47, 51.63, 50.54, 49.57, 40.27, 35.81, 34.65, 24.61, 23.98, 21.46, 20.48, 14.52, 9.94; ^{31}P NMR (162 MHz, D_2O) δ 18.66; HRMS calculated for $C_{22}H_{37}N_3O_7P$ ($M+H^+$) 486.2364 found 486.2533.

N-acetyl-L-isoleucyl-L-phenylalanine methyl ester (II-5a).

Synthesized using N-acetyl-L-isoleucine II-12 (112 mg, 0.65 mmol), L-phenylalanine methyl ester hydrochloride II-10 (104 mg, 0.68 mmol), HOBt (104 mg, 0.68 mmol), EDC (130 mg, 0.68 mmol) and 2,4,6-trimethylpyridine (172 μL, 1.30 mmol) in DMF (5 mL) using method A. White solid. Yield: 153 mg, 73.7%. ^{1}H NMR (400 MHz, $CDCl_3$) δ 7.30-7.20 (m, 3H), 7.10 (d, *J* = 7.1 Hz, 2H), 6.62 (d, *J* = 7.4 Hz, 1H), 6.33 (d, *J* = 8.5 Hz, 1H), 4.85 (q, *J* = 6.8 Hz, 1H), 4.32 (t, *J* = 8.2 Hz, 1H), 3.70 (s, 3H), 3.09 (ddd, *J* =19.8, 13.9, 6.2 Hz, 2H), 1.98 (s, 3H), 1.81-1.73 (m, 1H), 1.53-1.43 (m, 1H), 1.15-1.04 (m, 1H) 0.96-0.84 (m, 6H); ^{13}C NMR (100 MHz, $CDCl_3$) δ 171.54, 171.03, 169.94, 135.60, 129.19, 128.57, 127.12, 57.53, 53.25, 52.25, 37.83, 37.47, 24.90, 23.11, 15.12, 11.23; HRMS calculated for $C_{18}H_{27}N_2O_4$ ($M+H^+$) 335.1966 found 335.2163.

N-acetyl-L-isoleucyl-L-phenylalanine (II-5b).

Synthesized using N-acetyl-L-isoleucyl-L-phenylalanine methyl ester II-5a (220 mg, 0.658 mmol), acetonitrile (38 mL) and 3% Na_2CO_3 (57 mL) using method B. White solid. Yield: 171.0 mg, 80.7%. ^{1}H NMR (600 MHz, DMSO-d^6) δ 7.24-7.15 (m, 5H), 4.40-4.36 (m, 1H), 4.20-4.16 (m, 1H), 3.02 (dd, *J* = 13.8, 5.2 Hz, 1H), 2.87 (dd, *J* = 13.9, 9.1 Hz, 1H), 1.79 (s, 3H), 1.66-1.61 (m, 1H), 1.37-1.33 (m, 1H), 1.03-0.98 (m, 1H), 0.78-0.73 (m, 6H); ^{13}C NMR (150 MHz, DMSO-d^6) δ 172.75, 171.22, 171.14, 168.98, 168.87, 137.56, 129.01, 129.11, 126.37, 56.46-56.36, 53.32, 53.23, 36.67-36.54, 24.15, 22.45, 22.40, 15.22, 10.93; HRMS calculated for $C_{17}H_{25}N_2O_4$ ($M+H^+$) 321.1809 found 321.2011.

Diethyl N-(N-acetyl-L-isoleucyl-L-phenylalanyl)-1-amino-2-(4-benzyloxyphenyl)ethyl phosphonate (II-5c).

Synthesized using N-acetyl-L-isoleucyl-L-phenylalanine II-5b (117 mg, 0.365 mmol), diethyl 1-amino-2-(4-benxyloxyphenyl)ethylphosphonate II-8 (139 mg, 0.384 mmol), HOBt (58.7 mg, 0.384 mmol), EDC (73.3mg, 0.384 mmol) and 2,4,6-trimethylpyridine (95.6 μL, 0.73 mmol) in DMF (5 mL) using method A. The product was further purified by flash chromatography (4% methanol in DCM, R_f = 0.15) to give a mixture of diastereomers. White solid. Yield: 175 mg, 72.1 %. ^{1}H NMR (600 MHz, $CDCl_3$) δ 7.38-6.79(m, 14H), 5.05-5.00 (m, 1H), 4.97-4.90 (m, 2H), 4.70-4.62 (m, 1H), 4.38-4.32 (m, 1H), 4.15-3.91 (m, 4H), 3.18-3.11 (m, 1H), 3.05-3.00 (m, 0.5H), 2.90-2.65 (m, 2.5H), 2.01 (m, 1.5H), 2.00 (m, 1.5H), 1.76-1.67 (m, 1H), 1.50-1.42 (m, 1H), 1.32-1.23 (m, 6H), 1.11-0.99 (m, 1H), 0.85-0.78 (m, 4.5H), 0.76-0.70 (m, 1.5H); ^{13}C NMR

(150 MHz, $CDCl_3$) δ171.55, 171.20, 170.95-170.81, 170.40, 170.26, 157.97, 157.66, 137.04, 137.00, 136.44, 136.22, 130.58, 130.14, 129.58, 129.52, 129.36-129.18, 128.58, 128.39, 128.25, 127.96, 127.48, 127.44, 126.75, 114.95, 114.76, 70.08, 69.87, 63.14-62.42, 57.91, 57.83, 53.64, 53.45, 47.48, 47.30, 46.45, 46.26, 38.93, 38.83, 37.58, 37.46, 35.04, 34.83, 25.16, 25.08, 23.09, 23.04, 16.63-16.44, 15.46, 15.34, 11.43, 11.38; ^{31}P NMR (121 MHz, $CDCl_3$) δ 23.88, 23.68; HRMS calculated for $C_{26}H_{49}N_3O_7P$ ($M+H^+$) 666.3303 found 666.3700.

Diethyl N-(N-acetyl-L-isoleucyl-L-phenylalanyl)-1-amino-2-(4-hydoxyphenyl)ethyl phosphonate (II-5d).

Synthesized using diethyl N-(N-acetyl-L-isoleucyl-L-phenylalanyl)-1-amino-2-(4-benzyloxyphenyl)ethyl phosphonate II-5c (248 mg, 0.37 mmol), Pd/C (10% Pd, 25 mg) in methanol (5 mL) using method C, to yield a mixture of diastereomers. White solid. Yield: 169 mg, 79.0%. ^1H NMR (600 MHz, MeOD) δ 7.27-7.13 (m, 4H), 7.12-6.98 (m, 3H), 6.70 (dd, *J* = 23.8, 8.5 Hz, 2H), 4.68-4.62 (m, 1H), 4.57-4.51 (m, 1H), 4.20-4.05 (m, 5H), 3.16-3.08 (m, 1H), 3.05 (dd, *J* = 14.0, 5.2 Hz, 0.5H), 2.84-2.70 (m, 1.5H), 2.54 (dd, *J* = 14.2, 9.5 Hz, 0.5H), 1.95 (s, 1.5H), 1.93 (s, 1.5H), 1.71-1.66 (m, 1H), 1.36-1.29 (m, 6H), 1.10-1.02 (m, 1H), 0.83 (t, *J* = 7.3 Hz, 3H), 0.79 (d, *J* = 6.8 Hz, 1.5H), 0.70 (d, *J* = 6.8 Hz, 1.5 H); ^{13}C NMR (150 MHz, MeOD) δ 173.30, 173.25, 173.17, 157.52, 157.31, 138.21, 138.13, 131.33, 131.00, 130.41, 130.35, 129.39, 129.27, 129.00, 128.90, 127.68, 127.57, 116.34, 116.29, 64.51, 64.46, 64.23-64.11, 59.52, 59.40, 55.27, 55.03, 54.80, 48.15, 48.05, 39.29, 39.05, 37.65, 37.61, 35.17, 35.06, 25.84, 25.75, 22.47,

16.90-16.73, 15.85, 11.31, 11.25; ^{31}P NMR (162 MHz, MeOD) δ 26.93, 26.84; HRMS calculated for $C_{29}H_{43}N_3O_7P$ ($M+H^+$) 576.2834 found 576.3109.

SF2513C: N-(N-acetyl-L-isoleucyl-L-phenylalanyl)-1-amino-2-(4-hydoxyphenyl)ethyl phosphonic acid (II-5).

Synthesized using diethyl N-(N-acetyl-L-isoleucyl-L-phenylalanyl)-1-amino-2-(4-hydoxyphenyl)ethyl phosphonate II-5d (32.6 mg, 0.057 mmol), acetonitrile (6 mL), thioanisole (0.6 mL) and I-TMSi (3.0 mL) using method D. The phosphonate trimethylsilyl ester was hydrolyzed by treatment with 8:2 methanol in water (30 mL). Purified by HPLC, using a gradient of 5% acetonitrile in water to 25% acetonitrile in water containing ammonium acetate (10 mM) over 30 minutes. White solid. Yield: 5.15 mg, 17.5%. ^{1}H NMR (600 MHz, D_2O) δ 7.34-7.25 (m, 3H), 7.23 (d, *J* = 6.9 Hz, 2H), 7.15 (d, *J* = 8.5 Hz, 2H), 6.77 (d, *J* = 8.5 Hz, 2H), 4.64 (dd, *J* = 10.4, 4.1 Hz, 1H), 4.25-4.18 (m, 1H), 3.93 (d, *J* = 8.6 Hz, 1H), 3.19 (dt, *J* = 14.2, 3.1 Hz, 1H), 3.12 (dd, *J* = 14.1 Hz, 4.1 Hz, 1H), 2.76 (dd, *J* = 14.0, 10.4 Hz, 1H), 2.71-2.65 (m, 1H), 1.94 (s, 3H), 1.61-1.55 (m, 1H), 1.29-1.22 (m, 1H), 1.02-0.96 (m, 1H), 0.78 (t, *J* = 7.4 Hz, 3H) 0.58 (d, *J* = 6.8 Hz, 3H); ^{13}C NMR (150 MHz, D_2O) δ 173.47, 172.35, 171.58, 153.79, 136.52, 130.26, 130.10-130.00, 129.27, 128.38, 115.05, 58.00, 53.76, 50.59, 49.62, 37.74, 35.89, 34.75, 24.35, 21.56, 14.42, 9.93; ^{31}P NMR (162 MHz, D_2O) δ 18.69; HRMS calculated for $C_{25}H_{38}N_3O_7P$ ($M+H^+$) 520.2208 found 520.2441.

Diethyl N-(N-fluorenylmethyloxycarbonyl-L-glutamyl-5-tert-butyl ester)-1-amino-2-(4-benzyloxyphenyl)ethyl phosphonate (II-7b).

Synthesized using N-fluorenylmethyloxycarbonyl-glutamate-5-tert-butyl ester II-7a (252 mg, 0.593 mmol), diethyl 1-amino-2-(4-benxyloxyphenyl)ethylphosphonate II-8 (225 mg, 0.620 mmol), HOBt (94.9 mg, 0.620 mmol), EDC (119 mg, 0.620 mmol) and 2,4,6-trimethylpyridine (158 μL, 1.19 mmol) in DMF (6 mL) using method A. The reaction was dissolved in ethyl acetate and extracted with 1N citric acid, 1N $NaHCO_3$, and brine. The organic layer was then dried over $MgSO_4$, and then the product was further purified by flash chromatography (5% methanol in DCM, R_f = 0.21) to give a mixture of diastereomers. White solid. Yield: 360 mg, 78.8%. ^{1}H NMR (600 MHz, $CDCl_3$) δ 7.41-7.27 (m, 5H), 7.12 (dd, *J* = 13.2, 8.6 Hz, 2H), 6.87 (d, *J* = 8.6 Hz, 1H), 6.81 (d, *J* = 8.6 Hz, 1H), 5.00 (s, 1H), 4.95 (s, 1H), 4.70- 4.59 (m, 1.5H), 4.58-4.53 (m, 0.5H), 4.39- 4.34 (m, 1H), 415-4.02 (m, 4H), 3.22-3.13 (m, 1H), 2.87-2.77 (m, 1H), 2.23 (t, *J* = 7.7 Hz, 1H), 2.04 (s, 1.5H), 2.00 (s, 1.5H), 1.96-1.85 (m, 2H), 1.79-1.69 (m, 1.5H), 1.65-1.58 (m, 0.5H), 1.52-1.43 (m, 1H), 1.39 (s, 9H), 1.31-1.22 (m, 6H), 1.13-1.04 (m, 1H), 0.89-0.82 (m, 4.5H), 0.77 (d, *J* = 7.7 Hz, 1H);^{13}C NMR (600 MHz, $CDCl_3$) δ171.91, 172.80, 171.55, 171.31, 170.90, 170.87, 170.59, 170.34, 158.00, 157.86, 137.32, 137.24, 130.37, 130.26, 129.39-129.08, 128.74, 128.71, 128.12, 128.08, 127.65, 127.62, 115.07, 114.94, 80.93, 70.11, 70.06, 63.17-62.71, 57.99, 57.86, 52.42, 52.33, 47.51, 47.40, 46.48, 46.37, 34.93, 34.82, 31.51, 31.43, 28,67, 28.56, 28.27, 25.43, 25.37, 23.34, 23.33, 16.71-16.57, 15.61, 15.46,11.68; ^{31}P NMR (162 MHz, D_2O) δ 23.79, 23.61; HRMS calculated for $C_{36}H_{55}N_3O_9P$ ($M+H^+$) 704.3671 found 704.3667.

Diethyl N-(L-glutamyl-5-tert-butyl ester)-1-amino-2-(4-benzyloxyphenyl)ethyl phosphonate (II-7c).

Synthesized using diethyl N-(N-fluorenylmethyloxycarbonyl-L-glutamyl-5-tert-butyl ester)-1-amino-2-(4-benzyloxyphenyl)ethyl phosphonate II-7b (150 mg, 0.194 mmol) using method E. Clear oil. Yield: 65.0 mg, 60.5%. ^{1}H NMR (400 MHz $CDCl_3$) δ 7.43-7.25 (m, 5H), 7.12 (dd, *J* = 8.7, 2.4 Hz, 2H), 6.87 (dd, *J* = 8.5, 6.4 Hz, 2H), 5.01 (d, *J* = 2.1 Hz, 2H), 4.71-4.60 (m, 1H), 4.18-4.04 (m, 4H), 3.32-3.27 (m, 0.5H), 3.25-3.17 (m, 1.5H), 2.89-2.76 (m, 1H), 2.30-2.15 (m, 1H), 2.07 (t, *J* = 7.4 Hz, 1H), 1.96-1.86 (m, 0.5H), 1.86-1.66 (m, 1H), 1.62-1.52 (m, 0.5H), 1.41 (d, *J* = 3.3 Hz, 9H), 1.33-1.26 (m, 6H); ^{13}C NMR (100 MHz, $CDCl_3$) δ 173.88-173.78, 172.59, 172.57, 157.58, 157.52, 136.96, 136.93m 130.08, 130.03, 128.94-128.75, 128.43, 128.40, 1287.81, 127.76, 127.37, 127.31, 114.66, 80.37, 80.33, 69.82, 62.54-62.35, 54.39, 54.32, 46.58, 46.52, 45.03, 44.98, 34.75-34.56, 31.47, 31.42, 30.03, 29.88, 27.96, 16.37-16.25; ^{31}P NMR (162 MHz, D_2O) δ 25.51, 25.43; HRMS calculated for $C_{28}H_{42}N_2O_7P$ ($M+H^+$) 549.2725 found 549.2750.

Diethyl N-(N-acetyl-L-isoleucyl-L-glutamyl-5-tert-butyl ester)-1-amino-2-(4-benzyloxyphenyl)ethyl phosphonate (II-7d).

Synthesized using N-acetyl isoleucine II-12 (20.2 mg, 0.118 mmol), diethyl N-(L-glutamyl-5-tert-butyl ester)-1-amino-2-(4-benzyloxyphenyl)ethyl phosphonate 7c (62.0 mg, 0.113 mmol), HOBt (18 mg, 0.118 mmol), EDC (22.6 mg, 0.118 mmol) and 2,4,6-trimethylpyridine (36 μL, 0.23 mmol) in DMF (2 mL) using method A. The reaction was dissolved in ethyl acetate and extracted with 1N citric acid, 1N $NaHCO_3$, and brine. The

organic layer was then dried over $MgSO_4$, and then the product was further purified by flash chromatography (5% methanol in DCM, R_f = 0.23) to give a mixture of diastereomers. White solid. Yield: 60 mg, 75.4%. ^{1}H NMR (600 MHz, $CDCl_3$) δ 7.41-7.27 (m, 5H), 7.12 (dd, *J* = 13.2, 8.6 Hz, 2H), 6.87 (d, *J* = 8.6 Hz, 1H), 6.81 (d, *J* = 8.6 Hz, 1H), 5.00 (s, 1H), 4.95 (s, 1H), 4.70- 4.59 (m, 1.5H), 4.58-4.53 (m, 0.5H), 4.39- 4.34 (m, 1H), 415-4.02 (m, 4H), 3.22-3.13 (m, 1H), 2.87-2.77 (m, 1H), 2.23 (t, *J* = 7.7 Hz, 1H), 2.04 (s, 1.5H), 2.00 (s, 1.5H), 1.96-1.85 (m, 2H), 1.79-1.69 (m, 1.5H), 1.65-1.58 (m, 0.5H), 1.52-1.43 (m, 1H), 1.39 (s, 9H), 1.31-1.22 (m, 6H), 1.13-1.04 (m, 1H), 0.89-0.82 (m, 4.5H), 0.77 (d, *J* = 7.7 Hz, 1H);^{13}C NMR (600 MHz, $CDCl_3$) δ171.91, 172.80, 171.55, 171.31, 170.90, 170.87, 170.59, 170.34, 158.00, 157.86, 137.32, 137.24, 130.37, 130.26, 129.39-129.08, 128.74, 128.71, 128.12, 128.08, 127.65, 127.62, 115.07, 114.94, 80.93, 70.11, 70.06, 63.17-62.71, 57.99, 57.86, 52.42, 52.33, 47.51, 47.40, 46.48, 46.37, 34.93, 34.82, 31.51, 31.43, 28,67, 28.56, 28.27, 25.43, 25.37, 23.34, 23.33, 16.71-16.57, 15.61, 15.46,11.68; ^{31}P NMR (162 MHz, D_2O) δ 23.79, 23.61; HRMS calculated for $C_{36}H_{55}N_3O_9P$ ($M+H^+$) 704.3671 found 704.3667.

Diethyl N-(N-acetyl-L-isoleucyl-L-glutamyl-5-tert-butyl ester)-1-amino-2-(4-hydroxyphenyl)ethyl phosphonate (II-7e).

Synthesized using diethyl N-(N-acetyl-L-isoleucyl-L-glutamyl-5-tert-butyl ester)-1-amino-2-(4-benzyloxyphenyl) ethyl phosphonate II-7d (54 mg, 0.077 mmol), Pd/C (10% Pd, 6 mg) in methanol (2 mL) using method C, to yield a mixture of diastereomers. White solid. Yield: 41.4 mg,, 88.0%. ^{1}H NMR (600 MHz, MeOD) δ 7.08 (t, *J* = 7.4 Hz, 2H), 6.71 (dd, *J* = 13.9, 8.4 Hz, 4.62-4.52 (m, 1H), 4.47-4.36 (m, 1H), 4.24-4.13 (m, 4H),

3.20-3.10 (m, 1H), 2.86-2.74 (m, 1H), 2.33-2.27 (m, 1H), 2.03 (d, *J* = 2.60 Hz, 3H), 1.90-1.72 (m, 2H), 1.64-1.52 (m, 1H), 1.47 (d, *J* = 3.8 Hz, 9H), 1.39-1.32 (m, 6H), 1.28-1.11 (m, 1H), 0.98-0.89 (m, 4.5H), 0.81 (d, *J* = 6.8 Hz, 1.5 H); ^{13}C NMR (150 MHz, MeOD) δ 173.93, 173.80, 173.44-173.42, 172.94-172-80, 157.55, 157.27, 131.09. 130.92, 128.94-128.61, 116.28, 116.26, 81.72, 81.66, 64.47-64.04, 59.40, 53.34, 53.30, 47.66, 47.63, 37.82, 37.80, 35.07, 34.87, 32.28, 32.15, 29.08, 28.73, 28.33, 26.10, 25.99, 22.46, 22.44, 16.90-16.70, 15.97, 15.88; ^{31}P NMR (162 MHz, MeOD) δ 25.58, 25.51; HRMS calculated for $C_{29}H_{49}N_3O_9P$ ($M+H^+$) 614.3206 found 614.3263.

Diethyl N-(N-acetyl-L-isoleucyl-L-glutamyl)-1-amino-2-(4-hydroxyphenyl) ethyl phosphonate (II-7f).

Synthesized using diethyl N-(N-acetyl-L-isoleucyl-L-glutamyl-5-tert-butyl ester)-1-amino-2-(4-hydroxyphenyl)ethyl phosphonate II-7e (73.0 mg, 0.119 mmol) using method F, to yield a mixture of diastereomers. White solid. Yield: 50.2 mg, 75.8%. ^{1}H NMR (600 MHz, MeOD) δ 6.88 (t, *J* = 8.8 Hz, 2H), 6.51 (dd, *J* = 19.3, 8.4 Hz, 2H), 4.39-4.32 (m, 1H), 4.27-4.19 (m, 1H), 4.05-3.93 (m, 5H), 2.99-2.90 (m, 1H), 2.66-2.56 (m, 1H), 2.23-2.11 (m, 1H), 1.99-1.86 (m, 1H), 1.82 (d, *J* = 4.7 Hz, 3H), 1.72-1.56 (m, 2H), 1.46-1.27 (m, 2H), 1.20-1.13 (m, 6H), 1.08-0.94 (m, 1H), 0.76-0.70 (m, 4.5H), 0.61 (d, *J* = 6.8 Hz, 1.5H); ^{13}C NMR (150 MHz, MeOD) δ 176.57, 176.47, 173.56-173.49, 173.00, 172.90, 157.44, 157.27, 131.16, 130.97, 128.98-128.74, 116.35, 116.29, 64.50, 64.15, 29.54, 53.46, 53.43, 48.08, 48.01, 37.76, 37.74, 35.01, 34.90, 30.83, 30.58, 28.96, 28.59, 28.11, 28.01, 22.39, 16.88-16.66, 15.96, 15.88, 11.36, 11.33; ^{31}P NMR (162 MHz,

MeOD) δ 24.28, 24.13; HRMS calculated for $C_{25}H_{31}N_3O_9P$ ($M+H^+$) 558.2575 found 558.2586.

SF2513 D: N-(N-acetyl-L-isoleucyl-L-glutamyl)-1-amino-2-(4-hydroxyphenyl) phosphonic acid (II-7).

Synthesized using diethyl N-(N-acetyl-L-isoleucyl-L-glutamyl)-1-amino-2-(4-hydroxyphenyl) ethyl phosphonate II-7f (15.1 mg, 0.0271 mmol), acetonitrile (2 mL), thioanisole (0.2 mL) and I-TMSi (1.0 mL) using method D. The phosphonate trimethylsilyl ester was hydrolyzed by treatment with 8:2 isopropanoll in water (10 mL). Purified by HPLC using an isocratic method of 5% acetonitrile in water containing ammonium acetate (10 mM) for 10 minutes to yield a mixture of diastereomers. White solid. Yield: 5.15 mg, 17.5%. ^{1}H NMR (600 MHz, D_2O) δ 7.19-7.13 (m, 2H), 6.84-6.76 (m, 2H), 4.39-4.23 (m, 1.5H), 4.22-4.15 (m, 0.5H), 4.13-4.08 (m, 0.5H), 4.03-3.97 (m, 0.5H), 3.25-3.14 (m, 1H), 2.79-2.63 (m, 1H), 2.43-2.18 (m, 1.5H), 2.04 (s, 3H), 1.86-1.77 (m, 1H), 1.73-1.62 (m, 1H), 1.58-1.1.50 (m, 0.5H), 1.49-1.35 (m, 1H), 1.24-1.14 (m, 1H), 1.14-1.06 (m, 0.5H), 0.91-0.82 (m, 4.5H), 0.66-0.62 (m, 1.5H); ^{13}C NMR (150 MHz, D_2O) δ 179.27, 177.92, 174.39-171.96, 153.96, 153.78, 130.33, 130.24, 130.09-129.86, 115.24, 115.07, 64.19, 58.51, 58.41, 52.88, 52.52, 36.01, 35.93, 34.64, 34.58, 27.85, 27.35, 24.67, 24.45, 23.61, 21.55, 21.20, 14.67, 14.48, 10.19, 10.07; ^{31}P NMR (162 MHz, D_2O) δ17.55; HRMS calculated for $C_{21}H_{31}N_3O_9P$ ($M-H^+$) 500.1803 found 500.1755.

Co-crystallization of K-26 and ACE

Overexpression and purification of N-domain and C-domain of ACE constructs

Both the N- and C-domain ACE constructs were produced by expression in cultured CHO cells and purified as previously described.[102, 141]

Crystallization and data collection

The crystals of the C- and N-domain ACE complexes with K-26 were grown at 16°C by the hanging drop vapor diffusion method. C-domain ACE (11.5 mg/ml in 50 mM HEPES, pH 7.5) was pre-incubated with K-26 (II-1) (2 mM) at room temperature for two hours before crystallization. Pre-incubated sample was mixed with the reservoir solution consisting of 13.5 % PEG 4000, 50 mM sodium acetate, pH 4.7 and 10 μM $ZnSO_4$, and suspended above the well. Diffraction quality of co-crystals appeared after approximately 10 days. N-domain ACE (5 mg/ml in 50 mM HEPES, pH 7.5) was pre-incubated with K-26 (II-1) (2 mM) at room temperature for two hours before crystallization. Pre-incubated sample was mixed with the reservoir solution consisting of 30 % PEG 550MME/PEG 20000, 100 mM TRIS/Bicine pH 8.5 and 0.06M divalent cations (Molecular Dimensions Ltd, Suffolk, UK), and suspended above the well. Crystals appeared within 3 days. X-ray diffraction data for the C- and N-domain ACE-K-26 complexes were collected on the PX station IO3 at Diamond Light Source (Oxon, UK). A total of 100 and 250 images were collected using a Quantum-315 CCD detector (ADSC Systems, CA) for the C- and N- domain structures, respectively. 25% PEG 4000 was used as a cryoprotectant for C-domain ACE while no cryoprotectant was used for the N-domain. Crystal was kept at constant temperature (100K) under the liquid

nitrogen jet during data collection. Raw data images were indexed and scaled with HKL2000 [142] and the CCP4 program SCALA[143]. Initial phasing for structure solution was obtained using the molecular replacement routines of the program PHASER [144] The atomic coordinates of C-domain ACE (PDB code 108A)[133] and N-domain ACE (PDB code 3NXQ)[102] were used as a search model respectively. The resultant model was refined using REFMAC5[145] and adjustment of the model was carried out using COOT[146] Water molecules were added at positions where Fo–Fc electron density peaks exceeded 3σ and potential H-bonds could be made. Based on electron density interpretation, the inhibitor and sugar moieties were added in the complex structure and further refinement was carried out. The coordinate and parameter files for K-26 were taken from the AnCE-K-26 complex structure (PDB 2XHM)[120] and validated through the PRODRG server.[147] Validation of the protein structure was conducted with the aid of MOLPROBITY. [148] The structures presented 98% and 97% residues within the favored Ramachandran region for the C-domain and N-domain complexes, respectively. Figures were drawn with PyMOL (DeLano Scientific, San Carlos, CA, USA). Hydrogen bonds were verified with the program HBPLUS.[149] The detailed refinement statistics can be found in Table II-6.

	C-domain ACE	N-domain ACE	B- factor analysis		
				C-domain ACE	N-domain ACE
Resolution Å	1.85	2.1	**Whole protein atom**	22.7	43.2/38.2
Space group	$P2_12_12_1$	$P1$	**Main chain atom**	22.2	42.9/37.9
Cell	a=56.8, b=84.5, c=133.4Å α=β=γ=90.0°	a=73.0, b=77.3, c=82.0Å α=88.7, β=64.5, γ=75.2°	**Side chain atom**	23.2	43.5/38.5
No. of molecule in ASU	1	2	**Zinc ion**	18.7	35.4/37.0
Redundancy	4.2 (2.7)	1.8 (1.5)	**Chloride ion**	23.2	29.3/27.8
Total/unique number of reflection	939,579/55,751	763,835/90,926	**Inhibitor**	18.4	30.5/31.7
Completeness (%)	93.3 (65.4)	84.3 (71.7)	**Glycosylated sugar**	45.5	72.7/60.1
R_{symm} [a]	11.9 (57.6)	8.4 (49.9)	**Solvent**	30.6	34.6
I/σ(I)	10.2 (1.2)	7.8 (1.7)	**RCSB PDB code**	4BZR	4BZS
R_{cryst} [b]	21.4	23.5			
R_{free} [c]	25.1	27.7			
Rmsd in bond length	0.006	0.005			
Rmsd in bond angle	1.04	0.91			

Table II-6. Refinement statistics for crystal structures of K-26 in both C-domain and N-domain ACE. Values in parentheses are for last resolution shell. [a] $R_{symm}=\Sigma_h\Sigma_i[|I_i(h)- <I(h)>|/\Sigma_h\Sigma_i I_i(h)]$, where I_i is the ith measurement and $<I(h)>$ is the weighted mean of all the measurements of $I(h)$. [b] $R_{cryst} =\Sigma_h|F_o-F_c|/\Sigma_h F_o$, where F_o and F_c are observed and calculated structure factor amplitudes of reflection h, respectively. [c] R_{free} is equal to R_{cryst} for a randomly selected 5% subset of reflections.

Assays for ACE inhibition

Assay for inhibition of somatic ACE with substrate FAPGG

Somatic ACE was extracted from rabbit lung acetone powder. Turnover of the substrate FAPGG was monitored in triplicate in a 96-well plate in the presence of various concentrations of inhibitor by monitoring the corresponding change in absorbance at 340 nm.[127-128] IC_{50} was calculated by plotting the percent activity of the enzyme against the log of the concentration of the inhibitor. IC_{50} curves are available in Appendix B.

Assay for inhibition of N- and C- domains of ACE with substrate Z-FHL

Z-FHL turnover by purified N- and C- domain ACE constructs was monitored in triplicate with using fluorescence as previously described.[129-131] IC_{50} was calculated by plotting the percent activity of the enzyme against the log of the concentration of the inhibitor. The K_i value was obtained using a Dixon plot by performing the assay at two substrate concentrations (initial concentrations of 1mM and 0.2 mM Z-FHL) and plotting 1/v against the inhibitor concentration. IC_{50} curves and Dixon plots are available in Appendix B.

Assay for inhibition of bacterial dicarboxypeptidases by K-26 and captopril using substrate FAPGG

Purified dicarboxypeptidase in 50 mM sodium borate buffer containing 5% glycerol, pH = 8.3 (60 uL) was diluted to the appropriate concentration for use in the assay, combined with the inhibitor of known concentration (60 uL), and incubated for 5

minutes. The substrate FAPGG was added (100 uL of 1 mM FAPGG in 50 mM Tris buffer, pH 8.0 with 300 mM sodium chloride), and the turnover was monitored in triplicate in a 96-well plate by measuring the corresponding change in absorbance at 340 nm.[127-128] IC_{50} was calculated by plotting the percent activity of the enzyme against the log of the concentration of the inhibitor. IC_{50} curves are available in Appendix B.

Expression and Purification of Bacterial DCPs

Preparation of pET28_EcDCP and pET28_MR1DCP

The genes encoding EcDCP and MR1DCP were amplified by PCR from purified genomic DNA from *E.coli* and *Schwanella oneidensis str. MR- 1* using the appropriate forward and reverse primers with restriction enzyme sites (Table II-7). The PCR product was TOPO cloned and transformed into TOP10 cells (Invitrogen TOPO cloning kit) Cells were plated (LB agar with kanamycin (5 μg/mL) and spread with Xgal (40 uL, 40 mg/mL in DMF)) and colonies confirmed to contain the TOPO vector were selected, grown in liquid culture (LB with 5μg/mL kanamycin) and the plasmid DNA was harvested (QIAprep Spin Miniprep Kit). The plasmid DNA was digested using the appropriate restriction enzymes (New England Biolabs), purified on 1% agarose gel, extracted (Qiagen Gel Extraction Kit), and ligated into pET28a(+) treated with the same restriction enzymes to give the resulting vector pET28a_DCP, which codes for the bacterial dicarboxypeptidase with a N-terminal hexahistidine tag. All products were verified by sequencing.

	Strain Used		Primer	Restriction Enzyme
EcDCP	*Escherichia coli* st. K-12 sbstr. MG1655	Forward	5'-CATATGACAACAATGAATCCTTTCCTTGTGC-3'	NdeI
		Reverse	5'-GGATCCTTATATGTTCAAGCCACGATGTTGC-3'	BamHI
MR1DCP	*Schwanella oneidensis* str. MR-1	Forward	5'-CATATGGCTATTCTATTGAATCGTCCC-3'	NdeI
		Reverse	5'- GTCGACTTACCAGCCGCATTGACG-3'	SalI

Table II-7. PCR primers used for the cloning of EcDCP and MR1DCP from the given strain. Restriction enzyme sites are underlined for the corresponding restriction enzyme.

Preparation of pET28_K26DCP.

The K-26 dicarboxypeptidase gene from *Astrosporangium hypotensionis* was synthesized commercially (Mr. Gene) with NdeI and HindIII restriction enzyme sites in a generic kanamycin resistant vector. This vector was transformed into TOP10 *E. coli* cells, which were grown on LB agar supplemented with 50 µg/mL of kanamycin. Selected colonies were grown in 5 mL cultures of LB broth (with 50 µg/mL of kanamycin). Plasmids were harvested from these cells, digested using the appropriate restriction enzymes, and the resulting dicarboxypeptidase gene was ligated into an empty pET 28a(+) vector digested with the same restriction enzymes, introducing an N-terminal hexahistadine tag. The product was verified by sequencing.

Transformation, Expression and Purification of bacterial dicarboxypeptidase

Electrocompetent BL21DE3 *E. coli* cells were transformed with the pET28_DCP vector. LB media (1L with 50 mg/mL kanamycin) was inoculated (1%) with an overnight culture of BL21(DE3) cells containing the desired plasmid. This culture was shaken at 37^{o}C until an OD_{600} = 0.6-0.8 was reached. Dicarboxypeptidase expression was

induced by the addition of isopropyl β-D-1-thiogalactopyranoside (IPTG, 1mM final concentration) and was carried out at 30^{o}C overnight. Cells were harvested via centrifugation and frozen at -80 °C for subsequent purification. The cell pellet from 1L of liquid culture was resuspended in 20 mL of buffer A (10 mM imidazole, 50 mM Tris and 300 mM NaCl, pH 7.4) with DNAse added. Cells were disrupted with a French press (three times), centrifuged (12,000 rpm for 20 min) and the supernatant was applied to a 5 mL HiTrap nickel affinity column (GE Healthcare) equilibrated with buffer A. The column was washed with 10 column volumes of buffer A, then the desired His-tagged protein was eluted using a gradient of 100% buffer A to 100% buffer B (buffer A containing 500 mM imidazole) over 20 minutes. Gradient fractions having an absorbance at 280 nm were pooled and concentrated to 1 mL using an Amicon centrifugal filter (MWCO 10 kDa). Concentrated protein was desalted using a 5 mL HiTrap desalting column and eluted into 50 mM sodium borate buffer containing 5% glycerol (pH = 8.3). The overexpressed bacterial dicarboxypeptidase was immediately tested for FAPGG turnover.

Evolutionary relationships of taxa

The evolutionary history was inferred using the Neighbor-Joining method.[150] The optimal tree with the sum of branch length = 6.39523051 is shown (Figure 3). The evolutionary distances were computed using the Poisson correction method [151] and are in the units of the number of amino acid substitutions per site. The analysis involved 15 amino acid sequences. All positions containing gaps and missing data were eliminated.

There were a total of 548 positions in the final dataset. Evolutionary analyses were conducted in MEGA5. [152].

Acknowledgements

This work was originally published in *ACS Medicinal Chemistry Letters* under the citation, Glenna J. Kramer, Akif Mohd, Sylva L. U. Schwager, Geoffrey Masuyer, K. Ravi Acharya, Edward D. Sturrock, and Brian O. Bachmann, *ACS Med. Chem. Lett.*, **2014**, *5* (4), pp 346–351. This research would have not been possible without contributions from our collaborators in the laboratories of K. Ravi Acharya and Edward.D. Sturrock. K. Ravi Acharya, Akif Mohd and Geoffrey Masuyer are responsible for solving the crystal structures of K-26 in both the N-domain and the C-domain of ACE. Edward D. Sturrock and Sylva L. U. Schwager have graciously provided overexpressed C-domain and N-domain ACE along with guidance on the domain specific inhibition assays. Brian O. Bachmann provided immense amounts of guidance about experimental design. All authors provided input and feedback when writing the paper.

CHAPTER III

ACE INHIBITORY ACTIVITY OF A LIBRARY OF K-26 VARIANTS

Introduction

Natural products are a rich source of biologically active molecules and scaffolds which have widespread medicinal use.[153] One such example of a biologically active natural product is the metabolite K-26 (III-1) which is produced by the soil dwelling microbe, *Astrosporangium hypotensionis* (Figure III-1A).[7] This natural product has been noted for its selectivity for mammalian ACE and comparable activity to the widely prescribed antihypertensive drug, captopril, attributes at least partially ascribed to the non-proteogenic amino acid, AHEP (III-2). [50, 126]

ACE is a significant target for pharmacological regulation of blood pressure and has been discovered to have roles in a wide array of physiological processes from fibrosis to fluid balance regulation.[2] There are two isoforms of ACE present in humans, somatic ACE (sACE) and the tissue specific testicular ACE (tACE). sACE is comprised of two domains, referred to as the N-domain and the C-domain, each with their own HEXXH zinc binding sequence, substrate, and pharmacological inhibitor preference. tACE is nearly identical to the C-domain of sACE. Several inhibitors of this enzyme have been developed for treatment of hypertension, however, current ACE inhibitors have been attributed to side effects such as angioedema and a dry cough, a feature that has been associated with the inhibition of both ACE domains and potentially other off target enzymes.

Co-crystal structures of K-26 (II-1) in both N-domain and C-domain ACE have revealed that K-26 adopts a unique binding motif in the active site of ACE.[126] The phosphonic acid coordinates the zinc while the amino acid sidechains occupy solely the non-prime binding pockets. As all other known ACE inhibitors occupy the prime binding pockets, this binding motif is exclusive to K-26 and therefore focusing on the only the prime binding pockets is an unexplored realm for potent and selective ACE inhibitor design.[92-93, 101, 103]

As K-26 adopts an unusual binding conformation in the active site of ACE and exhibits selectivity for the mammalian enzyme, this natural product family is a relevant starting point for exploration for ACE inhibitor design. However, the current synthetic scheme would make obtaining a large library of synthetic variants difficult. As a result, we chose to use computational modeling to predict binding interactions of a set of AHEP (III-2) containing K-26 variants with both domains of ACE.

In this study, we opted to use the computational modeling suite Rosetta for the analysis of our set of variants. This powerful tool has been used in applications from *de novo* proteins structure determination, to studying protein-small molecule interactions, performing enzyme design and predicting the structure of biological macromolecules and complexes.[154-160] Rosetta has furthermore been shown to be an effective method of computational inhibitor study having been applied successfully in high-throughput library screening and ligand docking.[161-162] As the binding site of the K-26 inhibitor is known as the crystal structures of this small molecule with the human enzyme are available, utilizing Rosetta is an ideal approach to furthering structural activity relationship studies to identify inhibitors of interest based on the K-26 scaffold.

Using Rosetta, a binding energy will be calculated and used to select a handful of variants, with a spectrum of predicted inhibitory activities. These selected variants will be synthesized and experimentally assayed for inhibition of both domains of heterologously expressed human ACE. This analysis provides insight into the specific features of K-26 (II-1) and variants, potentially of pharmacological interest, which are responsible for the potent inhibition of the two individual domains of this enzyme.

Results

Rosetta prediction of K-26 variant binding

Although there are many options for modifications to the K-26 structure to optimize inhibitor binding, we chose to approach our study by evaluating the effect of different naturally occurring amino acids in two different positions in K-26 (III-1) (Figure III-1B). As previous studies have shown the importance of the AHEP (II-2) moiety for the pharmacological effect of the small molecule, we chose to leave the side-chain of the AHEP (III-2) untouched in our computational modeling experiments. Furthermore, as the N-terminal acetyl is deemed to be important for potent binding of K-26 (III-1) we chose to study inhibitors with this N-acetyl functionality. With our plan to evaluate each of the 20 natural amino acids in two different positions, a set of 400 different K-26 based in inhibitors would be evaluated for binding in each domain of ACE. Our approach entailed the use of Rosetta to predict the effect of these amino acid modifications by generating binding energies for each of the K-26 based inhibitors of interest.

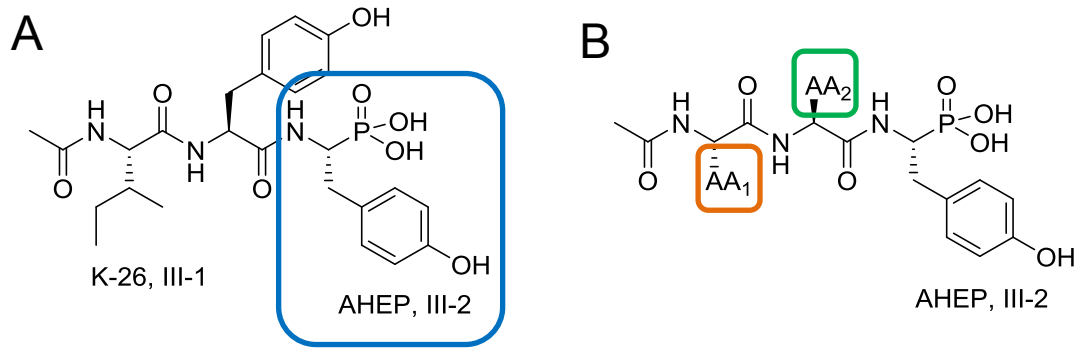

Figure III-1: K-26 and modifications for our computational study A. Structure of the ACE inhibitory natural product, K-26 (III-1). AHEP (III-2) is highlighted by a blue box. B. Amino acids modified in our computational study to give our set of 400 computationally studied variants. The side chains that are modified are highlighted in an orange and green box.

AHEP (III-2) was generated as a non-canonical amino acid that was utilized as the terminal amino acid in all K-26 tripeptide variants studied. The N-terminal acetyl group was appended to the K-26 variants by applying an N-acetyl patch. The coordinates for both the N-acetyl group and the AHEP were derived from the co-crystal structure of K-26 with tACE. Partial charges on the phosphonate of the AHEP were established based on the partial charges of phosphate. The initially generated K-26 was docked into the computationally relaxed structure with fixed zinc and zinc binding residues. The predicted binding conformation in both N-domain and C-domain ACE was compared to the crystal structures of K-26. As docking the K-26 ligand did not result in a pose that emulated the binding of the K-26 inhibitor in the crystal structure, the K-26 backbone was restrained as part of the optimization for inhibitor binding. With the restrained backbone, the optimized ligand superimposed with the crystal structure for both the C-domain and the N-domain of ACE (Figure III-2A,B).

Each of the 400 different K-26 variants were docked into the N-domain and the C-domain of ACE and the free energy of binding was calculated for each variant for the

collection of structures generated using the Rosetta energy function. The function is a linear combination of terms which model interaction forces between atoms, solvation effects and torsion energies.[163] The change in free energy of the inhibitor binding ($\Delta\Delta G_{predicted}$) predicted by Rosetta is calculated from the difference between the free energy of the inhibitor bound (ΔG_{bound}) and not bound ($\Delta G_{unbound}$) in the enzyme.

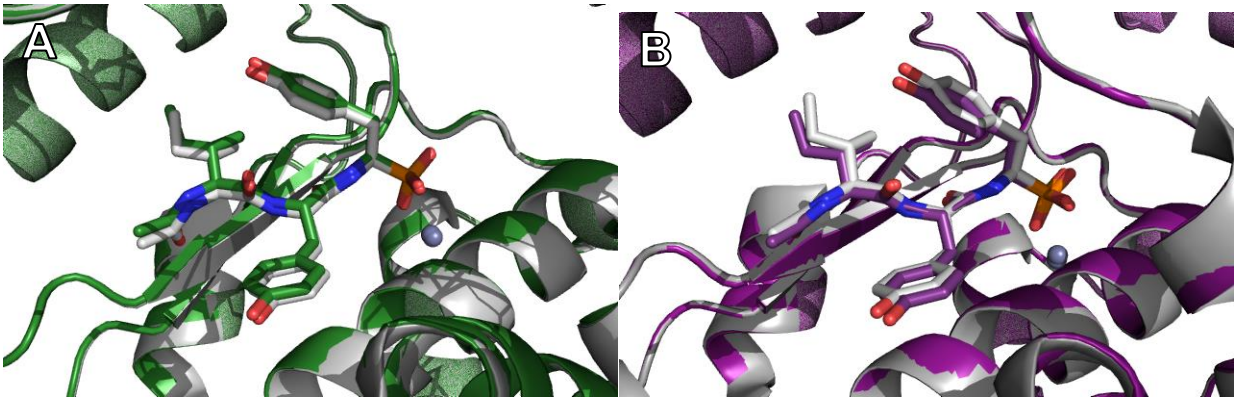

Figure III-2 Comparison of the low binding energy structure predicted by Rosetta (colored) and the crystal structure (grey). A. Low binding predicted by Rosetta for N-domain. ACE is shown in forest. B. Low binding energy structure predicted by Rosetta for C-domain. ACE is shown in deep purple.

Selection of K-26 variants for further study

For each of the 400 K-26 variants the Rosetta energy function was used to calculate the free energy for the inhibitor binding ($\Delta\Delta G_{predicted)}$ for both the C-domain and the N-domain of ACE (Figure III-3 A, B). As domain selectivity is a feature of interest to us in inhibitor development, we also compared the ratio of free energy ($\Delta\Delta G_{predicted}$) of binding for both the C-domain and the N-domain as a means to gain insight as to which variants may exhibit domain selective properties (Figure III-3 C).

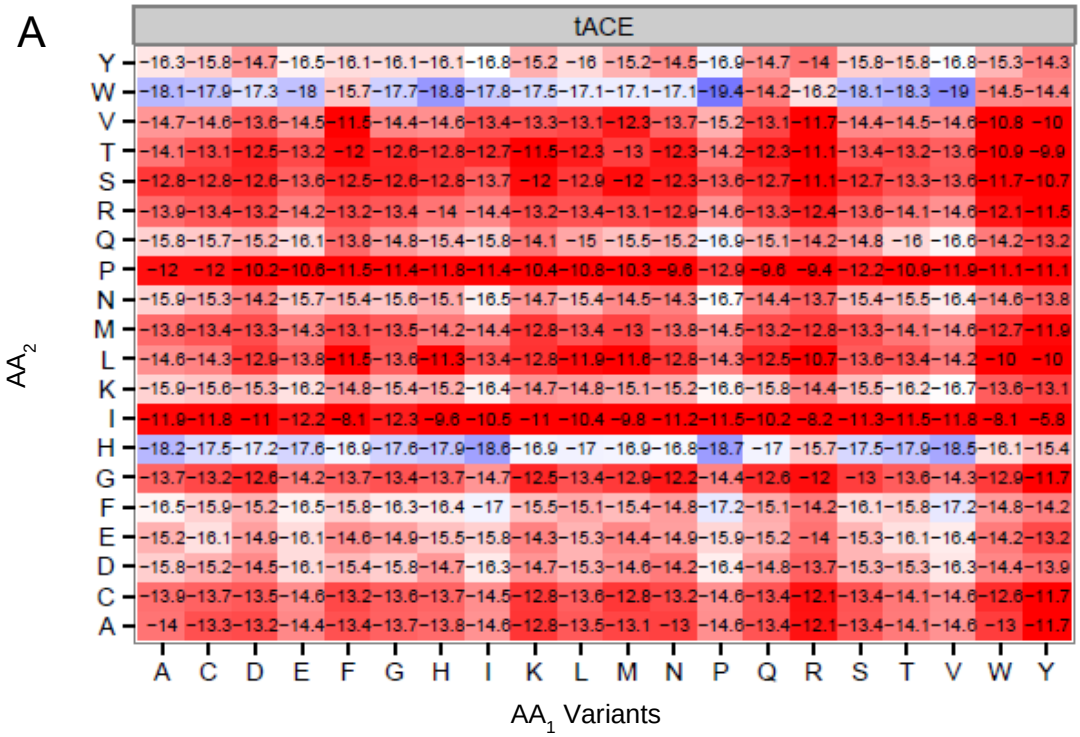
A
tACE
Y −16.3 −15.8 −14.7 −16.5 −16.1 −16.1 −16.1 −16.8 −15.2 −16 −15.2 −14.5 −16.9 −14.7 −14 −15.8 −15.8 −16.8 −15.3 −14.3
W −18.1 −17.9 −17.3 −18 −15.7 −17.7 −18.8 −17.8 −17.5 −17.1 −17.1 −17.1 −19.4 −14.2 −16.2 −18.1 −18.3 −19 −14.5 −14.4
V −14.7 −14.6 −13.6 −14.5 −11.5 −14.4 −14.6 −13.4 −13.3 −13.1 −12.3 −13.7 −15.2 −13.1 −11.7 −14.4 −14.5 −14.6 −10.8 −10
T −14.1 −13.1 −12.5 −13.2 −12 −12.6 −12.8 −12.7 −11.5 −12.3 −13 −12.3 −14.2 −12.3 −11.1 −13.4 −13.2 −13.6 −10.9 −9.9
S −12.8 −12.8 −12.6 −13.6 −12.5 −12.6 −12.8 −13.7 −12 −12.9 −12 −12.3 −13.6 −12.7 −11.1 −12.7 −13.3 −13.6 −11.7 −10.7
R −13.9 −13.4 −13.2 −14.2 −13.2 −13.4 −14 −14.4 −13.2 −13.4 −13.1 −12.9 −14.6 −13.3 −12.4 −13.6 −14.1 −14.6 −12.1 −11.5
Q −15.8 −15.7 −15.2 −16.1 −13.8 −14.8 −15.4 −15.8 −14.1 −15 −15.5 −15.2 −16.9 −15.1 −14.2 −14.8 −16 −16.6 −14.2 −13.2
P −12 −12 −10.2 −10.6 −11.5 −11.4 −11.8 −11.4 −10.4 −10.8 −10.3 −9.6 −12.9 −9.6 −9.4 −12.2 −10.9 −11.9 −11.1 −11.1
N −15.9 −15.3 −14.2 −15.7 −15.4 −15.6 −15.1 −16.5 −14.7 −15.4 −14.5 −14.3 −16.7 −14.4 −13.7 −15.4 −15.5 −16.4 −14.6 −13.8
M −13.8 −13.4 −13.3 −14.3 −13.1 −13.5 −14.2 −14.4 −12.8 −13.4 −13 −13.8 −14.5 −13.2 −12.8 −13.3 −14.1 −14.6 −12.7 −11.9
L −14.6 −14.3 −12.9 −13.8 −11.5 −13.6 −11.3 −13.4 −12.8 −11.9 −11.6 −12.8 −14.3 −12.5 −10.7 −13.6 −13.4 −14.2 −10 −10
K −15.9 −15.6 −15.3 −16.2 −14.8 −15.4 −15.2 −16.4 −14.7 −14.8 −15.1 −15.2 −16.6 −15.8 −14.4 −15.5 −16.2 −16.7 −13.6 −13.1
I −11.9 −11.8 −11 −12.2 −8.1 −12.3 −9.6 −10.5 −11 −10.4 −9.8 −11.2 −11.5 −10.2 −8.2 −11.3 −11.5 −11.8 −8.1 −5.8
H −18.2 −17.5 −17.2 −17.6 −16.9 −17.6 −17.9 −18.6 −16.9 −17 −16.9 −16.8 −18.7 −17 −15.7 −17.5 −17.9 −18.5 −16.1 −15.4
G −13.7 −13.2 −12.6 −14.2 −13.7 −13.4 −13.7 −14.7 −12.5 −13.4 −12.9 −12.2 −14.4 −12.6 −12 −13 −13.6 −14.3 −12.9 −11.7
F −16.5 −15.9 −15.2 −16.5 −15.8 −16.3 −16.4 −17 −15.5 −15.1 −15.4 −14.8 −17.2 −15.1 −14.2 −16.1 −15.8 −17.2 −14.8 −14.2
E −15.2 −16.1 −14.9 −16.1 −14.6 −14.9 −15.5 −15.8 −14.3 −15.3 −14.4 −14.9 −15.9 −15.2 −14 −15.3 −16.1 −16.4 −14.2 −13.2
D −15.8 −15.2 −14.5 −16.1 −15.4 −15.8 −14.7 −16.3 −14.7 −15.3 −14.6 −14.2 −16.4 −14.8 −13.7 −15.3 −15.3 −16.3 −14.4 −13.9
C −13.9 −13.7 −13.5 −14.6 −13.2 −13.6 −13.7 −14.5 −12.8 −13.6 −12.8 −13.2 −14.6 −13.4 −12.1 −13.4 −14.1 −14.6 −12.6 −11.7
A −14 −13.3 −13.2 −14.4 −13.4 −13.7 −13.8 −14.6 −12.8 −13.5 −13.1 −13 −14.6 −13.4 −12.1 −13.4 −14.1 −14.6 −13 −11.7
A C D E F G H I K L M N P Q R S T V W Y
AA2
AA1 Variants

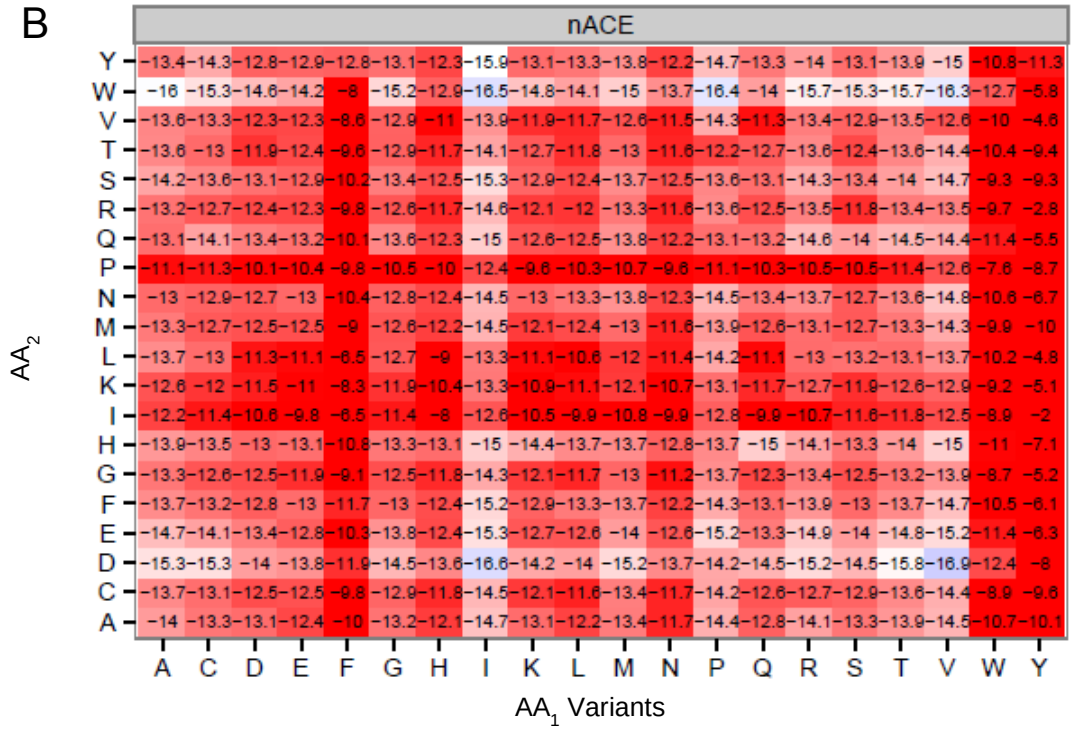
B
nACE
Y −13.4 −14.3 −12.8 −12.9 −12.8 −13.1 −12.3 −15.9 −13.1 −13.3 −13.8 −12.2 −14.7 −13.3 −14 −13.1 −13.9 −15 −10.8 −11.3
W −16 −15.3 −14.6 −14.2 −8 −15.2 −12.9 −16.5 −14.8 −14.1 −15 −13.7 −16.4 −14 −15.7 −15.3 −15.7 −16.3 −12.7 −5.8
V −13.6 −13.3 −12.3 −12.3 −8.6 −12.9 −11 −13.9 −11.9 −11.7 −12.6 −11.5 −14.3 −11.3 −13.4 −12.9 −13.5 −12.6 −10 −4.6
T −13.6 −13 −11.9 −12.4 −9.6 −12.9 −11.7 −14.1 −12.7 −11.8 −13 −11.6 −12.2 −12.7 −13.6 −12.4 −13.6 −14.4 −10.4 −9.4
S −14.2 −13.6 −13.1 −12.9 −10.2 −13.4 −12.5 −15.3 −12.9 −12.4 −13.7 −12.5 −13.6 −13.1 −14.3 −13.4 −14 −14.7 −9.3 −9.3
R −13.2 −12.7 −12.4 −12.3 −9.8 −12.6 −11.7 −14.6 −12.1 −12 −13.3 −11.6 −13.6 −12.5 −13.5 −11.8 −13.4 −13.5 −9.7 −2.8
Q −13.1 −14.1 −13.4 −13.2 −10.1 −13.6 −12.3 −15 −12.6 −12.5 −13.8 −12.2 −13.1 −13.2 −14.6 −14 −14.5 −14.4 −11.4 −5.5
P −11.1 −11.3 −10.1 −10.4 −9.8 −10.5 −10 −12.4 −9.6 −10.3 −10.7 −9.6 −11.1 −10.3 −10.5 −10.5 −11.4 −12.6 −7.6 −8.7
N −13 −12.9 −12.7 −13 −10.4 −12.8 −12.4 −14.5 −13 −13.3 −13.8 −12.3 −14.5 −13.4 −13.7 −12.7 −13.6 −14.8 −10.6 −6.7
M −13.3 −12.7 −12.5 −12.5 −9 −12.6 −12.2 −14.5 −12.1 −12.4 −13 −11.6 −13.9 −12.6 −13.1 −12.7 −13.3 −14.3 −9.9 −10
L −13.7 −13 −11.3 −11.1 −6.5 −12.7 −9 −13.3 −11.1 −10.6 −12 −11.4 −14.2 −11.1 −13 −13.2 −13.1 −13.7 −10.2 −4.8
K −12.6 −12 −11.5 −11 −8.3 −11.9 −10.4 −13.3 −10.9 −11.1 −12.1 −10.7 −13.1 −11.7 −12.7 −11.9 −12.6 −12.9 −9.2 −5.1
I −12.2 −11.4 −10.6 −9.8 −6.5 −11.4 −8 −12.6 −10.5 −9.9 −10.8 −9.9 −12.8 −9.9 −10.7 −11.6 −11.8 −12.5 −8.9 −2
H −13.9 −13.5 −13 −13.1 −10.8 −13.3 −13.1 −15 −14.4 −13.7 −13.7 −12.8 −13.7 −15 −14.1 −13.3 −14 −15 −11 −7.1
G −13.3 −12.6 −12.5 −11.9 −9.1 −12.5 −11.8 −14.3 −12.1 −11.7 −13 −11.2 −13.7 −12.3 −13.4 −12.5 −13.2 −13.9 −8.7 −5.2
F −13.7 −13.2 −12.8 −13 −11.7 −13 −12.4 −15.2 −12.9 −13.3 −13.7 −12.2 −14.3 −13.1 −13.9 −13 −13.7 −14.7 −10.5 −6.1
E −14.7 −14.1 −13.4 −12.8 −10.3 −13.8 −12.4 −15.3 −12.7 −12.6 −14 −12.6 −15.2 −13.3 −14.9 −14 −14.8 −15.2 −11.4 −6.3
D −15.3 −15.3 −14 −13.8 −11.9 −14.5 −13.6 −16.6 −14.2 −14 −15.2 −13.7 −14.2 −14.5 −15.2 −14.5 −15.8 −16.9 −12.4 −8
C −13.7 −13.1 −12.5 −12.5 −9.8 −12.9 −11.8 −14.5 −12.1 −11.6 −13.4 −11.7 −14.2 −12.6 −12.7 −12.9 −13.6 −14.4 −8.9 −9.6
A −14 −13.3 −13.1 −12.4 −10 −13.2 −12.1 −14.7 −13.1 −12.2 −13.4 −11.7 −14.4 −12.8 −14.1 −13.3 −13.9 −14.5 −10.7 −10.1
A C D E F G H I K L M N P Q R S T V W Y
AA2
AA1 Variants

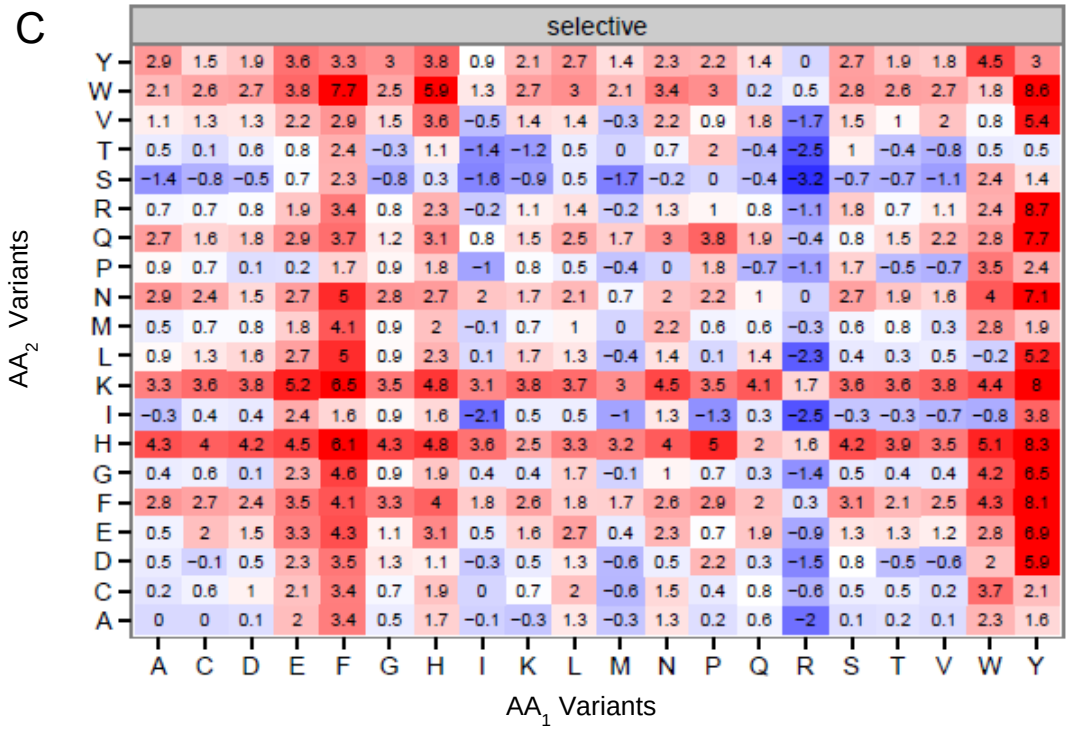

Figure III-3: Heat maps showing the Rosetta predicted ΔΔG of binding for the set of 400 K-26 variants analyzed in this study. A. ΔΔGpred for tACE. B. ΔΔGpred for N-domain ACE. C. Ratio of ΔΔGpred for tACE and N-domain ACE to show predicted domain selectivity for tACE (red) or N-domain (blue).

K-26 (III-1) and ten additional variants were selected for study, which are predicted to have a wide range of expected ACE inhibitory properties based on the Rosetta predicted ΔΔG values (Figure III-4). In addition to K-26 (III-1) and the two other naturally occurring AHEP containing compounds, SF 2513B (III-3) and SF 2513C (III-4), the variant Ac-Ile-Trp-AHEP (III-5) was selected as this inhibitor is predicted to be one of the most potent inhibitors of both domains of ACE. Comparison of the predicted ΔΔG values for tACE and the N-domain of ACE gave us a reason to select Ac-Ile-Ser-AHEP (III-6) as an inhibitor with a preference for the N-domain and Ac-Ile-His-AHEP (III-7), Ac-His-Trp-AHEP (III-8) and Ac-Leu-Tyr-AHEP (III-9) as inhibitors of tACE (C-domain). All of these potentially domain selective variants were chosen as they were also expected

to be reasonably good inhibitors based on the $\Delta\Delta G_{predicted}$ values. Due to less negative $\Delta\Delta G_{predicted}$ values, a middle of the spectrum inhibitor was selected, Ac-Leu-Ile-AHEP (III-10) and a poor inhibitor was selected, Ac-Tyr-Ile-AHEP (III-11). Ac-Tyr-Ile-AHEP is predicted to be one of the worst inhibitors of the variant set tested. Ac-Pro-Tyr-AHEP (III-12) was chosen for study as the rigid conformation of proline makes it unexpected that this variant would have $\Delta\Delta G_{predicted}$ only slightly worse than predicted values for the potent analog K-26 (III-1). The Rosetta predicted binding conformations for each variant selected for synthesis were visualized to ensure that the Rosetta energy predictions were structurally logical for the binding of the inhibitor in each ACE domain (Appendix C).

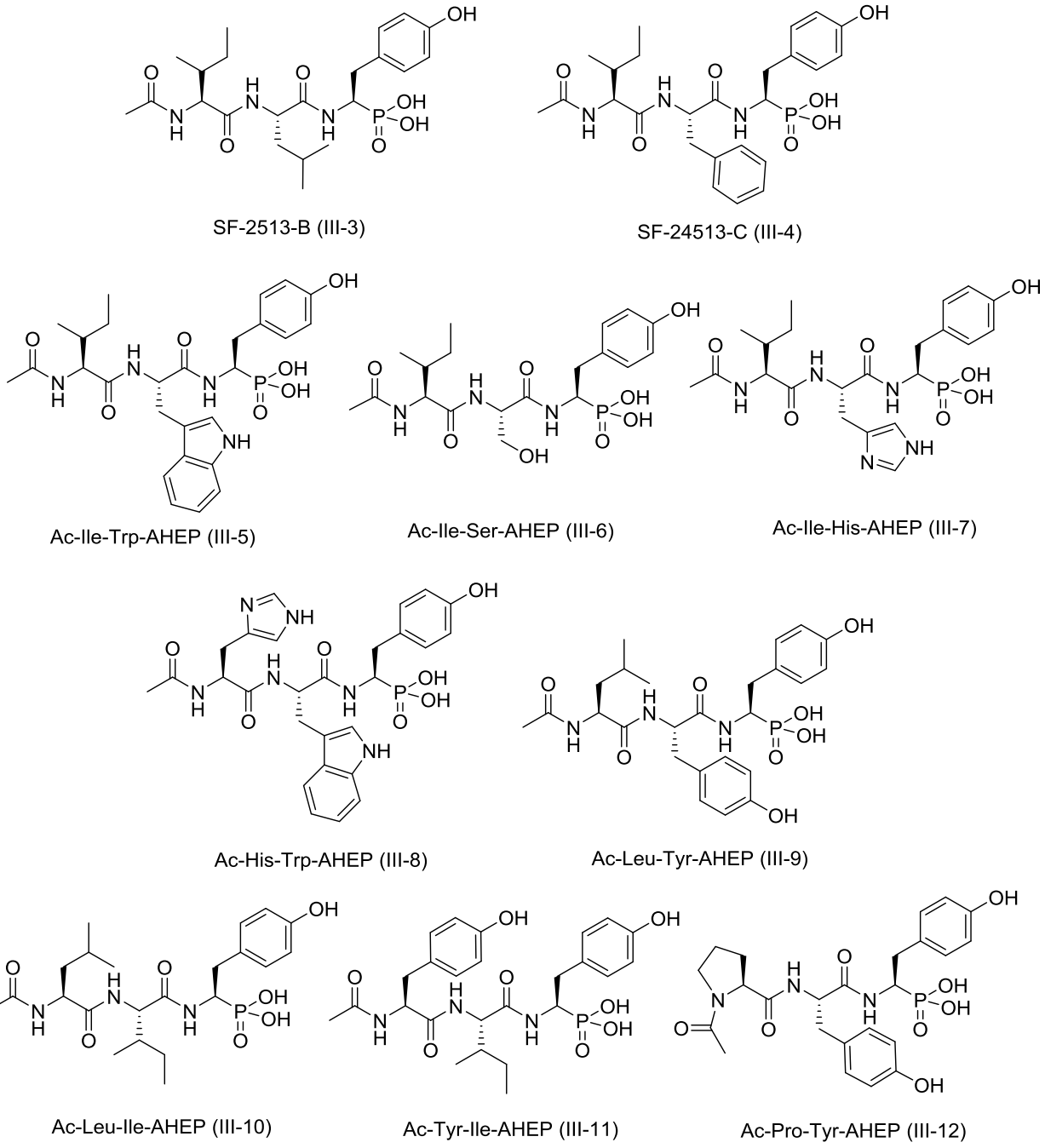

Figure III-4. K-26 variants selected for further study based on Rosetta ΔΔG predictions.

Synthesis of K-26 variants

The synthesis of all of the K-26 variant tripeptides, with the exception of Ac-Ile-His-AHEP (III-7), proceeded from the N-terminal to the AHEP phosphonate as

previously described (Scheme III-1A).[126-127] Ac-Ile-His-AHEP (III-7) was synthesized in the direction of the phosphonate towards the N-terminal of the peptide due to the commercial availability of the necessary amino acids for synthesis (Scheme III-2B) . Both of these schemes proceeded through two peptide coupling steps with HOBt and EDC with an intermediate deprotection, followed by global deprotection of the tripeptide. The synthesis yielded all K-26 variants as a mixture of two major diasteromers, which were separated and purified by preparative C_{18}-HPLC. K-26 (III-1), SF-2513-B (III-3) and SF-2513-C (III-4) had been synthesized and assayed for activity in a prior study.[50, 126] More details about the synthesis is given in the methods section and NMRs of structural intermediates can be found in Appendix D.

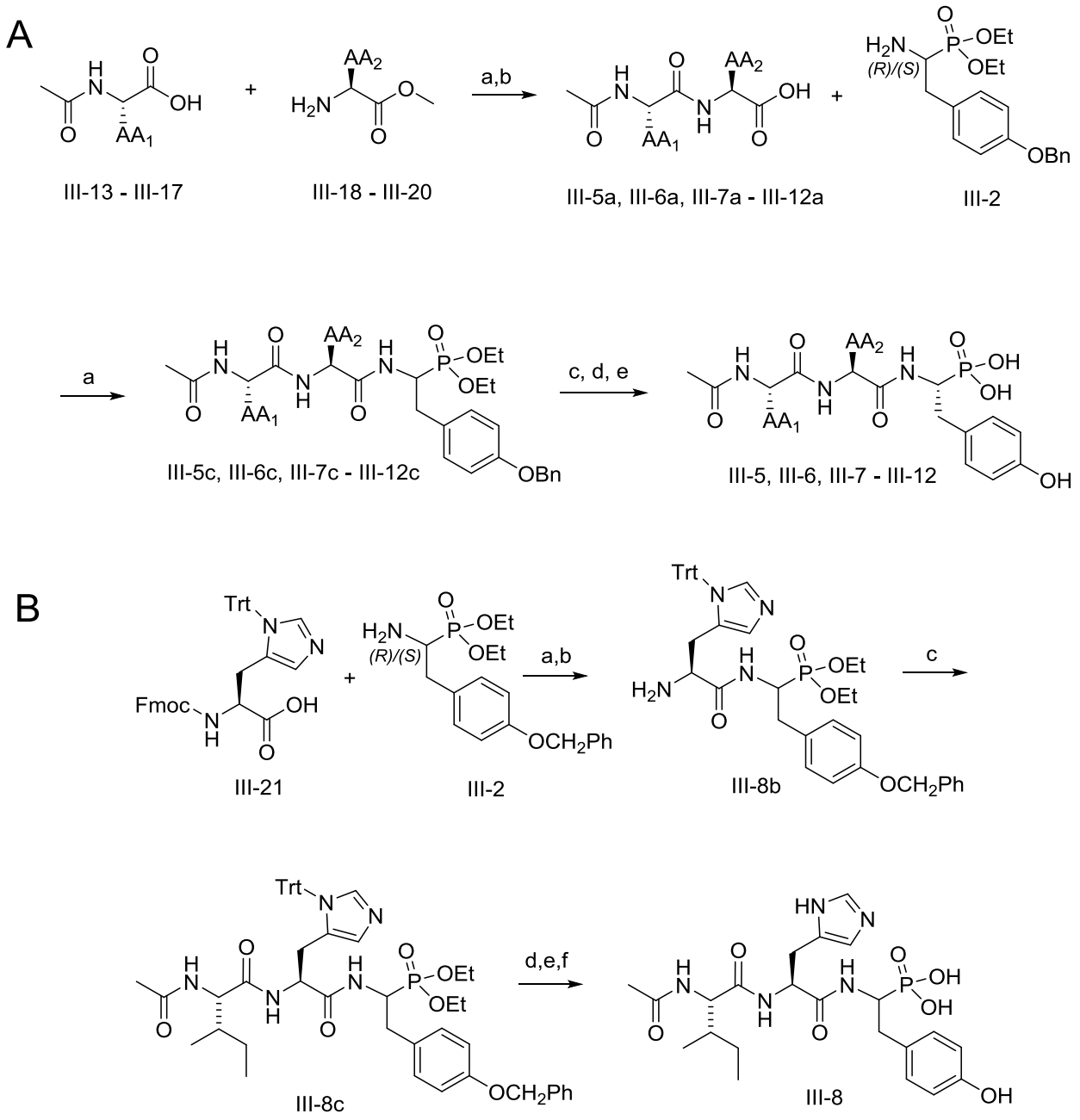

Scheme III-1. Chemical synthesis of K-26 variants. A. Reagents and conditions: (a) Method A. HOBt, EDC, 2,4,6-trimethylpyridine, DMF, 0°C for 1 hr, then rt overnight. (b) Method B. 5% NaOH, MeOH, rt, 2 hours. (c) Method A. 10% Pd/C, H_2, MeOH, rt overnight (d) Method F. TFA, DCM, rt, 30 min. (e) Method D. I-TMSi, thioanisole, CH_3CN, 0°C, 3 hours. Ac-Ile-Trp-AHEP (III-5): R_1 = Ile, R_2 = Trp, R_3 = Ile, R_4 = Trp. Ac-Ile-Ser-AHEP (III-6): R_1 = Ile, R_2 = Ser(OBzl), R_3 = Ile, R_4 = Ser. Ac-His-Ile-AHEP (III-7) R_1 = His(Trt), R_2 = Trp, R_3 = His, R_4 = Trp. Ac-Leu-Tyr-AHEP (III-9): R_1 = Leu, R_2 = Tyr(OBzl), R_3 = Leu, R_4 = Tyr. Ac-Leu-Ile-AHEP (III-10): R_1 = Leu, R_2 = Ile, R_3 = Leu, R_4 = Ile. Ac-Tyr-Ile-AHEP: R_1 = Tyr(tBu), R_2 = Ile, R_3 = Tyr, R_4 = Ile. Ac-Pro-Tyr-AHEP: R_1 = Pro, R_2 = Tyr(OBzl), R_3 = Pro, R_4 = Tyr. B. Reagents and conditions (a) Method A. HOBt, EDC, 2,4,6-trimethylpyridine, DMF, 0°C for 1 hr, then rt overnight. (b) Method E. TAEA, DCM, rt, 20 min. (c) Method A, N-Ac-Ile, HOBt, EDC, 2,4,6-trimethylpyridine, DMF, 0°C for 1 hr, then rt overnight. (d) Method C. 10% Pd/C, H_2, MeOH, rt overnight. (e) Method E. TFA, DCM, rt, 30 min. (f) Method D. I-TMSi, thioanisole, CH_3CN, 0°C, 3 hours.

Inhibitory activity of K-26 variants

Both diastereomers of the chemically synthesized K-26 family phosponotripeptides were initially assayed for mammalian ACE inhibition using the chromogenic substrate furylacryloyl-phenylalanyl-glycyl-glycine (FAPGG) and rabbit lung somatic ACE extract.[127-128] As previous studies suggest, diastereomers terminated by the naturally occurring (*R*)-AHEP amino acid are more potent than those terminated by *(S)*-AHEP, the most potent diastereomer was taken to contain the desired *(R)*-AHEP (Table III-1).[126-127]

K-26 Variant	IC_{50} (M)	
	(R)-AHEPdiastereomer	*(S)*-AHEP diastereomer
Ac-Ile-Trp-AHEP (III-5)	6.6×10^{-8}	2.8×10^{-7}
Ac-Ile-Ser-AHEP (III-6)	8.0×10^{-7}	4.1×10^{-6}
Ac-Ile-His-AHEP (III-7)	1.1×10^{-7}	5.2×10^{-6}
Ac-His-Trp-AHEP (III-8)	7.4×10^{-6}	8.2×10^{-6}
Ac-Leu-Tyr-AHEP (III-9)	1.3×10^{-6}	4.9×10^{-6}
Ac-Leu-Ile-AHEP (III-10)	4.5×10^{-5}	8.8×10^{-6}
Ac-Tyr-Ile-AHEP (III-11)	5.8×10^{-5}	1.2×10^{-4}
Ac-Pro-Tyr-AHEP (III-12)	7.3×10^{-7}	1.1×10^{-5}

Table III-1: Somatic ACE inhibition by both isolated diastereomers of the K-26 variants synthesized.

Correlation between Rosetta predictions and experimental measurements

Preliminary analysis was carried out correlating the experimental somatic ACE IC_{50} with the average of the $\Delta\Delta G_{predicted}$ for both the C-domain and the N-domain. The binding of the inhibitor to the enzyme can be given by the relationship $\Delta\Delta G = \Delta G_{bound} - \Delta G_{unbound}$. The ΔG_{bound} can be related to the K_i through the relationship $\Delta G_{bound} = RT \ln K_i$. where K_i is the inhibitory constant of the inhibitor enzyme complex. In our initial

analysis, the IC_{50} was used in place of the K_i as this value generally correlates well with the K_i when the enzyme is a potent inhibitor (Table III-2).[164]

K-26 Variant	IC_{50} Somatic ACE (M)	ΔΔGmeasured (kJ)	ΔΔGpredicted (kJ)		Average ΔΔGpredicted (kJ)
			C-domain ACE	N-domain ACE	
K-26 (III-1)	2.5×10^{-8}	-43.4	-16.8	-15.9	-16.35
SF2513B (III-3)	1.0×10^{-7}	-39.9	-13.4	-13.3	-13.35
SF2513C (III-4)	3.5×10^{-8}	-42.5	-17	-15.2	-16.1
Ac-Ile-Trp-AHEP (III-5)	6.6×10^{-8}	-41.1	-17.8	-16.5	-17.15
Ac-Ile-Ser-AHEP (III-6)	8.0×10^{-7}	-34.8	-13.7	-15.3	-14.5
Ac-Ile-His-AHEP (III-7)	1.1×10^{-7}	-39.7	-18.6	-15	-16.8
Ac-His-Trp-AHEP (III-8)	7.4×10^{-6}	-29.3	-16.8	-12.9	-14.85
Ac-Leu-Tyr-AHEP (III-9)	1.3×10^{-6}	-33.6	-16	-13.3	-14.65
Ac-Leu-Ile-AHEP (III-10)	4.5×10^{-5}	-24.8	-10.4	-9.9	-10.15
Ac-Tyr-Ile-AHEP (III-11)	5.8×10^{-5}	-24.2	-5.8	-2	-3.9
Ac-Pro-Tyr-AHEP (III-12)	7.3×10^{-7}	-35.0	-16.9	-14.7	-15.8

Table III-2. Measured IC_{50} values for each synthetic K-26 variant with somatic ACE and the corresponding $\Delta\Delta G_{predicted}$ and $\Delta\Delta G_{experimental}$ values. IC_{50} values for K-26 (III-1), SF 2513B (III-3) and SF 2513C (III-4) were published in Kramer et al.[126]

The average of the ΔΔG value predicted for each domain by Rosetta and the ΔΔG values calculated from our experimentally measured IC_{50} values for somatic ACE

inhibition were plotted to visualize a correlation between the data sets. These data sets do have a linear relationship with a $R^2 = 0.6184$ (Figure III-5).

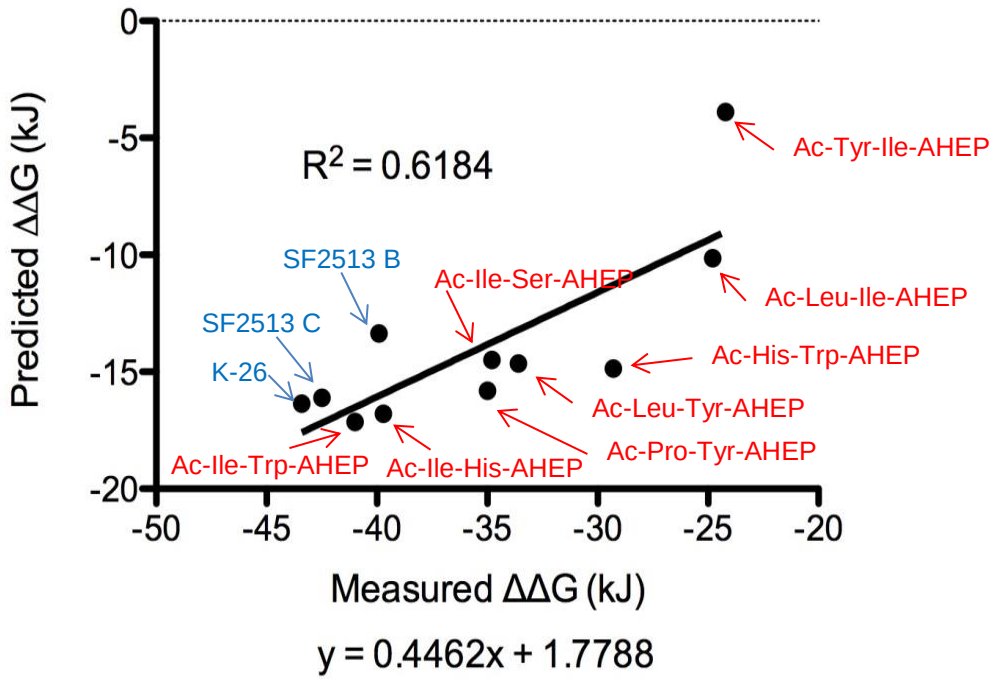

Figure III-5. Correlation plot of $\Delta\Delta G_{predicted\ and}$ $\Delta\Delta G_{measured}$ calculated from the experimental IC_{50} of each variant with somatic ACE. Natural product K-26 variants are shown in blue. Synthetic predicted variants are shown in red.

Discussion

In this study we describe the application of the computational modeling program Rosetta to predict binding affinities of a set of K-26 ACE inhibitor variants. Natural products in the K-26 family are among the most potent naturally occurring inhibitors of the two domain human enzyme of pharmacological relevance, ACE. As K-26 (III-1) has been shown in previous studies to exhibit an unusual binding mode in the active site of ACE, this molecule and variants are of interest in ACE inhibitor design. The solution phase synthesis of K-26 (III-1) and other AHEP (III-2) containing molecules is low

yielding and the final purification and identification of the resulting diastereomers is difficult making AHEP containing peptides a poor candidate for the generation of a large library of synthetic variants for structural activity relationship studies. However, as K-26 is a modified peptide, generation of an *in silico* library of variants is reasonable. As crystal structures are available for the natural product K-26 in both domains of ACE, this system an ideal candidate for a computational binding study.

Generating K-26 *in silico* was met with challenges. When docking the inhibitor into the active site of ACE it became necessary to fix both the backbone and the zinc in order to output a reasonable structure to emulate the crystal structure of this small molecule in ACE. Due to these constraints, all variants studied were generated using the fixed K-26 backbone with variation and full flexibility in the sidechains of the amino acids.

The Rosetta energy function was used to calculate the binding energy for the 400 variants of interest in both domains of ACE, with a small set of variants being selected for synthesis and further study. When selecting variants, we opted to choose not only variants that were predicted to be the most potent binders or particularly domain selective, but sampled molecules from across the spectrum of predicted binding energies to validate the ability of Rosetta to predict the specific activity of our inhibitors. Furthermore, when selecting variants for study, the rational analysis of structure of K-26 variant in the active site of ACE was important especially as the Rosetta energy function has known inaccuracies in the electrostatic portion of the analysis, which manifests itself particularly in poor handling of charged amino acids.[165] As a result, we also relied on

structural information to decide what analogs to select for further study, rather than simply using the Rosetta $\Delta\Delta G_{predicted}$.

The naturally occurring K-26 (III-1) was returned from our analysis as one of the most potent binders of all of the 400 variants studied, an interesting finding as this highlights the naturally occurring affinity of this microbially produced molecule for human ACE. However, several other analogs were predicted to have nearly comparable binding energies to the K-26 (III-1). These variants include another natural product from the K-26 family, SF2513C (III-4), along with the synthetic variants Ac-Ile-Trp-AHEP (III-5) and Ac-Ile-His-AHEP (III-7). Inhibition assays with somatic ACE have placed these inhibitors as the most potent of the variants tested suggesting the importance of the isoleucine residue in the AA_1 position and an aromatic residue present in the AA_2 position of the inhibitor. The AA_1 isoleucine fits comfortably in the binding pocket of the enzyme alongside Trp 357 (Trp 335 in N-domain), whereas the aromatic residues in the AA_2 position may have potential interactions with His 410 (His 388 in N-domain).

The variants with predicted poor binding, Ac-Leu-Ile-AHEP (III-10) and Ac-Tyr-Ile-AHEP (III-11) were also found to be the worst inhibitors based on assays with somatic ACE. Interestingly, these poor inhibitors are isomers of the natural products K-26 (III-1) and SF 2513BB (III-3) with sidechains of the residues in the AA_1 and AA_2 position reversed. The leucine and tyrosine present in the AA_1 position crowds the binding pocket where the AA_1 sidechain typically resides. The AA_2 isoleucine also crowds the binding pocket and has no favorable interactions with the histidine present suggesting that these poor steric interactions must be responsible for the lower affinity of these inhibitors (III-10 and III-11) compared to the native K-26 (III-1).

The variant with the constrained side chain residue in AA_1, Ac-Pro-Tyr-AHEP (III-12) although an unusual choice for an inhibitor, fits well in the binding pocket of the enzyme. The N-acetyl group is able to form important hydrogen bonds with the backbone of Asp 358 (Asp 336 in N-domain) while the Pro side chain occupies the binding pocket without a negative steric effect.

Analysis of the experimentally measured IC_{50} and correlation with the $\Delta\Delta G_{predicted}$ reveals a trendline describing the relationship between these two terms. That this trendline has an $R^2 = 0.6148$ is promising in that the binding energy function of Rosetta is effective at predicting the binding energy that would be measured from inhibition assays and therefore the K_i of the variant of interest. To confirm these results and to delve into the domain selective potential of these inhibitors, further analysis will be carried out using the inhibition constant (K_i) of each domain of ACE by the synthetic variants. After optimization of the Rosetta energy function for our data set, the validity of the Rosetta binding energy predictions for the determination of the binding affinity of the K-26 variants specifically in each of the individual domains of ACE will be evaluated.

Herein is described an interesting medicinal chemistry application of Rosetta. Variants of the K-26 family of natural products, with known potent activity towards the human pharmacological target, ACE, are computationally analyzed for binding energy. A handful of these peptide variants are synthesized and assayed for ACE inhibitory activity. The Rosetta predicted binding energy is shown to correlate with our experimental inhibition measurements showing promise for this type of approach in pharmacological inhibitor development.

Materials and Methods

Rosetta prediction of binding energy for K-26 variants

The coordinates of both tACE and the N-domain of ACE containing K-26 were obtained from the Protein Data Bank (PDB ID 4BZR, 4BZS). A collection of energy minimized structures were generated for both domains of ACE in the absence of K-26 using a protocol analogous to the Rosetta relax protocol. All side chains were repacked and minimized with backbone minimization in the immediate vicinity of the k26 binding site. Restraints were imposed on the zinc and zinc-coordinating residues to maintain the appropriate geometry and positioning of the metal binding site during minimization. The top model by score out of 100 models was carried forward.

A set of 400 K-26 variants were chosen for study. To model these variants, AHEP was generated as a non-canonical amino acid with a corresponding modification to the existing Rosetta code to accept non-canonical aminophosphonic acid residues.[166] Idealized internal coordinates for AHEP were established by minimization of N-acetyl, phosphonoxymethylated AHEP derived from k26 crystallized in tACE using the MMFF94x forcefield. Parameters, such as partial charge, for phosphonate atoms were approximated based on parameters for phosphate. All changes to the code and database are part of the current Rosetta repository. Experiments reported here were performed with revision 55456.

Coordinates for backbone and AHEP atoms of the co-crystallized k26 were transferred into the minimized enzyme to form the backbone of each tripeptide variant. First and second-shell side chains were repacked and minimized along with backbone atoms in the immediate vicinity of the tripeptide, as with the apo-enzyme. Models were scored

with the talaris2013 scoring function[163] and binding energies were calculated as the difference in energy between the tripeptide bound and unbound models ($\Delta\Delta G=\Delta G_{bound}-\Delta G_{unbound}$). Reported values are the average of the top ten binding energies from 25-50 models for each variant.

Chemical synthesis of variants

General synthesis.

Reactions were carried out in oven or flame dried glassware. All solvents were reagent grade. Amino acids and peptide coupling agents were purchased from EMD or Bachem. All reagents were commercially available and used without purification unless specified otherwise. AHEP (III-2) was synthesized as previously described.[127] HPLC purification was carried out using a Phenomonex C_{18} semi-preparative HPLC column on a Waters instrument using a flow rate of 5 mL/min. The purified analogs were tested for somatic ACE inhibitory activity using the substrate FAPGG using the described method. The most potent inhibitor was taken to be the desired (*R*)-diastereomer. All analogs were characterized by NMR and HRMS and quantitated, prior to inhibition studies, using an attenuated time delay proton NMR experiment (relaxation d_1 = 15 s) with dioxane or dimethylformamide added as an internal standard. NMR spectra were acquired on a Brucker AV-400, or AV-II-600 instrument. NMR spectra of synthetic intermediates and analogs are available in Appendix D.

Method A: Peptide Coupling[125, 127, 137]

The corresponding amino acids or peptides were dissolved in dimethylformamide (DMF) with N-hydroxybenzotriazole (HOBt) and the reaction mixture was cooled to 0 ^{o}C. Under inert atmosphere, 1-ethyl-3(3'-dimethylaminopropyl)carbodiimide hydrochloride (EDC) and 2,4,6-trimethylpyridine were added and the reaction was allowed to proceed for 1 hour at 0 ^{o}C and then overnight at room temperature. The reaction was dissolved in ethyl acetate and extracted with citric acid solution, 1N $NaHCO_3$, and brine. The organic layer was then dried over $MgSO_4$, and concentrated to give the desired product.

Method B: Saponification[167]

The corresponding dipeptide methyl ester was dissolved in methanol. Sodium hydroxide solution was added (5% w/v) and the reaction was stirred at room temperature for 2 hours. After evaporation of the solution, the residue was dissolved in ethyl acetate and washed with citric acid (2 x 20 mL), water (1 x 20 mL) and brine (1 x 20 mL). The organic layer was dried over $MgSO_4$ and concentrated to give the desired product.

Method C: Hydrogenation.[125]

The corresponding tripeptide and palladium on activated carbon (Pd/C) were combined in anhydrous methanol and allowed to stir overnight under 1atm hydrogen gas. After filtering through Celite, the filtrate was evaporated to give the product.

Method D: Phosphonate Deprotection.[127, 138]

The corresponding ethyl phosphonate was dissolved in anhydrous acetonitrile and thioanisole at 0 ^{o}C. Iodotrimethyl silane (I-TMSi) was added dropwise, and the reaction was allowed to proceed for 3 hours at 0 ^{o}C, after which the solvent was removed under vacuum to give a brown oily residue of the phosphonate trimethylsilyl ester. After hydrolysis of the trimethylsilyl ester, the solvent was evaporated and residue was redissolved in methanol ant the product was purified via preparative HPLC.

Method E: Fmoc Deprotection.[139]

The corresponding Fmoc protected dipeptide was dissolved in anhydrous DCM (5 mL) and under inert atmosphere tris(2-aminoethyl)amine (TAEA) (3.5 mL) was added dropwise. The reaction was allowed to stir for 30 minutes at room temperature then was dissolved in additional DCM, washed with brine and phosphate buffer (pH 5.5). The aqueous portion was collected and back extracted with additional DCM. The organic layers were pooled, dried over $MgSO_4$ and concentrated to give the product.

Method F: Acid Labile Protecting Group Deprotection.[140]

The corresponding protected peptide was dissolved in DCM (5 mL) and trifluoroacetic acid (TFA) (5 mL). The reaction was stirred for 30 minutes at room temperature and the solvent was removed in vaccuo to give the product.

N-acetyl-L-isoleucyl- L-tryptophan methyl ester (III-5a).

Synthesized using N-Ac-L-isoleucine-OH, III-13 (112 mg, 0.65 mmol), L-tryptophan methyl ester hydrochloride, III-18 (135 mg, 0.62 mmol), HOBt (104 mg, 0.68 mmol), EDC (130 mg, 0.68mmol) and 2,4,6-trimethylpyridine (172 μL, 1.3 mmol) in DMF (6 mL) using method A. White solid. Yield: 175 mg, 76%. Rotamers. ^{1}H NMR (400 MHz, $CDCl_3$) δ8.31 (s, 1H), 7.55-7.50 (m, 1H), 7.37-7.32 (m, 1H), 7.21-7.09 (m, 2H), 7.01 (d, *J* = 1.9Hz, 1H), 6.51 (s, 1H), 6.23 (s, 0.7H), 6.04 (s 0.3H), 4.94-4.87 (m, 1H), 4.43 (dd, *J* = 8.8, 5.5 Hz, 0.3 H), 4.30 (t, *J* = 7.8 Hz. 0.7 H), 3.68 (s, 3H), 3.31 (t, *J* = 5.3 Hz, 2H), 1.95 (s, 2H), 1.93 (s, 1H), 1.83-1.73 (m, 1H), 1.51-1.40 (m, 1H), 1.31-1.25 (m, 1H), 0.93-0.71 (m, 6H); ^{13}C NMR (100 MHz, $CDCl_3$) δ171.88, 170.99, 170.11, 136.12, 127.36, 123.24, 122.20, 119.65, 118.39, 111.33, 109.36, 57.60, 52.66, 52.37, 37.46, 27.48, 24.89, 23.14, 15.16, 11.26.

N-acetyl-L-isoleucyl- L-tryptophan (III-5b).

Synthesized using N-acetyl-L-isoleucyl- L-tryptophan methyl ester III-5a (170 mg, 0.46 mmol), methanol (16 mL) and 5% NaOH (4 mL) using method B. White solid. Yield: 108 mg, 65%. Rotamers. ^{1}H NMR (400 MHz, $CDCl_3$) δ7.54 (d, *J* = 7.9 Hz, 1H), 7.29 (d, *J* = 8.1 Hz, 1H), 7.09-6.96 (m, 3H), 4.70 (dd, *J* = 7.9, 5.1 Hz, 1H), 4.34 (d, *J* = 5.6 Hz, 0.2H), 4.19 (d, *J* = 8.0 Hz, 0.8H), 3.35-3.27 (m, 1H), 3.19-3.12 (m, 1H), 1.90 (s, 2.4H), 1.89 (s, 0.6H), 1.79-1.67 (m, 1H), 1.51-1.38 (m, 1H), 1.14-1.01 (m, 1H), 0.89-0.78 (m, 6H); ^{13}C NMR (100 MHz, $CDCl_3$) δ174.96, 173.58, 173.20, 137.93, 128.76, 124.60, 122.32, 119.81, 119.20, 112.19, 110.72, 59.16, 54.42, 37.93, 28.45, 25.77, 22.41, 15.73, 11.29.

Diethyl N-(N-acetyl-L-isoleucyl-L-tryptophanyl)-1-amino-2-(4-benzyloxyphenyl)ethyl phosphonate (III-5c)

Synthesized using N-acetyl-L-isoleucyl- L-tryptophan III-5b (200 mg, 0.56 mmol), AHEP III-2 (188 mg, 0.52 mmol), HOBt (90 mg, 0.59 mmol), EDC (113 mg, 0.59 mmol) and 2,4,6-trimethylpyridine (146 μL, 1.1 mmol) in DMF (6 mL) using method A to give a mixture of diastereomers. Tan foam. Yield: 190 mg, 48%. ^{1}H NMR (400 MHz, $CDCl_3$) δ7.46-7.19 (m, 7H), 7.18-6.47 (m, 3H), 6.48-6.76 (m, 2H), 6.78-6.68 (m, 2H), 5.04-4.98 (m, 1H), 4.86-4.84 (m, 1H), 4.83-4.57 (m, 2H), 4.55-4.47 (m, 1H), 4.21-4.03 (m, 4H), 3.85-3.71 (m, 0.5H), 3.30-3.05 (m, 1.5H), 3.02-2.73 (m, 2H), 2.06-1.93 (m, 3H), 1.83-1.62 (m, 1H), 1.44-1.24 (m, 7H), 1.13-0.67 (m, 7H); ^{13}C NMR (400 MHz, $CDCl_3$) δ172.41-171.76, 171.60-171.12, 170.89-170.60, 157.72-157.40, 137.05-136.91, 136.04-135.97, 130.36, 130.16-130.03, 129.42-129.29, 128.79-128.65, 128.48-128.34, 127.85-127.73, 127.41-127.31, 123.61, 121.28, 118.84, 117.98, 115.04-114.59, 111.19, 109.78-109.42, 69.88-69.72, 63.37-62.19, 57.77-57.62, 53.62-52.94, 47.78-44.06, 37.54-37.35, 34.96-34.41, 28.17-27.92, 25.08, 22.70-22.64, 16.35-16.17, 15.25-15.15, 11.25-11.12; ^{31}P NMR (162 MHz, D_2O) δ25.25, 25.11.

Diethyl N-(N-acetyl-L-isoleucyl-L-tryptophanyl)-1-amino-2-(4-hydoxyphenyl)ethyl phosphonate (III-5d)

Synthesized using diethyl N-(N-acetyl-L-isoleucyl-L-tryptophanyl)-1-amino-2-(4-benzyloxyphenyl)ethyl phosphonate III-5c (150 mg, 0.26 mmol), Pd/C (10% Pd, 15 mg) in methanol (5 mL) using method C, to yield a mixture of diastereomers. Yellowish oil. Yield: 126 mg, 81.0%. ^{1}H NMR (600 MHz, MeOD) δ 7.87 (dd, *J* = 19.6, 8.5 Hz, 1H),

7.56 (dd, *J* = 34.2, 7.7, 1H), 7.33 (dd, *J* = 13.6, 8.2 Hz, 1H), 7.14-7.04 (m, 3H), 6.93-6.89 (m, 1H), 6.76-6.70 (m, 2H), 4.79-4.71 (m, 1H), 4.63-4.52 (m, 1H), 4.21-3.99 (m, 5H), 3.23-3.19 (m, 0.5H), 3.15-3.06 (m, 1H), 3.01-2.96 (m, 0.5H), 2.94-2.88 (m, 0.5H), 2.84-2.72 (m, 1.5H), 2.01-1.92 (m, 3H), 1.74-1.67 (m, 0.5H), 1.59-1.50 (m, 0.5H), 1.40-1.25 (m, 7H), 1.10-1.02 (0.5H), 0.97-0.88 (m, 0.5H), 0.86-0.70 (m, 6H); ^{13}C NMR (150 MHz, MeOD) δ173.99-173.50, 173.43-173.31, 173.25-173.18, 157.36-157.21, 138.07-137.82, 131.31, 131.12-130.95, 128.99-128.66, 124.73-124.37, 122.37-122.26, 119.80-119.72, 119.32-119.21, 116.27-116.19, 112.23-112.11, 110.78-110.62, 64.20-64.03, 59.52, 59.44, 54.93, 54.83, 48.11, 47.84, 37.71-37.64, 35.20-35.04, 29.20-28.76, 25.81-25.71, 22.46, 22.42, 16.83-16.68, 15.80, 11.39; ^{31}P NMR (162 MHz, MeOD) δ25.13, 24.55.

Ac-Ile-Trp-AHEP: N-(N-acetyl-L-isoleucyl-L-tryptophanyl)-1-amino-2-(4-hydoxyphenyl)ethyl phosphonic acid (III-5)

Synthesized using diethyl N-(N-acetyl-L-isoleucyl-L-tryptophanyl)-1-amino-2-(4-hydoxyphenyl)ethyl phosphonate III-5d (32mg, 0.052 mmol), acetonitrile (6 mL), thioanisole (0.6 mL) and I-TMSi (3.0 mL) using method D. The phosphonate trimethylsilyl ester was hydrolyzed by treatment with 8:2 methanol in water (30 mL). Purified by HPLC, using a gradient of 5% acetonitrile in water to 25% acetonitrile in water containing ammonium acetate (10 mM) over 30 minutes. White solid. Yield: 2.1 mg, 7.2%. ^{1}H NMR (600 MHz, D_2O) δ7.67 (d, *J* = 8.0 Hz, 1H), 7.48 (d, *J* = 8.2 Hz, 1H), 7.24 (t, 7.5 Hz, 1H), 7.16 (s, 2H), 7.14 (d, *J* = 8.5 Hz, 2H), 6.78 (d, *J* = 8.46 Hz, 2H), 4.70 (dd, *J* = 9.8, 4.5 Hz, 1H), 4.28-4.22 (m, 1H), 3.92 (d, *J* = 7.9 Hz, 1H), 3.42 (dd, *J* =

14.9, 4.5 Hz, 1H), 3.22-3.17 (m, 1H), 2.95 (dd, *J* = 14.9, 9.8 Hz, 1H), 2.69 (dt, *J* = 12.7, 6.5 Hz, 1H), 1.90 (s, 3H), 1.58-1.50 (m, 1H), 1.16-1.09 (m, 1H), 0.94-0.85 (m, 1H), 0.73 (t, *J* = 7.3 Hz, 3H), 0.56 (d, *J* = 6.78 Hz, 3H); ^{13}C NMR (150 MHz, D_2O) δ173.53, 172.32, 171.92, 153.70, 135.84, 130.17, 130.00-129.90, 126.71, 124.28, 121.57, 119.03, 118.17, 114.93, 111.53, 109.02, 58.10, 53.39, 50.42, 49.45, 35.91, 34.64, 27.35, 24.02, 21.42, 14.21, 9.99; ^{31}P NMR (162 MHz, D_2O) δ18.65.

N-acetyl-L-isoleucyl-O-benzyl-L-serine methyl ester (III-6a)

Synthesized using N-Ac-L-isoleucine-OH III-13 (112 mg, 0.65 mmol), L-serine-O-benzyl methyl ester hydrochloride III-19 (152 mg, 0.62 mmol), HOBt (104.1 mg, 0.68 mmol), EDC (130.4 mg, 0.68 mmol) and 2,4,6-trimethylpyridine (172 µL, 1.30 mmol) in DMF (6 mL) using method A. White solid. Yield: 177 mg, 78.4%. ^{1}H NMR (400 MHz, $CDCl_3$) δ 7.35-7.24 (m, 5H), 6.81 (d, *J* = 8.2 Hz, 1H), 6.41 (d, *J* = 8.7 Hz, 1H), 4.75-4.70 (m, 1H), 4.55-4.40 (m, 3H), 3.90-3.84 (m, 1H), 3.73 (s, 3H), 3.67-3.61 (m, 1H), 1.99 (s, 3H), 1.88-1.78 (m, 1H), 1.56-1.49 (m, 1H), 1.27-1.06 (m, 1H), 0.96-0.85 (m, 6H); ^{13}C NMR (100 MHz, $CDCl_3$) δ 171.19, 170,26, 169.86, 137.28, 128.40, 127.85, 127.61, 73.20, 69.26, 57.39, 52.46, 52.43, 37.88, 24.89, 23.10, 15.06, 11.33.

N-acetyl-L-isoleucyl- O-benzyl-L-serine (III-6b)

Synthesized using N-acetyl-L-isoleucyl- O-benzyl-L-serine methyl ester III-6a (150 mg, 0.41 mmol), methanol (16 mL) and 5% NaOH (4 mL) using method B. White solid. Yield: 105mg, 70%. ^{1}H NMR (400 MHz, MeOD) δ 8.65 (d, *J* = 7.7 Hz, 1H) 8.30 (d, *J* = 9.1 Hz, 1H), 7.78-7.67 (m, 5H), 4.93-4.85 (m, 3H), 4.72 (dd, *J* = 9.0, 7.5 Hz, 1H),

4.15 (dd, *J* = 9.8, 5.8 Hz, 1H), 4.06 (dd, J 9.8, 4.2 Hz, 1H), 2.26 (s, 3H), 2.16-2.07 (m, 1H), 1.89-1.78 (m, 1H), 1.56-1.43 (m, 1H), 1.29-1.78 (m, 6H); ^{13}C NMR (100 MHz, MeOD) δ 171.37, 171.33, 169.02, 138.01, 128.19, 127.52, 127.46, 72.13, 69.31, 56.42, 52.25, 36.84, 24.22, 22.47, 15.24, 11.04.

Diethyl N-(N-acetyl-L-isoleucyl-O-benzyl-L-serinyl)-1-amino-2-(4-benzyloxyphenyl)ethyl phosphonate (III-6c)

Synthesized using N-acetyl-L-isoleucyl-O-benzyl-L-serine III-6b (80 mg, 0.23 mmol), AHEP III-2 (80 mg, 0.22 mmol), HOBt (37 mg, 0.24 mmol), EDC (45 mg, 0.24 mmol) and 2,4,6-trimethylpyridine (64 μL, 0.48 mmol) in DMF (3 mL) using method A to give a mixture of diastereomers. Clear oil. Yield: 117 mg, 74%. ^{1}H NMR (600 MHz, $CDCl_3$) δ7.45-7.18 (m, 1H), 7.16-7.01 (m, 2H), 6.90-6.72 (m, 2H), 5.97-4.89 (m, 2H), 4.80-4.71 (m, 0.5H), 4.71-4.58 (m, 1.5H), 4.45-4.24 (m, 2.5H), 4.23-3.94 (m, 4.5H), 3.81-3.74 (m, 0.5H), 3.73-3.65 (m, 0.5H), 3.59-3.47 (m, 1H), 3.22-3.07 (m, 1H), 2.96-2.73 (m, 1H), 2.09-1.97 (m, 3H), 1.89-1.73 (m, 1H), 1.59-1.39 (m, 1H), 1.37-1.04 (m, 8.5H), 0.97-0.79 (m, 4.5H); ^{13}C NMR (150 MHz, $CDCl_3$) δ 171.48-171.19, 170.36, 169.20-169.04, 157.52, 137.36, 137.35, 136.99, 136.91, 130.11, 130.03, 129.20-129.06, 128.97, 128.84, 128.44, 128.42, 128.36, 127.82-127.68, 127.49, 127.39, 127.37, 127.33, 114.63, 114.57, 73.17, 73.02, 69.79, 69.74, 69.09, 63.10-62.21, 58.31, 57.74, 52.83, 52.40, 47.91, 47.44, 46.36, 45.89, 37.49, 36.52, 34.68-34.37, 25.05, 22.94, 22.92, 16.42-16.25, 15.31, 15.22, 11.27, 11.05; ^{31}P NMR (162 MHz, $CDCl_3$) δ 24.88, 24.80, 23.69.

Diethyl N-(N-acetyl-L-isoleucyl-L-serinyl)-1-amino-2-(4-hydoxyphenyl)ethyl phosphonate (III-6d)

Synthesized using diethyl N-(N-acetyl-L-isoleucyl-L-serinyl)-1-amino-2-(4-benzyloxyphenyl)ethyl phosphonate III-6c (110 mg, 0.16 mmol), Pd/C (10% Pd, 13 mg) in methanol (4 mL) using method C, to yield a mixture of diastereomers. Clear oil. Yield: 69 mg, 81.0%. ^{1}H NMR (600 MHz, MeOD) δ7.08-7.00 (m, 2H), 6.71-6.65 (m, 2H), 4.59-4.35 (m, 2H), 4.20-4.06 (m, 5H), 3.71-3.40 (m, 2H), 3.15-3.02 (m, 1H), 2.92-2.74 (m, 1H), 2.05-1.96 (m, 3H), 1.91-1.72 (m, 1H), 1.62-1.42 (m, 1H), 1.35-1.26 (m, 6H), 1.26-1.11 (m, 1H), 0.96-0.80 (m, 6H). ^{13}C NMR (150 MHz, MeOD) δ174.06, 173.51, 171.59, 157.20, 131.11, 130.98, 129.08-128.74, 116.15, 64.52-64.15, 63.28-62.81, 59.86-59.58, 56.65-56.31, 38.09-37.28, 35.12-34.99, 27.10-27.05, 26.15-25.91, 24.18, 22.49, 16.84-16.66, 15.92-15.73, 11.48-11.27; ^{31}P NMR (162 MHz, MeOD) δ 25.36.

Ac-Ile-Ser-AHEP: N-(N-acetyl-L-isoleucyl-L-serinyl)-1-amino-2-(4-hydoxyphenyl)ethyl phosphonic acid (III-6)

Synthesized using diethyl N-(N-acetyl-L-isoleucyl-L-serinyl)-1-amino-2-(4-hydoxyphenyl)ethyl phosphonate III-6d (25 mg, 0.049 mmol), acetonitrile (6 mL), thioanisole (0.6 mL) and I-TMSi (3.0 mL) using method D. The phosphonate trimethylsilyl ester was hydrolyzed by treatment with 8:2 methanol in water (30 mL). Purified by HPLC, using a gradient of 5% acetonitrile in water to 25% acetonitrile in water containing ammonium acetate (10 mM) over 30 minutes. White solid. Yield: 2.8 mg, 12%. ^{1}H NMR (600 MHz, D_2O) δ7.14 (d, *J* = 8.5 Hz, 2H), 6.77 (d, *J* = 8.5 Hz, 2H), 4.48 (t, *J* = 5.5 Hz, 1H), 4.22-4.16 (m, 1H). 4.08 (d, *J* = 7.9 Hz, 1H), 3.78-3.70 (m, 2H),

2.66 (dt, *J* = 13.8, 6.3 Hz 1H), 2.30 (s, 3H) 1.73-1.68 (m, 1H), 1.42-1.37 (m, 1H), 1.13-1.06 (m, 1H), 0.84 (t, *J* = 7.4, 3H), 0.68 (d, *J* = 6.8 Hz, 3H); ^{13}C NMR (150 MHz, D2O) δ 173.94, 172.75, 169.78, 153.63, 130.10, 114.88, 61.58, 58.13, 54.50, 50.70, 49.72, 36.08, 34.62, 24.43, 21, 37, 14.32, 9.97; ^{31}P NMR (162 MHz, D2O) δ18.64.

Diethyl N-(N-fluorenylmethyloxycarbonyl-τ-trityl-L-histadyl-)-1-amino-2-(4-benzyloxyphenyl)ethyl phosphonate (III-7a)

Synthesized using N-(N- N-fluorenylmethyloxycarbonyl-τ-trityl-L-histadine) III-21 (150 mg, 0.27 mmol), AHEP III-2 (100 mg, 0.28 mmol), HOBt (44 mg, 0.28 mmol), EDC (55 mg, 0.28 mmol) and 2,4,6-trimethylpyridine (71 μL, 0.53 mmol) in DMF (3 mL) using method A to give a mixture of diastereomers. Tan foam. Yield: 117 mg, 85%. ^{1}H NMR (600 MHz, $CDCl_3$) δ7.76 (d, *J* = 7.6 Hz, 2H), 7.62-7.58 (m, 2H), 7.44-7.26 (m, 19H), 7.19-7.07 (m, 8H), 6.88-6.84 (m, 1H), 6.78 (d, *J* = 8.2 Hz, 1H), 6.72 (s, 1H), 4.94 (s, 2H), 4.75-4.69 (m, 1H), 4.55-4.48 (m, 1H), 4.35-4.25 (m, 1H), 4.20-4.02 (m, 5H), 3.27-3.15 (m, 1H), 3.07-3.01 (m, 0.5H), 2.95-2.86 (m, 1.5H), 2.77-2.67 (m, 1H), 1.32-1.26 (m, 6H); ^{13}C NMR (150 MHz, $CDCl_3$) δ171.23-171.11, 157.64-157.52, 143.96-143.92, 142.24-142.11, 138.18-138.02, 137.09, 137.00-136.89, 130.37, 129.74, 128.59, 128.13-128.11, 127.93, 127.72-127.71, 127.49-127.39, 127.15-127.12, 125.29, 119.96, 119.52-119.36, 114.73-114.67, 75.49-75.48, 69.99-69.83, 67.18-67.04, 62.96-62.48, 55.46-54.57, 47.35-46.32, 34.04-33.75, 31.30-30.66, 16.54-16.40; ^{31}P NMR (162 MHz, $CDCl_3$) δ25.25, 25.11.

Diethyl N-(τ-trityl-L-histadyl-)-1-amino-2-(4-benzyloxyphenyl)ethyl phosphonate (III-7b)

Synthesized using diethyl N-(N-fluorenylmethyloxycarbonyl- τ-trityl-L-histadyl-)-1-amino-2-(4-benzyloxyphenyl)ethyl phosphonate III-7a (170 mg, 0.18 mmol) using method E to yield a mixture of diastereomers. Yellowish foam. Yield: 104 mg, 62%. ^{1}H NMR (600 MHz, $CDCl_3$) δ7.76-7.73 (m, 1H), 7.70-7.60 (m, 1H), 7.33-7.19 (m, 14H), 7.05-7.02 (m, 7H), 6.77 (d, J = 3.3 Hz, 2H), 6.52 (d, J = 6.3 Hz, 1H), 4.92-4.87 (m, 2H), 4.62-4.53 (m, 1H), 4.06-3.96 (m, 5H), 3.47-3.35 (m, 0.5H), 3.18-3.05 (m, 1H), 2.80-2.71 (m, 1H), 2.57-2.53 (m, 0.5H), 2.43-2.32 (m, 1H), 1.22-1.17 (m, 6H); ^{13}C NMR (150 MHz, $CDCl_3$) δ174.18-174.20, 157.68-157.65, 142.44, 138.70, 138.45, 137.15, 130.41, 130.30, 129.80, 129.31-129.03, 128.82-128.69, 128.62-128.61, 128.16, 127.99-127.96, 127.59-127.47, 127.14-127.13, 119.35-119.34, 114.85-114.79, 75.36-75.35, 70.06-70.03, 62.70-62.54, 55.89, 48.23-47.88, 46.74-46.52, 45.71-45.49, 35.10-34.89, 33.29-32.98, 16.62-16.47; ^{31}P NMR (162 MHz, $CDCl_3$) δ25.59, 25.50.

Diethyl N-(N-acetyl-L-isoleucyl-τ-trityl-L-histadyl)-1-amino-2-(4-benzyloxyphenyl)ethyl phosphonate (III-7c)

Synthesized using N-Ac-L-isoleucine-OH III-13 (41 mg, 0.23 mmol), diethyl N-(τ-trityl-L-histadyl-)-1-amino-2-(4-benzyloxyphenyl)ethyl phosphonate III-7b (190 mg, 0.26 mmol), HOBt (42 mg, 0.27 mmol), EDC (53 mg, 0.27 mmol) and 2,4,6-trimethylpyridine (71 µL, 0.53 mmol) in DMF (3 mL) using method A to yield a mixture of diastereomers.. White solid. Yield: 144 mg, 62%. ^{1}H NMR (600 MHz, $CDCl_3$) δ7.64-7.59 (m, 2H), 7.29-7.18 (m, 14H), 7.04-6.97 (m, 7H), 6.93 (d, *J* = 8.6 Hz, 1H), 6.74 (d, *J* = 8.5 Hz, 1H), 6.65 (d, *J* = 6.66, 1H), 4.87-4.84 (m, 2H), 4.57-4.49 (m, 2H), 4.29-4.25 (m, 1H), 4.05-3.96 (m,

4H), 3.09-2.99 (m, 1H), 2.85-2.65 (m, 2H), 2.59-2.42 (m, 1H), 1.86-1.85 (m, 3H), 1.80-1.70 (m, 1H), 1.38-1.26 (m, 1H), 1.19-1.11 (m, 6H), 1.07-0.97 (m, 1H), 0.77-0.73 (m, 6H); ^{13}C NMR (150 MHz, $CDCl_3$) δ171.26, 170.87-170.56, 170.47-170.17, 157.57-157.53, 142.23-142.16, 138.04-137.83, 137.13-137.10, 136.81-136.70, 130.38-130.28, 129.77-129.76, 129.44-129.26, 128.77, 128.61-128.53, 128.21-128.17, 127.89-127.87, 127.51-127.42, 127.09, 119.77-119.36, 114.66, 107.81, 75.54-75.50, 69.97-69.88, 62.87-62.43, 58.21-57.83, 53.69-52.87, 47.70-46.47, 37.73-37.37, 34.97-34.68, 30.59-29.39, 25.04-24.67, 23.21-23.18, 16.50-16.36, 15.56-15.34, 11.64-11.59.^{31}P NMR (162 MHz, $CDCl_3$) δ25.21, 24.94.

Diethyl N-(N-acetyl-L-isoleucyl-τ-trityl-L-histadyl)-1-amino-2-(4-hydoxyphenyl)ethyl phosphonate (III-7d)

Synthesized using diethyl N-(N-acetyl-L-isoleucyl-τ-trityl-L-histadyl)-1-amino-2-(4-benzyloxyphenyl)ethyl phosphonate III-7c (120 mg, 0.13 mmol), Pd/C (10% Pd, 13 mg) in methanol (4 mL) using method C, to yield a mixture of diastereomers. White solid. Yield: 81 mg, 75%.^{1}H NMR (600 MHz, MeOD) δ7.73 (d, *J* = 7.3 Hz, 1H), 7.49-6.89 (m, 17H), 6.75-6.66 (m, 1H), 6.48-6.45 (m, 1H), 4.80-4.70 (m, 1H), 4.56-4.35 (m, 1H), 4.23-3.98 (m, 5H), 3.23-3.01 (m, 1.5H), 3.01-2.92 (m, 1H), 2.86-2.70 (m, 1.5H), 2.02-1.86 (m, 3H), 1.79-1.70 (m, 1H), 1.59-1.42 (m, 1H), 1.36-1.13 (m, 7H), 0.92-0.88 (m, 6H); ^{13}C NMR (150 MHz, MeOD) δ171.13-171.04, 170.86-170.84, 170.30, 157.38-157.25, 140.31-141.26, 137.31-137.23, 134.85-134.69, 131.39-131.35, 131.04-130.94, 130.89-130.79, 130.37, 130.11, 129.87-129.71, 129.19, 128.70, 128.50, 127.96-127.88, 127.23, 124.99, 120.67, 116.32-116.04, 80.01, 64.41-64.23, 60.11-59.78, 57.92, 53.17-

52.80, 48.19, 37.32-37.02, 35.20-34.82, 29.27-29.01, 26.37-26.12, 22.50-22.43, 16.89-16.75, 15.86-15.78, 11.33-11.25; ^{31}P NMR (162 MHz, MeOD) δ24.26, 23.93, 23.82.

Ac-Ile-His-AHEP: N-(N-acetyl-L-isoleucyl-L-histadyl)-1-amino-2-(4-hydoxyphenyl)ethyl phosphonic acid (III-7)

Synthesized by first treating diethyl N-(N-acetyl-L-isoleucyl-τ-trityl-L-histadyl)-1-amino-2-(4-hydoxyphenyl)ethyl phosphonate III-7d (57mg, 0.071 mmol) with method F. The resulting residue was concentrated in vaccuo and without further purification or characterization was treated with acetonitrile (6 mL), thioanisole (0.6 mL) and I-TMSi (3.0 mL) using method D. The resulting phosphonate trimethylsilyl ester was hydrolyzed by treatment with 8:2 isopropanol in water (30 mL). Purified by HPLC, using a gradient of 5% acetonitrile in water to 25% acetonitrile in water containing formic acid (0.1%) over 30 minutes. White solid. Yield: 2.9 mg, 8.1%.^{1}H NMR (600 MHz, D_2O) δ7.62 (s, 1H), 7.12 (d, *J*= 8.3 Hz, 2H), 6.83 (s, 1H), 6.73 (d, *J* = 8.3 Hz, 2H), 4.61-4.59 (m, 1H), 4.09-4.00 (m, 2H), 3.18 (d, *J* = 14.3 Hz, 1H), 3.09 (dd, *J* = 15.1, 4.1 Hz, 1H), 2.99-2.55 (m, 1H), 2.62-2.55 (m, 2H), 2.01 (s, 3H), 1.72-1.67 (m, 1H), 1.32-1.26 (m, 1H), 1.08-1.01 (m, 1H), 0.81 (t, *J* = 7.4 Hz, 3H), 0.69 (d, *J* = 6.3 Hz, 3H); ^{13}C NMR (150 MHz, D_2O) δ173.94, 127.58, 171.01, 154.46, 136.33, 131.03-130.94, 130.52-130.44, 130.30, 115.54-115.30, 115.24, 58.50-58.34, 52.45, 52.05, 51.13, 36.01, 35.96, 30.20, 24.38, 21.59, 14.60, 10.15; ^{31}P NMR (162 MHz, D_2O) δ16.70.

N-acetyl-(τ-trityl-L-histadyl)-L-tryptophan methyl ester (III-8a)

Synthesized using N-acetyl-(τ-trityl-L-histadyl)-OH III-14 (285 mg, 0.65 mmol), L-tryptophan methyl ester hydrochloride III-18 (135 mg, 0.62 mmol), HOBt (104.1 mg, 0.68 mmol), EDC (130.4 mg, 0.68 mmol) and 2,4,6-trimethylpyridine (172 µL, 1.30 mmol) in DMF (6 mL) using method A. White solid. Yield: 287 mg, 73%. ^{1}H NMR (600 MHz, $CDCl_3$) δ7.46 (dd, *J* = 19.6, 7.8 Hz, 2H), 7.34-7.24 (m, 12H), 7.10-7.07 (m, 7H), 7.03 (t, *J* = 7.6 Hz, 1H) 6.95 (s, 1H), 6.63 (s, 1H), 4.84-4.81 (m, 1H), 4.73-4.70 (m, 1H), 3.51 (s, 3H), 3.27 (dd, *J* = 14.8, 5.6 Hz, 1H), 3.19 (dd, *J* = 14.8, 5.3 Hz, 1H), 2.98 (dd, *J* = 14.9, 5.9 Hz, 1H), 2.91 (dd, *J* = 14.7, 5.5 Hz, 1H), 1.76 (s, 3H); ^{13}C NMR (150 MHz, $CDCl_3$) δ172.17, 171.15, 170.45, 142.32, 138.28, 136.85, 136.17, 129.80, 128.12, 127.52, 123.55, 121.88, 119.85, 119.36, 118.52, 111.39, 109.47, 75.45, 53.26, 53.11, 52.25, 30.18, 27.52, 23.03.

N-acetyl-(τ-trityl-L-histadyl) -L-tryptophan (III-8b)

Synthesized using N-acetyl-(τ-trityl-L-histadyl)-L-tryptophan methyl ester III-8a (170 mg, 0.27 mmol), methanol (16 mL) and 5% NaOH (4 mL) using method B. White solid. Yield: 95 mg, 57%. Rotamers. ^{1}H NMR (600 MHz, MeOD) δ8.42 (s, 1H), 8.02 (dd, J = 22.5, 7.9 Hz, 0.5 H), 7.77 (dd, J = 22.4, 7.5 Hz, 0.5 H), 7.56 (d, J = 7.9 Hz, 1H), 7.45-7.30 (m, 12H), 7.18-6.99 (m, 9H), 4.74-4.66 (m, 2H), 3.40-3.35 (m, 1H), 3.24-3.10 (m, 2H), 2.96-2.90 (m, 1H), 1.85 (s, 3H); ^{13}C NMR (150 MHz, MeOD) δ175.57-175.22, 173.71-173.17, 171.77-171.69, 141.63, 137.99-137.62, 132.34, 130.64, 130.02, 129.85, 129.71, 129.16, 128.73, 128.69-128.61, 128.17-128.03, 124.79-124.64, 122.92-121.99,

120.62-119.19, 112.35-112.29, 110.63-110.58, 79.45, 54.86-54.78, 53.41-53.32, 30.75, 28.86-28.25, 22.61-22.57.

Diethyl N-(N-acetyl-(τ-trityl-L-histadyl) -L-tryptophanyl)-1-amino-2-(4-benzyloxyphenyl)ethyl phosphonate (III-8c)

Synthesized using N-acetyl-(τ-trityl-L-histadyl) -L-tryptophan III-8b (40 mg, 0.064 mmol), AHEP III-2 (22 mg, 0.062 mmol), HOBt (10 mg, 0.068 mmol), EDC (13 mg, 0.068 mmol) and 2,4,6-trimethylpyridine (17 μL, 0.13 mmol) in DMF (1 mL) using method A to give a mixture of diastereomers. Tan foam. Yield: 40 mg, 64%. ^{1}H NMR (600 MHz, $CDCl_3$) δ7.64-7.58 (m, 0.5H), 7.54-7.43 (m, 0.5H), 7.40-7.17 (m, 16H), 7.15-7.07 (m, 1H), 7.06-6.99 (m, 6H), 6.95-6.84 (m, 2H), 6.80-6.69 (m, 4H), 6.68-6.54 (m, 1H), 4.98 -4.83 (m, 2H), 4.70-4.59 (m, 1.5H), 4.36-4.24 (m, 0.5H), 4.06-3.89 (m, 5H), 3.20-3.16 (m, 1H), 3.10-2.92 (m, 2H), 2.88-2.61 (m, 3H), 1.78 (s, 1.5H), 1.40 (s, 1.5H), 1.23-1.11 (m, 6H); ^{13}C NMR (150 MHz, $CDCl_3$) δ712.93-172.70, 172.31, 171.80-171.76, 159.73-159.62, 159.13, 144.13, 140.53, 139.03-139.00, 138.33-137.68, 132.19-123.07, 131.66, 130.72-130.71, 130.54-130.50, 130.21-130.14, 129.90-129.74, 129.47, 129.09-129.05, 128.89, 126.13-125.72, 123.89-123.73, 122.99, 122.12-121.36, 120.36-120.11, 116.81-116.75, 113.33-113.27, 110.68, 109.79, 77.51, 72.18-71.94, 65.08-64.39, 62.39, 56.32-55.87, 49.63-47.70, 36.71-35.59, 31.67-31.08, 28.12, 24.79-23.03, 18.51-18.39; ^{31}P NMR (162 MHz, $CDCl_3$) δ25.74, 25.33, 24.92, 24.82.

Ac-His-Trp-AHEP: N-(N-acetyl-L-histadyl-L-tryptophanyl)-1-amino-2-(4-hydoxyphenyl)ethyl phosphonic acid (III-8)

Synthesized by first treating diethyl N-(N-acetyl-(τ-trityl-L-histadyl) -L-tryptophanyl)-1-amino-2-(4-benzyloxyphenyl)ethyl phosphonate (III-8c) (35mg, 0.036 mmol) with Pd/C (10% Pd, 13 mg) in methanol (4 mL) using method C followed by method F without purification of characterization of the intermediates. The resulting residue was treated with acetonitrile (2 mL), thioanisole (0.2 mL) and I-TMSi (1.0 mL) using method D. The phosphonate trimethylsilyl ester was hydrolyzed by treatment with 8:2 isopropanol in water (30 mL). Purified by HPLC, using a gradient of 5% acetonitrile in water to 25% acetonitrile in water containing formic acid (0.1%) over 30 minutes. White solid. Yield: 0.77 mg, 2.6%. ^{1}H NMR (600 MHz,D_2O) δ8.46 (s, 2H), 7.59 (d, *J* = 8.0 Hz, 1H), 7.48 (d, *J* = 8.2 Hz, 1H), 7.24 (t, *J* = 7.3 Hz, 1H), 7.15 (t, *J* = 7.4 Hz, 1H), 7.11-7.09 (m, 3H), 6.75 (d, *J* = 8.1 Hz, 2H), 4.64-4.57 (m, 1H), 4.44-4.4qw20 (m, 1H), 4.16-4.11 (m, 1H), 3.22-3.17 (m, 2H), 2.87-2.80 (m, 2H), 2.75-2.70 (m, 1H), 2.64-2.58 (m, 1H), 1.74 (s, 3H); ^{13}C NMR (150 MHz,D_2O) δ173.43, 172.22, 171.02, 154.35, 136.00, 131.00, 130.51, 126.89, 124.26, 121.76, 119.20, 118.30, 115.24, 111.74, 109.32, 53.86, 53.14, 36.41, 28.34, 26.96, 23.24; ^{31}P NMR (162 MHz, D_2O) δ16.49.

N-acetyl-L-leucyl-O-benzyl-L-tyrosine methyl ester (III-9a)

Synthesized using N-Ac-L-leucine-OH III-15 (112 mg, 0.65 mmol), O-benzyl-L-tyrosine methyl ester hydrochloride III-20 (200 mg, 0.62 mmol), HOBt (104 mg, 0.68 mmol), EDC (130 mg, 0.68mmol) and 2,4,6-trimethylpyridine (172 μL, 1.3 mmol) in DMF (6 mL) using method A. White solid. Yield 185 mg, 68%. ^{1}H NMR (600 MHz, $CDCl_3$)

δ7.41 (d, J = 7.6 Hz, 2H), 7.37 (t, *J* = 7.3 Hz, 2H), 7.32 (t, *J* = 7.4 Hz, 1H), 7.03 (d, *J* = 8.5 Hz, 2H), 6.89 (d, *J* = 8.6 Hz, 2H), 6.73 (d, *J* = 7.8 Hz, 1H), 6.21 (d, *J* = 8.3 Hz, 1H), 5.02 (s, 3H), 4.79 (dd, *J* = 13.9, 6.2 Hz, 1H), 4.49-4.36 (m, 1H), 3.70 (s, 3H), 3.07 (dd, *J* = 14.0, 5.7 Hz, 1H), 3.00 (dd, *J* = 14.0, 6.5 Hz, 1H), 1.95 (s, 3H), 1.66-1.58 (m, 2H), 1.52-1.48 (m, 1H), 0.91 (t, *J* = 7.3 Hz, 6H); ^{13}C NMR (150 MHz, $CDCl_3$) δ171.05, 171.83, 170.25, 158.01, 137.08, 130.44, 128.68, 127.59, 115.02, 70.04, 52.53, 52.42, 51.68, 41.17, 37.15, 24.80, 23.15, 22.91, 22.31.

N-acetyl-L-leucyl-O-benzyl-L-tyrosine (III-9b)

Synthesized using N-acetyl-L-leucyl-O-benzyl-L-tyrosine methyl ester III-9a (178 mg, 0.40 mmol), methanol (16 mL) and 5% NaOH (4 mL) using method B. White solid. Yield: 153 mg, 90%.^{1}H NMR (400 MHz, MeOD) δ7.34 (d, *J* = 7.3 Hz, 2H), 7.28 (t, *J* = 7.1 Hz, 2H), 7.22 (t, *J* = 7.2 Hz, 1H), 7.05 (d, *J* = 8.6 Hz, 2H), 6.82 (d, *J* = 8.6 Hz, 2H), 4.96 (s, 2H), 4.54 (dd, *J* = 8.1, 5.2 Hz, 1H), 4.33 (dd, *J* = 9.3, 5.8 Hz, 1H), 3.06 (dd, *J* = 14.0, 5.2 Hz, 1H), 2.86 (dd, *J* = 13.6, 8.2 Hz, 1H), 1.94 (s, 3H), 1.60-1.49 (m, 1H), 1.48-1.37 (m, 2H), 0.84 (dd, J = 16.8, 6.5 Hz, 6H); ^{13}C NMR (100 MHz, MeOD) δ174.47-174.40, 173.46, 173.140173.03, 159.14, 138.77, 131.46, 130.39, 129.49, 115.32, 70.94, 54.95, 52.98, 41.69, 37.45, 25.82, 23.33, 22.42, 22.03.

Diethyl N-(N-acetyl-L-leucyl-O-benzyl-L-tyrosyl)-1-amino-2-(4-benzyloxyphenyl)ethyl phosphonate (III-9c)

Synthesized using N-acetyl-L-leucyl-O-benzyl-L-tyrosine III-9b (140 mg, 0.32 mmol), AHEP III-2 (109 mg, 0.30 mmol), HOBt (52 mg, 0.34 mmol), EDC (65 mg, 0.34

mmol) and 2,4,6-trimethylpyridine (84 μL, 0.63 mmol) in DMF (3 mL) using method A to give a mixture of diastereomers. Clear oil. Yield: 134 mg, 53%. ^{1}H NMR (600 MHz, $CDCl_3$) δ7.37-7.26 (m, 10H), 7.18-6.99 (m, 4H), 6.93-6.74 (m, 4H), 4.98-4.87 (m, 4H), 4.87-4.75 (m, 1H), 4.68-4.60 (m, 1H), 4.49-4.44 (m, 1H), 4.15-4.00 (m, 4H), 3.15-3.08 (m, 1H), 3.00-2.93 (m, 1H), 2.89-2.75 (m, 2H), 1.97-1.92 (m, 3H), 1.60-1.53 (m, 1H), 1.53-1.45 (m, 1H), 1.32-1.19 (m, 7H), 0.91-0.81 (m, 6H); ^{13}C NMR (150 MHz, $CDCl_3$) δ172.40-172.18, 171.26-170.87, 170.56-170.44, 157.95-157.68, 137.20-136.97, 130.65-130.42, 130.21, 129.13-129.05, 128.73-128.62, 128.61-128.55, 127.96-127.93, 127.54-127.49, 70.04-69.88, 63.76-62.53, 54.08-53.75, 51.83-51.70, 47.35-46.22, 41.45-40.93, 37.64-37.57, 35.07-34.70, 24.78, 22.96-22.87, 22.35-22.24, 22.07, 16.57-16.40; ^{31}P NMR (162 MHz, $CDCl_3$) δ25.09, 25.02.

Diethyl N-(N-acetyl-L-leucyl-O-benzyl-L-tyrosyl)-1-amino-2-(4-hydoxyphenyl)ethyl phosphonate (III-9d)

Synthesized using diethyl N-(N-acetyl-L-leucyl-O-benzyl-L-tyrosyl)-1-amino-2-(4-benzyloxyphenyl)ethyl phosphonate III-9c (120 mg, 0.15 mmol), Pd/C (10% Pd, 15 mg) in methanol (3 mL) using method C, to yield a mixture of diastereomers. Clear oil. Yield: 45 mg, 51%. ^{1}H NMR (600 MHz, MeOD) δ7.10-6.99 (m, 4H), 6.75-6.61 (m, 4H), 4.57-4.50 (m, 2H), 4.33-4.27 (m, 1H), 4.20-4.06 (m, 4H), 3.16-3.08 (m, 1H), 2.98-2.93 (m, 1H), 2.84-2.76 (m, 1H), 2.74-2.67 (m, 1H), 1.98-1.94 (m, 4H), 1.58-1.51 (m, 1H), 1.45-1.38 (m, 1H), 1.37-1.29 (m, 6H), 0.97-0.85 (m, 6H); ^{13}C NMR (150 MHz, D2O) δ174.56-174.15, 173.36, 173.18-173.09, 157.43-157.07, 131.35-131.28, 131.15-131.08, 128.98-128.88, 128.67-128.51, 116.31-115.99, 64.50-64.17, 55.68-55.18, 53.29-53.15, 48.33-

48.06, 41.69-48.06, 41.69-41.37, 38.22-38.12, 35.25-34.95, 25.76, 23.31-23.27, 22.43, 21.92, 16.85-16.71; ^{31}P NMR (162 MHz, MeOD) δ25.49.

Ac-Leu-Tyr-AHEP: N-(N-acetyl-L-leucyl-L-tyrosyl)-1-amino-2-(4-hydoxyphenyl)ethyl phosphonic acid (III-9)

Synthesized using diethyl N-(N-acetyl-L-leucyl-O-benzyl-L-tyrosyl)-1-amino-2-(4-hydoxyphenyl)ethyl phosphonate III-9d (21 mg, 0.036 mmol), acetonitrile (4 mL), thioanisole (0.4 mL) and I-TMSi (2.0 mL) using method D. The phosphonate trimethylsilyl ester was hydrolyzed by treatment with 8:2 methanol in water (20 mL). Purified by HPLC, using a gradient of 5% acetonitrile in water to 25% acetonitrile in water containing ammonium acetate (10 mM) over 30 minutes. White solid. Yield: 1.8 mg, 8.4%. ^{1}H NMR (600 MHz, D_2O) δ7.14 (d, *J* = 8.3 Hz, 2H), 7.07 (d, *J* = 8.3Hz, 2H), 6.79 (dd, *J* = 8.2, 4.6 Hz, 4H), 4.57 (dd, *J* = 10.3, 3.8 Hz, 1H), 4.25-4.15 (m, 2H), 3.19 (d, *J* = 13.9 Hz, 1H), 3.05 (dd, *J* = 14.1, 3.7 Hz, 1H), 2.69-2.63 (m, 2H), 1.94 (s, 3H), 1.46-1.39 (m, 1H), 1.38-1.33 (m, 1H), 1.24-1.19 (m, 1H), 0.86 (d, *J* = 6.6 Hz, 3H), 0.81 (d, *J* = 6.5 Hz, 3H); ^{13}C NMR (150 MHz, D_2O) δ 173.66, 173.57, 171.85, 157.09, 153.81, 130.62, 130.38, 128.49, 115.18, 115.07, 54.08, 52.03, 50.93, 49.99, 39.61, 36.60, 35.09, 24.15, 21.96, 21.58, 20.70; ^{31}P NMR (162 MHz,D_2O) δ18.02.

N-acetyl-L-leucyl-L-isoleucine methyl ester (III-10a)

Synthesized using N-Ac-L-leucine-OH III-15 (112 mg, 0.65 mmol), L-isoleucine methyl ester hydrochloride III-20 (99 mg, 0.62 mmol), HOBt (104 mg, 0.68 mmol), EDC (130 mg, 0.68mmol) and 2,4,6-trimethylpyridine (172 μL, 1.3 mmol) in DMF (6 mL)

using method A. White solid. Yield 150 mg, 81%. ^{1}H NMR (600 MHz, $CDCl_3$) δ7.73 (d, *J* = 8.1 Hz, 1H), 7.63 (d, *J* = 8.4 Hz, 1H), 4.72 (dd, *J* = 14.8, 8.6 Hz, 1H), 4.48 (dd, *J* = 8.1, 5.2 Hz, 1H), 3.74 (s, 3H), 1.95 (s, 3H), 1.89-1.84 (m, 1H), 1.71-1.65 (m, 1H), 1.63-1.58 (m, 1H), 1.57-1.52 (m, 1H), 1.44-1.37 (m, 1H), 1.24-1.16 (m, 1H), 0.92-0.84 (m, 12H); ^{13}C NMR (150 MHz, $CDCl_3$) δ173.27, 172.04, 170.40, 56.65, 51.87, 51.45, 41.21, 37.17, 24.97, 24.50, 22.70, 22.63, 22.12, 15.34, 11.52.

N-acetyl-L-leucyl-L-isoleucine (III-10b)

Synthesized using N-acetyl-L-leucyl-L-isoleucine methyl ester III-10a (138 mg, 0.46 mmol), methanol (16 mL) and 5% NaOH (4 mL) using method B. White solid. Yield: 108 mg, 82%.^{1}H NMR (400 MHz, MeOD) δ4.45 (dd, *J* = 9.0, 6.2 Hz, 1H), 4.37-4.33 (m, 1H), 1.97 (s, 3H), 1.94-1.85 (m, 1H), 1.73-1.63 (m, 1H), 1.60-1.47 (m, 3H), 1.30-1.20 (m, 1H), 0.98-0.90 (m, 12H); ^{13}C NMR (101 MHz, MeOD) δ174.89, 174.62, 173.27, 58.06, 53.14, 41.68, 38.38, 26.15, 25.85, 23.36, 22.33, 22.07, 15.98, 11.84.

Diethyl N-(N-acetyl-L-leucyl-L-isoleucyl)-1-amino-2-(4-benzyloxyphenyl)ethyl phosphonate (III-10c)

Synthesized using N-acetyl-L-leucyl-L-isoleucine III-10b (87 mg, 0.30 mmol), AHEP III-2 (104 mg, 0.29 mmol), HOBt (48 mg, 0.31 mmol), EDC (60 mg, 0.31 mmol) and 2,4,6-trimethylpyridine (80 μL, 0.60 mmol) in DMF (3 mL) using method A to give a mixture of diastereomers. Tan foam. Yield: 130 mg, 67%.^{1}H NMR (600 MHz, $CDCl_3$) δ7.41-7.27 (m, 5H), 7.16-7.11 (m, 2H), 6.89-6.80 (m, 2H), 5.01-4.90 (m, 2H), 4.71-4.48 (m, 2H), 4.13-4.01 (m, 5H), 3.21-3.02 (m, 1H), 2.91-2.79 (m, 1H), 2.03-1.98 (m, 3H),

1.78-1.69 (m, 0.5H), 1.67-1.58 (m, 1.5H), 1.58-1.51 (m, 1H), 1.51-1.42 (m, 1H), 1.40-1.19 (m, 7H), 1.12-0.99 (m, 1H), 0.98-0.77 (m, 6H); ^{13}C NMR (151 MHz, $CDCl_3$) δ172.55-172.33, 171.04-170.96, 170.45-170.32, 157.76-157.60, 137.14-137.00, 130.22-130.17, 130.10, 129.33-129.03, 128.58-128.50, 127.94-127.88, 127.48-127.40, 114.89-114.72, 70.03-69.83, 63.01-62.37, 57.61-56.63, 52.08-51.63, 47.37-45.90, 41.76-41.09, 37.98-37.19, 34.95-34.47, 24.85-24.70, 23.09-23.00, 22.89-22.82, 22.28-22.22, 16.61-16.36, 15.01-14.75, 11.77-11.55; ^{31}P NMR (162 MHz, $CDCl_3$) δ25.26, 25.16.

Diethyl N-(N-acetyl-L-leucyl-L-isoleucyl)-1-amino-2-(4-hydoxyphenyl)ethyl phosphonate (III-10d)

Synthesized using N-(N-acetyl-L-leucyl-L-isoleucyl)-1-amino-2-(4-benzyloxyphenyl)ethyl phosphonate III-10c (113 mg, 0.18 mmol), Pd/C (10% Pd, 15 mg) in methanol (3 mL) using method C, to yield a mixture of diastereomers. Clear oil. Yield: 56 mg, 58%. ^{1}H NMR (600 MHz, MeOD) δ7.08-7.02 (m, 2H), 6.69-6.66 (m, 2H), 4.61-4.49 (m, 1H), 4.40-4.34 (m, 1H), 4.20 (d, J = 7.5 Hz, 1H), 4.16-4.12 (m, 4H), 3.17-3.06 (m, 1H), 2.80-2.72 (m, 1H), 2.10-1.97 (m, 3H), 1.89-1.80 (m, 0.5H), 1.77-1.70 (m, 0.5H), 1.69-1.50 (m, 3H), 1.45-1.39 (m, 1H), 1.37-1.28 (m, 6H), 1.21-1.14 (m, 0.5H), 1,14-1.04 (m, 0.5H), 0.98-0.83 (m, 6H); ^{13}C NMR (150 MHz, MeOD) δ174.41-174.30, 173.39-173.31, 173.06, 157.37-157.21, 131.10-130.99, 128.98-128.83, 116.31-116.19, 64.28-64.03, 58.83-58.65, 53.19, 47.89-47.80, 41.71-41.35, 38.53-37.99, 34.90-34.65, 25.94-25.52, 23.48-23.13, 22.38-22.29, 21.84-21.79, 16.96-16.67, 15.64-15.44, 11.39-11.29; ^{31}P NMR (162 MHz, MeOD) δ25.72, 25.48.

Ac-Leu-Ile-AHEP: N-(N-acetyl-L-leucyl-L-isoleucine)-1-amino-2-(4-hydoxyphenyl)ethyl phosphonic acid (III-10)

Synthesized using diethyl N-(N-acetyl-L-leucyl-L-isoleucyl)-1-amino-2-(4-hydoxyphenyl)ethyl phosphonate III-10d (24 mg, 0.044 mmol), acetonitrile (4 mL), thioanisole (0.4 mL) and I-TMSi (2.0 mL) using method D. The phosphonate trimethylsilyl ester was hydrolyzed by treatment with 8:2 methanol in water (20 mL). Purified by HPLC, using a gradient of 5% acetonitrile in water to 25% acetonitrile in water containing ammonium acetate (10 mM) over 30 minutes. White solid. Yield: 1.9 mg, 8.9%. ^{1}H NMR (600 MHz, D_2O) δ7.22 (d, *J*= 8.5 Hz, 2H), 6.86 (d, *J*= 8.5 Hz, 2H), 4.32 (dd, *J* = 10.6, 4.4 Hz, 1H), 4.29-4.00 (m, 1H), 4.20 (d, *J* = 8.5 Hz, 1H), 3.25 (d, *J* = 14.1 Hz, 1H), 2.74 (t, *J* = 12.6 Hz, 1H), 2.10 (s, 3H), 1.84-1.76 (m, 1H), 1.70-1.59 (m, 2H), 1.41-1.33 (m, 2H), 1.16-1.09 (m, 1H), 1.01 (d, *J* = 6.5 Hz, 3H), 0.94 (d, *J* = 6.5 Hz, 3H), 0.92 (d, *J* = 6.9 Hz, 3H), 0.88 (t, *J* = 7.4 Hz, 3H); ^{13}C NMR (151 MHz, D_2O) δ174.05, 173.86, 172.19, 153.72, 130.30, 130.11, 115.06, 57.75, 52.28, 50.58, 49.60, 39.37, 36.56, 34.67, 24.27, 23.99, 22.13, 21.44, 20.46, 14.55, 9.78; ^{31}P NMR (162 MHz,D_2O) δ18.68.

N-acetyl-O-tert-butyl-L-tyrosyl-L-isoleucine methyl ester (III-11a)

Synthesized using N-acetyl-O-tert-butyl-L-tyrosine III-16 (182 mg, 0.65 mmol), L-isoleucine methyl ester hydrochloride III-20 (90 mg, 0.62 mmol), HOBt (104 mg, 0.68 mmol), EDC (130 mg, 0.68mmol) and 2,4,6-trimethylpyridine (172 μL, 1.3 mmol) in DMF (6 mL) using method A. Clear oil. Yield: 223 mg, 89%. ^{1}H NMR (400 MHz, $CDCl_3$) δ 7.08 (d, *J* = 8.2 Hz, 2H), 6.86 (dd, *J* = 8.3, 1.1 Hz, 2H), 4.82-4.68 (m, 1H), 4.44 (dd, *J* =

8.3, 5.1 Hz, 1H), 3.68 (s, 3H), 2.97 (d, *J* = 7.2 Hz, 2H), 1.93 (s, 3H), 1.86-1.68 (m, 1H), 1.41-1.24 (m, 1H), 1.29 (s, 9H), 1.15-0.96 (m, 1H), 0.88-0.71 (m, 6H); ^{13}C NMR (100 MHz, $CDCl_3$) δ 171.72, 171.51, 170.06, 154.18, 131.23, 129.56, 124.07, 78.20, 56.58, 54.42, 51.91, 37.53, 28.70, 25.00, 22.88, 15.25, 11.41.

N-acetyl-O-tert-butyl-L-tyrosyl-L-isoleucine (III-11b)

Synthesized using of N-acetyl-O-tert-butyl-L-tyrosyl-L-isoleucine methyl ester III-11a (205 mg, 0.51 mmol), methanol (20 mL) and 5% NaOH (5 mL) using method B. Clear oil. Yield: 184 mg, 52%. ^{1}H NMR (400 MHz, MeOD) δ 7.08 (d, *J* = 8.4 Hz, 2H), 6.81 (dd, *J* = 8.5, 2.1 Hz, 2H), 4.67-4.59 (m, 1H), 4.30 (d, *J* = 5.5 Hz, 0.7H). 4.23 (d, *J* = 5.4 Hz, 0.3H), 3.04-2.92 (m, 2H), 2.81-2.70 (m, 2H), 1.83 (s, 0.7H), 1.81 (s, 2.3 H), 1.85-1.64 (m, 1H), 1.49-1.37 (m, 1H), 1.22 (s, 9H), 1.33-1.11 (m, 0.5H), 1.06-0.93 (m, 0.5H), 0.86-0.71 (m, 6H); ^{13}C NMR (100 MHz, MeOD) δ174.40, 173.69, 173.19-172.90, 155.24-155.08, 133.53, 130.82, 130.79, 125.12, 79.50-79.42, 58.06-57.97, 55.99-55.90, 38.23-38.12, 38.58, 29.16, 26.12, 22.41-22.34, 15.97, 11.86.

Diethyl N-(N-acetyl-O-tert-butyl-L-tyrosyl-L-isoleucyl)-1-amino-2-(4-benzyloxyphenyl)ethyl phosphonate (III-11c)

Synthesized using N-acetyl-O-tert-butyl-L-tyrosyl-L-isoleucine III-11b (184 mg, 0.47 mmol), AHEP III-2 (163 mg, 0.45 mmol), HOBt (75 mg, 0.49 mmol), EDC (95 mg, 0.49 mmol) and 2,4,6-trimethylpyridine (130 μL, 0.99 mmol) in DMF (5 mL) using method A to give a mixture of diastereomers. Yellowish foam. Yield: 172 mg, 52%. ^{1}H NMR (400 MHz, $CDCl_3$) δ7.43-7.19 (m, 5H), 7.18-7.06 (m, 4H), 6.90-6.78 (m, 4H), 5.02-

4.91 (m, 2H), 4.83-4.66 (m, 1H), 4.65-4.51 (m, 1H), 4.20-3.98 (m, 5H), 3.24-3.00 (m, 2H), 3.00-2.79 (m, 2H), 2.00-1.85 (m, 3H), 1.81-1.49 (m, 1H), 1.48-1.33 (m, 0.5H), 1.34-1.20 (m, 15H), 1.21-0.93 (1.5H), 0.91-0.30 (6H); ^{13}C NMR (100 MHz, $CDCl_3$) δ171.68, 171.41-170.64, 170.36-169.98, 157.79-157.46, 154.28-153.95, 137.09-136.82, 131.92-131.27, 130.11, 129.80-129.60, 129.52-128.64, 128.56-128.34, 127.91-127.69, 127.48-127.26, 124.12-123.85, 114.84-114.58, 78.26-78.04, 69.91, 63.66-63.08, 62.90-62.10, 57.79-56.44, 55.39-54.30, 47.75-47.00, 45.90-45.45, 44.21-43.96, 38.06-36.91, 34.97-34.22, 28.72, 25.92-24.23, 22.88-22.58, 16.58-16.28, 14.19-14.09, 11.74-11.34; ^{31}P NMR (162 MHz, $CDCl_3$) δ 25.37-24.79.

Diethyl N-(N-acetyl-O-tert-butyl-L-tyrosyl-L-isoleucyl)-1-amino-2-(4-hydoxyphenyl)ethyl phosphonate (III-11d)

Synthesized using diethyl N-(N-acetyl-O-tert-butyl-L-tyrosyl-L-isoleucyl)-1-amino-2-(4-benzyloxyphenyl)ethyl phosphonate III-11c (165 mg, 0.22 mmol), Pd/C (10% Pd, 20 mg) in methanol (5 mL) using method C, to yield a mixture of diastereomers. Yellowish oil. Yield: 77 mg, 76%. ^{1}H NMR (400 MHz, MeOD) δ 7.21-7.13 (m, 2H), 7.11-7.05 (m, 2H), 6.96-6.89 (m, 2H), 6.75-6.67 (m, 2H), 4.68-4.43 (m, 2H), 4.28-4.11 (m, 5H), 3.20-3.00 (m, 2H) 2.99-2.70 (m, 2H), 2.02-1.80 (m, 3H), 1.83-1.68 (m, 1H), 1.68-1.51 (m, 0.5H), 1.40 -1.29 (m, 15H), 1.24-1.03 (m, 1.5H), 1.00-0.84 (m, 2H), 0.84-0.68 (m, 2H), 0.68-0.45 (m, 2H); ^{13}C NMR (100 MHz, MeOD) δ174.02-173.42, 173.41-173.06, 171.05-172.51, 157.46-157.05, 155.35-154.99, 133.83-133.73, 131.42-130.95, 130.78-130.59, 129.23-128.51, 125.15, 116.44-116.01, 79.34-79.32, 65.20-65.04, 64.33-64.06, 59.27-58.56, 56.86-55.86, 49.46-47.44, 38.39-37.63, 35.14-34.48, 29.15,

27.19-24.89, 22.45-22.32, 16.78-16.67, 15.77-15.45, 11.99-11.30; ^{31}P NMR (162 MHz, MeOD) δ 25.77-25.15.

Diethyl N-(N-acetyl-L-tyrosyl-L-isoleucyl)-1-amino-2-(4-hydoxyphenyl)ethyl phosphonate (III-11e)

Synthesized using diethyl N-(N-acetyl-O-tert-butyl-L-tyrosyl-L-isoleucyl)-1-amino-2-(4-hydoxyphenyl)ethyl phosphonate III-11d (80 mg, 0.12 mmol) using method F, to yield a mixture of diastereomers. Yellowish oil. Yield: 47 mg, 64%. ^{1}H NMR (600 MHz, MeOD) δ 6.92-6.87 (m, 4H), 6.55-6.49 (m, 4H), 4.46-4.30 (m, 2H), 4.08-3.94 (m, 5H), 2.96-2.88 (m, 1H), 2.85-2.71 (m, 1H)2.68-2.50 (m, 2H), 1.84-1.70 (m, 3H), 1.62-1.52 (m, 0.5H), 1.52-1.44 (m, 0.25H), 1.42-1.34 (m, 0.25H), 1.28-1.05 (m, 7H), 1.05-0.94 (m, 0.5H), 0.93-0.83 (m, 0.5H), 0.76-0.25 (m, 6H); ^{13}C NMR (150 MHz, MeOD) 174.14-173.57, 173.35, 173.35-173.06, 160.55-159.64, 157.40-157.12, 131.32-131.21, 131.17-131.08, 129.30-128.50, 116.31-116.17, 65.20-65.04, 64.51-64.02, 59.29-57.79, 57.11-56.20, 48.32-46.49, 38.49-36.98, 35.34-34.50, 27.01-24.95, 22.51-22.31, 16.87-16.59, 15.81-15.46, 12.02-11.26; ^{31}P NMR (162 MHz, MeOD) δ 25.67, 25.45, 25.17.

Ac-Tyr-Ile-AHEP: N-(N-acetyl-L-tyrosyl-L-isoleucyl)-1-amino-2-(4-hydoxyphenyl)ethyl phosphonic acid (III-11)

Synthesized using diethyl N-(N-acetyl-L-tyrosyl-L-isoleucyl)-1-amino-2-(4-hydoxyphenyl)ethyl phosphonate III-11e (23 mg, 0.039 mmol), acetonitrile (4 mL), thioanisole (0.4 mL) and I-TMSi (2.0 mL) using method D. The phosphonate trimethylsilyl ester was hydrolyzed by treatment with 8:2 methanol in water (20 mL).

Purified by HPLC, using a gradient of 5% acetonitrile in water to 25% acetonitrile in water containing ammonium acetate (10 mM) over 30 minutes. White solid. Yield: 2.5 mg, 12%. ^{1}H NMR (600 MHz, D_2O) δ7.16 (d, *J* = 8.4 Hz, 2H), 7.07 (d, *J* = 8.5 Hz, 2H), 6.83 (d, *J* = 8.5 Hz, 2H), 6.78 (d, *J* = 8.5 Hz, 2H), 4.43 (dd, *J* = 9.8, 5.2 Hz, 1H), 4.28-4.22 (m, 1H), 4.11 (d, *J* = 8.8 Hz, 1H), 3.19 (d, *J* = 14.2 Hz, 1H), 2.84 (dd, *J* = 14.3, 5.1 Hz, 1H), 2.75-2.65 (m, 1H), 1.91 (s, 3H), 1.72-1.66 (m, 1H), 1.27-1.21 (m, 1H), 1.04-0.96 (m, 1H), 0.82 (d, *J* = 6.8, 3H), 0.78 (t, *J* = 7.32 Hz, 3H); ^{13}C NMR (150, D_2O) 173.91, 172.62, 172.03, 154.23, 153.89, 130.41, 128.60, 115.37, 115.12, 57.99, 55.09, 50.65, 49.63, 26.43, 26.14, 24.67, 24.04, 21.46, 14.54, 9.82; ^{31}P NMR (162 MHz, D_2O) δ 18.67.

N-acetyl-L-prolinyl-O-benzyl-L-tyrosine methyl ester (III-12a)

Synthesized using N-acetyl-L-proline III-17 (102 mg, 0.65 mmol), O-benzyl-L-tyrosine methyl ester hydrochloride III-20 (200 mg, 0.62 mmol), HOBt (104 mg, 0.68 mmol), EDC (130 mg, 0.68 mmol) and 2,4,6-trimethylpyridine (172 μL, 1.3 mmol) in DMF (6 mL) using method A. Clear oil. Yield: 191 mg, 73%. Rotamers. ^{1}H NMR (400 MHz, $CDCl_3$) δ7.37-7.26 (m, 5H), 7.06-6.99 (m, 2H), 6.89-6.81 (m, 2H), 4.99 (s, 0.6H), 4.97 (s, 1.4H), 4.79-4.75 (m, 0.3H), 4.75-4.70 (m, 0.7H), 4.49 (dd, *J* = 8.0, 1.7 Hz, 0.7 H), 4.18 (dd, *J* = 8.7, 2.2 Hz, 0.3H), 3.68 (s, 0.7H), 3.65 (s, 2.3 H), 3.45-3.41 (m, 0.5H), 3.24 (dd, *J* = 8.0, 5.4 Hz, 1.5H), 3.17-3.05 (m, 1H), 2.95-2.85 (m, 1H), 2.30-2.24 (m, 1H), 1.95 (s, 0.7H), 1.93 (s, 2.3H), 1.91-1.81 (m, 2H), 1.75-1.67 (m, 1H); ^{13}C NMR (100 MHz, $CDCl_3$) δ171.78, 170.80, 170.62, 157.56, 136.95, 130.21, 129.92, 128.44, 127.81,

127.29, 114.86, 114.59, 69.80, 69.76. 59.20, 53.20, 53.06, 52.24, 52.12, 47.92, 36.88, 27.08, 24.69, 22.29-22.13.

N-acetyl-L-prolinyl-O-benzyl-L-tyrosine (III-12b)

Synthesized using N-acetyl-L-prolinyl-O-benzyl-L-tyrosine methyl ester III-12a (220 mg, 0.52 mmol), methanol (12 mL) and 5% NaOH (3 mL) using method B. White solid. Yield: 134 mg, 63%. ^{1}H NMR (600 MHz, MeOD) δ7.42-7.39 (m, 2H), 7.34 (t, *J* = 7.4 Hz, 2H), 7.28 (t, *J* = 7.3 Hz, 1H), 7.14 (t, *J* = 8.76 Hz, 2H), 6.89 (dd, *J* = 8.5, 6.6 Hz, 2H), 5.04 (s, 2H), 4.71 (dd, *J* = 10.9, 4.4 Hz, 0.5H), 4.61 (dd, *J* = 7.5, 5.5 Hz, 0.5H), 4.42 (dd, *J* = 8.8, 3.4 Hz, 0.5H), 4.26 (dd, *J* = 8.8, 2.8 Hz, 0.5H), 3.54-3.46 (m, 1H), 3.42-3.37 (m, 1H), 3.25 (dd, *J* = 14.2, 4.5 Hz, 0.5H), 3.11 (dd, *J* = 14.1, 5.4 Hz, 0.5H), 2.96 (dd, *J* = 14.1, 7.6 Hz, 0.5H), 2.89-2.85 (m, 0.5H), 2.23-2.18 (m, 0.5H), 2.09-2.02 (m, 0.5H), 2.04 (s, 1.5H), 2.00 (s, 1.5H), 1.99-1.93 (m, 0.5H), 1.92-1.85 (m, 1.5H), 1.78-1.72 (m, 0.5H), 1.71-1.66 (m, 0.5H); ^{13}C NMR (100 MHz, MeOD) δ176.77, 174.40-174.13, 173.48, 159.13-159.11, 138.85-138.77, 131.49, 131.18, 130.84, 130.38, 129.49-129.48, 128.83-128.81, 128.49-128.47, 115.96, 115.84, 74.14, 70.91-70.90, 62.56, 60.99, 55.03, 54.67, 47.90, 37.39, 37.22, 23.92, 30.43, 25.50, 23.62, 22.19, 22.07.

Diethyl N-(N-acetyl-L-prolinyl-O-benzyl-L-tyrosyl)-1-amino-2-(4-benzyloxyphenyl)ethyl phosphonate (III-12c)

Synthesized using N-acetyl-L-prolinyl-O-benzyl-L-tyrosine III-12b (134 mg, 0.33 mmol), AHEP III-2 (112 mg, 0.31 mmol), HOBt (52 mg, 0.34 mmol), EDC (65 mg, 0.34 mmol) and 2,4,6-trimethylpyridine (90 μL, 0.68 mmol) in DMF (4 mL) using method A to

give a mixture of diastereomers. Clear oil. Yield: 126 mg, 50%. ^{1}H NMR (400 MHz, $CDCl_3$) δ7.40-7.26 (m, 10H), 7.18-7.12 (m, 2H), 7.05-6.93 (m, 2H), 6.91-6.83 (m, 2H), 6.83-6.73 (m, 2H), 5.02-4.94 (m, 4H), 4.82-4.67 (m, 1H), 4.67-4.55 (m, 1H), 4.43-4.32 (m, 0.5H), 4.18-4.02 (m, 4.5H), 3.43-3.36 (m, 0.5H), 3.27-3.07 (m, 2.5H), 3.03-2.96 (m, 0.5H), 2.93-2.77 (m, 1.5H), 2.76-2.67 (m, 1H), 2.19-2.12 (m, 0.5H), 2.12-1.97 (m, 2H), 1.92 (s, 0.5H), 1.88-1.83 (m, 1.5H), 1.83-1.67 (m, 2.5H), 1.36-1.22 (m, 6H); ^{13}C NMR (100 MHz, $CDCl_3$) δ171.15-171.12, 170.92-170.87, 170.69-170.65, 157.73-157.46, 137.09-137.03, 130.35, 130.21, 130.17, 129.25, 129.14-129.06, 128.57-128.50, 127.96-127.83, 127.47-127.39, 114.80-114.50, 39.95-69.87, 63.23-62.46, 59.88-59.68, 53.56, 48.00, 47.23-45.69, 36.57-36.00, 34.51-34.39, 27.95, 27.47, 24.73-24.69, 22.33-22.30, 16.51-16.37; ^{31}P NMR (162 MHz, $CDCl_3$) δ25.19, 24.84.

Diethyl N-(N-acetyl-L-prolinyl-O-benzyl-L-tyrosyl)-1-amino-2-(4-hydoxyphenyl)ethyl phosphonate (III-12d)

Synthesized using diethyl N-(N-acetyl-L-prolinyl-O-benzyl-L-tyrosyl)-1-amino-2-(4-benzyloxyphenyl)ethyl phosphonate III-12c (110 mg, 0.14 mmol), Pd/C (10% Pd, 15 mg) in methanol (3 mL) using method C, to yield a mixture of diastereomers. Clear oil. Yield: 52 mg, 65%.^{1}H NMR (400 MHz, MeOD) δ7.12-7.01 (m, 3H), 6.96-6.82 (m, 1H), 6.76-6.65 (m, 4H), 4.62-4.53 (m, 1.5H), 4.38-4.32 (m, 0.5H), 4.24-4.05 (m, 5H), 3.59-3.46 (1.5H), 3.39-3.35 (m, 0.5H), 3.20-3.10 (m, 1.5H), 3.05-2.97 (m, 0.5H), 2.88-2.68 (m, 2H), 2.14-1.96 (m, 4H), 1.96-1.70 (m, 3H), 1.4-1.31 (m, 6H); ^{13} CNMR (600 MHz, MeOD) δ 173.94-173.84, 173.35-173.11, 172.80, 157.38-157.10, 131.29-131.02, 129.98-128.60, 116.30-116.04, 64.36-64.22, 62.10, 61.54-61.45, 55.71-55.21, 47.94,

38.84-37.70, 35.20-37.93, 33.02, 30.46-30.41, 35.56-25.48, 23.73-23.60, 22.36-21.99, 16.88-16.65; ^{1}P NMR (400 MHz, MeOD) δ25.35 (broad).

Ac-Pro-Tyr-AHEP: N-(N-acetyl-L-prolinyl-L-tyrosyl)-1-amino-2-(4-hydoxyphenyl)ethyl phosphonic acid (III-12)

Synthesized using diethyl N-(N-acetyl-L-prolinyl-O-benzyl-L-tyrosyl)-1-amino-2-(4-hydoxyphenyl)ethyl phosphonate III-12d (21 mg, 0.036 mmol), acetonitrile (4 mL), thioanisole (0.4 mL) and I-TMSi (2.0 mL) using method D. The phosphonate trimethylsilyl ester was hydrolyzed by treatment with 8:2 methanol in water (20 mL). Purified by HPLC, using a gradient of 5% acetonitrile in water to 25% acetonitrile in water containing ammonium acetate (10 mM) over 30 minutes. White solid. Yield: 1.8 mg, 9.7%. ^{1}H NMR (600 MHz, D_2O) δ7.16-7.12 (m, 3H), 7.05 (d, *J* = 8.5Hz, 1H), 6.82-6.80 (m, 3H), 6.76 (d, *J* = 8.7 Hz, 1H), 4.65 (dd, *J* = 11.7, 3.7 Hz, 0.5H), 4.54 (dd, *J* = 9.5, 4.9 Hz, 0.5H), 4.28 (dd, *J* = 8.5, 4.1 Hz, 1H), 4.22-4.20 (m, 1H), 3.54-3.46 (m, 1H), 3.40-3.35 (m, 1H), 3.20 (d, *J* = 13.7Hz, 1H), 3.12 (dd, *J* = 14.1, 3.6 Hz, 0.5H), 2.99 (dd, *J* = 14.3, 4.8 Hz, 0.5H), 2.68-2.64 (m, 2H), 2.18-2.12 (m, 0.5H), 2.08 (s, 1.5H), 2.08-2.00 (m, 0.5H), 2.00 (s, 1.5H), 1.91-1.86 (m, 0.5H), 1.85-1.79 (m, 0.5H), 1.76-1.58 (m, 2H); ^{13}C NMR (150 MHz, D_2O) δ173.56-173.52, 172.81, 172.08-171.85, 154.18, 154.14, 153.88, 153.78, 130.47, 130.42, 130.28, 130.18, 128.67, 128.48, 115.38, 115.30, 115.09, 114.94, 61.17, 59.81, 54.17, 54.04, 48.51, 46.96, 36.70, 36.10, 35.08, 34.91, 31.51, 29.20, 24.04, 22.41, 21.37, 20.64; ^{31}P NMR (162 MHz, D_2O) δ18.71.

Assay for ACE inhibition

Assay for inhibition of somatic ACE with substrate FAPGG

Somatic ACE was extracted from rabbit lung acetone powder. Turnover of the substrate FAPGG was monitored in triplicate in a 96-well plate in the presence of various concentrations of inhibitor by monitoring the corresponding change in absorbance at 340 nm.[127-128] IC_{50} was calculated by plotting the percent activity of the enzyme against the log of the concentration of the inhibitor. IC_{50} curves are available in Appendix E.

Acknowledgements

This research would have not been possible without our collaboration with the laboratory of Jens Meiler. David Nannemann has performed much of the computational work that was described herein. Brian Bachmann, David Nannemann and Jens Meiler have provided guidance and insight in experimental design.

CHAPTER IV

K-26 CHEMICAL PROBE DEVELOPMENT

Introduction

Affinity chromatography is one of the most widely used methods for small molecule target-identification.[168-170] In this classic approach, structural activity relationship studies are used to determine which functional groups are expendable while still retaining activity of the small molecule of interest. These dispensable functional groups are then used as points for modification of the drug for attachment to a solid matrix or linker. This chemical probe is then able to interact directly with the protein target, which can subsequently be identified. This method has successfully been applied for discovery of potential drug targets and small molecule enzymatic interactions, with a possible role in giving insight into the biosynthesis and discovery of mechanism of action of a small molecule.[170]

Our small molecule of interest, K-26, has an unknown target and mechanism of biosynthesis. Although ACE is a central enzyme in blood pressure and fluid balance regulation in mammals and a target of pharmaceutical treatment of cardiovascular disease, it is unlikely that mammalian ACE would be the environmental target of the microbially produced tripeptide, K-26 (IV-1).[126] Furthermore, the unique terminal phosphonic acid, a structural feature of the non-proteogenic amino acid, *(R)*-1-amino-2-(4-hydroxyphenyl) ethylphosphonic acid *(R)*-AHEP (II-2) is interesting from a biosynthetic perspective as the unique carbon-phosphorus bond must be synthesized

by unprecedented mechanism.[49, 59] Although phosphonate containing natural products are common, all examples with known biosynthesis utilize a phosphoenol pyruvate (PEP) mutase which catalyzes the intramolecular rearrangement of phosphoenolpyruvate to phosphonopyruvate, a precursor in carbon-phosphorus bond formation in all known examples.[59] Furthermore, it is not clear how the appropriate intermediate necessary in carbon-phosphorus bond formation could result from a precursor of AHEP in a PEP mutase catalyzed process.[49] Lastly, there is no PEP mutase identifiable in the annotated genome of the K-26 producing organism, leading us to believe that the biosynthesis of this natural product must proceed through an alternate and novel mechanism.

K-26 is an ideal candidate for development of a chemical probe as there have been previous structural activity relationship studies of this small molecule with ACE. These studies of K-26 revealed that both *(R)*-AHEP and the N-acetyl tail are imperative for potent ACE inhibitory activity (Figure II-1).[50] If *(R)*-AHEP is replaced with *(S)*-AHEP the inhibition of ACE drops 10 fold (IV-4), removing AHEP in favor of a tyrosine residue results in a 1500 fold decrease in ACE inhibition (IV-5), and protecting the AHEP phosphonate with ethyl esters results in a 25000 fold drop in activity (IV-6). Additionally removal of the N-acetyl tail results in a 15 fold decrease in activity (IV-3, IV-7).

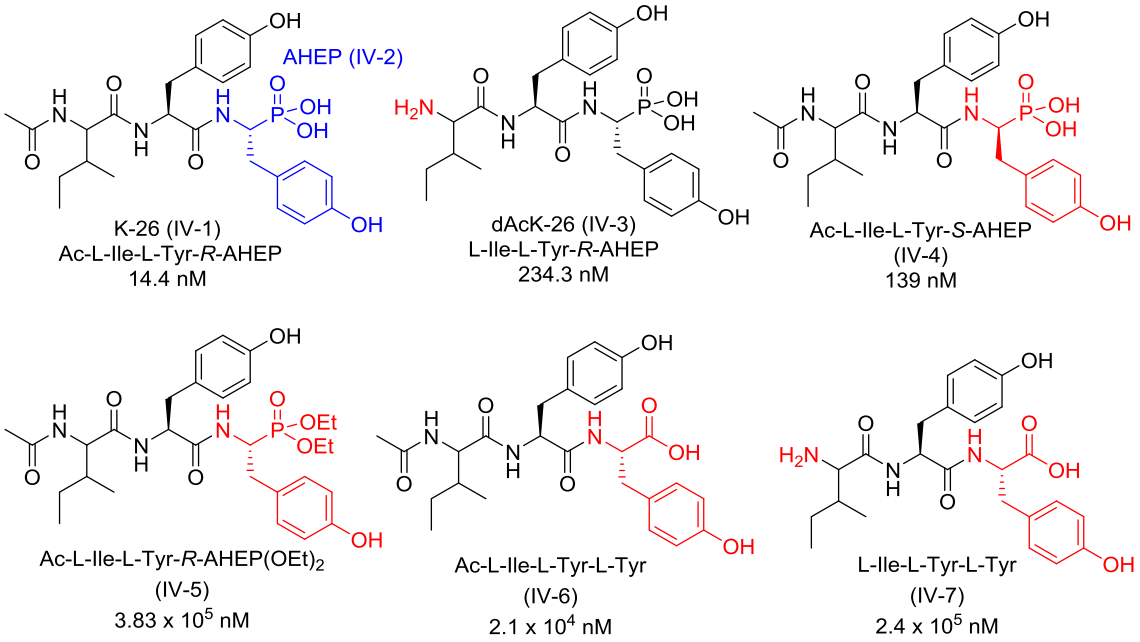

Figure IV-1: Important structural features of K-26 and analogs for ACE inhibition. Both the *S*-AHEP and N-acetyl functionalities are important for potent ACE inhibition by this small molecule. AHEP (IV-2) is shown in blue. Modifications of from the original K-26 (IV-1) structure are highlighted in red.

Based on those prior SAR studies, a chemical probe design must leave *(R)*-AHEP untouched and would build off the N-terminal end of the peptide. The linker would be attached to the N-terminal end of dAcK-26 (IV-3), a K-26 derivative without the N-acetyl tail. The linker was designed to restore the amide functionality of the N-acetyl group of K-26, when coupled to dAcK-26 (IV-3). Thus we were able to obtain probes with the essential *(R)*-AHEP and an extended derivative of the N-acetyl functionality intact. This would presumably give a chemical probe with the highest degree of ACE inhibitory activity possible giving ACE a utility as an enzymatic target in probe development experiments. Also, the unmodified *(R)*-AHEP would be left free to target the enzymatic machinery responsible for the biosynthesis of this unique amino acid and natural product.

Results

Probe design and synthesis

In the design of a K-26 affinity probe, we initially chose to pursue a probe with a PEG linker and a biotin tag to be used as a handle for affinity purification with streptavidin, systems both widely used in affinity chromatography (IV-8, Figure IV-2).[171-174] A probe of this type has the advantage of being un-tethered until the addition of solid phase avidin, which has a strong affinity interaction with the biotin. As a result, this probe can be purified, quantified and the inhibitory activity can be tested allowing verification that potent inhibitory activity remains even after the addition of the linker. Furthermore, biotin has been used with the ACE inhibitor lisinopril (IV-9) to develop a chemical probe.[175] The second system chosen was a linker bound directly to sepharose (IV-10), which has been used with the ACE inhibitor lisinopril as a standard method for affinity purification of ACE (IV-11).[176]

K-26 functionality was imparted on both probes by linking the free amino terminal of the K-26 derivative, dAcK-26 (IV-3) to the respective linkers through an aqueous coupling with an N-hydroxysuccinimide ester (NHS, IV-12) (SchemeIV-1).[176-177] Coupling of the primary amine in dAcK-26 (IV-3) to the commercially available NHS-PEG_{12}-biotin linker yielded free biotin-K-26 (IV-8) which was purified by LC-MS, and characterized then quantitated by NMR prior to use. The sepharose-K-26 probe (IV-10) was synthesized in a fashion similar to the affinity resin used in the well precedented and common ACE affinity purification method, which uses the potent ACE inhibitor lisinopril (IV-9) tethered to a sepharose bead by a 6-(4-aminobenzamido)hexanoic acid linker (IV-11). Here, we coupled a 6-(4-aminobenzamino)hexanoic acid linker to epoxy

activated Sepharose 6B. After the linker was functionalized with N-hydroxysuccinimide (IV-12), we coupled dAcK-26 (IV-3) to the linker under aqueous conditions to yield Sepharose-K-26 (IV-10).

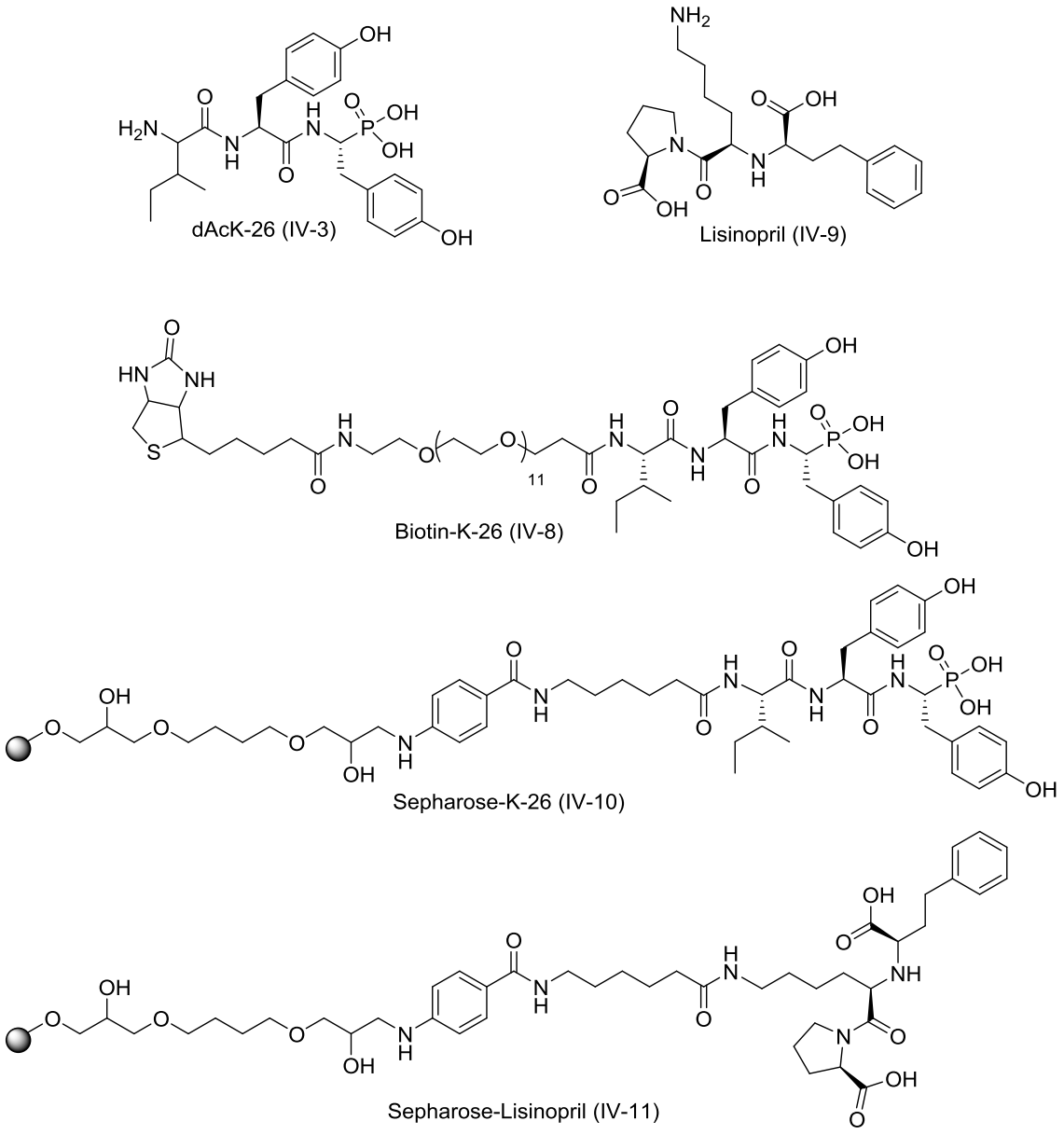

Figure IV-2: Inhibitors and probes of interest in this study.

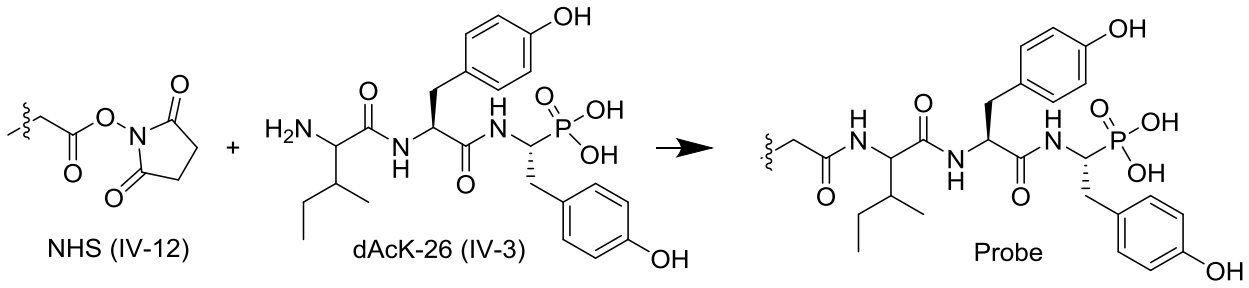

Scheme IV-1: Aqueous coupling of dAcK-26 to linker bound N-hydroxysuccinimide to yield K-26 affinity resin.

Biotin-K-26 probe evaluation

After synthesis, the free biotin-K-26 (IV-8) was evaluated for the ability to potently inhibit ACE using both the substrate FAPGG to assay for inhibition of somatic ACE and the substrate Z-FHL to assay for inhibition of purified N-domain and C-domain ACE constructs.[127-128] The biotin-K-26 probe was determined to still be a mid-nanomolar inhibitor of somatic ACE (IC_{50} = 93.5 nM) (Figure IV-3A). The relative long linker resulted in approximately a 7-fold drop in activity compared to free K-26 (IC_{50} = 12.5 nM), but restored some of the potency compared to dAcK-26 (IC_{50} = 234 nM),[127] with the biotin-K-26 probe having about 3 times the activity of dAcK-26. We did expect the bulky linker to have an effect on the ACE inhibition compared to free K-26. Furthermore, the biotin-K-26 probe was tested as an inhibitor of the individual C- and N- domains of ACE using overexpressed and purified ACE constructs with the substrate Z-FHL (Figure IV-3B,C).[102, 129-131, 141] The biotin-K-26 (IV-8) was found to be a potent mid-nanomolar inhibitor of both domains of ACE, with a very slight preference for the N- domain.

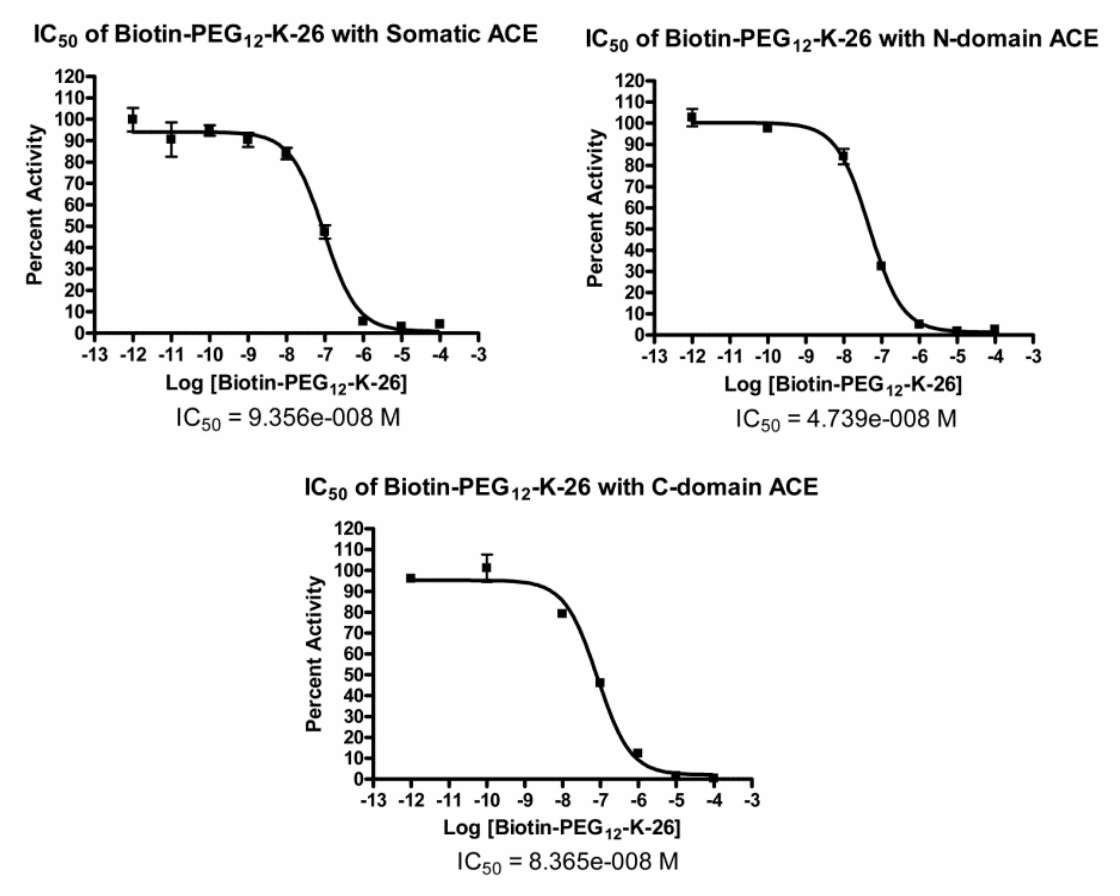

Figure IV-3. IC_{50} curves for inhibition of ACE by the biotin-K-26 probe. A. Inhibition of rabbit lung somatic ACE by free biotin-K-26 using the substrate FAPGG. B. Inhibition of purified N-domain ACE by free biotin-K-26 using the substrate Z-FHL. C. Inhibition of purified C-domain ACE by free biotin-K-26 using the substrate Z-FHL.

Next, to determine if biotin retained the ability to bind to avidin in the biotin-K-26 probe, we used a colorimetric assay with 4'-hydroxyazobenzene-2-carboxylic acid (HABA).[178] HABA is displaced from the biotin binding sites on avidin in when increasing amounts of a biotinylated probe or free biotin is added, a process which can be monitored by a decrease in absorbance at 500 nm. This titration experiment with HABA indicated that the probe effectively binds to avidin, although it appears to be approximately two-fold less efficient than biotin alone (Figure IV-4). The results of the HABA assay confirmed that adding the K-26 to the biotin-PEG linker did not interfere

with the affinity interaction between the biotin and the avidin and biotin-K-26 is indeed able to bind to NeutrAvidin.

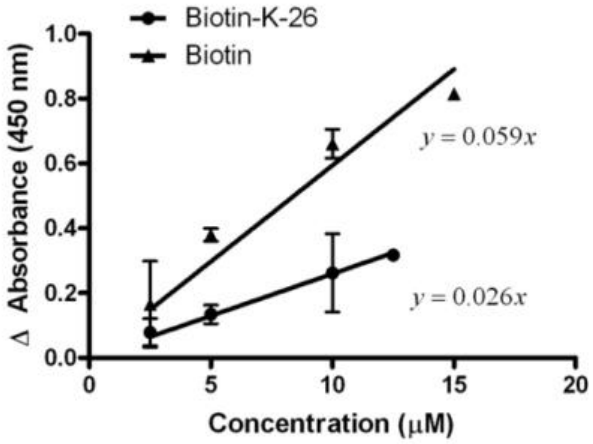

Figure IV-4. HABA colorimetric assay evaluating the ability of biotin and biotin-K-26 to bind to soluble avidin.

General pull-down schematic

The ability of K-26 probe conjugates to bind and purify ACE was first assessed via competition experiments using authentic K-26 (IV-1). Two tACE containing samples were prepared by spiking in 5 µg/mL of the heterologous enzyme into cell culture media (Figure IV-5). An excess of K-26 (IV-1) was added to one of these sample replicates as a preblocked control sample, denoted as K-26 (+), while an equal volume of buffer was added to the other sample, denoted K-26 (-). The K-26 concentration in the control replicate was 5 µM in solution, a concentration high enough to entirely abolish ACE activity and prevent ACE, or any other proteins with a high specific affinity to the chemical probe, from binding. After a brief incubation period, the K-26 probe conjugate (IV-8, IV-10) was added. The supernatant was removed and retained for activity testing

and the beads were thoroughly washed with buffer to remove non-specifically binding proteins. A portion of denaturing SDS-page loading buffer was added to the beads, and boiled to denature bound proteins. These bound proteins were analyzed via gel chromatography, western blotting or by a spectral counting proteomics method.

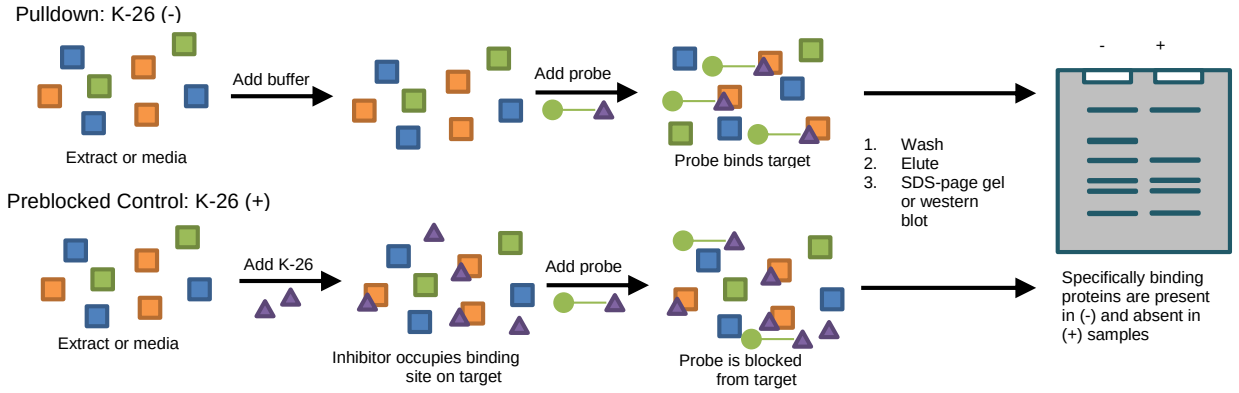

Figure IV-5. General pull-down experimental design. Free K-26 is added to block the binding of the target proteins in the K-26 (+) sample. Non-specific proteins bind to the probe in both cases with (+) and without (-) free K-26.

Mutually exclusive binding of biotin-K-26

Although our free biotin-K-26 probe (IV-8) was found to be a mid-nanomolar inhibitor of both domains of ACE and was shown to retain the high affinity interaction between the biotin and the avidin, when the probe was bound to the solid phase, no binding of tACE was observed and only a slight depletion in ACE activity was noted upon addition of the probe to ACE containing media. The pull-down with the biotin-K-26 chemical probe (IV-8) remained ineffective under a variety of incubation conditions, (ranging from 1 hour to 48 hours at 0 ^{o}C and at room temperature) and buffer ionic strengths. Furthermore, the pull-down efficacy was not increased when the biotin-K-26 chemical probe (IV-8) was incubated with ACE in solution prior to adding the

NeutrAvidin to pullout the chemical probe. In light of that unexpected result, we explored the possibility of an unfavorable NeutrAvidin/K-26 interaction, we evaluated the ability of the biotin-K-26 probe to inhibit ACE in the presence of soluble avidin (Figure IV-6).

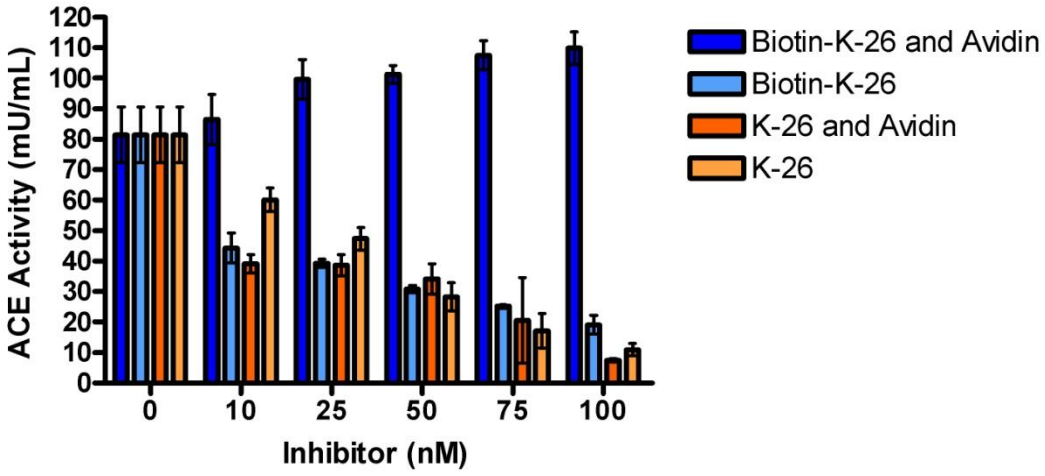

Figure IV-6. ACE activity when incubated with biotin-K-26 (IV-8) and avidin, biotin-K-26, K-26 (IV-1) and avidin or K-26 alone. ACE activity decreases in the presence of the inhibitor K-26, K-26 with avidin and biotin-K-26 alone, however biotin-K-26 (IV-8) in the presence of avidin does not inhibit ACE.

Both free biotin-K-26 (IV-8) and K-26 (IV-1) were shown to inhibit ACE potently, with increasing concentrations of both molecules causing a decrease in ACE activity, as expected. When soluble avidin was added to the system, K-26 (IV-1) was still capable of potently inhibiting ACE as shown by the decrease in ACE activity with the increase in K-26 (IV-1) concentration. However, adding avidin to the system rendered the biotin-K-26 (IV-8) incapable of inhibiting ACE. Surprisingly, ACE showed no degree of inhibition when incubated with 100 nM of biotin-K-26 (IV-8) in the presence of avidin. In the absence of avidin, 100 nM of biotin-K-26 (IV-8) was shown to nearly abolish ACE

activity, confirming that our biotin-K-26 (IV-8) probe is only able to bind the avidin and the target ACE in a mutually exclusive fashion.

Pull-downs of heterologously expressed ACE with sepharose-K-26 (IV-10)

The poor performance of the biotinylated probe (IV-8) prompted us to investigate the use of alternative affinity probes, particularly ones where the K-26 (IV-1) would be linked directly linked to a solid phase, abrogating the mutually exclusive binding interactions of avidin and ACE. We investigated the use of a Sepharose resin probe based on a previously developed lisinopril resin (IV-11), which is used as a standard method for the purification of heterologously expressed ACE.[176] Initial characterization of K-26-sepharose (IV-10) using activity assays and western blots revealed a much lower ACE affinity than the corresponding lisinopril resin (Figure IV-7A,B).

As our K-26 chemical probe (IV-10) is unique with respect to the lisinopril probe (IV-11) due to the K-26 phosphonate moiety which is negatively charged at neutral pH, the ionic strength of the enzyme containing solution was an important aspect to consider in these pull-down experiments. We rationalized that increasing the ionic strength of the media or buffer by adding sodium chloride would reduce the ability of the K-26 functionality to non-specifically bind with other charged species and in turn increase the ability that the probe to specifically bind with the target enzymes. Modifying the ionic strength of the solution by increasing the NaCl concentration was successful in dramatically increasing the affinity of the K-26 probe (IV-10) of ACE and in turn the pull-down efficiency (Figure IV-7C). Importantly, affinity pull-down of ACE spiked culture media supplemented with 1 M NaCl, was shown to be significantly more effective with K-26-sepharose (IV-10) than

with the corresponding biotin-K-26 (IV-8) resin (Figure IV-7D). Additionally, the observation that an excess of authentic K-26 (IV-1) is able to block binding to sepharose-K-26 (IV-10) suggests that the interaction is specific.

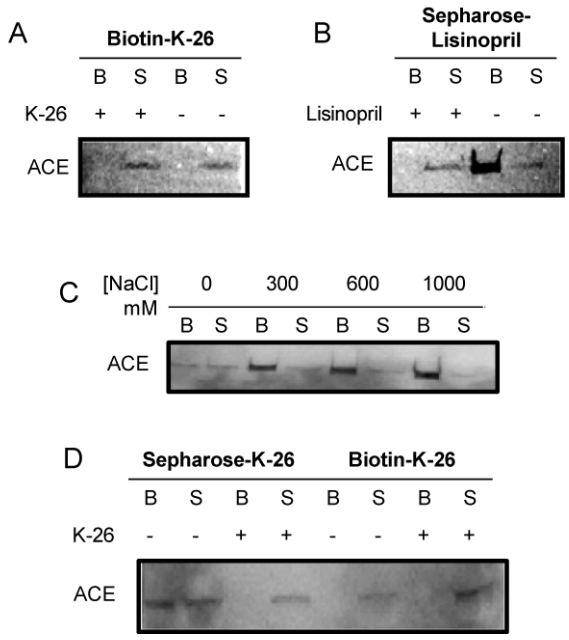

Figure IV-7. Western blots of preliminary pull downs with tACE A. Western blot of pull-down with biotin-K-26 (IV-8) from media with 5µg/mL of tACE. B. Western blot of pull-down with sepharose-lisinopril (IV-11) from media with 5µg/mL of tACE. C. Western blot of pull-down with K-26 functionalized sepharose (IV-10) in media with 5µg/mL of tACE and different ionic strengths. D. Western blot of pull-down with K-26 (IV-1) with either K-26 functionalized sepharose (IV-10) or biotin-K-26 (IV-8) from media with 1000 mM of NaCl and 5 µg/mL of tACE. Western blots were imaged for ACE using a polyclonal anti C-domain antibody. K-26 (+) samples have had the inhibitor K-26 (IV-1) added prior to the addition of the probe. Lanes with the notation B contain the protein which was denatured off of the affinity resin (bead) after the pull-down. Lanes with the designation S correspond to the analysis of the proteins remaining in solution after incubation with the affinity resin.

Using tACE spiked into buffer, the amount of enzyme the probe was able to bind was evaluated (Figure IV-8A). When 25 µg/mL of tACE was spiked into buffer, a visible amount of tACE was pulled out with the probe, however a significant amount of tACE remained in solution. With 10 µg/mL of tACE spiked into buffer, the amount of tACE remaining in solution was less than the sample of tACE bound to the beads, showing

tACE enrichment on the beads. With the samples containing 5 µg/mL and 1 µg/mL of ACE, only a small amount of ACE was detected suggesting that 10 µg/mL of tACE was optimal for visualization of tACE on the coomasie gel. K-26 was then shown to effectively compete for tACE and prevent the enzyme from binding to the probe when 10 µg/mL of tACE was spiked in to the buffer (Figure IV-8B).

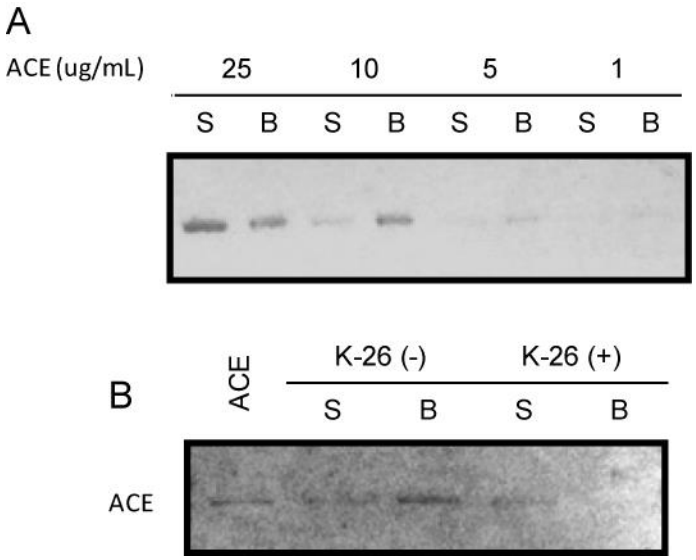

Figure IV-8. Western blots of pull downs of tACE with sepharose-K-26 probe A. Coomasie stained gel of pull-down using sepharose-K-26 (IV-10) with various concentrations of tACE spiked into buffer. Remaining tACE in the buffer after incubation is shown in the S lanes. B. Coomasie stained gel of pull-down using sepharose-K-26 (IV-10) with 10 µg/mL of tACE spiked into buffer showing that binding of tACE can be blocked through the addition of the competitive inhibitor K-26 (IV-1). Lanes with the notation B contain the protein which was denatured off of the affinity resin (bead) after the pull-down. Lanes with the designation S correspond to the analysis of the proteins remaining in solution after incubation with the affinity resin.

These results were further confirmed using a spectral counting proteomics method to analyze proteins pulled out of cell media spiked with 5 µg/mL of tACE.[179-180] The data was analyzed using fold change between the number of normalized spectral counts between the K-26 (+) and K-26 (-) samples. A protein was defined as a hit if there was at least a 2 fold difference between the K-26 (-) and K-26 (+) samples and the

K-26 (-) sample had at least 5 spectral counts. As a point of comparison we conducted the same experiment using the Pantoliano sepharose-lisinopril affinity resin (IV-11) in which pre-blocking with lisinopril (IV-9) was used as a control. As expected, both probes were found to only specifically bind tACE, The sepharose-K-26 probe (IV-10) exhibited a 3.5 fold difference in spectral counts between the K-26 (+) and K-26 (-) samples. whereas, the sepharose-lisinopril (IV-11) resin had 5.22 fold more spectral counts in the lisinopril (-) sample, when compared to the lisinopril pre-blocked control (+) (Table IV-1).

Probe Used	Protein	Accession Number	MW kDa	Normalized Spectral Counts		Binding Ratio
				Competitive Inhibitor (-)	Competitive Inhibitor (+)	
Lisinopril	tACE	2IUL:A| PDBID tACE	68	141	27	5.22
	Angiotensin-converting enzyme *Heterocephalus glaber*	tr|G5BDK0|G5BDK0_HETGA	150	49	14	3.5
	Uncharacterized protein *Spermophilus tridecemlineatus*	tr|I3MDG2|I3MDG2_SPETR	151	47	14	3.36
	Angiotensin-converting enzyme *Mus musculus*	sp|P09470|ACE_MOUSE (+5)	151	21	0	-
K-26	tACE	2IUL:A|PDBID tACE	68	49	16	3.06

Table IV-1: Summary of Proteomics Hits for K-26 (IV-10) and Lisinopril (IV-11) probe with overexpressed ACE in media. Binding to the lisinopril probe was blocked by the competitive inhibitor, lisinopril. Binding to the K-26 probe was blocked by the competitive inhibitor K-26.

As a next step in probe validation, we decided to examine if the sepharose-K-26 probe (IV-10) was able to pull low levels of ACE out of a complex sample mixture. We spiked ACE into bacterial cell free extracts at level which we would expect to be a closer

representation the physiological expression levels of a possible target enzyme. As degradation of ACE by proteases present in the bacterial extracts is a possibility, we added PMSF to the cell free extracts and examined the time course necessary to achieve a depletion of ACE activity after the addition of the probe. Using the substrate FAPGG, we assayed for ACE activity and compared the ACE activity to a sample without the probe added, which had been incubated under the same conditions. We examined the ability of the probe to deplete the spiked in ACE activity in cell free extracts of both *E. coli* and the producing actinomycete in comparison to ACE spiked into buffer (Figure IV-9). Addition of the probe depleted the ACE activity to one third of the levels seen in the sample without beads added. When ACE was spiked into bacterial cell free extracts, the ACE activity was not depleted as drastically as the respective sample without beads added. However there was a significant decrease in ACE activity suggesting that the enzyme is indeed binding to the probe. Despite the decrease in measured ACE activity in the samples, when the bound proteins were eluted off of the beads, a corresponding protein band was not visible on a coomassie stained gel and proteomics analysis of the elutant from the beads did not return ACE as a hit. This likely is the result of low abundance of ACE in the bacterial extract or due to ACE degradation by proteases present in the bacterial cell free extracts despite the addition of PMSF and the short time course of the incubation.

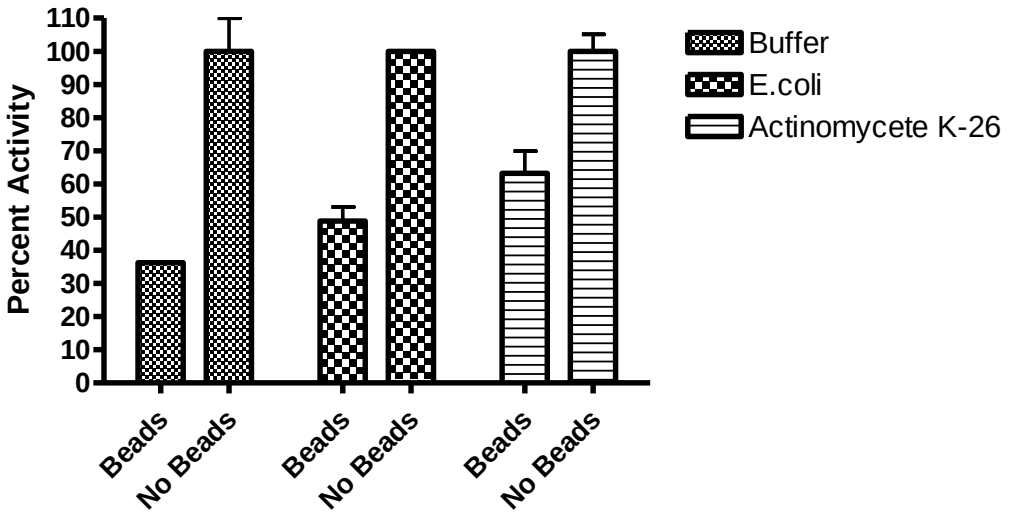

Figure IV-9. Depletion of activity of ACE spiked into buffer, *E.coli* or actinomycete K-26 cell free extract by the addition of the sepharose-K-26 probe (beads). ACE activity was monitored using the substrate FAPGG in samples in which the probe (IV-10) had been added (beads) and compared to a control sample where a volume of buffer had been added in place of the beads (no beads). All samples were incubated under identical conditions before ACE activity was measured. Activity of the no beads control was set to 100%.

Application of sepharose-K-26 (IV-10) in preliminary target ID experiments

The sepharose-K-26 probe (IV-10) was then applied in a preliminary target identification experiment using cell free extract from both *E. coli* and the K-26 producing organism. Our first attempt of a pull-down of was using cell free extract from *E. coli* with the goal of determining if the K-26 probe (IV-10) was able to target any enzymes in this cell free extract, particularly the *E. coli* dicarboxypeptidase (EcDCP) which has been characterized as a bacterial ACE-like enzyme[126] and to use these results as a possible control to eliminate non-specific enzymatic hits from future pull-down experiments. The experiment did not return results suggesting that EcDCP is a target for K-26, which is not surprising given the known low affinity of K-26 for EcDCP and furthermore did not reveal any potential K-26 target (Table IV-2).

Protein	Accession Number	MW kDa	Normalized Spectral Counts		Binding Ratio
			K-26 (-)	K-26 (+)	
30S ribosomal protein S1	RS1_ECOLI	61	26	17	1.53
DNA-directed RNA polymerase subunit beta	RPOB_ECOLI	151	17	11	1.55
Translation initiation factor IF-2	IF2_ECOLI	97	12	8	1.50
Pyruvate dehydrogenase E1 component	ODP1_ECOLI	100	11	7	1.57
DNA-directed RNA polymerase subunit beta	RPOC_ECOLI	155	11	6	1.83
Glycerophosphoryl diester phosphodiesterase	GLPQ_ECOLI	41	8	2	4.00
Uracil phosphoribosyltransferase	UPP_ECOLI	23	8	1	8.00
50S ribosomal protein L1	RL1_ECOLI	25	7	4	1.75
Chaperone protein htpG	HTPG_ECOLI	71	7	2	3.50
50S ribosomal protein L6	RL6_ECOLI	19	6	4	1.50
Transcription elongation protein nusA	NUSA_ECOLI	55	5	3	1.67
Enolase	ENO_ECOLI	46	5	1	5.00

Table IV-2: Hits from pull-down with sepharose-K-26 (IV-10) in *E.coli* cell free extract.

Next we carried out a pull-down experiment with actinomycete K-26 cell free extract, with the goal of determining the endogenous target of K-26 (IV-1), if any, and to glean information about the biosynthetic pathway of this small molecule. In the target ID experiments with actinomycete K-26 extract, to increase the probability of successfully targeting a protein of interest, we first determined that the actinomycete was indeed producing the small molecule K-26 (IV-1) using mass spectrometry.[49] The presence of K-26 (IV-1) in the liquid culture of the actinomycete would ensure that the enzymes responsible for the biosynthesis of this small molecule were being produced. Cell free extract from the actinomycete culture determined to produce K-26 (IV-1) was used in the target identification experiment. Despite the fact that K-26 was in known production by the actinomycete and 11 protein hits were identified in the experiment, no enzymes

were identified which have a discernible role in the biosynthesis of K-26 (IV-1) or an explainable role as a target (Table IV-3).

Protein	Accession Number	MW kDa	Normalized Spectral Counts		Binding Ratio
			K-26 (-)	K-26 (+)	
Cytosol aminopeptidase family, catalytic domain protein	pak26.polypeptide.98805.1 (+1)	49	7	3	2.33
response regulator	pak26.polypeptide.97571.2 (+1)	23	6	3	2
glutamine synthetase, type I	pak26.polypeptide.102241.1 (+1)	51	6	2	3
Xylose isomerase-like TIM barrel family protein	pak26.polypeptide.102749.1 (+1)	37	6	1	6
3-deoxy-7-phosphoheptulonate synthase	pak26.polypeptide.102496.1 (+1)	49	6	1	6
RibD C-terminal domain protein	pak26.polypeptide.98395.1 (+1)	21	5	2	2.5
hypothetical protein	pak26.polypeptide.99216.1 (+1)	116	5	2	2.5
isoleucyl-tRNA synthetase	pak26.polypeptide.100171.1 (+1)	116	5	1	5
pyruvate dehydrogenase e1 component, beta subunit (ec 1.2.4.1).	pak26.polypeptide.103166.1 (+1)	35	5	1	5
valyl-tRNA synthetase	pak26.polypeptide.101480.1 (+1)	95	5	1	5
amidotransferase) (gmp synthetase).	pak26.polypeptide.102625.1 (+1)	56	5	1	5

Table IV-3: Summary of proteomics hits for K-26 probe (IV-10) applied for target identification with actinomycete K-26 cell free extract.

Discussion

Target identification with a chemical probe based on the microbial natural product K-26 (IV-1) has presented several challenges. The development of the biotin-K-26 probe (IV-8) appeared to progress as expected as our untethered probe still retained

low nanomolar affinity for ACE. However, this probe was unexpectedly unable to pull ACE out of media even under a variety of incubation conditions and solution ionic strengths. Troubleshooting the system allowed us to come to the conclusion that the biotin-K-26 probe (IV-8) retains its ability to independently bind avidin and inhibit ACE; however this interaction is mutually exclusive.

As avidin does not affect the inhibitory effect of free K-26 (IV-1) on ACE, the mutually exclusive interaction of biotin-K-26 (IV-8) binding must not be due to potential charge-charge interactions between the K-26 (IV-1) and avidin. A literature search reveals an ACE affinity resin consisting of an avidin tethered biotinylated-lisinopril, which has been shown to similarly be unable to bind to ACE despite the high affinity of the biotin-lisinopril alone for ACE.[175] The shortcomings of this previously described biotinylated-lisinopril affinity resin are attributed to a linker of insufficient length. This 20 angstrom long linker is presumed to be too short to accommodate both of the deeply recessed binding sites which are located in a cleft on both avidin and in ACE. Our biotin-K-26 probe (IV-8), in contrast, contains 12 PEG units, giving the probe spacer arm an overall length of 56.0 angstroms, a length more than sufficient to reach the active sites of both ACE and avidin simultaneously when the probe is extended.

A computational modeling study does, however, suggest that PEG chains may hydrogen bond with water and form a helical structure.[181] If this is indeed the case, it would greatly reduce the overall length of the linker. If the linker length were reduced, it could perhaps be too short to extend into the recessed ACE active site after the biotin is bound to the avidin or streptavidin and potentially explain the obtained results. Regardless, as the biotin-PEG linker system used on this probe is a widely employed

system for small molecule target identification experiments the ineffectiveness of the biotin-K-26 probe to pull the ACE out of solution is unexpected given the mid-nanomolar inhibition by the free biotin-K-26 probe (IV-8), and inevitably led us to choose to develop an alternate affinity sepharose-K-26 probe (IV-10).

This sepharose-K-26 probe (IV-10) was found to be significantly more effective than the corresponding biotin-K-26 probe (IV-8) at targeting ACE spiked into buffer and media. However, this probe was not able to definitively pullout low abundance ACE spiked into a complex protein mixture of a cell free extract. As there are many other enzymes present it is possible that ACE was outcompeted for the binding sites on the probe. Also, it is presumed that ACE is degraded quickly as an unnaturally occurring enzyme in the cell free extract and with only a low abundance of the ACE spiked in initially, perhaps it is possible that only a small amount, less than the limits of detection of the spectral counting mass spectrometry experiment, was pulled out.

Target identification experiments using the sepharose-K-26 probe (IV-10) in the actinomycete K-26 extract also did not return any obvious hits for the small molecule target or biosynthetic enzymes. Interestingly, the isoleucyl tRNA synthetase 100171 is a shared hit from a previously carried out pyrophosphate exchange assay to identify biosynthetic enzymes in K-26.[182] Although recent literature has pointed to a role of tRNA synthetases in peptide bond formation of a phosphonate containing natural product, it is unclear at this time why this isoleucyl tRNA synthetase, would have an affinity for the phosphonate moiety of K-26.[183] Possibilities include that the isoleucyl tRNA synthetase may be a high abundance protein co-purifying with a lower abundance biosynthetic target, however previous experiments examining the gene cluster

containing the isoleucyl tRNA synthetase have all but eliminated those enzymes has having a role in K-26 biosynthesis.[182] Regardless, the endogenous target and biosynthesis of the fascinating metabolite, K-26 (IV-1), specifically of the biosynthetically unprecedented carbon-phosphorus linkage in the AHEP moiety remains elusive.

Materials and Methods

Chemical Synthesis

General Probe Synthesis

Reactions were carried out in oven or flame dried glassware. All solvents were reagent grade. Amino acids and peptide coupling agents were purchased from EMD or Bachem. All reagents were commercially available and used without purification unless specified otherwise. Purification was carried out using a Phenomonex C18 semi-preparative HPLC column on a Waters HPLC or a Thermo HPLC-MS instrument using a flow rate of 5 mL/min. Where possible, characterization was completed by NMR and HRMS. Quantitation of synthetic products were carried out using an attenuated time delay proton experiment (d1=15s) with dioxane or DMF added as an internal standard. NMR spectra were acquired on a Brucker DRX-400, AV-400, DRX-500, or AV-II-600 instrument. High resolution mass spectral data were acquired at Vanderbilt University by Cody Goodwin.

Synthesis of N-(N-acetyl-L-isoleucyl-L-tyrosyl)-1-(R)-amino-2-(4-hydroxyphenyl)ethyl phosphonic acid (K-26, IV-1)

Synthesis and HPLC purification was carried out as previously described.[50] The synthetic product was verified and quantitated by NMR.

Synthesis of N-(L-isoleucyl-L-tyrosyl)-1-(R)-amino-2-(4-hydroxyphenyl)ethyl phosphonic acid (dAcK-26, IV-3)

Synthesis and HPLC purification was carried out as previously described.[50] The synthetic product was verified and quantitated by NMR.

Synthesis of Biotin-PEG_{12}-K26 (IV-8)

N-(L-isoleucyl-L-tyrosyl)-1-*(R)*-amino-2-(4-hydroxyphenyl)ethyl phosphonic acid (dAcK-26 (IV-3), 939 μg,1.9 μmol) was dissolved in 3.6 mL of 100 mM phosphate buffer, pH=8.0. Under argon atmosphere, 45 μL of a biotin-PEG_{12}-NHS (250 mM, Pierce) dissolved in DMF was added. The reaction was stirred for 5 hours at room temperature. After reducing the volume in vaccuo the product was purified by HPLC-MS using a linear gradient of water to acetonitrile (ranging from 95:5 to 70:30 over 30 minutes) containing 10 mM ammonium acetate. Evaporation of the HPLC solvents yielded the product (31%, 776 μg). ^{1}H NMR spectra is included in Appendix F. ^{1}H NMR (600 MHz, D_2O) δ7.13 (dd, *J* = 13.3, 8.5 Hz, 4H), 6.76 (dd, *J* = 17.8, 8.5 Hz, 4H), 4.62-4.59 (m, 1H), 4.59-4.56 (m, 1H), 4.43-4.41 (m, 1H), 4.09-4.03 (m, 1H), 4.03 (d *J* = 8.6 Hz, 1H), 3.84-3.74 (m, 2H), 3.74-3.66 (m, 42 H), 3.66-3.61 (m, 5H), 3.42-3.39 (m, 2H), 3.35-3.31 (m, 1H), 3.24-3.18 (m, 1H), 3.16-3.11 (m, 1H), 3.01-2.98 (m, 1H), 2.67-2.60

(m, 2H), 2.56-2.44 (m, 2H), 2.30-2.67 (m, 2H), 1.77-1.70 (m, 1H), 1.70-1.55 (m, 4H), 1.47-1.40 (m, 2H), 1.23-1.18 (m, 1H), 1.01-0.94 (m, 1H), 0.79 (t, *J* = 7.3 Hz, 3H), 0.63 (d, *J* = 6.8 Hz, 3H); HRMS calculated for $C_{60}H_{101}N_6O_{22}PS$ ($M + 2H^+$) 660.3208, found 660.3320.

Functionalization of NeutrAvidin with biotin-PEG_{12}-K26 probe (IV-8)

A solution of Biotin-PEG_{12}-K-26 (IV-8) (0.758 mM, 100 µL) in 10 mM HEPES buffer (pH=7.5 with 30 mM KCl and 100 µM $ZnCl_2$) was incubated with 250 µL of Neutravidin beads and an additional 150 µL of HEPES buffer overnight at 4^{o}C with gentle mixing on a lab rotator. After the incubation, the beads were allowed to settle out of solution and the supernatant was removed. The beads were washed 5 times with cold HEPES buffer (750 µL) to remove any unbound probe, then stored at 4^{o}C in 250 µL of HEPES buffer as a 50% slurry.

Preparation of Sepharose-K26 (IV-10)

Preparation of sepharose-K-26 (IV-10) was carried out similarly to that of sepharose bound lisinopril, using free dAcK-26 (IV-3) in place of free lisinopril (IV-9),[176, 184-185] (Scheme IV-2). Specifically, epoxy activated sepharose 6B (0.5 g) was first washed with water (75 mL) in a sintered glass funnel. The swollen gel was mixed with N-(p-aminobenzoyl)-6-aminocaproic acid (90 mM) in 0.1 M NaOH (pH = 12.9, 2.5 mL) overnight at 45^{o}C. After blocking unreacted sites through a 4 hour incubation with ethanolamine (1M final concentration), the resin was washed with HCl (10 mM, 75 mL), dioxane (35 mL), and DMF (14 mL). The linker was then functionalized with an N-

hydrozysuccinimide through a 4 hour room temperature incubation with NHS (0.2 M final concentration) and diisopropylcarbodiimide (DIPCl, 0.2 M final conc) in DMF (2.5 mL). After washing the NHS activated sepharose (IV-15) with dioxane (35 mL), dAcK-26 (IV-3) (0.067 M) in 7.5 mL of sodium bicarbonate (0.1 M, pH = 10.2) was loaded onto sepharose by incubating the functionalized sepharose with the dAcK-26 (IV-3) for 16 hours at 4^{o}C under gentle agitation. After the incubation, the beads were washed with 150 mL of Tris (100 mM, pH = 7.5) buffer in a fritted funnel to ensure that all unbound dAcK-26 (IV-3) was removed. Washes were collected and the amount of dAcK-26 (IV-3) remaining was quantitated by NMR using an attenuated time delay proton experiment (d1=15s) with dioxane added as an internal standard to ensure that dAcK-26 (IV-3) was indeed coupling to the linker. Sepharose-K-26 (IV-10) was stored at 4^{o}C in 100 mM Tris buffer, which would aid in blocking unreacted N-hydroxysuccinimide sites on the linker.

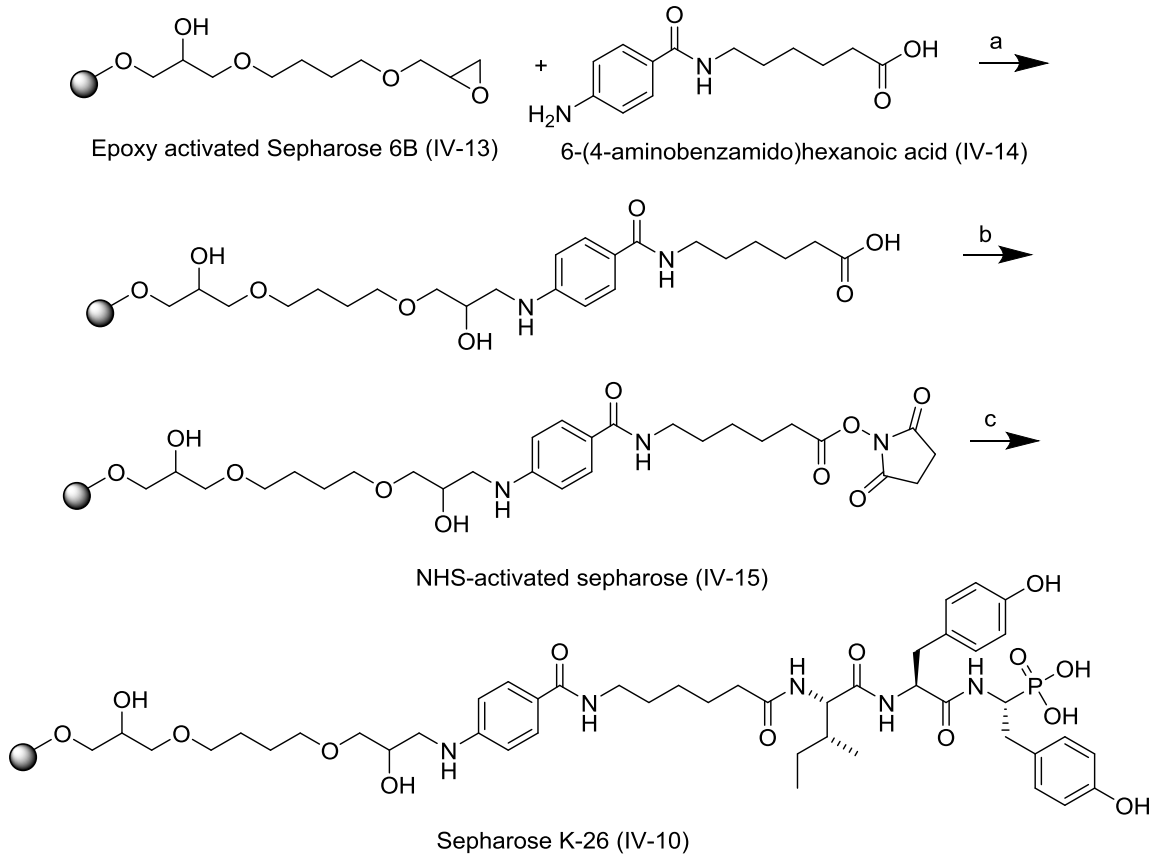

Scheme IV-2. Synthesis of sepharose K-26 (IV-10). a.1 M NaOH, pH 12.9, 45°C 16 hours. Unreacted sites blocked with ethanolamine then resin washed with HCl, water, dioxane and DMF. b. DMF, NHS, DIPCl, 2 hours, RT. c. dAcK-26, 100 mM $NaHCO_3$ pH 10.2, 4°C 16 hours.

Analysis of Biotin-PEG12-K-26 Probe (IV-8)

Determining IC_{50} of biotin-PEG_{12}-K-26 with somatic ACE with substrate FAPGG

Somatic ACE was extracted from rabbit lung acetone powder. Turnover of the substrate FAPGG was monitored in a 96-well plate in the presence of various concentrations of biotin-K-26 (IV-8) inhibitor by monitoring the corresponding change in absorbance at 340 nm as previously described.[127-128] IC_{50} was calculated by plotting the percent activity of the enzyme against the log of the concentration of the inhibitor.

Determining IC_{50} of biotin-PEG_{12}-K-26 with N- and C- domains of ACE with substrate Z-FHL

Z-FHL turnover by heterologously expressed N-domain and tACE in the presence of various concentrations of biotin-K-26 (IV-8) was monitored using fluorescence as previously described.[129-131] IC_{50} was calculated by plotting the percent activity of the enzyme against the log of the concentration of the inhibitor.

Evaluation of biotinylated probe affinity to avidin

The ability of the biotinylated probe to bind to avidin was performed essentially as previously described.[178] Briefly, the dye 4-Hydroxybenzene-2'-carboxylic acid (HABA) binds to avidin with a low dissociation constant, and its stoichiometric displacement by biotin can be followed by a change in absorbance at 450 nm. The binding experiments were performed in a total volume of 150 µL with a final concentration of 0.25 mg/mL Avidin and 1 mM HABA, with a range of different biotin concentrations.

Evaluation of the simultaneous binding of K-26 and avidin to the biotin-K-26 probe

The ability of the biotinylated probe to bind both avidin and heterologously expressed tACE G13 simultaneously was evaluated by pre-incubating various concentrations of either the biotin-K-26 probe or free K-26 with a 15-fold excess of avidin, followed by incubation with tACE G13. After the incubation, the catalytic activity of the tACE was evaluated using a fluorogenic assay with Z-FHL as substrate.[186]

Pull-downs with chemical probes

General pull-down procedure

The pull-downs were conducted using a batch method. To the two samples containing the desired proteins to be evaluated (1 mL, each) was added either K-26 (IV-1) (5 µM final concentration) or an equal volume of buffer. These samples were designated K-26 (+) and K-26 (-), respectively. An additional portion of the protein sample was retained for catalytic activity testing. These samples were allowed to incubate for 5 minutes on ice and then 50 µL of either the solid phase bound biotin-K-26 or streptavidin-K-26, or free biotin-K-26 (10 µL of 1 mg/mL probe, 0.758 mM) was added to both the K-26 (+) and the K-26 (-) sample. In the case where free biotin-K-26 was added, 50 µL of Neutravidin beads were added after an additional 5 minute incubation. The samples were incubated at 4^{o}C with gentle agitation, after which point the supernatant above the beads was removed and retained for catalytic activity testing and other analysis. The beads were washed three times with 500 µL portions of cold HEPES buffer (10 mM, pH=7.5 with 30 mM KCl and 100 µM $ZnCl_2$) to remove specifically bound proteins, centrifuging briefly (10 sec at 300 rpm) between each wash to hasten the settling of the beads in solution. After the last wash, residual solution was removed from the beads and then the beads were boiled in a portion of SDS-page loading buffer to denature bound proteins, which were analyzed by a coomassie stained gel, a western blot using polyclonal anti-C-domain antibodies, or through a mass spectrometry based spectral counting proteomics method. Retained solution samples were analyzed for ACE catalytic activity, with the rationale that the lower the catalytic activity, the less ACE that remained in the solution, by monitoring the turnover of either

the substrate Z-FHL or FAPGG using one of the previously described assays.

Pull-down of recombinanatly expressed tACE in media

General pull-down procedure was followed using samples of tissue culture media, spiked with approximately 5 µg/mL of tACE G13, a minimally glycosylated recombinant human ACE variant (tACE G13) with wild-type activity (expressed and purified as previously described.[187] After addition of the K-26 (IV-1) to block binding, the probe was added and the samples were incubated overnight at 4^{o}C. The pull-down was run in parallel with the previously described lisinopril-sepharose,[176] which was blocked with free lisinopril (IV-9) (5 µM total concentration) to give lisinopril (+) and lisinopril (-) samples. Supernatant samples were analyzed for ACE catalytic activity and both denatured bead samples and supernatant samples were analyzed via western blot.

Pull-down of recombinanatly expressed tACE under various ionic strengths

General pull-down procedure was followed using samples of tissue culture media containing NaCl (0 mM 300 mM, 600 mM or 1000 mM), spiked with approximately 5 µg/mL of tACE G13. Pull-down was conducted using both the sepharose K-26 probe (IV-10), with which K-26 (IV-1) was used to block binding, or lisinopril-sepharose (IV-11), which was blocked with free lisinopril (IV-9) (5 µM) as a control. Supernatant samples were analyzed for ACE catalytic activity and both the supernatant and the denatured bead samples were analyzed via a western blot.

Pull-down of recombinanatly expressed tACE with 1000 mM salt by both biotin-K-26 (IV-8) and sepharose-K-26 (IV-10)

General pull-down procedure was followed using samples of tissue culture media containing 1000 mM NaCl spiked with approximately 5 µg/mL of tACE G13. Pull-down was conducted using both the sepharose K-26 probe and biotin-K-26 functionalized Neutravidin, blocked with K-26 as a control (5 µM total concentration). Supernatant samples were analyzed for ACE catalytic activity and both the supernatant and denatured bead samples were analyzed via a western blot. The sepharose (+) and sepharose (-) samples were submitted to the Vanderbilt Proteomics core for analysis by a mass spectrometry spectral counting method.

Preparation of Astrosporangium hypotensionis extracts

The actinomycete K-26 was grown as previously described.[7] The K-26 production cultures were tested for K-26 production after 48, 60, 72, 84 and 96 hours of growth, to determine when the K-26 producing enzymes would be at their maximum levels. Relative K-26 levels were determined via mass spectrometry using Ile-Tyr-Tyr as an internal standard.[188] As K-26 production seemed to peak at 84 hours, 2 g of cells from that time point were used to prepare the lysate for the target identification experiment. The given mass of cells were resuspended in 20 mL of cold Tris buffer (50 mM, pH = 7.5, 100 mM NaCl) and lysed by French press with 1 mM PMSF.

Application of probe with bacterial extracts

Prepared bacterial extracts (1 mL), with spiked in tACE (2.5 ng/mL) either spiked

with free K-26 (IV-1) (5 µM) or buffer (50 mM Tris buffer, pH = 7.5 with 300 mM NaCl). An additional portion of the protein sample was retained for catalytic activity testing. After mixing and incubating on ice for 5 minutes, sepharose-K-26 (IV-10) was added (50 µL). The bead slurry was mixed with the extract on an end over end lab rotator at 4^{o}C for 30 minutes, to reduce non-specific binding, after which point the supernatant was removed. After briefly centrifuging, the supernatant was removed and retained for analysis. The beads were washed with 3 x 500 µL of cold HEPES buffer (10 mM, pH=7.5 with 30 mM KCl and 100 µM $ZnCl_2$) buffer, centrifuging between washes. The beads were denatured by boiling in SDS loading buffer and the resulting denatured proteins were run on a 10% SDS- page gel. Retained protein samples and supernatants were analyzed for catalytic ACE activity using FAPGG as a substrate in a previously described assay. Bead samples were submitted to the Vanderbilt proteomics core for analysis via a mass spectroscopy based spectral counting method to identify specific proteins bound under the project ID 3230 and 3632

Quantitative Proteomics Analysis

Shotgun proteomic analysis of filtrate was performed by first resolving eluted proteins approximately 1cm using a 10% Novex precast gel, and then performing in-gel tryptic digestion to recover peptides. Resulting peptides were analyzed by a 70 minute data dependent LC-MS/MS analysis. Briefly, peptides were autosampled onto a 200 mm by 0.1 mm (Jupiter 3 micron, 300A), self-packed analytical column coupled directly to an LTQ (ThermoFisher) using a nanoelectrospray source and resolved using an aqueous to organic gradient. A series of a full scan mass spectrum followed by 5 data-

dependent tandem mass spectra (MS/MS) was collected throughout the run and dynamic exclusion was enabled to minimize acquisition of redundant spectra. MS/MS spectra were searched via SEQUEST against either an *E .coli* or *Astrosporangium hypotensionis* database that also contained reversed version for each of the entries. (http://www.ncbi.nlm.nih.gov/pubmed/7741214). Identifications were filtered and collated into spectral count numbers at the protein level using Scaffold (Proteome Software)

Acknowledgements

This work was only possible due to our collaborators in the Sturrock lab at University of Cape Town. J. Albert Abrie has conducted several of the pull-down experiments with recombinantly expressed tACE. Both J. Albert Abrie and E.D. Sturrock have provided input with regards to troubleshooting and experimental design. Hayes McDonald in the Vanderbilt proteomic core has also kindly provided guidance and insight into pull-down controls and spectral counting proteomic analysis. Lastly, Brian O. Bachmann has provided an immense amount of insight, feedback and guidance along the entire course of this study.

CHAPTER V

FUTURE DIRECTIONS

Natural products are a rich source of pharmaceutically active molecules. The K-26 family of microbial metabolites is a class of natural products which are among the most potent natural product inhibitors of human ACE. This pharmacologically relevant enzyme consists of two tissue specific isoforms, the single domain testicular ACE and somatic ACE which is comprised of two domains, each with differing physiological roles in processes including blood pressure, fluid balance and fibrosis regulation. In the previous chapters of this dissertation, research centered around the K-26 family of potent ACE-inhibitors has been described.

Structural activity studies of K-26 and related tripeptides were facilitated by the crystal structures of K-26 in both domains of a heterologously expressed mammalian ACE construct. These structures reveal that K-26 adopts an unusual binding motif in the active site of the enzyme, occupying only the non-prime binding pockets, making this metabolite a unique and interesting subject for ACE inhibitor design and study. Naturally occurring members of the K-26 family and a set of selected AHEP containing tripeptides from a computational modeling experiment of 400 of these tripeptides have been synthesized and evaluated for somatic ACE inhibition. Of all analogs evaluated, K-26 is still taken to be the most potent AHEP containing ACE inhibitor. Imminent studies on the ACE inhibitory properties will give more relevant data pertaining to the domain selectivity of these variants.

Interestingly, K-26 has been established to exhibit selectivity for mammalian ACE. This microbial natural product is not a potent inhibitor of closely related ACE-like enzymes that have been studied from bacterial sources, an unexpected result given the high sequence similarity between mammalian and bacterial ACE-like enzymes. The widely prescribed and pharmacologically relevant ACE inhibitor captopril, however, is a potent inhibitor of these bacterial ACE-like enzymes.

Furthermore two chemical probes have been developed using K-26 by using heterologously expressed ACE to validate the probes. The first of these affinity probes, a biotin based probe, was determined to be a potent nanomolar inhibitor ACE. This probe, however, was ineffective at pulling ACE out of solution as there seems to be a mutually exclusive relationship between binding the solid phase streptavidin and the target ACE. A K-26 affinity probe tethered directly to a solid phase sepharose was deemed to be more effective through validation with overexpressed mammalian ACE. This chemical probe was applied in a preliminary pull-down experiment to glean information about a possible endogenous target or biosynthetic enzymes responsible for assembly of the AHEP moiety with inconclusive results.

Despite these and previous studies on K-26, many questions remain about this fascinating small molecule. These questions, along with potential approaches for furthering research on this small molecule, will be discussed in the following paragraphs.

The structural activity studies conducted in this dissertation have only begun to examine the potential structural modifications to K-26 that could aid in the design of inhibitors with increased potency and domain selectivity to human ACE. As K-26 only occupies

the S1, S2 and S3 binding pockets, one approach would be to design inhibitors that build off of the tripeptidic K-26 scaffold. This could be accomplished by building off of either the N-terminus of K-26 or the phosphonate in AHEP. This extended inhibitor would utilize additional binding pockets within the active site of ACE. Also, as only naturally occurring amino acids were used in this study, incorporating non-proteogenic amino acids into the tripeptidic structure of K-26 may be a fruitful outlet for more potent and selective inhibitor design.

The synthesis and purification of K-26 and other AHEP containing tripeptides has been a challenge of this research. Due to the limitations of the current synthetic approach, the development of a method for the enantoselective synthesis of AHEP or for the attachment of AHEP onto the solid phase for solid phase peptide synthesis would undoubtedly simply the process. Additionally, discovery of the biosynthetic process for AHEP and K-26 may allow for biosynthetic methods to be adopted. Any study which would rely on the synthesis of K-26 and variants would be expedited and this would make larger and more diverse libraries of these AHEP based molecules obtainable.

Aside from the pharmacological applications of this ACE inhibitory peptide, two interesting, but large, questions remain unanswered about K-26: How this small molecule made and what is its function in nature? The chemical probe developed in this study was applied in preliminary experiments with cell free extract of the actinomycete, with the goal of beginning to shed light on some of these important questions. Despite the high affinity of K-26 for mammalian ACE and the probe validation with ACE, no enzymes were unambiguously identified from the actinomycete that would logically have a role in either the biosynthesis of AHEP or as an endogenous

target. It would be reasonable to conclude that our possible target of interest is expressed at low levels by the actinomycete, especially given the low production levels of the small molecule K-26 by the actinomycete. This may render the affinity probe ineffective as it is not capable of capturing enough of the target enzyme for proteomics analysis. This could be remedied in two ways: the abundance of the target can be increased or the probe can be made more effective.

One approach would be to modify the actinomycete culture conditions to increase the production levels of K-26. This increase in K-26 would likely be associated with a corresponding increase in the levels of relevant biosynthetic enzymes, raising the likelihood that our probe will bind these enzymes in high enough abundance to return a proteomics hit. Furthermore, to aid in the identification of lower abundance proteins, the knowledge gained from the development of our current affinity probe could be applied to generate a similar covalently binding chemical probe. A probe of this type could make use of an aryl azide, diazarine or benzophenone functionality. [189] In particular, an aliphatic diazarine may be a favorable option to consider for incorporation in place of the isoleucine in K-26.[190-191] When exposed to UV light, the generated radical would form a covalent linkage with a functionality present in the active site of the enzyme, irreversibly tethering the enzyme target to the probe. This would allow for the capture and identification of low abundance proteins or protein targets with lower affinity for the chemical probe.

Due to this covalent linkage, the enzymatic target of the K-26 probe could be denatured before pulling out of solution. This would possibly be an effective method to eliminate the mutually exclusive binding relationship which was apparent with the biotin

K-26 affinity probe. Therefore, biotin may remain a suitable choice in covalent binding K-26 probe design. The use of biotin in chemical probe design has associated benefits, such as the potential for cell permeability of the probe and the ability to utilize the streptavidin-biotin relationship for identification and purification of the target. [170] Undoubtedly, this would increase the likelihood of an unambiguous proteomics hit, raising the chance of success of these experiments.[192-193]

In this study, the N-acetyl portion of the molecule was chosen for the placement of the handle in chemical probe development. This would allow the AHEP portion and phosphonic acid to be unhindered and to presumably interact with the biosynthetic machinery responsible for its assembly. Attachment of the handle to a different portion of K-26 may render the probe capable of capturing biosynthetic enzymes and enzymatic targets that interact with other regions of this natural product.

Furthermore, any chemical probe based on K-26 could be broadly applied to a wide range of organisms in environmental target identification experiments. However, a study of this sort may be challenging without additional information about potential organisms that the actinomycete K-26 commonly co-inhabits with in the environment.

REFERENCES

1. Newman, D. J.; Cragg, G. M., Natural products as sources of new drugs over the 30 years from 1981 to 2010. *J Nat Prod* **2012,** *75*, 311-35.

2. Shen, X. Z.; Ong, F. S.; Bernstein, E. A.; Janjulia, T.; Blackwell, W. L.; Shah, K. H.; Taylor, B. L.; Gonzalez-Villalobos, R. A.; Fuchs, S.; Bernstein, K. E., Nontraditional roles of angiotensin-converting enzyme. *Hypertension* **2012,** *59*, 763-8.

3. CDC High blood pressure facts. http://www.cdc.gov/bloodpressure/facts.htm (accessed June 15, 2014).

4. WHO A global brief on hypertension: Silent killer, global public health crisis. http://www.who.int/cardiovascular_diseases/publications/global_brief_hypertension/en/ (accessed July 1, 2014).

5. Morimoto, T.; Gandhi, T. K.; Fiskio, J. M.; Seger, A. C.; So, J. W.; Cook, E. F.; Fukui, T.; Bates, D. W., An evaluation of risk factors for adverse drug events associated with angiotensin-converting enzyme inhibitors. *J Eval Clin Pract* **2004,** *10*, 499-509.

6. Dictionary of Natural Products. http://dnp.chemnetbase.com.

7. Yamato, M.; Koguchi, T.; Okachi, R.; Yamada, K.; Nakayama, K.; Kase, H.; Karasawa, A.; Shuto, K., K-26, a novel inhibitor of angiotensin I converting enzyme produced by an actinomycete K-26. *J Antibiot (Tokyo)* **1986,** *39*, 44-52.

8. Nakagomi, K.; Ebisu, H.; Sadakane, Y.; Fujii, N.; Akizawa, T.; Tanimura, T., Properties and human origin of two angiotensin-I-converting enzyme inhibitory peptides isolated from a tryptic hydrolysate of human serum albumin. *Biol Pharm Bull* **2000,** *23*, 879-83.

9. Nakagomi, K.; Fujimura, A.; Ebisu, H.; Sakai, T.; Sadakane, Y.; Fujii, N.; Tanimura, T., Acein-1, a novel angiotensin-I-converting enzyme inhibitory peptide isolated from tryptic hydrolysate of human plasma. *FEBS Lett* **1998,** *438*, 255-7.

10. Nakagomi, K.; Yamada, R.; Ebisu, H.; Sadakane, Y.; Akizawa, T.; Tanimura, T., Isolation of acein-2, a novel angiotensin-I-converting enzyme inhibitory peptide derived from a tryptic hydrolysate of human plasma. *FEBS Lett* **2000,** *467*, 235-8.

11. Kohama, Y.; Matsumoto, S.; Oka, H.; Teramoto, T.; Okabe, M.; Mimura, T., Isolation of angiotensin-converting enzyme inhibitor from tuna muscle. *Biochem Biophys Res Commun* **1988,** *155*, 332-7.

12. Kohama, Y.; Oka, H.; Matsumoto, S.; Nakagawa, T.; Miyamoto, T.; Mimura, T.; Nagase, Y.; Satake, M.; Takane, T.; Fujita, T., Biological properties of angiotensin-converting enzyme inhibitor derived from tuna muscle. *J Pharmacobiodyn* **1989,** *12*, 566-71.

13. Matsumura, N.; Fujii, M.; Takeda, Y.; Shimizu, T., Isolation and characterization of angiotensin I-converting enzyme inhibitory peptides derived from bonito bowels. *Biosci Biotechnol Biochem* **1993,** *57*, 1743-4.

14. Matsumura, N.; Fujii, M.; Takeda, Y.; Sugita, K.; Shimizu, T., Angiotensin I-converting enzyme inhibitory peptides derived from bonito bowels autolysate. *Biosci Biotechnol Biochem* **1993,** *57*, 695-7.

15. Ferreira, L. A.; Henriques, O. B.; Lebrun, I.; Batista, M. B.; Prezoto, B. C.; Andreoni, A. S.; Zelnik, R.; Habermehl, G., A new bradykinin-potentiating peptide (peptide P) isolated from the venom of Bothrops jararacussu (jararacucu tapete, urutu dourado). *Toxicon* **1992,** *30*, 33-40.

16. Kato, H.; Suzuki, T., Bradykinin-potentiating peptides from the venom of Agkistrodon halys blomhoffi. Isolation of five bradykinin potentiators and the amino acid sequences of two of them, potentiators B and C. *Biochemistry* **1971,** *10*, 972-80.

17. Komori, Y.; Sugihara, H., Purification and physiological study of a hypotensive factor from the venom of Vipera aspis aspis (aspic viper). *Toxicon* **1990,** *28*, 359-69.

18. Hyoung Lee, D.; Ho Kim, J.; Sik Park, J.; Jun Choi, Y.; Soo Lee, J., Isolation and characterization of a novel angiotensin I-converting enzyme inhibitory peptide derived from the edible mushroom Tricholoma giganteum. *Peptides* **2004,** *25*, 621-7.

19. Jang, J. H.; Jeong, S. C.; Kim, J. H.; Lee, Y. H.; Ju, Y. C.; Lee, J. S., Characterisation of a new antihypertensive angiotensin I-converting enzyme inhibitory peptide from Pleurotus cornucopiae. *Food Chem* **2011,** *127*, 412-8.

20. Huang, W. Y.; Davidge, S. T.; Wu, J., Bioactive natural constituents from food sources-potential use in hypertension prevention and treatment. *Crit Rev Food Sci Nutr* **2013,** *53*, 615-30.

21. Murray, B. A.; Fitzgerald, R. J., Angiotensin converting enzyme inhibitory peptides derived from food proteins: biochemistry, bioactivity and production. *Curr Pharm Des* **2007,** *13*, 773-91.

22. Morigiwa, A.; Kitabatake, K.; Fujimoto, Y.; Ikekawa, N., Angiotensin converting enzyme-inhibitory triterpenes from Ganoderma lucidum. *Chem Pharm Bull (Tokyo)* **1986,** *34*, 3025-8.

23. Boh, B.; Berovic, M.; Zhang, J.; Zhi-Bin, L., Ganoderma lucidum and its pharmaceutically active compounds. *Biotechnol Annu Rev* **2007,** *13*, 265-301.

24. Somanadhan, B.; Smitt, U. W.; George, V.; Pushpangadan, P.; Rajasekharan, S.; Duus, J. O.; Nyman, U.; Olsen, C. E.; Jaroszewski, J. W., Angiotensin converting enzyme (ACE) inhibitors from Jasminum azoricum and Jasminum grandiflorum. *Planta Med* **1998,** *64*, 246-50.

25. Hansen, K.; Adsersen, A.; Christensen, S. B.; Jensen, S. R.; Nyman, U.; Smitt, U. W., Isolation of an angiotensin converting enzyme (ACE) inhibitor from Olea europaea and Olea lancea. *Phytomedicine* **1996,** *2*, 319-25.

26. Ando, T.; Okada, S.; Uchida, I.; Hemmi, K.; Nishikawa, M.; Tsurumi, Y.; Fujie, A.; Yoshida, K.; Okuhara, M., WF-10129, a novel angiotensin converting enzyme inhibitor produced by a fungus, Doratomyces putredinis. *J Antibiot (Tokyo)* **1987,** *40*, 468-75.

27. Baldwin, J. E., Adlington, R. M., Andrew, R. T., Smith M. L., Carbon based mucleophilic ring opening of activated monocyclic B-lactams; Synthesis and sterochemical assignment of the ACE inhibitor WF-10129. *Tetrahedron* **1995,** *51*, 4733-4762.

28. Bush, K.; Henry, P. R.; Souser-Woehleke, M.; Trejo, W. H.; Slusarchyk, D. S., Phenacein--an angiotensin-converting enzyme inhibitor produced by a streptomycete. I. Taxonomy, fermentation and biological properties. *J Antibiot (Tokyo)* **1984,** *37*, 1308-12.

29. Liu, W. C.; Parker, W. L.; Brandt, S. S.; Atwal, K. S.; Ruby, E. P., Phenacein--an angiotensin-converting enzyme inhibitor produced by a streptomycete. II. Isolation, structure determination and synthesis. *J Antibiot (Tokyo)* **1984,** *37*, 1313-9.

30. Nakatsukasa, W. M.; Wilgus, R. M.; Thomas, D. N.; Mertz, F. P.; Boeck, L. D., Angiotensin converting enzyme inhibitors produced by Streptomyces chromofuscus. Discovery, taxonomy and fermentation. *J Antibiot (Tokyo)* **1985,** *38*, 997-1002.

31. Mynderse, J. S.; Samlaska, S. K.; Fukuda, D. S.; Du Bus, R. H.; Baker, P. J., Isolation of A58365A and A58365B, angiotensin converting enzyme inhibitors produced by Streptomyces chromofuscus. *J Antibiot (Tokyo)* **1985,** *38*, 1003-7.

32. Umezawa, H.; Aoyagi, T.; Ogawa, K.; Obata, T.; Iinuma, H.; Naganawa, H.; Hamada, M.; Takeuchi, T., Foroxymithine, a new inhibitor of angiotensin-converting enzyme, produced by actinomycetes. *J Antibiot (Tokyo)* **1985,** *38*, 1813-5.

33. Huang, L.; Albers-Schonberg, G.; Monaghan, R. L.; Jakubas, K.; Pong, S. S.; Hensens, O. D.; Burg, R. W.; Ostlind, D. A.; Conroy, J.; Stapley, E. O., Discovery, production and purification of the Na+, K+ activated ATPase inhibitor, L-681,110 from the fermentation broth of Streptomyces sp. MA-5038. *J Antibiot (Tokyo)* **1984,** *37*, 970-5.

34. Hensens, O. D.; Liesch, J. M., Structure elucidation of angiotensin converting enzyme inhibitor L-681,176 from Streptomyces sp. MA 5143a. *J Antibiot (Tokyo)* **1984,** *37*, 466-8.

35. Kodani, S.; Ohnishi-Kameyama, M.; Yoshida, M.; Ochi, K., A New Siderophore Isolated from Streptomyces sp TM-34 with Potent Inhibitory Activity Against Angiotensin-Converting Enzyme. *Euro J Org Chem* **2011**, 3191-3196.

36. Kido, Y.; Hamakado, T.; Yoshida, T.; Anno, M.; Motoki, Y.; Wakamiya, T.; Shiba, T., Isolation and characterization of ancovenin, a new inhibitor of angiotensin I converting enzyme, produced by actinomycetes. *J Antibiot (Tokyo)* **1983,** *36*, 1295-9.

37. Wakamiya, T.; Ueki, Y.; Shiba, T.; Kido, Y.; Motoki, Y., The Structure of Ancovenin, a New Peptide Inhibitor of Angiotensin-I Converting Enzyme. *Tetrahedron Lett* **1985,** *26*, 665-668.

38. Singh, P. D.; Johnson, J. H., Muraceins--muramyl peptides produced by Nocardia orientalis as angiotensin-converting enzyme inhibitors. II. Isolation and structure determination. *J Antibiot (Tokyo)* **1984,** *37*, 336-43.

39. Bush, K.; Henry, P. R.; Slusarchyk, D. S., Muraceins--muramyl peptides produced by Nocardia orientalis as angiotensin-converting enzyme inhibitors. I. Taxonomy, fermentation and biological properties. *J Antibiot (Tokyo)* **1984,** *37*, 330-5.

40. Ishida, K.; Kato, T.; Murakami, M.; Watanabe, M.; Watanabe, M. F., Microginins, zinc metalloproteases inhibitors from the cyanobacterium Microcystis aeruginosa. *Tetrahedron* **2000,** *56*, 8643-8656.

41. Kodani, S.; Suzuki, S.; Ishida, K.; Murakami, M., Five new cyanobacterial peptides from water bloom materials of lake Teganuma (Japan). *FEMS Microbiology Letters* **1999,** *178*, 343-348.

42. Kraft, M.; Schleberger, C.; Weckesser, J.; Schulz, G. E., Binding structure of the leucine aminopeptidase inhibitor microginin FR1. *FEBS Letters* **2006,** *580*, 6943-6947.

43. Matsuura, F.; Hamada, Y.; Shioiri, T., Total Synthesis of Microginin, an Angiotensin-Converting Enzyme-Inhibitory Pentapeptide from the Blue-Green-Alga Microcystis-Aeruginosa. *Tetrahedron* **1994,** *50*, 11303-11314.

44. Neumann, U.; Forchert, A.; Flury, T.; Weckesser, J., Microginin FR1, a linear peptide from a water bloom of Microcystis species. *FEMS Microbiology Letters* **1997,** *153*, 475-478.

45. Okino, T.; Matsuda, H.; Murakami, M.; Yamaguchi, K., Microginin, an Angiotensin-Converting Enzyme-Inhibitor from the Blue-Green-Alga Microcystis-Aeruginosa. *Tetrahedron Lett* **1993,** *34*, 501-504.

46. Kase, H.; Kaneko, M.; Yamada, K., K-13, a novel inhibitor of angiotensin I converting enzyme produced by Micromonospora halophytica subsp. exilisia. I. Fermentation, isolation and biological properties. *J Antibiot (Tokyo)* **1987,** *40*, 450-4.

47. Yasuzawa, T.; Shirahata, K.; Sano, H., K-13, a novel inhibitor of angiotensin I converting enzyme produced by Micromonospora halophytica subsp. exilisia. II. Structure determination. *J Antibiot (Tokyo)* **1987,** *40*, 455-8.

48. Hirayama, N.; Kasai, M.; Shirahata, K., Structure and conformation of a novel inhibitor of angiotensin I converting enzyme--a tripeptide containing phosphonic acid. *Int J Pept Protein Res* **1991,** *38*, 20-4.

49. Ntai, I.; Manier, M. L.; Hachey, D. L.; Bachmann, B. O., Biosynthetic origins of C-P bond containing tripeptide K-26. *Org Lett* **2005,** *7*, 2763-5.

50. Ntai, I.; Bachmann, B. O., Identification of ACE pharmacophore in the phosphonopeptide metabolite K-26. *Bioorg Med Chem Lett* **2008,** *18*, 3068-71.

51. Ohuchi, I.; Kurihara, K.; Shinohara, A.; Takei, T.; Yoshida, J.; Amano, S.; Miyadoh, S.; Matsuhashi, Y.; Shomure, T.; Sezaki, M., Studies on new angiotensin converting enzyme inhibitors, SF2513 A, B and C, Produced by *Streptosporangium nondiastaticum*. *Sci. Reports of Meiji Seiki Kaisha* **1988,** *27*, 46-54.

52. Koguchi, T.; Yamada, K.; Yamato, M.; Okachi, R.; Nakayama, K.; Kase, H., K-4, a novel inhibitor of angiotensin I converting enzyme produced by Actinomadura spiculosospora. *J Antibiot (Tokyo)* **1986,** *39*, 364-71.

53. Kido, Y.; Hamakado, T.; Anno, M.; Miyagawa, E.; Motoki, Y.; Wakamiya, T.; Shiba, T., Isolation and characterization of I5B2, a new phosphorus containing inhibitor of angiotensin I converting enzyme produced by Actinomadura sp. *J Antibiot (Tokyo)* **1984,** *37*, 965-9.

54. Hidaka, T.; Shimotohno, K. W.; Morishita, T.; Seto, H., Studies on the biosynthesis of bialaphos (SF-1293). 18. 2-phosphinomethylmalic acid synthase: a descendant of (R)-citrate synthase? *J Antibiot (Tokyo)* **1999,** *52*, 925-31.

55. Mirakhur, A.; Gallagher, M. J.; Ledson, M. J.; Hart, C. A.; Walshaw, M. J., Fosfomycin therapy for multiresistant Pseudomonas aeruginosa in cystic fibrosis. *J Cyst Fibros* **2003,** *2*, 19-24.

56. Morikawa, K.; Nonaka, M.; Yoshikawa, Y.; Torii, I., Synergistic effect of fosfomycin and arbekacin on a methicillin-resistant Staphylococcus aureus-induced biofilm in a rat model. *Int J Antimicrob Agents* **2005,** *25*, 44-50.

57. Tempera, G.; Mirabile, M.; Mangiafico, A.; Caccamo, M.; Bonfiglio, G., Fosfomycin tromethamine in uncomplicated urinary tract infections: an epidemiological survey. *J Chemother* **2004,** *16*, 216-7.

58. Wiesner, J.; Borrmann, S.; Jomaa, H., Fosmidomycin for the treatment of malaria. *Parasitol Res* **2003,** *90 Suppl 2*, S71-6.

59. Metcalf, W. W.; Van Der Donk, W. A., Biosynthesis of phosphonic and phosphinic acid natural products. *Annu Rev Biochem* **2009,** *78*, 65-94.

60. Freeman, S.; Seidel, H. M.; Schwalbe, C. H.; Knowles, J. R., Phosphonate Biosynthesis - the Stereochemical Course of Phosphoenolpyruvate Phosphomutase. *Journal of the American Chemical Society* **1989,** *111*, 9233-9234.

61. Mcqueney, M. S.; Lee, S. L.; Swartz, W. H.; Ammon, H. L.; Mariano, P. S.; Dunawaymariano, D., Evidence for an Intramolecular, Stepwise Reaction Pathway for Pep Phosphomutase Catalyzed P-C Bond Formation. *Journal of Organic Chemistry* **1991,** *56*, 7121-7130.

62. Liu, S. J.; Lu, Z. B.; Jia, Y.; Dunaway-Mariano, D.; Herzberg, O., Dissociative phosphoryl transfer in PEP mutase catalysis: Structure of the enzyme/sulfopyruvate complex and kinetic properties of mutants. *Biochemistry* **2002,** *41*, 10270-10276.

63. Ntai, I.; Phelan, V. V.; Bachmann, B. O., Phosphonopeptide K-26 biosynthetic intermediates in Astrosporangium hypotensionis. *Chem Commun (Camb)* **2006**, 4518-20.

64. Skeggs, L. T., Jr., Discovery of the two angiotensin peptides and the angiotensin converting enzyme. *Hypertension* **1993,** *21*, 259-60.

65. Skeggs, L. T., Jr.; Kahn, J. R.; Shumway, N. P., The preparation and function of the hypertensin-converting enzyme. *J Exp Med* **1956,** *103*, 295-9.

66. Bernstein, K. E.; Martin, B. M.; Edwards, A. S.; Bernstein, E. A., Mouse angiotensin-converting enzyme is a protein composed of two homologous domains. *J Biol Chem* **1989,** *264*, 11945-51.

67. Soubrier, F.; Alhenc-Gelas, F.; Hubert, C.; Allegrini, J.; John, M.; Tregear, G.; Corvol, P., Two putative active centers in human angiotensin I-converting enzyme revealed by molecular cloning. *Proc Natl Acad Sci U S A* **1988,** *85*, 9386-90.

68. Cushman, D. W.; Cheung, H. S., Concentrations of angiotensin-converting enzyme in tissues of the rat. *Biochim Biophys Acta* **1971,** *250*, 261-5.

69. El-Dorry, H. A.; Bull, H. G.; Iwata, K.; Thornberry, N. A.; Cordes, E. H.; Soffer, R. L., Molecular and catalytic properties of rabbit testicular dipeptidyl carboxypeptidase. *J Biol Chem* **1982,** *257*, 14128-33.

70. Das, M.; Hartley, J. L.; Soffers, R. L., Serum angiotensin-converting enzyme. Isolation and relationship to the pulmonary enzyme. *J Biol Chem* **1977,** *252*, 1316-9.

71. Wei, L.; Alhenc-Gelas, F.; Soubrier, F.; Michaud, A.; Corvol, P.; Clauser, E., Expression and characterization of recombinant human angiotensin I-converting enzyme. Evidence for a C-terminal transmembrane anchor and for a proteolytic processing of the secreted recombinant and plasma enzymes. *J Biol Chem* **1991,** *266*, 5540-6.

72. Naim, H. Y., Angiotensin-converting enzyme of the human small intestine. Subunit and quaternary structure, biosynthesis and membrane association. *Biochem J* **1992,** *286 (Pt 2)*, 451-7.

73. Allinson, T. M.; Parkin, E. T.; Condon, T. P.; Schwager, S. L.; Sturrock, E. D.; Turner, A. J.; Hooper, N. M., The role of ADAM10 and ADAM17 in the ectodomain shedding of angiotensin converting enzyme and the amyloid precursor protein. *Eur J Biochem* **2004,** *271*, 2539-47.

74. Oppong, S. Y.; Hooper, N. M., Characterization of a secretase activity which releases angiotensin-converting enzyme from the membrane. *Biochem J* **1993,** *292 (Pt 2)*, 597-603.

75. Parkin, E. T.; Turner, A. J.; Hooper, N. M., Secretase-mediated cell surface shedding of the angiotensin-converting enzyme. *Protein Pept Lett* **2004,** *11*, 423-32.

76. Bernstein, K. E.; Ong, F. S.; Blackwell, W. L.; Shah, K. H.; Giani, J. F.; Gonzalez-Villalobos, R. A.; Shen, X. Z.; Fuchs, S.; Touyz, R. M., A modern understanding of the traditional and nontraditional biological functions of angiotensin-converting enzyme. *Pharmacol Rev* **2013,** *65*, 1-46.

77. Bernstein, K. E.; Shen, X. Z.; Gonzalez-Villalobos, R. A.; Billet, S.; Okwan-Duodu, D.; Ong, F. S.; Fuchs, S., Different in vivo functions of the two catalytic domains of angiotensin-converting enzyme (ACE). *Curr Opin Pharmacol* **2011,** *11*, 105-11.

78. Gonzalez-Villalobos, R. A.; Shen, X. Z.; Bernstein, E. A.; Janjulia, T.; Taylor, B.; Giani, J. F.; Blackwell, W. L.; Shah, K. H.; Shi, P. D.; Fuchs, S.; Bernstein, K. E., Rediscovering ACE: novel insights into the many roles of the angiotensin-converting enzyme. *J Mol Med (Berl)* **2013,** *91*, 1143-54.

79. Zou, K.; Maeda, T.; Watanabe, A.; Liu, J.; Liu, S.; Oba, R.; Satoh, Y.; Komano, H.; Michikawa, M., Abeta42-to-Abeta40- and angiotensin-converting activities in different domains of angiotensin-converting enzyme. *J Biol Chem* **2009,** *284*, 31914-20.

80. Eckman, E. A.; Adams, S. K.; Troendle, F. J.; Stodola, B. A.; Kahn, M. A.; Fauq, A. H.; Xiao, H. D.; Bernstein, K. E.; Eckman, C. B., Regulation of steady-state beta-amyloid levels in the brain by neprilysin and endothelin-converting enzyme but not angiotensin-converting enzyme. *J Biol Chem* **2006,** *281*, 30471-8.

81. Wolozin, B.; Bednar, M. M., Interventions for heart disease and their effects on Alzheimer's disease. *Neurol Res* **2006,** *28*, 630-6.

82. Rousseau, A.; Michaud, A.; Chauvet, M. T.; Lenfant, M.; Corvol, P., The hemoregulatory peptide N-acetyl-Ser-Asp-Lys-Pro is a natural and specific substrate of the N-terminal active site of human angiotensin-converting enzyme. *J Biol Chem* **1995,** *270*, 3656-61.

83. Bonnet, D.; Lemoine, F. M.; Khoury, E.; Pradelles, P.; Najman, A.; Guigon, M., Reversible inhibitory effects and absence of toxicity of the tetrapeptide acetyl-N-Ser-Asp-Lys-Pro (AcSDKP) in human long-term bone marrow culture. *Exp Hematol* **1992,** *20*, 1165-9.

84. Liao, T. D.; Yang, X. P.; D'ambrosio, M.; Zhang, Y.; Rhaleb, N. E.; Carretero, O. A., N-acetyl-seryl-aspartyl-lysyl-proline attenuates renal injury and dysfunction in hypertensive rats with reduced renal mass: council for high blood pressure research. *Hypertension* **2010,** *55*, 459-67.

85. Lin, C. X.; Rhaleb, N. E.; Yang, X. P.; Liao, T. D.; D'ambrosio, M. A.; Carretero, O. A., Prevention of aortic fibrosis by N-acetyl-seryl-aspartyl-lysyl-proline in angiotensin II-induced hypertension. *Am J Physiol Heart Circ Physiol* **2008,** *295*, H1253-H1261.

86. Peng, H.; Carretero, O. A.; Brigstock, D. R.; Oja-Tebbe, N.; Rhaleb, N. E., Ac-SDKP reverses cardiac fibrosis in rats with renovascular hypertension. *Hypertension* **2003,** *42*, 1164-70.

87. Wei, L.; Alhenc-Gelas, F.; Corvol, P.; Clauser, E., The two homologous domains of human angiotensin I-converting enzyme are both catalytically active. *J Biol Chem* **1991,** *266*, 9002-8.

88. Fuchs, S.; Frenzel, K.; Hubert, C.; Lyng, R.; Muller, L.; Michaud, A.; Xiao, H. D.; Adams, J. W.; Capecchi, M. R.; Corvol, P.; Shur, B. D.; Bernstein, K. E., Male fertility is dependent on dipeptidase activity of testis ACE. *Nat Med* **2005,** *11*, 1140-2; author reply 1142-3.

89. Yu, X. C.; Sturrock, E. D.; Wu, Z.; Biemann, K.; Ehlers, M. R.; Riordan, J. F., Identification of N-linked glycosylation sites in human testis angiotensin-converting

enzyme and expression of an active deglycosylated form. *J Biol Chem* **1997,** *272*, 3511-9.

90. O'neill, H. G.; Redelinghuys, P.; Schwager, S. L.; Sturrock, E. D., The role of glycosylation and domain interactions in the thermal stability of human angiotensin-converting enzyme. *Biol Chem* **2008,** *389*, 1153-61.

91. Voronov, S.; Zueva, N.; Orlov, V.; Arutyunyan, A.; Kost, O., Temperature-induced selective death of the C-domain within angiotensin-converting enzyme molecule. *FEBS Lett* **2002,** *522*, 77-82.

92. Corradi, H. R.; Schwager, S. L.; Nchinda, A. T.; Sturrock, E. D.; Acharya, K. R., Crystal structure of the N domain of human somatic angiotensin I-converting enzyme provides a structural basis for domain-specific inhibitor design. *J Mol Biol* **2006,** *357*, 964-74.

93. Natesh, R.; Schwager, S. L.; Sturrock, E. D.; Acharya, K. R., Crystal structure of the human angiotensin-converting enzyme-lisinopril complex. *Nature* **2003,** *421*, 551-4.

94. Erdos, E. G., The ACE and I: how ACE inhibitors came to be. *FASEB J* **2006,** *20*, 1034-1038.

95. Smith, C. G.; Vane, J. R., The discovery of captopril. *FASEB J* **2003,** *17*, 788-789.

96. Koh, C. Y.; Kini, M., From snake venom toxins to therapeutics - Cardiovascular examples. *Toxicon* **2012,** *59*, 497-506.

97. Natesh, R.; Schwager, S. L.; Evans, H. R.; Sturrock, E. D.; Acharya, K. R., Structural details on the binding of antihypertensive drugs captopril and enalaprilat to human testicular angiotensin I-converting enzyme. *Biochemistry* **2004,** *43*, 8718-24.

98. Akif, M.; Masuyer, G.; Schwager, S. L.; Bhuyan, B. J.; Mugesh, G.; Isaac, R. E.; Sturrock, E. D.; Acharya, K. R., Structural characterization of angiotensin I-converting enzyme in complex with a selenium analogue of captopril. *FEBS J* **2011,** *278*, 3644-50.

99. Dive, V.; Cotton, J.; Yiotakis, A.; Michaud, A.; Vassiliou, S.; Jiracek, J.; Vazeux, G.; Chauvet, M. T.; Cuniasse, P.; Corvol, P., RXP 407, a phosphinic peptide, is a potent inhibitor of angiotensin I converting enzyme able to differentiate between its two active sites. *Proc Natl Acad Sci U S A* **1999,** *96*, 4330-5.

100. Georgiadis, D.; Cuniasse, P.; Cotton, J.; Yiotakis, A.; Dive, V., Structural determinants of RXPA380, a potent and highly selective inhibitor of the angiotensin-converting enzyme C-domain. *Biochemistry* **2004,** *43*, 8048-54.

101. Kroger, W. L.; Douglas, R. G.; O'neill, H. G.; Dive, V.; Sturrock, E. D., Investigating the domain specificity of phosphinic inhibitors RXPA380 and RXP407 in angiotensin-converting enzyme. *Biochemistry* **2009,** *48*, 8405-12.

102. Anthony, C. S.; Corradi, H. R.; Schwager, S. L.; Redelinghuys, P.; Georgiadis, D.; Dive, V.; Acharya, K. R.; Sturrock, E. D., The N domain of human angiotensin-I-converting enzyme: the role of N-glycosylation and the crystal structure in complex with an N domain-specific phosphinic inhibitor, RXP407. *J Biol Chem* **2010,** *285*, 35685-93.

103. Corradi, H. R.; Chitapi, I.; Sewell, B. T.; Georgiadis, D.; Dive, V.; Sturrock, E. D.; Acharya, K. R., The structure of testis angiotensin-converting enzyme in complex with the C domain-specific inhibitor RXPA380. *Biochemistry* **2007,** *46*, 5473-8.

104. Macours, N.; Poels, J.; Hens, K.; Francis, C.; Huybrechts, R., Structure, evolutionary conservation, and functions of angiotensin- and endothelin-converting enzymes. *Int Rev Cytol* **2004,** *239*, 47-97.

105. Baig, M. S.; Kumar, A.; Siddiqi, M. I.; Goyal, N., Characterization of dipeptidylcarboxypeptidase of Leishmania donovani: a molecular model for structure based design of antileishmanials. *J Comput Aided Mol Des* **2010,** *24*, 77-87.

106. Cunha, C. E.; Magliarelli Hde, F.; Paschoalin, T.; Nchinda, A. T.; Lima, J. C.; Juliano, M. A.; Paiva, P. B.; Sturrock, E. D.; Travassos, L. R.; Carmona, A. K., Catalytic properties of recombinant dipeptidyl carboxypeptidase from Escherichia coli: a comparative study with angiotensin I-converting enzyme. *Biol Chem* **2009,** *390*, 931-40.

107. Riviere, G.; Michaud, A.; Corradi, H. R.; Sturrock, E. D.; Ravi Acharya, K.; Cogez, V.; Bohin, J. P.; Vieau, D.; Corvol, P., Characterization of the first angiotensin-converting like enzyme in bacteria: Ancestor ACE is already active. *Gene* **2007,** *399*, 81-90.

108. Cornell, M. J.; Williams, T. A.; Lamango, N. S.; Coates, D.; Corvol, P.; Soubrier, F.; Hoheisel, J.; Lehrach, H.; Isaac, R. E., Cloning and expression of an evolutionary conserved single-domain angiotensin converting enzyme from Drosophila melanogaster. *J Biol Chem* **1995,** *270*, 13613-9.

109. Taylor, C. A.; Coates, D.; Shirras, A. D., The Acer gene of Drosophila codes for an angiotensin-converting enzyme homologue. *Gene* **1996,** *181*, 191-7.

110. Williams, T. A.; Michaud, A.; Houard, X.; Chauvet, M. T.; Soubrier, F.; Corvol, P., Drosophila melanogaster angiotensin I-converting enzyme expressed in Pichia pastoris resembles the C domain of the mammalian homologue and does not require glycosylation for secretion and enzymic activity. *Biochem J* **1996,** *318 (Pt 1)*, 125-31.

111. Riviere, G.; Michaud, A.; Deloffre, L.; Vandenbulcke, F.; Levoye, A.; Breton, C.; Corvol, P.; Salzet, M.; Vieau, D., Characterization of the first non-insect invertebrate

functional angiotensin-converting enzyme (ACE): leech TtACE resembles the N-domain of mammalian ACE. *Biochem J* **2004,** *382*, 565-73.

112. Laurent, V.; Salzet, M., Biochemical properties of the angiotensin-converting-like enzyme from the leech Theromyzon tessulatum. *Peptides* **1996,** *17*, 737-45.

113. Hooper, N. M., Families of zinc metalloproteases. *FEBS Lett* **1994,** *354*, 1-6.

114. Miyoshi, S.; Shinoda, S., Microbial metalloproteases and pathogenesis. *Microbes Infect* **2000,** *2*, 91-8.

115. Donoghue, M.; Hsieh, F.; Baronas, E.; Godbout, K.; Gosselin, M.; Stagliano, N.; Donovan, M.; Woolf, B.; Robison, K.; Jeyaseelan, R.; Breitbart, R. E.; Acton, S., A novel angiotensin-converting enzyme-related carboxypeptidase (ACE2) converts angiotensin I to angiotensin 1-9. *Circ Res* **2000,** *87*, E1-9.

116. BLAST: Basic Local Sequence Alignment Search Tool. http://blast.ncbi.nlm.nih.gov/Blast.cgi.

117. Multiple Sequence Alignment by CLUSTALW. http://www.genome.jp/tools/clustalw/.

118. Kim, H. M.; Shin, D. R.; Yoo, O. J.; Lee, H.; Lee, J. O., Crystal structure of Drosophila angiotensin I-converting enzyme bound to captopril and lisinopril. *FEBS Lett* **2003,** *538*, 65-70.

119. Akif, M.; Georgiadis, D.; Mahajan, A.; Dive, V.; Sturrock, E. D.; Isaac, R. E.; Acharya, K. R., High-resolution crystal structures of Drosophila melanogaster angiotensin-converting enzyme in complex with novel inhibitors and antihypertensive drugs. *J Mol Biol* **2010,** *400*, 502-17.

120. Akif, M.; Ntai, I.; Sturrock, E. D.; Isaac, R. E.; Bachmann, B. O.; Acharya, K. R., Crystal structure of a phosphonotripeptide K-26 in complex with angiotensin converting enzyme homologue (AnCE) from Drosophila melanogaster. *Biochem Biophys Res Commun* **2010,** *398*, 532-6.

121. Newman, D. J.; Cragg, G. M., Natural products as sources of new drugs over the 30 years from 1981 to 2010. *J. Nat. Prod.* **2012,** *75*, 311-335.

122. Crawford, J. M.; Clardy, J., Bacterial symbionts and natural products. *Chem. Commun. (Camb)* **2011,** *47*, 7559-7566.

123. Koguchi, T.; Yamada, K.; Yamato, M.; Okachi, R.; Nakayama, K.; Kase, H., K-4, a novel inhibitor of angiotensin I converting enzyme produced by *Actinomadura spiculosospora*. *J. Antibiot. (Tokyo)* **1986,** *39*, 364-371.

124. Yamato, M.; Koguchi, T.; Okachi, R.; Yamada, K.; Nakayama, K.; Kase, H.; Karasawa, A.; Shuto, K., K-26, a novel inhibitor of angiotensin I converting enzyme produced by an actinomycete K-26. *J. Antibiot. (Tokyo)* **1986,** *39*, 44-52.

125. Kido, Y.; Hamakado, T.; Anno, M.; Miyagawa, E.; Motoki, Y.; Wakamiya, T.; Shiba, T., Isolation and characterization of I5B2, a new phosphorus containing inhibitor of angiotensin I converting enzyme produced by Actinomadura sp. *J. Antibiot. (Tokyo)* **1984,** *37*, 965-969.

126. Kramer, G. J.; Mohd, A.; Schwager, S. L.; Masuyer, G.; Acharya, K. R.; Sturrock, E. D.; Bachmann, B. O., Interkingdom pharmacology of Angiotensin-I converting enzyme inhibitor phosphonates produced by actinomycetes. *ACS Med Chem Lett* **2014,** *5*, 346-51.

127. Ntai, I.; Bachmann, B. O., Identification of ACE pharmacophore in the phosphonopeptide metabolite K-26. *Bioorg Med Chem Lett* **2008,** *18*, 3068-3071.

128. Holmquist, B.; Bunning, P.; Riordan, J. F., A continuous spectrophotometric assay for angiotensin converting enzyme. *Anal Biochem* **1979,** *95*, 540-548.

129. Friedland, J.; Silverstein, E., A sensitive fluorimetric assay for serum angiotensin-converting enzyme. *Am\. J Clin Path* **1976,** *66*, 416-424.

130. Nchinda, A. T.; Chibale, K.; Redelinghuys, P.; Sturrock, E. D., Synthesis of novel keto-ACE analogues as domain-selective angiotensin I-converting enzyme inhibitors. *Bioorg Med Chem Lett* **2006,** *16*, 4612-4615.

131. Schwager, S. L.; Carmona, A. K.; Sturrock, E. D., A high-throughput fluorimetric assay for angiotensin I-converting enzyme. *Nat Protoc* **2006,** *1*, 1961-1964.

132. Natesh, R.; Schwager, S. L.; Evans, H. R.; Sturrock, E. D.; Acharya, K. R., Structural details on the binding of antihypertensive drugs captopril and enalaprilat to human testicular angiotensin I-converting enzyme. *Biochemistry* **2004,** *43*, 8718-8724.

133. Natesh, R.; Schwager, S. L.; Sturrock, E. D.; Acharya, K. R., Crystal structure of the human angiotensin-converting enzyme-lisinopril complex. *Nature* **2003,** *421*, 551-554.

134. Cunha, C. E.; Magliarelli Hde, F.; Paschoalin, T.; Nchinda, A. T.; Lima, J. C.; Juliano, M. A.; Paiva, P. B.; Sturrock, E. D.; Travassos, L. R.; Carmona, A. K., Catalytic properties of recombinant dipeptidyl carboxypeptidase from *Escherichia coli:* a comparative study with angiotensin I-converting enzyme. *Biol Chem* **2009,** *390*, 931-940.

135. Miyoshi, S.; Shinoda, S., Microbial metalloproteases and pathogenesis. *Microbes Infect* **2000,** *2*, 91-98.

136. Williams, T. A.; Michaud, A.; Houard, X.; Chauvet, M. T.; Soubrier, F.; Corvol, P., Drosophila melanogaster angiotensin I-converting enzyme expressed in Pichia pastoris resembles the C domain of the mammalian homologue and does not require glycosylation for secretion and enzymic activity. *Biochem J* **1996,** *318 (Pt 1)*, 125-131.

137. Carpino, L. A.; El-Faham, A.; Albericio, F., Efficiency in peptide coupling: 1-Hydroxy-7-azabenzotriazole vs 3,4-Dihydro-3-hydroxy-4-oxo-1,2,3-benzotriazine. *J Org Chem* **1995,** *60*, 3561-3564.

138. Oishi, S.; Karki, R. G.; Kang, S. U.; Wang, X.; Worthy, K. M.; Bindu, L. K.; Nicklaus, M. C.; Fisher, R. J.; Burke, T. R., Jr., Design and synthesis of conformationally constrained Grb2 SH2 domain binding peptides employing alpha-methylphenylalanyl based phosphotyrosyl mimetics. *J Med Chem* **2005,** *48*, 764-772.

139. Carpino, L. A.; Sadat-Aalaee, D.; Beyermann, M., Tris(2-aminoethy1)amine as a substitute for 4-(Aminomethy1)piperidine in the FMOC/polyamine approach to rapid peptide synthesis. *J Org Chem* **1990,** *55*, 1673-1675.

140. Boger, D. L. Y., D., Total synthesis of deoxybouvardin and RA-VII: Macrocyclization via an intramolecular Ullmann reaction *J Am Chem Soc* **1991,** *113*, 1427-1429.

141. Gordon, K.; Redelinghuys, P.; Schwager, S. L.; Ehlers, M. R.; Papageorgiou, A. C.; Natesh, R.; Acharya, K. R.; Sturrock, E. D., Deglycosylation, processing and crystallization of human testis angiotensin-converting enzyme. *Biochem J* **2003,** *371*, 437-442.

142. Otwinowski, W.; Minor, W., Processing of X-ray diffraction data collected in oscillation mode. In *Macromolecular Crystallography, part A*, Carter Jr., C. W.; Sweet, R. M., Eds. Academic Press: New York, 1997; pp 307-326.

143. CCP4, The CCP4 Suite: Programs for protein crystallography. *Acta. Crystallogr., Sect. D: Biol. Crystallogr.* **1994,** *50*, 760-763.

144. Mccoy, A. J.; Grosse-Kunstleve, R. W.; Adams, P. D.; Winn, M. D.; Storoni, L. C.; Read, R. J., Phaser Crystallographic Software. *J Appl Crystallogr* **2007,** *40*, 658-674.

145. Murshudov, G. N.; Vagin, A. A.; Dodson, E. J., Refinement of macromolecular structures by the maximum-likelihood method. *Acta Crystallogr, Sect D: Biol Crystallogr* **1997,** *53*, 240-255.

146. Emsley, P.; Cowtan, K., COOT: Model-building tools for molecular graphics. *Acta Crystallogr, Sect D: Biol Crystallogr* **2004,** *60*, 2126-2132.

147. Schuttelkopf, A. W.; Van Aalten, D. M., PRODRG: a tool for high-throughput crystallography of protein-ligand complexes. *Acta Crystallogr, Sect D: Biol Crystallogr* **2004,** *60*, 1355-1363.

148. Davis, I. W.; Leaver-Fay, A.; Chen, V. B.; Block, J. N.; Kapral, G. J.; Wang, X.; Murray, L. W.; Arendall, W. B., 3rd; Snoeyink, J.; Richardson, J. S.; Richardson, D. C., MolProbity: All-atom contacts and structure validation for proteins and nucleic acids. *Nucleic Acids Res.* **2007,** *35*, W375-W383.

149. Mcdonald, I. K.; Thornton, J. M., Satisfying hydrogen bonding potential in proteins. *J Mol Biol* **1994,** *238*, 777-793.

150. Saitou, N.; Nei, M., The neighbor-joining method: a new method for reconstructing phylogenetic trees. *Mol Biol Evol* **1987,** *4*, 406-425.

151. Bryson, V.; Vogel, H. J., Evolutionary divergence and convergence in proteins. In *Evolving Genes and Proteins*, Zuckerkandl, E.; Pauling, L., Eds. Academic Press: New York, 1965; pp 97-166.

152. Tamura, K.; Peterson, D.; Peterson, N.; Stecher, G.; Nei, M.; Kumar, S., MEGA5: molecular evolutionary genetics analysis using maximum likelihood, evolutionary distance, and maximum parsimony methods. *Mol Biol Evol* **2011,** *28*, 2731-2739.

153. Li, J. W.; Vederas, J. C., Drug discovery and natural products: end of an era or an endless frontier? *Science* **2009,** *325*, 161-5.

154. Rohl, C. A.; Strauss, C. E.; Misura, K. M.; Baker, D., Protein structure prediction using Rosetta. *Methods Enzymol* **2004,** *383*, 66-93.

155. Siegel, J. B.; Zanghellini, A.; Lovick, H. M.; Kiss, G.; Lambert, A. R.; St Clair, J. L.; Gallaher, J. L.; Hilvert, D.; Gelb, M. H.; Stoddard, B. L.; Houk, K. N.; Michael, F. E.; Baker, D., Computational design of an enzyme catalyst for a stereoselective bimolecular Diels-Alder reaction. *Science* **2010,** *329*, 309-13.

156. Kuhlman, B.; Dantas, G.; Ireton, G. C.; Varani, G.; Stoddard, B. L.; Baker, D., Design of a novel globular protein fold with atomic-level accuracy. *Science* **2003,** *302*, 1364-8.

157. Davis, I. W.; Raha, K.; Head, M. S.; Baker, D., Blind docking of pharmaceutically relevant compounds using RosettaLigand. *Protein Sci* **2009,** *18*, 1998-2002.

158. Davis, I. W.; Baker, D., RosettaLigand docking with full ligand and receptor flexibility. *J Mol Biol* **2009,** *385*, 381-92.

159. Misura, K. M.; Chivian, D.; Rohl, C. A.; Kim, D. E.; Baker, D., Physically realistic homology models built with ROSETTA can be more accurate than their templates. *Proc Natl Acad Sci U S A* **2006,** *103*, 5361-6.

160. Das, R.; Baker, D., Macromolecular modeling with rosetta. *Annu Rev Biochem* **2008,** *77*, 363-82.

161. Ballester, P. J.; Westwood, I.; Laurieri, N.; Sim, E.; Richards, W. G., Prospective virtual screening with Ultrafast Shape Recognition: the identification of novel inhibitors of arylamine N-acetyltransferases. *J R Soc Interface* **2010,** *7*, 335-42.

162. Perola, E.; Walters, W. P.; Charifson, P. S., A detailed comparison of current docking and scoring methods on systems of pharmaceutical relevance. *Proteins* **2004,** *56*, 235-49.

163. Leaver-Fay, A.; O'meara, M. J.; Tyka, M.; Jacak, R.; Song, Y.; Kellogg, E. H.; Thompson, J.; Davis, I. W.; Pache, R. A.; Lyskov, S.; Gray, J. J.; Kortemme, T.; Richardson, J. S.; Havranek, J. J.; Snoeyink, J.; Baker, D.; Kuhlman, B., Scientific benchmarks for guiding macromolecular energy function improvement. *Methods Enzymol* **2013,** *523*, 109-43.

164. Cheng, Y.; Prusoff, W. H., Relationship between the inhibition constant (K1) and the concentration of inhibitor which causes 50 per cent inhibition (I50) of an enzymatic reaction. *Biochem Pharmacol* **1973,** *22*, 3099-108.

165. Nannemann, D. P.; Kaufmann, K. W.; Meiler, J.; Bachmann, B. O., Design and directed evolution of a dideoxy purine nucleoside phosphorylase. *Protein Eng Des Sel* **2010,** *23*, 607-16.

166. Renfrew, P. D.; Campbell, G.; Strauss, C. E.; Bonneau, R., The 2010 Rosetta developers meeting: macromolecular prediction and design meets reproducible publishing. *PLoS One* **2011,** *6*, e22431.

167. Katukojvala, S.; Barlett, K. N.; Lotesta, S. D.; Williams, L. J., Spirodiepoxides in total synthesis: epoxomicin. *J Am Chem Soc* **2004,** *126*, 15348-9.

168. Kawatani, M.; Osada, H., Affinity-based target identification for bioactive small molecules. *Medchemcomm* **2014,** *5*, 277-287.

169. Leslie, B. J.; Hergenrother, P. J., Identification of the cellular targets of bioactive small organic molecules using affinity reagents. *Chem Soc Rev* **2008,** *37*, 1347-60.

170. Ziegler, S.; Pries, V.; Hedberg, C.; Waldmann, H., Target identification for small bioactive molecules: finding the needle in the haystack. *Angew Chem Int Ed Engl* **2013,** *52*, 2744-92.

171. Wulff, J. E.; Siegrist, R.; Myers, A. G., The natural product avrainvillamide binds to the oncoprotein nucleophosmin. *J Am Chem Soc* **2007,** *129*, 14444-51.

172. Wang, G.; Shang, L.; Burgett, A. W.; Harran, P. G.; Wang, X., Diazonamide toxins reveal an unexpected function for ornithine delta-amino transferase in mitotic cell division. *Proc Natl Acad Sci U S A* **2007,** *104*, 2068-73.

173. Emami, K. H.; Nguyen, C.; Ma, H.; Kim, D. H.; Jeong, K. W.; Eguchi, M.; Moon, R. T.; Teo, J. L.; Kim, H. Y.; Moon, S. H.; Ha, J. R.; Kahn, M., A small molecule inhibitor of beta-catenin/CREB-binding protein transcription [corrected]. *Proc Natl Acad Sci U S A* **2004,** *101*, 12682-7.

174. Statsuk, A. V.; Bai, R.; Baryza, J. L.; Verma, V. A.; Hamel, E.; Wender, P. A.; Kozmin, S. A., Actin is the primary cellular receptor of bistramide A. *Nat Chem Biol* **2005,** *1*, 383-8.

175. Bernstein, K. E.; Welsh, S. L.; Inman, J. K., A deeply recessed active site in angiotensin-converting enzyme is indicated from the binding characteristics of biotin-spacer-inhibitor reagents. *Biochem Biophys Res Commun* **1990,** *167*, 310-6.

176. Pantoliano, M. W.; Holmquist, B.; Riordan, J. F., Affinity chromatographic purification of angiotensin converting enzyme. *Biochemistry* **1984,** *23*, 1037-42.

177. Zhu, J.; Wan, Q.; Danishefsky, S. J., Synthesis of Biotinylated Tumor-Associated Carbohydrate Antigens for Immunological Studies. *Tetrahedron Lett* **2009,** *50*, 712-714.

178. Green, N. M., Spectrophotometric determination of avidin and biotin. In *Methods in Enzymol.*, Academic Press: New York, 1970; Vol. XVIII, p 418.

179. Li, M.; Gray, W.; Zhang, H.; Chung, C. H.; Billheimer, D.; Yarbrough, W. G.; Liebler, D. C.; Shyr, Y.; Slebos, R. J., Comparative shotgun proteomics using spectral count data and quasi-likelihood modeling. *J Proteome Res* **2010,** *9*, 4295-305.

180. Choi, H.; Fermin, D.; Nesvizhskii, A. I., Significance analysis of spectral count data in label-free shotgun proteomics. *Mol Cell Proteomics* **2008,** *7*, 2373-85.

181. Xue, Y.; O'mara, M. L.; Surawski, P. P.; Trau, M.; Mark, A. E., Effect of poly(ethylene glycol) (PEG) spacers on the conformational properties of small peptides: a molecular dynamics study. *Langmuir* **2011,** *27*, 296-303.

182. Phelan, V. V., Biosynthetic Investigations of the Peptide Natural Products K-26 and Anthramycin. 2011.

183. Bougioukou, D. J.; Mukherjee, S.; Van Der Donk, W. A., Revisiting the biosynthesis of dehydrophos reveals a tRNA-dependent pathway. *Proc Natl Acad Sci U S A* **2013,** *110*, 10952-7.

184. Cuatrecasas, P.; Parikh, I., Adsorbents for affinity chromatography. Use of N-hydroxysuccinimide esters of agarose. *Biochemistry* **1972,** *11*, 2291-9.

185. Cuatrecasas, P., Affinity chromatography of macromolecules. *Adv Enzymol Relat Areas Mol Biol* **1972,** *36*, 29-89.

186. Schwager, S. L.; Carmona, A. K.; Sturrock, E. D., A high-throughput fluorimetric assay for angiotensin I-converting enzyme. *Nat Protoc* **2006,** *1*, 1961-4.

187. Gordon, K.; Redelinghuys, P.; Schwager, S. L.; Ehlers, M. R.; Papageorgiou, A. C.; Natesh, R.; Acharya, K. R.; Sturrock, E. D., Deglycosylation, processing and crystallization of human testis angiotensin-converting enzyme. *Biochem J* **2003,** *371*, 437-42.

188. Ntai, I.; Manier, M. L.; Hachey, D. L.; Bachmann, B. O., Biosynthetic origins of C-P bond containing tripeptide K-26. *Org Lett* **2005,** *7*, 2763-2765.

189. Geurink, P. P.; Prely, L. M.; Van Der Marel, G. A.; Bischoff, R.; Overkleeft, H. S., Photoaffinity labeling in activity-based protein profiling. *Top Curr Chem* **2012,** *324*, 85-113.

190. Shi, H.; Zhang, C. J.; Chen, G. Y.; Yao, S. Q., Cell-based proteome profiling of potential dasatinib targets by use of affinity-based probes. *J Am Chem Soc* **2012,** *134*, 3001-14.

191. Das, J., Aliphatic diazirines as photoaffinity probes for proteins: recent developments. *Chem Rev* **2011,** *111*, 4405-17.

192. Wang, R. E.; Hunt, C. R.; Chen, J.; Taylor, J. S., Biotinylated quercetin as an intrinsic photoaffinity proteomics probe for the identification of quercetin target proteins. *Bioorg Med Chem* **2011,** *19*, 4710-20.

193. Ishikawa, F.; Kakeya, H., Specific enrichment of nonribosomal peptide synthetase module by an affinity probe for adenylation domains. *Bioorg Med Chem Lett* **2014,** *24*, 865-9.

APPENDIX A

NMR SPECTRA

OF SYNTHETIC INTERMEDIATES

FROM CHAPTER II

NMR spectra of K-4 (II-2) and synthetic intermediates (II-2a - II-2d)

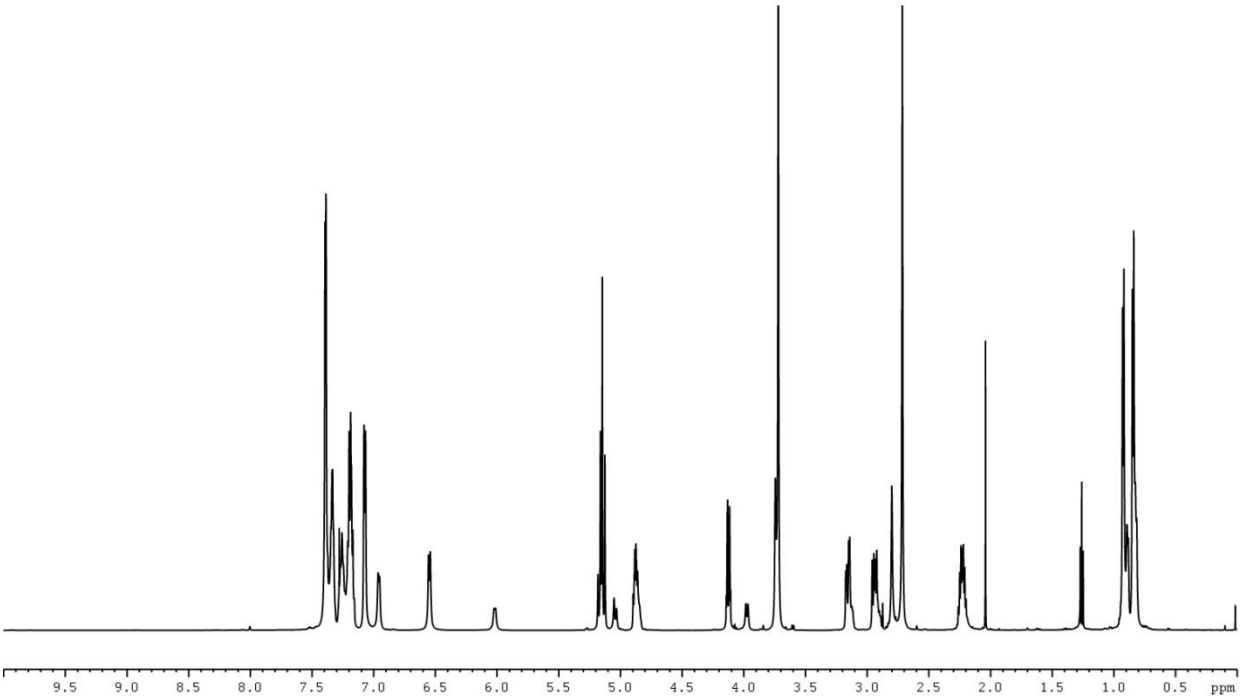

^{1}HNMR Spectrum (600 MHz) of N-benzyloxycarbonyl-N-methyl-L-valyl-L-phenylalanine methyl ester (II-2a) in $CDCl_3$

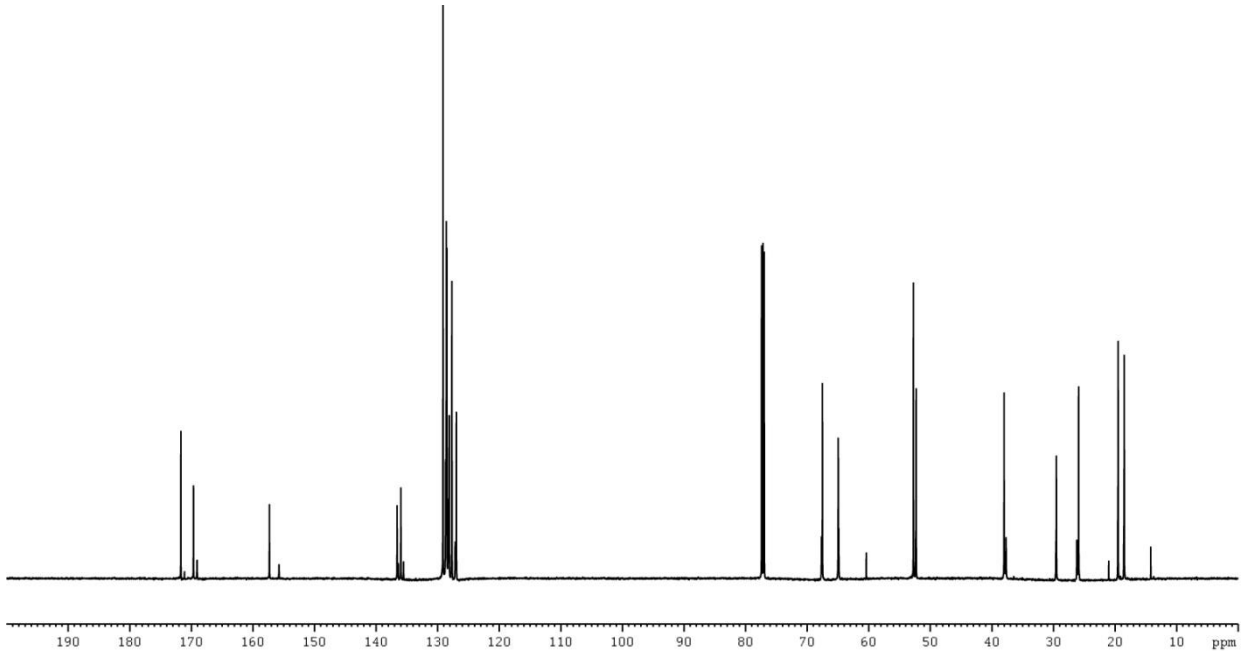

^{13}CNMR Spectrum (150 MHz) of N-benzyloxycarbonyl-N-methyl-L-valyl-L-phenylalanine methyl ester (II-2a) in $CDCl_3$

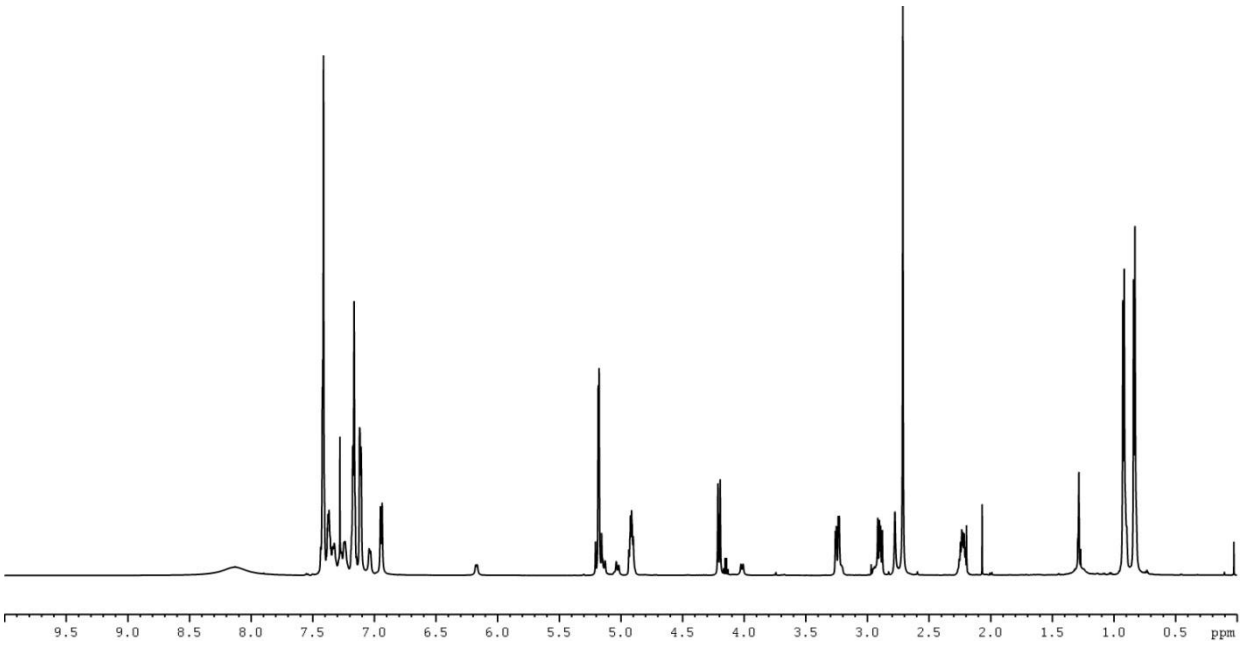

^{1}HNMR Spectrum (600 MHz) of N-benzyloxycarbonyl-N-methyl-L-valyl-L-phenylalanine (II-2b) in $CDCl_3$

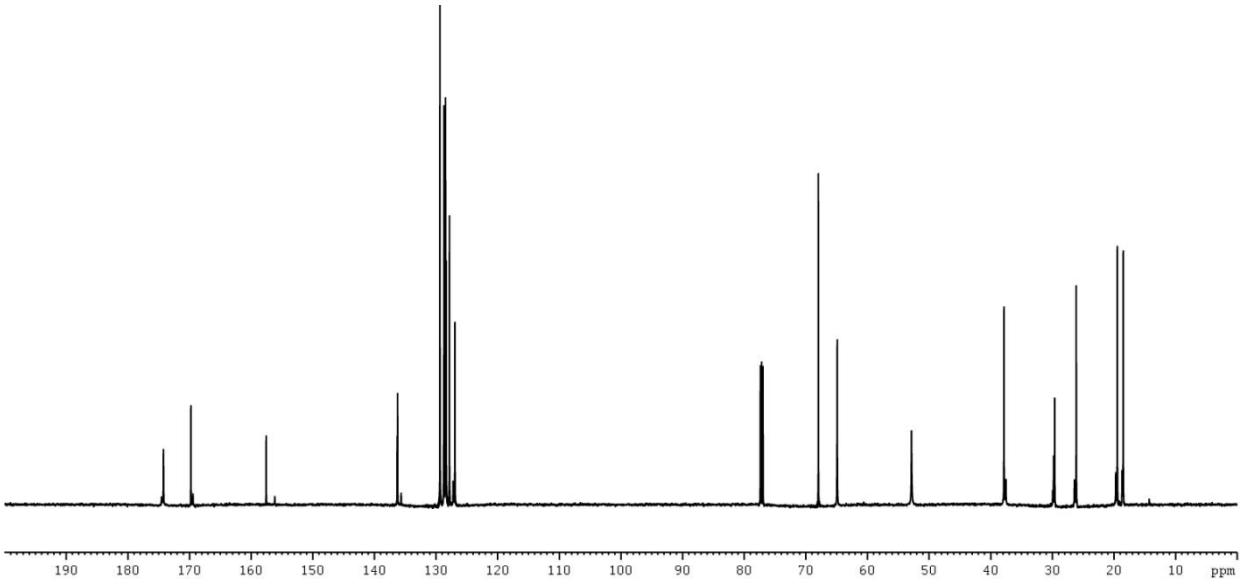

^{13}CNMR Spectrum (150 MHz) of N-benzyloxycarbonyl-N-methyl-L-valyl-L-phenylalanine (II-2b) in $CDCl_3$

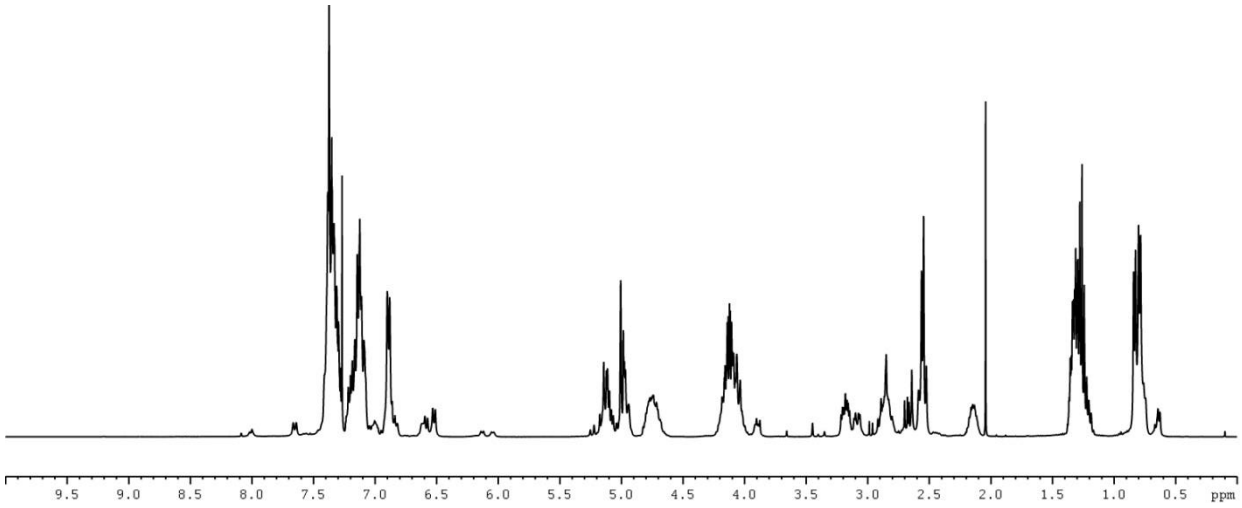

^{1}HNMR Spectrum (400 MHz) of N-(N-benzyloxycarbonyl-N-methyl-L-valyl-L-phenylalanyl)-1-amino-2-(4-benzyloxyphenyl)ethyl phosphonate (II-2c) in $CDCl_3$

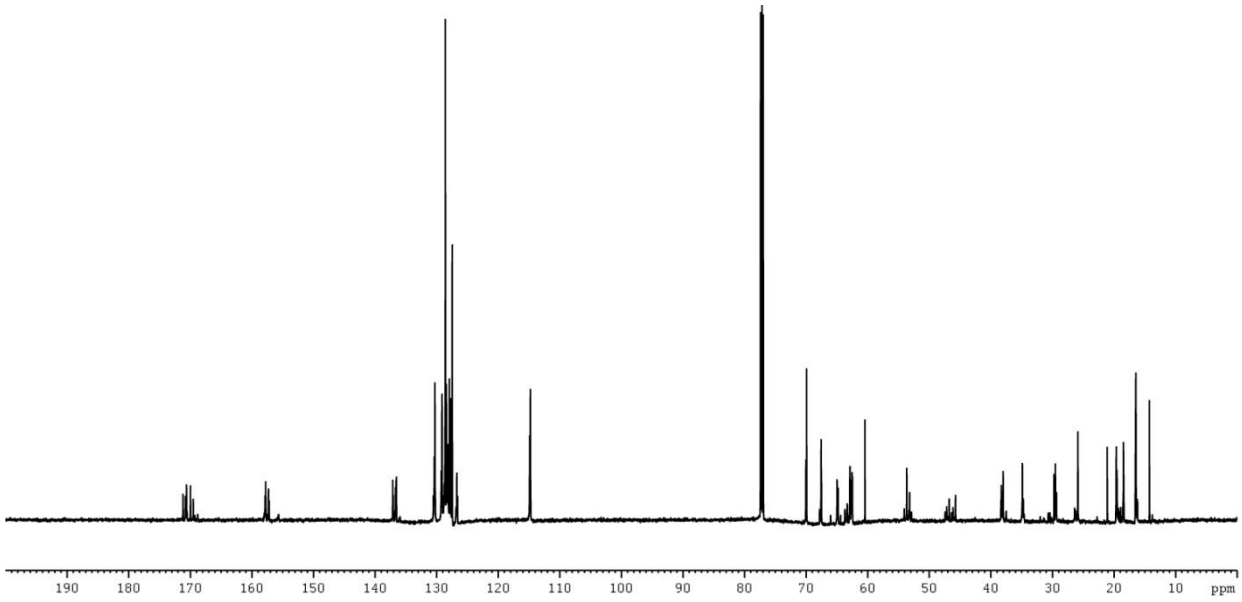

^{13}CNMR Spectrum (150 MHz) of N-(N-benzyloxycarbonyl-N-methyl-L-valyl-L-phenylalanyl)-1-amino-2-(4-benzyloxyphenyl)ethyl phosphonate (II-2c) in $CDCl_3$

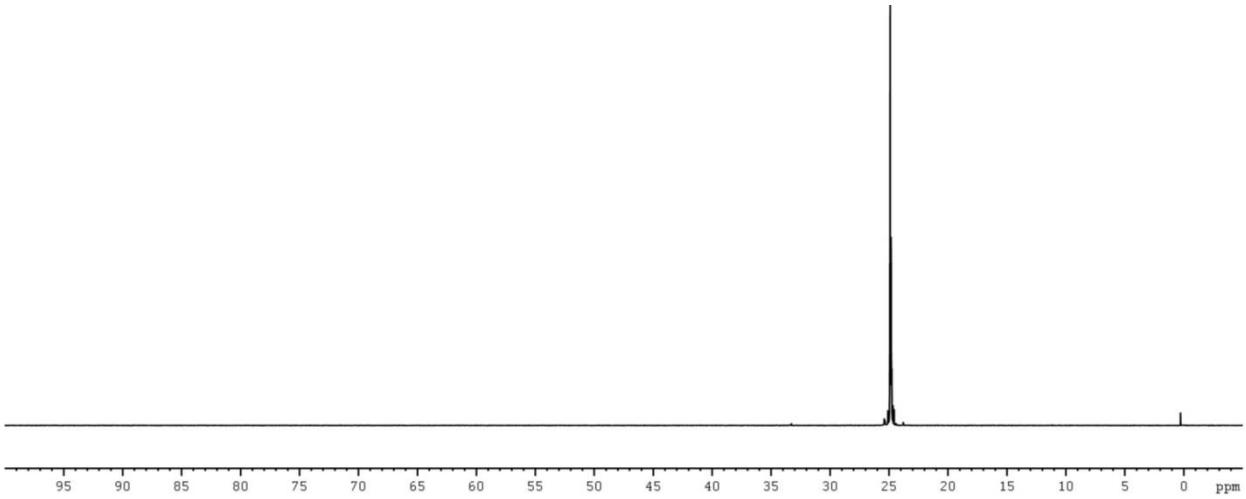

^{31}PNMR Spectrum (162 MHz) of N-(N-benzyloxycarbonyl-N-methyl-L-valyl-L-phenylalanyl)-1-amino-2-(4-benzyloxyphenyl)ethyl phosphonate (II-2c) in $CDCl_3$

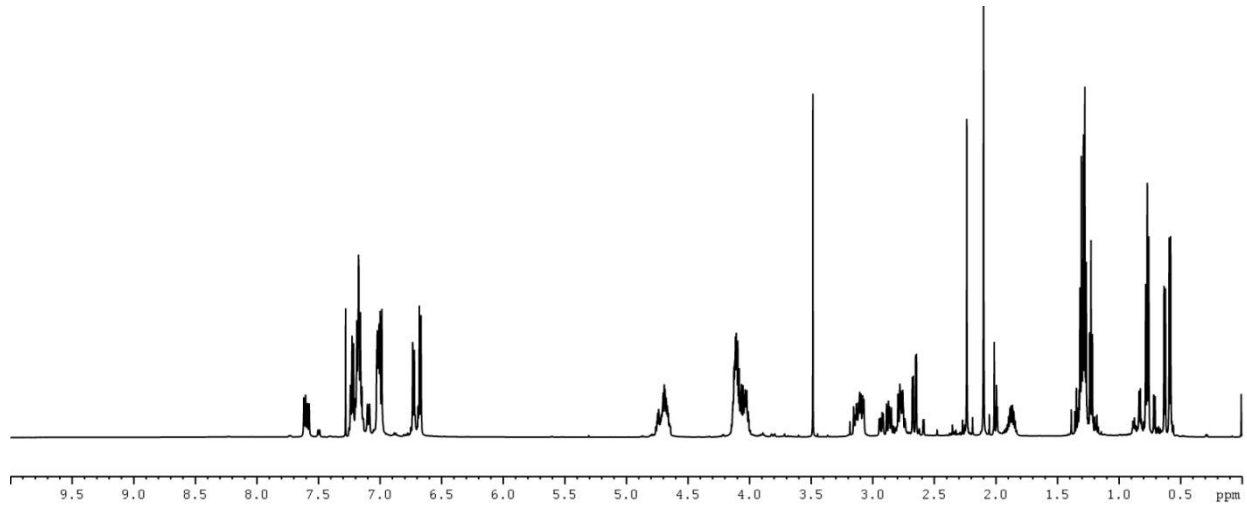

^{1}HNMR Spectrum (600 MHz) of diethyl N-(N-methyl-L-valyl-L-phenylalanyl)-1-amino-2-(4-hydoxyphenyl)ethyl phosphonate (II-2d) in $CDCl_3$

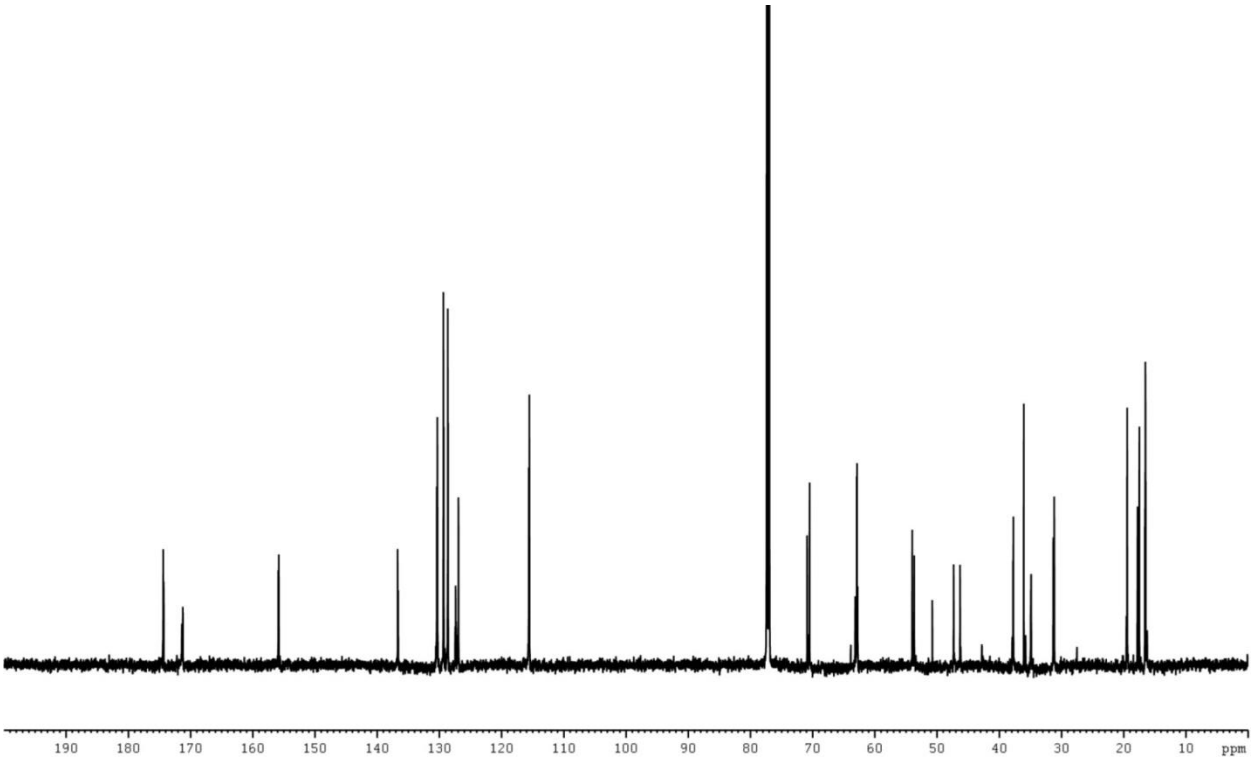

^{13}CNMR Spectrum (150 MHz) of diethyl N-(N-methyl-L-valyl-L-phenylalanyl)-1-amino-2-(4-hydoxyphenyl)ethyl phosphonate (II-2d) in $CDCl_3$

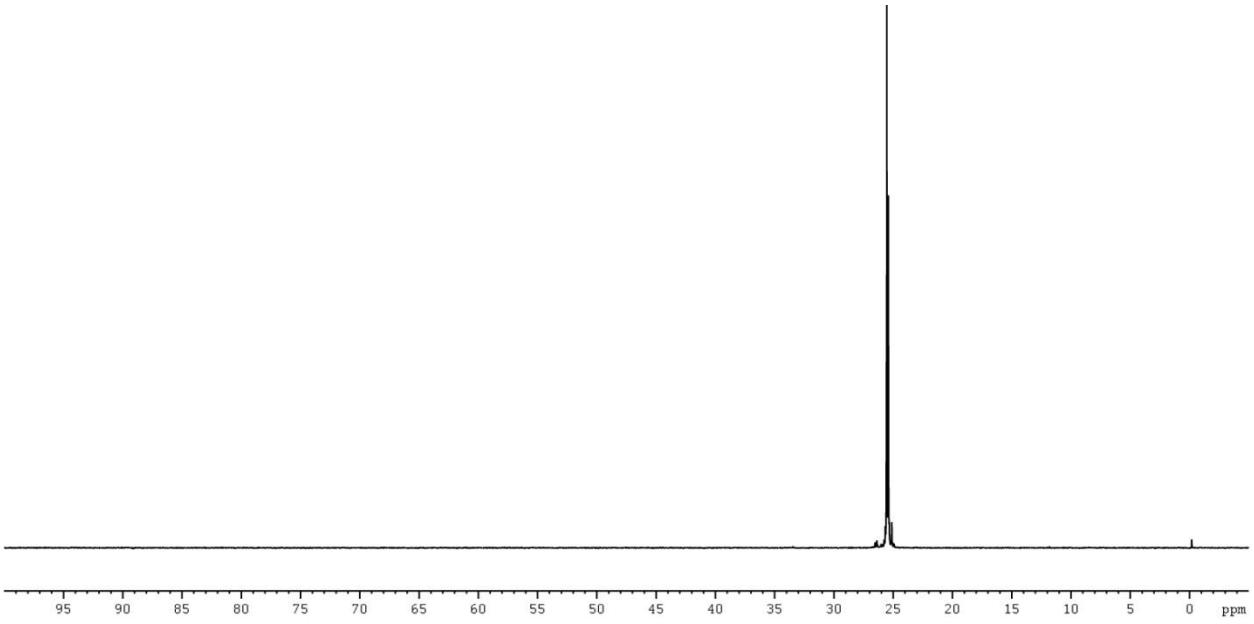

^{31}PNMR Spectrum (162 MHz) of diethyl N-(N-methyl-L-valyl-L-phenylalanyl)-1-amino-2-(4-hydoxyphenyl)ethyl phosphonate (II-2d) in $CDCl_3$

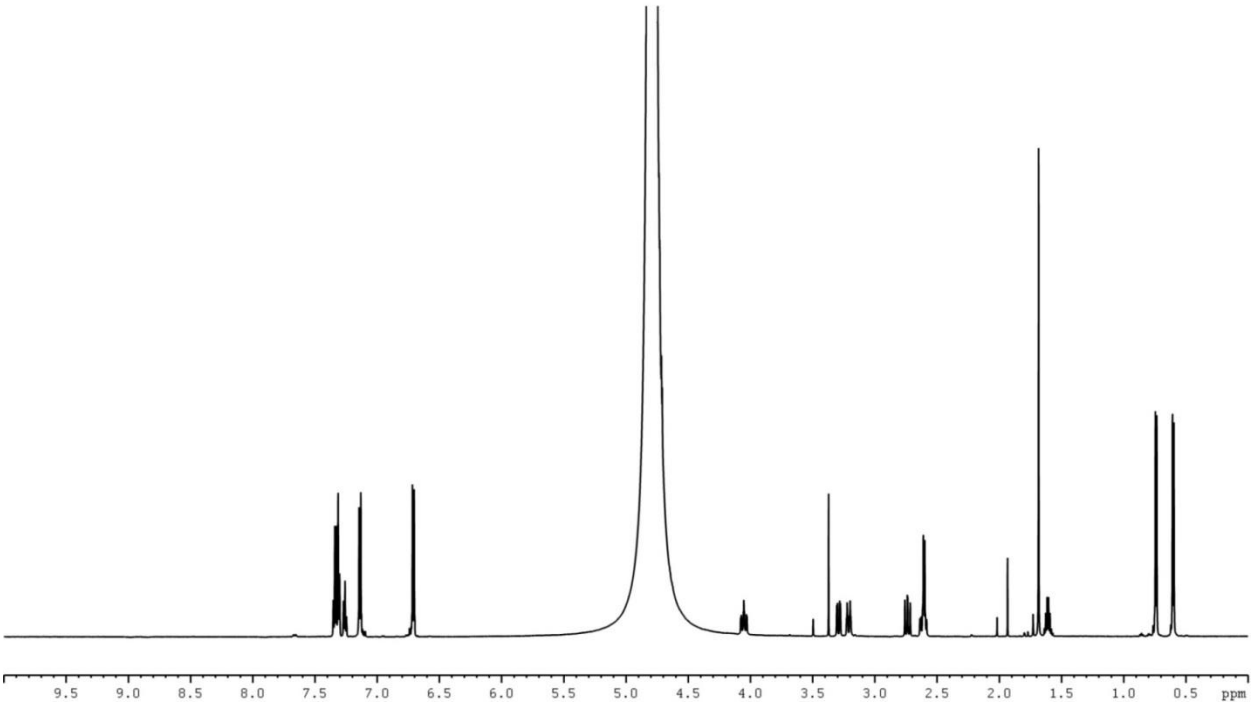

^{1}HNMR Spectrum (600 MHz) of K-4: N-(N-methyl-L-isoleucyl-L-phenylalanyl)-1-amino-2-(4-hydoxyphenyl)ethyl phosphonic acid (II-2) in D_2O, pD = 11.9

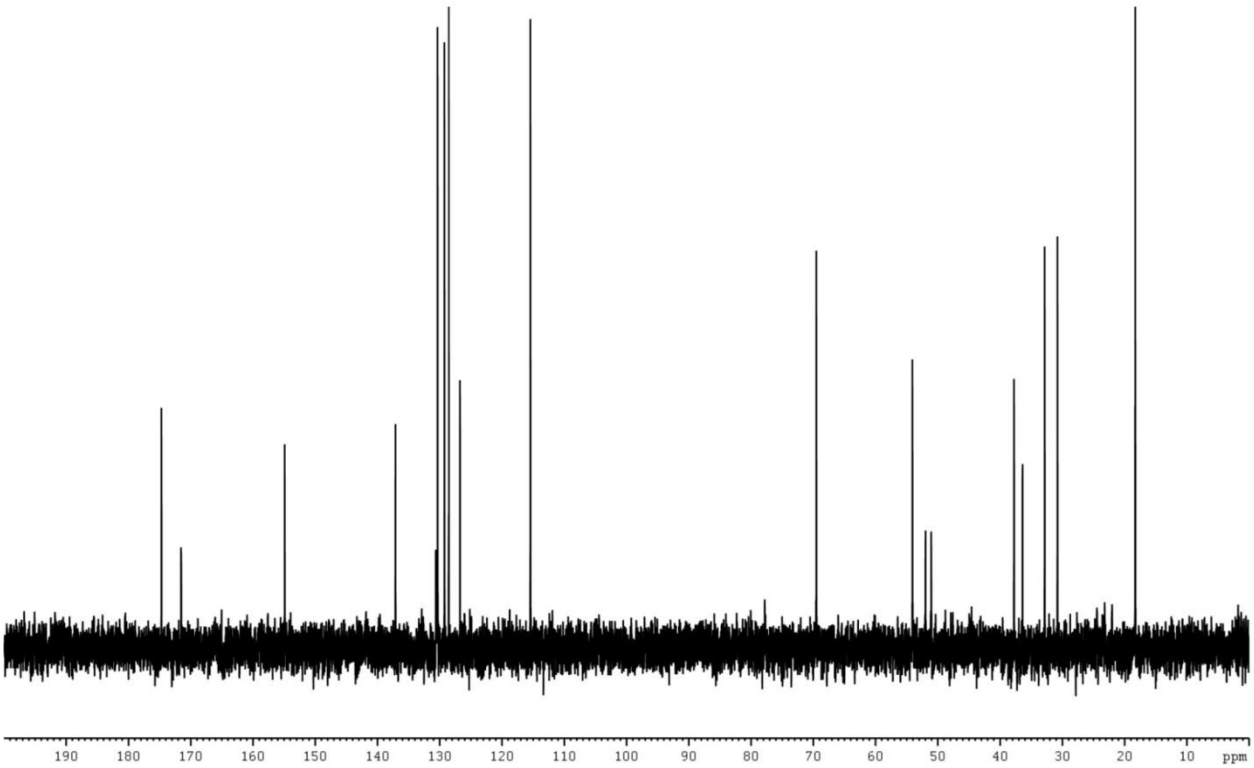

^{13}CNMR Spectrum (150 MHz) of K-4: N-(N-methyl-L-isoleucyl-L-phenylalanyl)-1-amino-2-(4-hydoxyphenyl)ethyl phosphonic acid (II-2) in D_2O, pD = 11.9

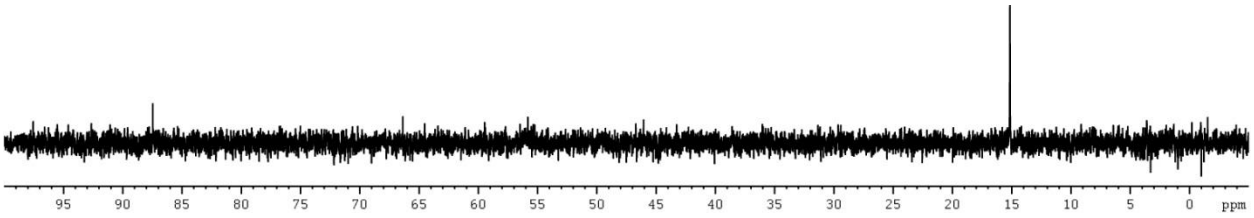

^{31}PNMR Spectrum (162 MHz) of K-4: N-(N-methyl-L-isoleucyl-L-phenylalanyl)-1-amino-2-(4-hydoxyphenyl)ethyl phosphonic acid (II-2) in D_2O, pD = 11.9

NMR spectra of 15-B-2 (II-3) and synthetic intermediates (II-3a - II-3d)

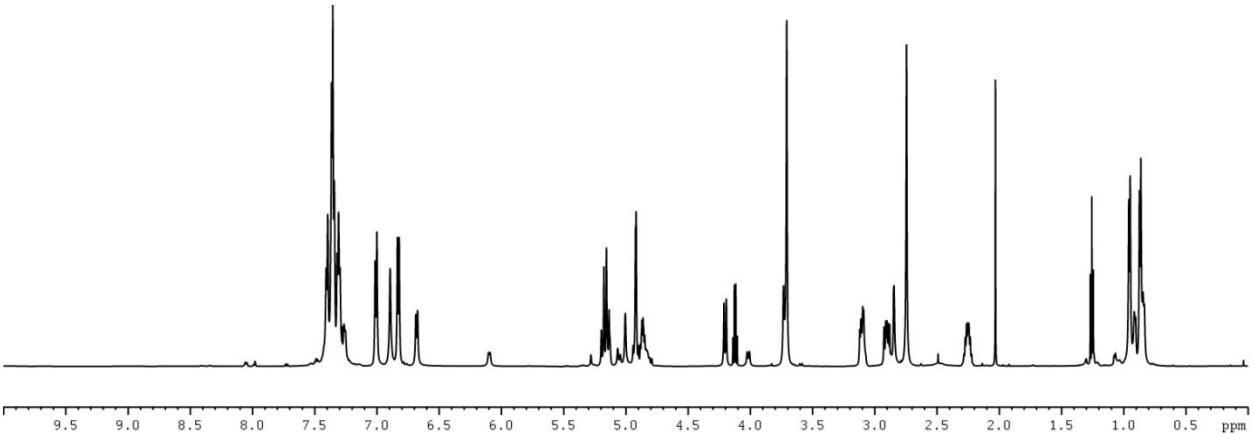

^{1}HNMR Spectrum (600 MHz) of N-benzyloxycarbonyl-N-methyl-L-valyl-O-benzyl-L-tyrosine methyl ester (II-3a) in $CDCl_3$

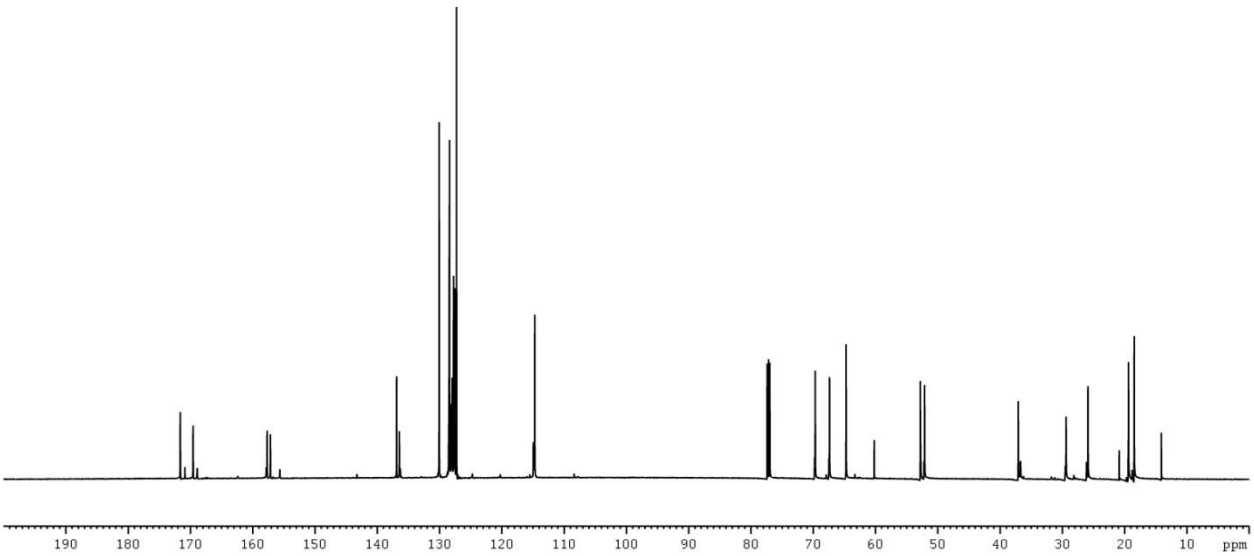

^{13}CNMR Spectrum (150 MHz) of N-benzyloxycarbonyl-N-methyl-L-valyl-O-benzyl-L-tyrosine methyl ester (II-3a) in $CDCl_3$

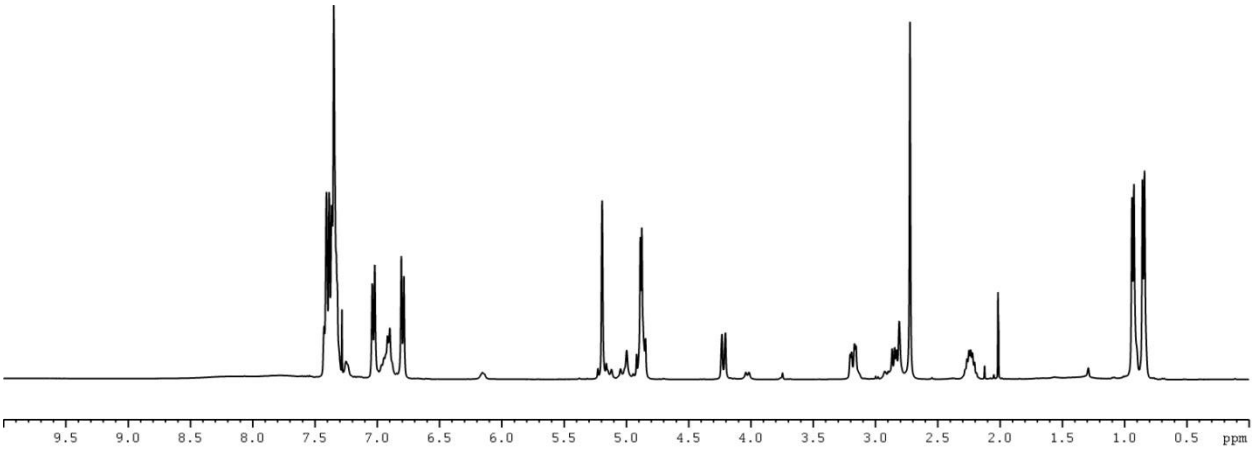

^{1}HNMR Spectrum (400 MHz) of N-benzyloxycarbonyl-N-methyl-L-valyl-O-benzyl-L-tyrosine (II-3b) in $CDCl_3$

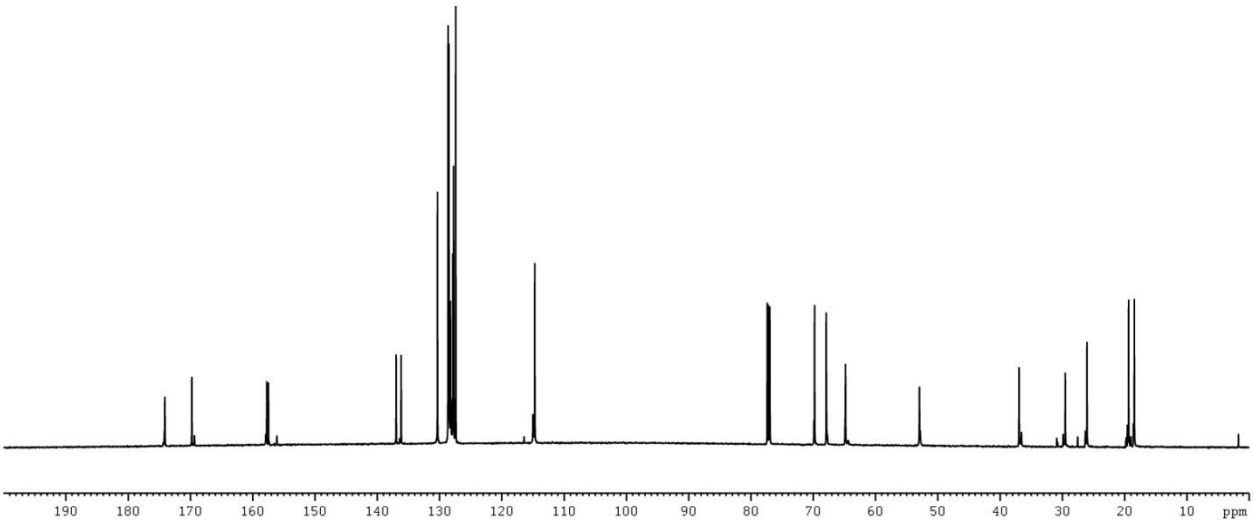

^{13}CNMR Spectrum (150 MHz) of N-benzyloxycarbonyl-N-methyl-L-valyl-O-benzyl-L-tyrosine (II-3b) in $CDCl_3$

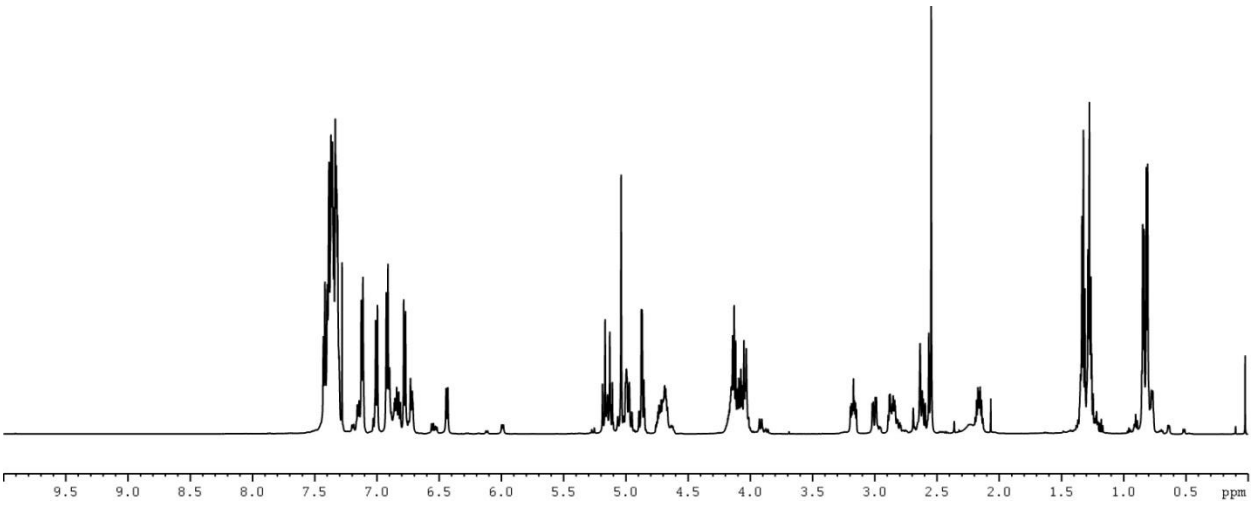

^{1}HNMR Spectrum (600 MHz) of diethyl N-(N-benzyloxycarbonyl-N-methyl-L-valyl-O-benzyl-L-tyrosyl)-1-amino-2-(4-benzyloxyphenyl)ethyl phosphonate (II-3c) in $CDCl_3$

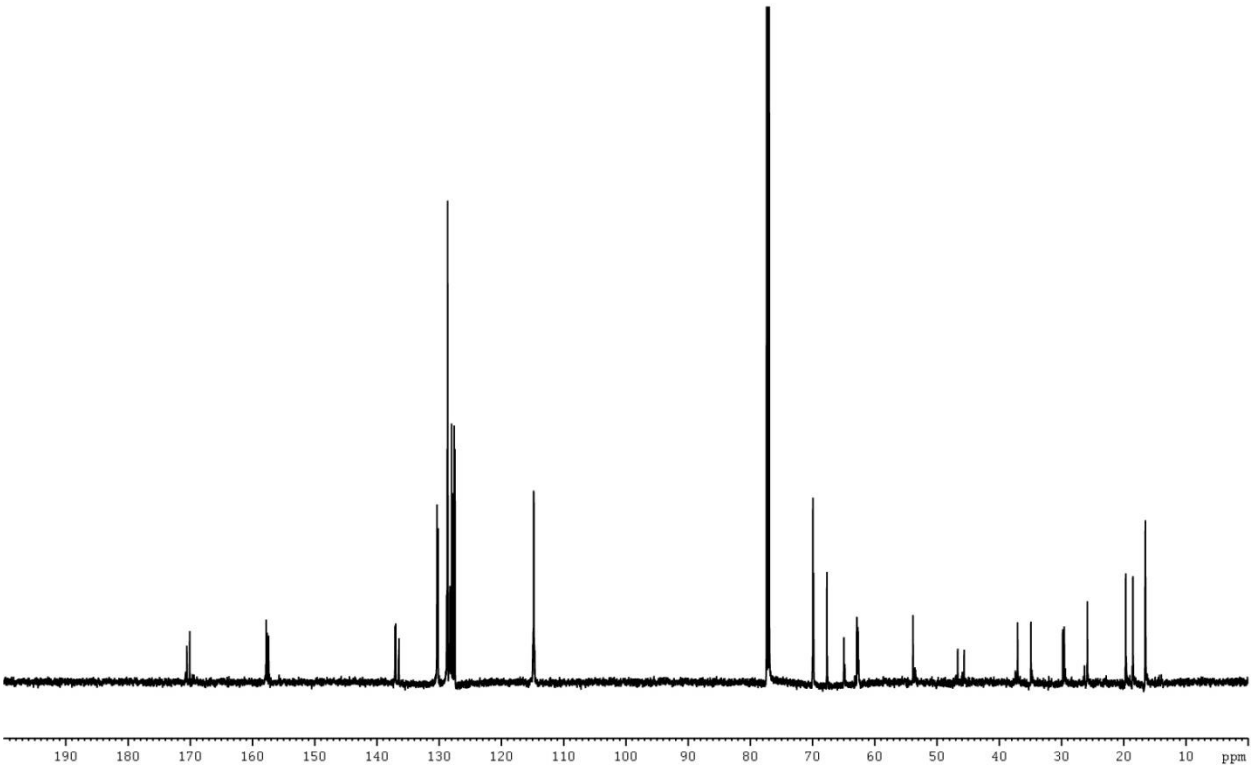

^{13}CNMR Spectrum (150 MHz) diethyl N-(N-benzyloxycarbonyl-N-methyl-L-valyl-O-benzyl-L-tyrosyl)-1-amino-2-(4-benzyloxyphenyl)ethyl phosphonate (II-3c) in $CDCl_3$

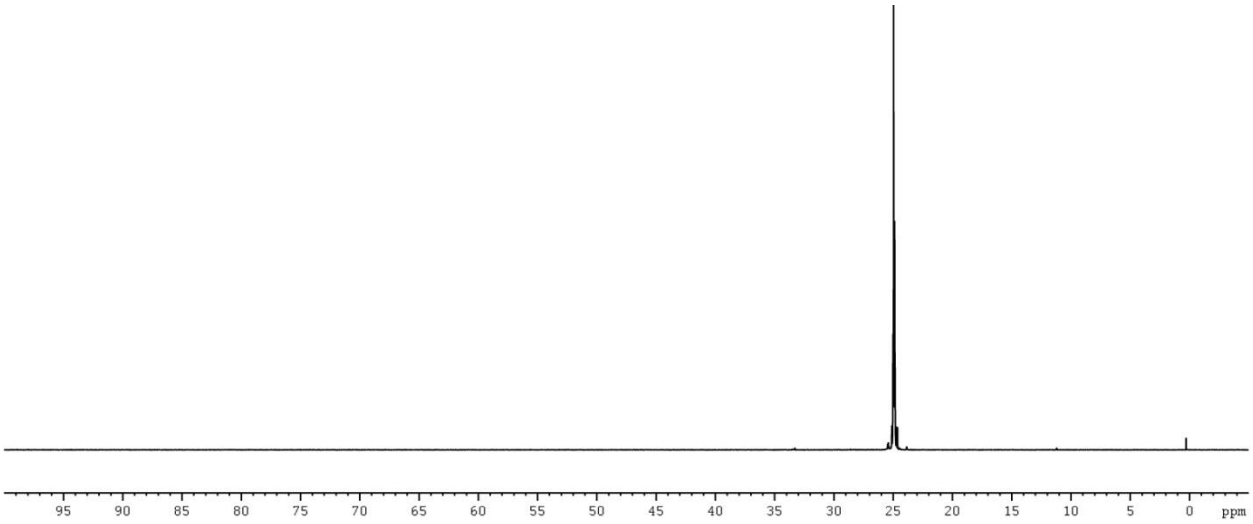

^{31}PNMR Spectrum (162 MHz) of diethyl N-(N-benzyloxycarbonyl-N-methyl-L-valyl-O-benzyl-L-tyrosyl)-1-amino-2-(4-benzyloxyphenyl)ethyl phosphonate (II-3c) in $CDCl_3$

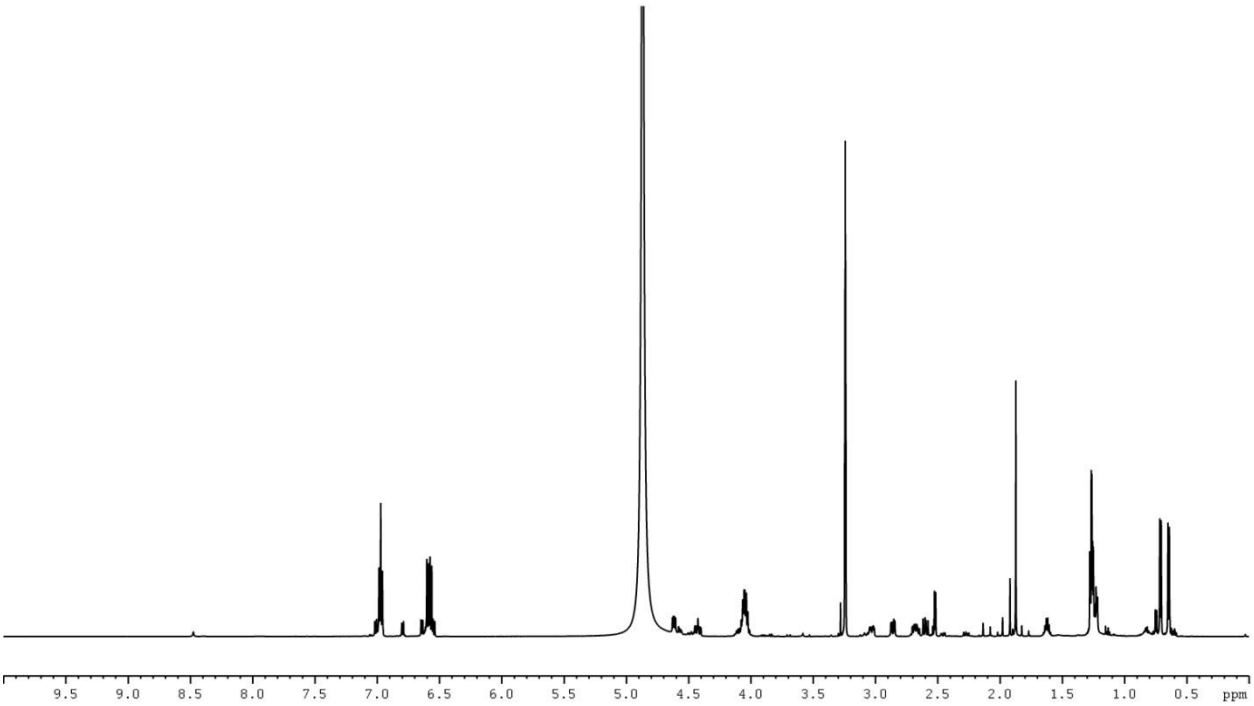

^{1}HNMR Spectrum (600 MHz) of diethyl N-(N-methyl-L-valyl-L-tyrosyl)-1-amino-2-(4-hydoxyphenyl)ethyl phosphonate (II-3d) in MeOD

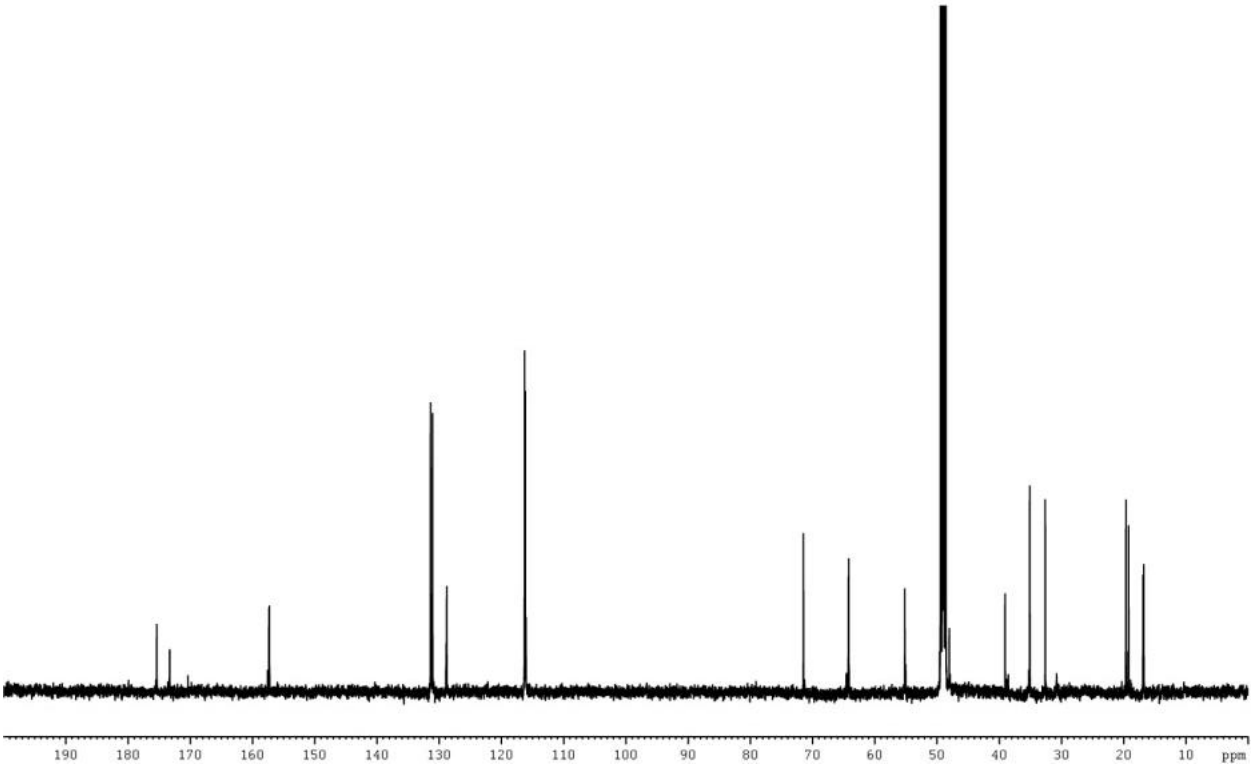

^{13}CNMR Spectrum (150 MHz) diethyl N-(N-methyl-L-valyl-L-tyrosyl)-1-amino-2-(4-hydoxyphenyl)ethyl phosphonate (II-3d) in MeOD

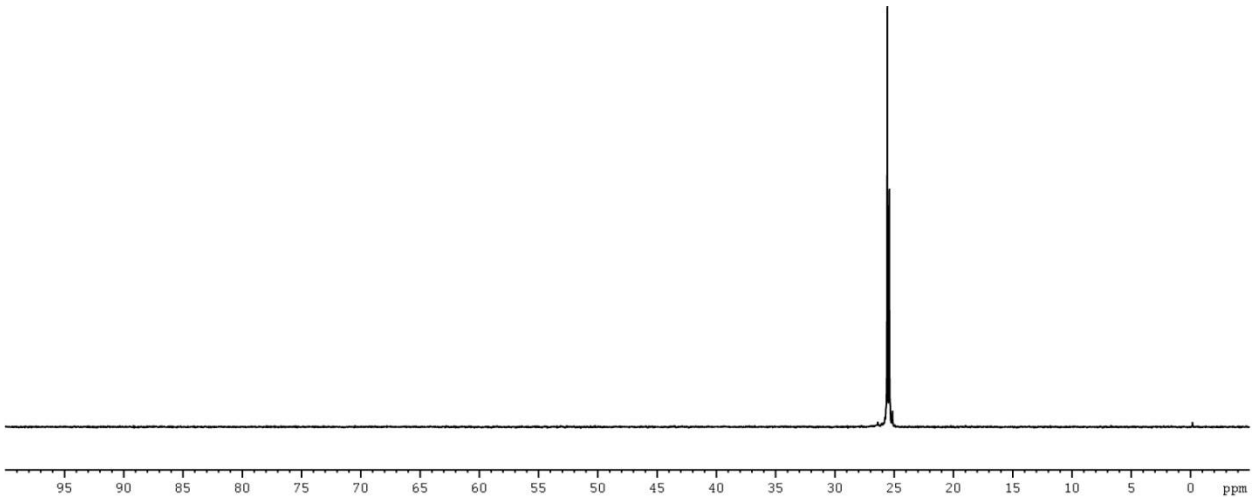

^{31}PNMR Spectrum (162 MHz) of diethyl N-(N-methyl-L-valyl-L-tyrosyl)-1-amino-2-(4-hydoxyphenyl)ethyl phosphonate (II-3d) in MeOD

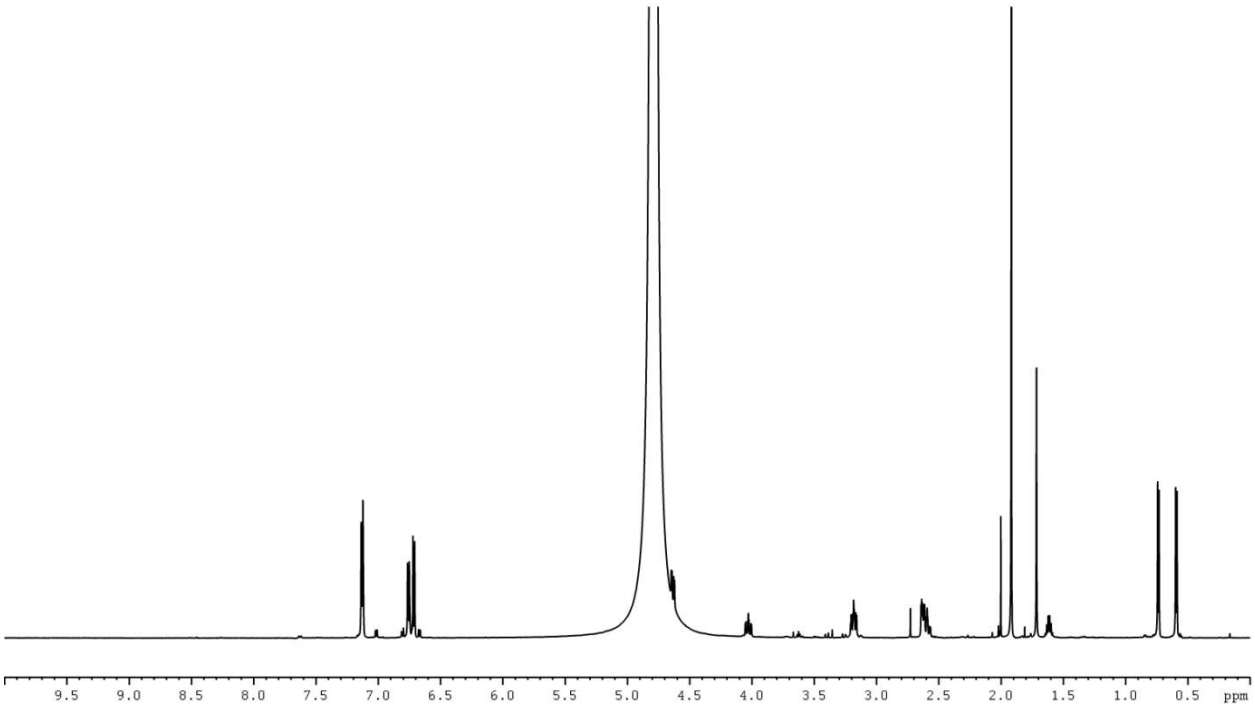

^{1}HNMR Spectrum (600 MHz) of 15-B-2: N-(N-methyl-L-valyl-L-tyrosyl)-1-amino-2-(4-hydoxyphenyl)ethyl phosphonic acid (II-3) in D_2O, pD = 11.9

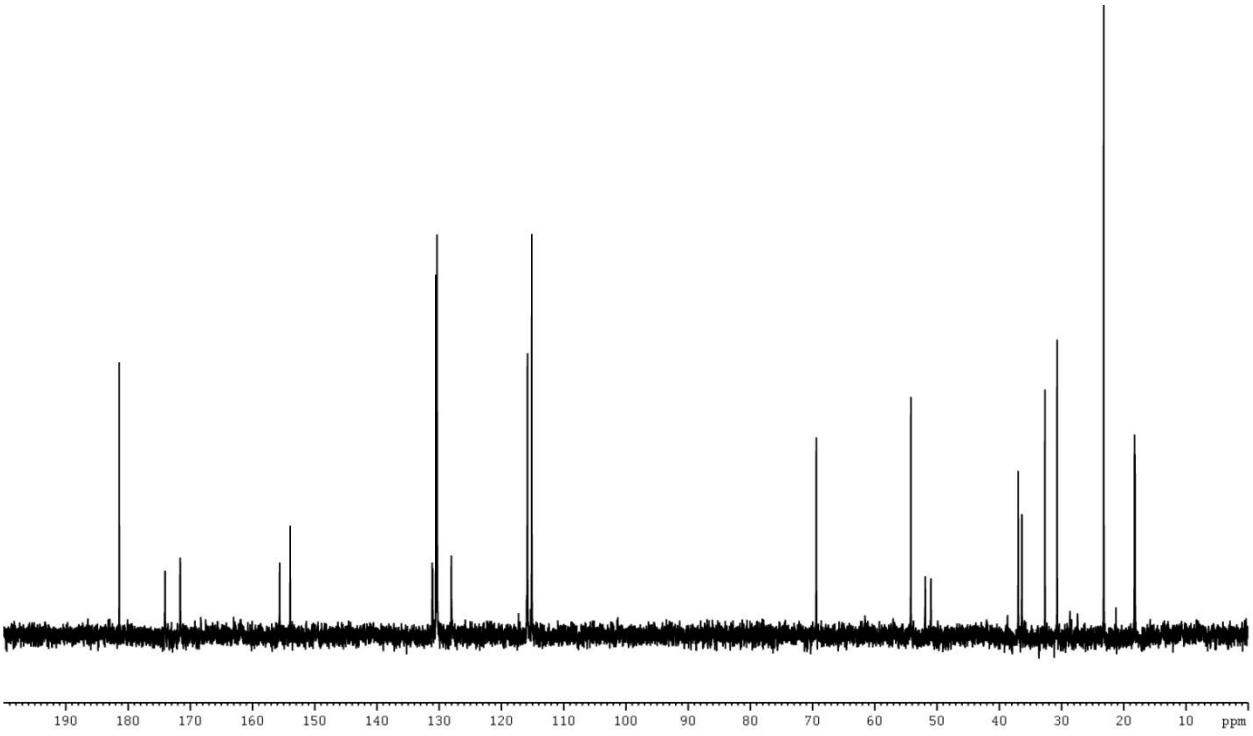

^{13}CNMR Spectrum (150 MHz) of 15-B-2: N-(N-methyl-L-valyl-L-tyrosyl)-1-amino-2-(4-hydoxyphenyl)ethyl phosphonic acid (II-3) in D_2O, pD = 11.9

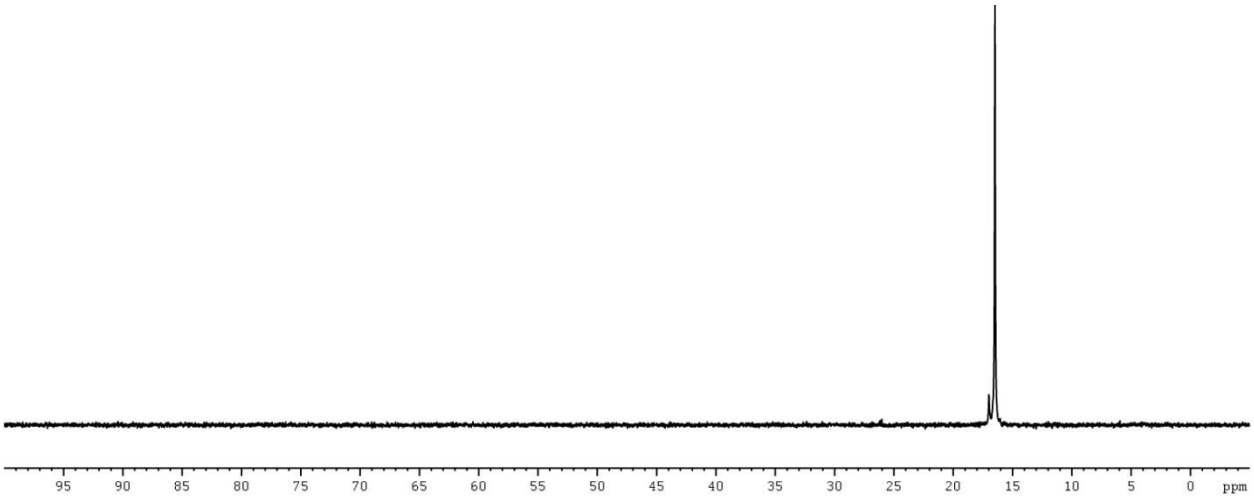

^{31}PNMR Spectrum (162 MHz) of 15-B-2: N-(N-methyl-L-valyl-L-tyrosyl)-1-amino-2-(4-hydoxyphenyl)ethyl phosphonic acid (II-3) in D_2O, pD = 11.9

NMR spectra of SF2513 B (II-4) and synthetic intermediates (II-4a - II-4d)

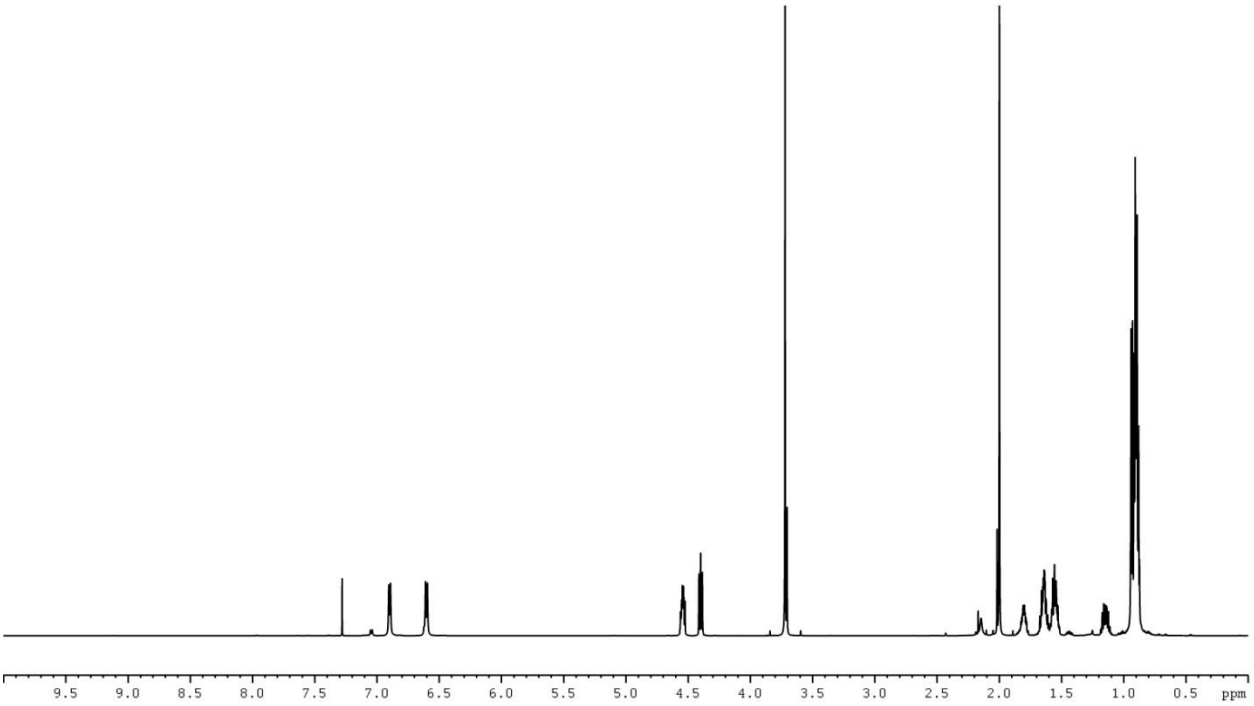

^{1}HNMR Spectrum (600 MHz) of N-acetyl-L-isoleucyl-L-leucine methyl ester (II-4a) in $CDCl_3$

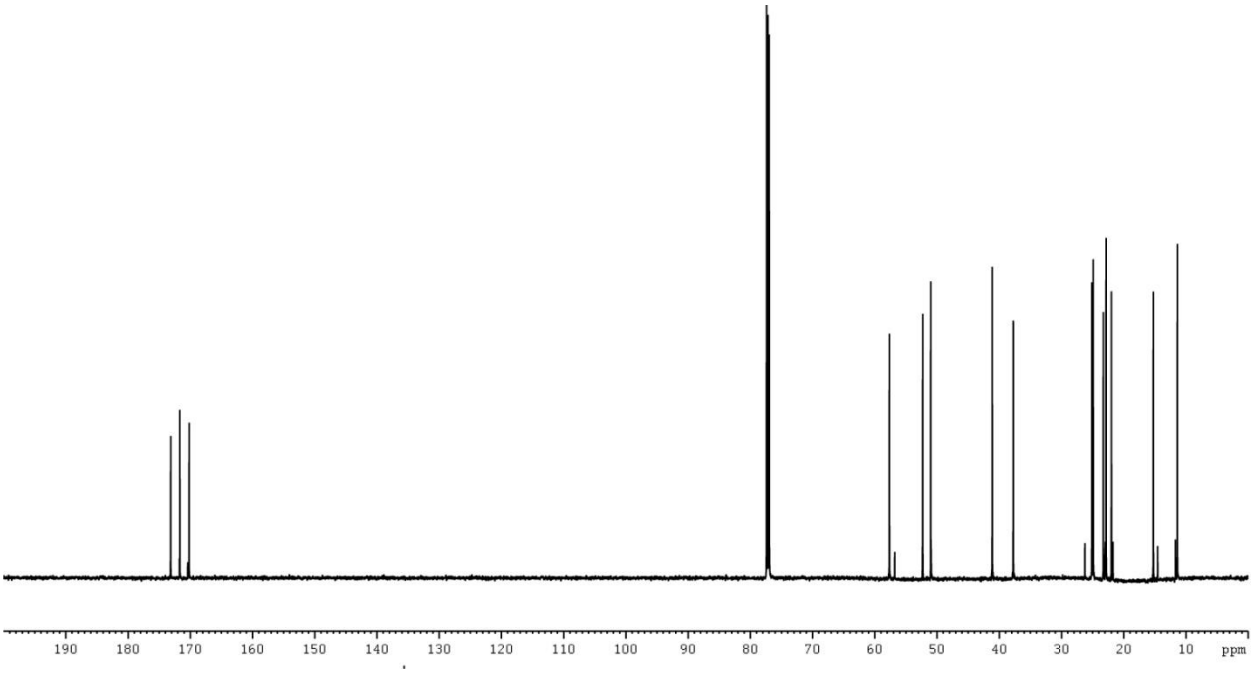

^{13}CNMR Spectrum (150 MHz) of N-acetyl-L-isoleucyl-L-leucine methyl ester (II-4a) in $CDCl_3$

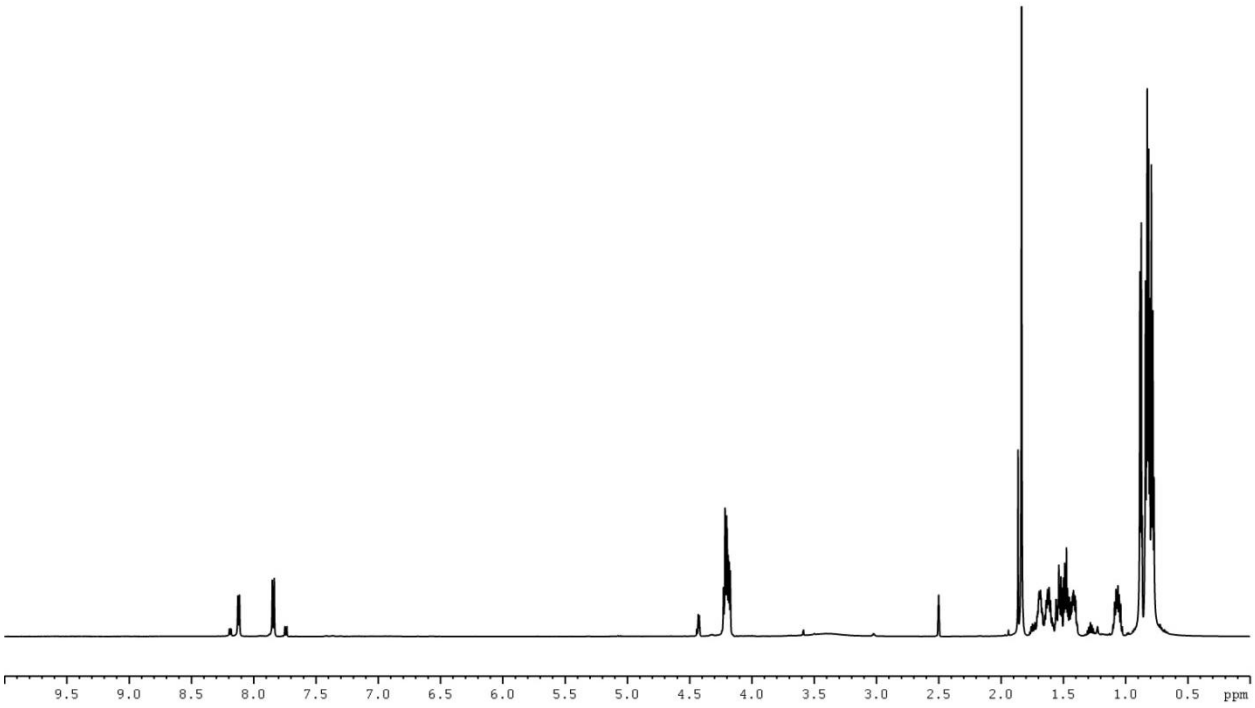

^{1}HNMR Spectrum (600 MHz) of N-acetyl-L-isoleucyl-L-leucine (II-4b) in DMSO-d^{6}

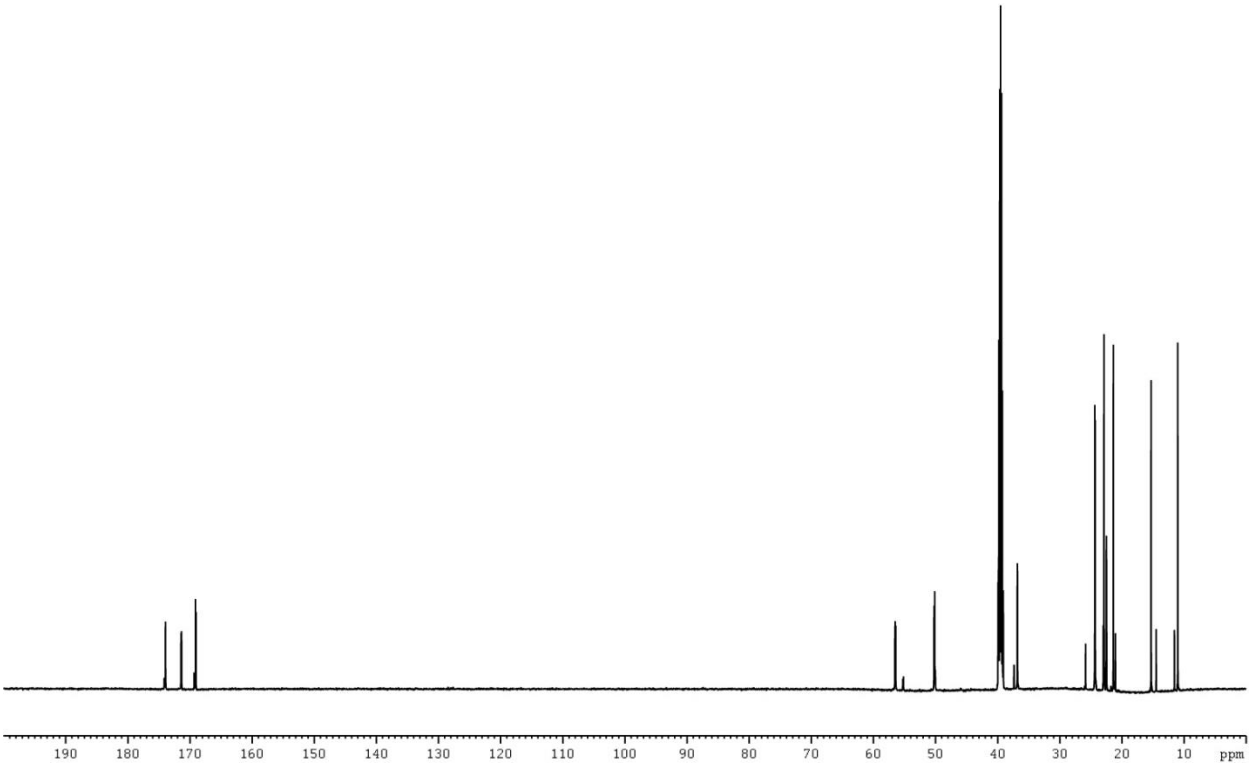

^{13}CNMR Spectrum (150 MHz) of N-acetyl-L-isoleucyl-L-leucine (II-4b) in DMSO-d^{6}

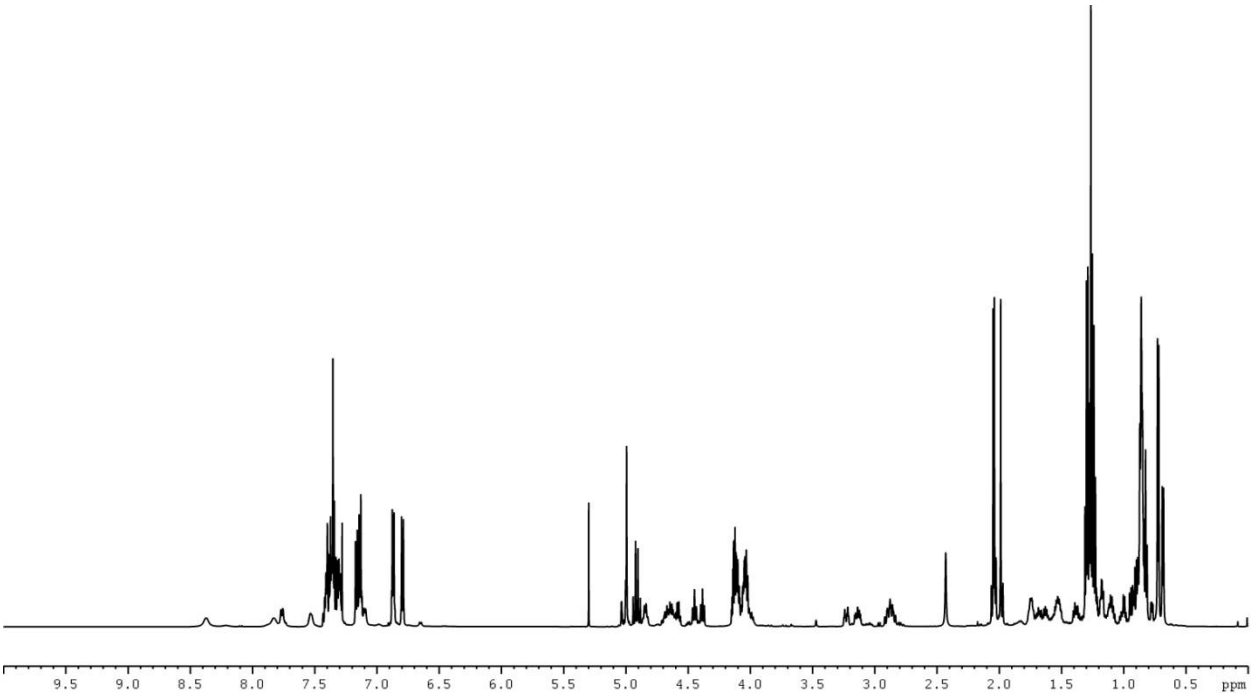

^{1}HNMR Spectrum (600 MHz) of diethyl N-(N-acetyl-L-isoleucyl-L-leucyl)-1-amino-2-(4-benzyloxyphenyl)ethyl phosphonate (II-4c) in $CDCl_3$

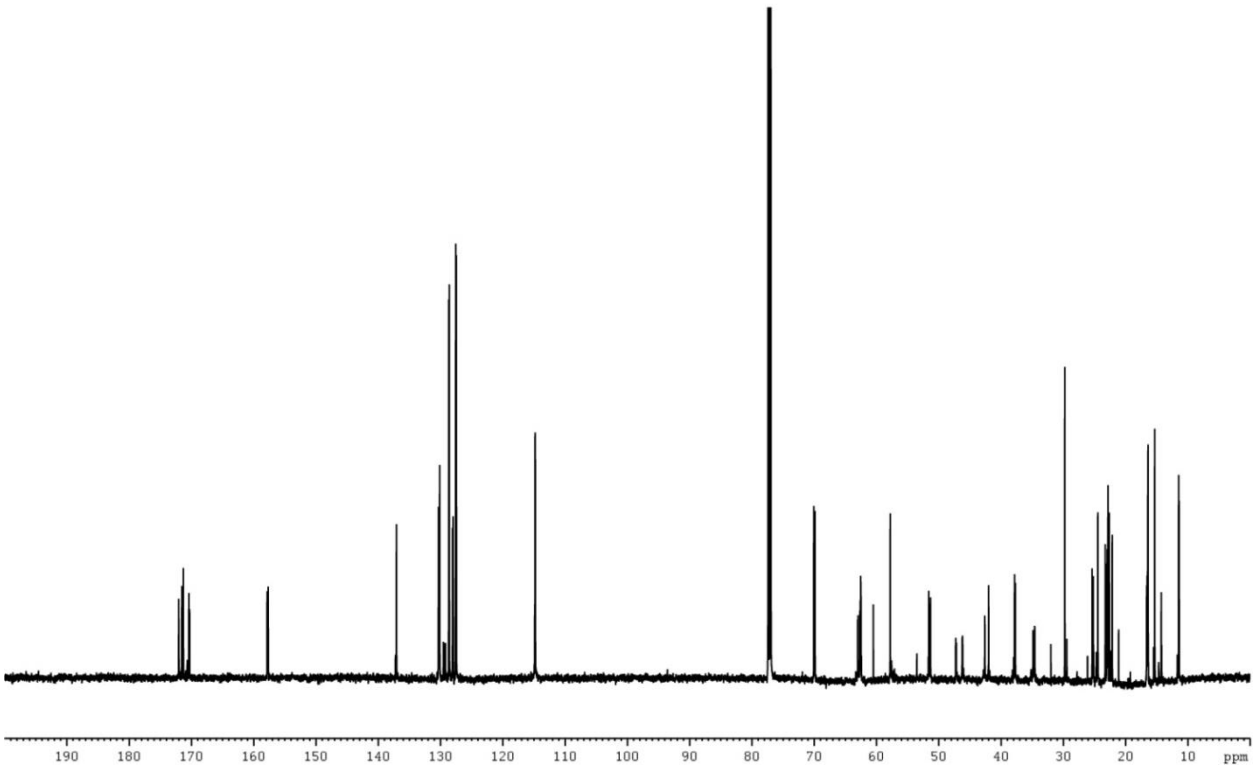

^{13}CNMR Spectrum (150 MHz) of diethyl N-(N-acetyl-L-isoleucyl-L-leucyl)-1-amino-2-(4-benzyloxyphenyl)ethyl phosphonate (II-4c) in $CDCl_3$

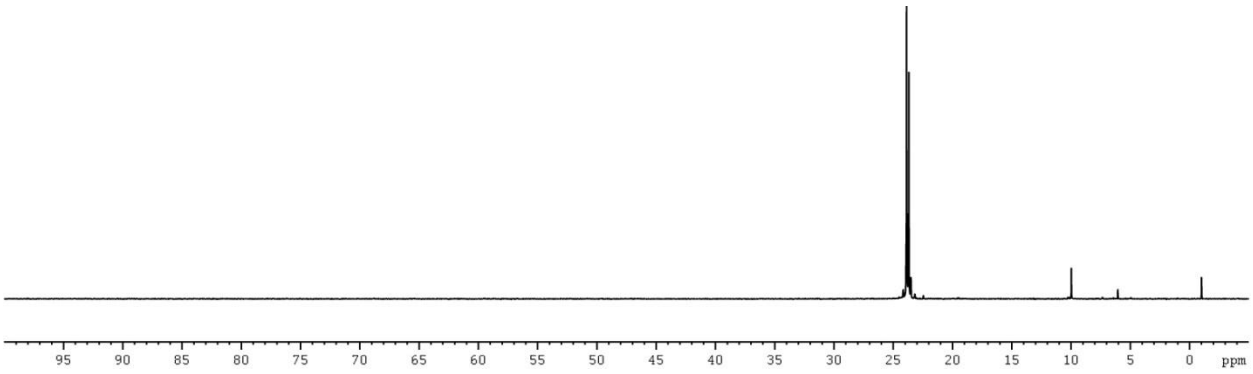

^{31}PNMR Spectrum (121 MHz) diethyl N-(N-acetyl-L-isoleucyl-L-leucyl)-1-amino-2-(4-benzyloxyphenyl)ethyl phosphonate (II-4c) in $CDCl_3$

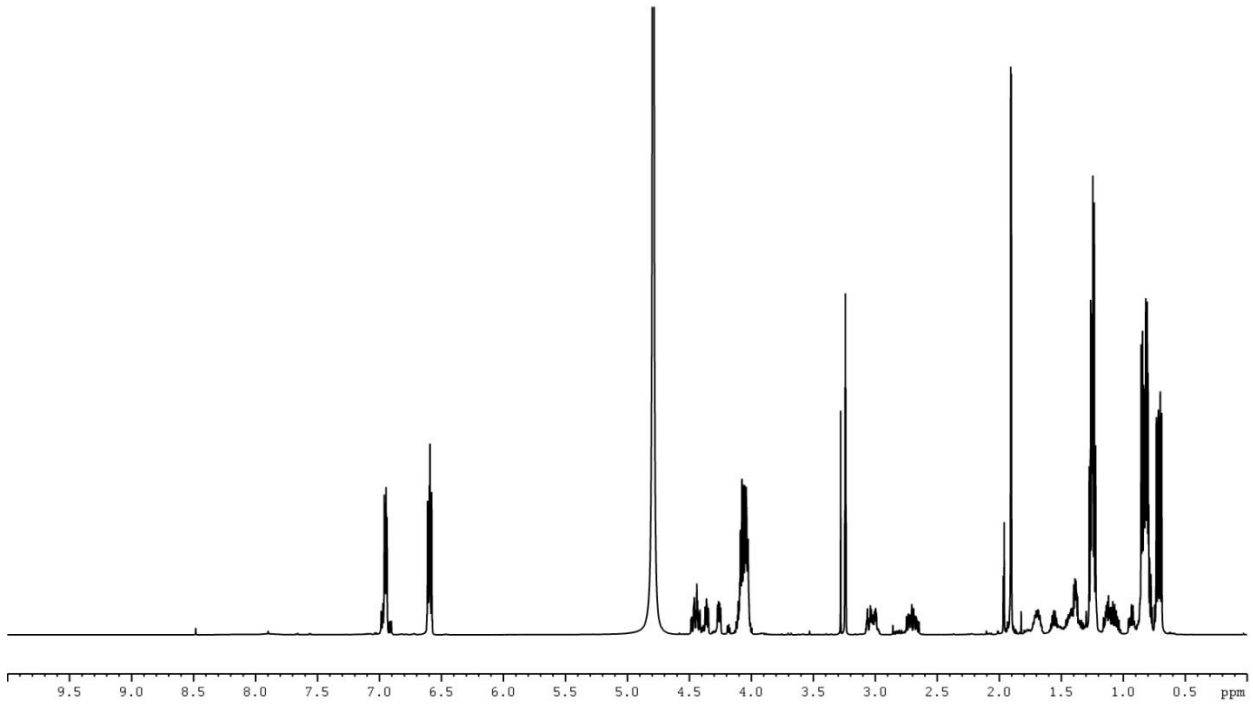

^{1}HNMR Spectrum (600 MHz) of diethyl N-(N-acetyl-L-isoleucyl-L-leucyl)-1-amino-2-(4-hydoxyphenyl)ethyl phosphonate (II-4d) in MeOD

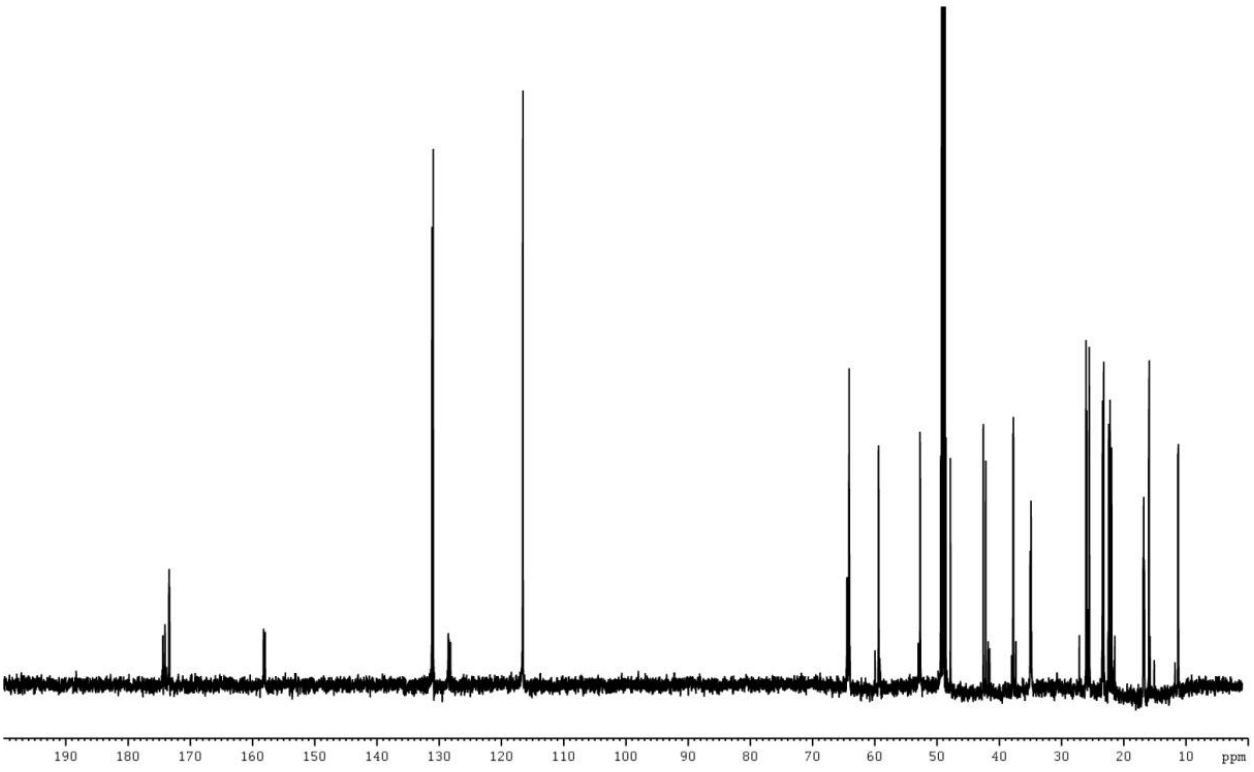

^{13}CNMR Spectrum (150 MHz) of diethyl N-(N-acetyl-L-isoleucyl-L-leucyl)-1-amino-2-(4-hydoxyphenyl)ethyl phosphonate (II-4d) in MeOD

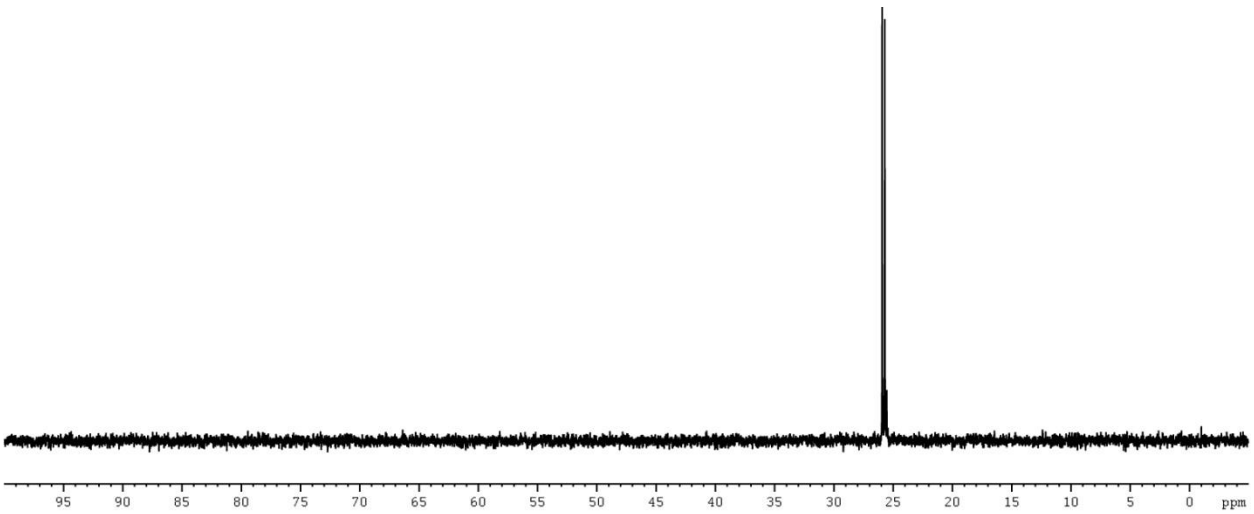

^{31}PNMR Spectrum (121 MHz) diethyl N-(N-acetyl-L-isoleucyl-L-leucyl)-1-amino-2-(4-hydoxyphenyl)ethyl phosphonate (II-4d) in MeOD

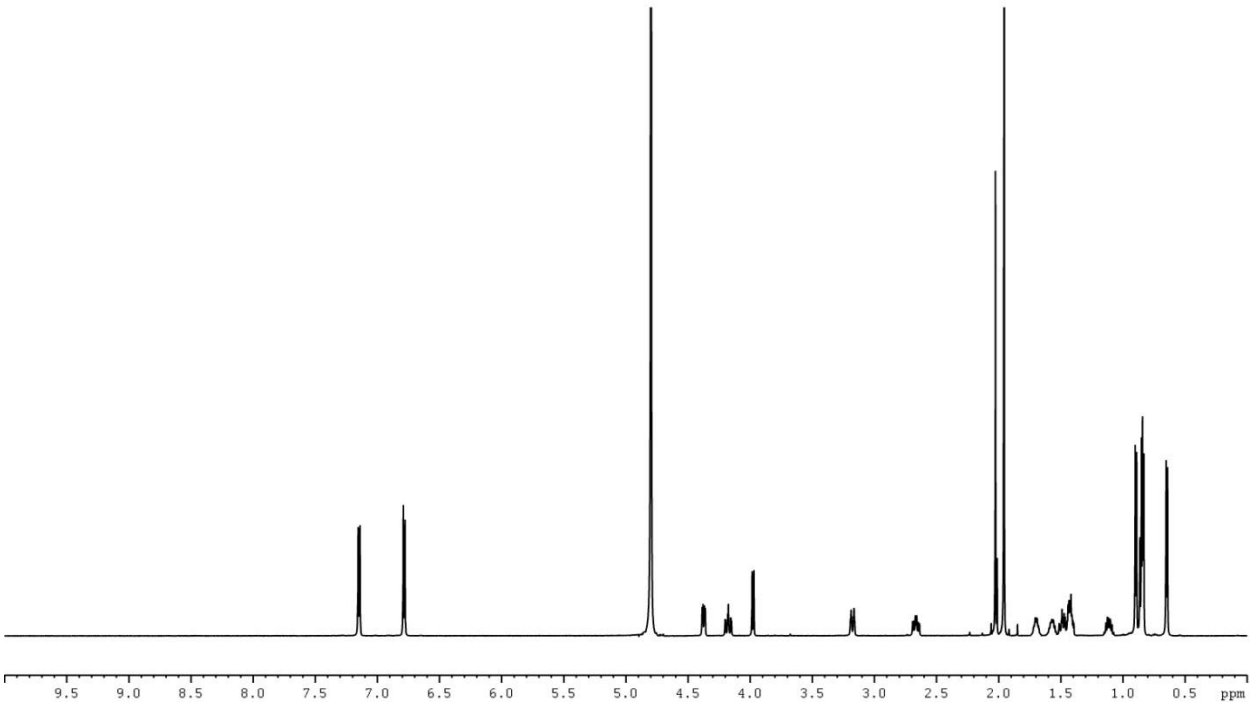

^{1}HNMR Spectrum (600 MHz) of SF2513 B: N-(N-acetyl-L-isoleucyl-L-leucyl)-1-amino-2-(4-hydoxyphenyl)ethyl phosphonic acid (II-4) in D_2O

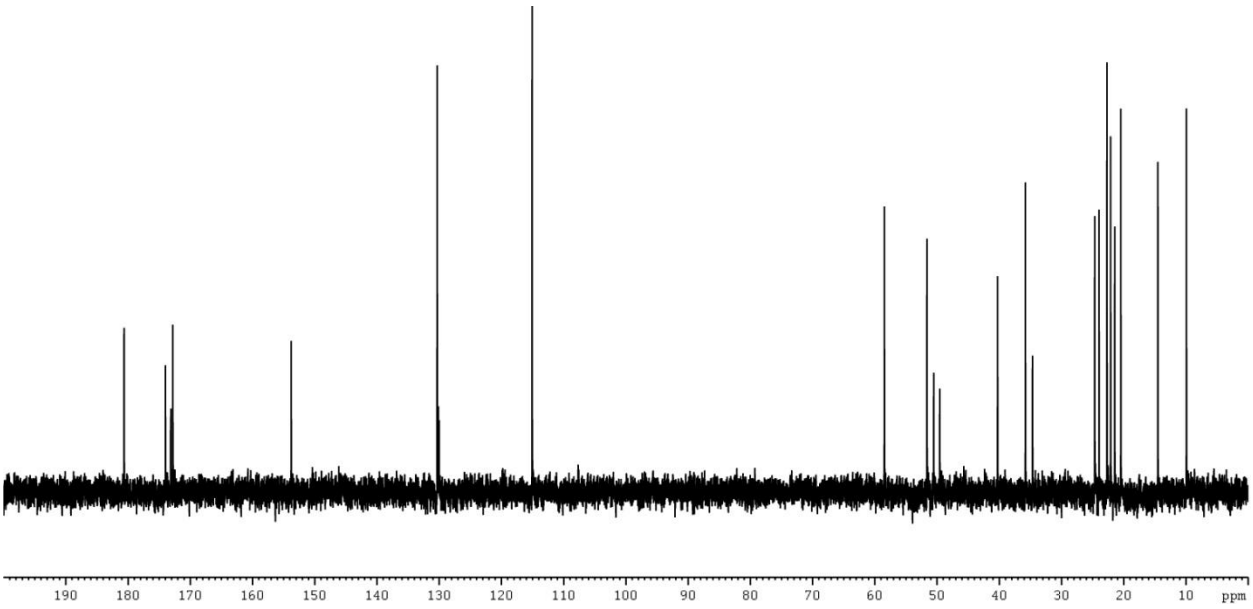

^{13}CNMR Spectrum (150 MHz) of SF2513 B: N-(N-acetyl-L-isoleucyl-L-leucyl)-1-amino-2-(4-hydoxyphenyl)ethyl phosphonic acid (II-4) in D_2O

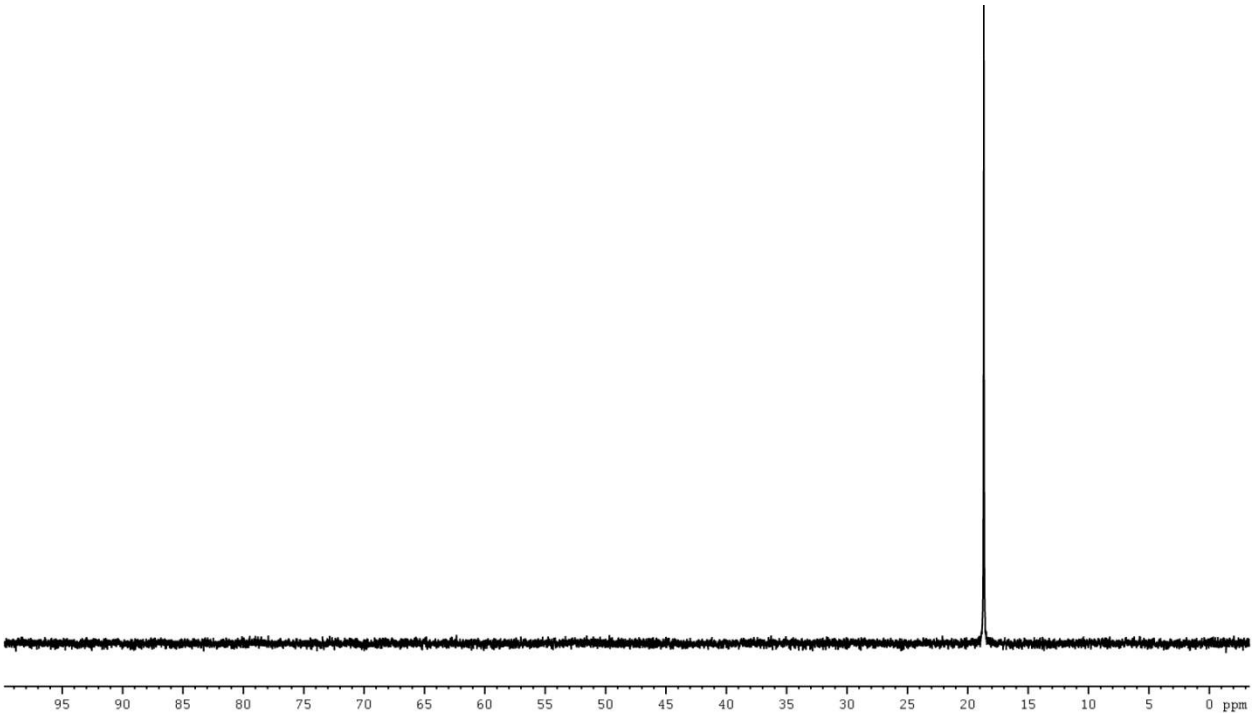

^{31}PNMR Spectrum (162 MHz) of SF2513 B: N-(N-acetyl-L-isoleucyl-L-leucyl)-1-amino-2-(4-hydoxyphenyl)ethyl phosphonic acid (II-4) in D_2O

NMR spectra of SF2513 C (II-5) and synthetic intermediates (II-5a - II-5d)

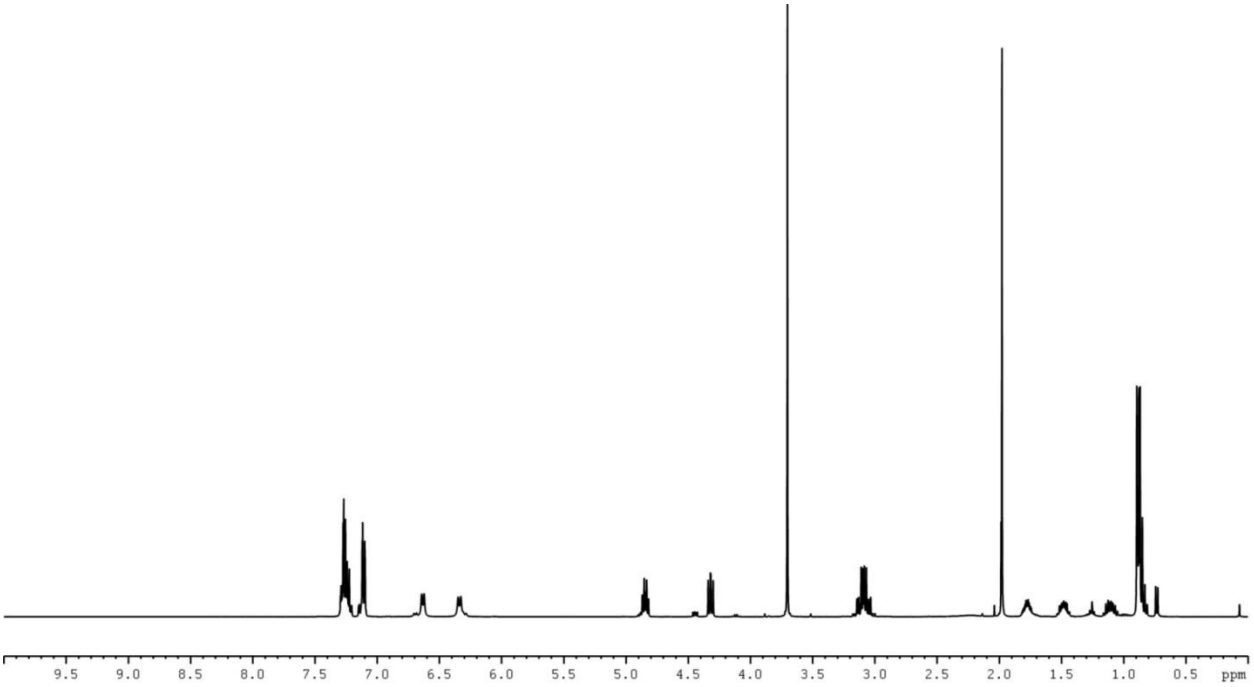

^{1}HNMR Spectrum (400 MHz) of N-acetyl-L-isoleucyl-L-phenylalanine methyl ester (II-5a) in $CDCl_3$

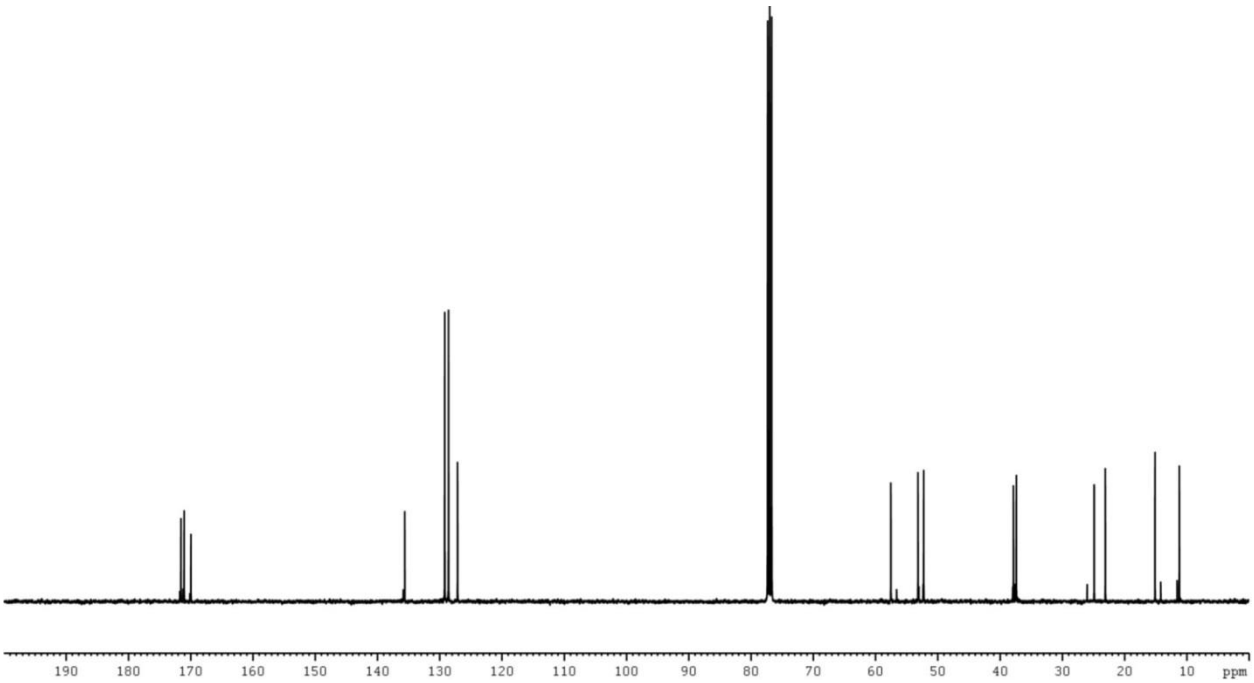

^{13}CNMR Spectrum (100 MHz) of N-acetyl-L-isoleucyl-L-phenylalanine methyl ester (II-5a) in $CDCl_3$

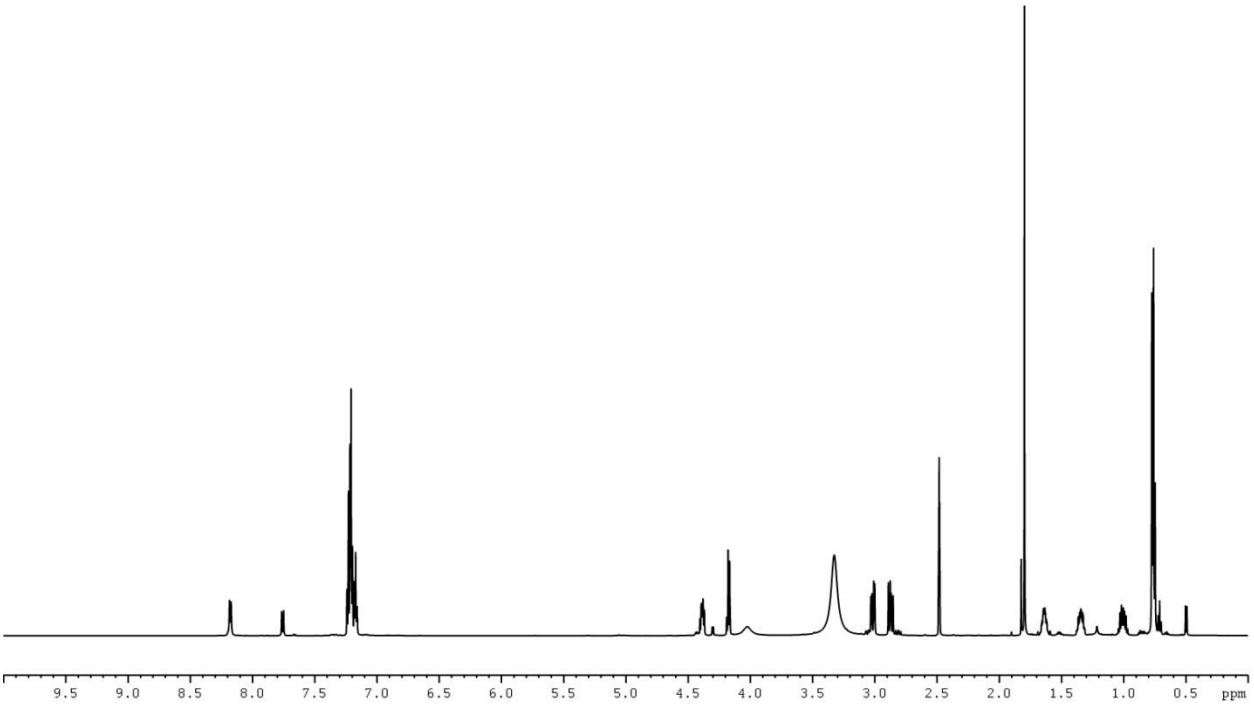

^{1}HNMR Spectrum (600 MHz) of N-acetyl-L-isoleucyl-L-phenylalanine (II-5b) in DMSO-d^{6}

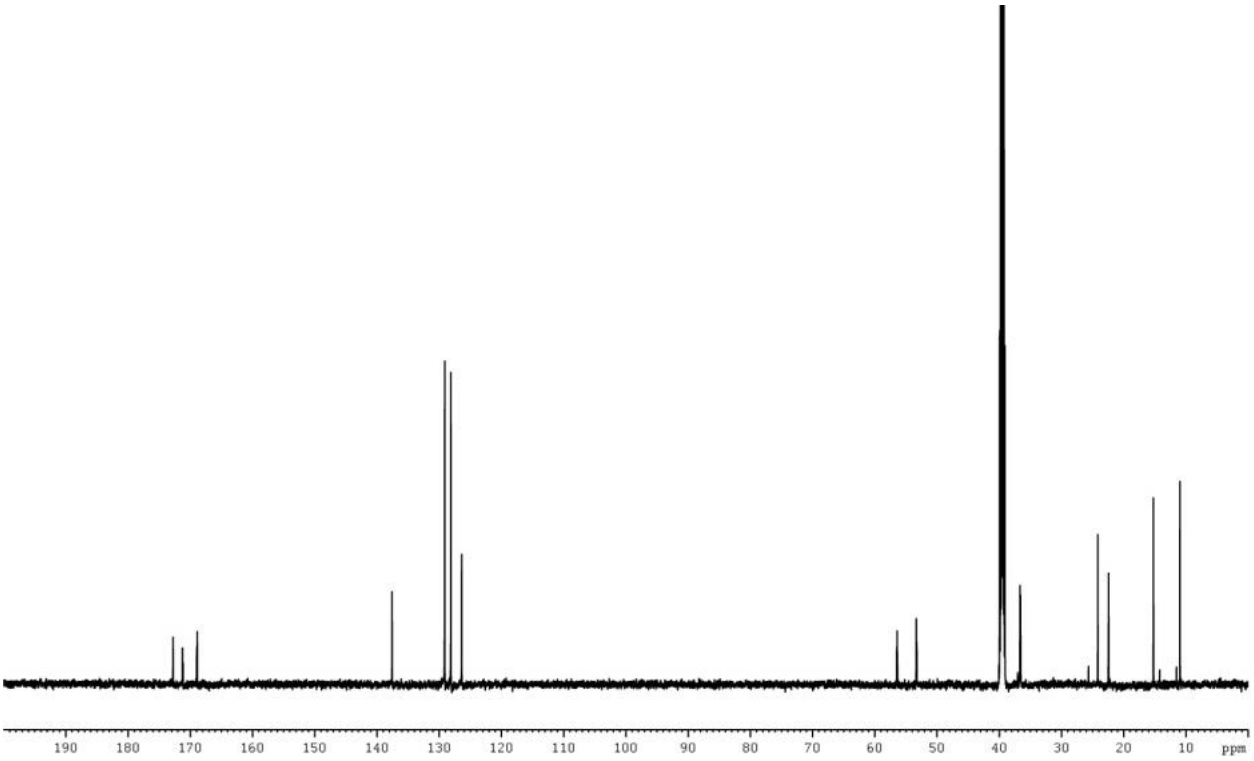

^{13}CNMR Spectrum (1II-50 MHz) of N-acetyl-L-isoleucyl-L-phenylalanine (II-5b) in DMSO-d^{6}

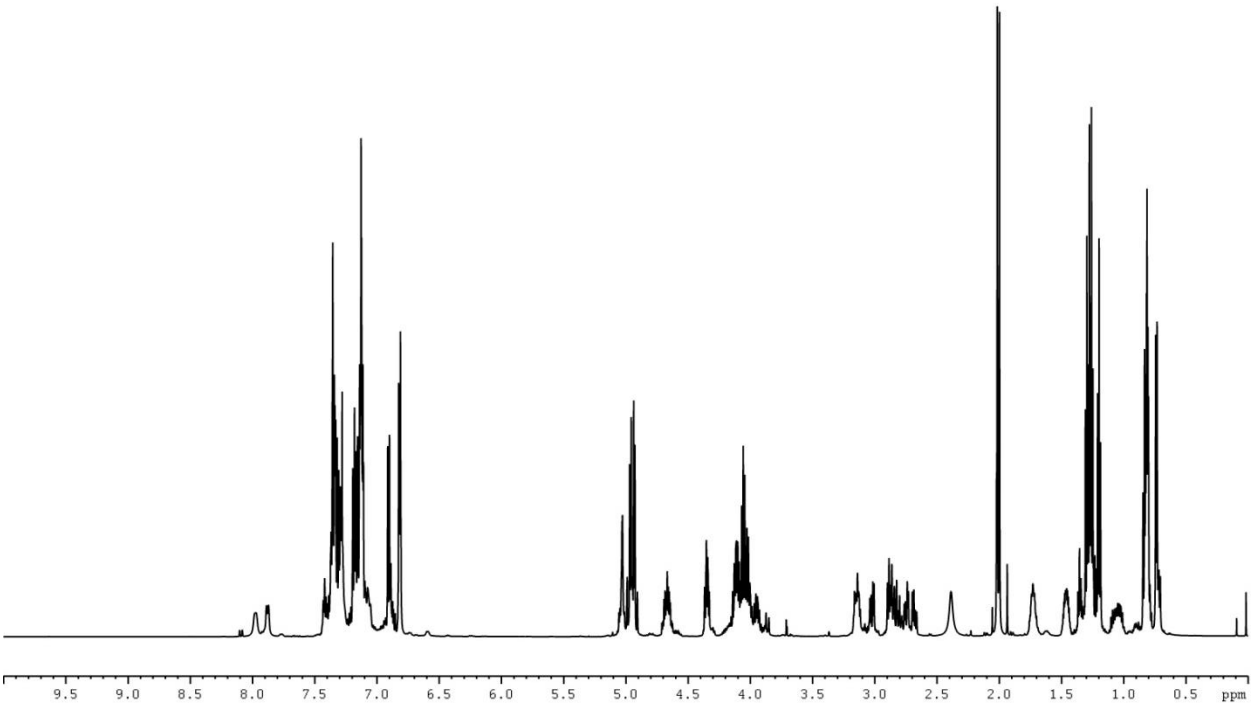

^{1}HNMR Spectrum (600 MHz) of diethyl N-(N-acetyl-L-isoleucyl-L-phenylalanyl)-1-amino-2-(4-benzyloxyphenyl)ethyl phosphonate (II-5c) in $CDCl_3$

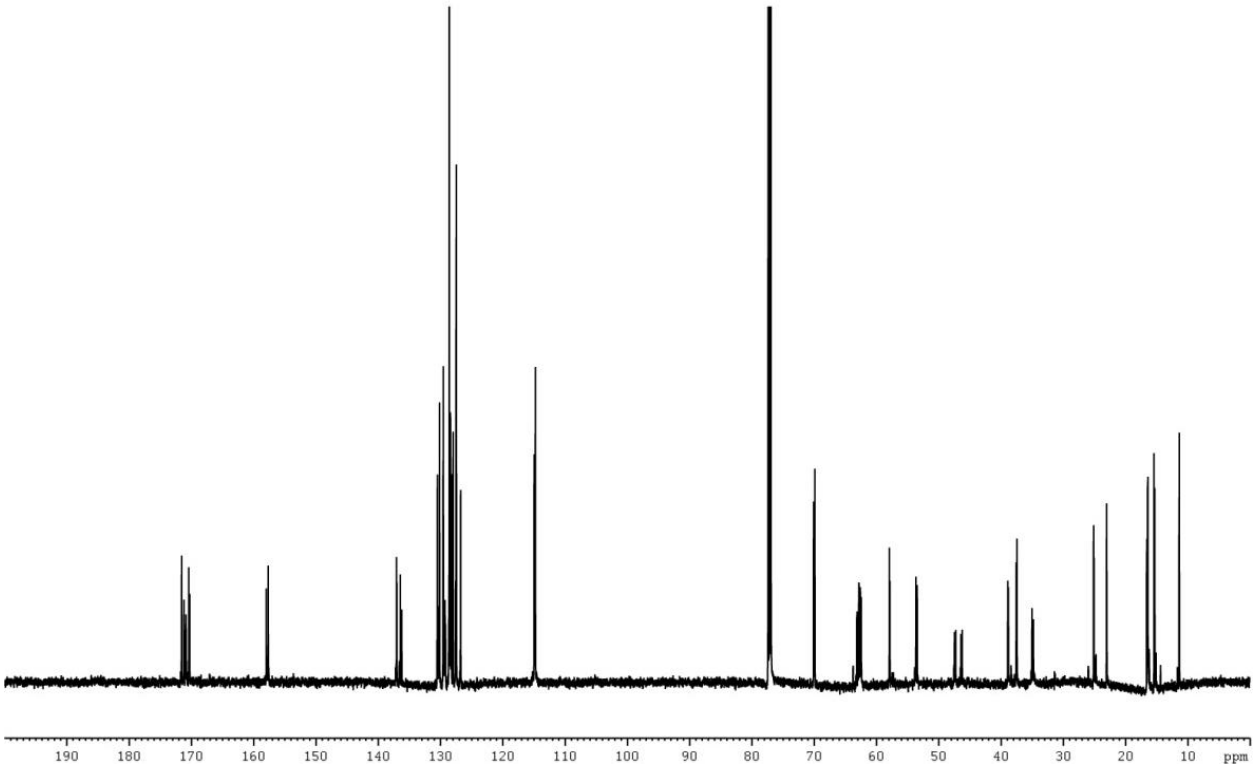

^{13}CNMR Spectrum (150 MHz) of diethyl N-(N-acetyl-L-isoleucyl-L-phenylalanyl)-1-amino-2-(4-benzyloxyphenyl)ethyl phosphonate (II-5c) in $CDCl_3$

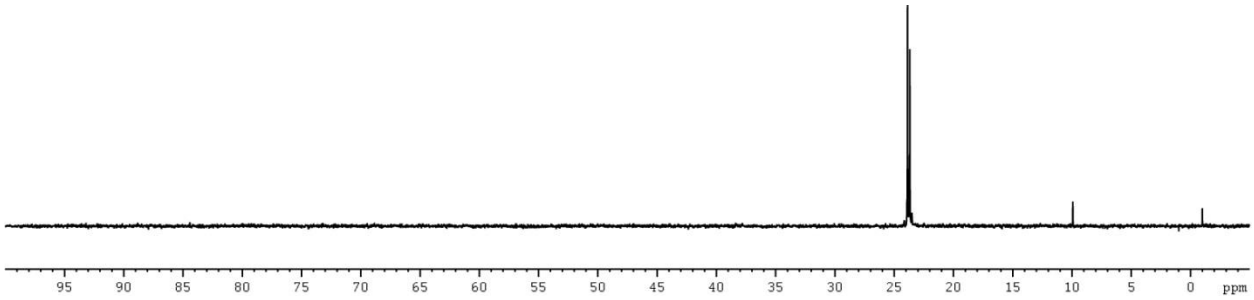

^{31}PNMR Spectrum (121 MHz) of diethyl N-(N-acetyl-L-isoleucyl-L-phenylalanyl)-1-amino-2-(4-benzyloxyphenyl)ethyl phosphonate (II-5c) in $CDCl_3$

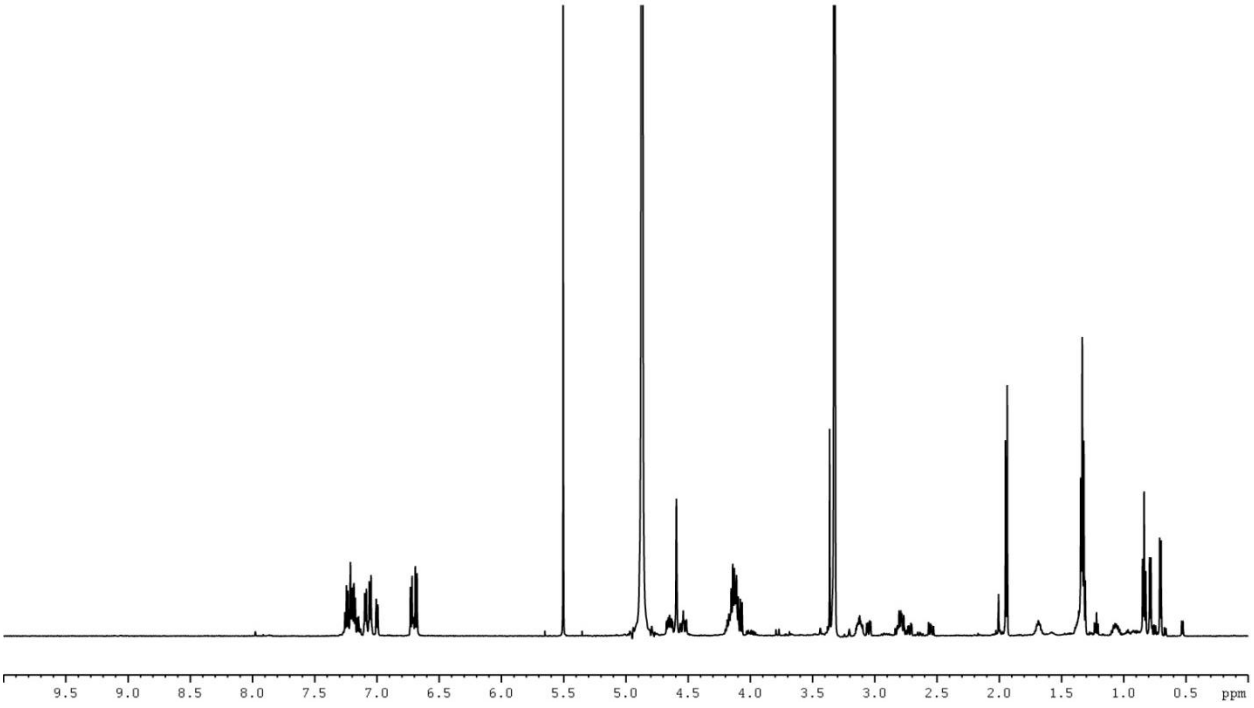

^{1}HNMR Spectrum (600 MHz) of diethyl N-(N-acetyl-L-isoleucyl-L-phenylalanyl)-1-amino-2-(4-hydoxyphenyl)ethyl phosphonate (II-5d) in MeOD

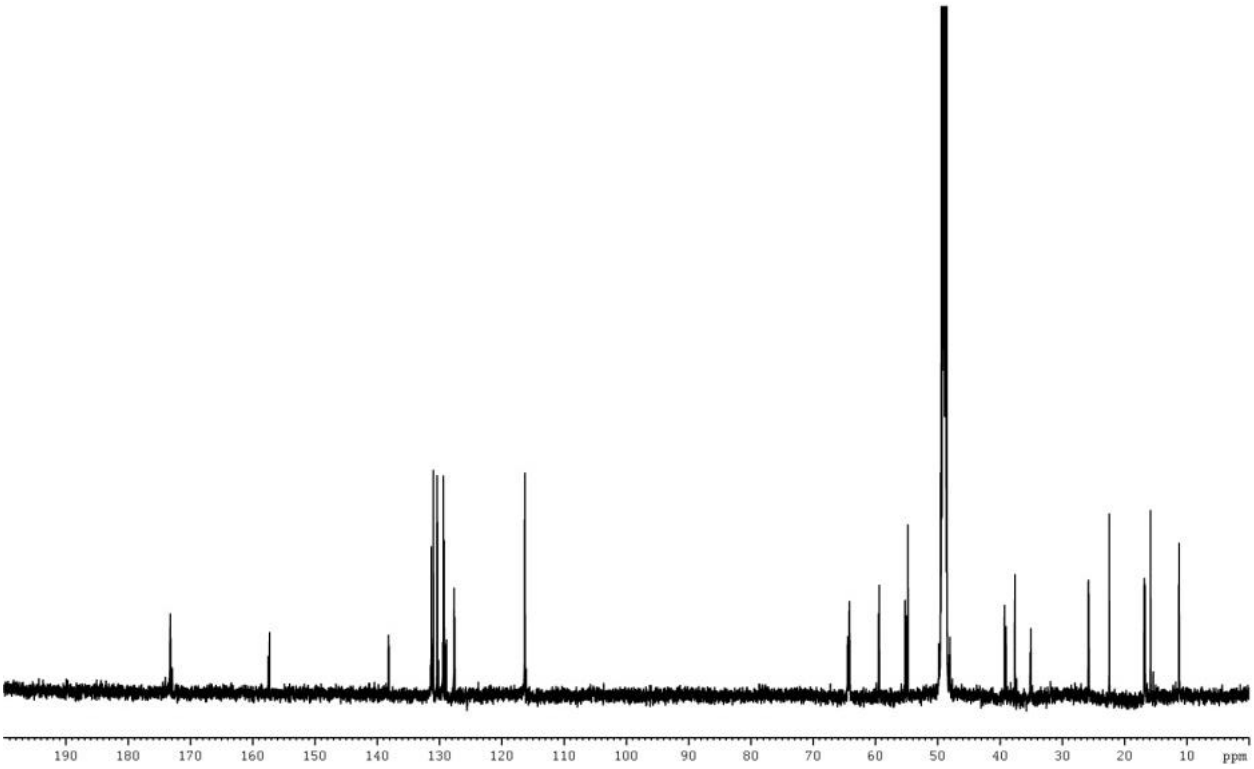

^{13}CNMR Spectrum (150 MHz) of diethyl N-(N-acetyl-L-isoleucyl-L-phenylalanyl)-1-amino-2-(4-hydoxyphenyl)ethyl phosphonate (II-5d) in MeOD

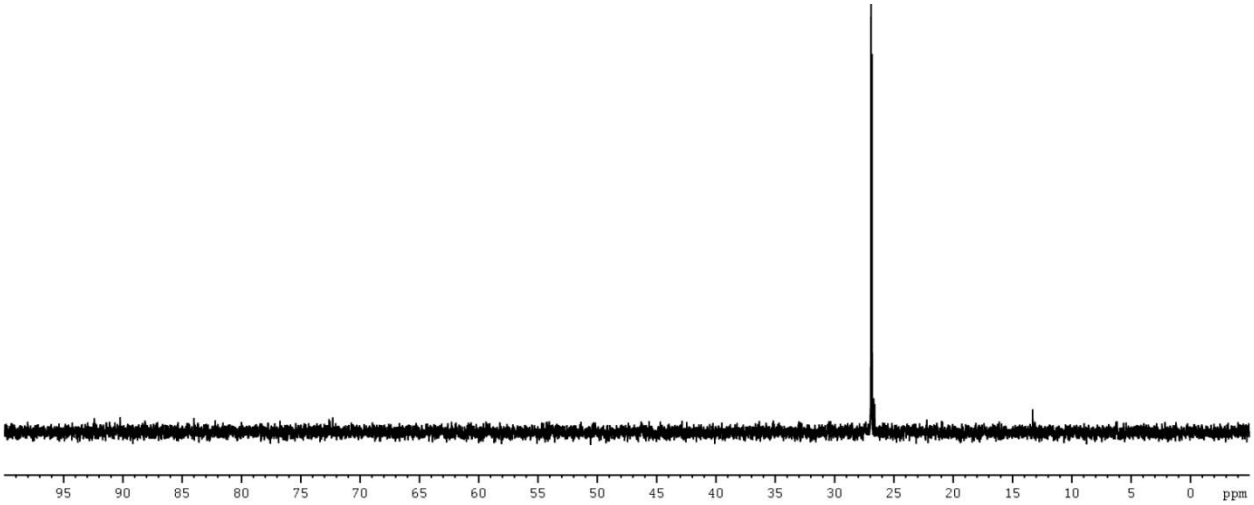

^{31}PNMR Spectrum (162 MHz) of diethyl N-(N-acetyl-L-isoleucyl-L-phenylalanyl)-1-amino-2-(4-hydoxyphenyl)ethyl phosphonate (II-5d) in MeOD

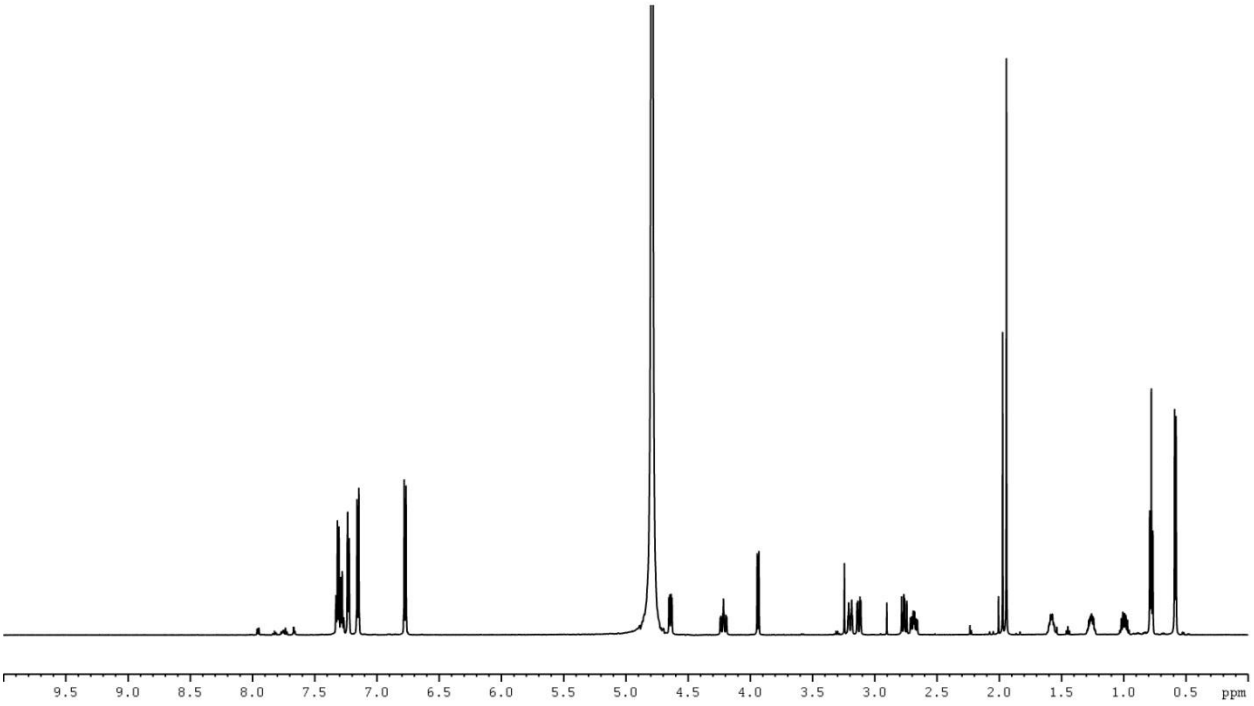

^{1}HNMR Spectrum (600 MHz) of SF2513 C: N-(N-acetyl-L-isoleucyl-L-phenylalanyl)-1-amino-2-(4-hydoxyphenyl)ethyl phosphonic acid (II-5) in D_2O

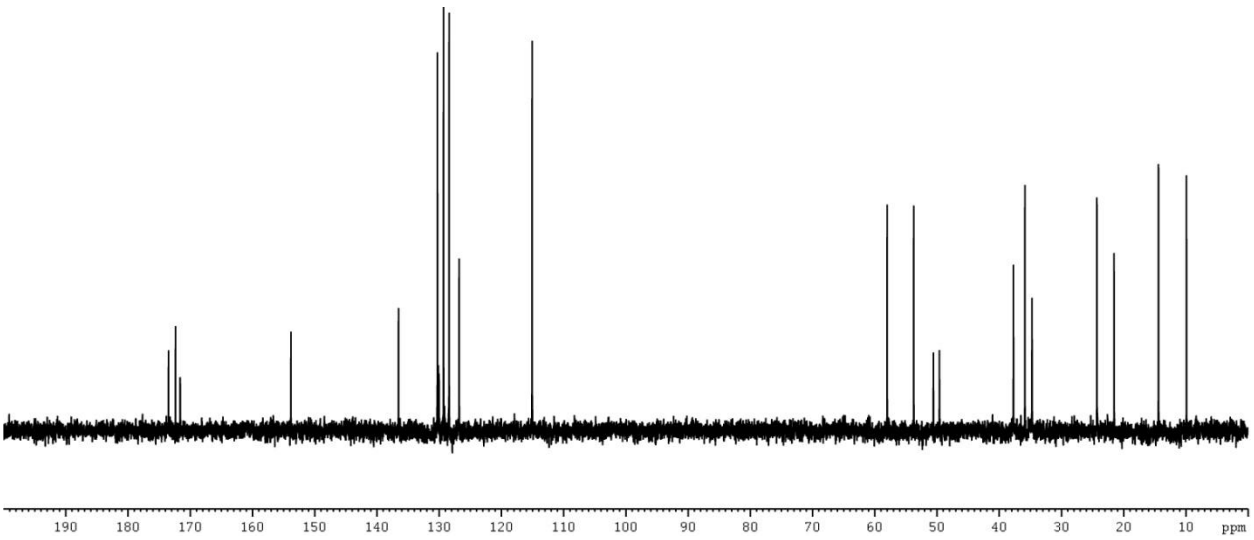

^{13}CNMR Spectrum (150 MHz) of SF2513 C: N-(N-acetyl-L-isoleucyl-L-phenylalanyl)-1-amino-2-(4-hydoxyphenyl)ethyl phosphonic acid (II-5) in D_2O

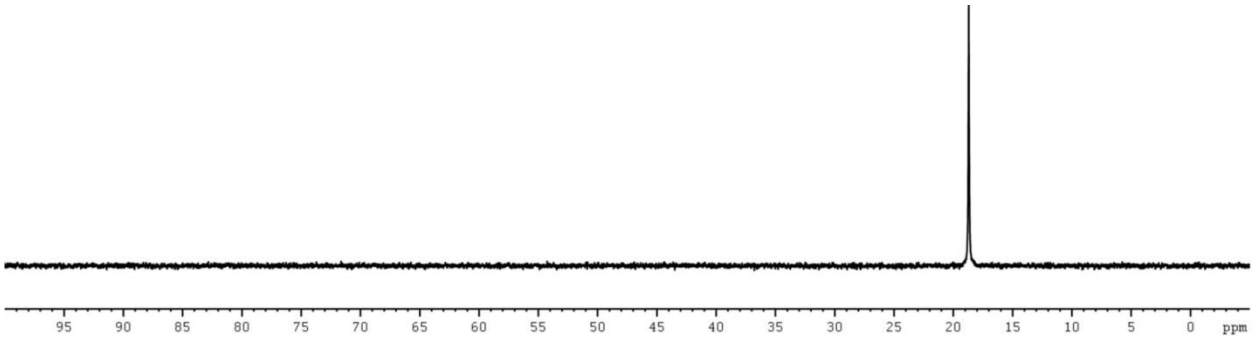

^{31}PNMR Spectrum (162 MHz) of SF2513 C: N-(N-acetyl-L-isoleucyl-L-phenylalanyl)-1-amino-2-(4-hydoxyphenyl)ethyl phosphonic acid (II-5) in D_2O

NMR spectra of SF2513 D (II-7) and synthetic intermediates (II-7b – II-7e)

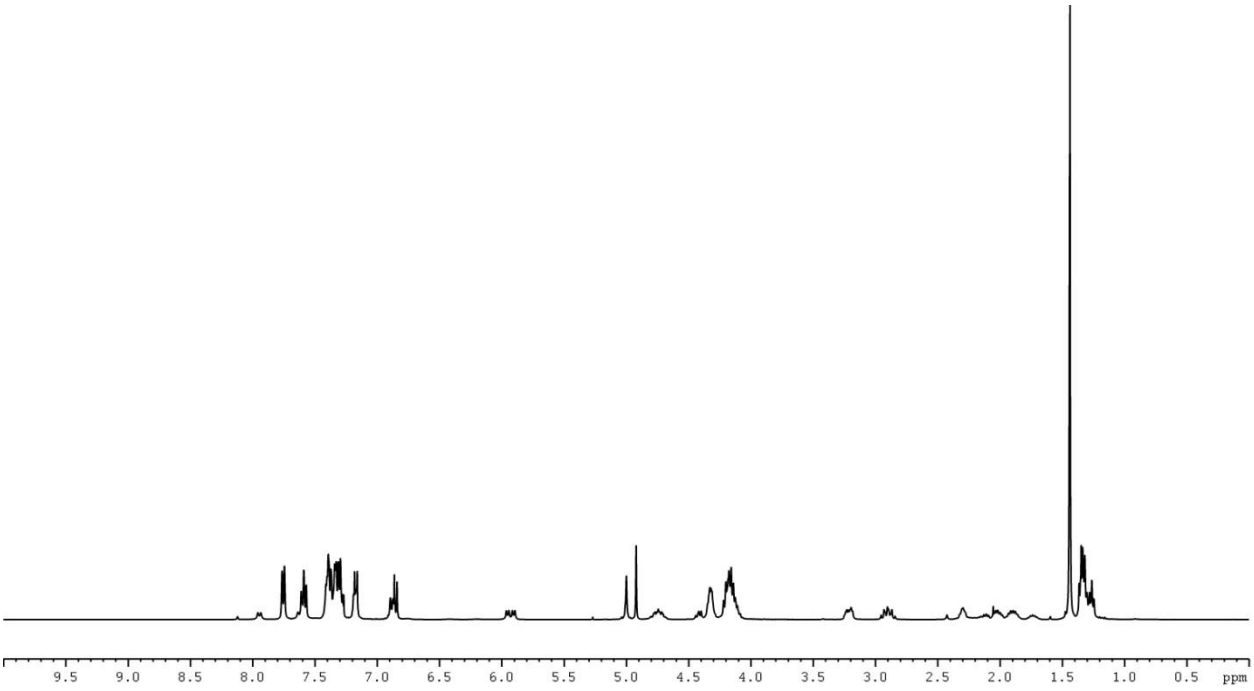

^{1}HNMR Spectrum (400 MHz) of diethyl N-(N-fluorenylmethyloxycarbonyl-L-glutamyl-5-tert-butyl ester)-1-amino-2-(4-benzyloxyphenyl)ethyl phosphonate (II-7b) in $CDCl_3$

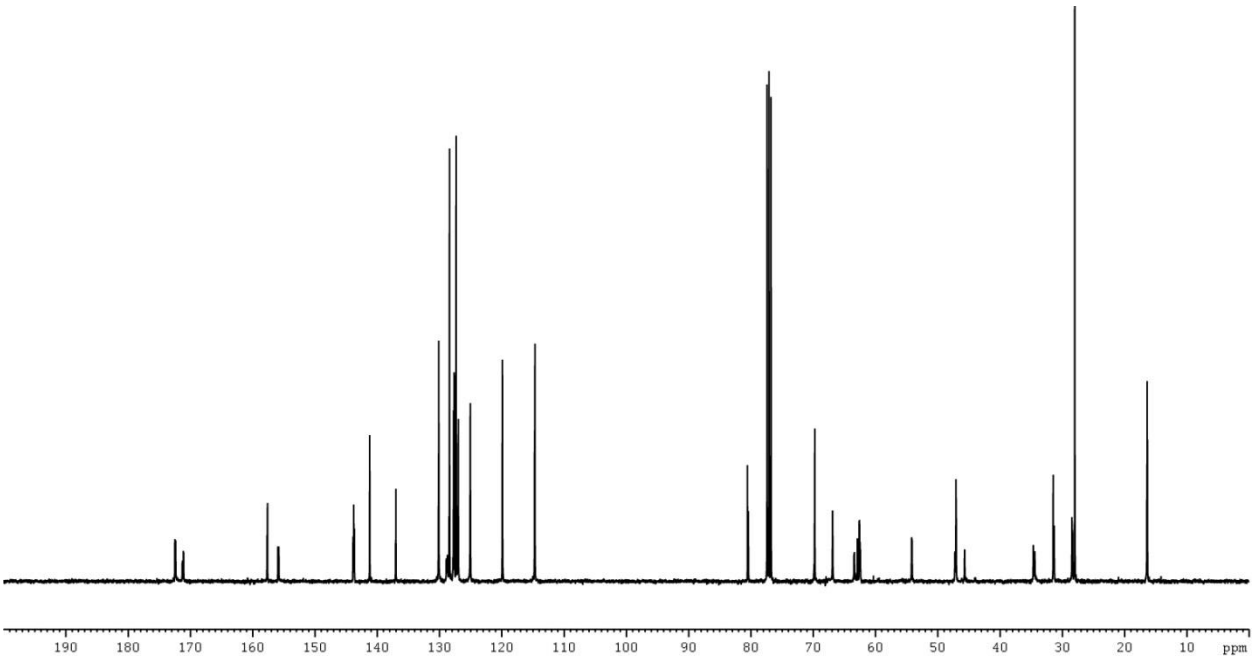

^{13}CNMR Spectrum (100 MHz) of diethyl N-(N-fluorenylmethyloxycarbonyl-L-glutamyl-5-tert-butyl ester)-1-amino-2-(4-benzyloxyphenyl)ethyl phosphonate (II-7b) in $CDCl_3$

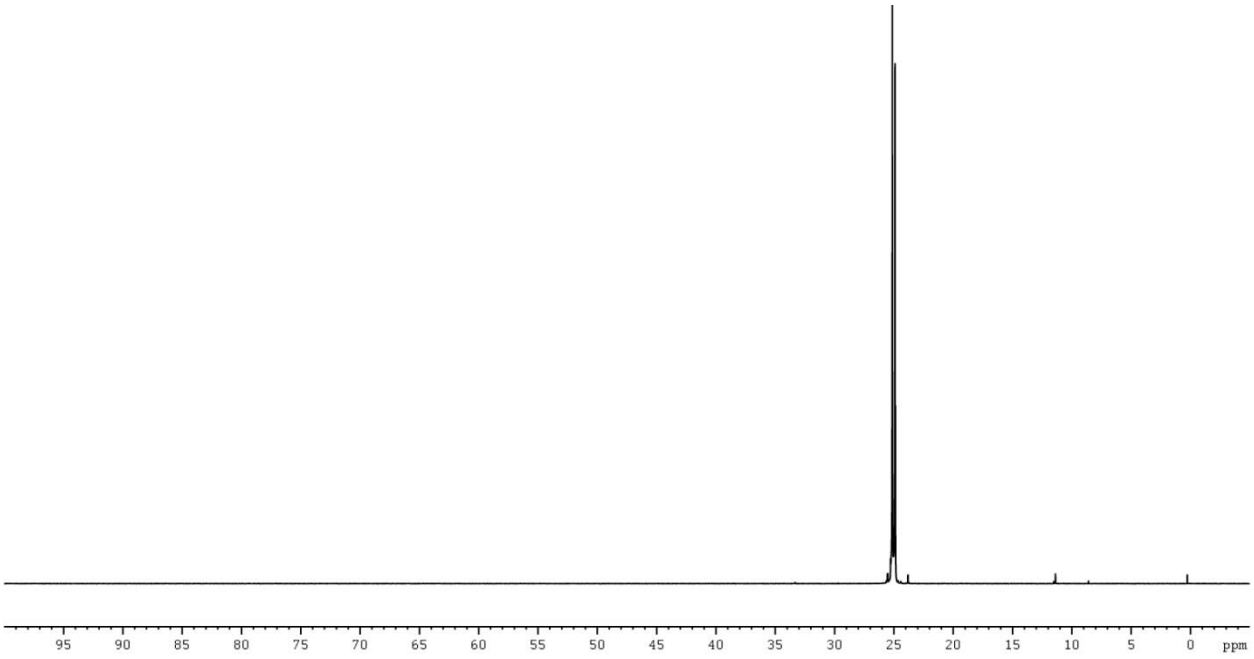

^{31}PNMR Spectrum (162 MHz) of diethyl N-(N-fluorenylmethyloxycarbonyl-L-glutamyl-5-tert-butyl ester)-1-amino-2-(4-benzyloxyphenyl)ethyl phosphonate (II-7b) in $CDCl_3$

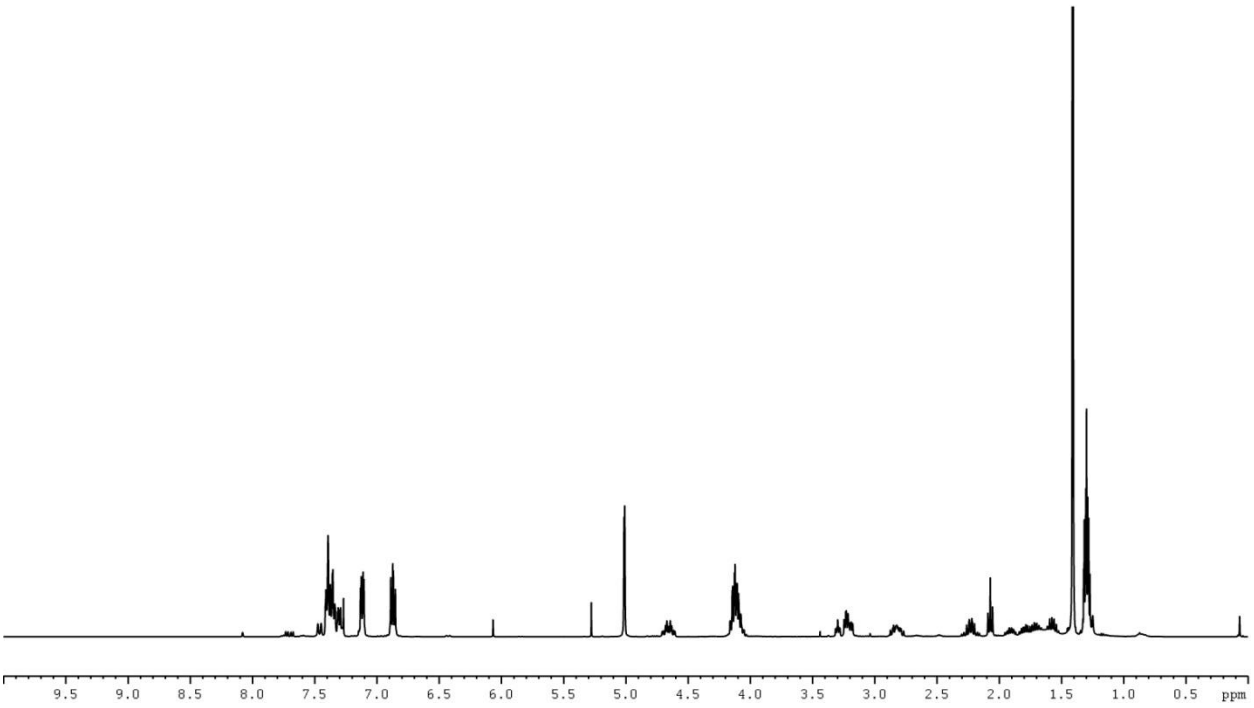

^{1}HNMR Spectrum (400 MHz) of diethyl N-(L-glutamyl-5-tert-butyl ester)-1-amino-2-(4-benzyloxyphenyl)ethyl phosphonate (II-7c) in $CDCl_3$

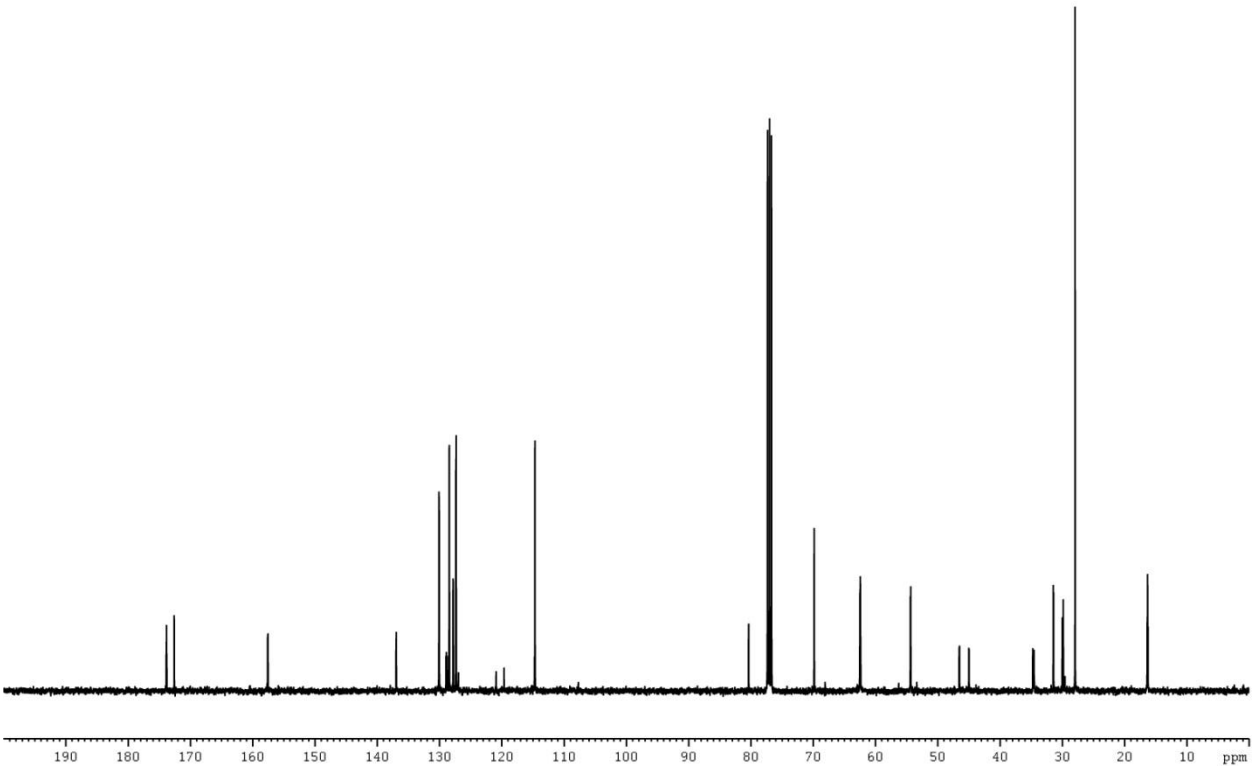

^{13}CNMR Spectrum (100 MHz) of diethyl N-(L-glutamyl-5-tert-butyl ester)-1-amino-2-(4-benzyloxyphenyl)ethyl phosphonate (II-7c) in $CDCl_3$

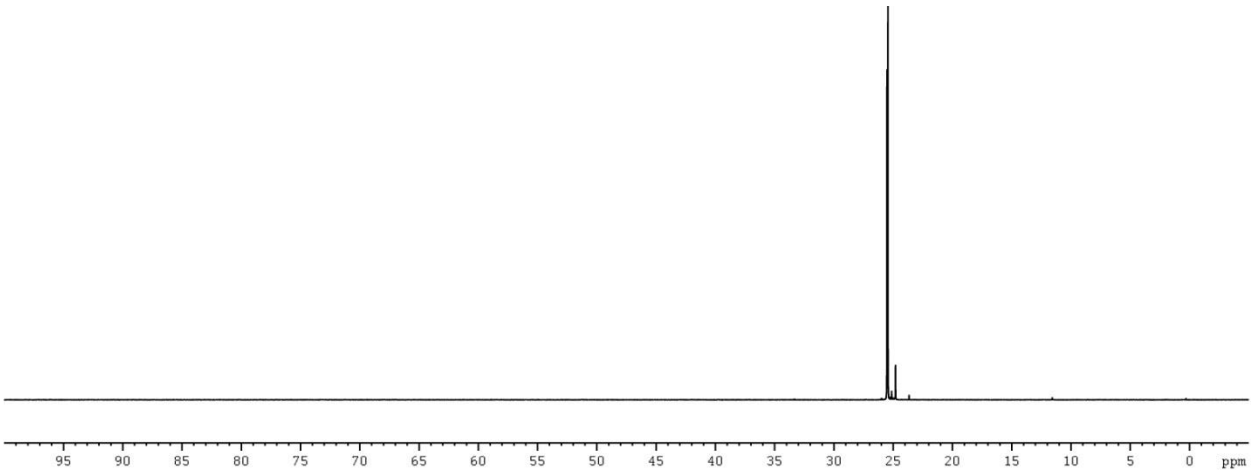

^{31}PNMR Spectrum (162 MHz) of diethyl N-(L-glutamyl-5-tert-butyl ester)-1-amino-2-(4-benzyloxyphenyl)ethyl phosphonate (II-7c) in $CDCl_3$

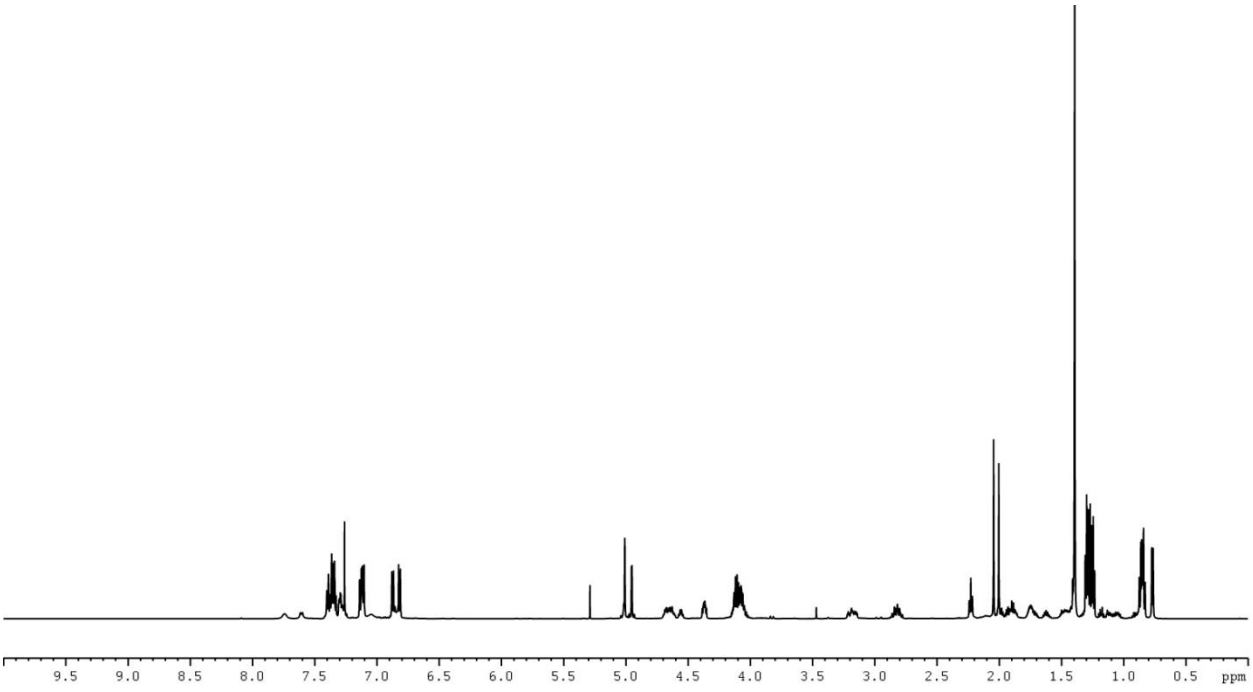

^{1}HNMR Spectrum (600 MHz) diethyl N-(N-acetyl-L-isoleucyl-L-glutamyl-5-tert-butyl ester)-1-amino-2-(4-benzyloxyphenyl)ethyl phosphonate (II-7d) in $CDCl_3$

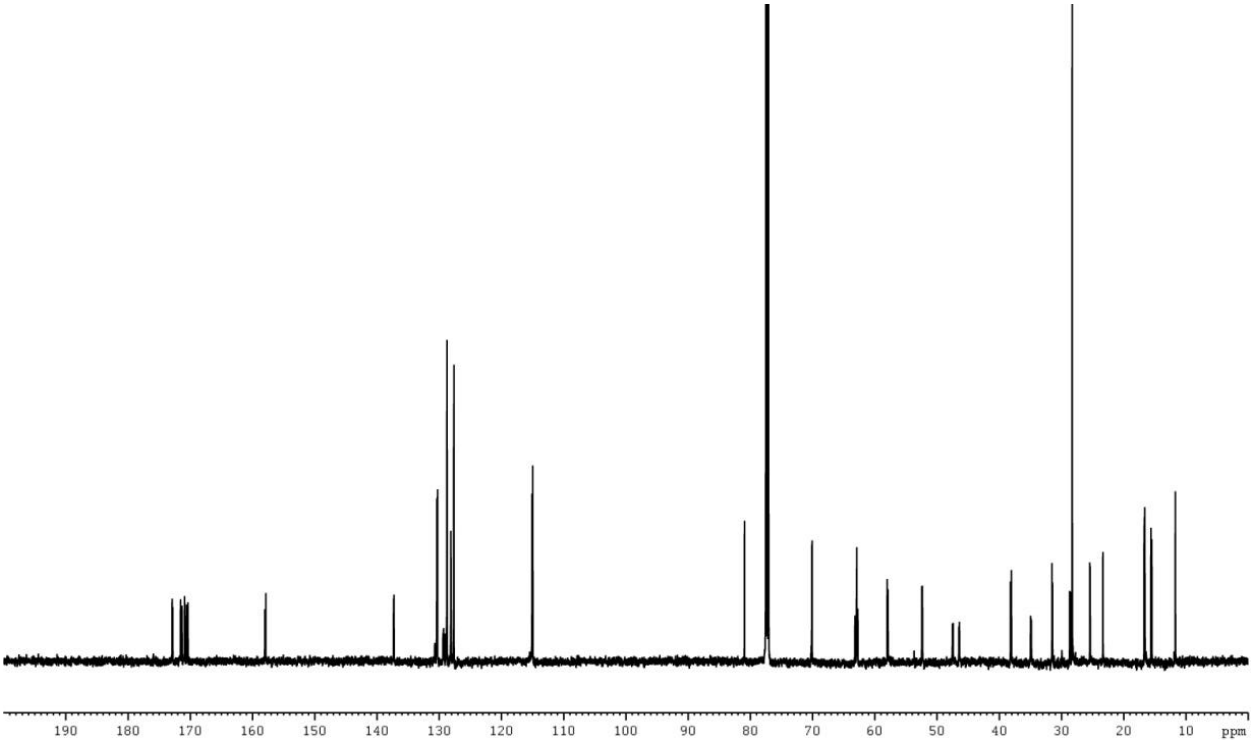

^{13}CNMR Spectrum (150 MHz) of diethyl N-(N-acetyl-L-isoleucyl-L-glutamyl-5-tert-butyl ester)-1-amino-2-(4-benzyloxyphenyl)ethyl phosphonate (II-7d) in $CDCl_3$

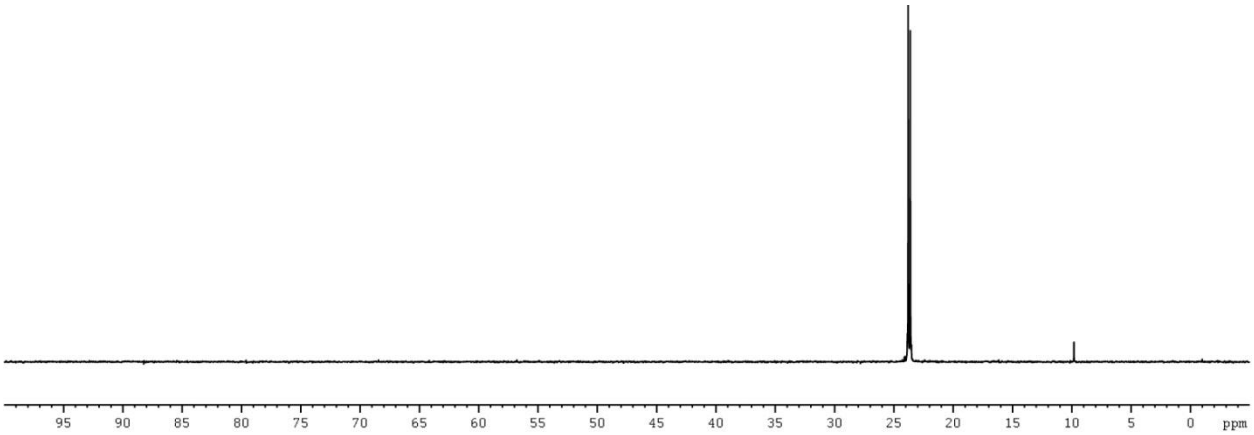

^{31}PNMR Spectrum (162 MHz) of diethyl N-(N-acetyl-L-isoleucyl-L-glutamyl-5-tert-butyl ester)-1-amino-2-(4-benzyloxyphenyl)ethyl phosphonate (II-7d) in $CDCl_3$

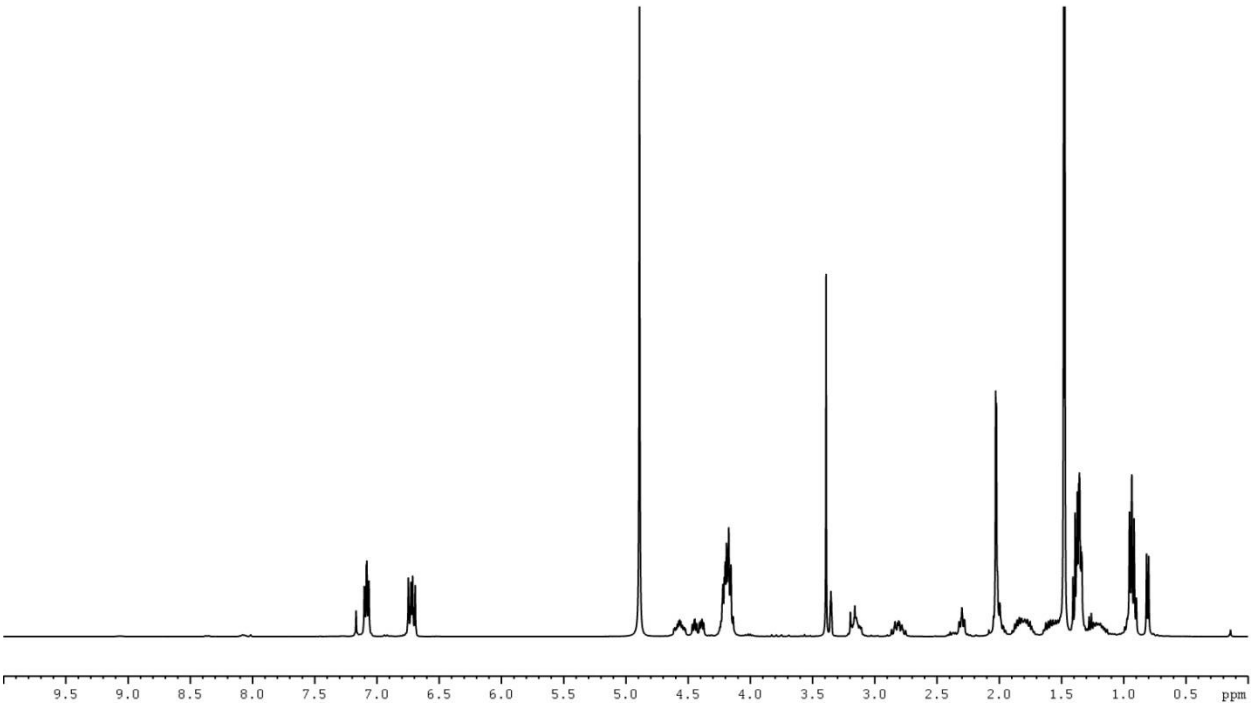

^{1}HNMR Spectrum (600 MHz) of diethyl N-(N-acetyl-L-isoleucyl-L-glutamyl)-1-amino-2-(4-benzyloxyphenyl)ethyl phosphonate (II-7e) in MeOD

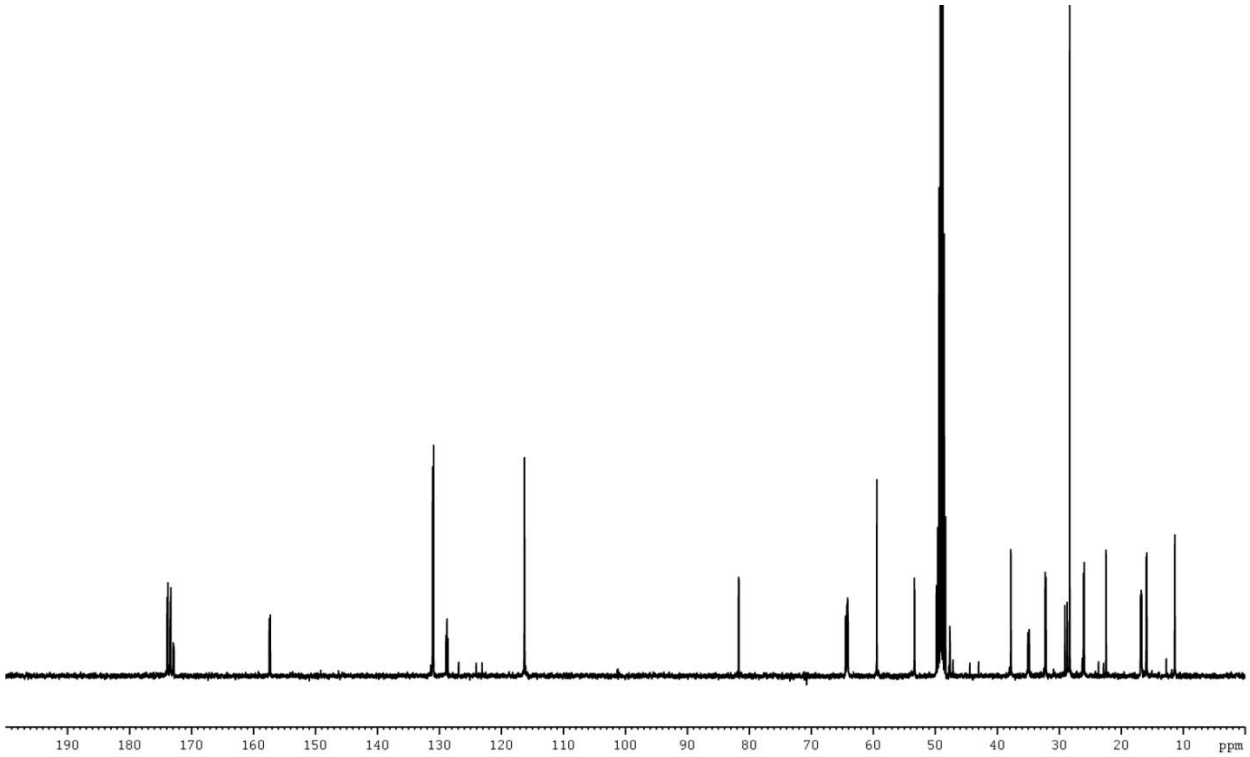

^{13}CNMR Spectrum (150 MHz) of diethyl N-(N-acetyl-L-isoleucyl-L-glutamyl)-1-amino-2-(4-benzyloxyphenyl)ethyl phosphonate (II-7e) in MeOD

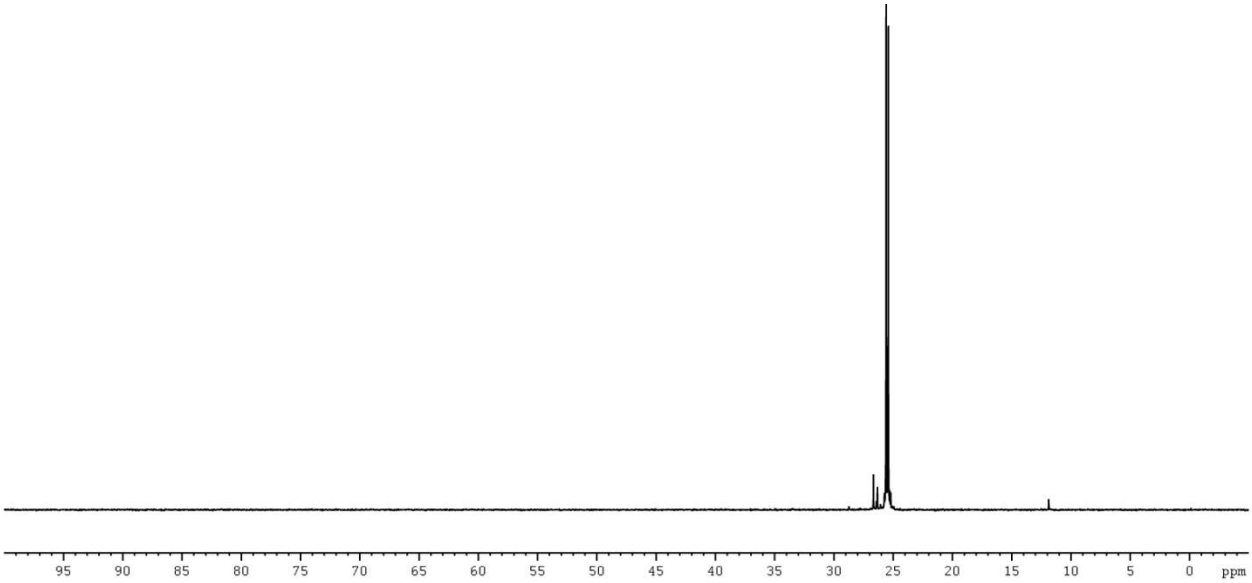

^{31}PNMR Spectrum (162 MHz) of diethyl N-(N-acetyl-L-isoleucyl-L-glutamyl)-1-amino-2-(4-benzyloxyphenyl)ethyl phosphonate (II-7e) in MeOD

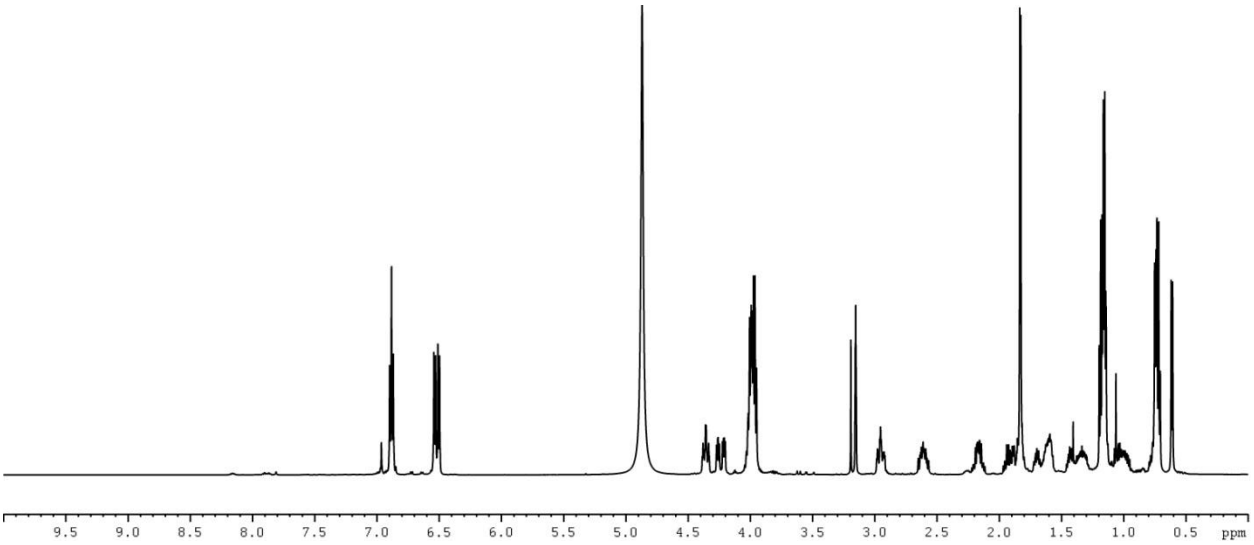

^{1}HNMR Spectrum (600 MHz) of diethyl N-(N-acetyl-L-isoleucyl-L-glutamyl)-1-amino-2-(4-hydroxyphenyl) ethyl phosphonate (II-7f) in MeOD

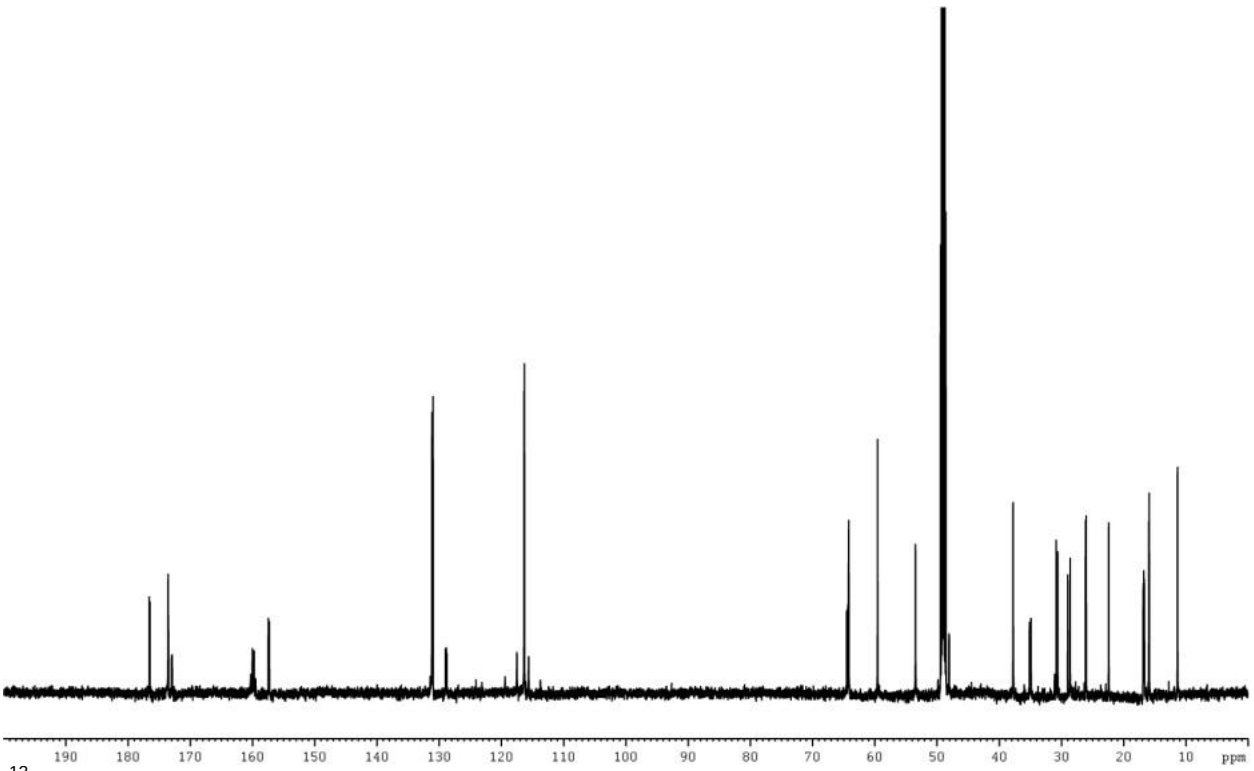

^{13}CNMR Spectrum (150 MHz) of diethyl N-(N-acetyl-L-isoleucyl-L-glutamyl)-1-amino-2-(4-hydroxyphenyl) ethyl phosphonate (II-7f) in MeOD

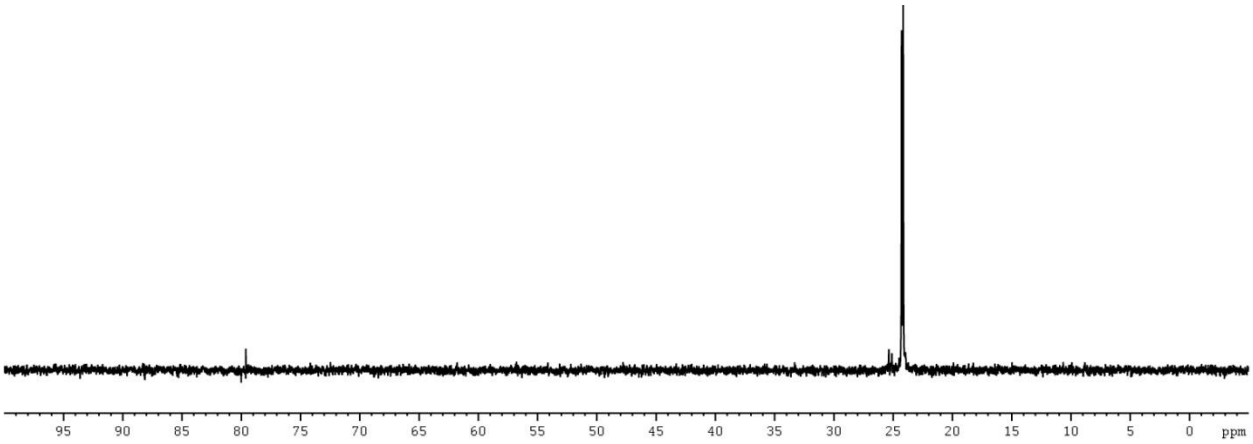

^{31}PNMR Spectrum (162 MHz) of diethyl N-(N-acetyl-L-isoleucyl-L-glutamyl)-1-amino-2-(4-hydroxyphenyl) ethyl phosphonate (II-7f) in MeOD

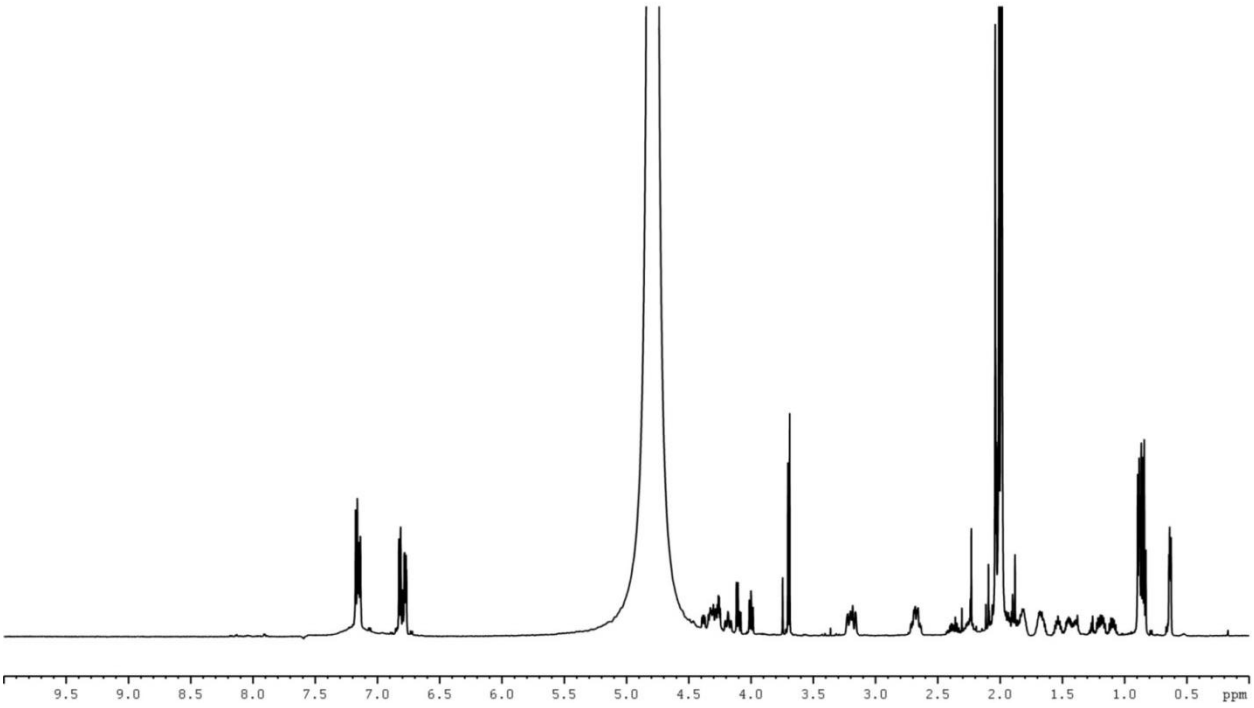

^{1}HNMR Spectrum (600 MHz) of SF2513 D: N-(N-acetyl-L-isoleucyl-L-glutamyl)-1-amino-2-(4-hydroxyphenyl) phosphonic acid (II-7) in D_2O

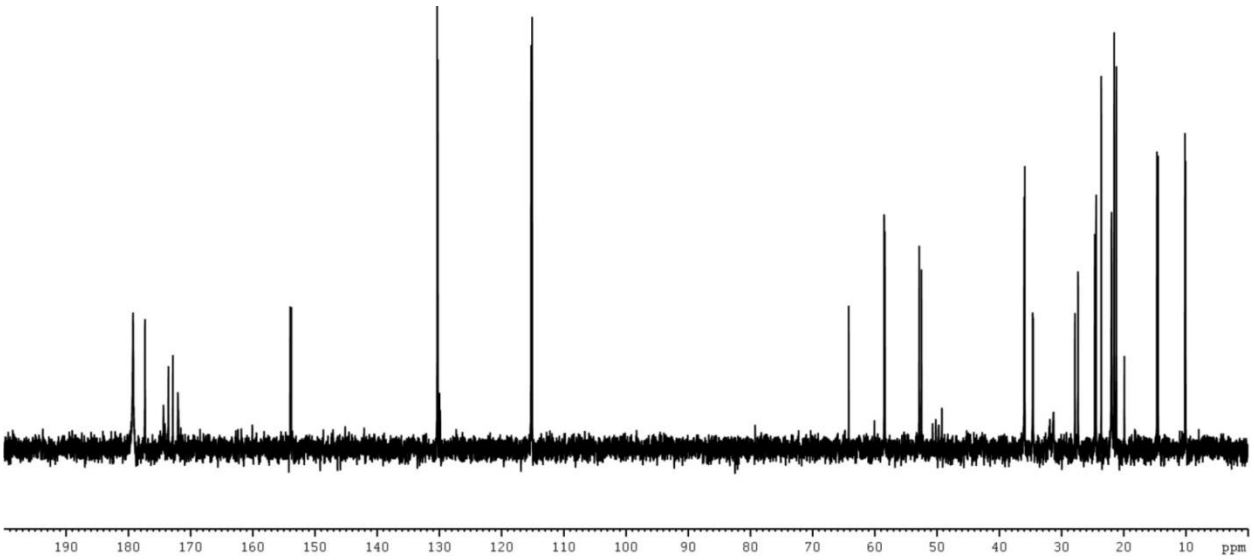

^{13}CNMR Spectrum (150 MHz) of SF2513 D: N-(N-acetyl-L-isoleucyl-L-glutamyl)-1-amino-2-(4-hydroxyphenyl) phosphonic acid (II-7) in D_2O

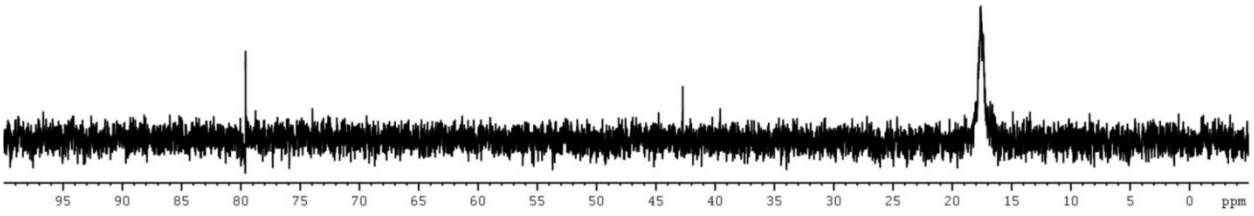

^{31}PNMR Spectrum (162 MHz) of SF2513 D: N-(N-acetyl-L-isoleucyl-L-glutamyl)-1-amino-2-(4-hydroxyphenyl) phosphonic acid (II-7) in D_2O

APPENDIX B

GRAPHS USED IN IC_{50} AND K_I CALCULATIONS

FROM CHAPTER II

IC_{50} curves for inhibition of somatic ACE by the K-26 analog

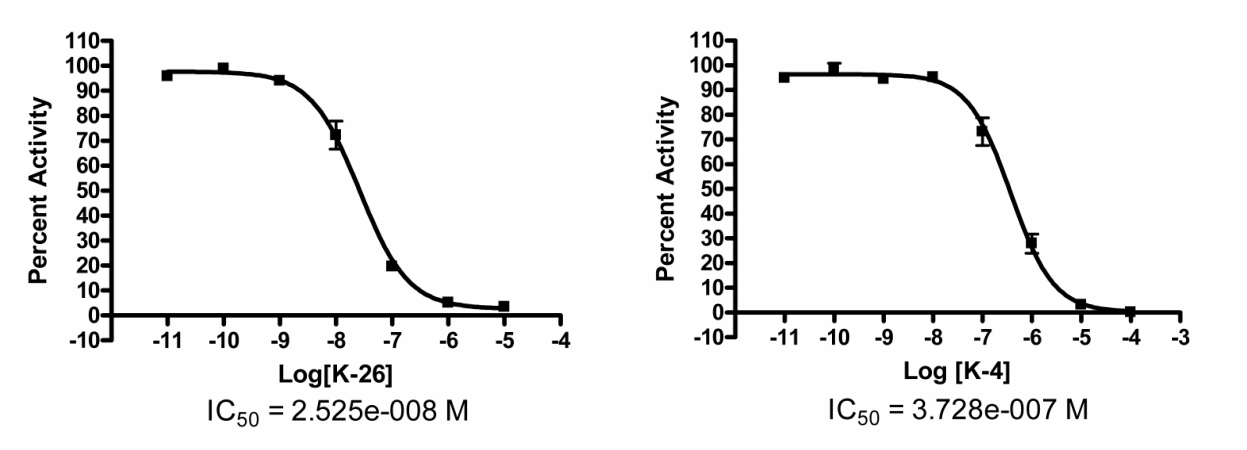

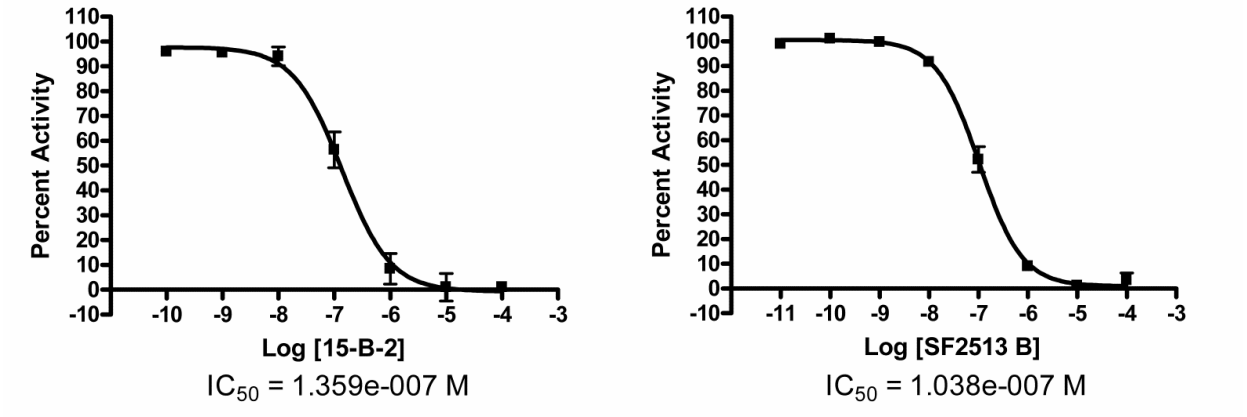

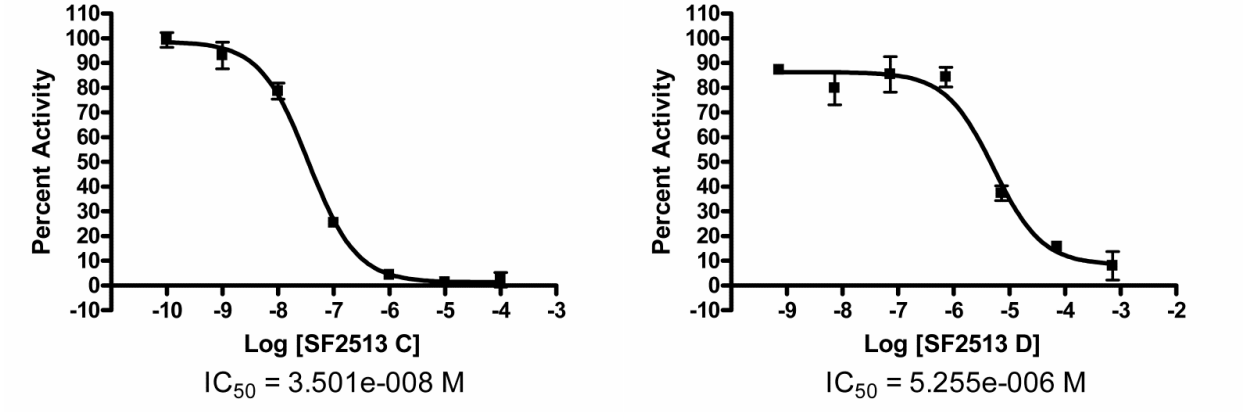

IC_{50} curves for the inhibition of C-domain ACE by the K-26 analog

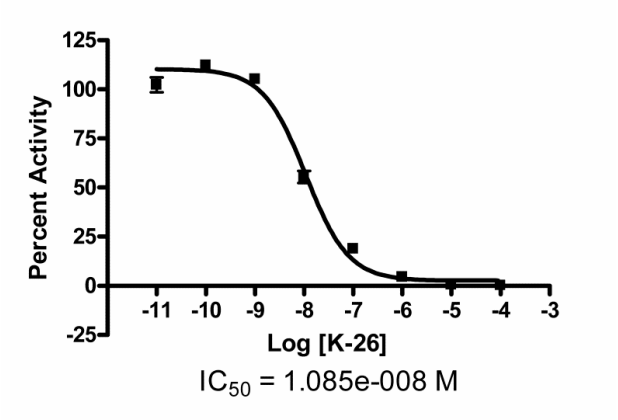

IC_{50} = 1.085e-008 M

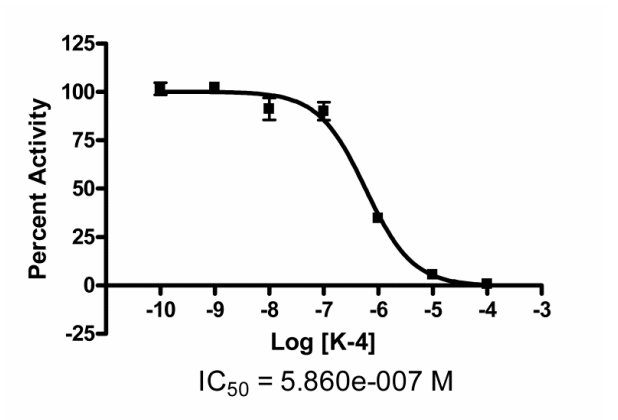

IC_{50} = 5.860e-007 M

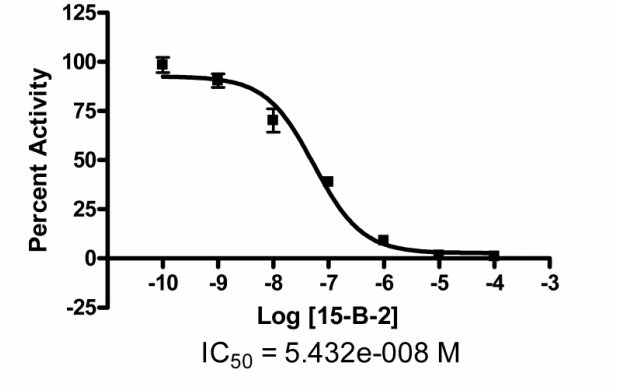

IC_{50} = 5.432e-008 M

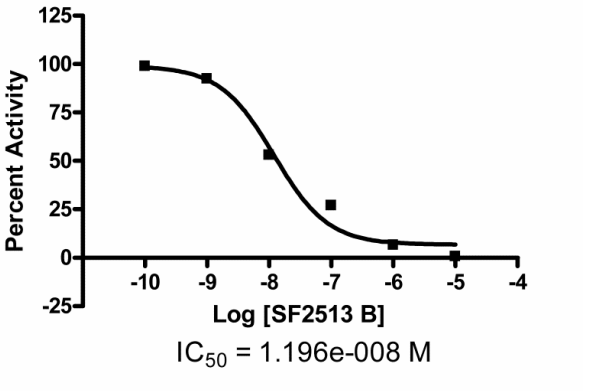

IC_{50} = 1.196e-008 M

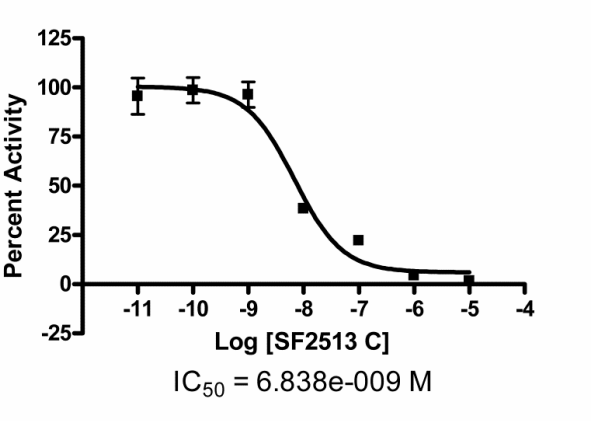

IC_{50} = 6.838e-009 M

IC_{50} curves for the inhibition of N-domain ACE by the K-26 analog

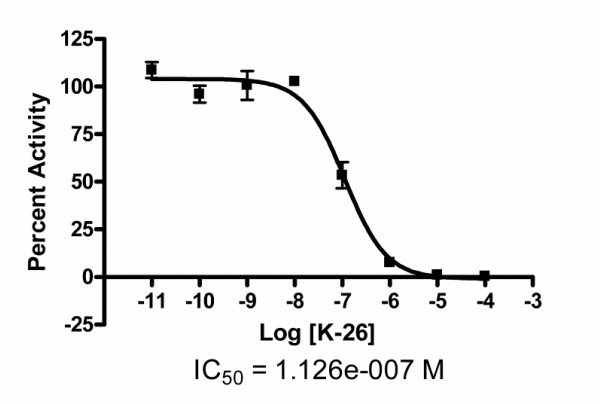

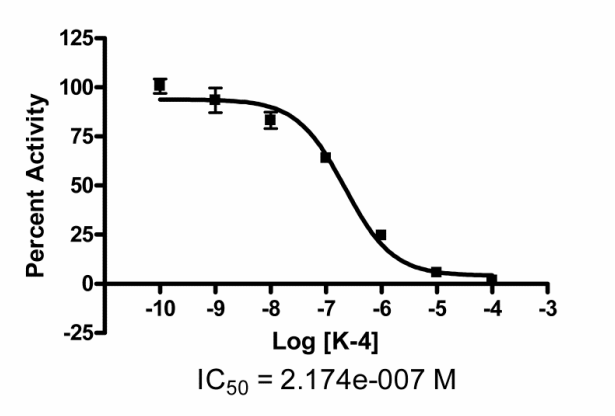

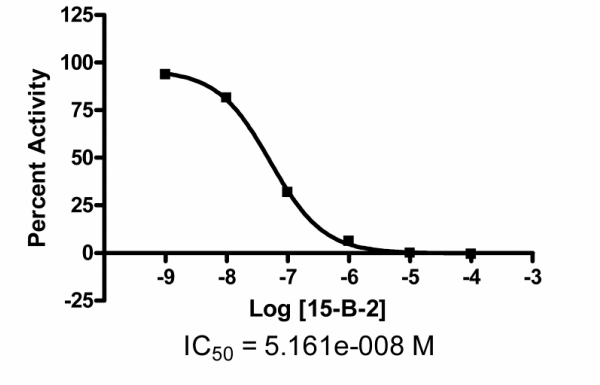

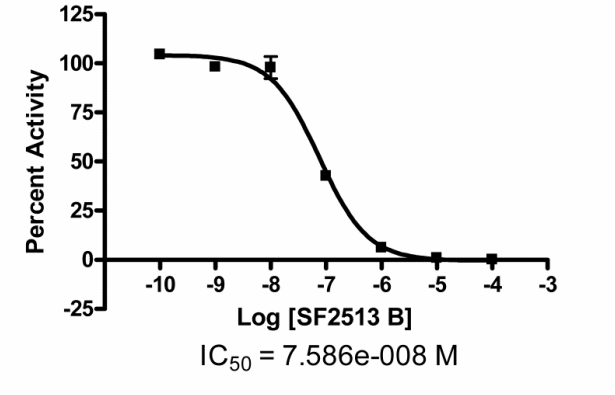

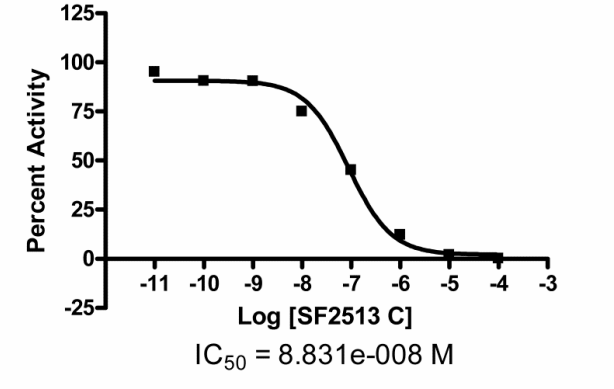

Dixon plot to determine K_i the inhibition of C-domain ACE by the K-26 analog

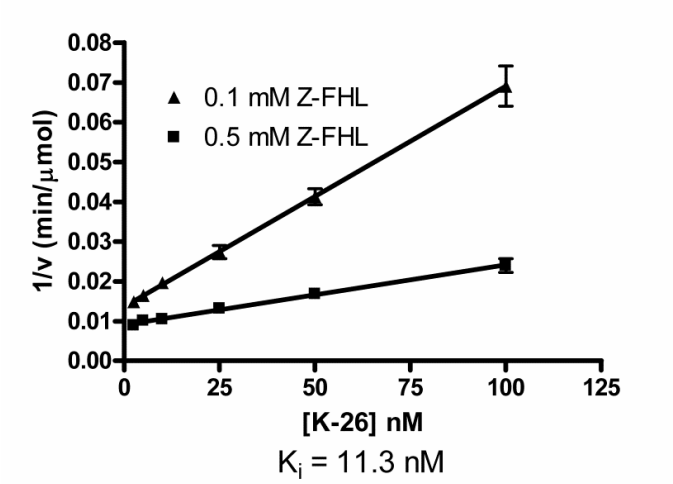

K_i = 11.3 nM

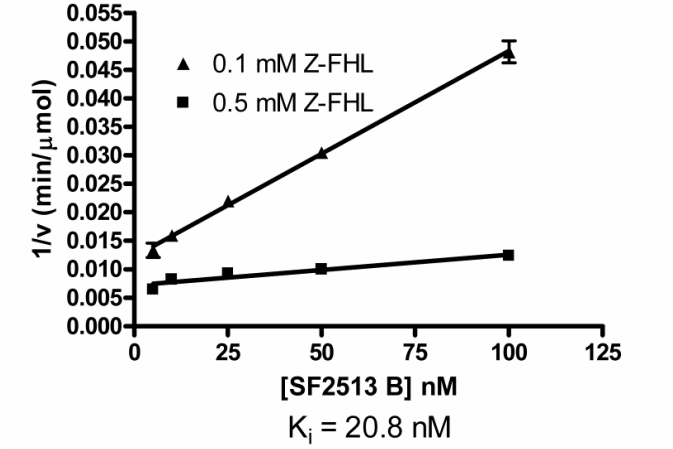

K_i = 20.8 nM

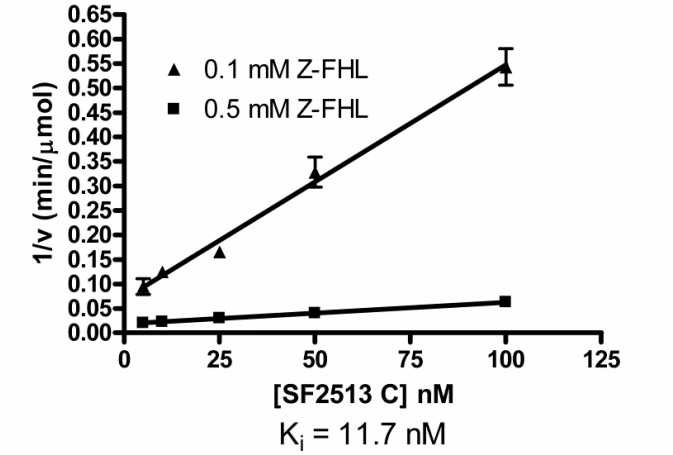

K_i = 11.7 nM

Dixon plot to determine K_i the inhibition of N-domain ACE by the K-26 analog

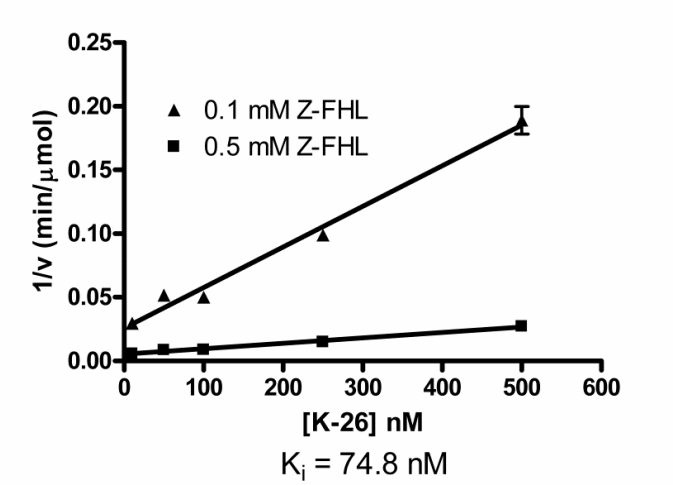

K_i = 74.8 nM

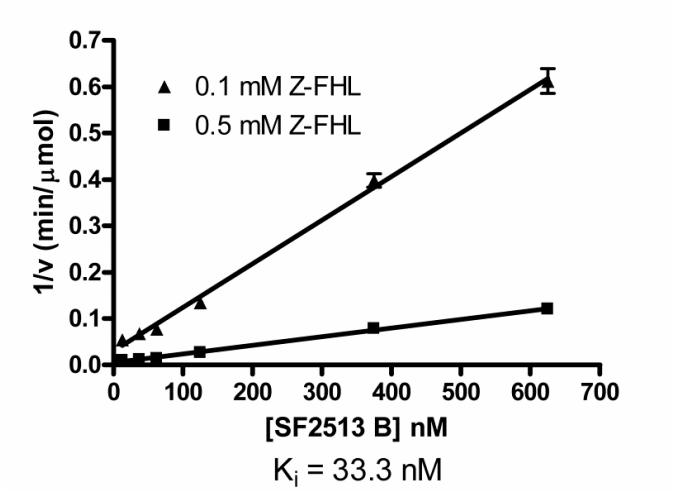

K_i = 33.3 nM

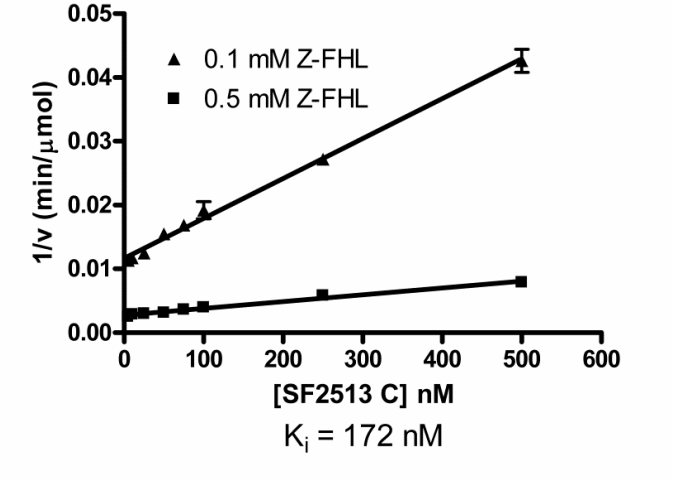

K_i = 172 nM

IC_{50} curves for the inhibition of bacterial DCPs by K-26 and captopril

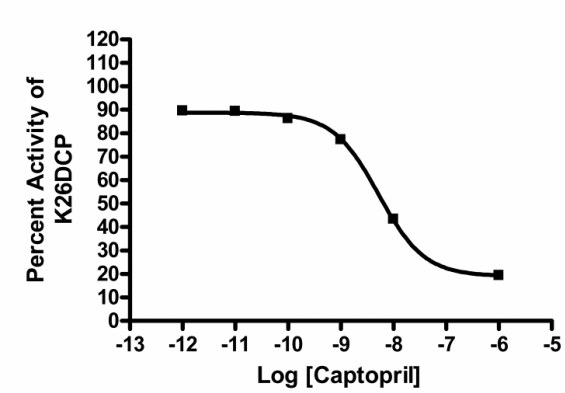

IC_{50} = 5.220e-009 M

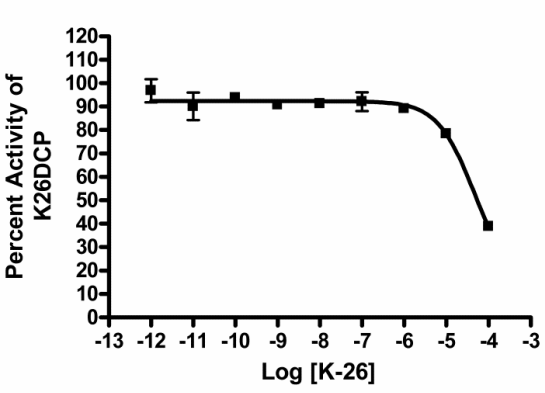

IC_{50} = 4.491e-005 M

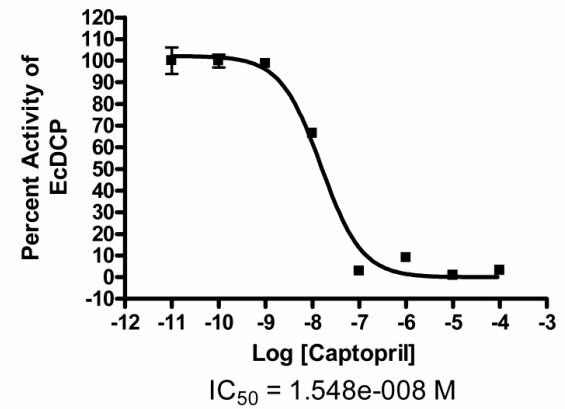

IC_{50} = 1.548e-008 M

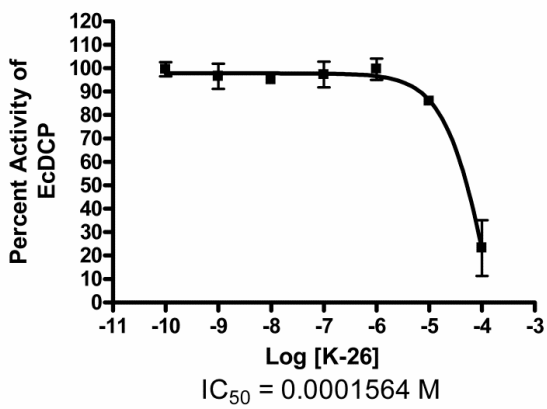

IC_{50} = 0.0001564 M

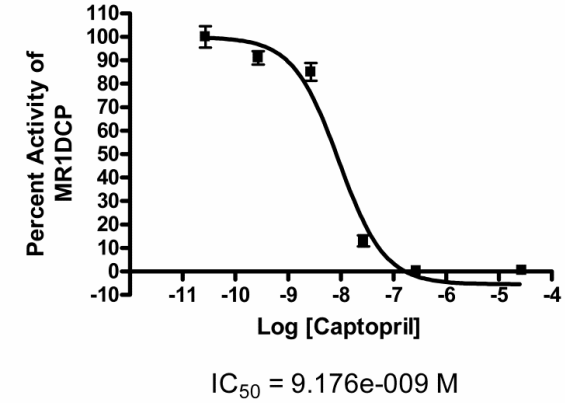

IC_{50} = 9.176e-009 M

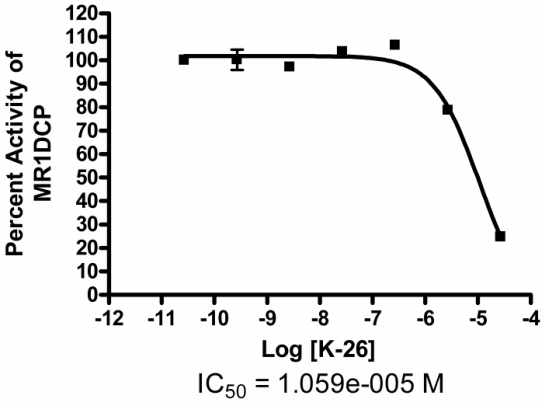

IC_{50} = 1.059e-005 M

APPENDIX C

ROSETTA PREDICTED BINDING CONFORMATIONS OF K-26 VARIANTS

FROM CHAPTER III

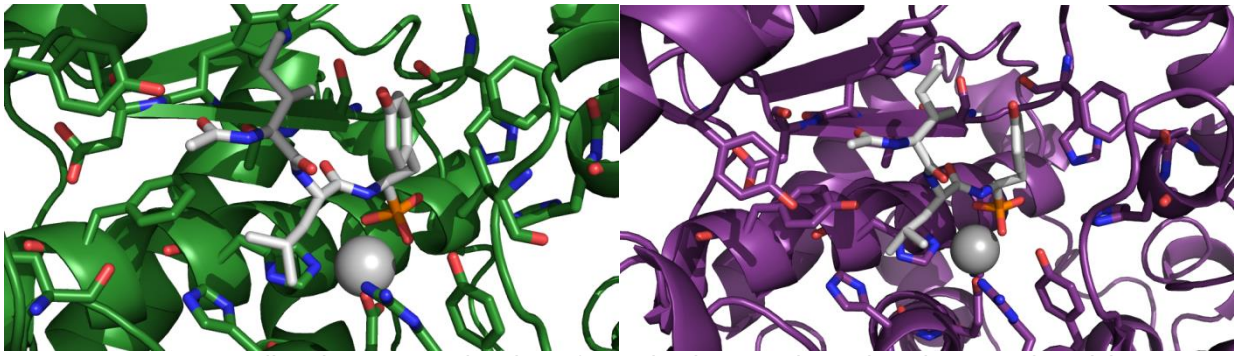

Rosetta predicted SF 2513B (III-3) conformation in tACE (green) and N-ACE (purple)

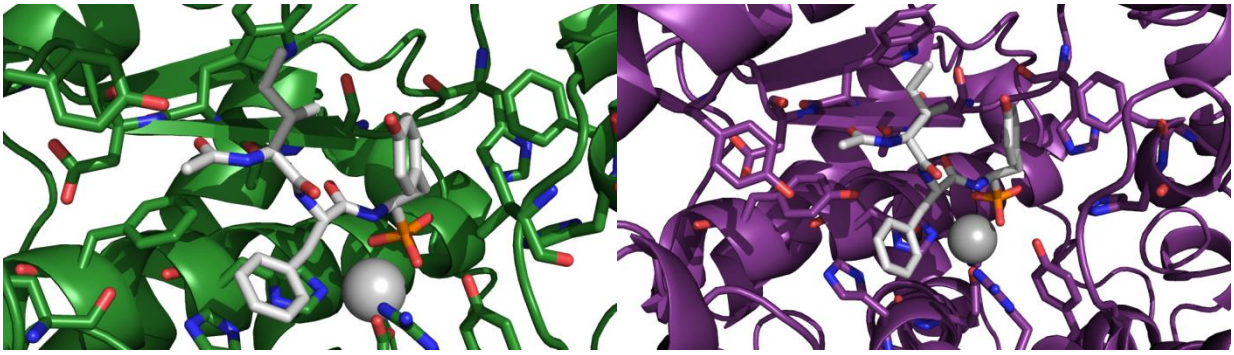

Rosetta predicted SF 2513C (III-4) conformation in tACE (green) and N-ACE (purple)

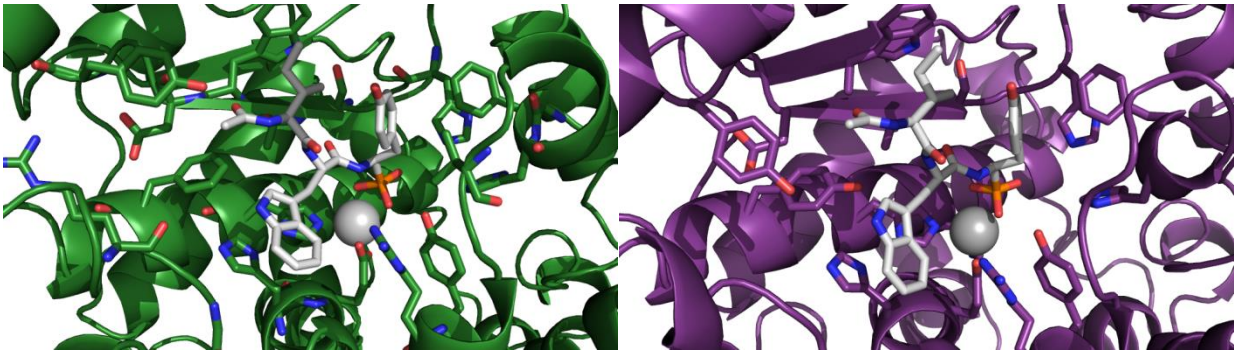

Rosetta predicted Ac-Ile-Trp-AHEP (III-5) conformation in tACE (green) and N-ACE (purple)

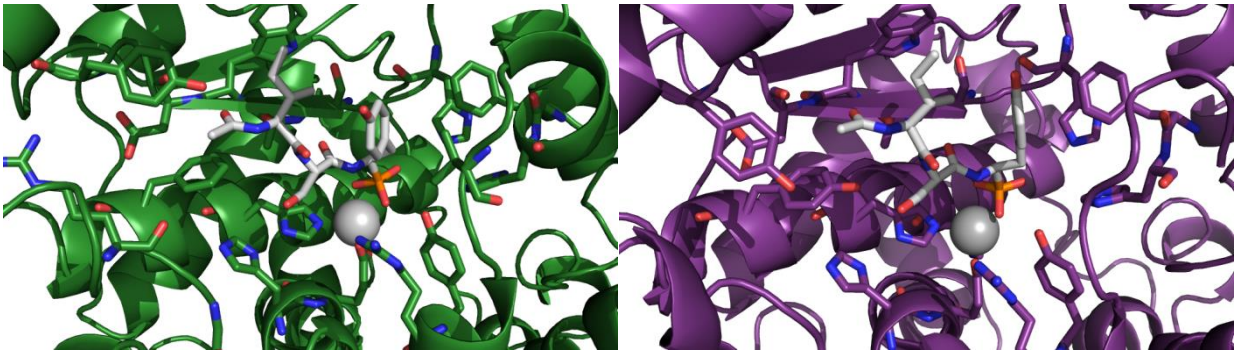

Rosetta predicted Ac-Ile-Ser-AHEP (III-6) conformation in tACE (green) and N-ACE (purple)

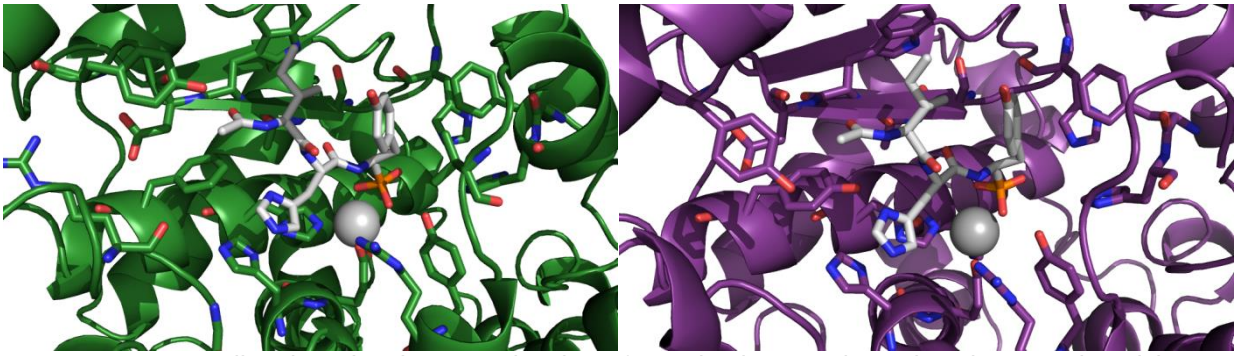

Rosetta predicted Ac-Ile-His-AHEP (III-7) conformation in tACE (green) and N-ACE (purple)

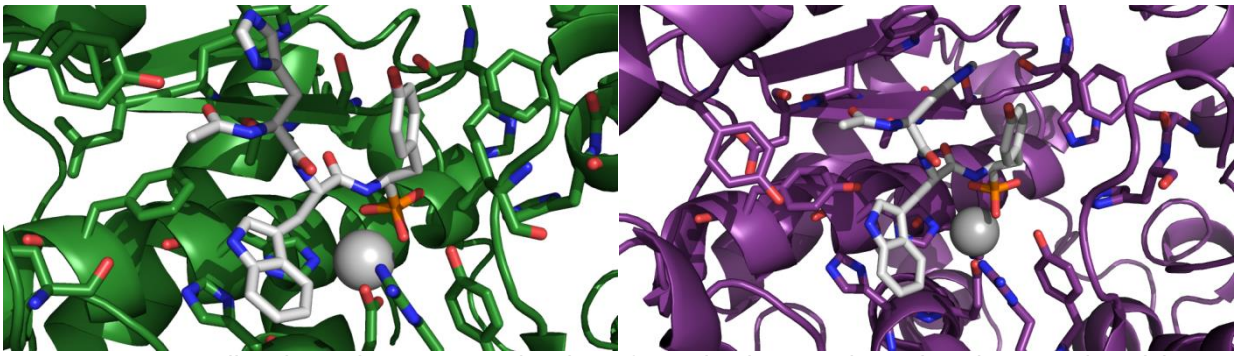

Rosetta predicted Ac-His-Trp-AHEP (III-9) conformation in tACE (green) and N-ACE (purple)

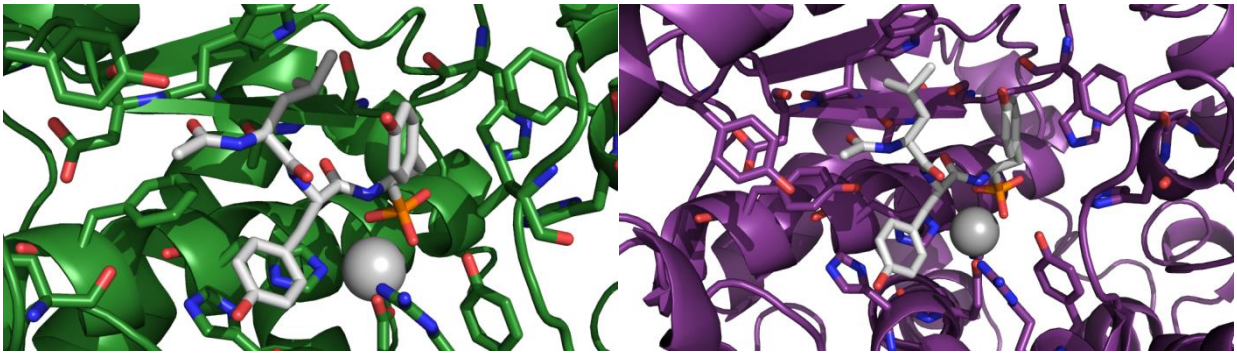

Rosetta predicted Ac-Leu-Tyr-AHEP (III-9) conformation in tACE (green) and N-ACE (purple)

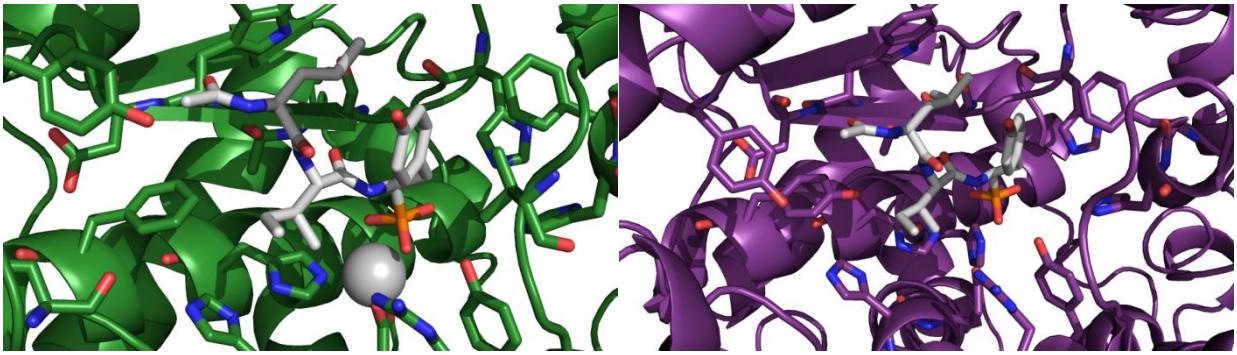

Rosetta predicted Ac-Leu-Ile-AHEP (III-10) conformation in tACE (green) and N-ACE (purple)

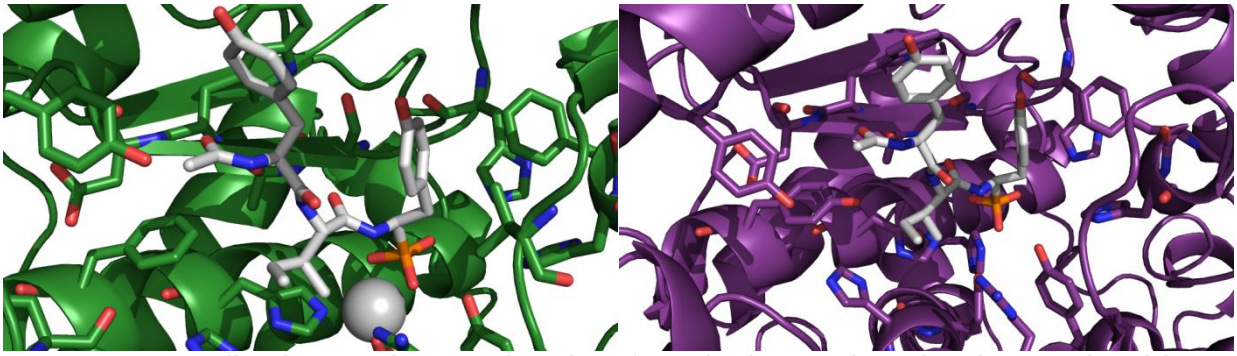

Rosetta predicted Ac-Tyr-Ile-AHEP (III-11) conformation in tACE (green) and N-ACE (purple)

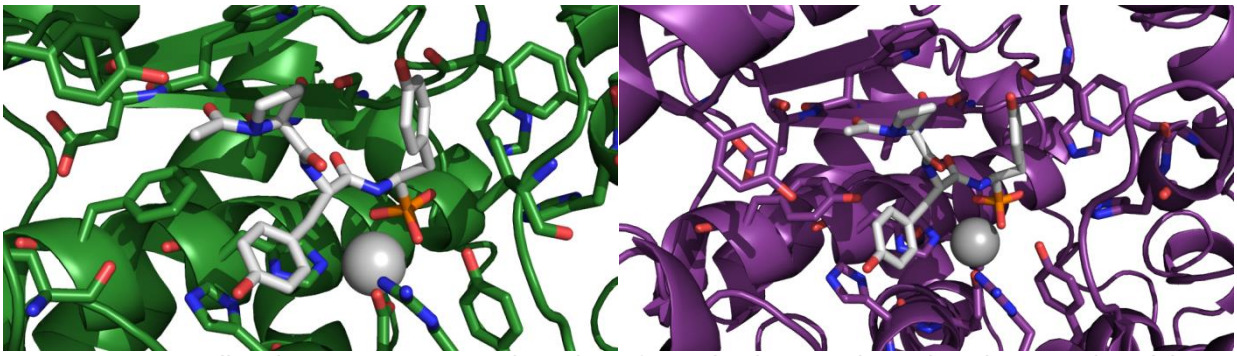

Rosetta predicted Ac-Pro-Tyr-AHEP (III-12) conformation in tACE (green) and N-ACE (purple)

APPENDIX D

NMR SPECTRA

OF SYNTHETIC INTERMEDIATES

FROM CHAPTER III

NMR spectra of Ac-Ile-Trp-AHEP (III-3) and synthetic intermediates (III-3a - III-3d)

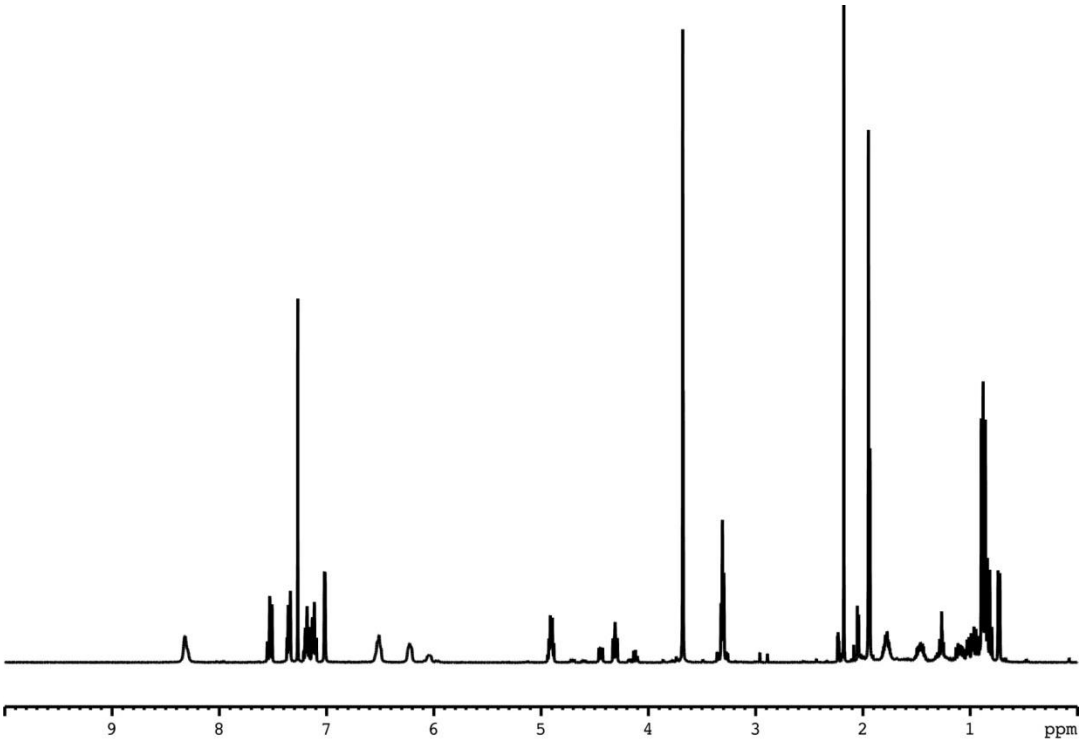

^{1}HNMR Spectrum (400 MHz) of N-acetyl-L-isoleucyl-L-tryptophan methyl ester (III-3a) in $CDCl_3$

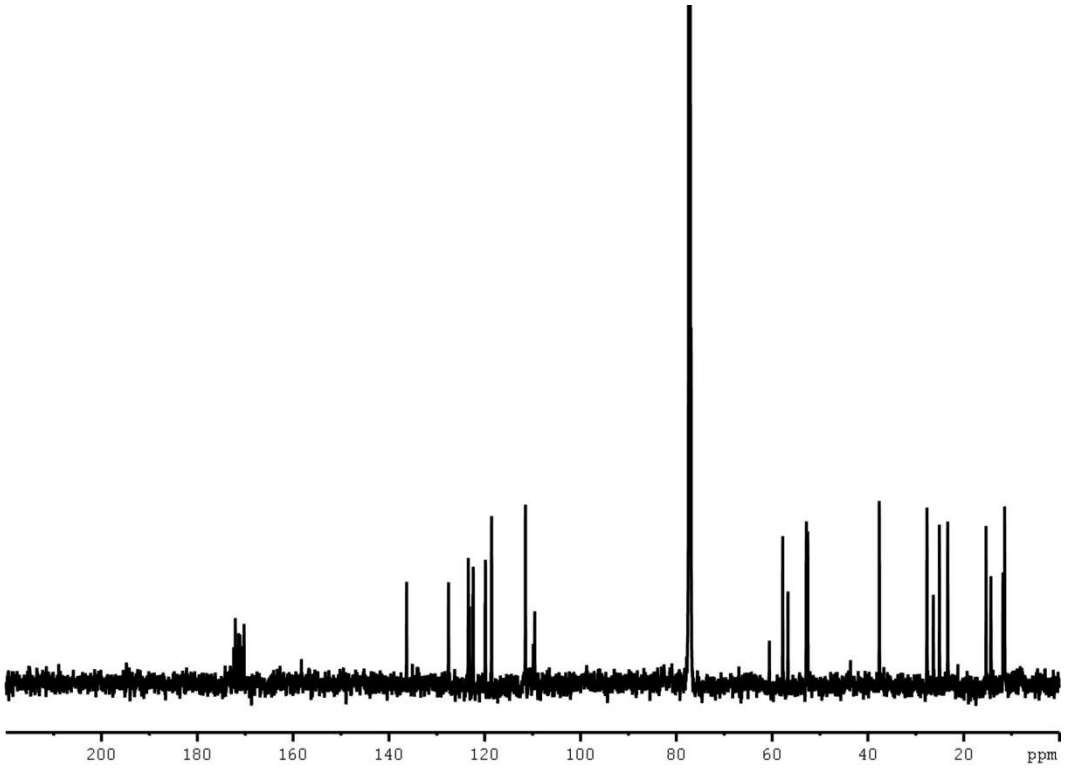

^{13}CNMR Spectrum (100 MHz) of N-acetyl-L-isoleucyl-L-tryptophan methyl ester (III-3a) in $CDCl_3$

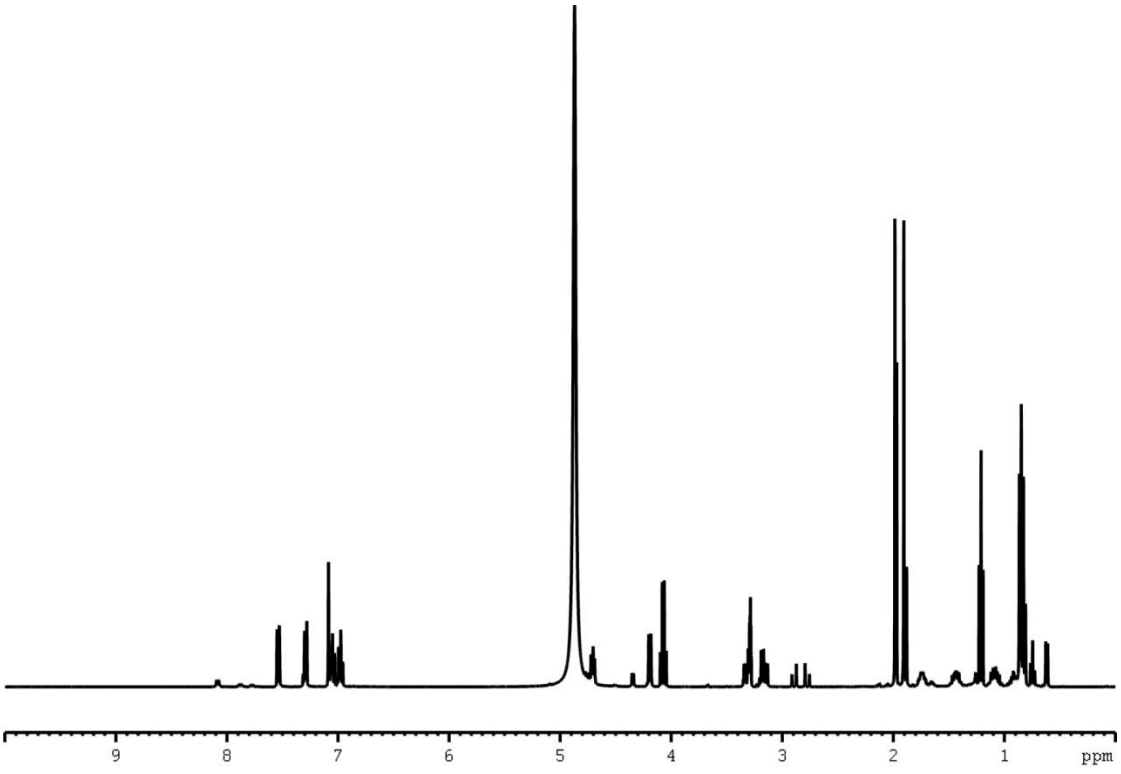

^{1}HNMR Spectrum (400 MHz) of N-acetyl-L-isoleucyl-L-tryptophan (III-3b) in MeOD

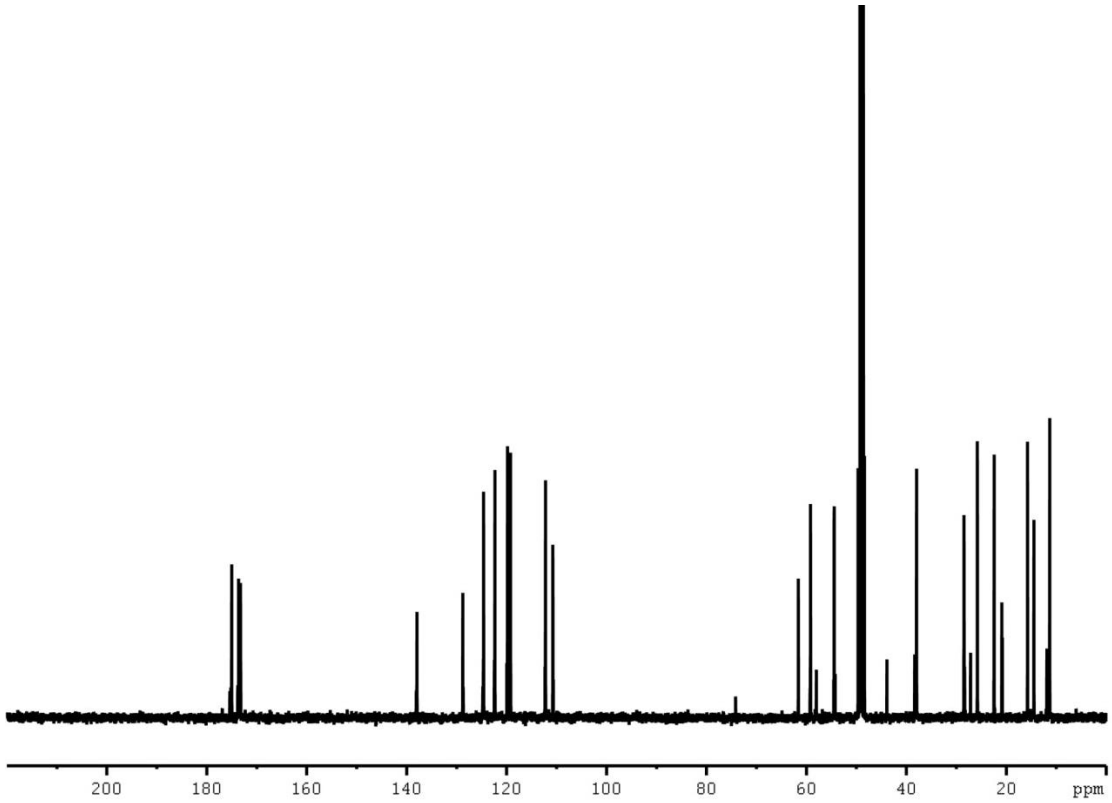

^{13}CNMR Spectrum (100 MHz) of N-acetyl-L-isoleucyl-L-tryptophan (III-3b) in MeOD

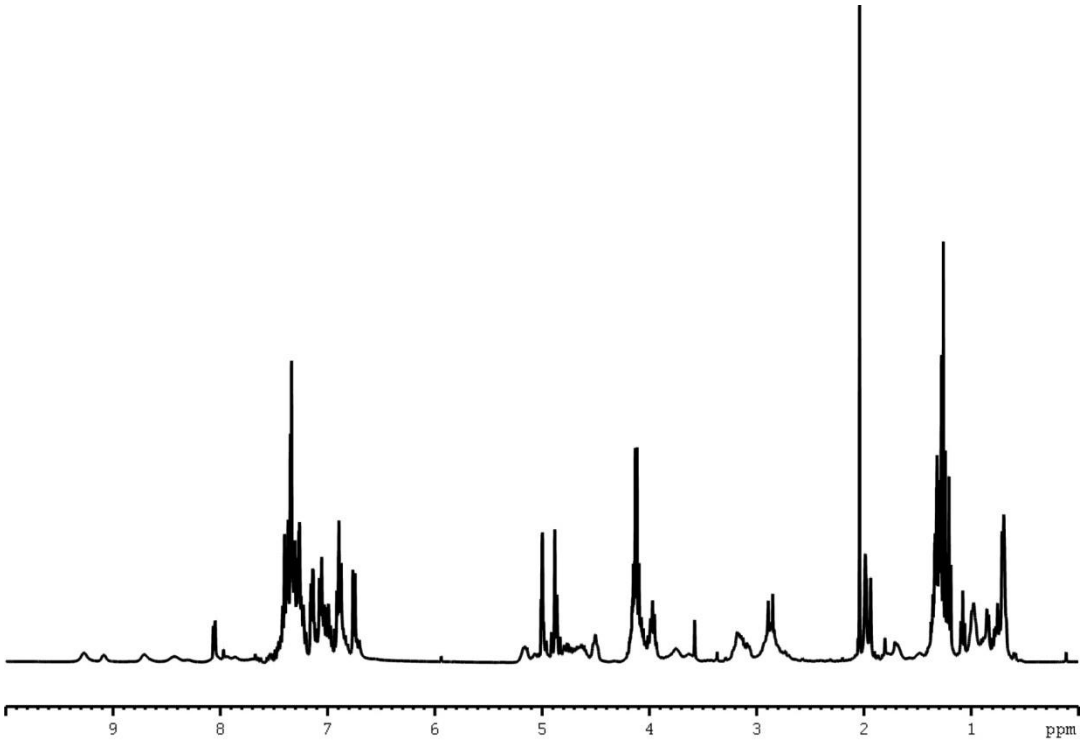

^{1}HNMR Spectrum (600 MHz) of diethyl N-(N-acetyl-L-isoleucyl-L-tryptophanyl)-1-amino-2-(4-benzyloxyphenyl)ethyl phosphonate (III-3c) in $CDCl_3$

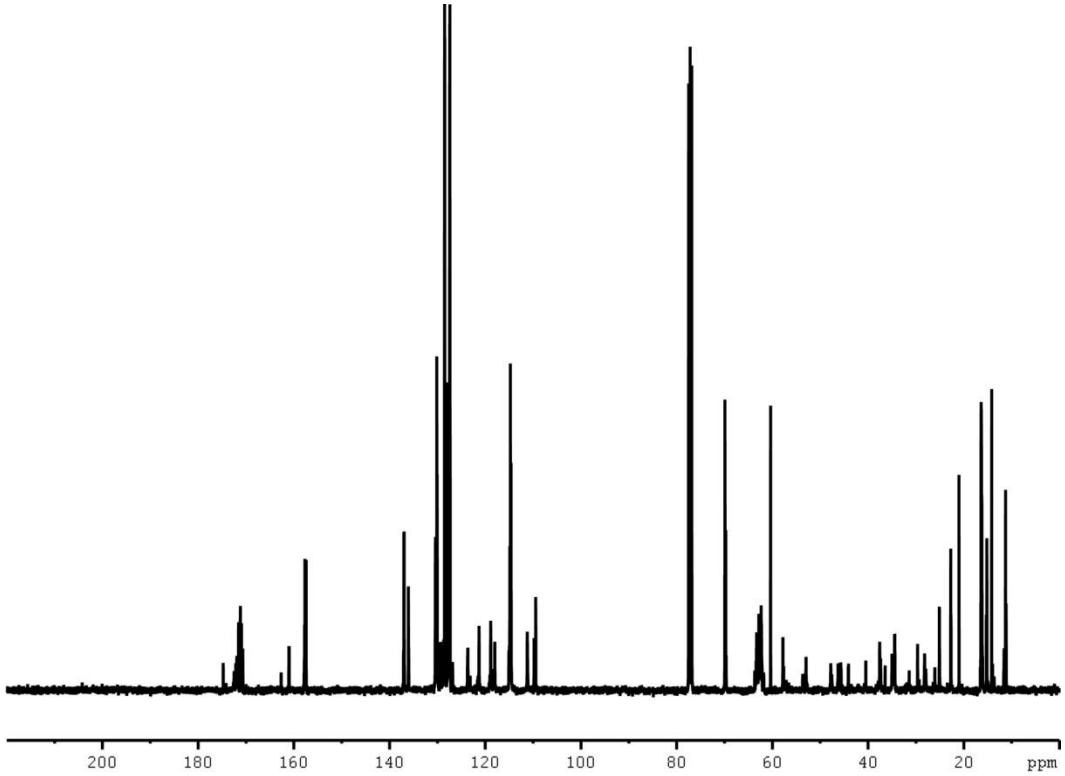

^{13}CNMR Spectrum (150 MHz) of diethyl N-(N-acetyl-L-isoleucyl-L-tryptophanyl)-1-amino-2-(4-benzyloxyphenyl)ethyl phosphonate (III-3c) in $CDCl_3$

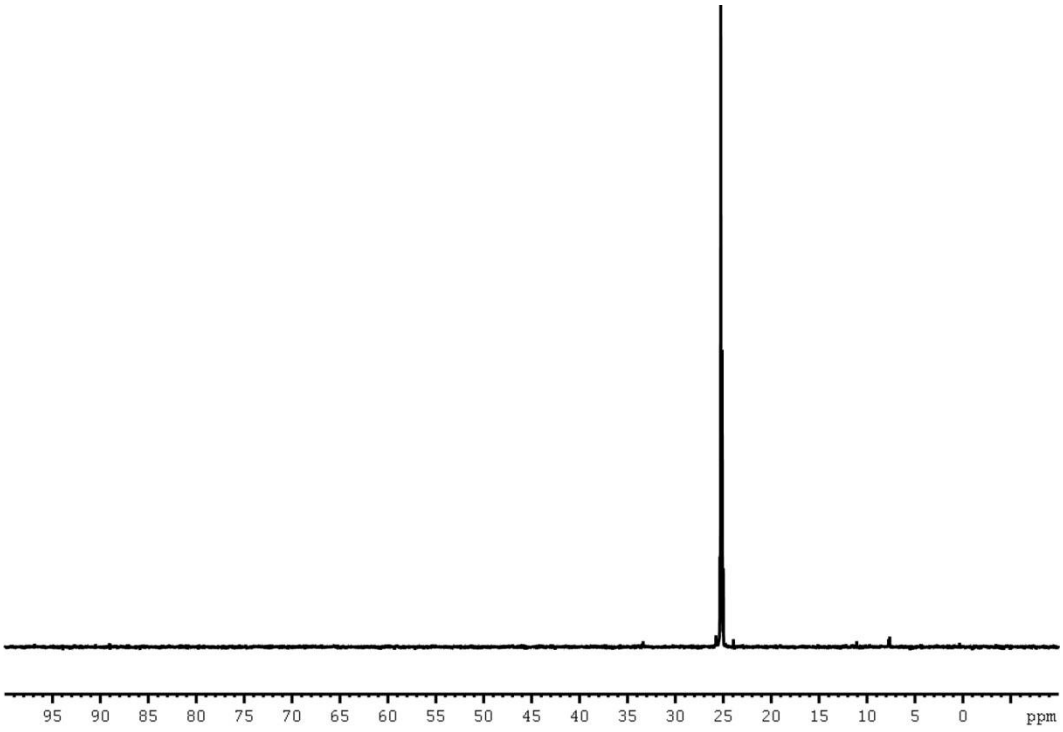

^{31}PNMR Spectrum (162 MHz) of diethyl N-(N-acetyl-L-isoleucyl-L-tryptophanyl)-1-amino-2-(4-benzyloxyphenyl)ethyl phosphonate (III-3c) in $CDCl_3$

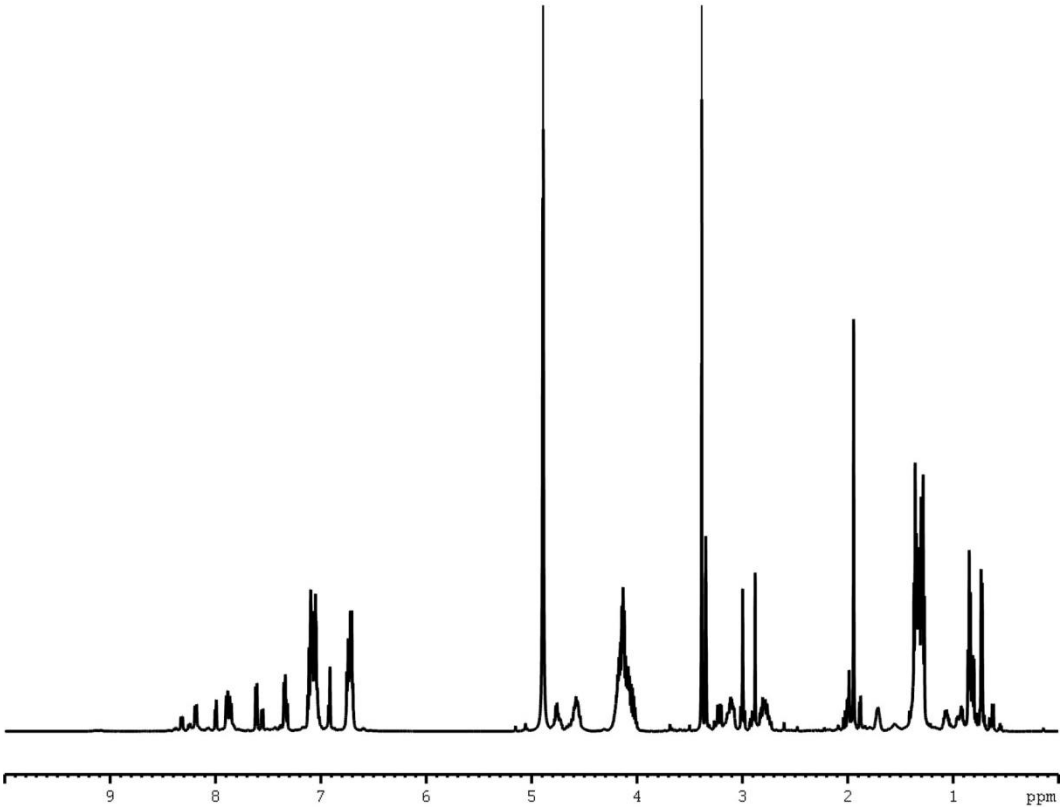

^{1}HNMR Spectrum (600 MHz) of diethyl N-(N-acetyl-L-isoleucyl-L-leucyl)-1-amino-2-(4-hydoxyphenyl)ethyl phosphonate (III-3d) in MeOD

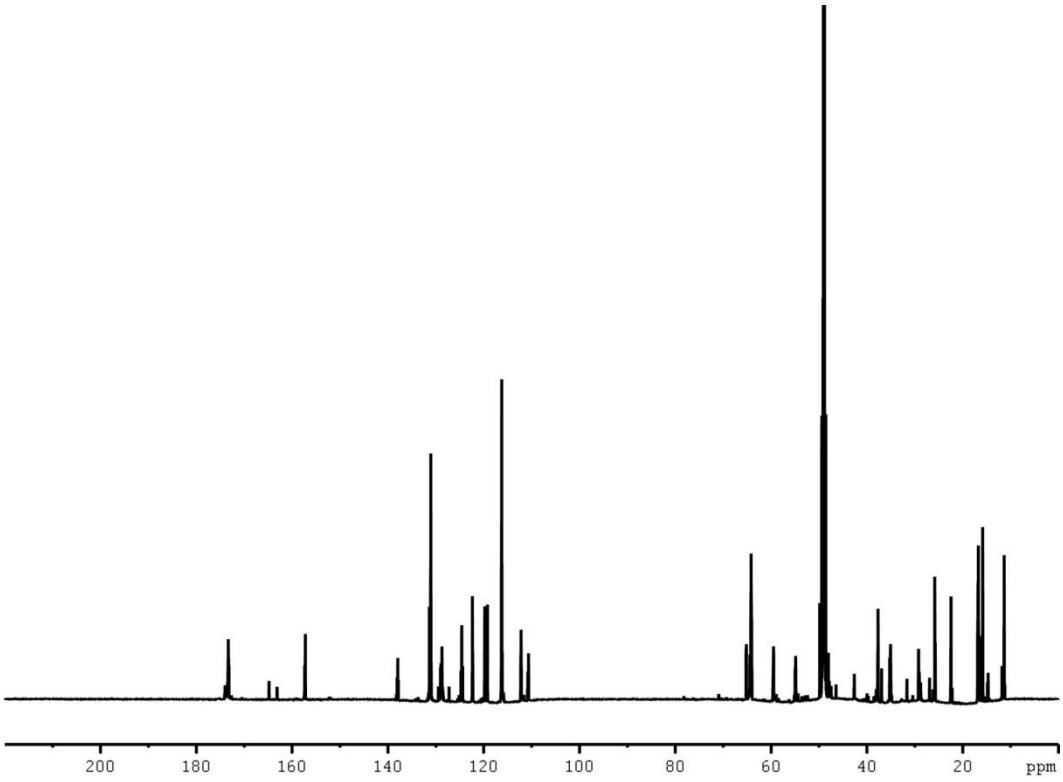

^{13}CNMR Spectrum (150 MHz) of diethyl N-(N-acetyl-L-isoleucyl-L-tryptophanyl)-1-amino-2-(4-hydoxyphenyl)ethyl phosphonate (III-3d) in MeOD

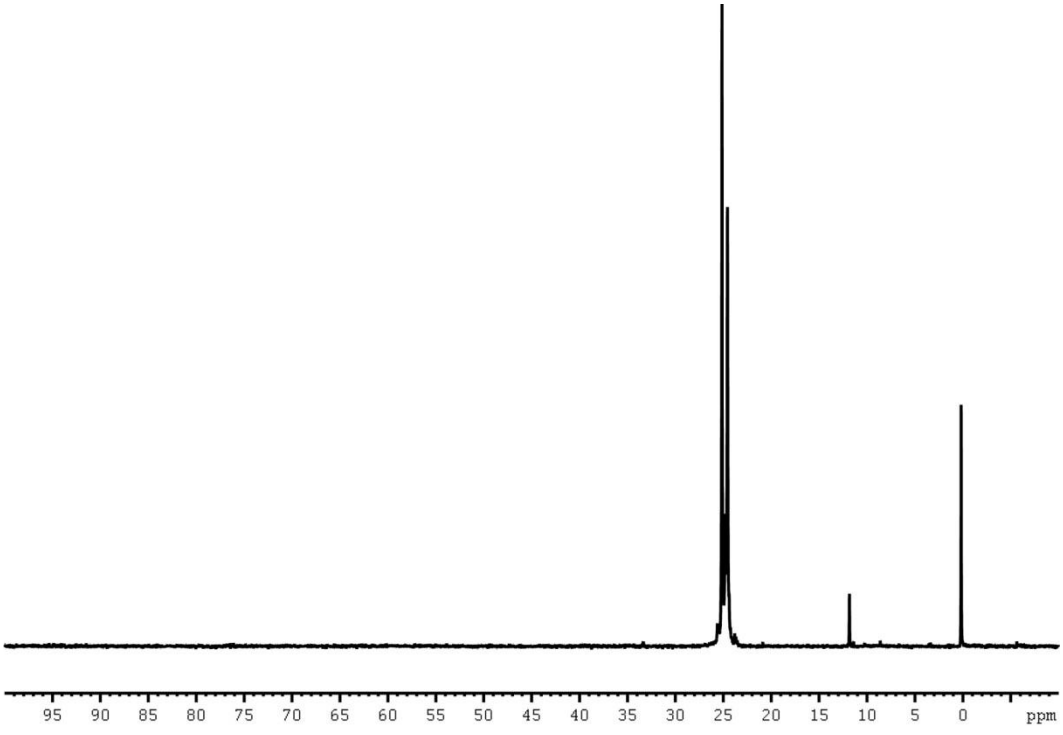

^{31}PNMR Spectrum (121 MHz) diethyl N-(N-acetyl-L-isoleucyl-L-tryptophanyl)-1-amino-2-(4-hydoxyphenyl)ethyl phosphonate (III-3d) in MeOD

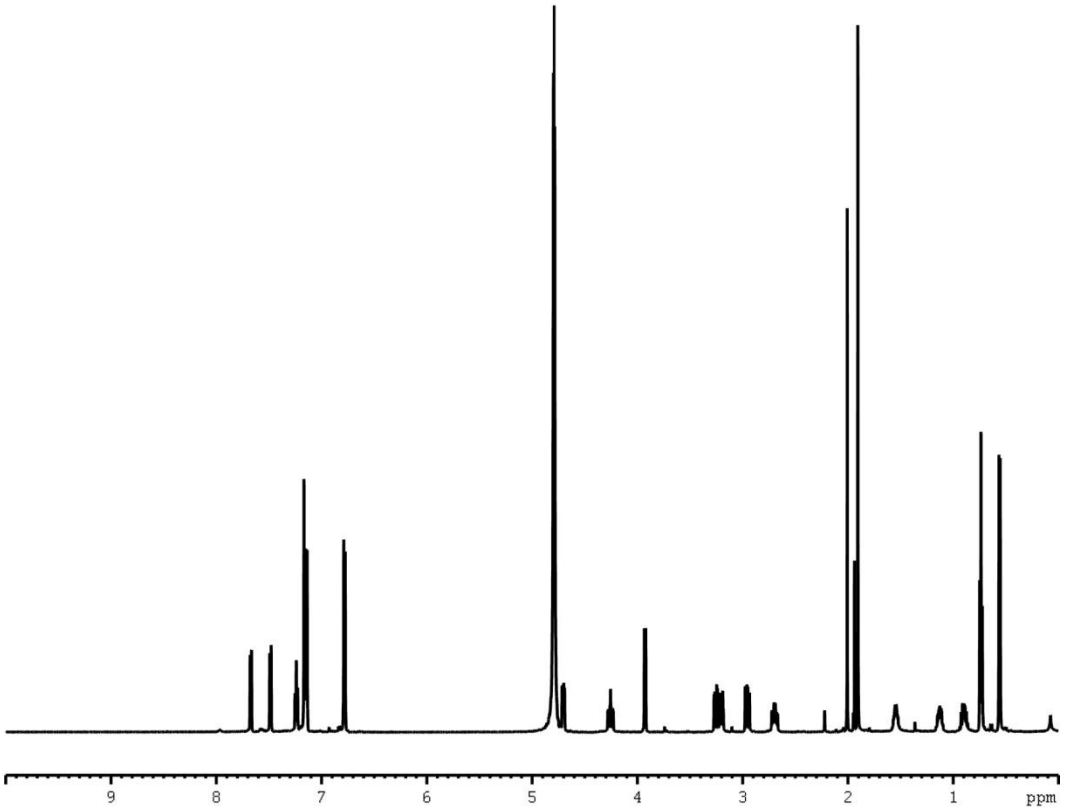

^{1}HNMR Spectrum (600 MHz) of Ac-Ile-Trp-AHEP: N-(N-acetyl-L-isoleucyl-L-tryptophanyl)-1-amino-2-(4-hydoxyphenyl)ethyl phosphonic acid (III-3) in D_2O

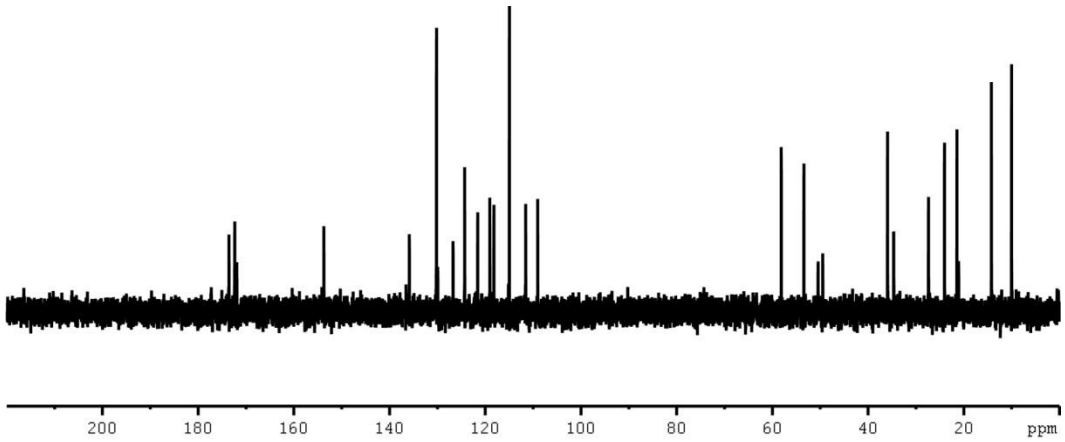

^{13}CNMR Spectrum (150 MHz) of Ac-Ile-Trp-AHEP: N-(N-acetyl-L-isoleucyl-L-tryptophanyl)-1-amino-2-(4-hydoxyphenyl)ethyl phosphonic acid (III-3) in D_2O

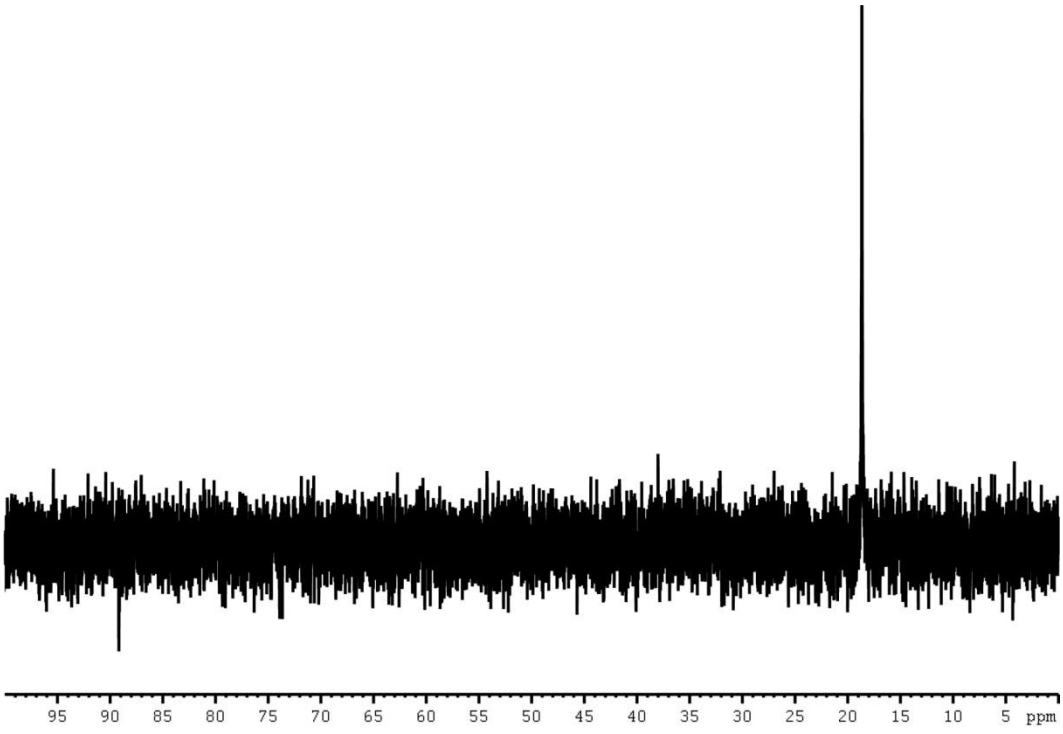

^{31}PNMR Spectrum (162 MHz) of Ac-Ile-Trp-AHEP: N-(N-acetyl-L-isoleucyl-L-tryptophanyl)-1-amino-2-(4-hydoxyphenyl)ethyl phosphonic acid (III-3) in D_2O

NMR spectra of Ac-Ile-Ser-AHEP (III-4) and synthetic intermediates (III-4a - III-4d)

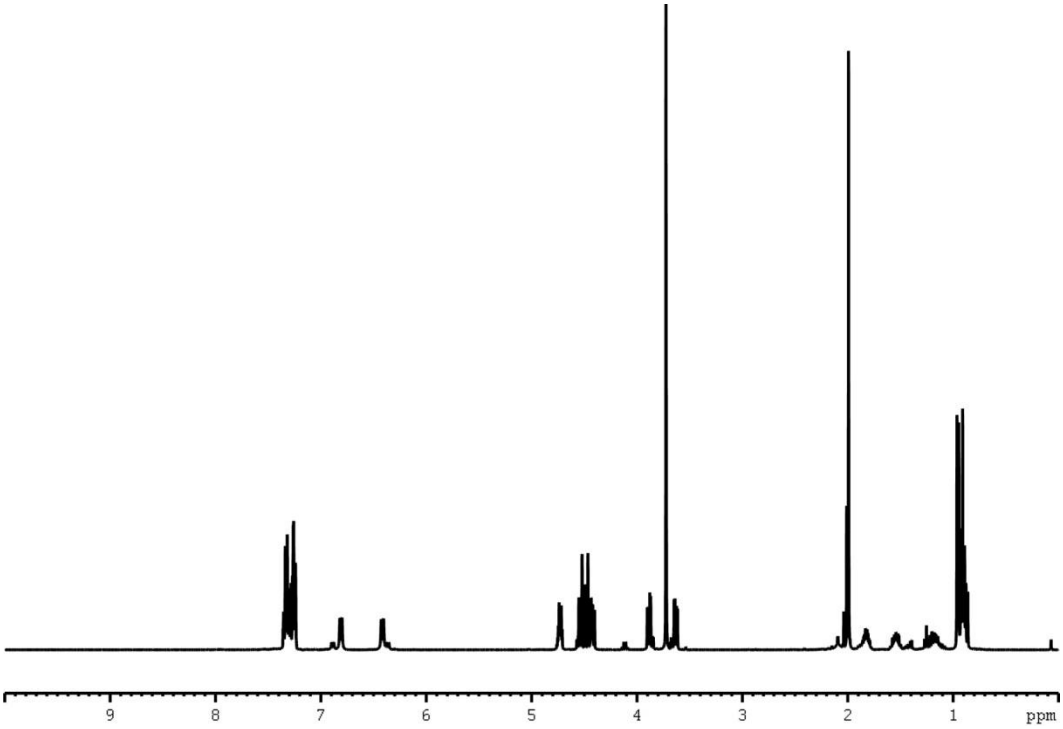

^{1}HNMR Spectrum (400 MHz) of N-acetyl-L-isoleucyl-O-benzyl-L-serine methyl ester (III-4a) in $CDCl_3$

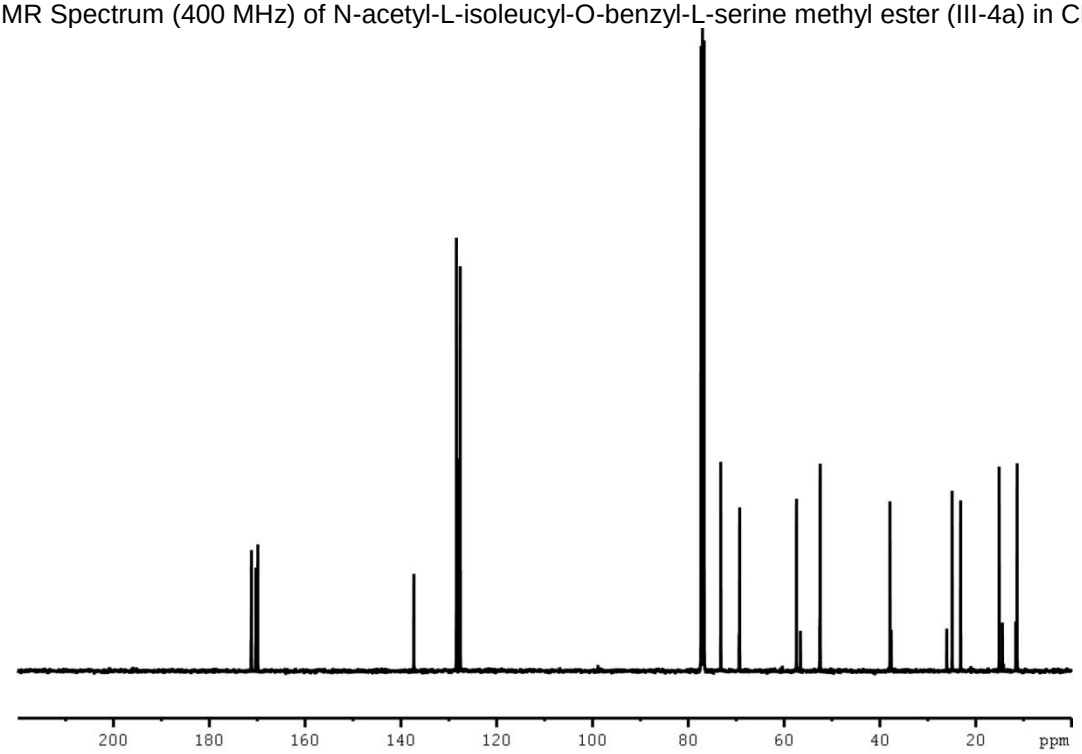

^{13}CNMR Spectrum (100 MHz) of N-acetyl-L-isoleucyl- O-benzyl-L-serine methyl ester (III-4a) in $CDCl_3$

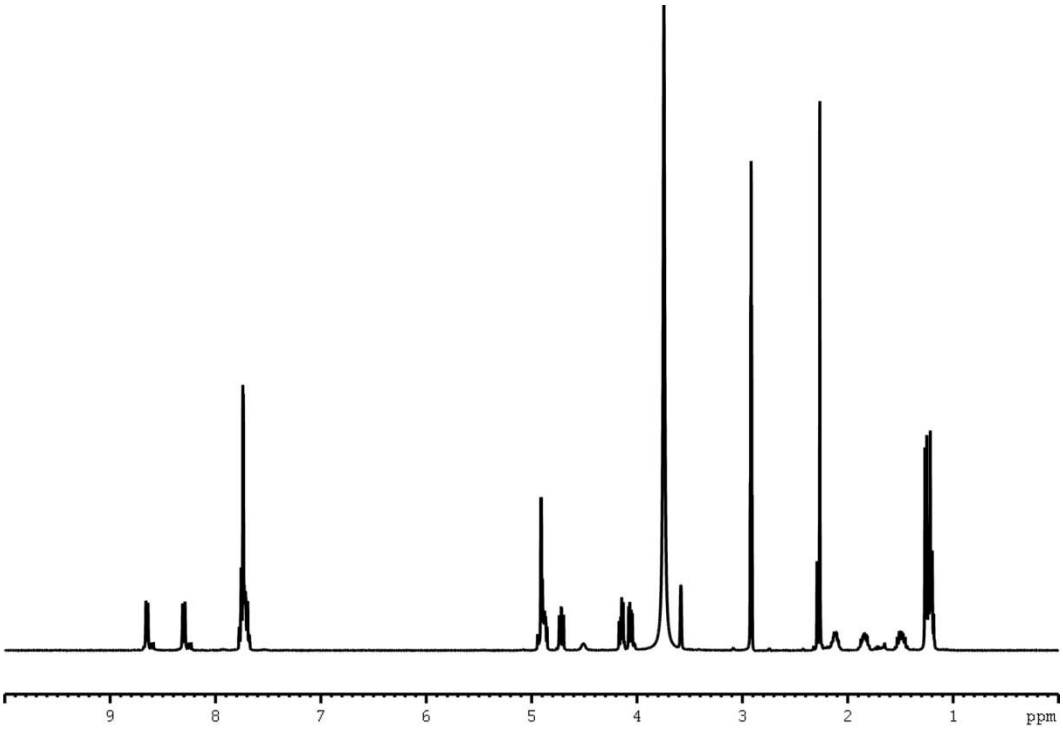

^{1}HNMR Spectrum (400 MHz) of N-acetyl-L-isoleucyl- O-benzyl-L-serine (III-4b) in MeOD

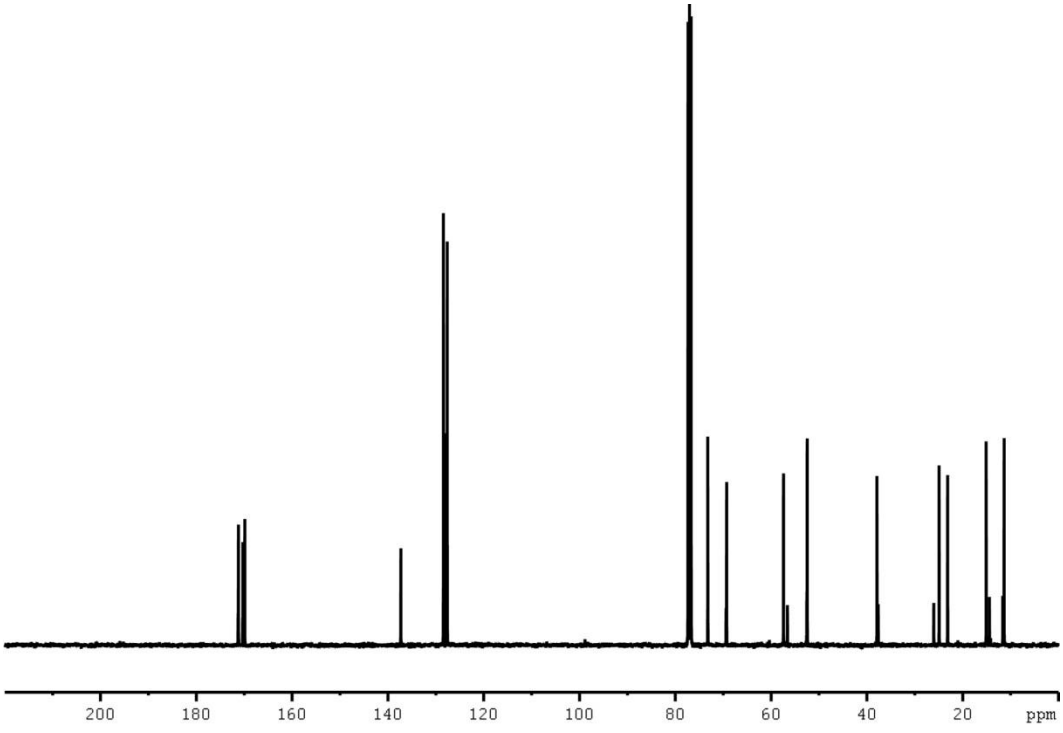

^{13}CNMR Spectrum (100 MHz) of N-acetyl-L-isoleucyl- O-benzyl-L-serine (III-4b) in MeOD

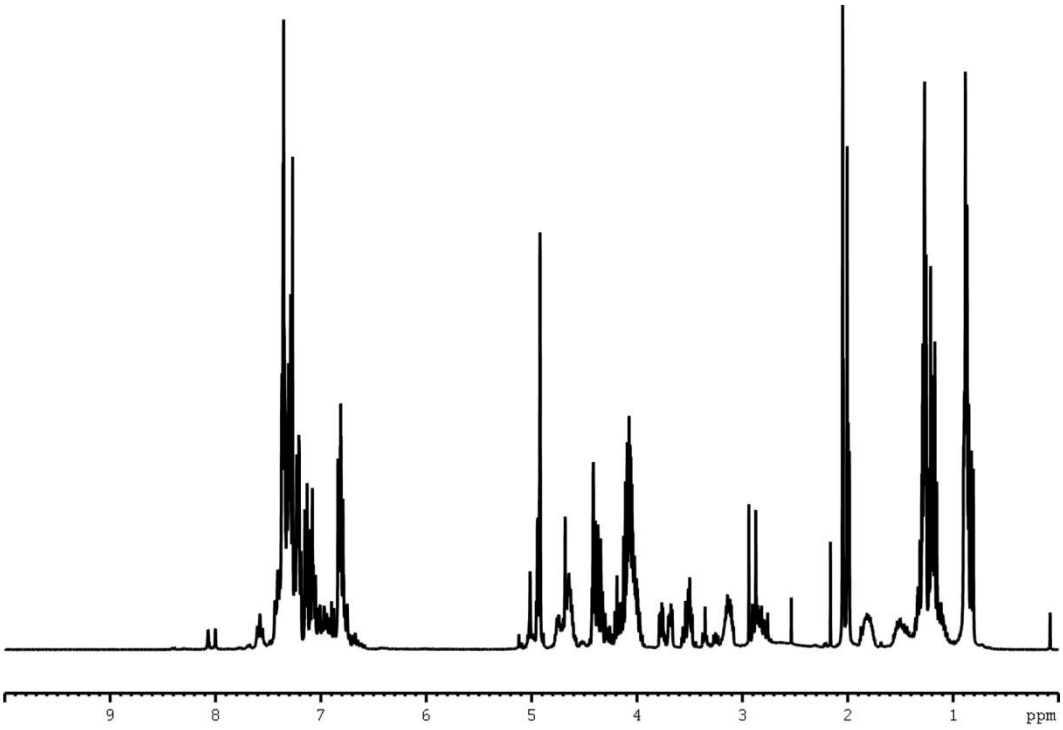

^{1}HNMR Spectrum (600 MHz) of diethyl N-(N-acetyl-L-isoleucyl-O-benzyl-L-serinyl)-1-amino-2-(4-benzyloxyphenyl)ethyl phosphonate (III-4c) in $CDCl_3$

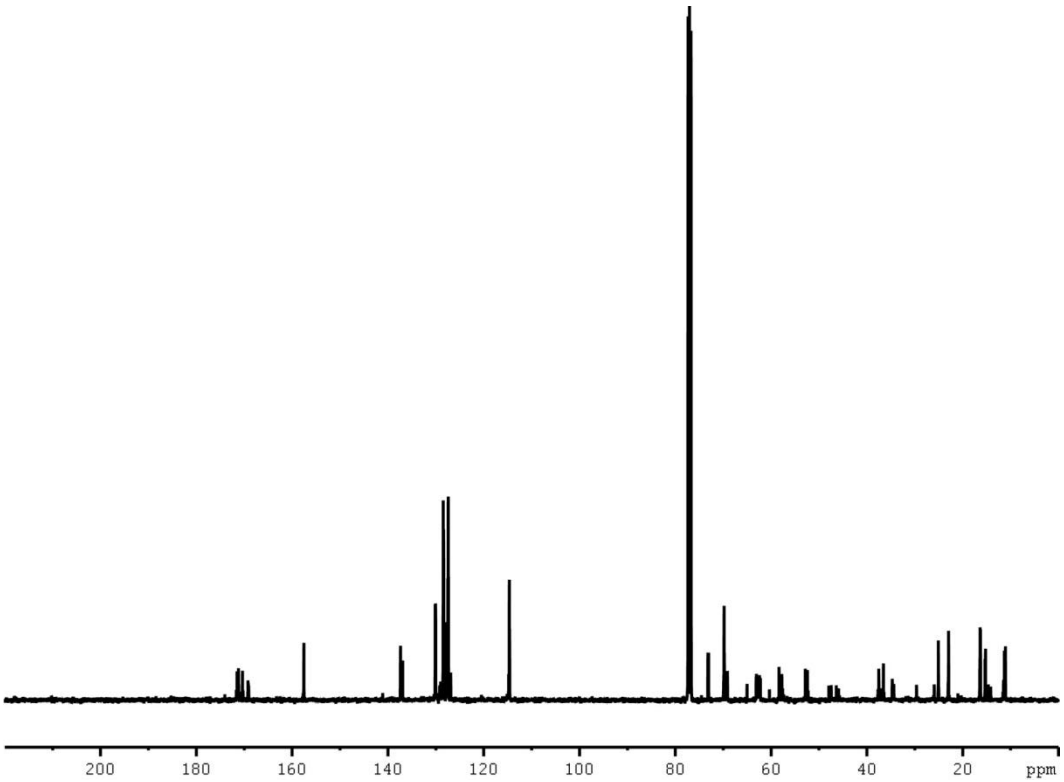

^{13}CNMR Spectrum (150 MHz) of diethyl N-(N-acetyl-L-isoleucyl-O-benzyl-L-serinyl)-1-amino-2-(4-benzyloxyphenyl)ethyl phosphonate (III-4c) in $CDCl_3$

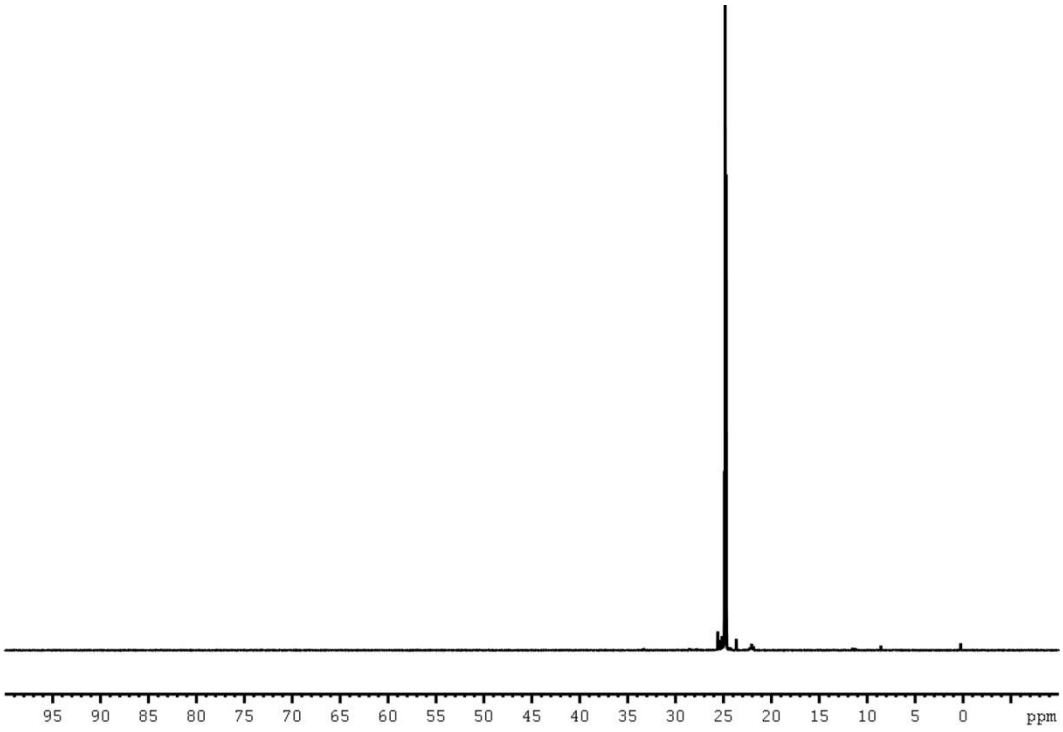

^{31}PNMR Spectrum (162 MHz) of diethyl N-(N-acetyl-L-isoleucyl-O-benzyl-L-serinyl)-1-amino-2-(4-benzyloxyphenyl)ethyl phosphonate (III-4c) in $CDCl_3$

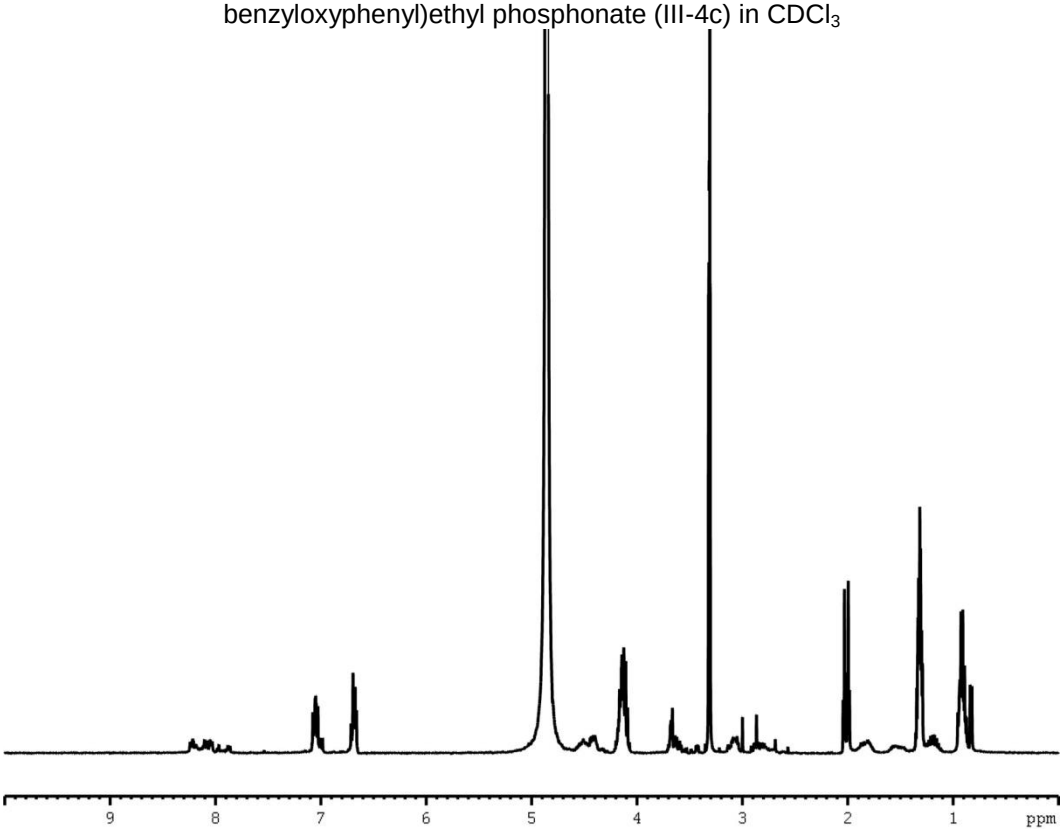

^{1}HNMR Spectrum (600 MHz) of diethyl N-(N-acetyl-L-isoleucyl-L-serinyl)-1-amino-2-(4-hydoxyphenyl)ethyl phosphonate (III-4d) in MeOD

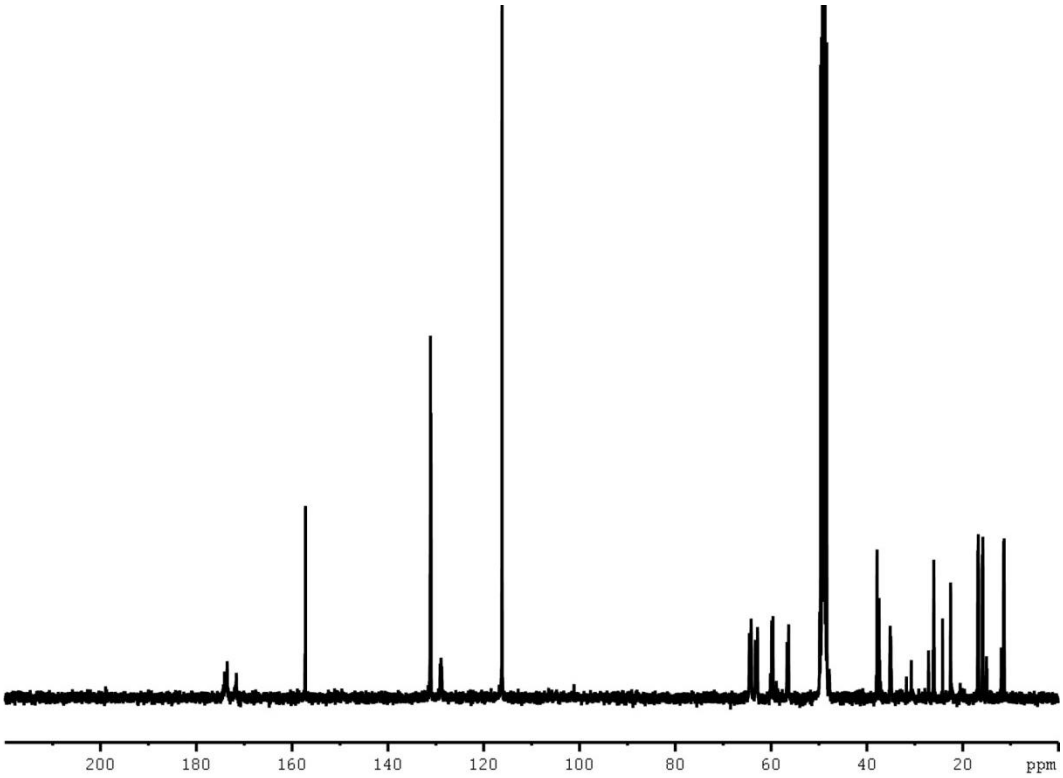

^{13}CNMR Spectrum (150 MHz) of diethyl N-(N-acetyl-L-isoleucyl-L-serinyl)-1-amino-2-(4-hydoxyphenyl)ethyl phosphonate (III-4d) in MeOD

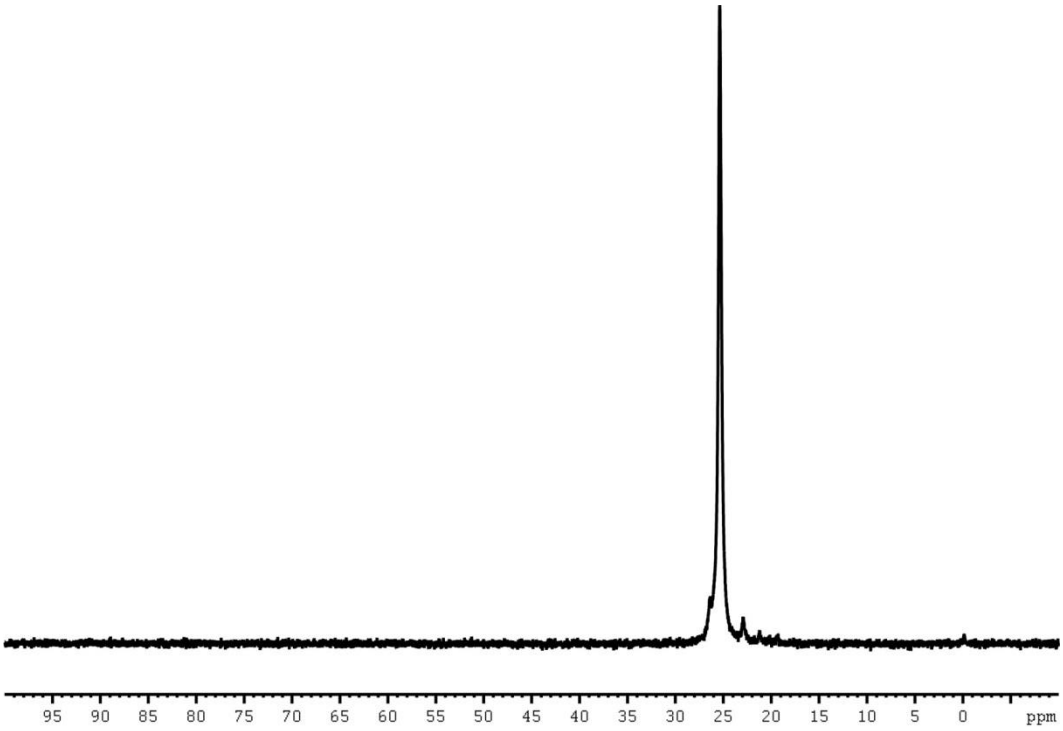

^{31}PNMR Spectrum (121 MHz) diethyl N-(N-acetyl-L-isoleucyl-L-serinyl)-1-amino-2-(4-hydoxyphenyl)ethyl phosphonate (III-4d) in MeOD

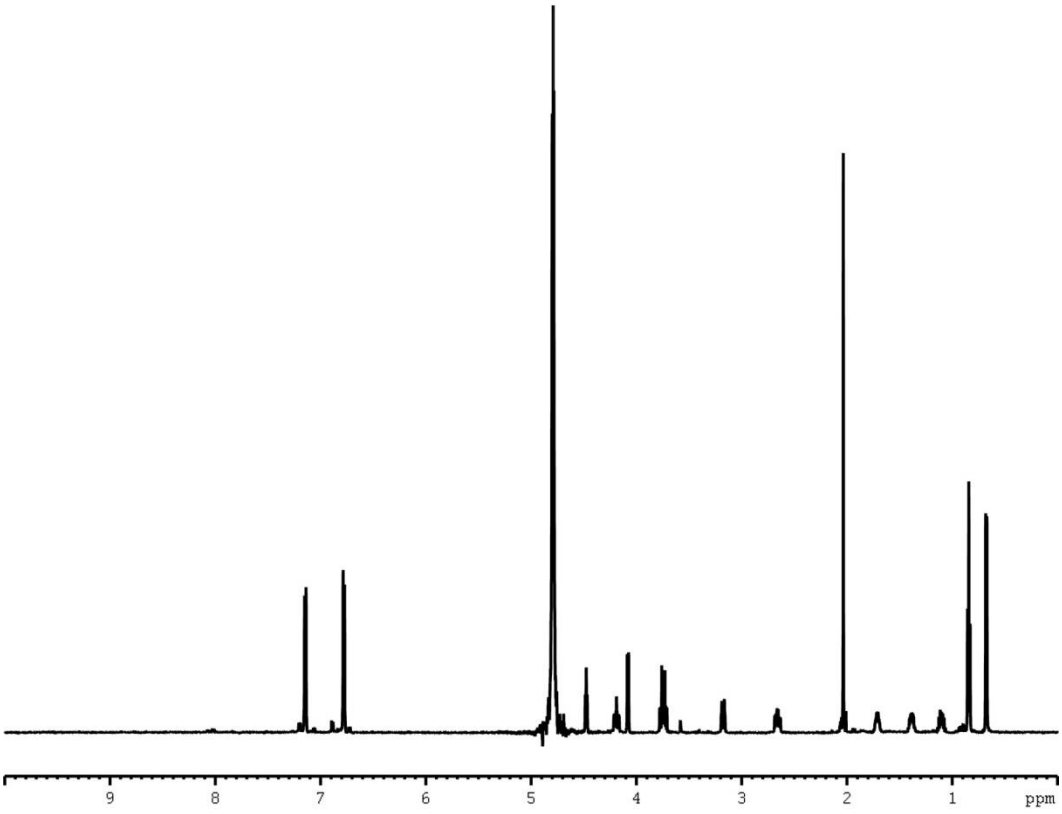

^{1}HNMR Spectrum (600 MHz) of Ac-Ile-Ser-AHEP: N-(N-acetyl-L-isoleucyl-L-serinyl)-1-amino-2-(4-hydoxyphenyl)ethyl phosphonic acid (III-4) in D_2O

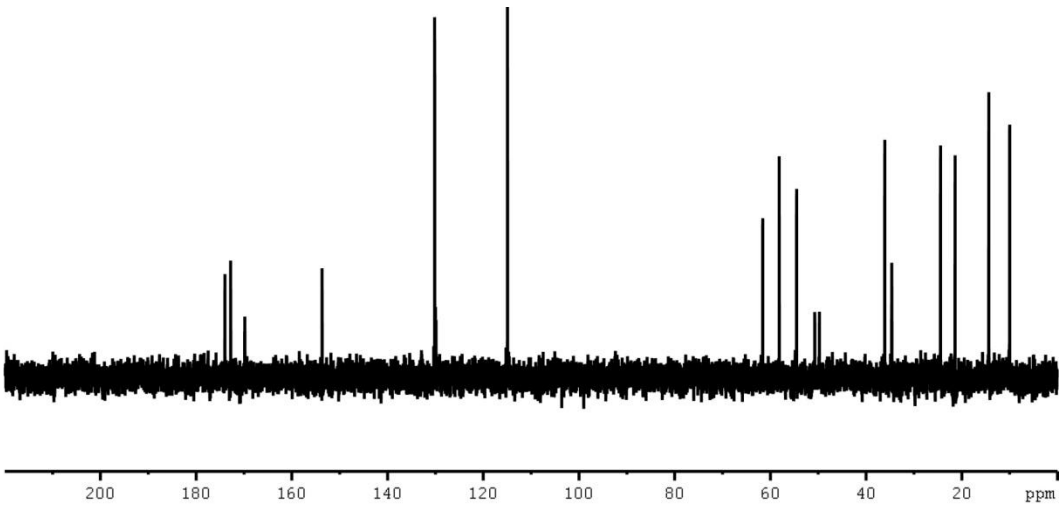

^{13}CNMR Spectrum (150 MHz) of Ac-Ile-Ser-AHEP: N-(N-acetyl-L-isoleucyl-L-serinyl)-1-amino-2-(4-hydoxyphenyl)ethyl phosphonic acid (III-4) in D_2O

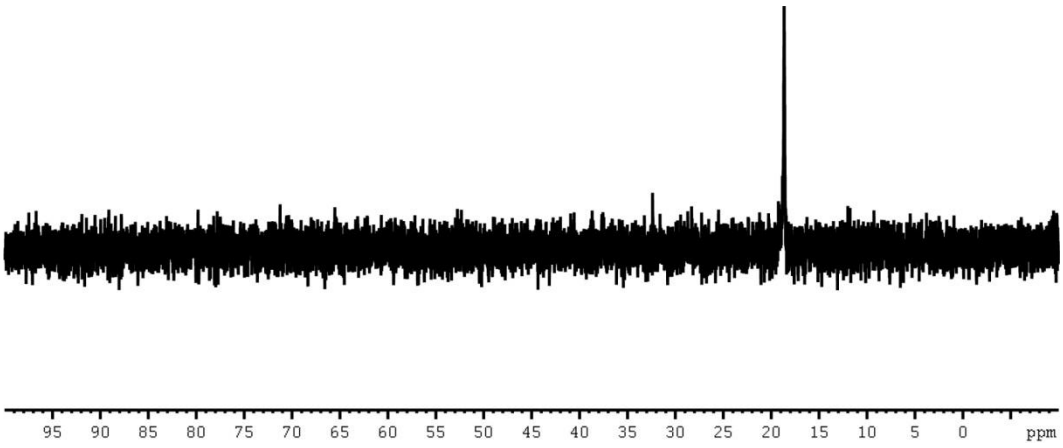

^{31}PNMR Spectrum (162 MHz) of Ac-Ile-Ser-AHEP: N-(N-acetyl-L-isoleucyl-L-serinyl)-1-amino-2-(4-hydoxyphenyl)ethyl phosphonic acid (III-4) in D_2O

NMR spectra of Ac-Ile-His-AHEP (III-5) and synthetic intermediates (III-5a - III-5d)

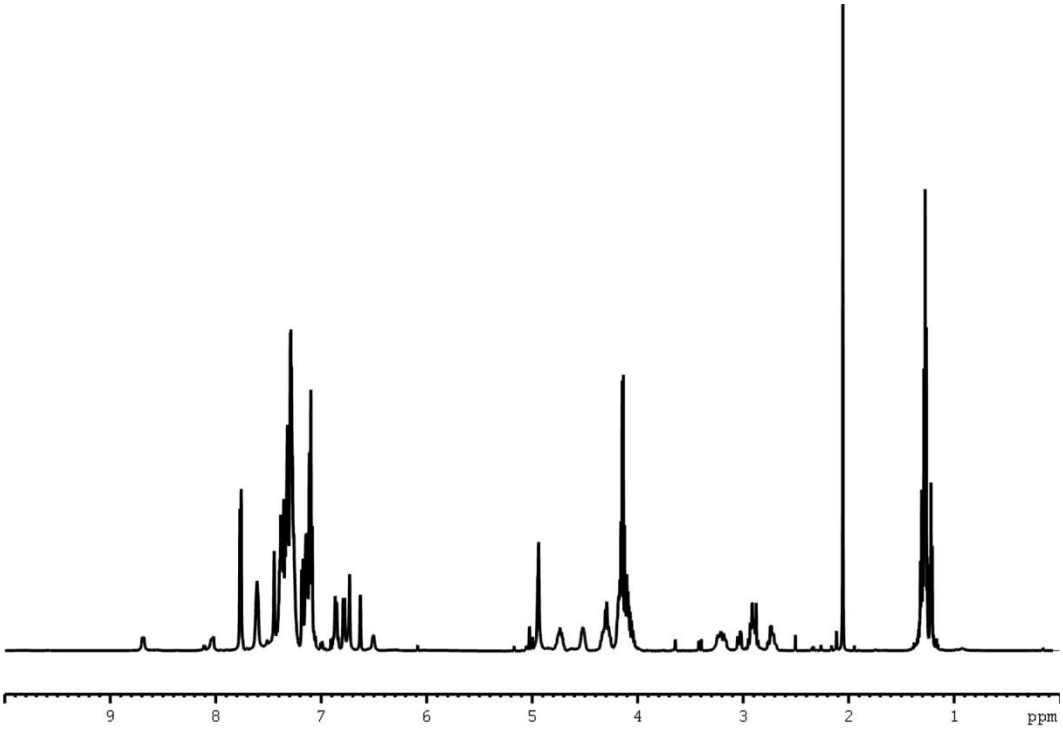

^{1}HNMR Spectrum (400 MHz) of diethyl N-(N-fluorenylmethyloxycarbonyl-T-trityl-L-histadyl-)-1-amino-2-(4-benzyloxyphenyl)ethyl phosphonate (III-5a) in $CDCl_3$

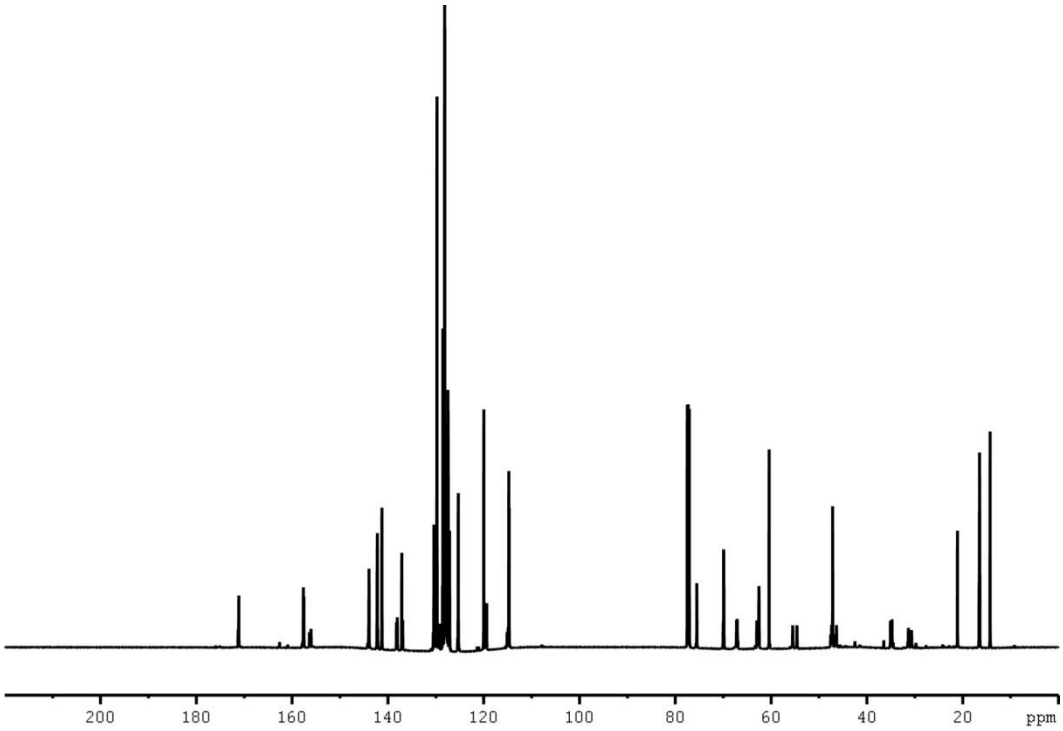

^{13}CNMR Spectrum (100 MHz) of diethyl N-(N-fluorenylmethyloxycarbonyl-T-trityl-L-histadyl-)-1-amino-2-(4-benzyloxyphenyl)ethyl phosphonate (III-5a) in $CDCl_3$

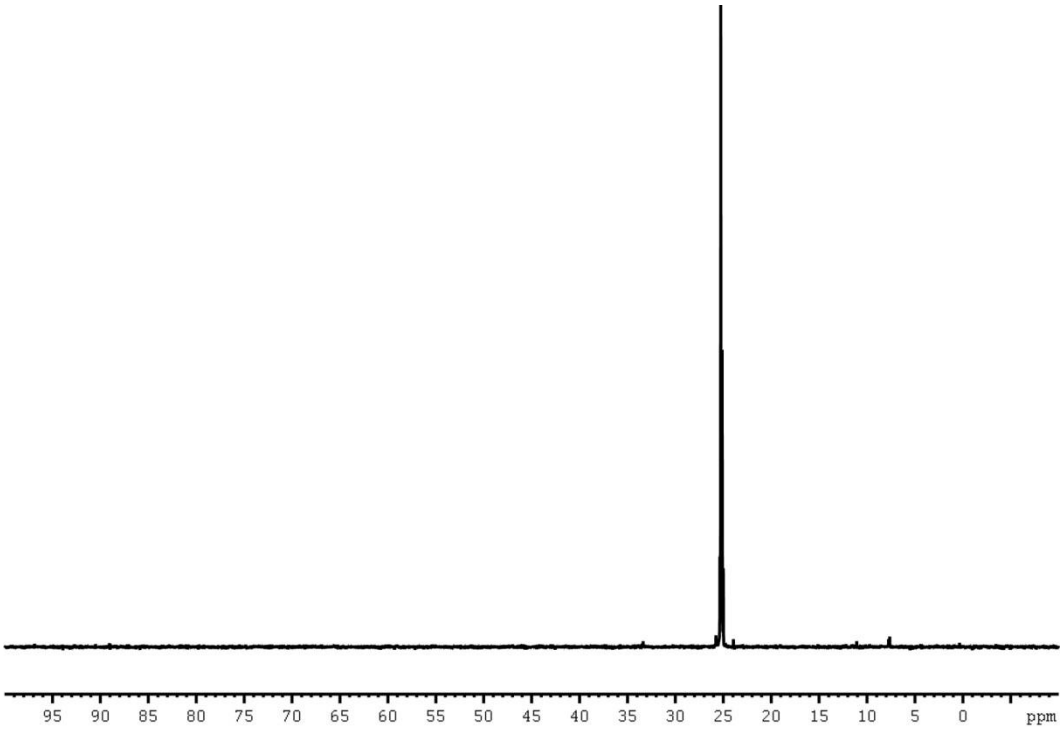

^{31}PNMR Spectrum (162 MHz) of diethyl N-(N-fluorenylmethyloxycarbonyl-T-trityl-L-histadyl-)-1-amino-2-(4-benzyloxyphenyl)ethyl phosphonate (III-5a) in $CDCl_3$

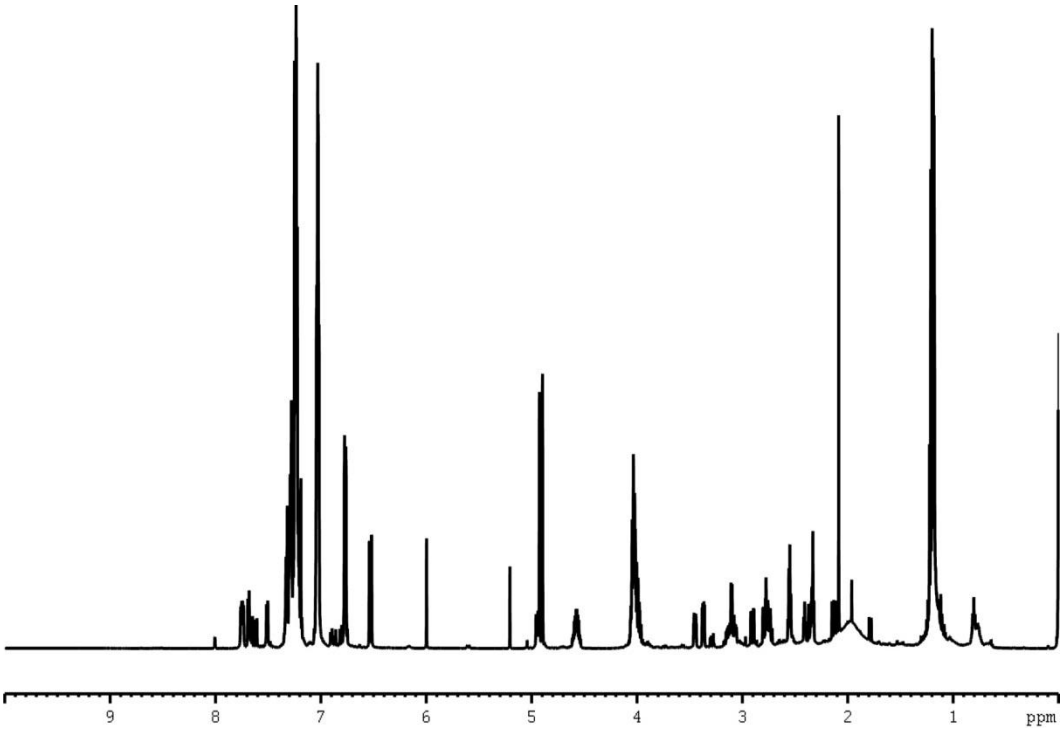

^{1}HNMR Spectrum (400 MHz) of diethyl N-(T-trityl-L-histadyl-)-1-amino-2-(4-benzyloxyphenyl)ethyl phosphonate (III-3b) in $CDCl_3$

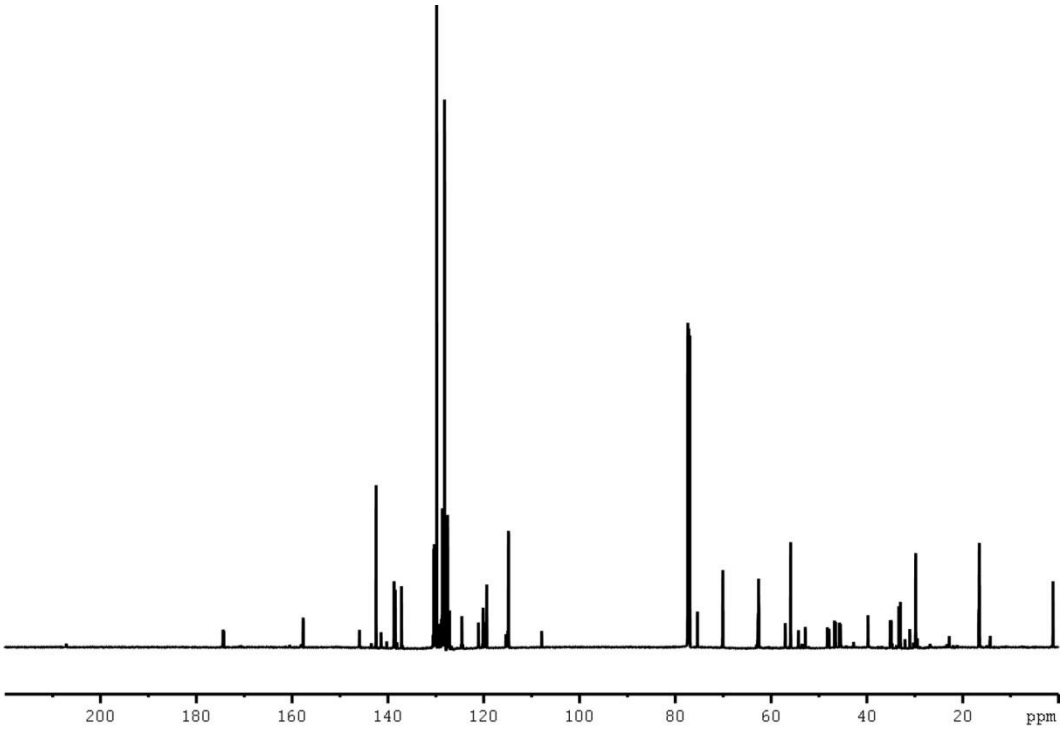

^{13}CNMR Spectrum (100 MHz) of diethyl N-(T-trityl-L-histadyl-)-1-amino-2-(4-benzyloxyphenyl)ethyl phosphonate (III-3b) in $CDCl_3$

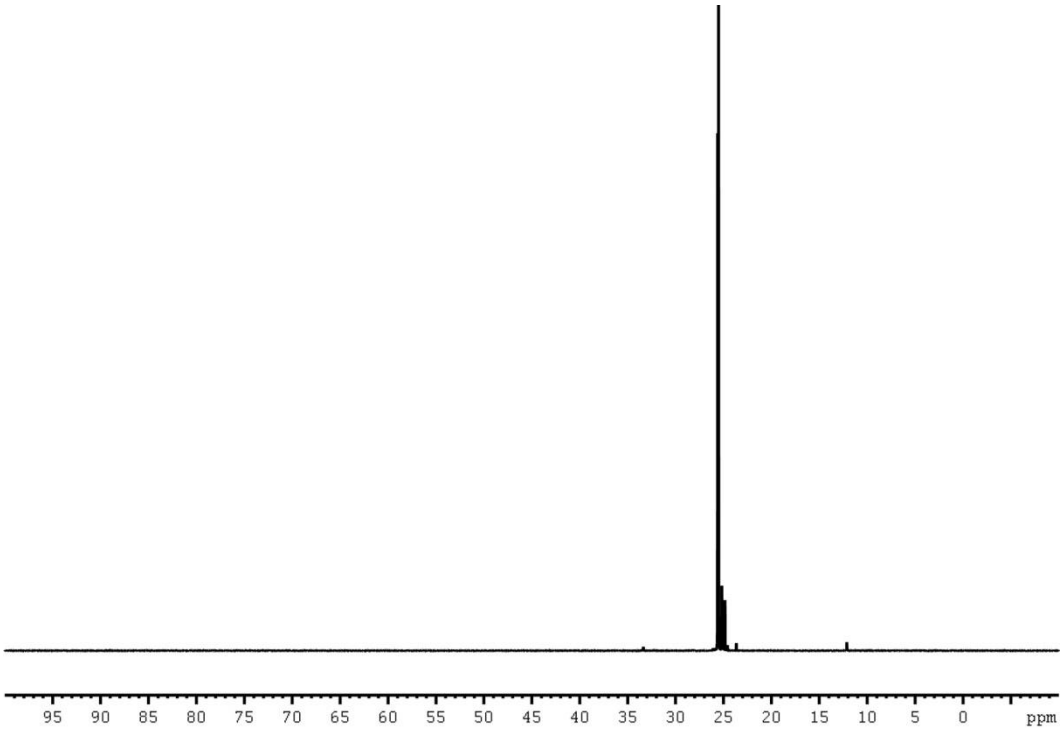

^{31}PNMR Spectrum (162 MHz) of diethyl N-(T-trityl-L-histadyl-)-1-amino-2-(4-benzyloxyphenyl)ethyl phosphonate (III-5b) in $CDCl_3$

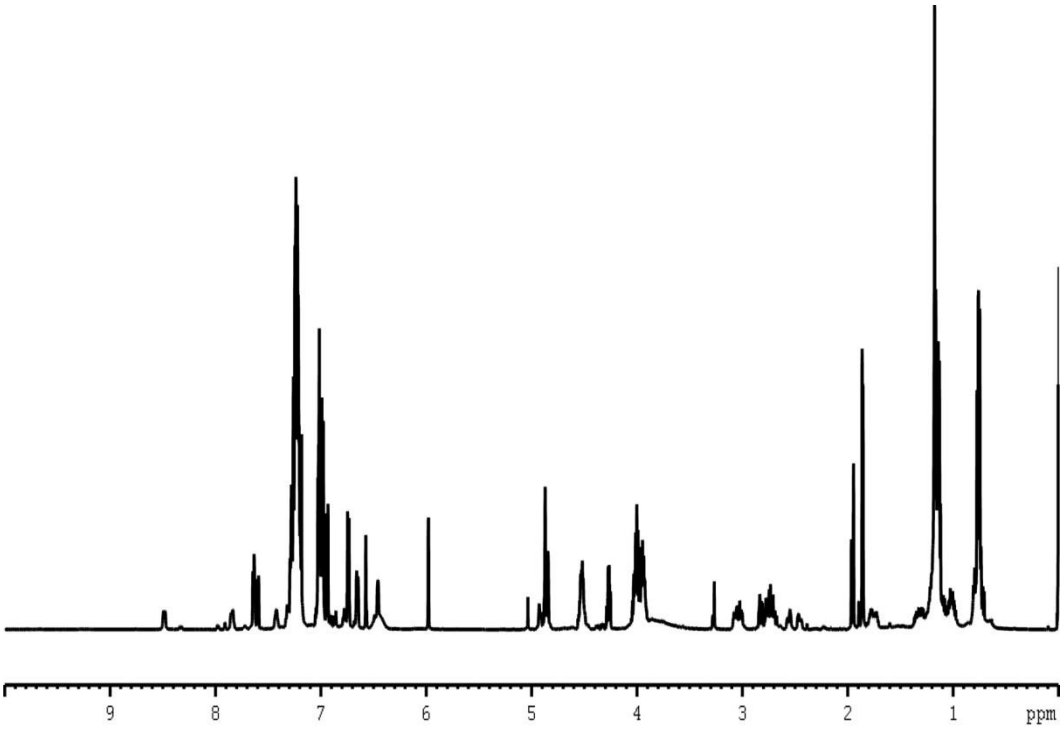

^{1}HNMR Spectrum (600 MHz) of diethyl N-(N-acetyl-L-isoleucyl- T-trityl-L-histadyl)-1-amino-2-(4-benzyloxyphenyl)ethyl phosphonate (III-5c) in $CDCl_3$

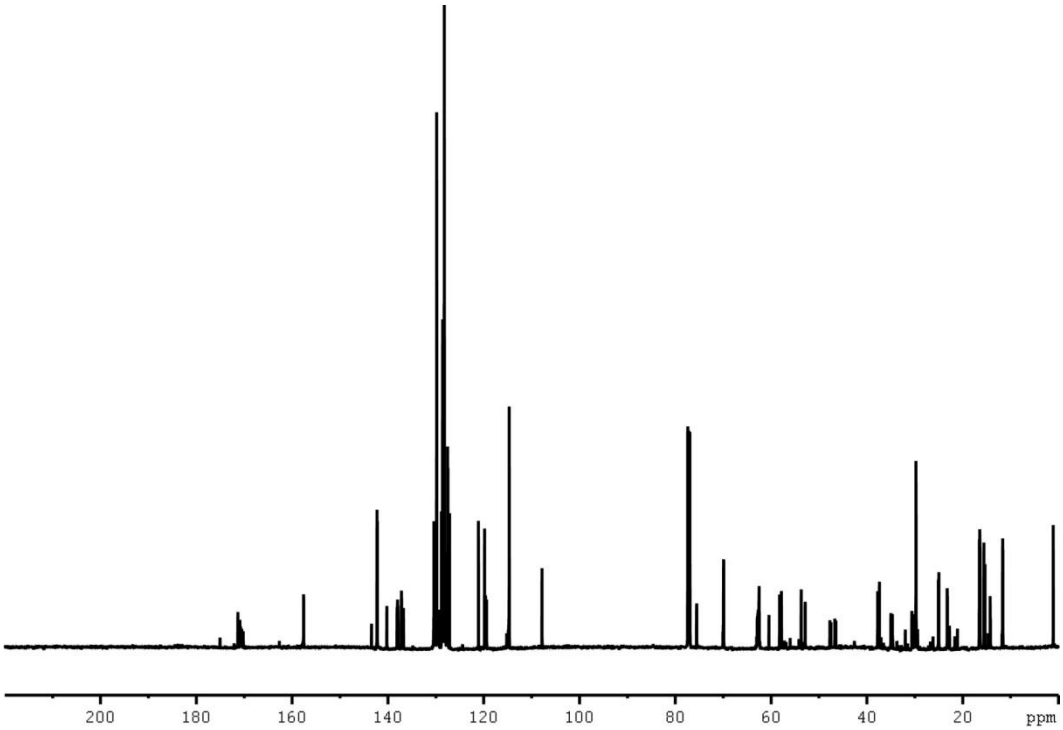

^{13}CNMR Spectrum (150 MHz) of diethyl N-(N-acetyl-L-isoleucyl- T-trityl-L-histadyl)-1-amino-2-(4-benzyloxyphenyl)ethyl phosphonate (III-5c) in $CDCl_3$

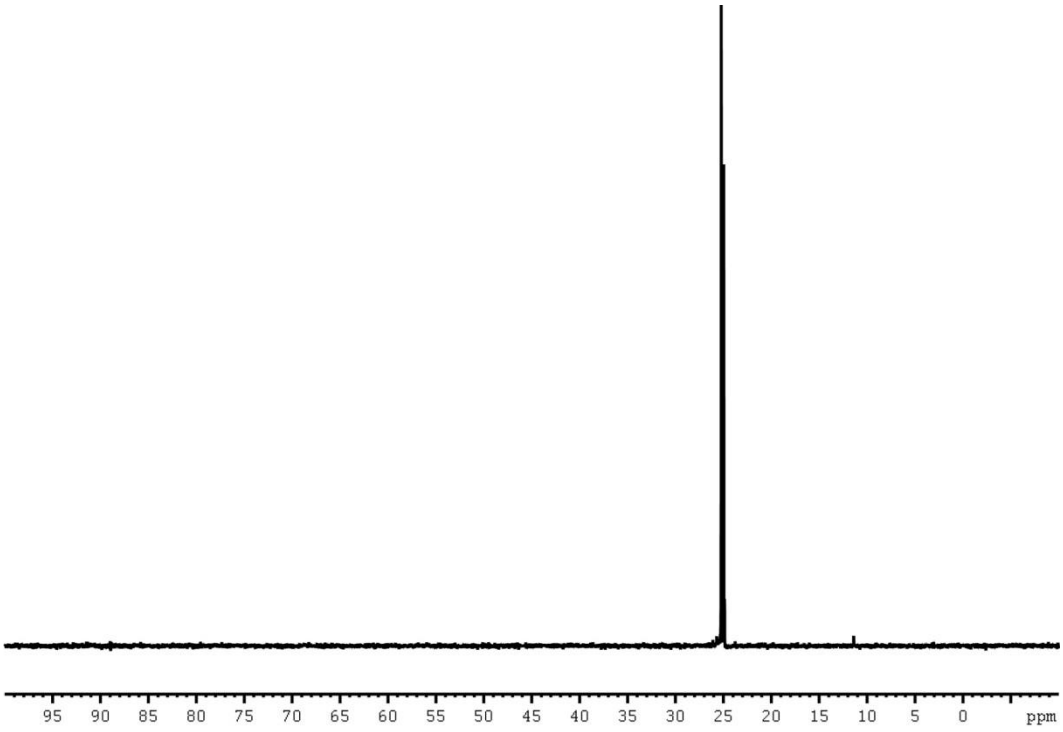

^{31}PNMR Spectrum (162 MHz) of diethyl N-(N-acetyl-L-isoleucyl- T-trityl-L-histadyl)-1-amino-2-(4-benzyloxyphenyl)ethyl phosphonate (III-5c) in $CDCl_3$

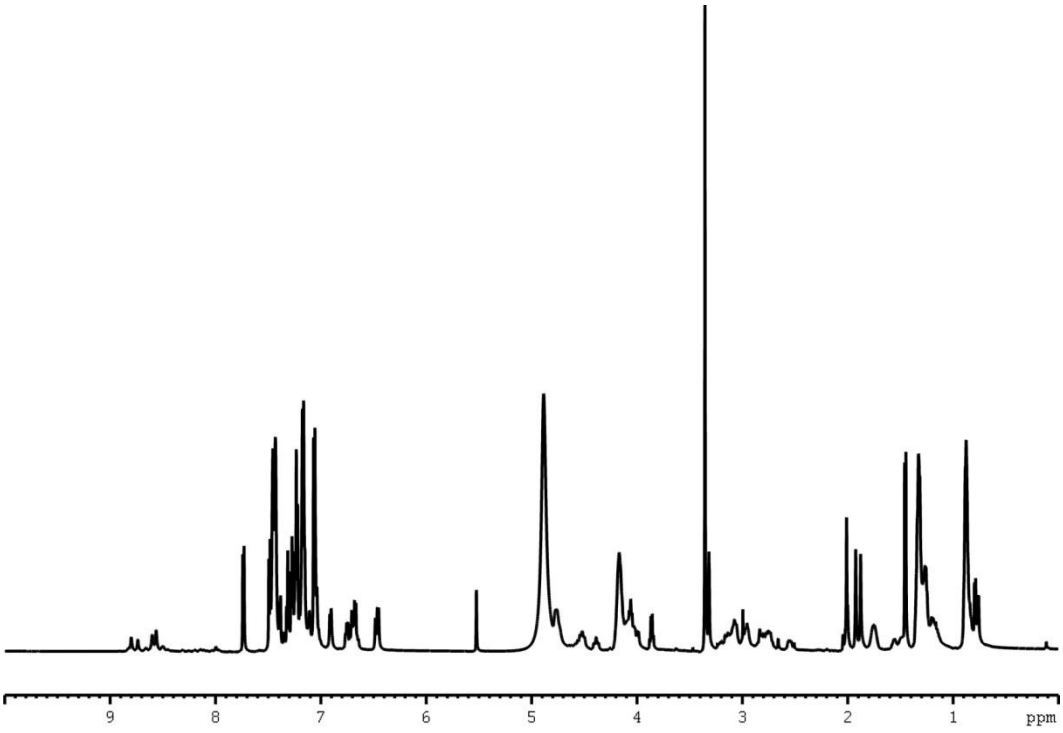

^{1}HNMR Spectrum (600 MHz) of diethyl N-(N-acetyl-L-isoleucyl- T-trityl-L-histadyl)-1-amino-2-(4-hydoxyphenyl)ethyl phosphonate (III-5d) in MeOD

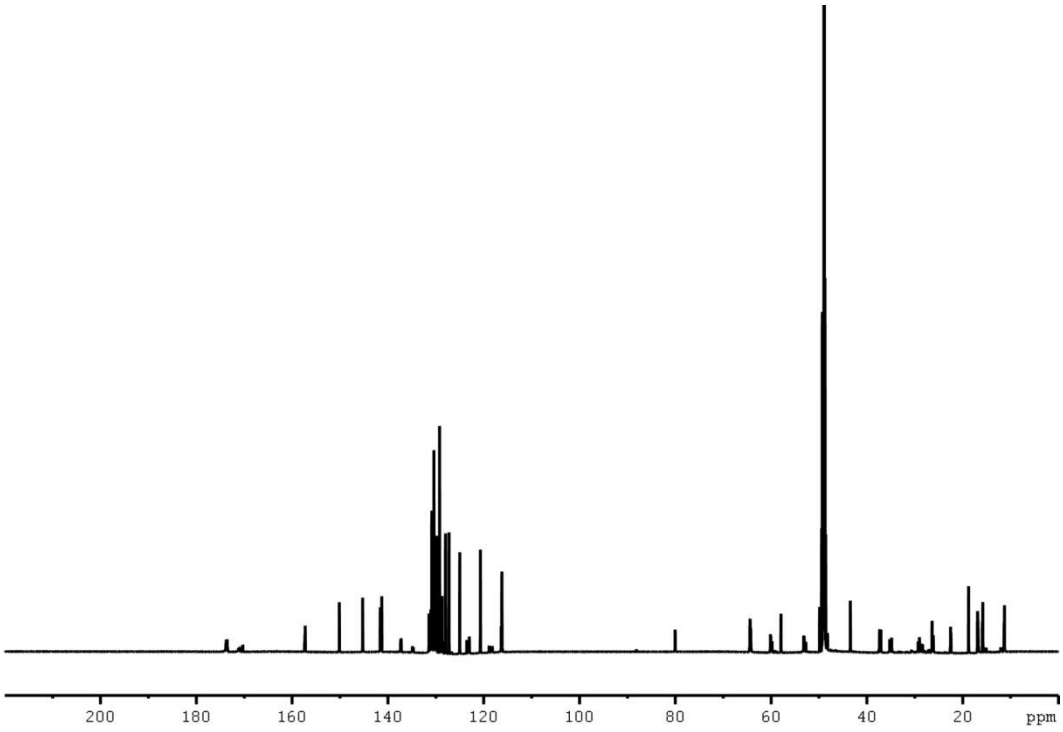

^{13}CNMR Spectrum (150 MHz) of diethyl N-(N-acetyl-L-isoleucyl- T-trityl-L-histadyl)-1-amino-2-(4-hydoxyphenyl)ethyl phosphonate (III-5d) in MeOD

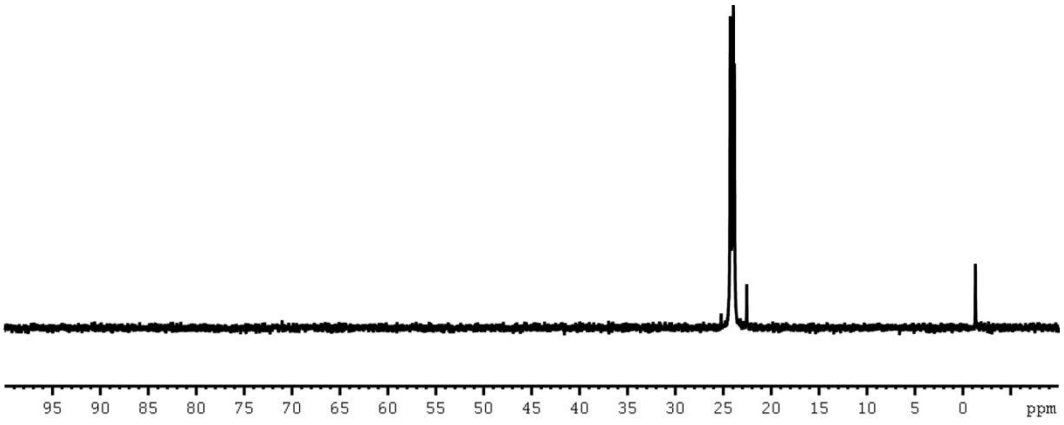

^{31}PNMR Spectrum (162 MHz) diethyl N-(N-acetyl-L-isoleucyl- T-trityl-L-histadyl)-1-amino-2-(4-hydoxyphenyl)ethyl phosphonate (III-5d) in MeOD

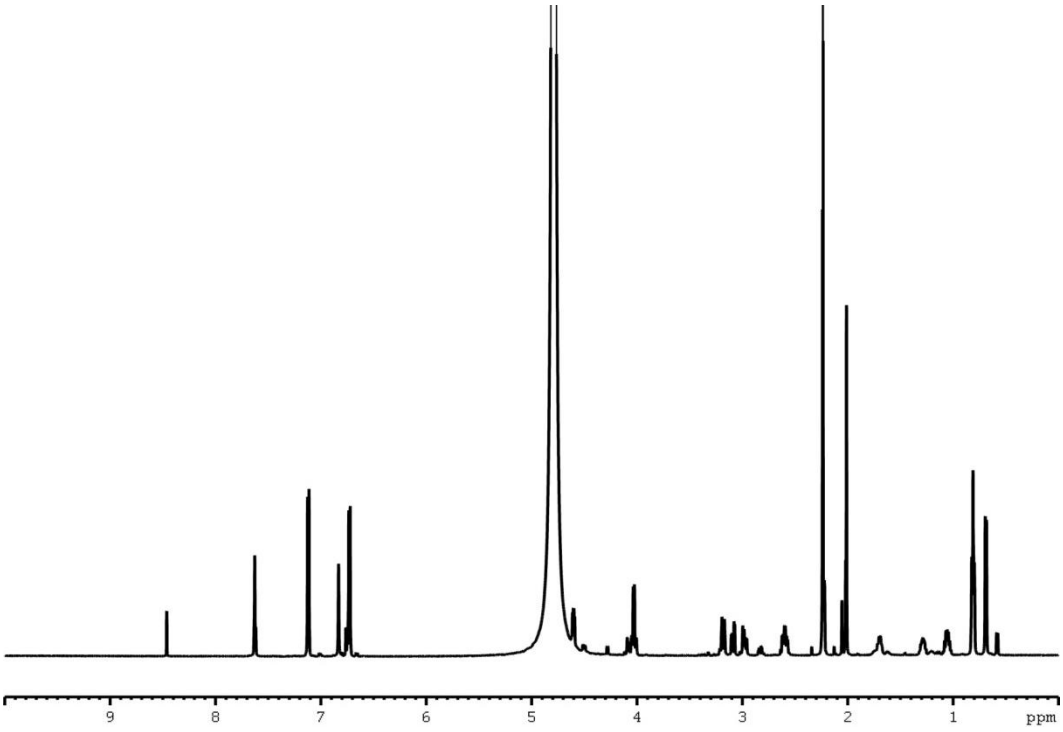

^{1}HNMR Spectrum (600 MHz) of Ac-Ile-His-AHEP: N-(N-acetyl-L-isoleucyl-L-histadyl)-1-amino-2-(4-hydoxyphenyl)ethyl phosphonic acid (III-5) in D_2O

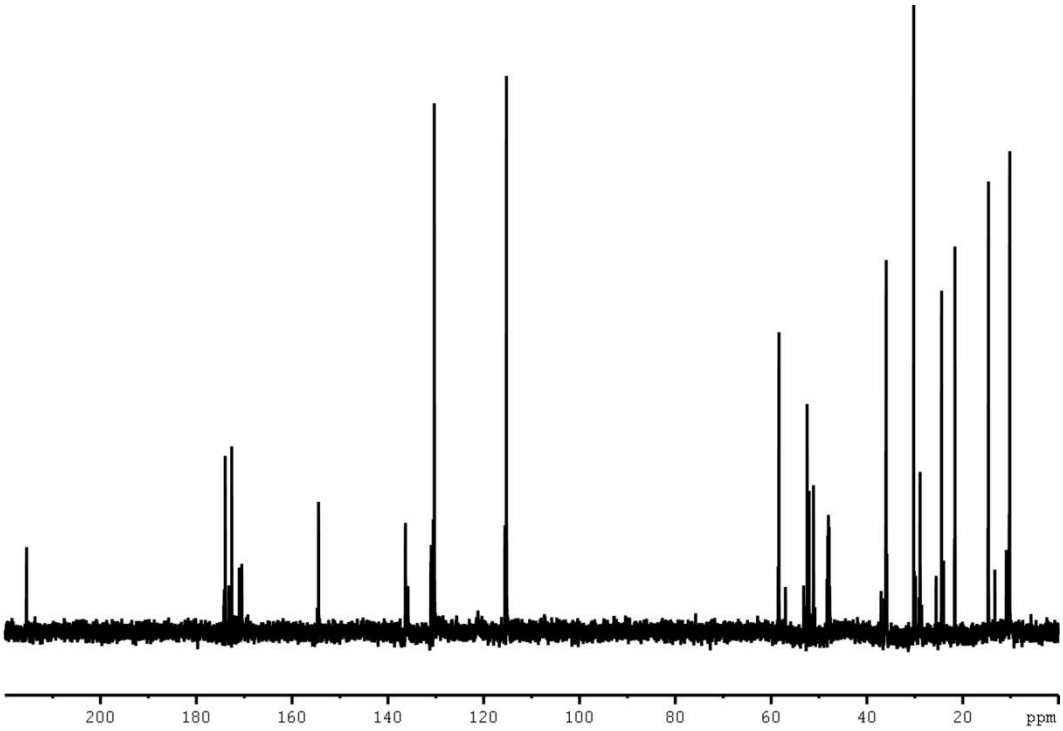

^{13}CNMR Spectrum (150 MHz) of Ac-Ile-His-AHEP: N-(N-acetyl-L-isoleucyl-L-histadyl)-1-amino-2-(4-hydoxyphenyl)ethyl phosphonic acid (III-5) in D_2O

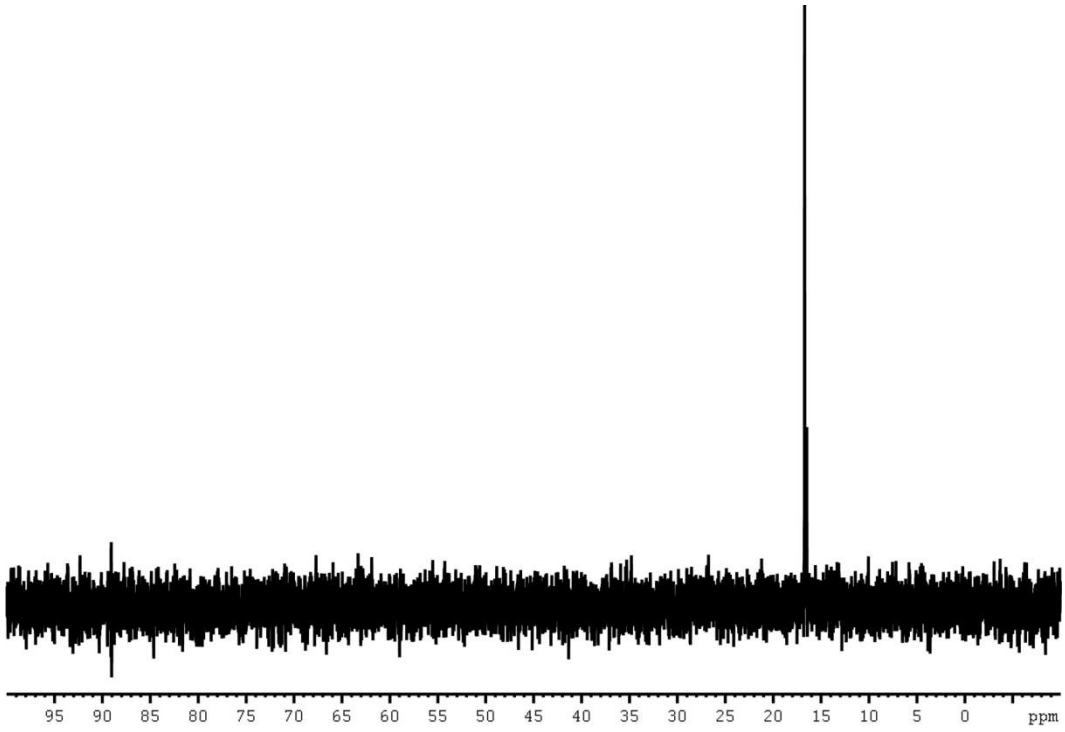

^{31}PNMR Spectrum (162 MHz) of Ac-Ile-His-AHEP: N-(N-acetyl-L-isoleucyl-L-histadyl)-1-amino-2-(4-hydoxyphenyl)ethyl phosphonic acid (III-5) in D_2O

NMR spectra of Ac-His-Trp-AHEP (III-6) and synthetic intermediates (III-6a - III-6c)

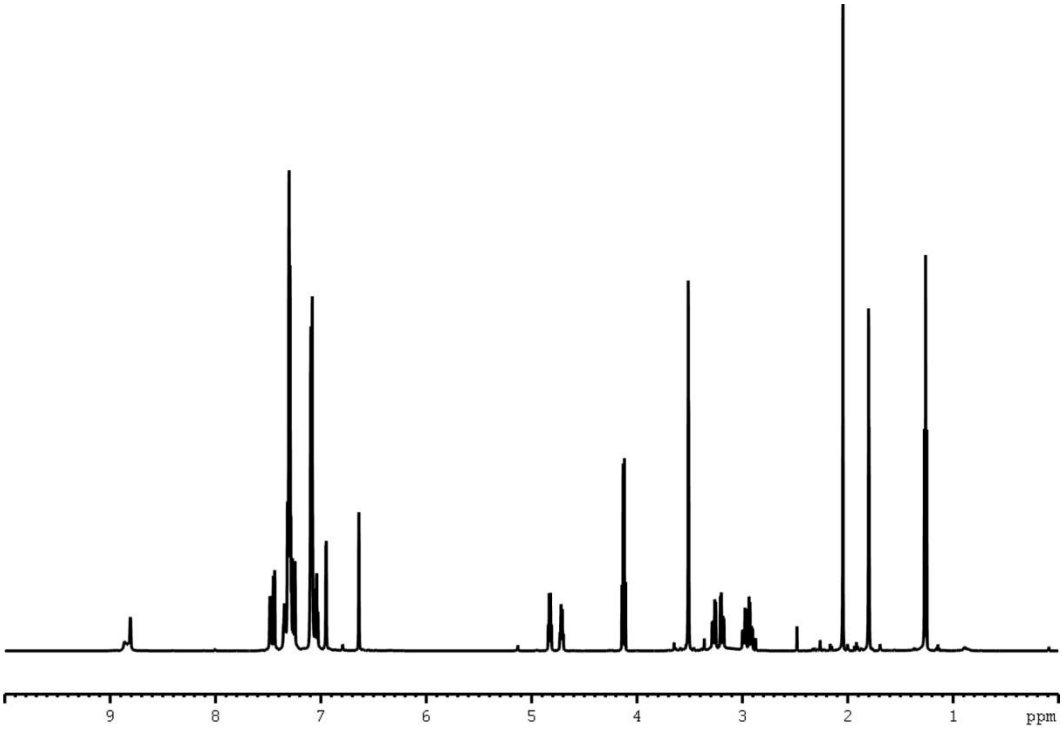

^{1}HNMR Spectrum (400 MHz) of N-acetyl-(T-trityl-L-histady)l-L-tryptophan methyl ester (III-6a) in $CDCl_3$

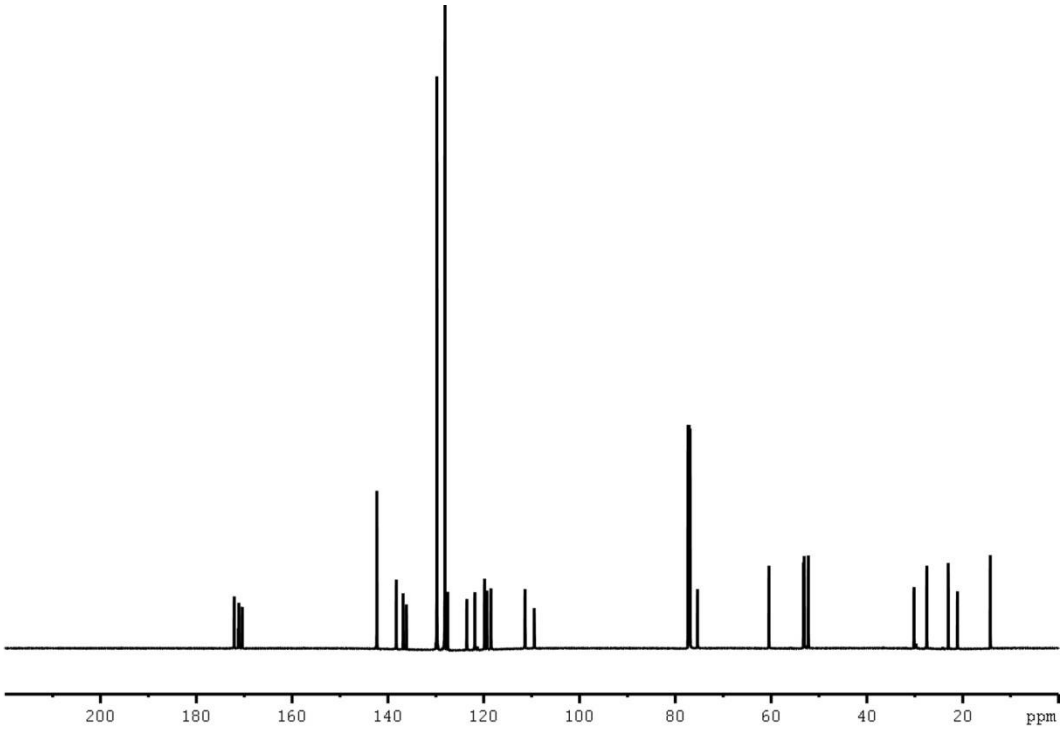

^{13}CNMR Spectrum (100 MHz) of N-(T-trityl-L-histadyl)-L-tryptophan methyl ester (III-6a) in $CDCl_3$

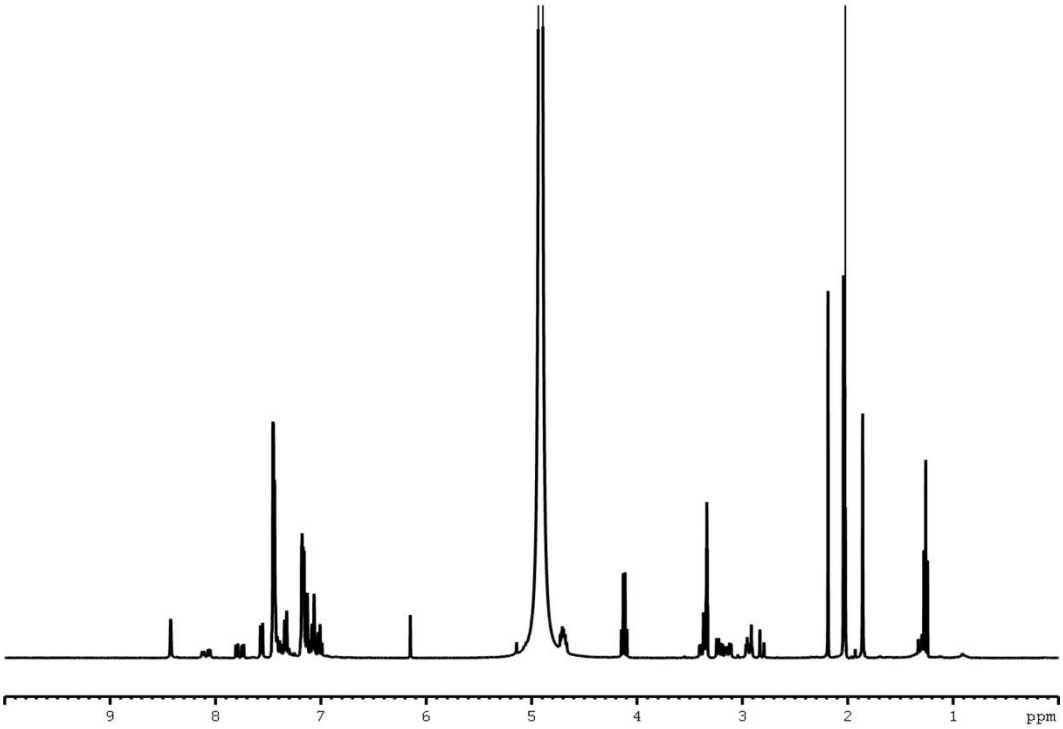

^{1}HNMR Spectrum (400 MHz) of N-acetyl-(T-trityl-L-histady)l-L-tryptophan (III-6b) in MeOD

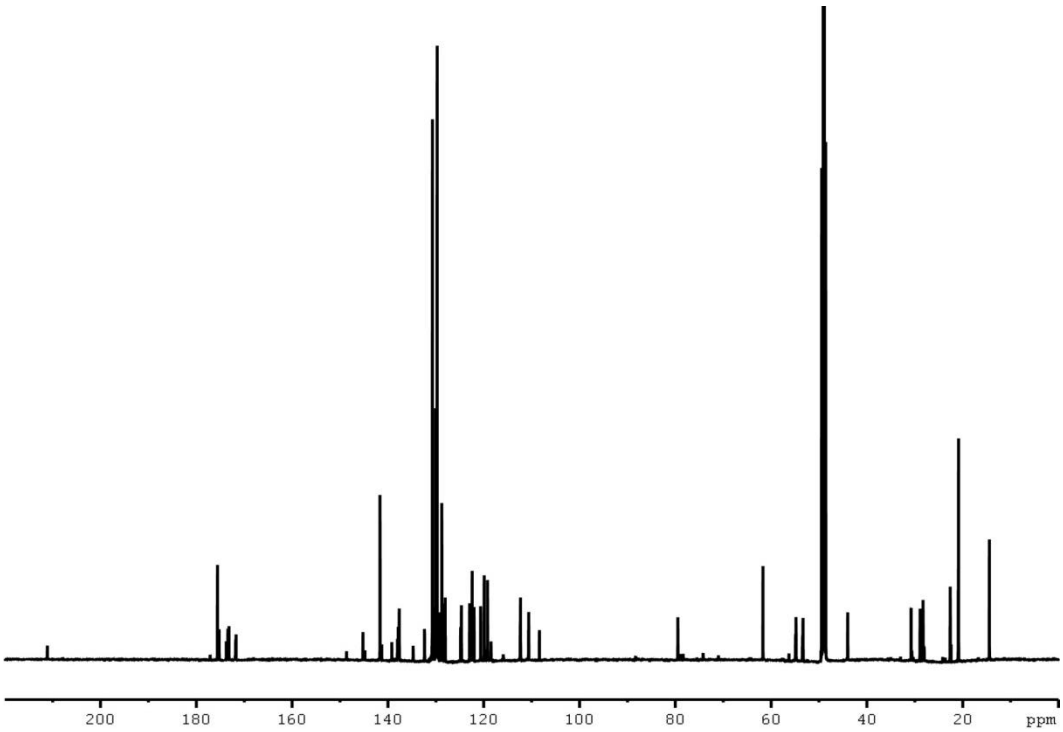

^{13}CNMR Spectrum (100 MHz) of N-acetyl-(T-trityl-L-histadyl) -L-tryptophan (III-6b) in MeOD

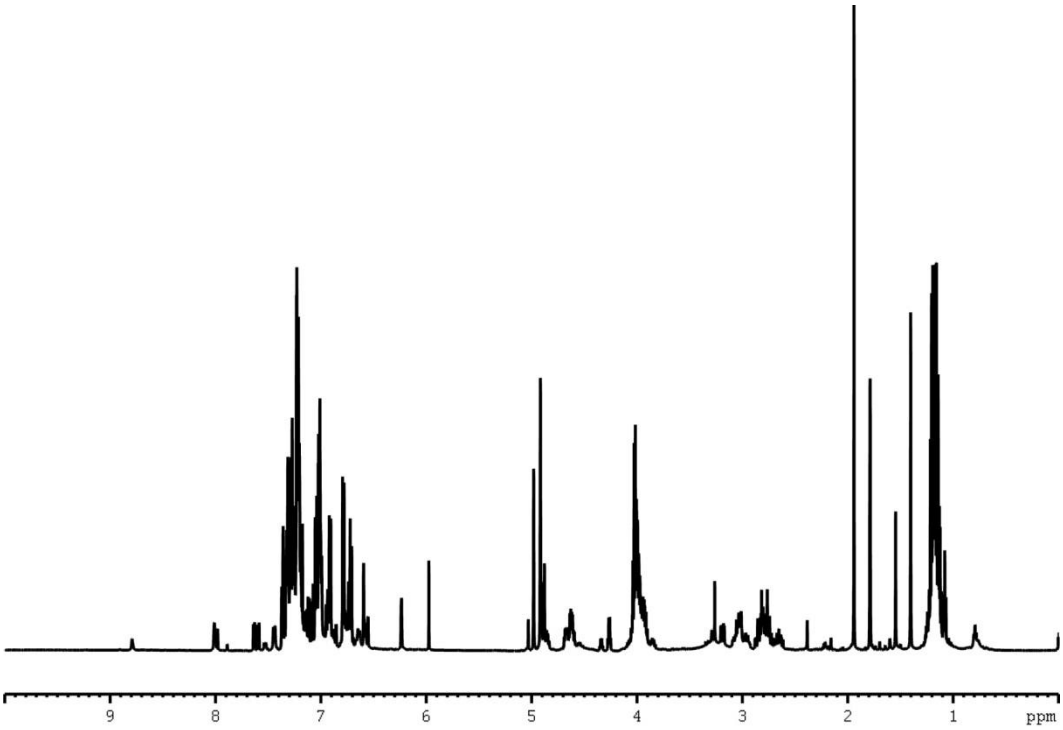

^{1}HNMR Spectrum (600 MHz) of diethyl N-(N-acetyl-(T-trityl-L-histadyl) -L-tryptophanyl)-1-amino-2-(4-benzyloxyphenyl)ethyl phosphonate (III-6c) in $CDCl_3$

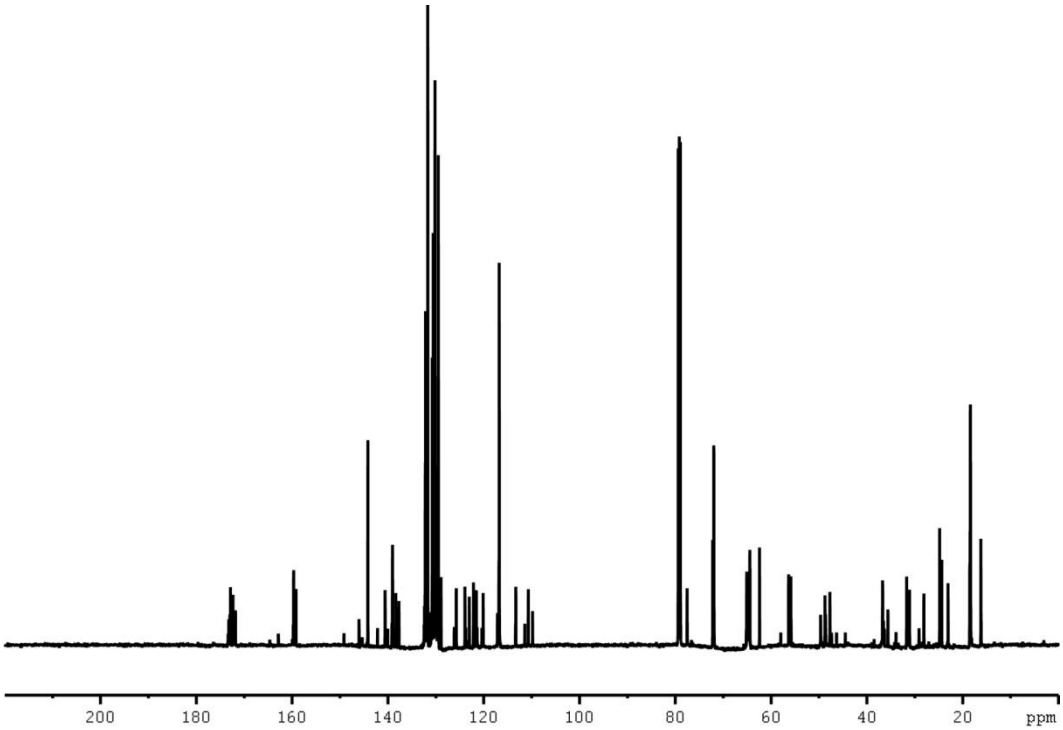

^{13}CNMR Spectrum (150 MHz) of diethyl N-(N-acetyl-(T-trityl-L-histadyl)-L-tryptophanyl)-1-amino-2-(4-benzyloxyphenyl)ethyl phosphonate (III-6c) in $CDCl_3$

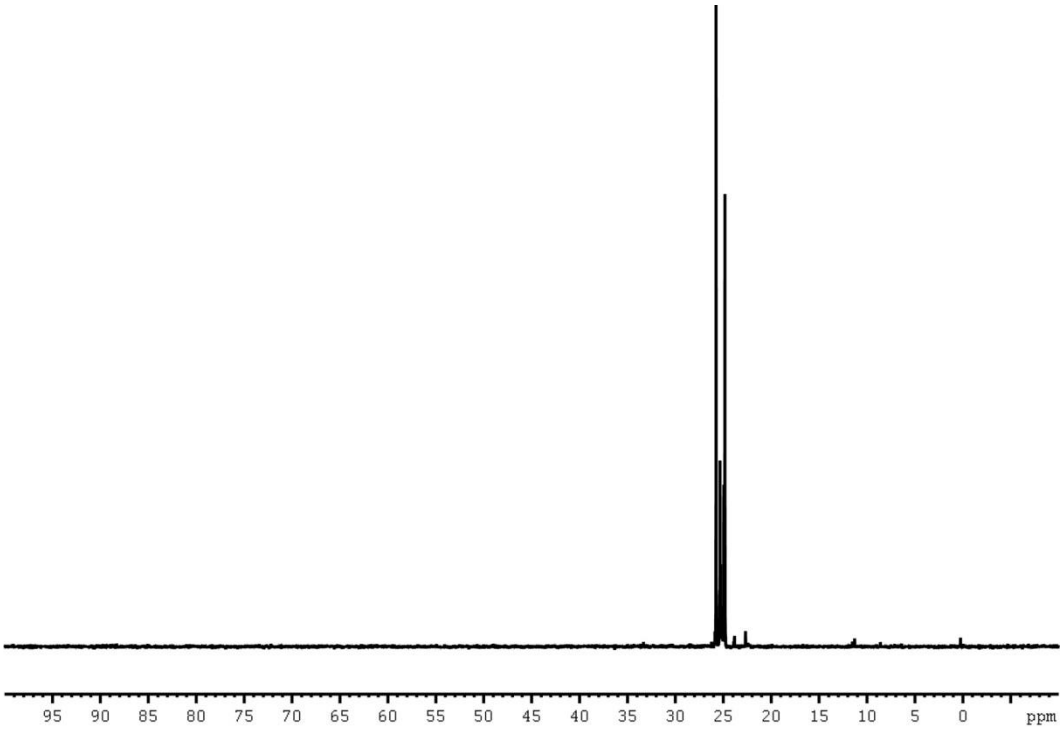

^{31}PNMR Spectrum (162 MHz) of diethyl N-(N-acetyl-(T-trityl-L-histadyl)-L-tryptophanyl)-1-amino-2-(4-benzyloxyphenyl)ethyl phosphonate (III-6c) in $CDCl_3$

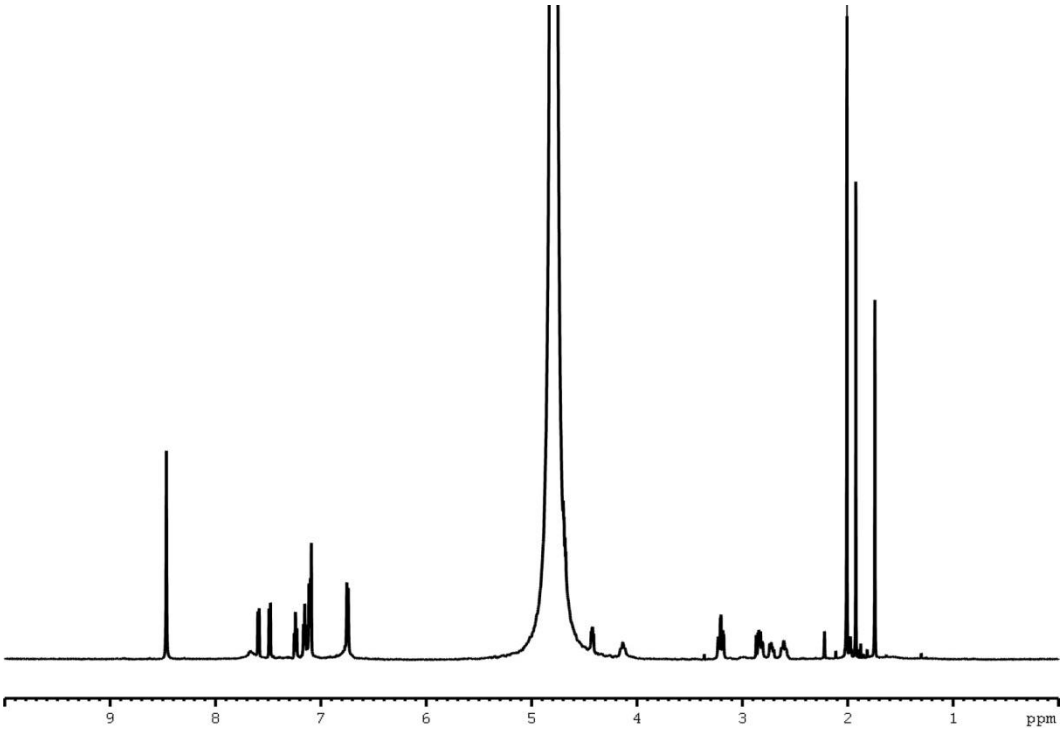

^{1}HNMR Spectrum (600 MHz) of Ac-His-Trp-AHEP: N-(N-acetyl-L-histadyl-L-tryptophanyl)-1-amino-2-(4-hydoxyphenyl)ethyl phosphonic acid (III-6) in D_2O

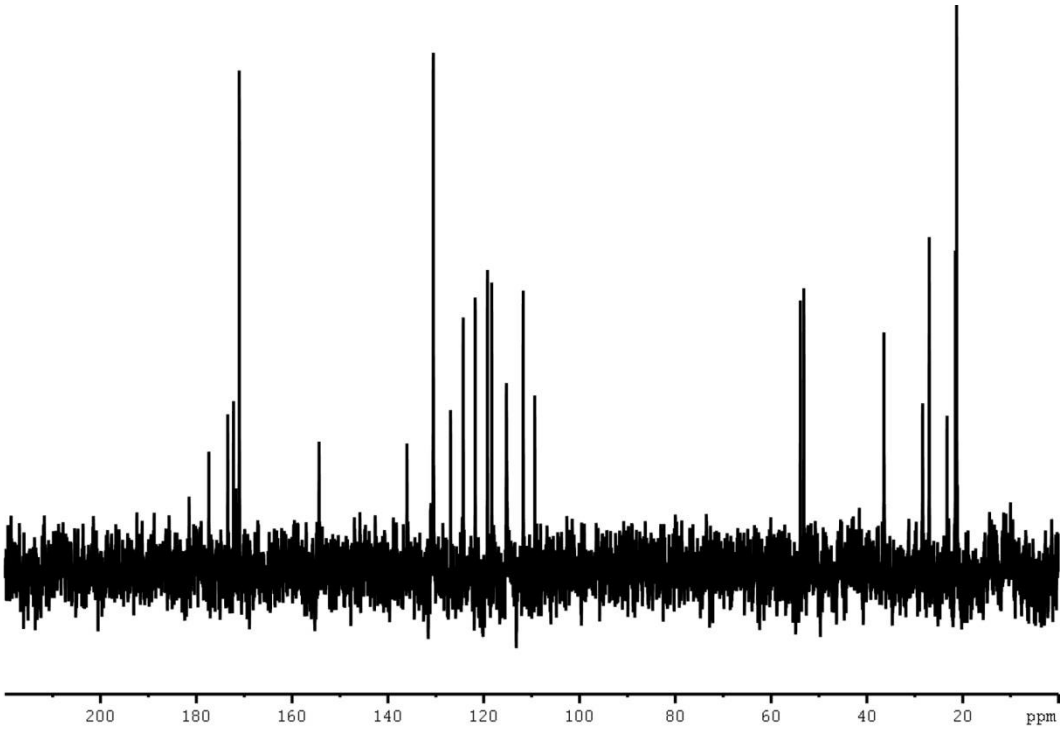

^{13}CNMR Spectrum (150 MHz) of Ac-His-Trp-AHEP: N-(N-acetyl-L-histadyl-L-tryptophanyl)-1-amino-2-(4-hydoxyphenyl)ethyl phosphonic acid (III-6) in D_2O

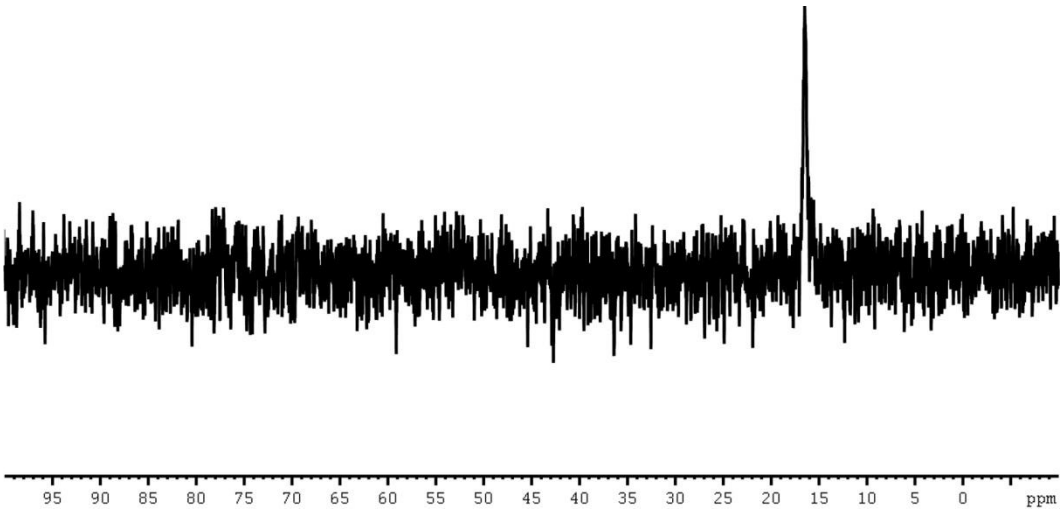

^{31}PNMR Spectrum (162 MHz) of Ac-His-Trp-AHEP: N-(N-acetyl-L-histadyl-L-tryptophanyl)-1-amino-2-(4-hydoxyphenyl)ethyl phosphonic acid (III-6) in D_2O

NMR spectra of Ac-Leu-Tyr-AHEP (III-7) and synthetic intermediates (III-7a - III-7d)

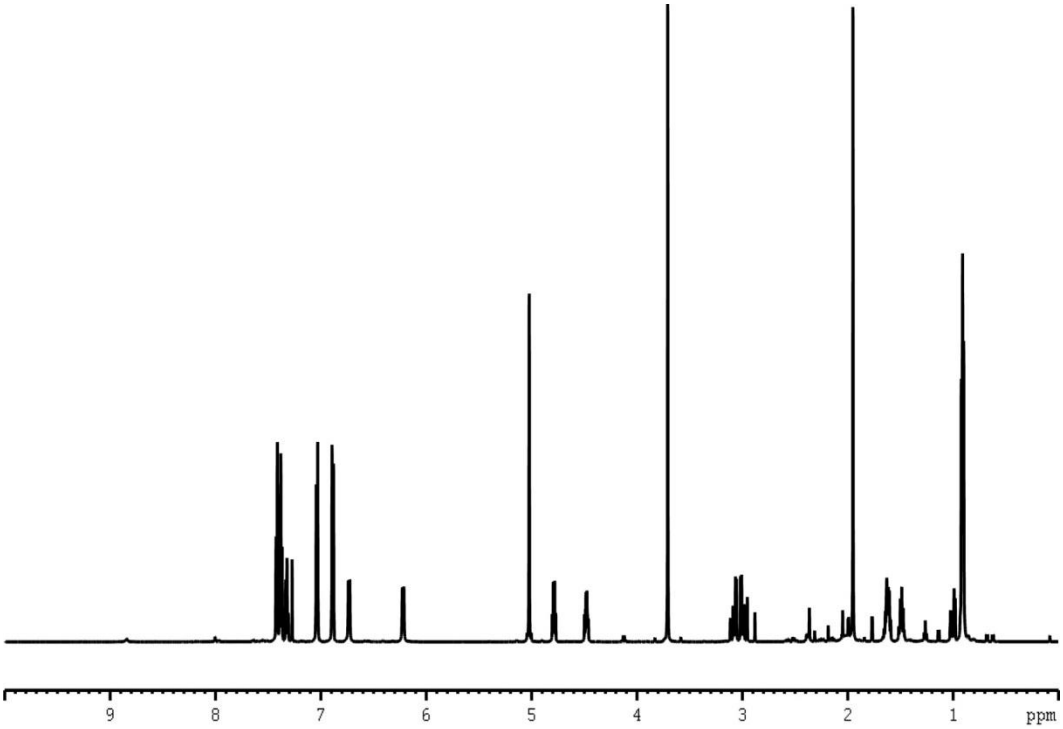

^{1}HNMR Spectrum (400 MHz) of N-acetyl-L-leucyl-O-benzyl-L-tyrosine methyl ester (III-7a) in $CDCl_3$

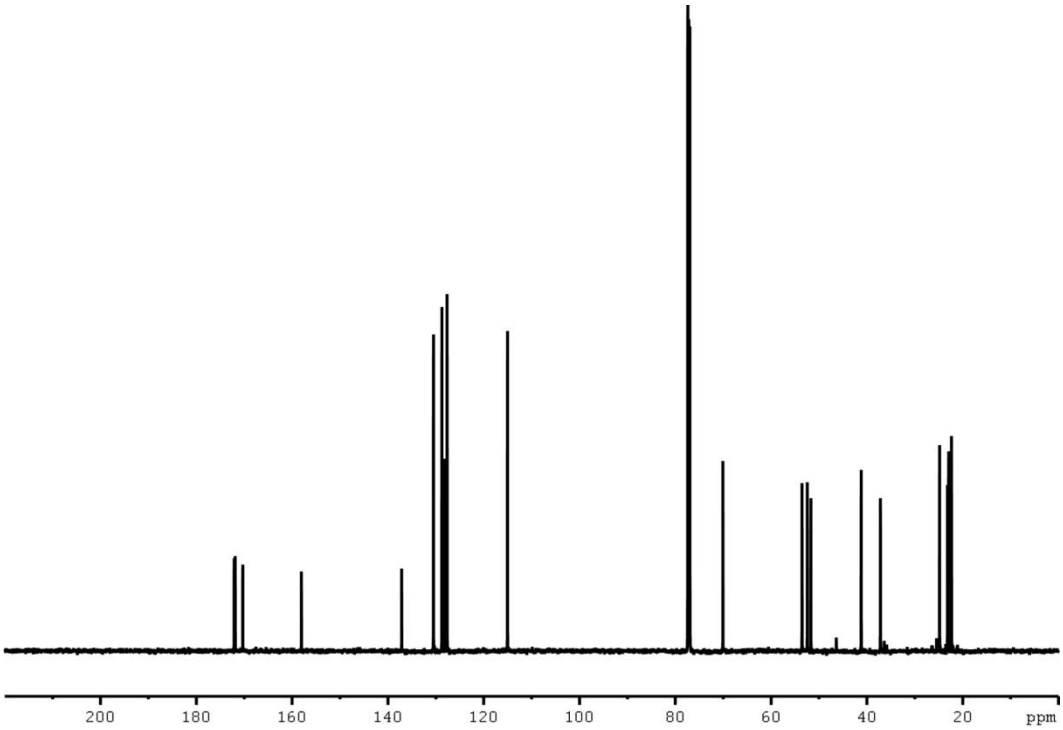

^{13}CNMR Spectrum (100 MHz) of N-acetyl-L-leucyl-O-benzyl-L-tyrosine methyl ester (III-7a) in $CDCl_3$

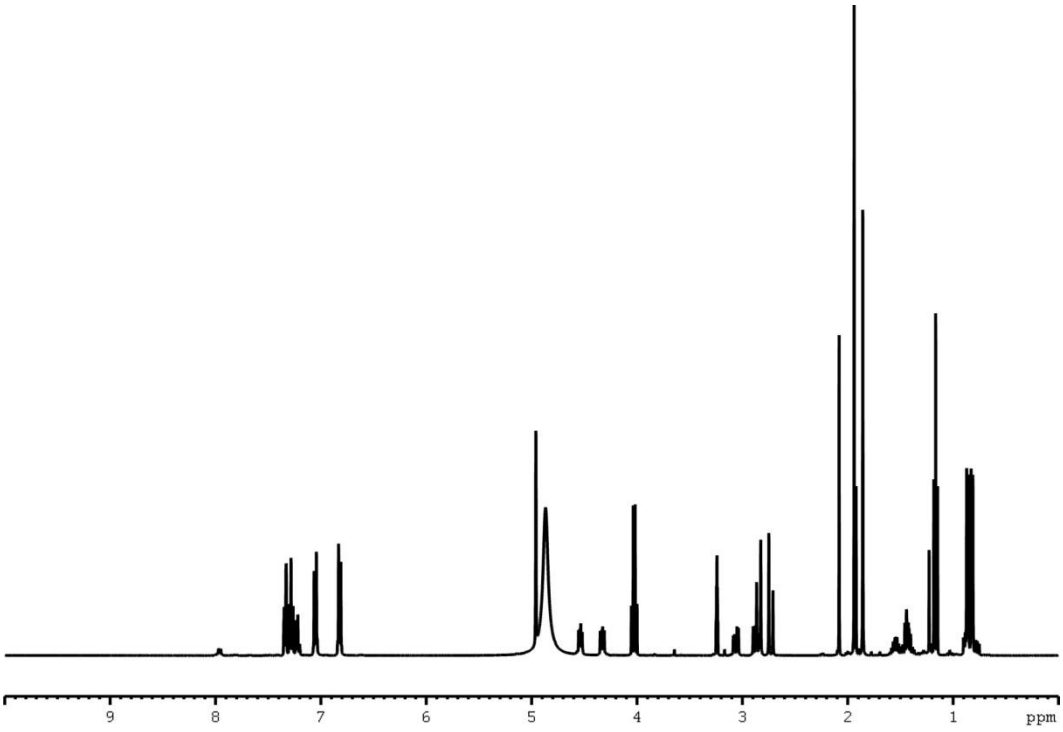

^{1}HNMR Spectrum (400 MHz) of N-acetyl-L-leucyl-O-benzyl-L-tyrosine (III-7b) in MeOD

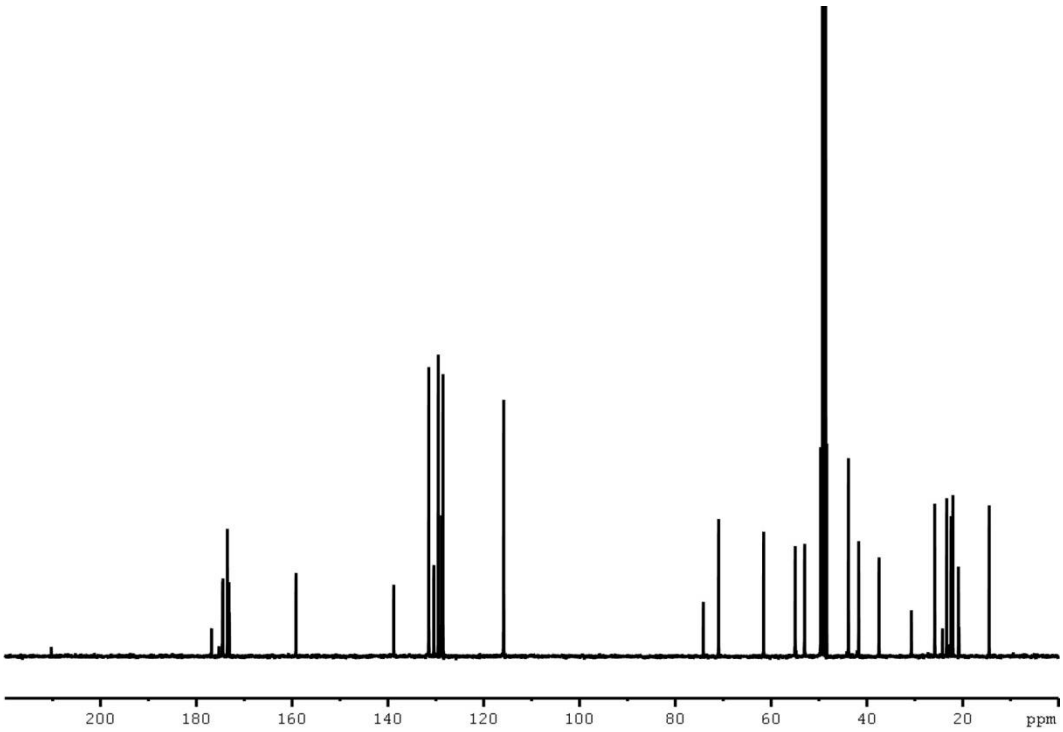

^{13}CNMR Spectrum (100 MHz) of N-acetyl-L-leucyl-O-benzyl-L-tyrosine (III-7b) in MeOD

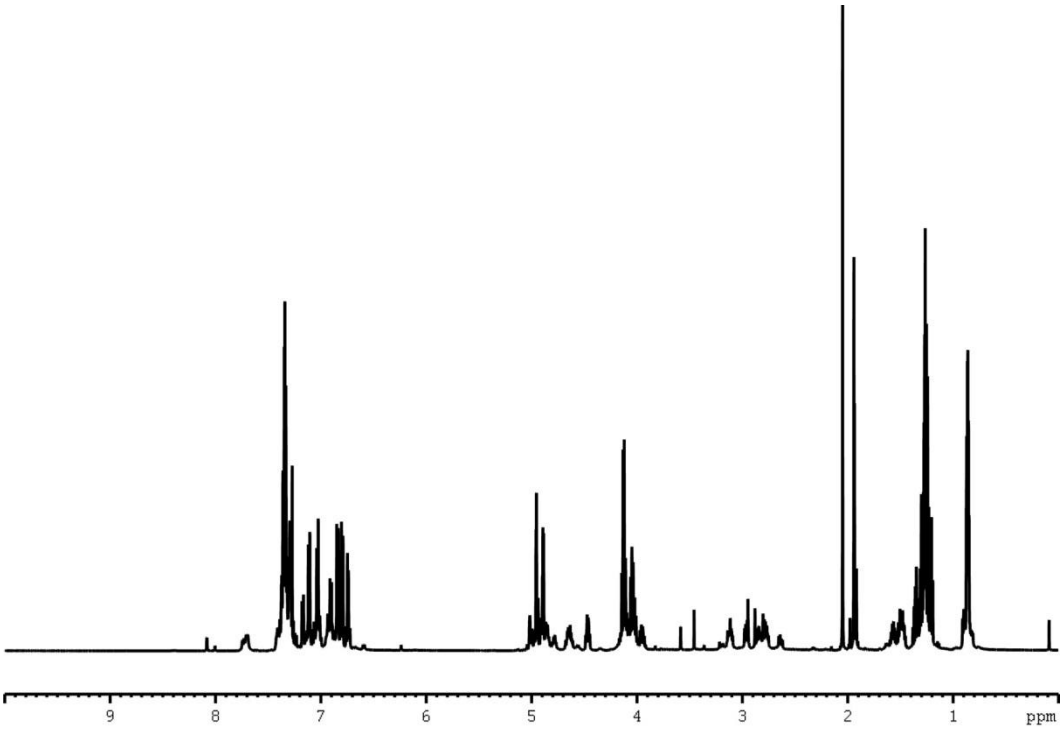

^{1}HNMR Spectrum (600 MHz) of diethyl N-(N-acetyl-L-leucyl-O-benzyl-L-tyrosyl)-1-amino-2-(4-benzyloxyphenyl)ethyl phosphonate (III-7c) in $CDCl_3$

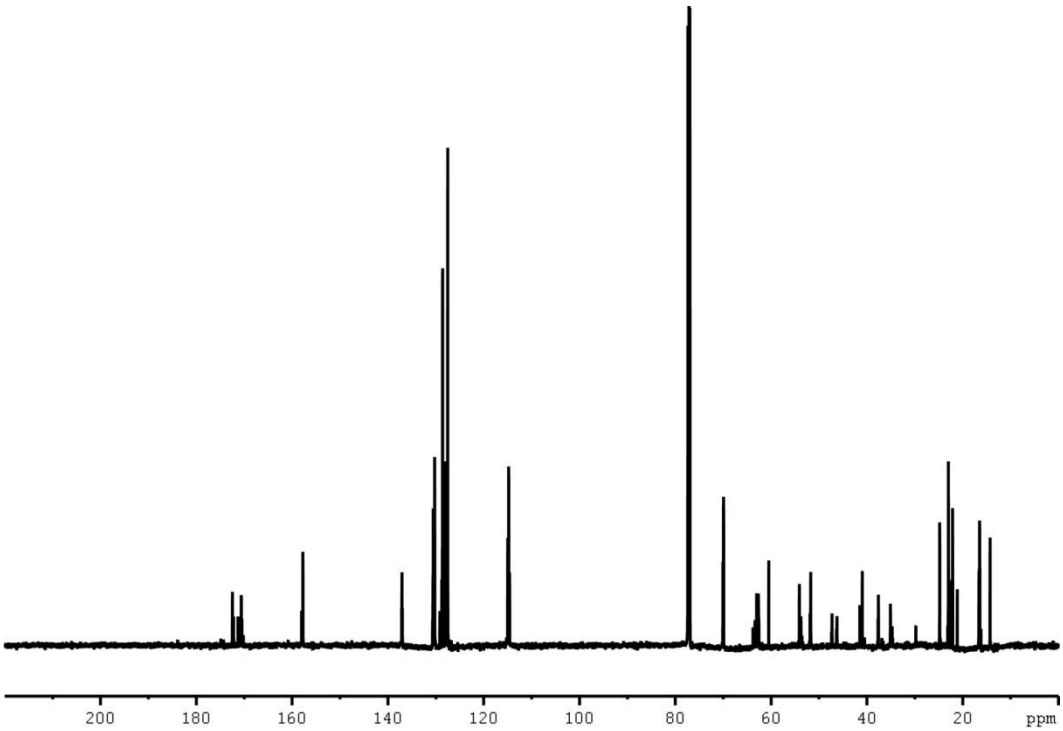

^{13}CNMR Spectrum (150 MHz) of diethyl N-(N-acetyl-L-leucyl-O-benzyl-L-tyrosyl)-1-amino-2-(4-benzyloxyphenyl)ethyl phosphonate (III-7c) in $CDCl_3$

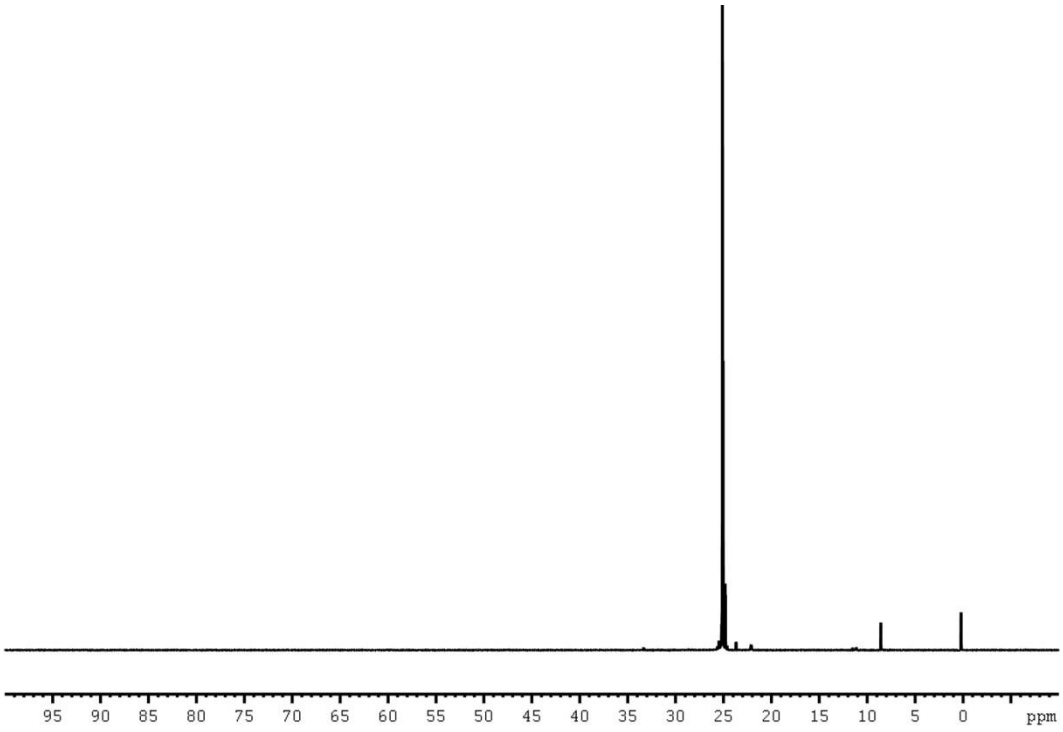

^{31}PNMR Spectrum (162 MHz) of diethyl N-(N-acetyl-L-leucyl-O-benzyl-L-tyrosyl)-1-amino-2-(4-benzyloxyphenyl)ethyl phosphonate (III-7c) in $CDCl_3$

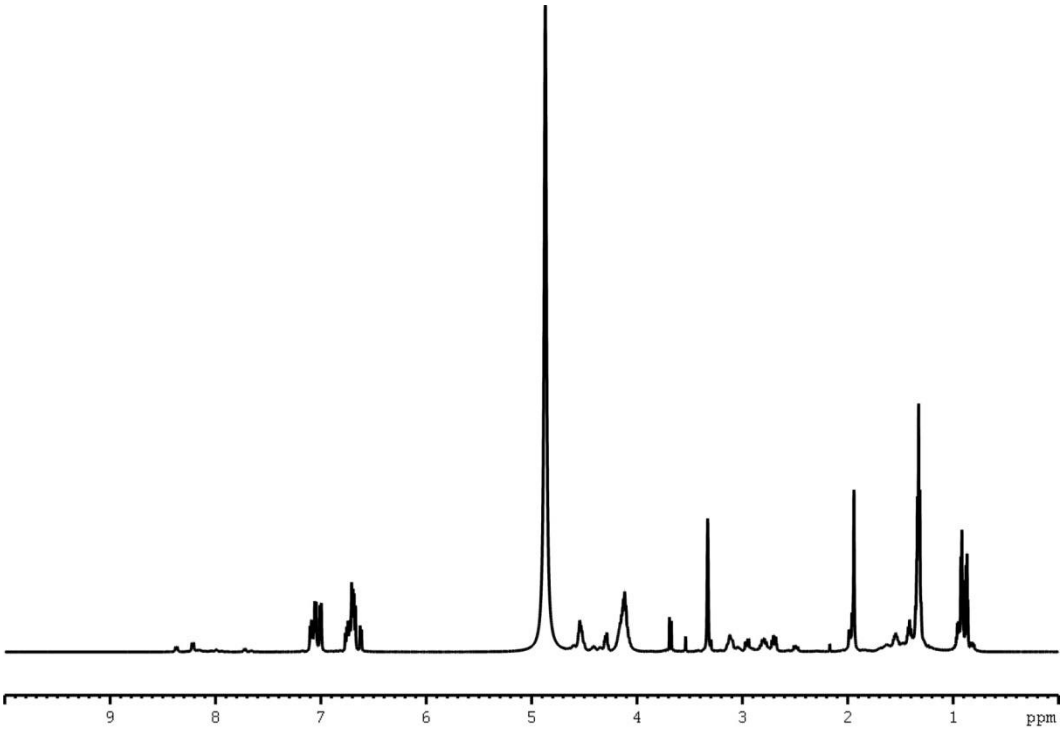

^{1}HNMR Spectrum (600 MHz) of diethyl N-(N-acetyl-L-leucyl-O-benzyl-L-tyrosyl)-1-amino-2-(4-hydoxyphenyl)ethyl phosphonate (III-7d) in MeOD

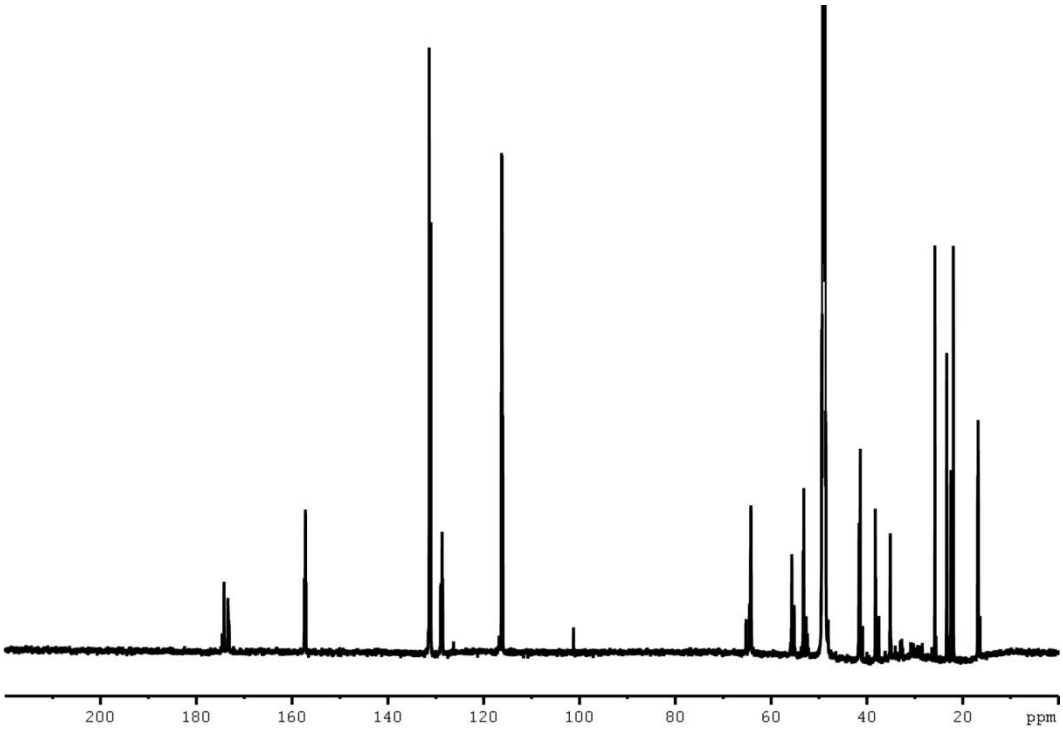

^{13}CNMR Spectrum (150 MHz) of diethyl N-(N-acetyl-L-leucyl-O-benzyl-L-tyrosyl)-1-amino-2-(4-hydoxyphenyl)ethyl phosphonate (III-7d) in MeOD

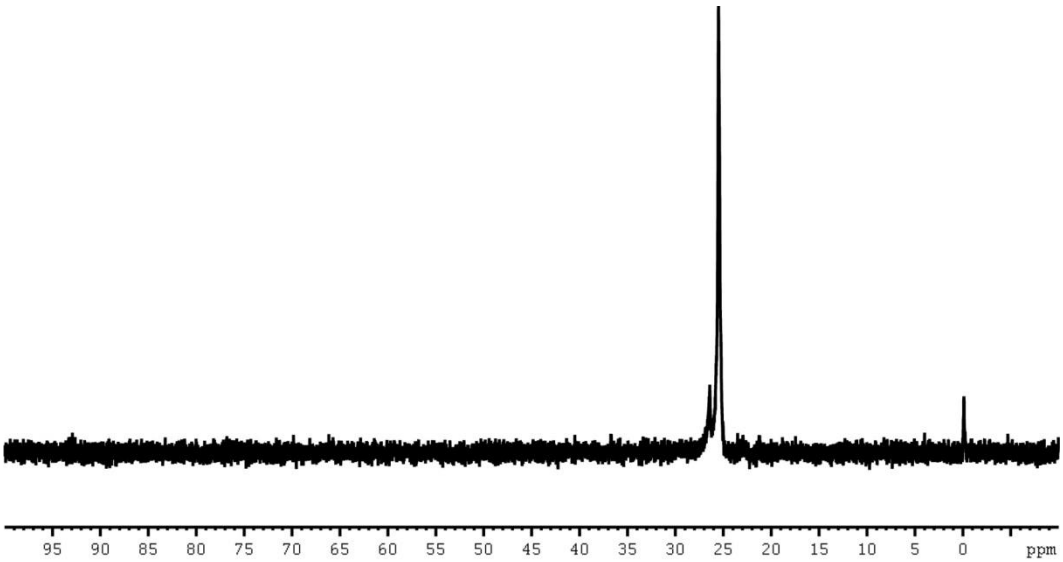

^{31}PNMR Spectrum (121 MHz) diethyl N-(N-acetyl-L-leucyl-O-benzyl-L-tyrosyl)-1-amino-2-(4-hydoxyphenyl)ethyl phosphonate (III-7d) in MeOD

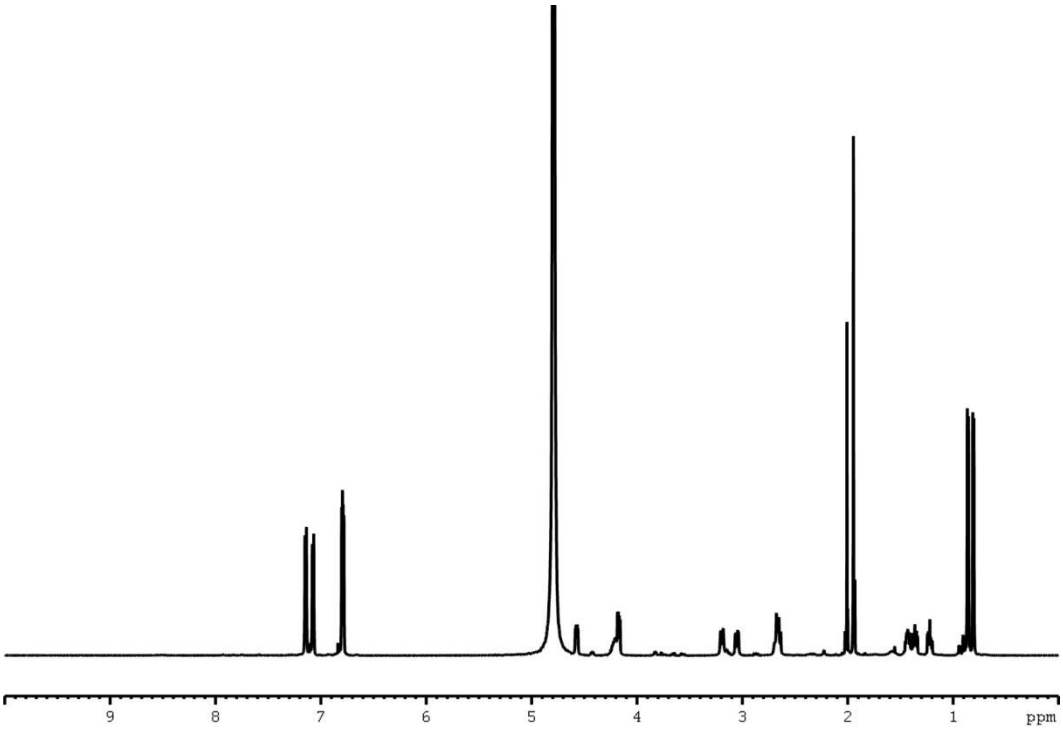

^{1}HNMR Spectrum (600 MHz) of Ac-Leu-Tyr-AHEP: N-(N-acetyl-L-leucyl-L-tyrosyl)-1-amino-2-(4-hydoxyphenyl)ethyl phosphonic acid (III-7) in D_2O

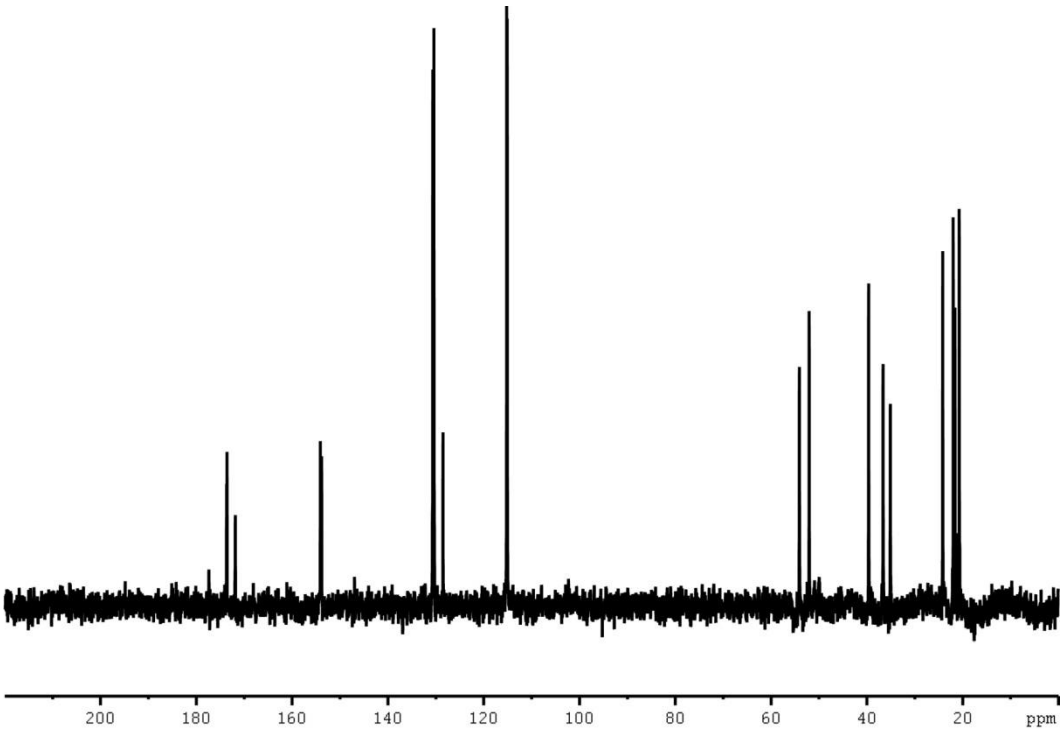

^{13}CNMR Spectrum (150 MHz) of Ac-Leu-Tyr-AHEP: N-(N-acetyl-L-leucyl-L-tyrosyl)-1-amino-2-(4-hydoxyphenyl)ethyl phosphonic acid (III-7) in D_2O

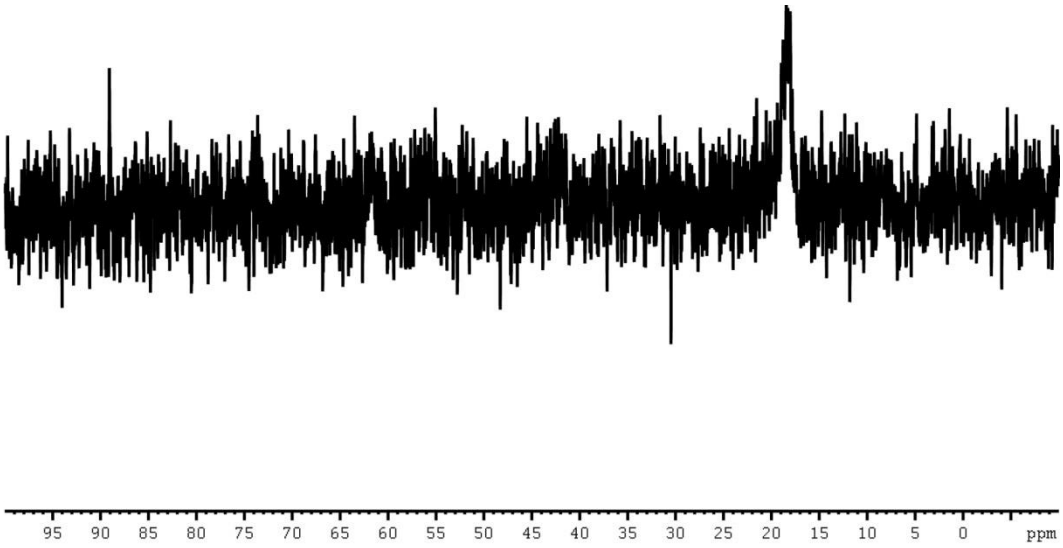

^{31}PNMR Spectrum (162 MHz) of Ac-Leu-Tyr-AHEP: N-(N-acetyl-L-leucyl-L-tyrosyl)-1-amino-2-(4-hydoxyphenyl)ethyl phosphonic acid (III-7) in D_2O

NMR spectra of Ac-Leu-Ile-AHEP (III-8) and synthetic intermediates (III-8a - III-8d)

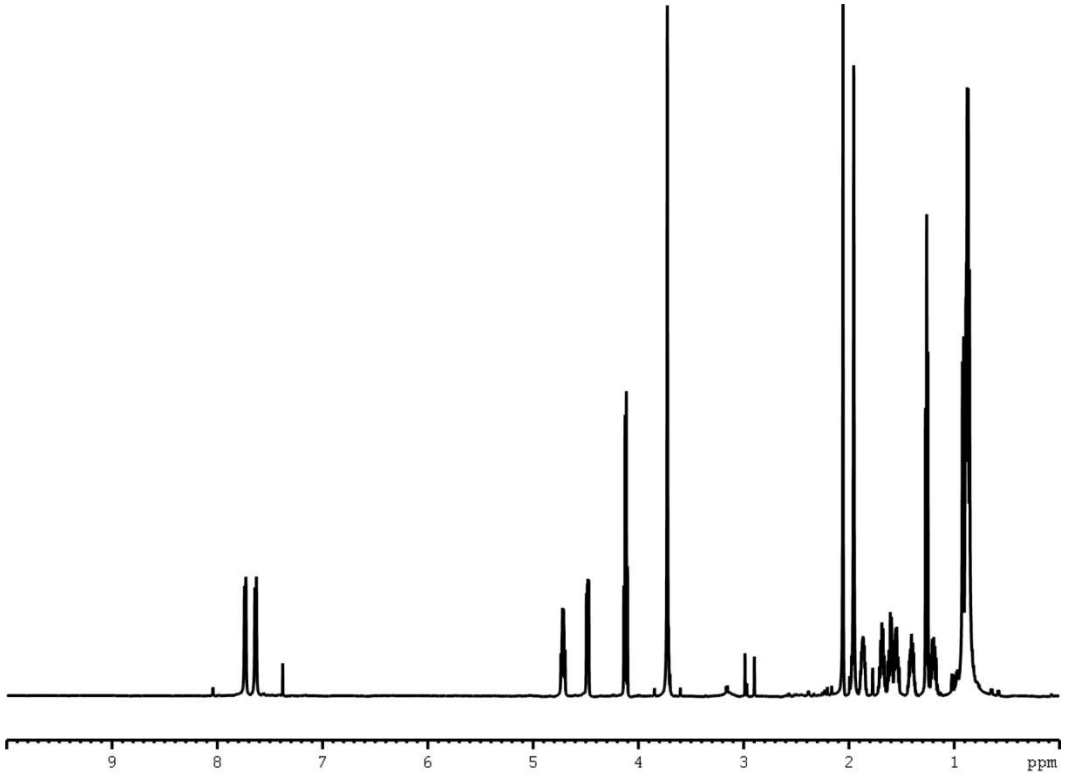

^{1}HNMR Spectrum (400 MHz) of N-acetyl-L-leucyl-L-isoleucine methyl ester (III-8a) in $CDCl_3$

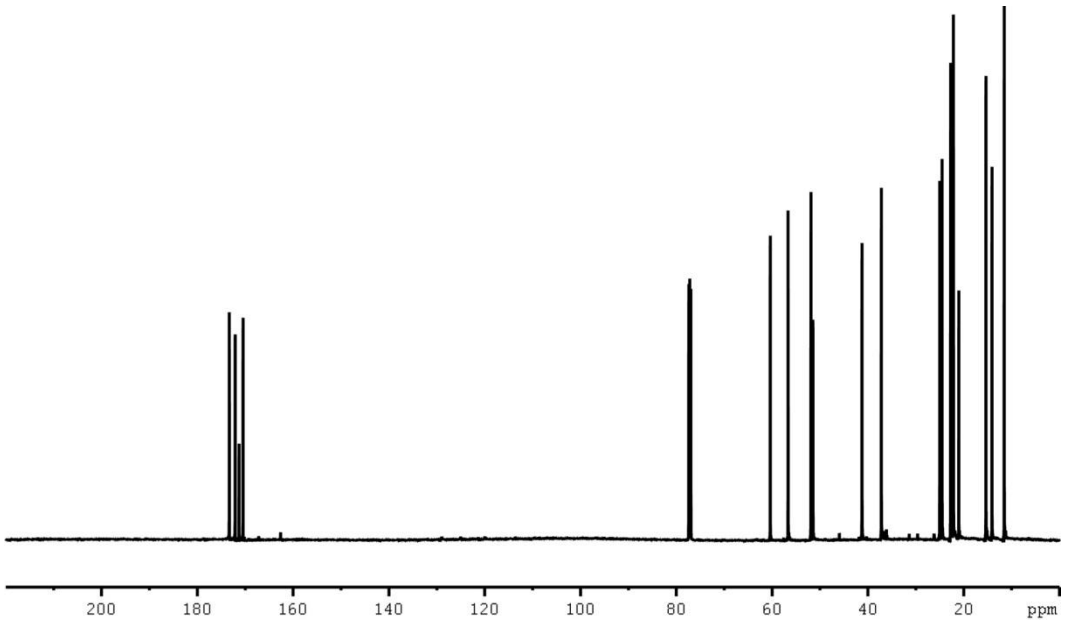

^{13}CNMR Spectrum (100 MHz) of N-acetyl-L-leucyl-L-isoleucine methyl ester (III-8a) in CDCl3

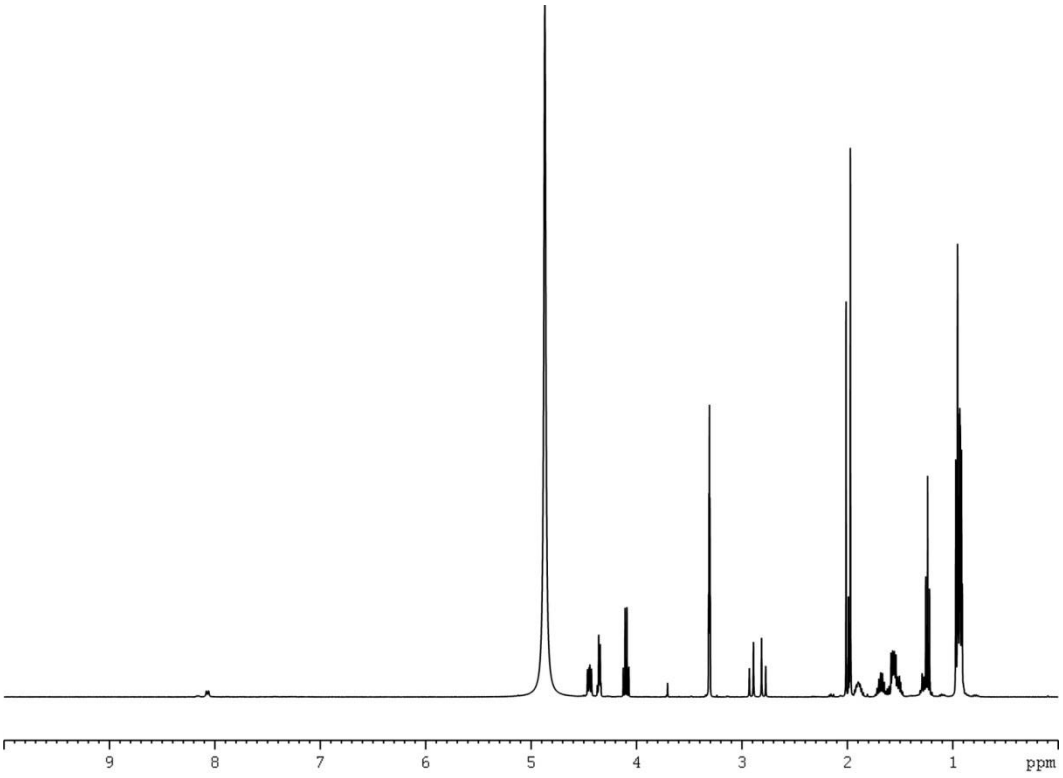

^{1}HNMR Spectrum (400 MHz) of N-acetyl-L-leucyl-L-isoleucine (III-8b) in MeOD

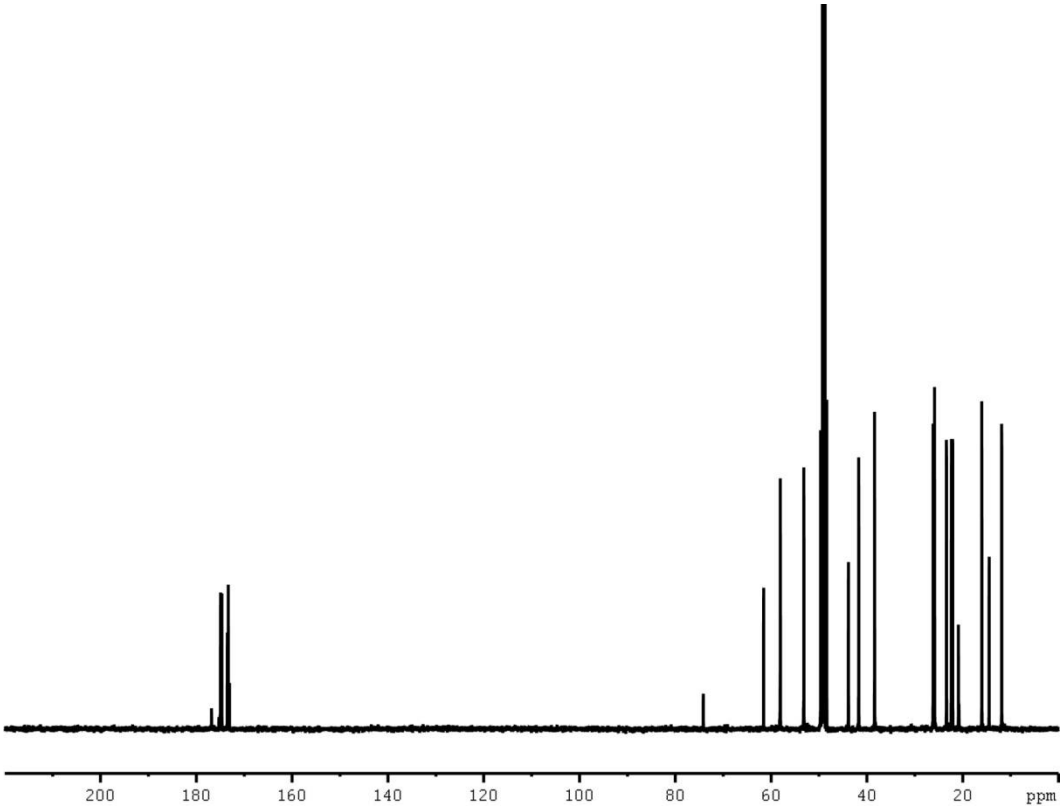

^{13}CNMR Spectrum (100 MHz) of N-acetyl-L-leucyl-L-isoleucine (III-8b) in MeOD

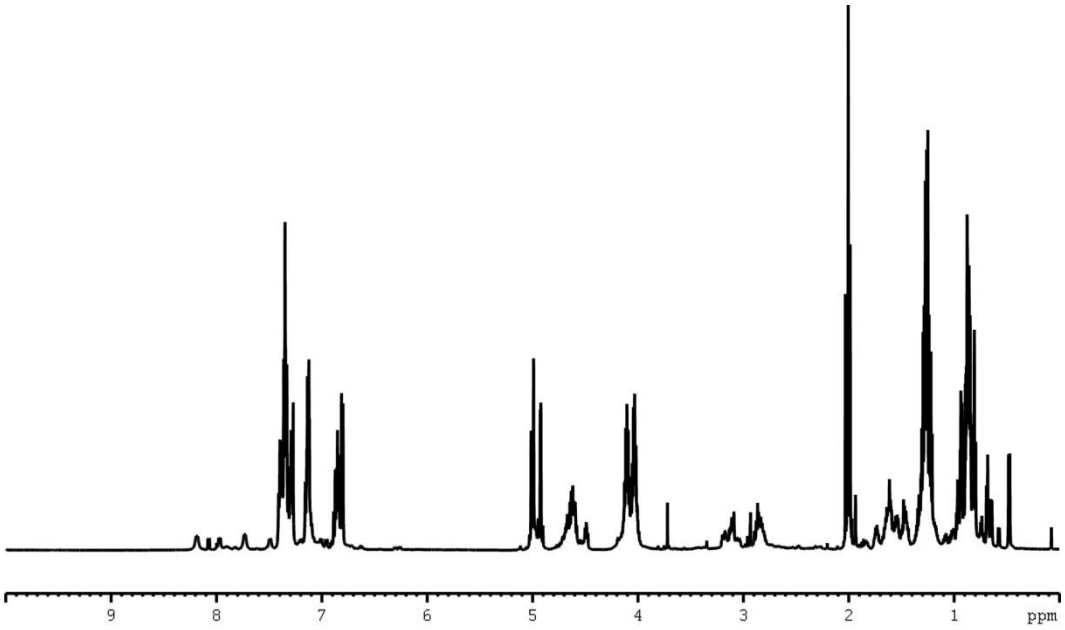

^{1}HNMR Spectrum (600 MHz) of diethyl N-(N-acetyl-L-leucyl-L-isoleucyl)-1-amino-2-(4-benzyloxyphenyl)ethyl phosphonate (III-8c) in $CDCl_3$

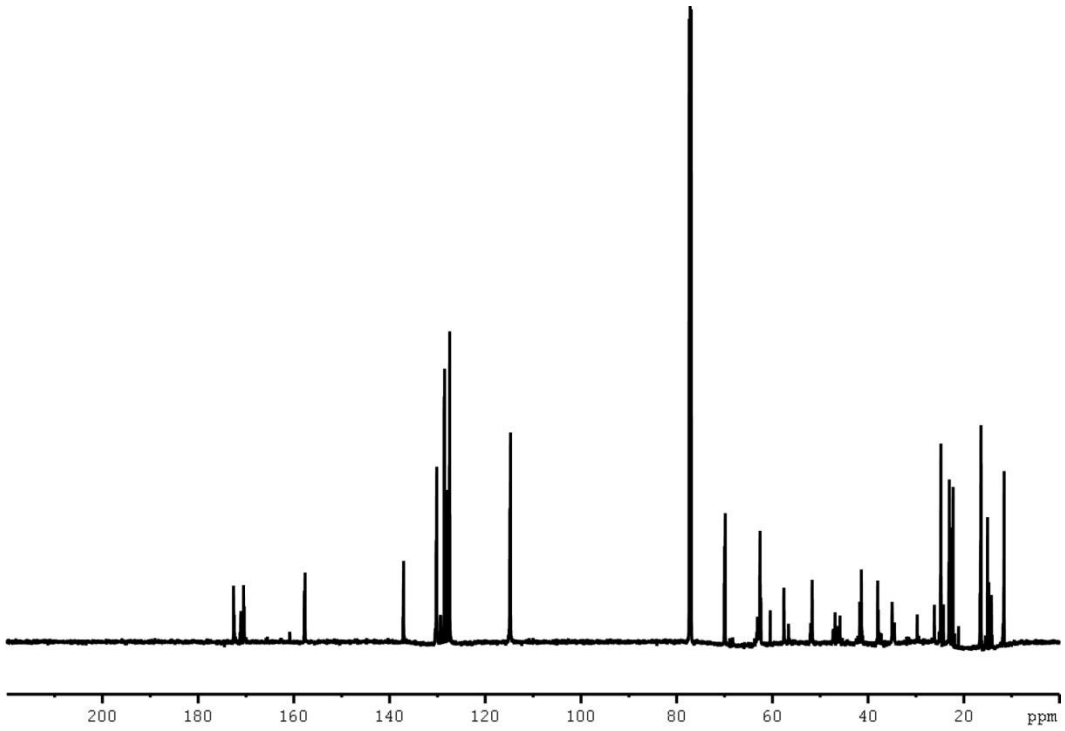

^{13}CNMR Spectrum (150 MHz) of diethyl N-(N-acetyl-L-leucyl-L-isoleucyl)-1-amino-2-(4-benzyloxyphenyl)ethyl phosphonate (III-8c) in $CDCl_3$

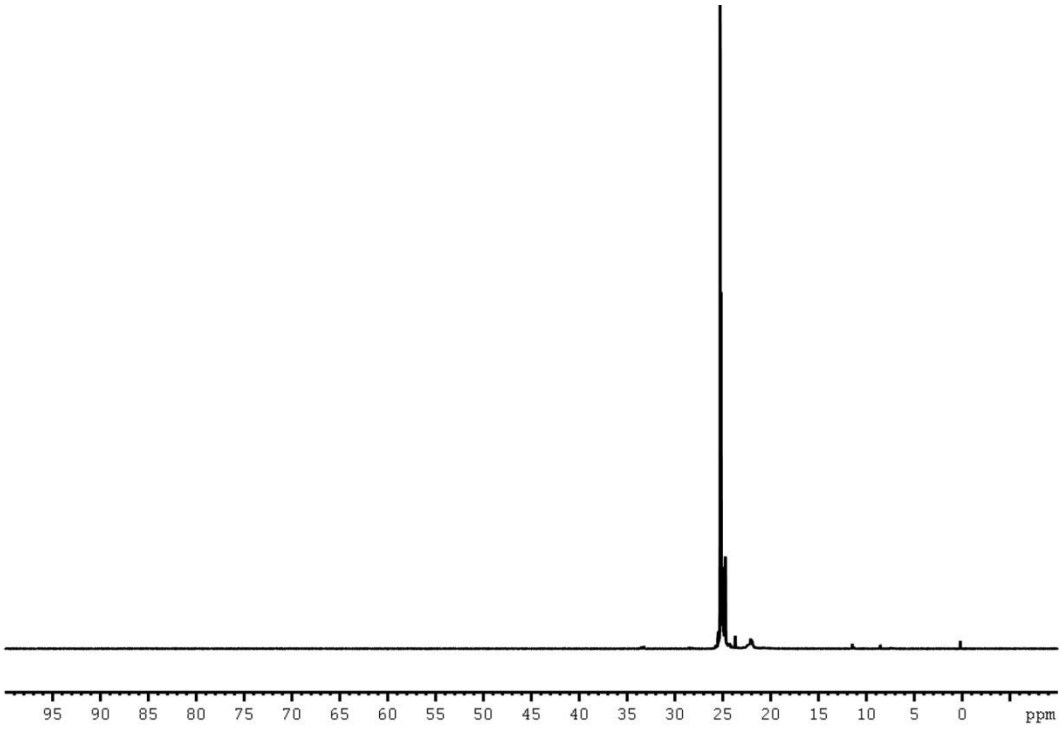

^{31}PNMR Spectrum (162 MHz) of diethyl N-(N-acetyl-L-leucyl-L-isoleucyl)-1-amino-2-(4-benzyloxyphenyl)ethyl phosphonate (III-8c) in $CDCl_3$

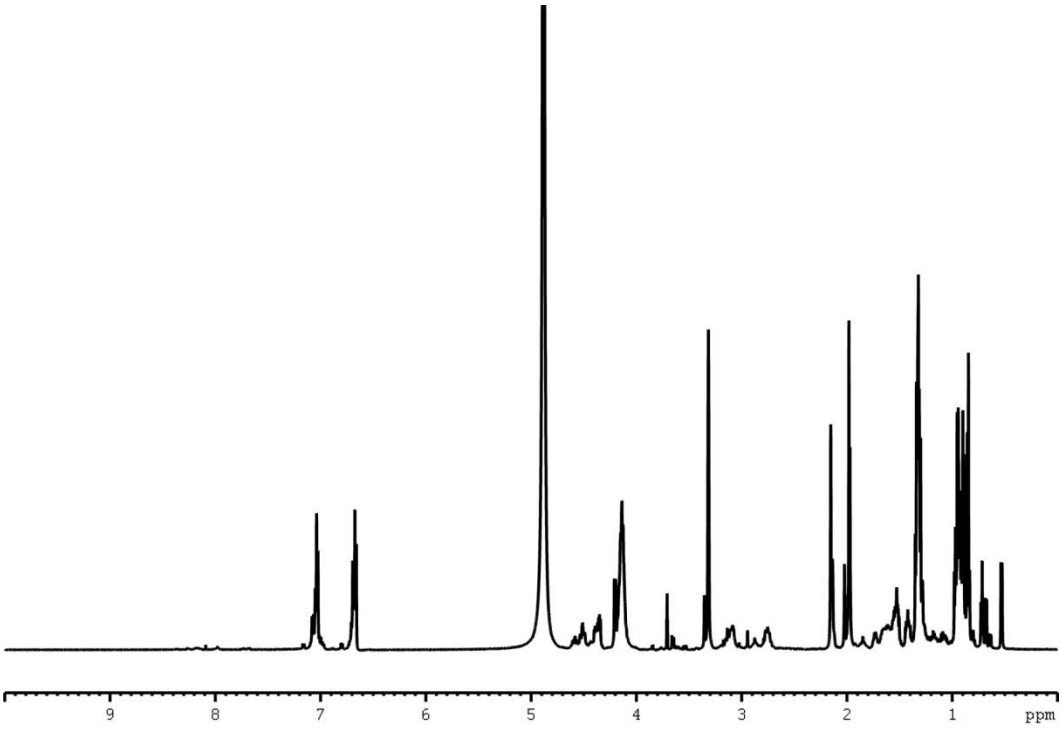

^{1}HNMR Spectrum (600 MHz) of diethyl N-(N-acetyl-L-leucyl-L-isoleucyl)-1-amino-2-(4-hydoxyphenyl)ethyl phosphonate (III-8d) in MeOD

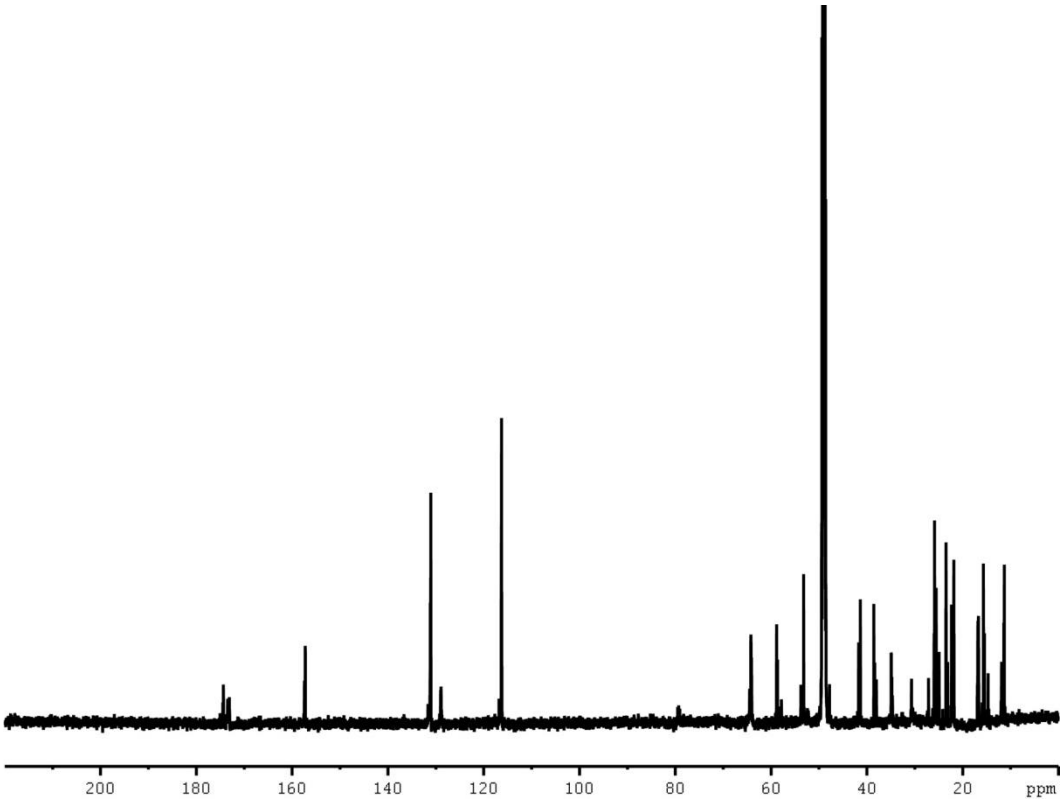

^{13}CNMR Spectrum (150 MHz) of diethyl N-(N-acetyl-L-leucyl-L-isoleucyl)-1-amino-2-(4-hydoxyphenyl)ethyl phosphonate (III-8d) in MeOD

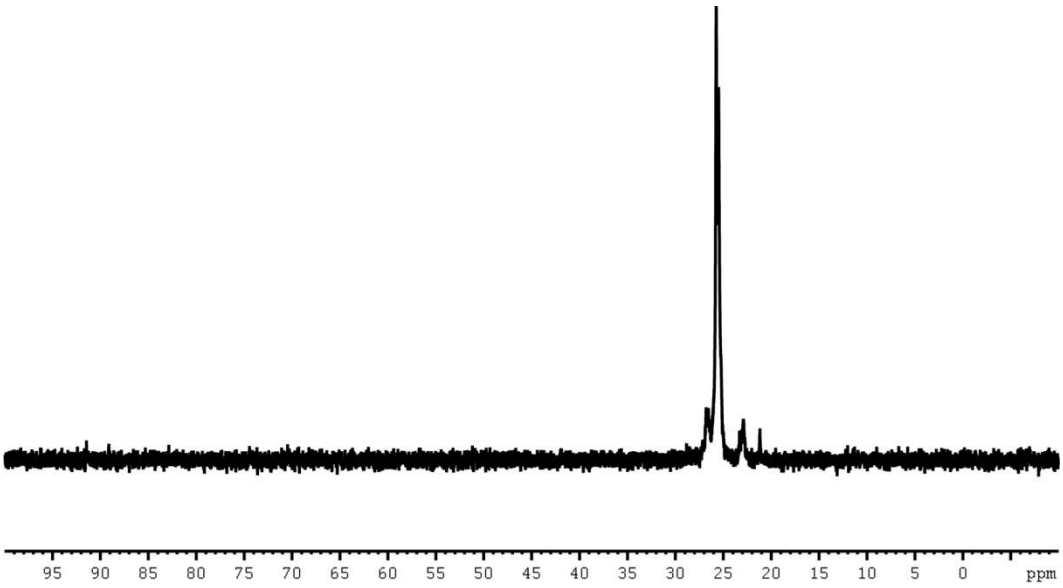

^{31}PNMR Spectrum (121 MHz) diethyl N-(N-acetyl-L-leucyl-L-isoleucyl)-1-amino-2-(4-hydoxyphenyl)ethyl phosphonate (III-8d) in MeOD

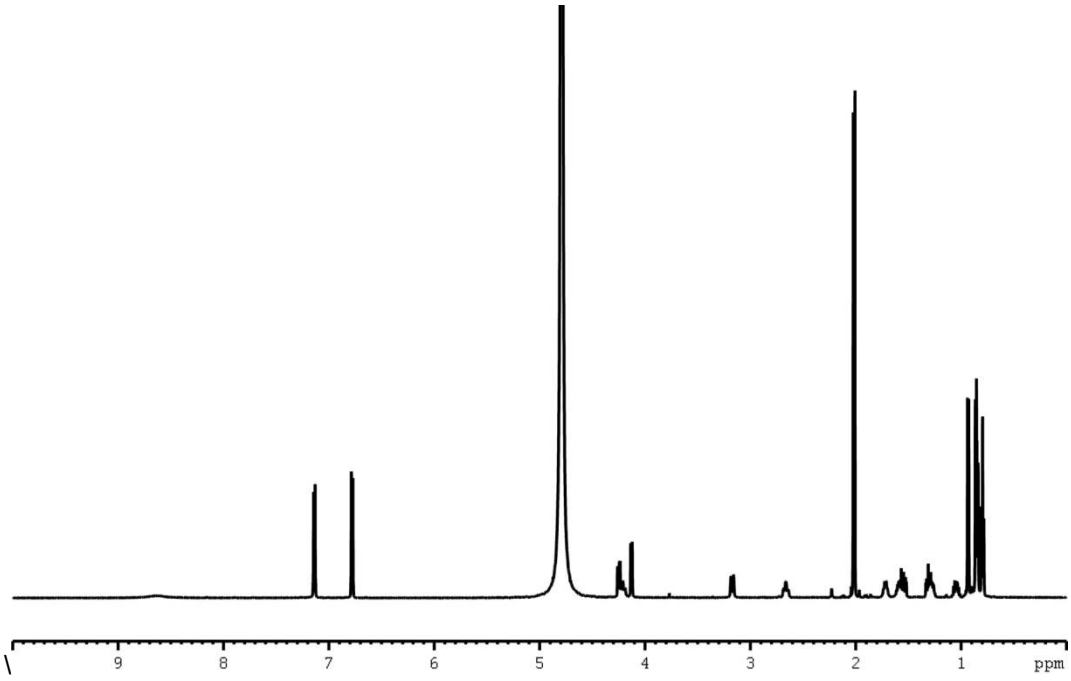

^{1}HNMR Spectrum (600 MHz) of Ac-Leu-Ile-AHEP: N-(N-acetyl-L-leucyl-L-isoleucine)-1-amino-2-(4-hydoxyphenyl)ethyl phosphonic acid (III-8) in D_2O

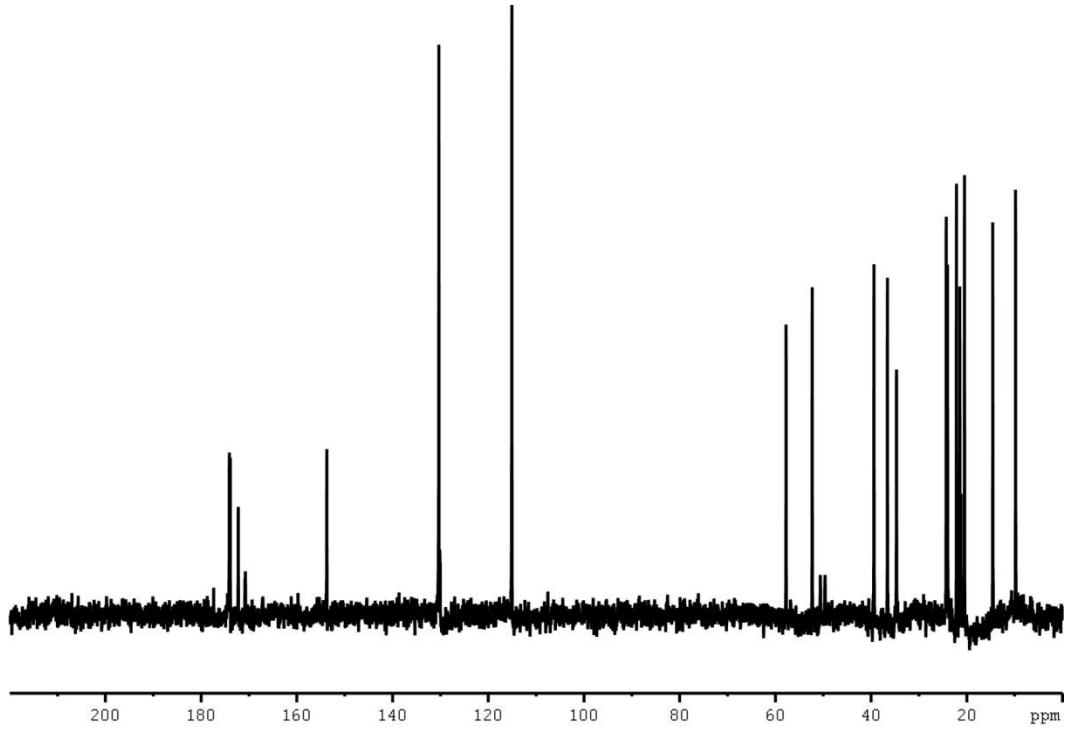

^{13}CNMR Spectrum (150 MHz) of Ac-Leu-Ile-AHEP: N-(N-acetyl-L-leucyl-L-isoleucine)-1-amino-2-(4-hydoxyphenyl)ethyl phosphonic acid (III-8) in D_2O

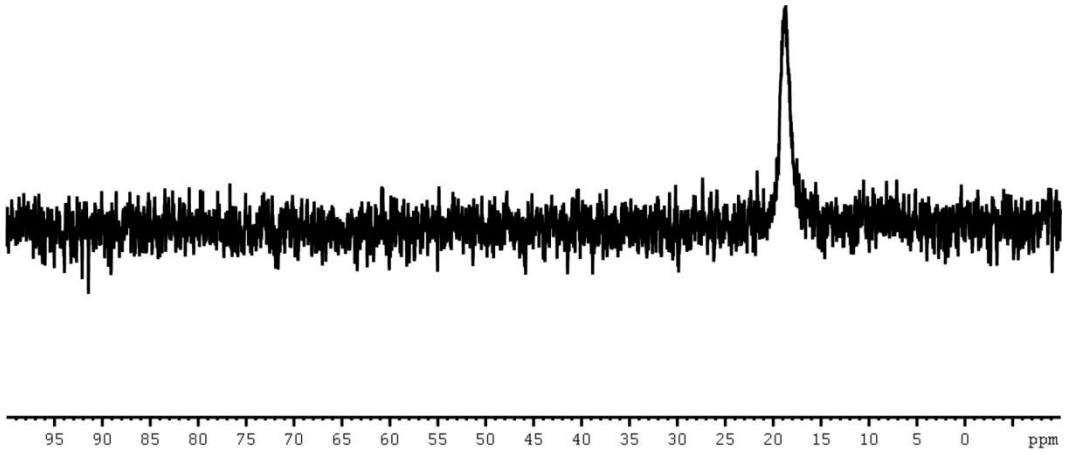

^{31}PNMR Spectrum (162 MHz) of Ac-Leu-Ile-AHEP: N-(N-acetyl-L-leucyl-L-isoleucine)-1-amino-2-(4-hydoxyphenyl)ethyl phosphonic acid (III-8) in D_2O

NMR spectra of Ac-Tyr-Ile-AHEP (III-9) and synthetic intermediates (III-9a - III-9e)

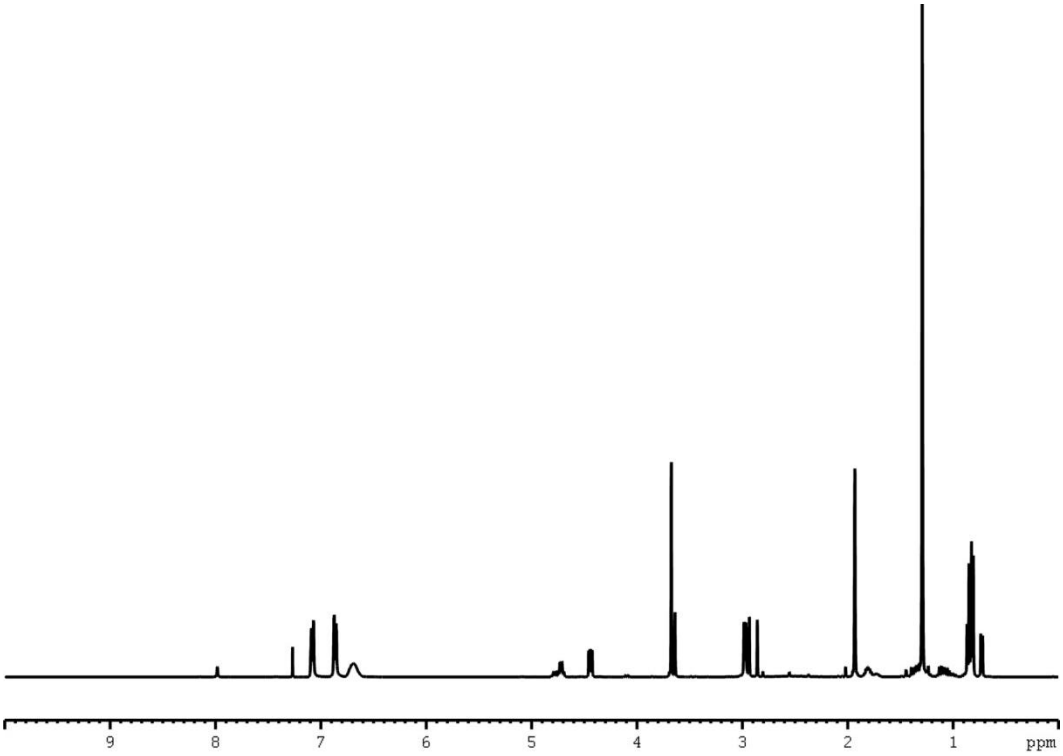

^{1}HNMR Spectrum (400 MHz) of N-acetyl-O-tert-butyl-L-tyrosyl-L-isoleucine methyl ester (III-9a) in $CDCl_3$

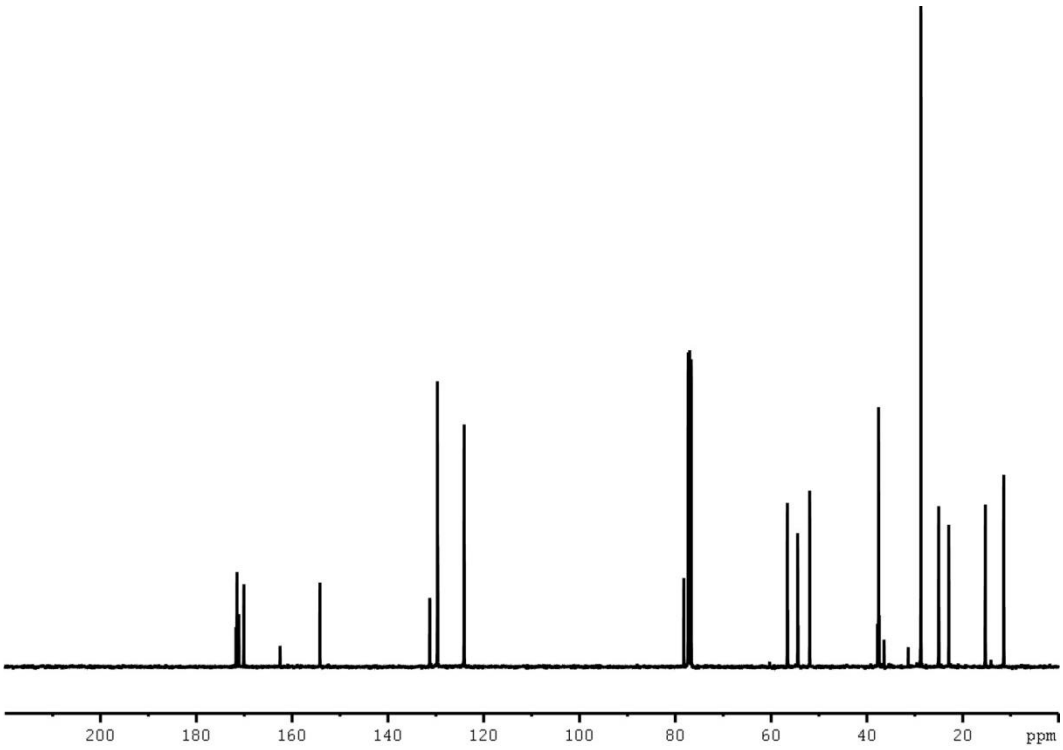

^{13}CNMR Spectrum (100 MHz) of N-acetyl-O-tert-butyl-L-tyrosyl-L-isoleucine methyl ester (III-9a) in $CDCl_3$

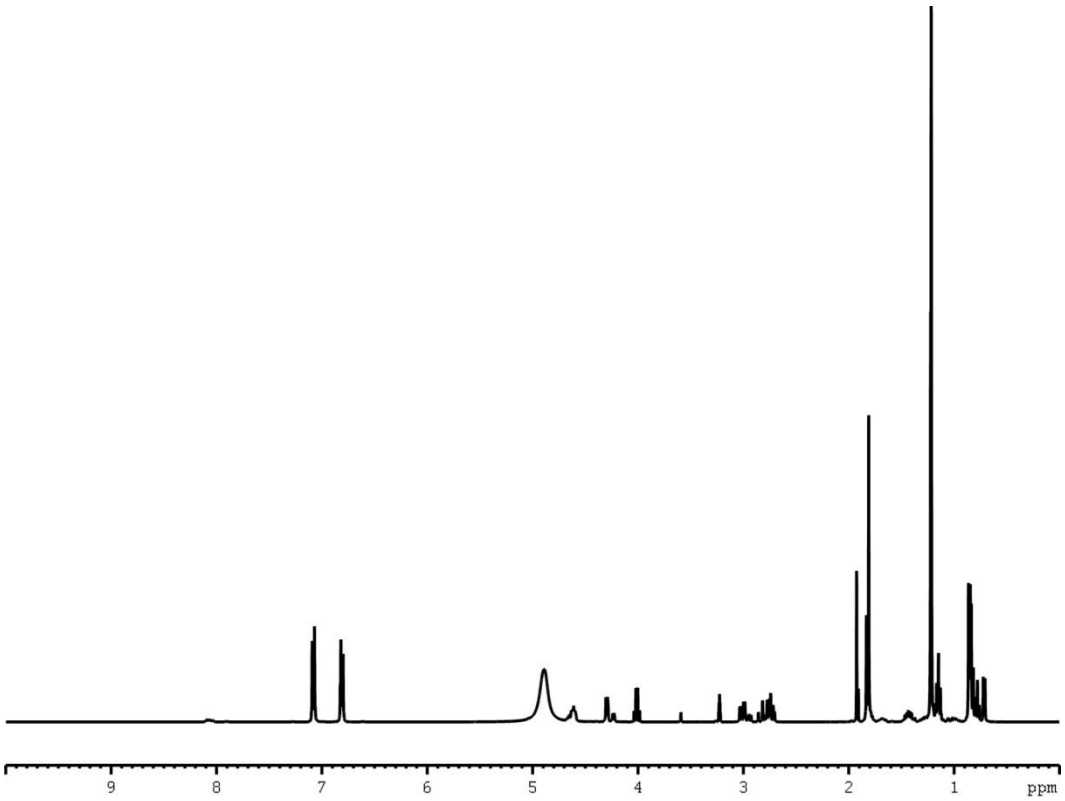

^{1}HNMR Spectrum (400 MHz) of N-acetyl-O-tert-butyl-L-tyrosyl-L-isoleucine (III-9b) in MeOD

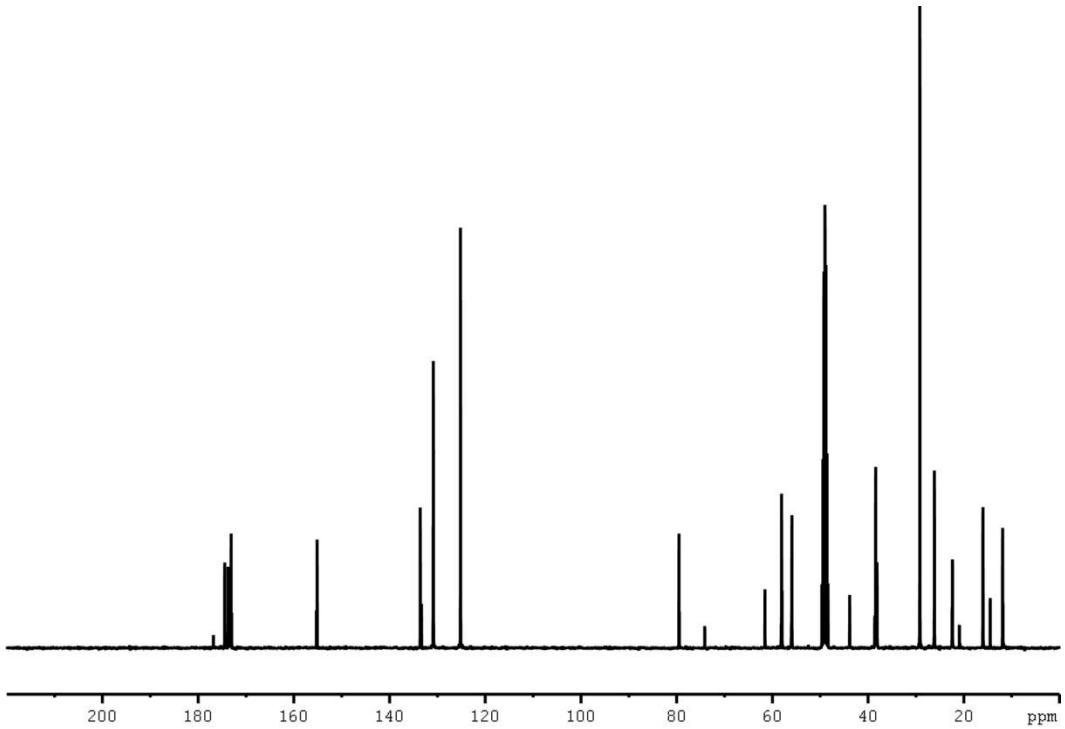

^{13}CNMR Spectrum (100 MHz) of N-acetyl-O-tert-butyl-L-tyrosyl-L-isoleucine (III-9b) in MeOD

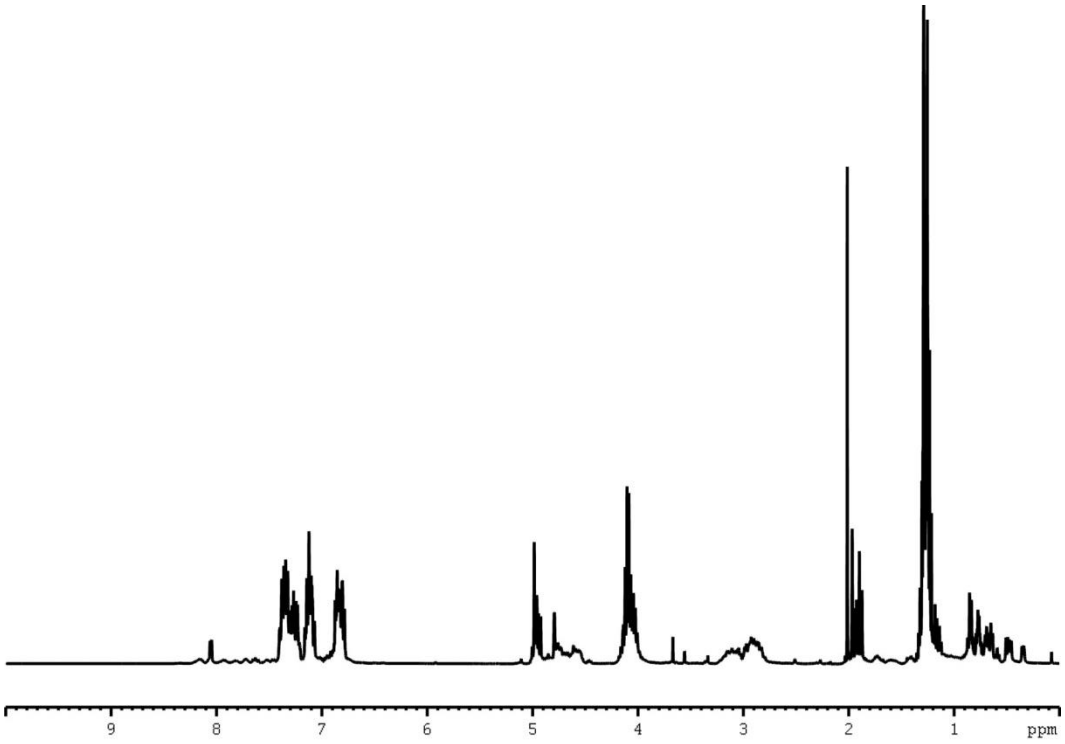

^{1}HNMR Spectrum (600 MHz) of diethyl N-(N-acetyl-O-tert-butyl-L-tyrosyl-L-isoleucyl)-1-amino-2-(4-benzyloxyphenyl)ethyl phosphonate (III-9c) in $CDCl_3$

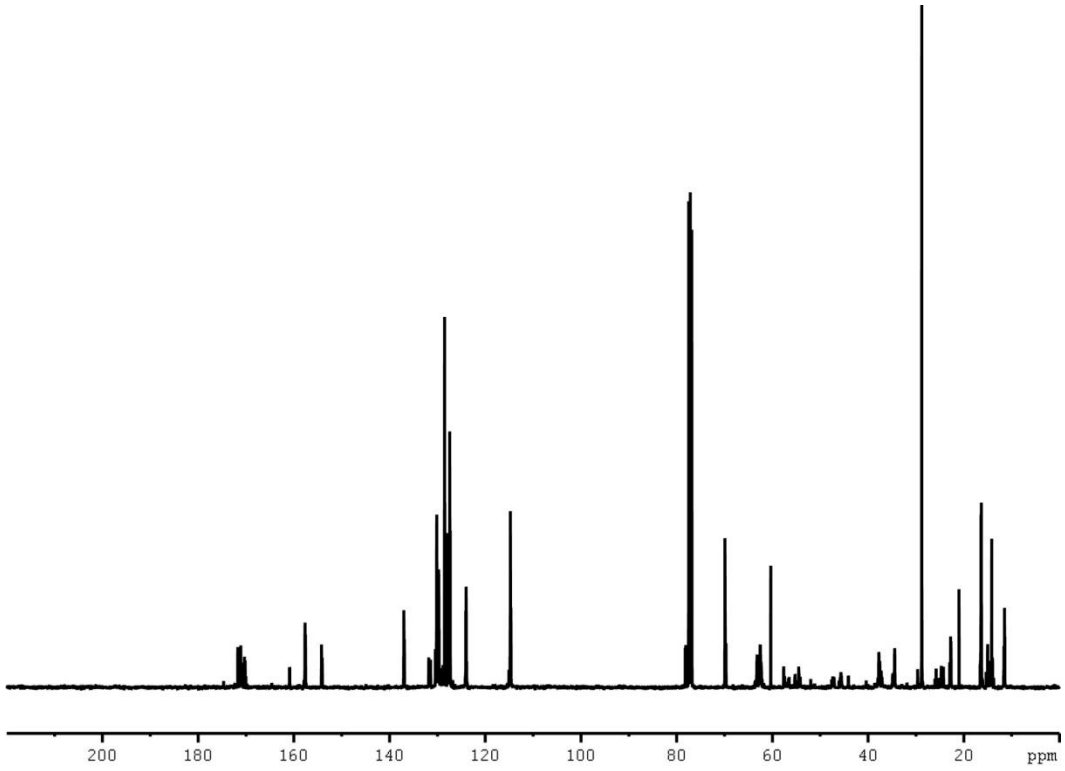

^{13}CNMR Spectrum (150 MHz) of diethyl N-(N-acetyl-O-tert-butyl-L-tyrosyl-L-isoleucyl)-1-amino-2-(4-benzyloxyphenyl)ethyl phosphonate (III-9c) in $CDCl_3$

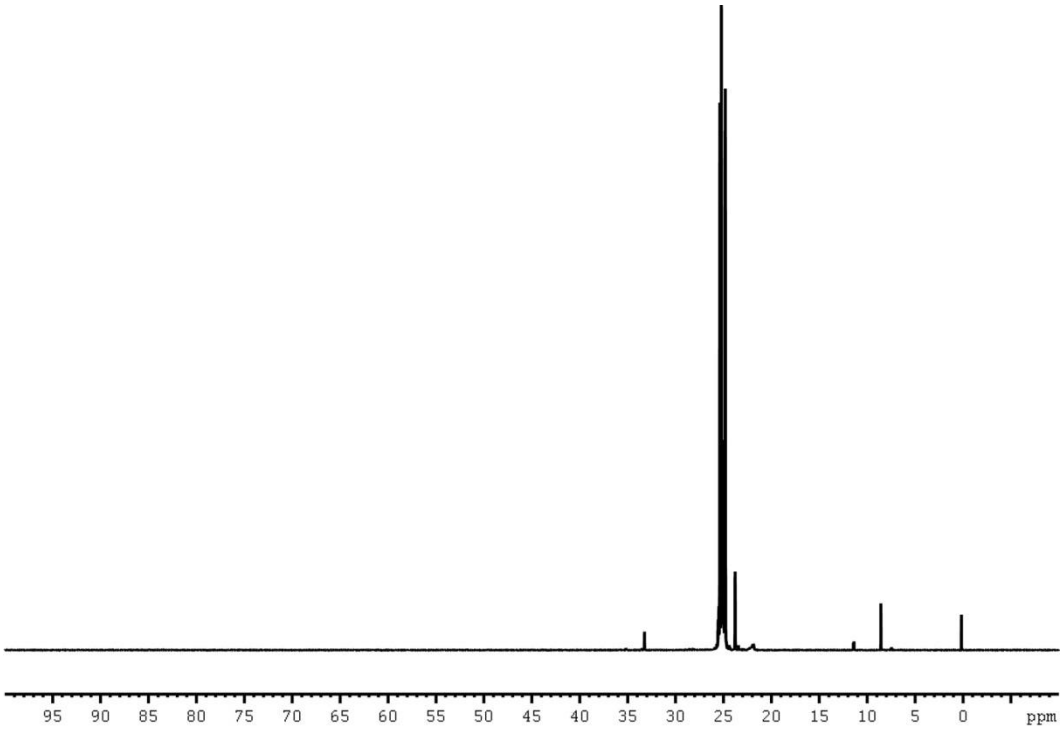

^{31}PNMR Spectrum (162 MHz) of diethyl N-(N-acetyl-O-tert-butyl-L-tyrosyl-L-isoleucyl)-1-amino-2-(4-benzyloxyphenyl)ethyl phosphonate (III-9c) in $CDCl_3$

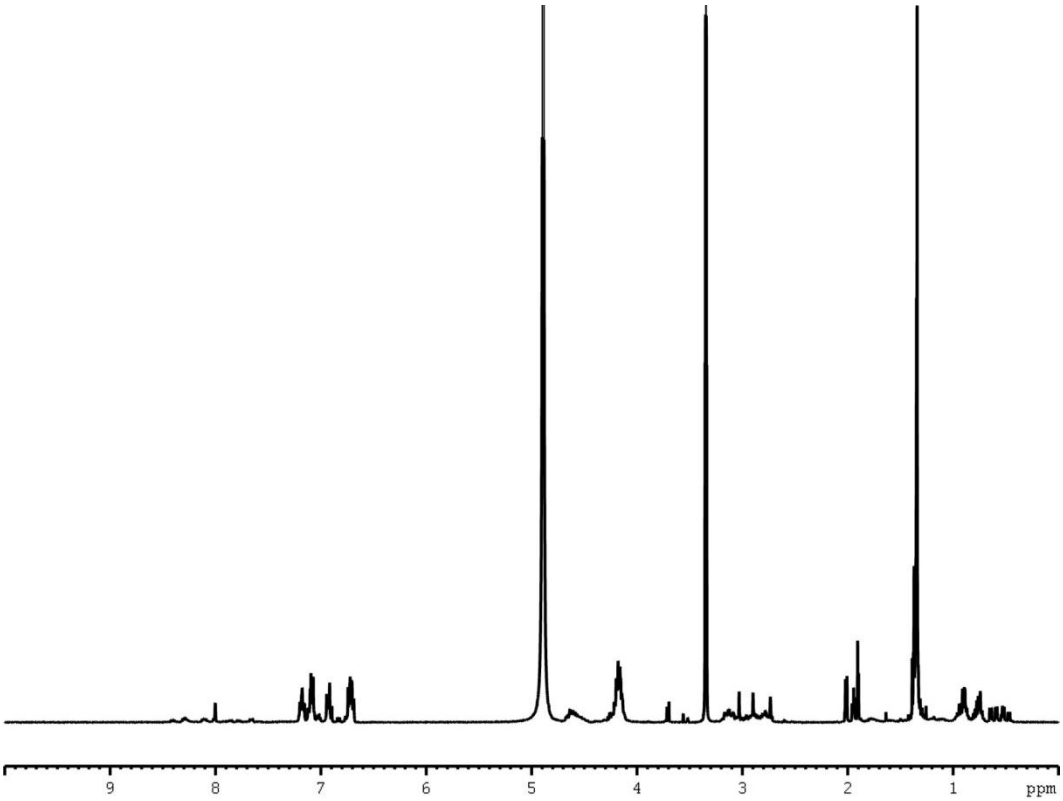

^{1}HNMR Spectrum (600 MHz) of diethyl N-(N-acetyl-O-tert-butyl-L-tyrosyl-L-isoleucyl)-1-amino-2-(4-hydoxyphenyl)ethyl phosphonate (III-9d) in MeOD

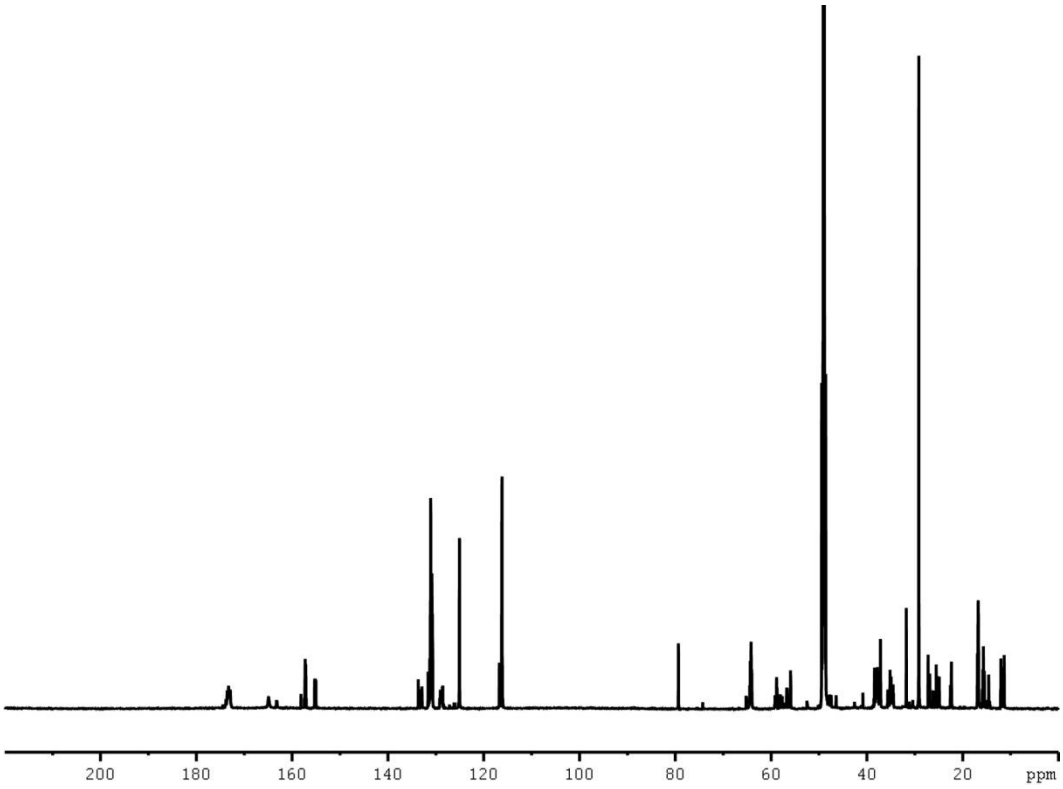

^{13}CNMR Spectrum (150 MHz) of diethyl N-(N-acetyl-O-tert-butyl-L-tyrosyl-L-isoleucyl)-1-amino-2-(4-hydoxyphenyl)ethyl phosphonate (III-9d) in MeOD

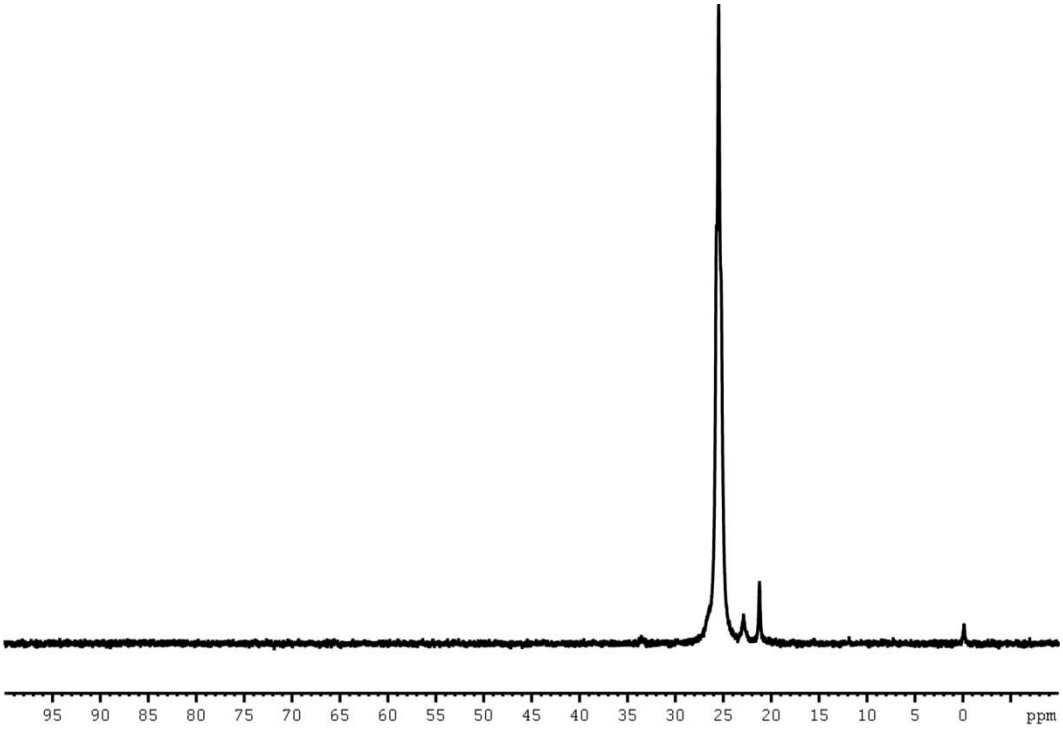

^{31}PNMR Spectrum (162 MHz) of diethyl N-(N-acetyl-O-tert-butyl-L-tyrosyl-L-isoleucyl)-1-amino-2-(4-hydoxyphenyl)ethyl phosphonate (III-9d) in MeOD

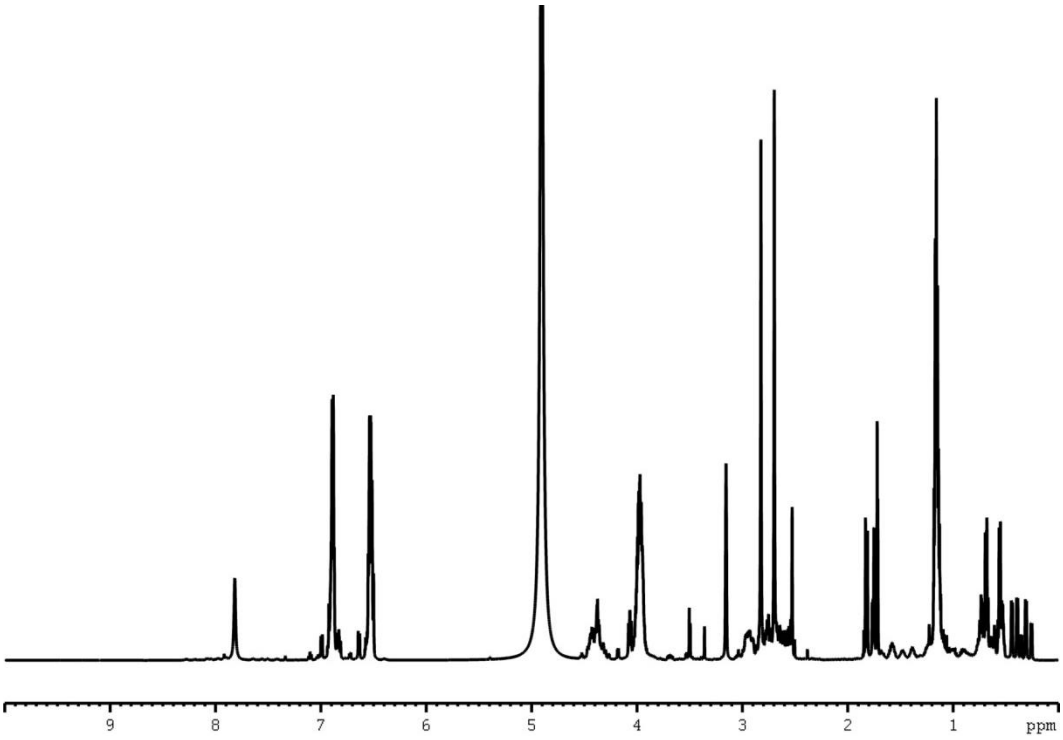

^{1}HNMR Spectrum (600 MHz) of diethyl N-(N-acetyl-L-tyrosyl-L-isoleucyl)-1-amino-2-(4-hydoxyphenyl)ethyl phosphonate (III-9e) in MeOD

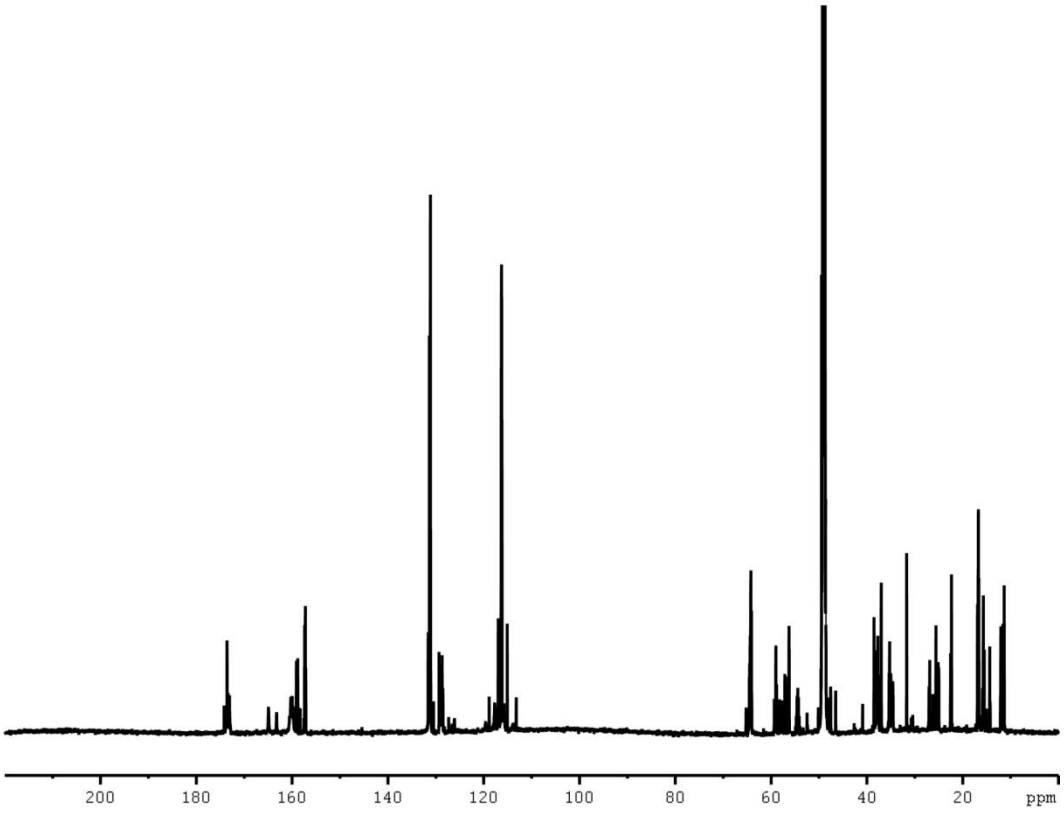

^{13}CNMR Spectrum (150 MHz) of diethyl N-(N-acetyl-L-tyrosyl-L-isoleucyl)-1-amino-2-(4-hydoxyphenyl)ethyl phosphonate (III-9e) in MeOD

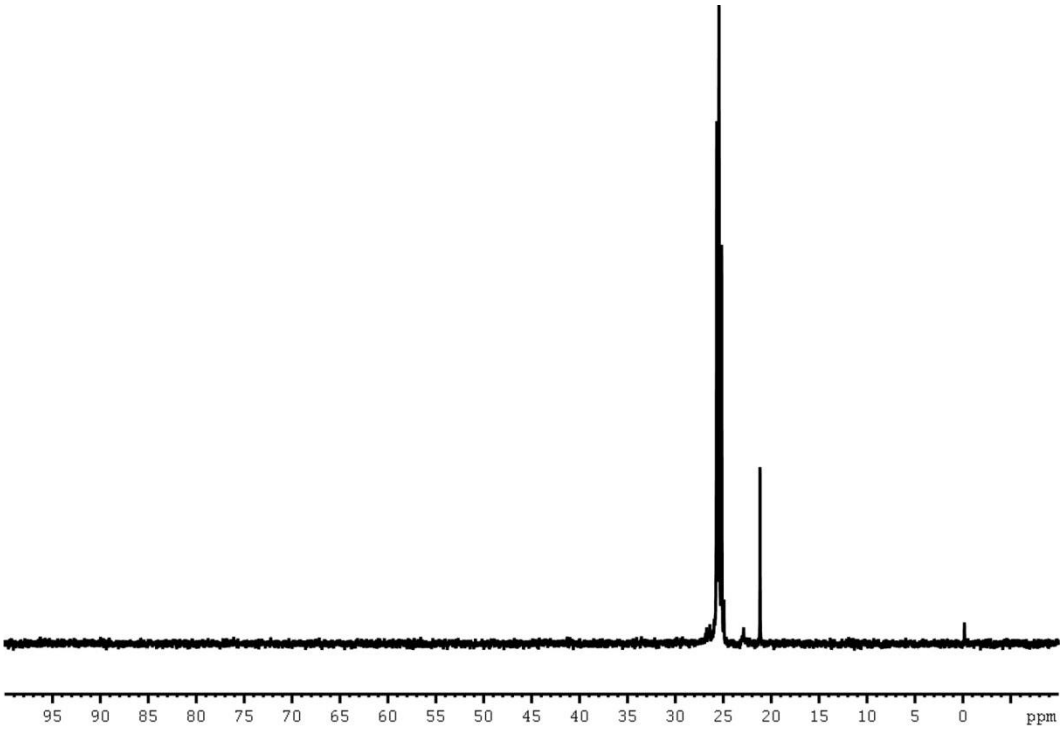

^{31}PNMR Spectrum (162 MHz) of diethyl N-(N-acetyl-L-tyrosyl-L-isoleucyl)-1-amino-2-(4-hydoxyphenyl)ethyl phosphonate (III-9e) in MeOD

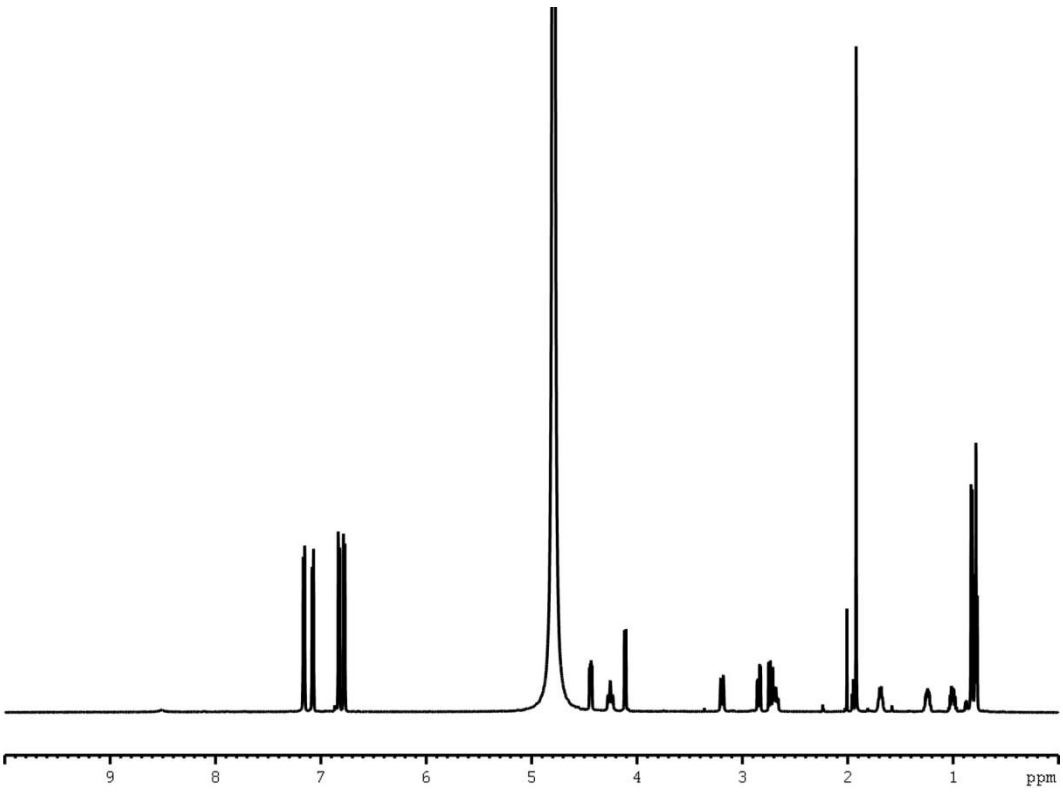

^{1}HNMR Spectrum (600 MHz) of Ac-Tyr-Ile-AHEP: N-(N-acetyl-L-tyrosyl-L-isoleucyl)-1-amino-2-(4-hydoxyphenyl)ethyl phosphonic acid (III-9) in D_2O

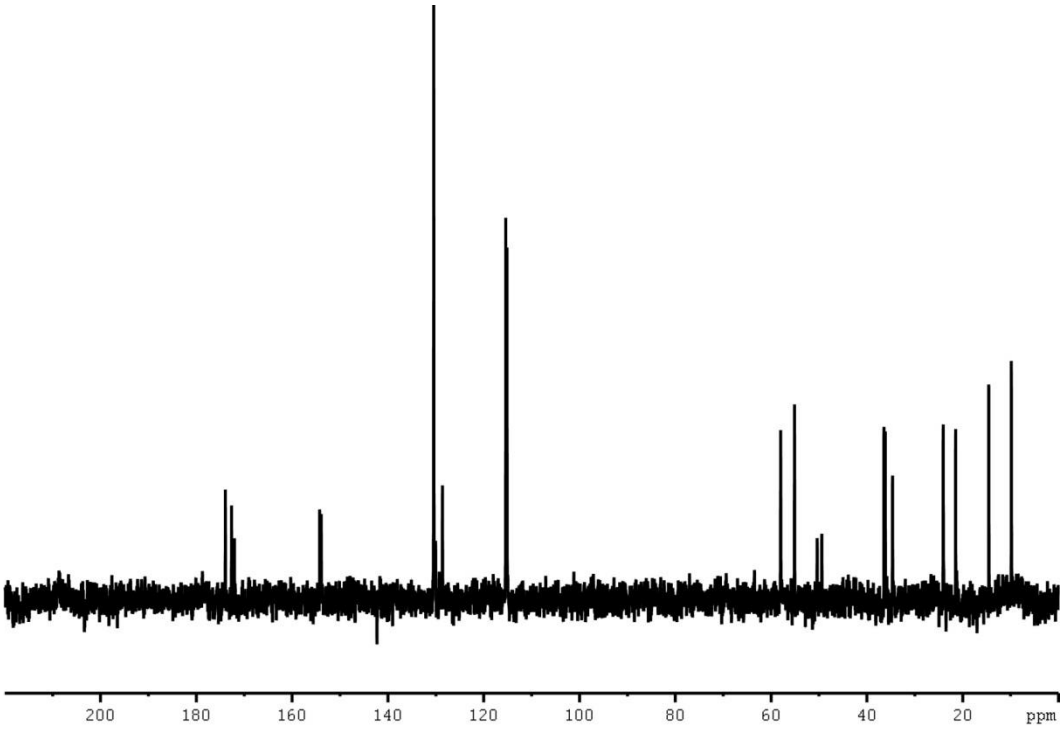

^{13}CNMR Spectrum (150 MHz) of Ac-Tyr-Ile-AHEP: N-(N-acetyl-L-tyrosyl-L-isoleucyl)-1-amino-2-(4-hydoxyphenyl)ethyl phosphonic acid (III-9) in D_2O

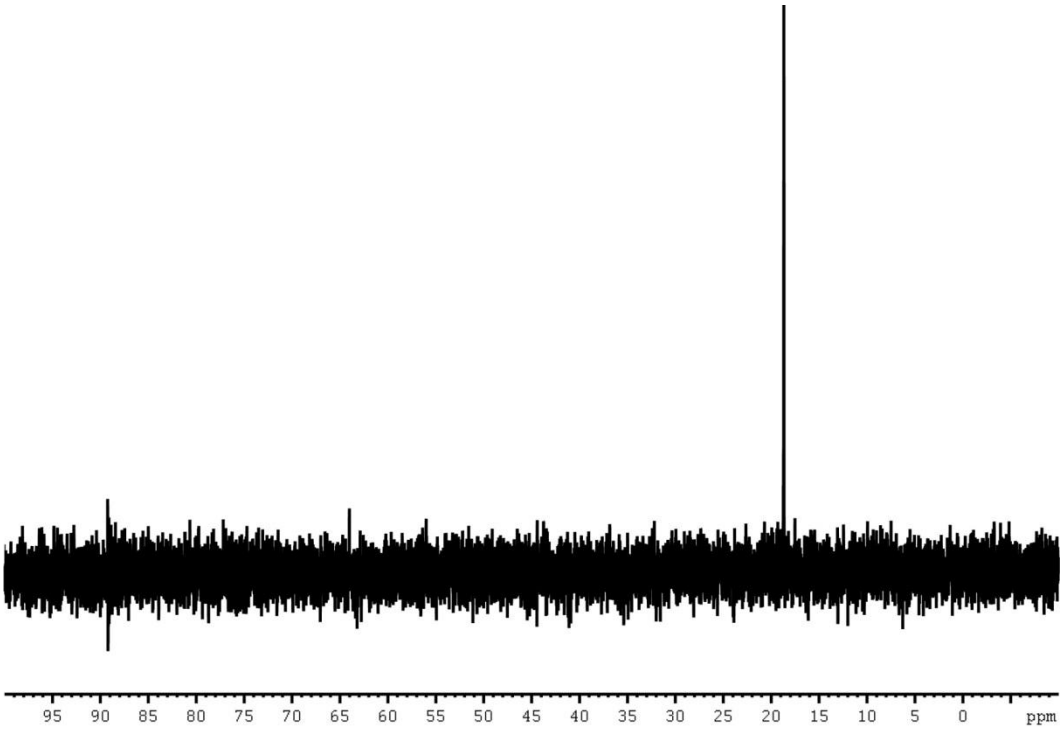

^{31}PNMR Spectrum (162 MHz) of Ac-Ile-Trp-AHEP of Ac-Tyr-Ile-AHEP: N-(N-acetyl-L-tyrosyl-L-isoleucyl)-1-amino-2-(4-hydoxyphenyl)ethyl phosphonic acid (III-9) in D_2O

NMR spectra of Ac-Pro-Tyr-AHEP (III-10) and synthetic intermediates (III-10a - III-10d)

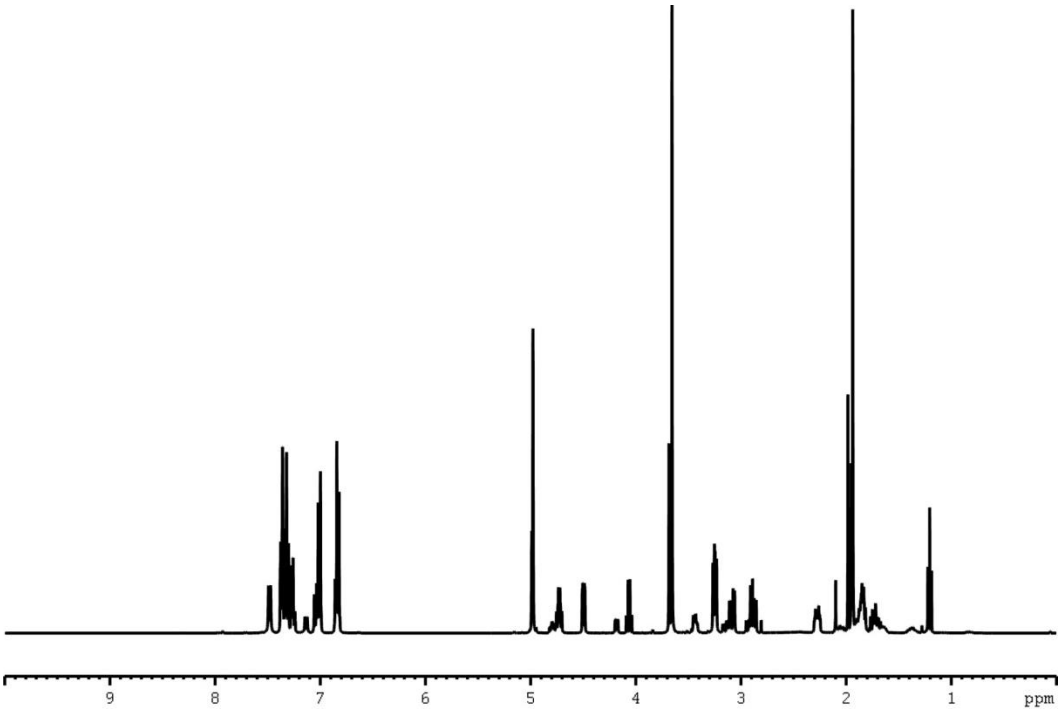

^{1}HNMR Spectrum (400 MHz) of N-acetyl-L-prolinyl-O-benzyl-L-tyrosine methyl ester (III-10a) in $CDCl_3$

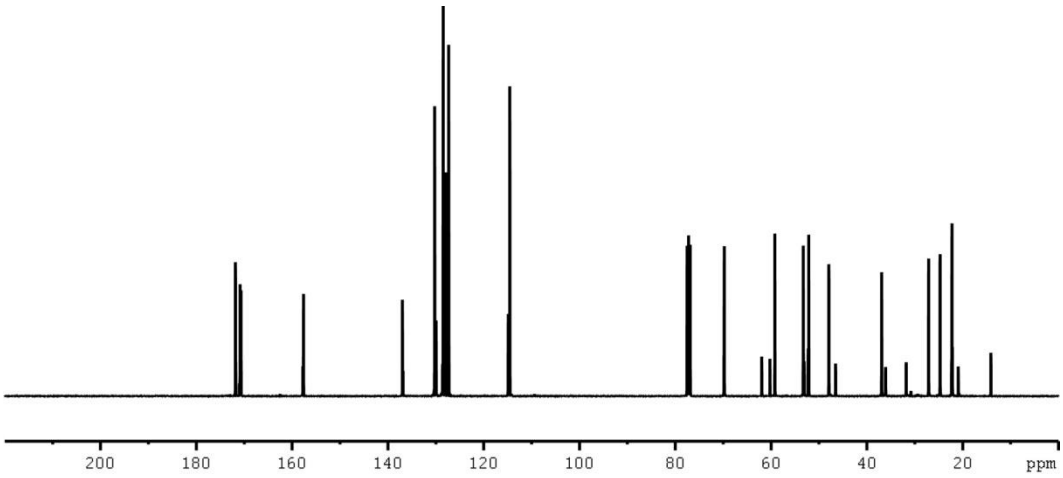

^{13}CNMR Spectrum (100 MHz) of N-acetyl-L-prolinyl-O-benzyl-L-tyrosine methyl ester (III-10a) in $CDCl_3$

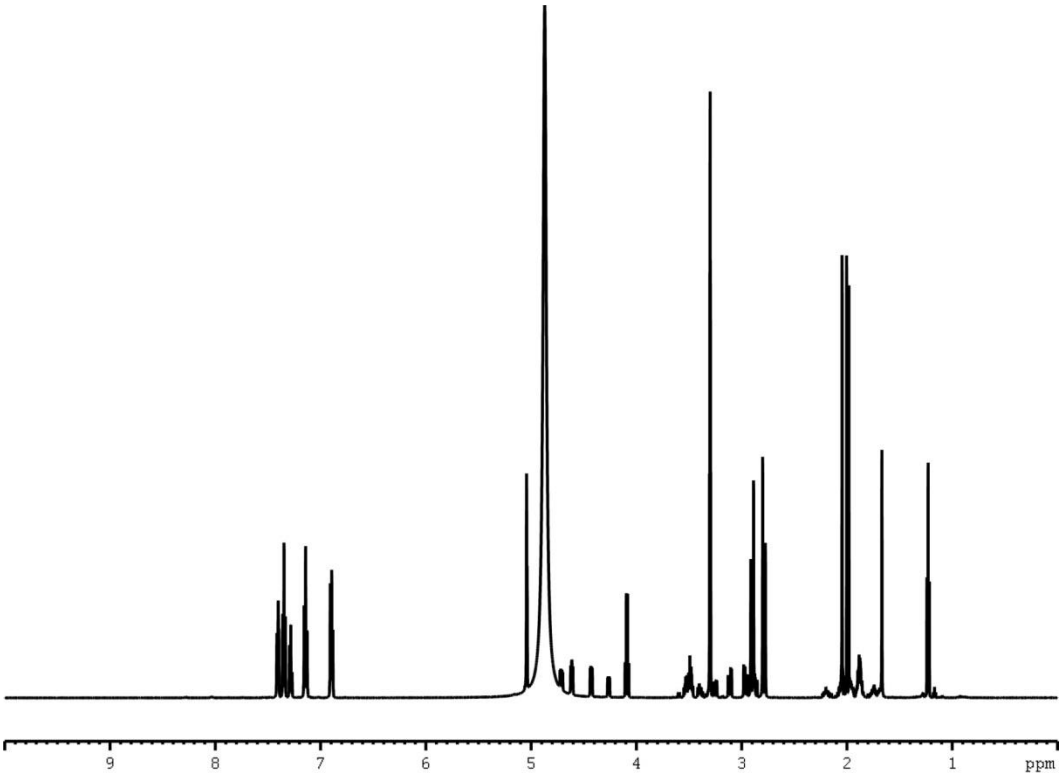

^{1}HNMR Spectrum (400 MHz) of N-acetyl-L-prolinyl-O-benzyl-L-tyrosine (III-10b) in MeOD

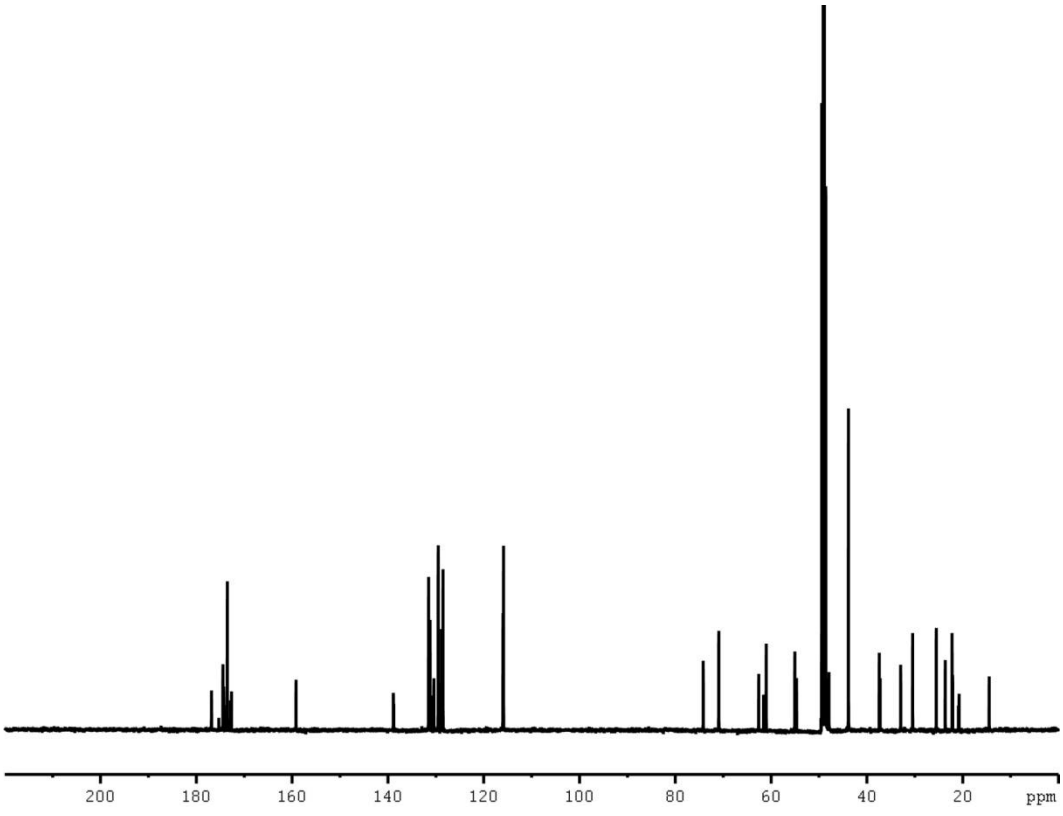

^{13}CNMR Spectrum (100 MHz) of N-acetyl-L-prolinyl-O-benzyl-L-tyrosine (III-10b) in MeOD

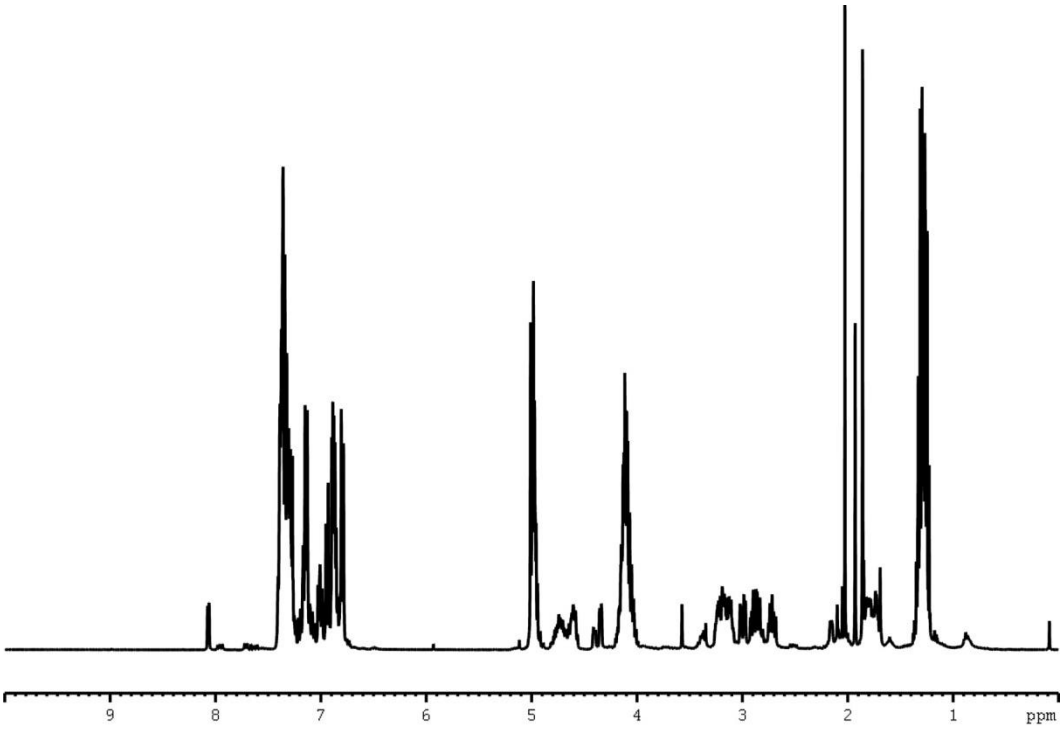

^{1}HNMR Spectrum (600 MHz) of diethyl N-(N-acetyl-L-prolinyl-O-benzyl-L-tyrosyl)-1-amino-2-(4-benzyloxyphenyl)ethyl phosphonate (III-10c) in $CDCl_3$

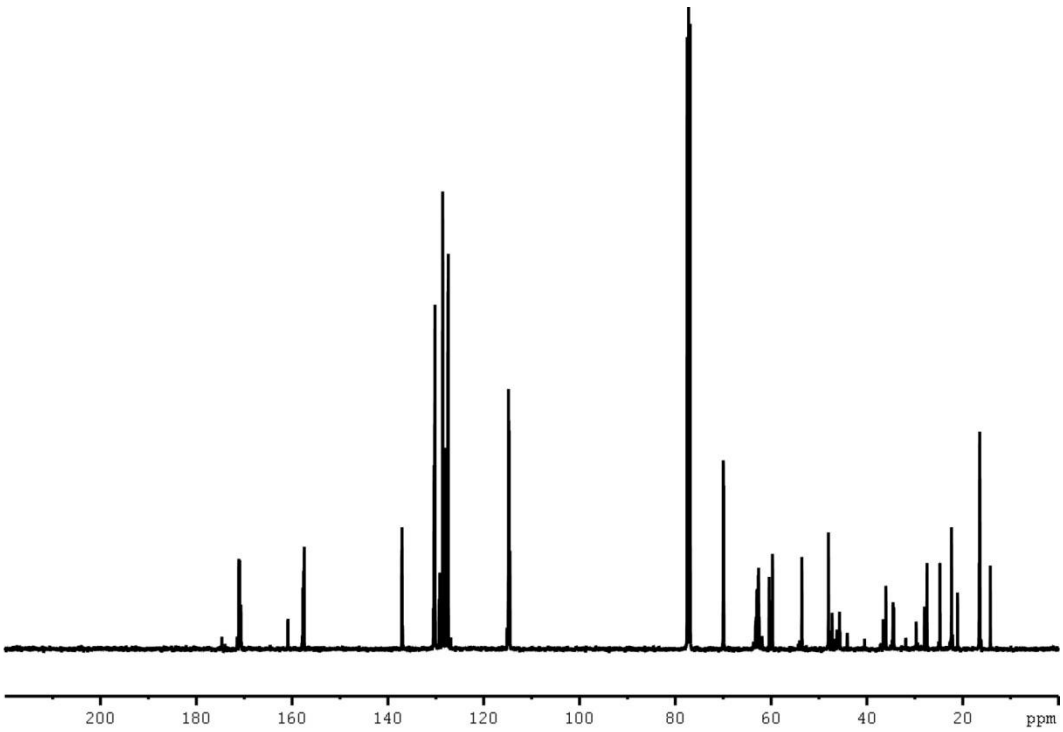

^{13}CNMR Spectrum (150 MHz) of diethyl N-(N-acetyl-L-prolinyl-O-benzyl-L-tyrosyl)-1-amino-2-(4-benzyloxyphenyl)ethyl phosphonate (III-10c) in $CDCl_3$

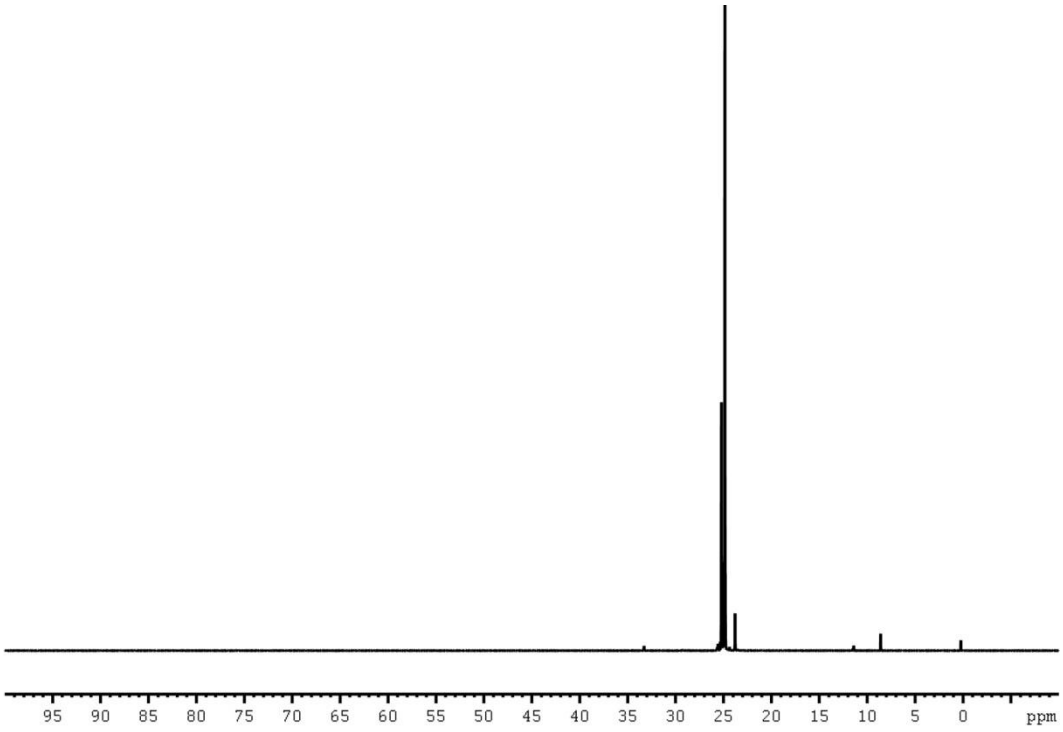

^{31}PNMR Spectrum (162 MHz) of diethyl N-(N-acetyl-L-prolinyl-O-benzyl-L-tyrosyl)-1-amino-2-(4-benzyloxyphenyl)ethyl phosphonate (III-10c) in $CDCl_3$

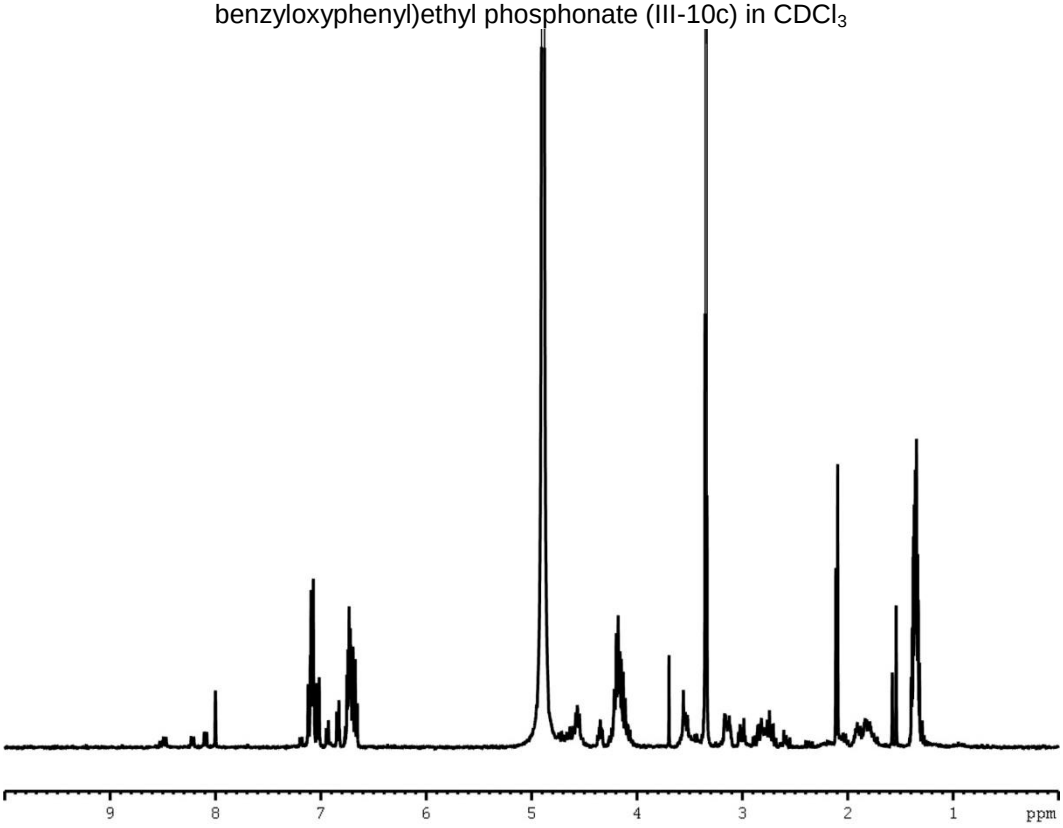

^{1}HNMR Spectrum (600 MHz) of diethyl N-(N-acetyl-L-prolinyl-O-benzyl-L-tyrosyl)-1-amino-2-(4-hydoxyphenyl)ethyl phosphonate (III-10d) in MeOD

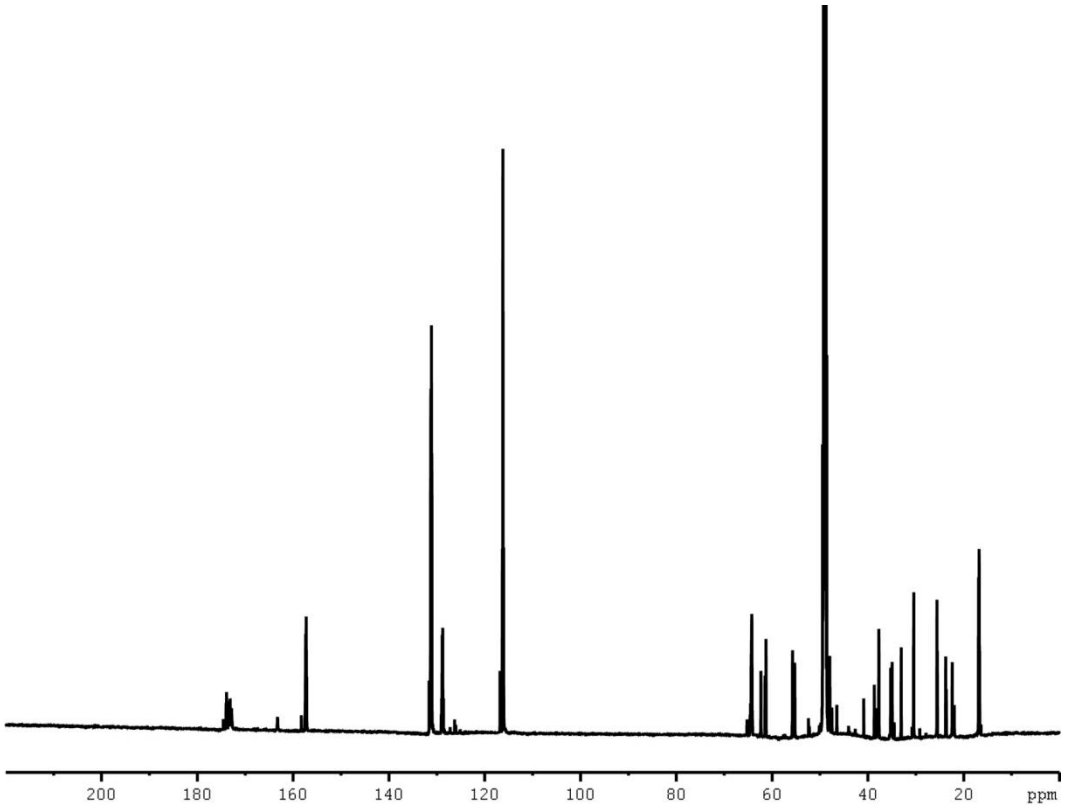

^{13}CNMR Spectrum (150 MHz) of diethyl N-(N-acetyl-L-prolinyl-O-benzyl-L-tyrosyl)-1-amino-2-(4-hydoxyphenyl)ethyl phosphonate (III-10d) in MeOD

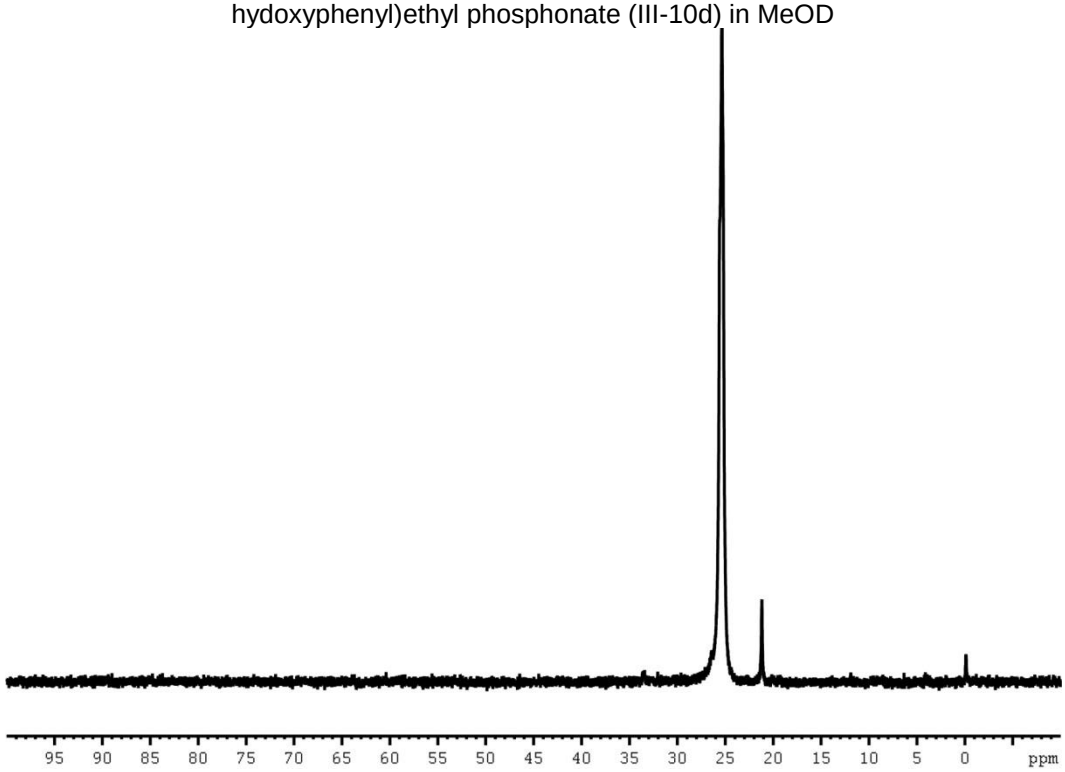

^{31}PNMR Spectrum (121 MHz) diethyl N-(N-acetyl-L-prolinyl-O-benzyl-L-tyrosyl)-1-amino-2-(4-hydoxyphenyl)ethyl phosphonate (III-10d) in MeOD

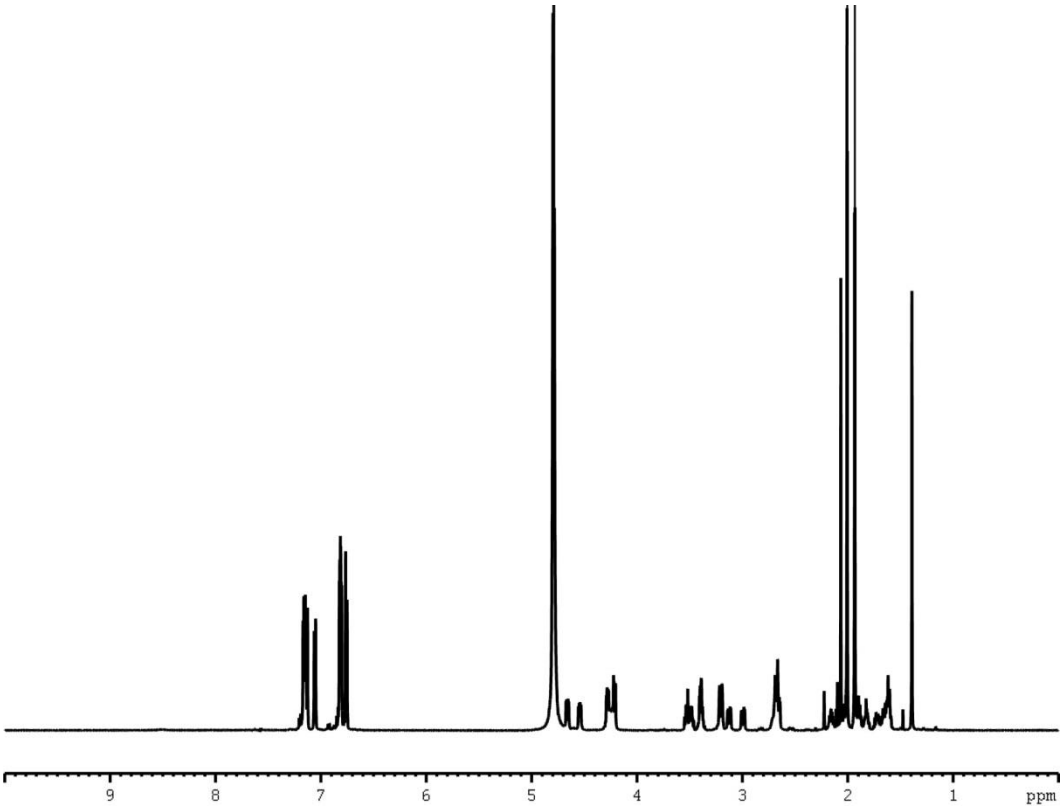

^{1}HNMR Spectrum (600 MHz) of Ac-Leu-Tyr-AHEP: N-(N-acetyl-L-prolinyl-L-tyrosyl)-1-amino-2-(4-hydoxyphenyl)ethyl phosphonic acid (III-10) in D_2O

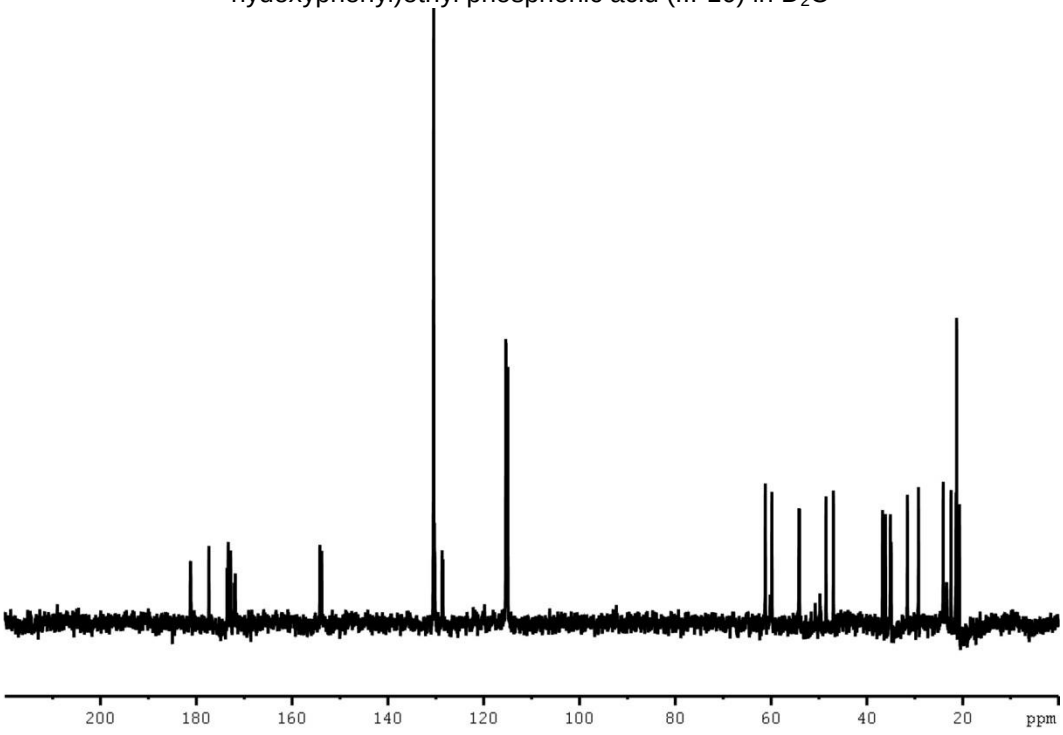

^{13}CNMR Spectrum (150 MHz) of Ac-Leu-Tyr-AHEP: N-(N-acetyl-L-prolinyl-L-tyrosyl)-1-amino-2-(4-hydoxyphenyl)ethyl phosphonic acid (III-10) in D_2O

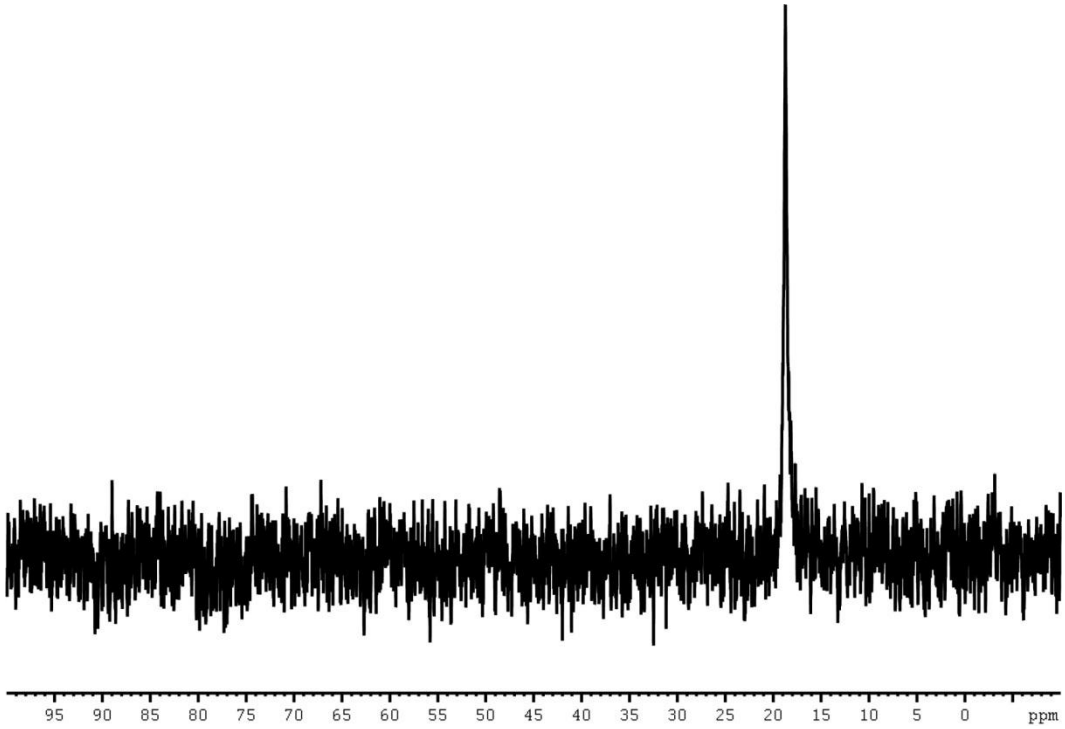

^{31}PNMR Spectrum (162 MHz) of Ac-Leu-Tyr-AHEP: N-(N-acetyl-L-prolinyl-L-tyrosyl)-1-amino-2-(4-hydoxyphenyl)ethyl phosphonic acid (III-10) in D_2O

APPENDIX E

GRAPHS USED IN IC_{50} CALCULATIONS

FROM CHAPTER III

IC_{50} curves for inhibition of somatic ACE by K-26 variant

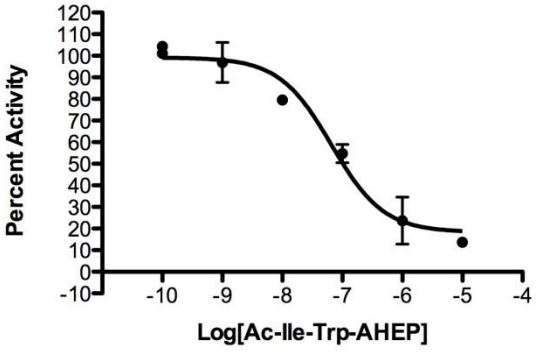

IC_{50} = 6.569e-008 M

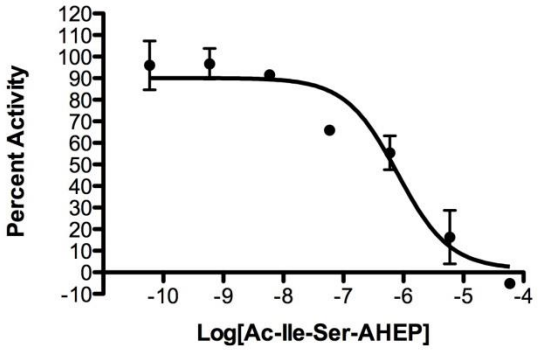

IC_{50} = 7.996e-007 M

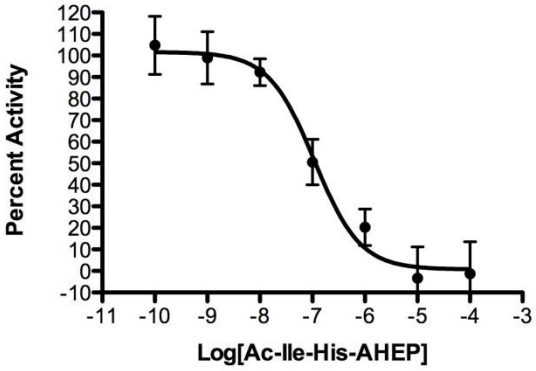

IC_{50} = 1.093e-007 M

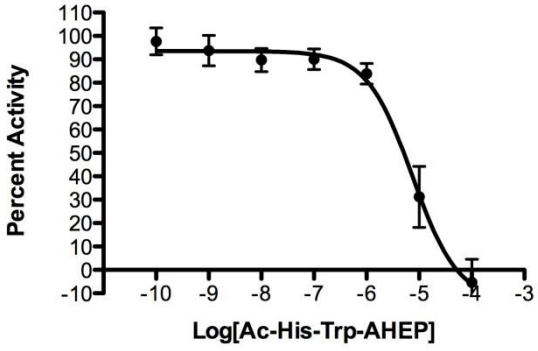

IC_{50} = 7.433e-006M

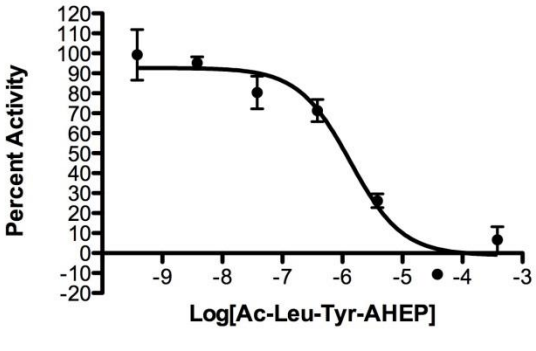

IC_{50} = 1.352e-006 M

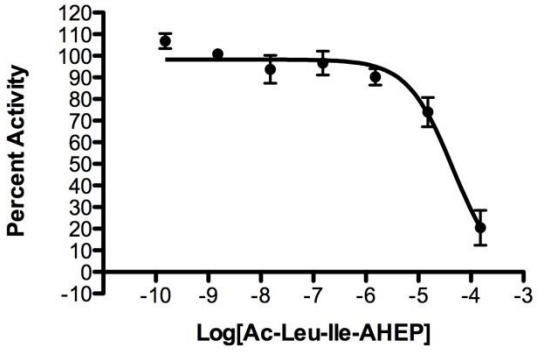

IC_{50} = 4.551e-005 M

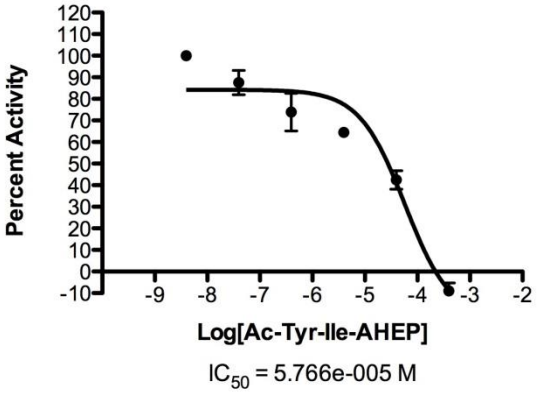
Percent Activity
120
110
100
90
80
70
60
50
40
30
20
10
0
-10
-9
-8
-7
-6
-5
-4
-3
-2
Log[Ac-Tyr-Ile-AHEP]
IC50 = 5.766e-005 M

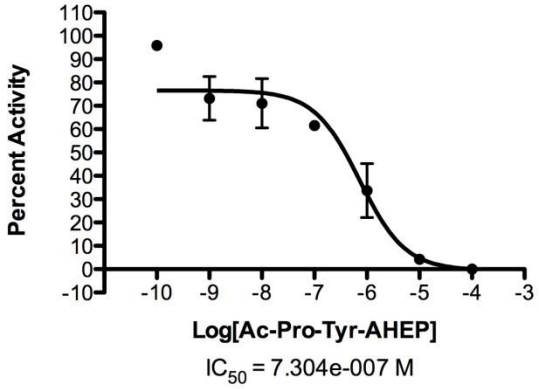
Percent Activity
110
100
90
80
70
60
50
40
30
20
10
0
-10
-10
-9
-8
-7
-6
-5
-4
-3
Log[Ac-Pro-Tyr-AHEP]
IC50 = 7.304e-007 M

APPENDIX F

NMR SPECTRA

OF BIOTIN PROBE

FROM CHAPTER IV

^{1}H NMR of Biotin-PEG$_{12}$-K-26 (IV-8)